frontiers | Research Topics

Recent highlights in the development of therapeutic antiviral strategies

Edited by
Gaëtan Ligat, Cécile E. Malnou, William Rawlinson and Stuart T. Hamilton

Published in
Frontiers in Microbiology

ISSN 1664-8714
ISBN 978-2-8325-4161-6
DOI 10.3389/978-2-8325-4161-6

About Frontiers

Frontiers is more than just an open access publisher of scholarly articles: it is a pioneering approach to the world of academia, radically improving the way scholarly research is managed. The grand vision of Frontiers is a world where all people have an equal opportunity to seek, share and generate knowledge. Frontiers provides immediate and permanent online open access to all its publications, but this alone is not enough to realize our grand goals.

Frontiers journal series

The Frontiers journal series is a multi-tier and interdisciplinary set of open-access, online journals, promising a paradigm shift from the current review, selection and dissemination processes in academic publishing. All Frontiers journals are driven by researchers for researchers; therefore, they constitute a service to the scholarly community. At the same time, the *Frontiers journal series* operates on a revolutionary invention, the tiered publishing system, initially addressing specific communities of scholars, and gradually climbing up to broader public understanding, thus serving the interests of the lay society, too.

Dedication to quality

Each Frontiers article is a landmark of the highest quality, thanks to genuinely collaborative interactions between authors and review editors, who include some of the world's best academicians. Research must be certified by peers before entering a stream of knowledge that may eventually reach the public - and shape society; therefore, Frontiers only applies the most rigorous and unbiased reviews. Frontiers revolutionizes research publishing by freely delivering the most outstanding research, evaluated with no bias from both the academic and social point of view. By applying the most advanced information technologies, Frontiers is catapulting scholarly publishing into a new generation.

What are Frontiers Research Topics?

Frontiers Research Topics are very popular trademarks of the *Frontiers journals series*: they are collections of at least ten articles, all centered on a particular subject. With their unique mix of varied contributions from Original Research to Review Articles, Frontiers Research Topics unify the most influential researchers, the latest key findings and historical advances in a hot research area.

Find out more on how to host your own Frontiers Research Topic or contribute to one as an author by contacting the Frontiers editorial office: frontiersin.org/about/contact

Recent highlights in the development of therapeutic antiviral strategies

Topic editors

Gaëtan Ligat — INSERM UMR1291 Institut Toulousain des Maladies Infectieuses et Inflammatoires, France

Cécile E. Malnou — Université Toulouse III Paul Sabatier, France

William Rawlinson — New South Wales Health Pathology, Australia

Stuart T. Hamilton — University of New South Wales, Australia

Citation

Ligat, G., Malnou, C. E., Rawlinson, W., Hamilton, S. T., eds. (2023). *Recent highlights in the development of therapeutic antiviral strategies*. Lausanne: Frontiers Media SA. doi: 10.3389/978-2-8325-4161-6

Table of contents

05 Editorial: Recent highlights in the development of therapeutic antiviral strategies
Cécile E. Malnou and Gaëtan Ligat

07 Multiple functions of stress granules in viral infection at a glance
Yuelin Guan, Yan Wang, Xudong Fu, Guannan Bai, Xue Li, Jianhua Mao, Yongbin Yan and Lidan Hu

18 Dextran sulfate from *Leuconostoc mesenteroides* B512F exerts potent antiviral activity against SARS-CoV-2 *in vitro* and *in vivo*
Sabina Andreu, Cayetano von Kobbe, Pilar Delgado, Inés Ripa, María José Buzón, Meritxell Genescà, Núria Gironès, Javier del Moral-Salmoral, Gustavo A. Ramírez, Sonia Zúñiga, Luis Enjuanes, José Antonio López-Guerrero and Raquel Bello-Morales

35 Combination therapy of therapeutic antibody and vaccine or entecavir in HBV carrier mice
Ruoyao Qi, Jiali Cao, Yangtao Wu, Xing Lei, Jinhang He, Liang Zhang, Rao Fu, Feng Chen, Yingbin Wang, Tianying Zhang, Ningshao Xia and Quan Yuan

47 The FDA-approved drug nitazoxanide is a potent inhibitor of human seasonal coronaviruses acting at postentry level: effect on the viral spike glycoprotein
Sara Piacentini, Anna Riccio, Silvia Santopolo, Silvia Pauciullo, Simone La Frazia, Antonio Rossi, Jean-Francois Rossignol and M. Gabriella Santoro

60 Mechanism of *Lactiplantibacillus plantarum* regulating Ca^{2+} affecting the replication of PEDV in small intestinal epithelial cells
Zifei Kan, Shujuan Zhang, Guisong Liao, Zheng Niu, Xiangyang Liu, Zhiwei Sun, Xia Hu, Yiling Zhang, Shasha Xu, Jingyi Zhang, Hong Zou, Xingcui Zhang and Zhenhui Song

73 Hantavirus: an overview and advancements in therapeutic approaches for infection
Samia Afzal, Liaqat Ali, Anum Batool, Momina Afzal, Nida Kanwal, Muhammad Hassan, Muhammad Safdar, Atif Ahmad and Jing Yang

95 Corrigendum: Hantavirus: an overview and advancements in therapeutic approaches for infection
Samia Afzal, Liaqat Ali, Anum Batool, Momina Afzal, Nida Kanwal, Muhammad Hassan, Muhammad Safdar, Atif Ahmad and Jing Yang

101 Antiviral activity of zinc against hepatitis viruses: current status and future prospects
Shiv Kumar, Shabnam Ansari, Sriram Narayanan, C. T. Ranjith-Kumar and Milan Surjit

122 Functional epitopes and neutralizing antibodies of vaccinia virus
Fenghao Peng, Naijing Hu, Yingjun Liu, Cong Xing, Longlong Luo, Xinying Li, Jing Wang, Guojiang Chen, He Xiao, Chenghua Liu, Beifen Shen, Jiannan Feng and Chunxia Qiao

131 Anti-CMV therapy, what next? A systematic review
Claire Gourin, Sophie Alain and Sébastien Hantz

162 Lactic acid bacterial surface display of scytovirin inhibitors for anti-ebolavirus infection
Joshua Wiggins, Ngan Nguyen, Wenzhong Wei, Leah Liu Wang, Haley Hollingsead Olson and Shi-Hua Xiang

frontiers | Frontiers in Microbiology

TYPE Editorial
PUBLISHED 05 December 2023
DOI 10.3389/fmicb.2023.1338999

OPEN ACCESS

EDITED AND REVIEWED BY
Anna Kramvis,
University of the Witwatersrand, South Africa

*CORRESPONDENCE
Gaëtan Ligat
✉ gaetan.ligat@inserm.fr

RECEIVED 15 November 2023
ACCEPTED 23 November 2023
PUBLISHED 05 December 2023

CITATION
Malnou CE and Ligat G (2023) Editorial: Recent highlights in the development of therapeutic antiviral strategies.
Front. Microbiol. 14:1338999.
doi: 10.3389/fmicb.2023.1338999

Editorial: Recent highlights in the development of therapeutic antiviral strategies

Cécile E. Malnou and Gaëtan Ligat*

Institut Toulousain des Maladies Infectieuses et Inflammatoires (Infinity), Université de Toulouse, Institut national de la santé et de la recherche médicale (INSERM), Centre national de la recherche scientifique (CNRS), Université Toulouse III - Paul Sabatier (UPS), Toulouse, France

KEYWORDS

antiviral strategies, viral inhibitor, vesicles, miRNA, genes editing and silencing

Editorial on the Research Topic
Recent highlights in the development of therapeutic antiviral strategies

Recent developments in antiviral therapies are at the forefront of medical research, shaping the landscape of viral disease management and offering new hope in the fight against viral infections. Biotherapies, in the realm of antiviral treatments represent a cutting-edge approach to combat viral infections. These therapies leverage biological agents such as antibodies, interferons, or engineered immune cells to directly target viruses, or host factors, to improve the immune response. One notable example is the development of monoclonal antibodies, which have shown remarkable effectiveness in neutralizing viruses like SARS-CoV-2. The development of interferon-based therapies is another notable recent innovation. These treatments stimulate the host immune response, which improves its capacity to fight viral infections such as Hepatitis B Virus (HBV) infection. Recently, nucleic acid technologies have revolutionized antiviral strategies. mRNA vaccines, exemplified by those designed to combat COVID-19, have demonstrated effectiveness and adaptability against emerging viral variants. However, challenges persist in the pursuit of effective antiviral treatments. New therapeutic strategies need to be developed to overcome viral resistance. Beyond therapeutic strategies, a comprehensive approach to antiviral efforts includes a focus on prevention, early detection, and public education. Vaccination campaigns, innovative strategies for rapid viral detection, and public awareness programs all contribute to the fight against viral infections and improve global health outcomes.

In this Research Topic, we have collected original research and review articles covering many different aspects of therapeutic antiviral strategies.

Among them, several manuscripts mainly focused on antiviral therapies against coronaviruses. In an elegant study, Andreu et al. report for the first time the broad-spectrum antiviral activity of a Dextran sulfate-based extrapolymeric substance produced by the lactic acid bacterium *Leuconostoc mesenteroides* B512F. They evaluated the toxicity and antiviral efficacy upon inhalation of this exopolysaccharide substance in mouse models susceptible to SARS-CoV-2 infection, and demonstrated a strong inhibition of SARS-CoV-2 infection *in vivo*. Moreover, they also demonstrated a broad-spectrum antiviral activity of this substance against several enveloped viruses such as SARS-CoV-2, HCoV229E, HSV-1, in *in vitro* models and in human lung tissue. In another study, Piacentini et al. showed that the anti-infective drug nitazoxanide has a potent antiviral activity against three human seasonal coronaviruses HCoV-229E, -NL63, and OC43 in cell culture. Nitazoxanide does not affect HCoV adsorption, entry or uncoating, but acts at post-entry level, interfering with the

spike glycoprotein maturation. Together, these two studies propose promising tools for the treatment of seasonal coronavirus infections. Finally, Guan et al. summarized the antiviral mechanisms of stress granules (SGs) and provided new insights into the development of SG-targeted antiviral drugs according to different pathways, particularly in the context of SARS-CoV-2.

Apart from the example of the study of Andreu et al. using a bacterium deriving molecule as antiviral treatment, other works presented in this Research Topic have used such antiviral approaches. In an interesting study, Wiggins et al. engineered two bacterial strains (*Lactobacillus casei* and *Lactococcus lactis*) for expressing scytovirin, a lectin deriving from cyanobacteria, on the bacterial surface. They demonstrated that both bacterial strains neutralize pseudotyped Ebolavirus in a cell-based assay. In a similar way, Kan et al. proposed a potential new drug to treat porcine epidemic diarrhea virus (PEDV) infection, by using *Lactiplantibacillus plantarum* supernatant. This acts by promoting the balance of intra- and extracellular Ca 2+ concentrations, thereby inhibiting PEDV proliferation with depends on intracellular Ca 2+ level.

In another work, Qi et al. evaluated the potential for synergistic effects of combination therapies to treat chronic hepatitis B infection. They presented two combination approaches aiming to target HBsAg and HBV-DNA. The first involved the use of antibodies followed by the administration of a therapeutic vaccine. The second combined antibodies with Entecavir. In both cases, they have shown that they constitute promising strategies to treat hepatitis B.

Finally, three reviews present current knowledge in antiviral approaches for chosen viruses. In the first one, Peng et al. presented functional epitopes and neutralizing antibodies of vaccinia virus, and discussed their potential value in the context of smallpox prevention and treatment. In a second manuscript, Afzal et al. reviewed current advances in therapeutic strategies, immune-based therapies and vaccine candidates for Hantavirus infections. Lastly, Gourin et al. presented the state of the current knowledge about anti-human cytomegalovirus (HCMV) therapies. They described the various molecules developed against HCMV with their mode of action, preclinical tests, clinical studies and possible resistance.

Significant progress has been made over the past decades in the development of new antiviral therapeutic approaches. In addition to the discovery and development of treatments for viral infections for which we do not yet have a strategy, the main challenge is to develop therapeutic approaches to overcome resistance mutations and toxicity of approved therapies. Overall, this Research Topic covered a large panel of antiviral strategies including new drugs, immune-based therapies, therapeutic antibody, and vaccine, and offer new perspectives for therapeutic intervention.

Author contributions

CEM: Writing — original draft, Writing — review & editing. GL: Writing — original draft, Writing — review & editing.

Funding

The author(s) declare financial support was received for the research, authorship, and/or publication of this article. CM received financial support from the ANR Corofet grant (ANR-21-CE14-0030), the Défi Clé Cell Based Biotherapies Occitanie (EXOBARRIER), and the Défi Clé Risques Infectieux et Vecteurs Occitanie (ZIKEV-sf). GL received financial support from the Défi Clé Cell Based Biotherapies Occitanie (INTERCYTE). Our team received institutional grants from INSERM, CNRS, and Toulouse III University.

Acknowledgments

The authors would like to thank the authors and reviewers of this Research Topic for their contribution and quick respond in all stages of the revision process.

Conflict of interest

The authors declare that the research was conducted in the absence of any commercial or financial relationships that could be construed as a potential conflict of interest.

Publisher's note

frontiers | Frontiers in Microbiology

TYPE Review
PUBLISHED 01 March 2023
DOI 10.3389/fmicb.2023.1138864

OPEN ACCESS

EDITED BY
Gaëtan Ligat,
Université Toulouse III Paul Sabatier,
France

REVIEWED BY
Sourish Ghosh,
Indian Institute of Chemical Biology (CSIR),
India
Zhen Luo,
Jinan University,
China
Jia Xue,
China Agricultural University,
China

*CORRESPONDENCE
Yongbin Yan
✉ ybyan@tsinghua.edu.cn
Lidan Hu
✉ hulidan@zju.edu.cn

†These authors have contributed equally to this work

SPECIALTY SECTION
This article was submitted to Virology, a section of the journal Frontiers in Microbiology

RECEIVED 06 January 2023
ACCEPTED 08 February 2023
PUBLISHED 01 March 2023

CITATION
Guan Y, Wang Y, Fu X, Bai G, Li X, Mao J, Yan Y and Hu L (2023) Multiple functions of stress granules in viral infection at a glance. *Front. Microbiol.* 14:1138864. doi: 10.3389/fmicb.2023.1138864

Multiple functions of stress granules in viral infection at a glance

Yuelin Guan[1†], Yan Wang[1†], Xudong Fu[2,3], Guannan Bai[1], Xue Li[4], Jianhua Mao[1], Yongbin Yan[5*] and Lidan Hu[1*]

[1]The Children's Hospital, Zhejiang University School of Medicine, National Clinical Research Center for Child Health, Hangzhou, China, [2]Center of Stem Cell and Regenerative Medicine, and Bone Marrow Transplantation Center of the First Affiliated Hospital, Zhejiang University School of Medicine, Hangzhou, Zhejiang, China, [3]Zhejiang Laboratory for Systems and Precision Medicine, Zhejiang University Medical Center, Hangzhou, Zhejiang, China, [4]Department of Big Data in Health Science School of Public Health and The Second Affiliated Hospital, Zhejiang University School of Medicine, Hangzhou, Zhejiang, China, [5]State Key Laboratory of Membrane Biology, School of Life Sciences, Tsinghua University, Beijing, China

Stress granules (SGs) are distinct RNA granules induced by various stresses, which are evolutionarily conserved across species. In general, SGs act as a conservative and essential self-protection mechanism during stress responses. Viruses have a long evolutionary history and viral infections can trigger a series of cellular stress responses, which may interact with SG formation. Targeting SGs is believed as one of the critical and conservative measures for viruses to tackle the inhibition of host cells. In this systematic review, we have summarized the role of SGs in viral infection and categorized their relationships into three tables, with a particular focus on Severe Acute Respiratory Syndrome Coronavirus 2 (SARS-CoV-2) infection. Moreover, we have outlined several kinds of drugs targeting SGs according to different pathways, most of which are potentially effective against SARS-CoV-2. We believe this review would offer a new view for the researchers and clinicians to attempt to develop more efficacious treatments for virus infection, particularly for the treatment of SARS-CoV-2 infection.

KEYWORDS

stress granule, viral infection, SARS-CoV-2, drug design, antiviral drugs

1. Introduction

In eukaryotic cells, the membraneless organelles composed of mRNA and proteins are called RNA granules (Anderson and Kedersha, 2009). Stress granules (SGs), one type of RNA granules, transiently form in the cytoplasm during cellular stress and are evolutionarily conservative in animals and plants (Spector, 2006; Reineke and Neilson, 2019). SGs are involved in the regulation of transcription and translation which is essential for maintaining cellular homeostasis. Life is full of transient stress, and eukaryotic cells have developed sophisticated coping mechanisms to deal with a bombardment of cellular challenges (Morimoto, 2011; Li et al., 2013). SG formation appears to be a prudent and essential mechanism during stress responses; it reduces energy use, restores cellular homeostasis, and increases cell viability under damaging conditions (Mahboubi and Stochaj, 2017).

SGs are composed of multiple factors including translation initiation factors, polyadenylated RNA, small ribosomal subunits, and numerous RNA binding proteins (RBPs; Thomas et al., 2011; Aulas and Vande Velde, 2015). These components can be divided into three grades (Fan

and Leung, 2016). The innermost part exists in almost all SGs induced by various stress conditions. It consists of a 48S pre-initiation complex, along with stalled mRNA transcripts, such as poly (A)-binding protein-1 (PABP-1), eukaryotic initiation factor 3 (eIF3), eukaryotic initiation factor 4B (eIF4B), eukaryotic initiation factor 4F (eIF4F), and eukaryotic initiation factor 4A (eIF4A), etc., (Anderson and Kedersha, 2002). The middle part contains some scaffold proteins, such as GTPase-activating protein SH3 domain-binding protein 1/2 (G3BP1/2) and T cell intracellular antigen 1 (TIA-1; Matsuki et al., 2013). The outermost part contains variant signaling proteins based on the various cellular environment. Various amounts and sizes of SGs with specific stress-related components (i.e., protein and RNA) would be formed differently depending on the cell types, stress situations, and changes in action time (Moeller et al., 2004). In brief, as a rapid response signaling hub, SG with complex structures plays an important regulatory role in a variety of stress injuries. Along with this, it is reasonable to speculate that misregulated SG dynamics may induce an inaccurate cellular state of physiological activity of both RNA metabolism and protein homeostasis (Li et al., 2013; Portz et al., 2021).

Abnormal metabolism of SGs has been found in a variety of diseases, including but not limited to cancer, neurodegenerative diseases (NDs), viral infections, autoimmune disease, cataracts, glaucoma, diabetes, and brain ischemia (Moujaber et al., 2017). Given that SGs have drawn widespread concern in recent years, the correlations between cancer or NDs and SGs have already been widely described (Chen and Liu, 2017; Gao et al., 2019; Hu et al., 2022), while reviews about the role of SGs in viral infections are less understood. Some studies point out that viral infections can trigger a series of cellular stress reactions and consequently regulate the assembly or disassembly of SGs (McInerney et al., 2005), suggesting the importance of SGs in balancing the translation of host-and virus-encoded mRNAs (Reineke and Neilson, 2019; Eiermann et al., 2020). In this review, we mainly focus on recent advances in the correlation between viruses and SGs, which may provide insight into developing new effective antiviral treatments in clinical application.

To better understand the relationship between SGs and anti-virus, this review first briefly describes the background of SGs and the information about viruses. Based on the interactions between SG and viruses, viruses were categorized into three main groups, i.e., inhibition, promotion, and temporary promotion of SG formation. Secondly, this review further recapitulates the role of SGs in the regulation of antiviral response, especially for several important antiviral function pathways of SGs are also highlighted. In particular, given that Severe Acute Respiratory Syndrome Coronavirus 2 (SARS-CoV-2) has made the most far-reaching impact in the world since 2019, this review also summarizes the current evidence regarding the connection between SARS-CoV-2 and SGs, aiming to provide insights into developing novel SG-based drugs for clinical treatment of SARS-CoV-2 infection.

2. The dynamic processes of SGs

SG formation appears to be a conservative and essential mechanism during stress responses. Once the cell recovers to its normal situation, SGs would transiently disassemble. The assembly and disassembly of SGs are regulated by environmental and physiological factors (Protter and Parker, 2016; Moujaber et al., 2017). By adjusting the balance between the translational repression mRNA and translating mRNAs, SG formation can handle the timely and appropriate response to stress conditions (Protter and Parker, 2016). The biogenesis of SGs under normal physiological conditions is usually divided into five phases based on the specific composition and localization of mRNPs (Anderson and Kedersha, 2008). Phase one: stalled initiation and ribosome runoff. Phase two: primary aggregation and nucleation. Phase three: secondary aggregation. Phase four: integration and signaling. Phase five: mRNA triage. SG disassembly is the reverse process. Large SGs are decomposed into small particles, and these small particles are subsequently depolymerized or removed (Kedersha et al., 2005). Along with the disappearance of stress, SGs are decomposed rapidly from the cytoplasm of cells through the chaperone pathway or autophagy pathway (Wheeler et al., 2016). These phases occur sequentially in normal conditions (the flow chart shown in Figure 1). Moreover, in some pathological conditions, such as hypoxia, a common feature of numerous pathological conditions, including myocardial infarction, stroke, inflammation, and malignant tumors, SG formation may inhibit cell apoptosis through translation arrest, prevention of unfolded proteins accumulation (Arimoto et al., 2008). Besides, SGs share many components with neuronal granules in neurons, which clearly indicates that SGs affect neurodegenerative diseases, amyotrophic lateral sclerosis (ALS) disease, frontotemporal lobar degeneration (FTLD), Alzheimer's disease (AD) and Spinal muscular atrophy (SMA; Anderson et al., 2015; Brownsword and Locker, 2022; Hu et al., 2022).

Once SGs are absent in cells for some reasons, it may cause various abnormal physiological activities and even the occurrence of diseases (Gao et al., 2019). For instance, the deficiency of G3BP1 leads to abnormal synaptic plasticity, calcium homeostasis in neurons, and increases apoptotic cell death (Zekri et al., 2005; Martin et al., 2013). TIA-1 knockout (KO) mice worsen hepatic steatosis and fibrosis (Dolicka et al., 2022) and dysregulate expression of lipid storage and membrane dynamics factors in nervous tissue (Heck et al., 2014). In the case of viral infections, in G3BP1 KO cells, the replication efficiency of mammalian orthoreovirus (MRV) is significantly improved (Carroll et al., 2014). In murine TIA-1-related protein (TIAR) KO cells, West Nile virus (WNV) growth is decreased (Li et al., 2002). In the following texts, we will mainly focus on the relationship between SGs and viral infection.

3. Viral infection regulates the SG formation in double ended manners

During the process of viral infection, the assembly and disassembly of SGs are intensively regulated (McCormick and Khaperskyy, 2017). There has been evidence showing that viral infection could interfere with SG formation through various mechanisms (White and Lloyd, 2012), such as inhibiting translational initiation (Linero et al., 2011), sequestering SG components (such as TIA-1, and G3BP1/2) (Nikolic et al., 2016), and interacting with key SG proteins to form stable viral ribonucleoprotein (RNP) complexes (Abrahamyan et al., 2010). However, some viruses have developed mechanisms to blunt host responses and manipulate SGs to evade host defenses (Kim et al., 2016). Viruses can regulate SG formation by three major manners: inducing SG formation, inducing SG transient formation, or inhibiting SG formation. Protein kinase R (PKR), one of the major innate immune mechanisms, is the primary sensor

10.3389/fmicb.2023.1138864

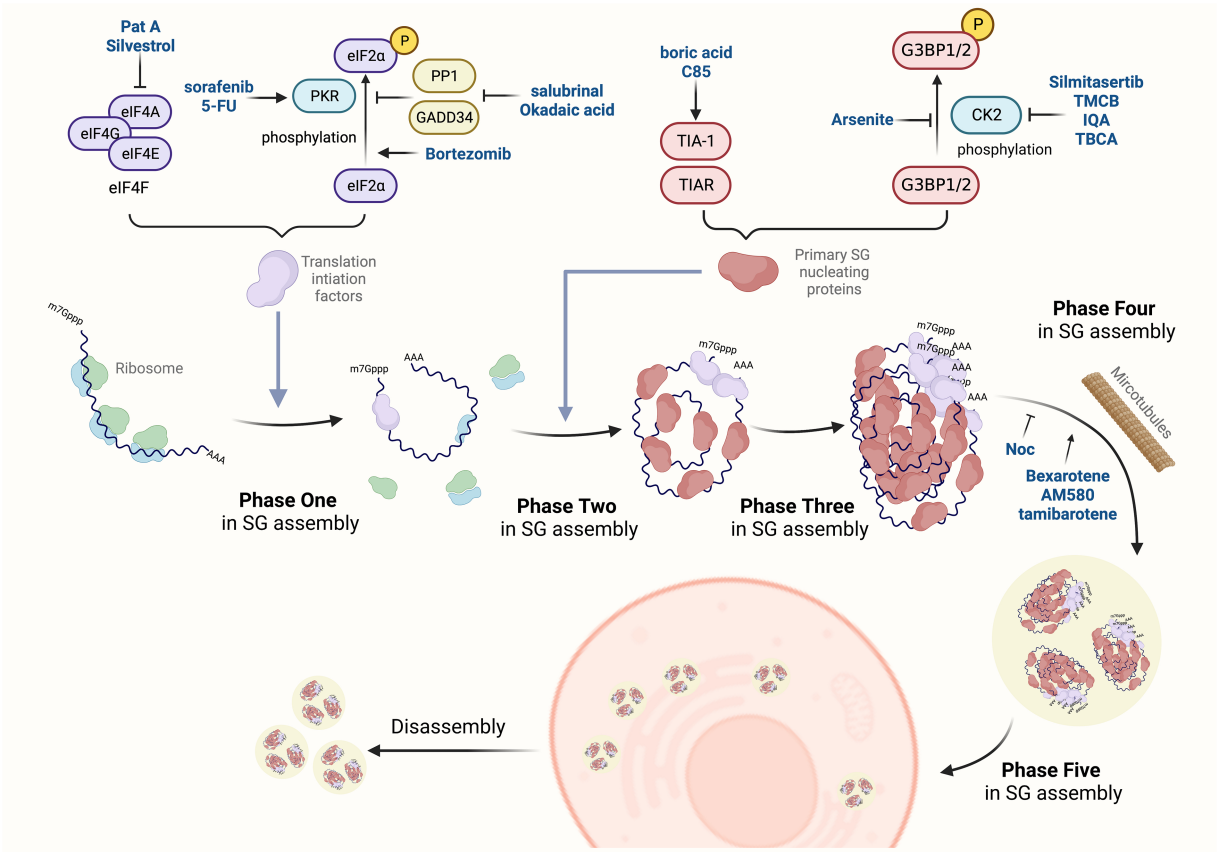

FIGURE 1
SGs-targeted antiviral drugs. The dynamic change of SGs is a complex process regulated by many post-translational modifications, protein remodeling complexes, and microtubule networks. The assembly of SG is divided into five phases. Phase one: SG assembly begins with stalled translation initiation, and ribosomes flow out to convert into mRNPs. Phase two: primary aggregation and nucleation occur when heterogeneous 48S-bound transcripts bind to self-aggregation RNA-binding proteins, such as G3BP1/2, TIA-1, tristetraprolin (TTP), and fragile X mental retardation protein (FMRP). Phase three: secondary aggregation and crosslinking occur when PABP-1 is bound to poly(A)-containing transcripts and smaller oligomers crosslink to assemble microscopic invisible aggregates. Phase four: some transcripts bind to multiple SG nucleating proteins, which enhance the cross-linking process to form progressively larger SGs, and then recruit non-RNA-binding proteins (e.g., TRAF2, plakophilins, SRC3, FAST). Phase five: specific transcripts are sorted out of SGs by translation initiation, assembling into other RNA granules. The disassembly of SGs is the reverse process. Novel drugs have been identified to affect the process of SGs assembly *via* different mechanisms.

responsible for host defense against invading viral pathogens *via* rapid inhibition of SG formation upon viral infection (Gao et al., 2022). And PKR is activated by double-stranded RNA (dsRNA) viruses. For the specific way of inducing SG transient formation, some RNA viruses activate the PKR pathway, resulting in the phosphorylation of eukaryotic initiator factor 2A (eIF2α) and promoting SG formation at the early stage of viral infection. Nevertheless, in the later stage of infection, they utilize several mechanisms to antagonize SG formation, such as G3BP1/2 cleavage and PKR inactivation to inhibit SG formation in turn (Ng et al., 2013; Okonski and Samuel, 2013). In the following text, we describe these three categories of viruses in detail.

3.1. Viruses induce SG formation

The first type of virus induces SG formation to aid viral RNA replication (Table 1). The "induced SGs" viruses are dedicated to activating eIF2α and/or recruiting SGs' core components.

Many viruses target the PKR/eIF2α pathway to trigger SG assembly and destroy the homeostasis of cells. For example, Sindbis virus (SINV) and Respiratory syncytial virus (RSV) infection activate PKR and induce eIF2α phosphorylation, which lead to SG assembly (Lindquist et al., 2011; Jefferson et al., 2019). Under oxidative stress and RSV infection, exposure to polyhexamethylene guanidine phosphate (PHMG-p) remarkably increases eIF2α phosphorylation and significantly increases SG formation (Choi et al., 2022). Given the limited space available, more targeted proteins of viruses are listed in Table 1. Beyond PKR, the virus can also activate other eIF2α kinases in cells. Porcine reproductive and respiratory syndrome virus (PRRSV) alternatively activates PKR-like endoplasmic reticulum kinase (PERK) to phosphorylate eIF2α and consequently stimulates cells to produce SGs (Zhou et al., 2017). Porcine hemagglutinating encephalomyelitis virus (PHEV) infection induces endoplasmic reticulum (ER) stress, activates the UPR, then activate PERK/PKR-eIF2α axis, as a result, promoting SG formation (Shi et al., 2022). Rift Valley fever virus (RVFV) reduces the PKB/mTOR (the protein kinase B, mechanistic target of rapamycin) signaling pathway, thereby increasing the activity of eIF4E binding protein 1/2 (4EBP1/2) to inhibit the translation process, and then cause transient SG assembly (Hopkins et al., 2015). Vesicular stomatitis virus (VSV) infection of

TABLE 1 Viruses induce SG formation.

Species	Type	Mechanism of formation	Refs
CSFV	(+) ssRNA	PKR phosphorylation, eIF2α phosphorylation	Liu et al. (2015)
HSV-2	dsDNA	Deletion of virion host shutoff protein (Vhs) inhibits elF2α phosphorylation	Finnen et al. (2014)
PRRSV	(+) ssRNA	eIF2α phosphorylation by PERK activation	Zhou et al. (2017)
PHEV	(+) ssRNA	activated PERK/PKR-eIF2α axis	Shi et al. (2022)
RSV	(−) ssRNA	PKR-mediated aggregation of SGs	Lindquist et al. (2011)
RVFV	(−) ssRNA	Down-regulation of PKB/mTOR signaling pathways and increased the activity of 4EBP1/2 proteins	Hopkins et al. (2015)
SINV	(+) ssRNA	Activation of GCN2 through its viral RNA; infection induces eIF2α phosphorylation, which leads to SG assembly	Jefferson et al. (2019)
TBEV	(+) ssRNA	Recruitment of TIA-1 and TIAR	Albornoz et al. (2014)
TGEV	(+) ssRNA	TIA-1/TIAR aggregation and elF2α phosphorylation	Sola et al. (2011)
VSV	(−) ssRNA	elF2α phosphorylation and SG-like particle formation and aggregation	Dinh et al. (2013)
VV	dsDNA	Deletion of E3L activates PKR	Simpson-Holley et al. (2011)

HSV-2, Herpes simplex virus type 2

TABLE 2 Viruses trigger SG formation temporarily.

Species	Type	Mechanism of formation	Refs
HCV	(+) ssRNA	Phosphorylation level of elF2α determines SG formation and depolymerization	Ruggieri et al. (2012)
MHV	(+) ssRNA	Addition of eIF2α phosphorylation	Raaben et al. (2007)
MRV	dsRNA	The high phosphorylation level of elF2α and interaction between G3BP1 and μNS	Qin et al. (2009), Qin et al. (2011) and Carroll et al. (2014)
PEDV	(+) ssRNA	Caspase-8-mediated cleavage of G3BP1 inhibits SG assembly and SG assembly is impaired by silencing G3BP1	Sun et al. (2021) and Guo et al. (2022)
PV	(+) ssRNA	Protease 2A can induce the generation of SGs at first, and the cleavage of G3BP1 by PV3C protease leads to SG depolymerization later	Dougherty et al. (2015) and Yang et al. (2018)
WNV	(+) ssRNA	W956IC can efficiently induce SGs through PKR activation	Courtney et al. (2012)

host cells will induce elF2α phosphorylation and promote SG-like particle formation and assembly (Dinh et al., 2013).

Besides, TIA-1/TIAR can be recruited to their replication sites to form SGs when host cells are infected by tick-borne encephalitis virus (TBEV) (Albornoz et al., 2014). Porcine transmissible gastroenteritis virus (TGEV) infection will also induce TIA-1/TIAR aggregation and elF2α phosphorylation, resulting in SG assembly at the late stage (Sola et al., 2011). Given that the regulation of SG formation is crucial for the replication of infected viruses, drugs that inhibit SGs by bypassing PKR (or other kinases) and/or eIF2α phosphorylation may have therapeutic potential to control the virus replication.

3.2. Viruses trigger SG formation temporarily

The second type of virus is featured to temporarily trigger SG formation in the early replication cycle but limit SG formation in the late replication cycle (Table 2).

The vast majority of these viruses regulate SG dynamics by regulating elF2α phosphorylation. Hepatitis C virus (HCV) infection rapidly induces the production of SGs in the early stage, and then the depolymerization of SGs occurs later, and this change happens depending on the phosphorylation level of elF2α (Ruggieri et al., 2012). In the early stage of infection, mouse hepatitis coronavirus (MHV) causes SG formation by promoting the elF2α phosphorylation (Raaben et al., 2007). MRV induces SG formation (Qin et al., 2009) in the early stage of infection, but the SG formation is reduced in the late stage of infection, regardless of the high elF2α phosphorylation (Qin et al., 2011). Although natural WNV infection does not induce SGs, the W956IC (a lineage 2/1 chimeric WNV infectious clone) efficiently induces SGs through PKR activation to phosphorylate elF2α at the early infection stage (Courtney et al., 2012).

Overexpression of G3BP may induce spontaneous SG formation (White and Lloyd, 2012). It has also been reported that MRV can recruit the viral non-structural protein μNS to interact with G3BP1, which interferes with SG assembly (Carroll et al., 2014). Epidemic diarrhea virus (PEDV) infection results in the cleavage of G3BP1 and this process is mediated by caspase-8 (Sun et al., 2021). And PEDV replication is significantly enhanced when SG assembly is impaired by silencing G3BP1 (Guo et al., 2022). Besides, protease 2A of poliovirus (PV) induces the generation of SGs at first, and the cleavage of G3BP1 by PV3C protease leads to SG disassembly later (Yang et al., 2018).

3.3. Viruses inhibit SG formation

Contrary to the above mechanisms, a prevalent group of viruses impinges on SG formation throughout the process of infection in Table 3.

TABLE 3 Viruses inhibit SG formation.

Species	Type	Mechanism of inhibition	Refs
CHIKV	(+) ssRNA	GADD34 to enhance the dephosphorylation of elF2α	Clavarino et al. (2012)
CVB3	(+) ssRNA	G3BP1 cleavage	Fung et al. (2013)
DENV	(+) ssRNA	recruit TIA/TIAR to replication complexes	Emara and Brinton (2007)
EBOV	(−) ssRNA	Inhibition of PKR pathway by VP35	Le Sage et al. (2017)
EMCV	(+) ssRNA	G3BP1 cleavage	Ng et al. (2013)
FCV	(+) ssRNA	The viral protease NSP6 to cleave G3BP1	Humoud et al. (2016)
FMDV	(+) ssRNA	L protein to stably interact with G3BP1	Visser et al. (2019)
HCMV	dsDNA	Encodement of pTRS1 to interact with PKR	Vincent et al. (2017)
HIV-1	ssRNA-RT	Assembly of SHRNP	Abrahamyan et al. (2010)
HSV	dsDNA	Inhibition of PERK activation and elF2α phosphorylation by surface glycoprotein gB; UL41 interferes with SG formation through its endoribonuclease activity	Mulvey et al. (2007) and Finnen et al. (2016)
HTLV-1	ssRNA-RT	Interaction with HDAC6 through Tax	Legros et al. (2011)
IAV	(−) ssRNA	Inhibition of PKR activation by NS1; Regulation of SGs assembly by DDX3X	Khaperskyy et al. (2012), Khaperskyy et al. (2014) and Kesavardhana et al. (2021)
IBV	(+) ssRNA	Inhibition of PKR activation through NSP2 ; Up-regulation of GADD34 ; Increase dephosphorylated activity of PP1	Wang et al. (2009) and Burgess and Mohr (2018)
JEV	(+) ssRNA	G3BP1 isolation and interaction with CAPRIN1	Katoh et al. (2013)
KSHV	dsDNA	Expression of ORF57 to bind to PKR	Sharma et al. (2017) and Sharma and Zheng (2021)
Mengovirus	(+) ssRNA	PKR-dependent aggregation of G3BP1 by L protein	Reineke et al. (2015)
MERS-CoV	(+) ssRNA	Inhibition of PKR-mediated elF2α phosphorylation	Nakagawa et al. (2018)
MeV	(−) ssRNA	Inhibition of PKR-dependent SG aggregation by protein-C	Randall and Goodbourn (2008)
PRV	dsRNA	Dephosphorylation of elF2α	Xu et al. (2020)
Rotavirus	dsRNA	Block the PKR-eIF2α phosphorylation; Transferation of PABP from cytoplasm to nucleus	Montero et al. (2008), Lopez and Arias (2012) and Dhillon and Rao (2018)
SARS-CoV-2	(+) ssRNA	The N protein attenuates SG formation by localizing to the SGs and sequestering G3BP1/2 from their interacting proteins	Bouhaddou et al. (2020) and Gordon et al. (2020b)
SEV	ssRNA-RT	The transcription product interacts with TIAR to inhibit the generation of SGs	Iseni et al. (2002)
TMEV	(+) ssRNA	Expression of leader (L) protein to stably interact with G3BP1	Borghese and Michiels (2011)
WNV	(+) ssRNA	Interaction with TIA-1 and TIAR to inhibit SG formation	Li et al. (2002) and Emara and Brinton (2007)
ZIKV	(+) ssRNA	Hijack of G3BP1 and CAPRIN1	Hou et al. (2017)

Some viruses encode PKR inhibitors, thereby avoiding PKR-mediated phosphorylation of eIF2α and SG formation (Malinowska et al., 2016). Given the limited space available, only some mediate proteins of viruses were described in detail, and we have listed more target proteins of viruses in Table 3. For example, influenza A virus (IAV) and infectious bronchitis virus (IBV) inhibit the activity of PKR to block the phosphorylation of eIF2α by the non-structural protein 1 (NSP1) and non-structural protein 2 (NSP2), respectively, which in turn inhibits SG formation (Khaperskyy et al., 2014; Burgess and Mohr, 2018). Intriguingly, Middle East respiratory syndrome Coronavirus (MERS-CoV) inhibits the SG formation by inhibiting PKR-mediated elF2α phosphorylation, while lacking subunits 4a and 4b MERS-CoV induces the SG formation (Nakagawa et al., 2018). For rotavirus-infected host cells, it blocks host protein synthesis, PKR activation, eIF2α phosphorylation, and modification of cellular translation machinery (Lopez and Arias, 2012). Beyond the PKR pathway, there are other pathways, e.g., PERK pathway, regulating the phosphorylation of eIF2α. Herpes simplex virus (HSV), as a dsDNA virus, inhibits the activation of PERK and hinders the eIF2α phosphorylation through the surface glycoprotein B (Mulvey et al., 2007). In addition, several other viruses regulate the eIF2α dephosphorylation. Chikungunya virus (CHIKV) induces the expression of DNA-damage-inducible 34 (GADD34) to increase the dephosphorylation of eIF2α (Clavarino et al., 2012). And Pseudorabies virus (PRV) infection significantly inhibits the SG formation by dephosphorylating eIF2α, such as Chikungunya virus (CHIKV) and Pseudorabies virus (PRV; Xu et al., 2020).

Moreover, except for regulating the phosphorylation of eIF2α, viruses can inhibit SG formation *via* interaction with SG components, especially the scaffold proteins, e.g., G3BP1 and TIA-1. For example, Theiler's murine encephalomyelitis virus (TMEV) and foot-and-mouth disease virus (FMDV; Visser et al., 2019) interfere with SG formation by leader (L) protein to stably sequester G3BP1. Similarity,

the Japanese encephalitis virus (JEV) and Zika virus (ZIKV) sequester G3BP1 by interacting with the cell cycle-associated protein 1 (CAPRIN1; Hou et al., 2017). Moreover, feline calicivirus (FCV), encephalomyocarditis virus (EMCV; Ng et al., 2013), and coxsackievirus B3 (CVB3; Fung et al., 2013) can produce the viral protease to cleave G3BP1, thereby disrupting the assembly of SGs (Humoud et al., 2016). In addition to G3BP1, TIA-1/TIAR are also targeted by viruses to interfere with SG formation. The 3′ stem-loop structure in WNV, Sendai virus's (SEV) transcription product, and dengue virus (DENV) could interact with TIA/TIAR which inhibit SG formation (Li et al., 2002; Emara and Brinton, 2007). Beyond scaffold proteins, other SG core components are also involved in viral infection (Iseni et al., 2002; Emara and Brinton, 2007; more detail in Table 1). Human immunodeficiency virus type 1 (HIV-1) significantly inhibits SG formation by assembling the Staufen1-containing HIV-1-dependent ribonucleoproteins (SHRNP) in host cells (Abrahamyan et al., 2010). Moreover, the host DEAD-box box helicase 3X-linked protein (DDX3X) also coordinates various antiviral responses in IAV infection, including regulation of SG assembly (Kesavardhana et al., 2021). Taken together, the core components of SGs (G3BP1, TIA-1/TIAR, HDAC6, SHRNP, DDX3X, GADD34, PP1) can be regulated by viruses to eventually affect SG formation.

It is worth mentioning that SARS-CoV-2 can also inhibit SG formation. Given the global pandemic caused by SARS-CoV-2, this review makes effort to elaborate on the interactive relationship between SARS-CoV-2 and SGs. SARS-CoV-2, a positive-sense single-stranded RNA (ssRNA) virus (Zhang et al., 2019), includes 30 kb of genomic RNA and four structural proteins (the crown spike (S) glycoprotein, the membrane (M) protein, ion channels envelope (E) protein, and nucleocapsid (N) protein; Wang Q. et al., 2020). And post-translational modifications (PTMs) related to SARS-CoV-2, like glycosylation and phosphorylation, are also pathogenic (Cheng et al., 2022). The S protein consists of two subunits, S1 and S2, which play a key role in receptor recognition and virus-cell membrane fusion. The glycosylation of SARS-CoV-2 mainly occurs on the S protein, which mediates the interaction with cellular receptors angiotensin-converting enzyme 2 (ACE2). After binding to ACE2, the S protein would alter its conformation, then resulting in viral membrane fusion (Zhou et al., 2020). As for the N protein, it has two distinct RNA-binding domains, involved in multiple aspects of the viral life cycle, including viral genomic RNA replication and virion assembly. The RNA intercalator mitoxantrone disrupts N protein assembly *in vitro* and in cells (Somasekharan and Gleave, 2021). Furthermore, the N protein is highly produced in infected cells to increase the efficiency of subgenomic viral RNA transcription, regulate host cell metabolism (Liu W. et al., 2020), and mediate the suppression of host antiviral responses (Nabeel-Shah et al., 2022; Wang et al., 2022). The interaction between the N protein and G3BP1/2 supports SARS-CoV-2 infection. Some studies agree that the N protein could disrupt SG formation by sequestering G3BP1/2 from interacting with other proteins (Stukalov et al., 2021; Kim et al., 2022). The non-structural protein 1 (Nsp1) of the virus can decrease the level of G3BP1, which is associated with nuclear accumulation of the SG-nucleating protein TIAR (Dolliver et al., 2022). Besides, methyltransferases 1 (PRMT1) methylates SARS-CoV-2 N protein at residues R95 and R177. It is reported that the methylation of R95 can regulate the ability of N protein to suppress SG formation (Cai T. et al., 2021). Meanwhile, the phosphorylation of the N protein can also interfere with the SG formation (Cheng et al., 2022). For instance, the inhibition of SG formation by SARS-CoV-2 may be mediated through the interaction of N protein with casein kinase 2 (CK2) subunits, like G3BP1/2, casein kinase 2 beta/casein kinase 2 alpha 2 (CSNK2B/CSNK2A2; Gordon et al., 2020b).

To summarize, viruses have evolved several mechanisms to counteract the restrictive effect of translational repression. Some viruses, mainly ssRNA viruses, replicate by inducing or controlling SG formation (Tables 1, 2). Other viruses achieve efficient replication by preventing SG formation *via* a variety of mechanisms. This strategy is the most popular choice for viruses, including ssRNA viruses, dsRNA viruses, dsDNA viruses, and retroviruses (Table 3).

4. The antiviral effect of SGs

As described above, SGs can interact with virus replication *via* multiple mechanisms, which might be promising targets for antiviral intervention. Given that SARS-CoV-2 belongs to the type of virus that inhibits SG formation, in this section, we outline the reported small molecules that can trigger SG formation and discuss the prospects for developing antiviral drugs (Figure 1).

4.1. The pathways involved in anti-virus

It is generally believed that SG formation can affect translation, which will inhibit viral replication (Nikolic et al., 2016). The translation of some viruses is strictly dependent on the 40S subunit and eIF4G, and these translation initiation factors are retained in SGs, which is not conducive to the translation of viral proteins (Liu Y. et al., 2020). PKR and PERK are the two enzymes related to translation and PKR activation during certain viral infections. Meanwhile, the assembly of the viral replication complex is affected when G3BP1 or TIA-1/TIAR remains in the SG, (Fritzlar et al., 2019). For instance, the 3′ terminal neck structure of WNV, TBEV, ZIKV, and JEV can interact with TIA-1/TIAR to regulate viral replication (Bonenfant et al., 2019). Some viruses like Vaccinia virus (VV), MRV, and DENV recruit G3BP1 to assist the replication of viruses around the viral replication complex. The RNA recognition receptor retinoic acid-inducible gene-I (RIG-I) is retained in SG and activated by dsRNA in SG to activate the innate immune response of cells (McInerney et al., 2005). In both human and mouse cells, the deletion of G3BP1 leads to insufficient binding of RNA by RIG-I (Cai H. et al., 2021). In conclusion, the cell can sense the virus from multiple aspects, inhibit its translation, and resist viral infection. It is the SG that can provide a platform for the recognition of pathogene-related molecular patterns, activates the immune signaling pathway of host cells. Therefore, SGs are generally considered to have antiviral effects upon viral infection (Yang et al., 2019; Zhang et al., 2019).

4.2. SG-targeted antiviral small molecules

4.2.1. miRNAs targeted gene coded SG-associated protein

Previous studies have found that miRNAs can be used as targeting SGs. Three miRNAs have been reported, hsa-miR-615-3p, hsa-miR-221-3p, and hsa-miR-124-3p, which target at least two of the five key

genes coded SG scaffold proteins (Prasad et al., 2021). One of the studies have shown that mitogen-activated protein kinase-activated protein kinase 2 (MAPKAPK2) in the lungs of SARS-CoV-2 patients could be reduced by hsa-miR-615-3p (Jafarinejad-Farsangi et al., 2020). The hsa-miR-221-3p, which targets ADAM17 (a disintegrin and metallo protease 17), is upregulated in hamster lung tissue infected by SARS-CoV-2 (Kim et al., 2020). It has been shown that SARS-CoV-2 hijacks DEAD box polypeptide 58 (DDX58), but hsa-miR-124-3p binds to DDX58 and inhibits SARS-CoV-2 genome replication eventually (Arora et al., 2020). Besides, hsa-miR-124-3p is found to be down-regulated in JEV-infected human neural stem cells (Mukherjee et al., 2019) and reduced pro-inflammatory cytokines Interleukin 6 (IL-6) and tumor necrosis factor alpha (TNFα) to prevent lung injury (Liang et al., 2020).

4.2.2. Compounds targeted phase one in SG assembly

The major signaling pathways that regulate SG formation include the eIF2α and eIF4F pathways, and mTOR. As we mentioned in the background, PKR and eIF2α kinases are responsible for SG formation under different stresses, which provide effective drug targets for therapeutic intervention (Wang F. et al., 2020). Several small molecules have been reported to induce eIF2α phosphorylation. The RAF1/MEK/ERK kinase (Rubisco assembly factor 1, mitogen-activated protein kinase kinase, extracellular signal-regulated kinase) inhibitor sorafenib (Abdelgalil et al., 2019) and the anti-tumor drug 5-fluorouracil (5-FU; Kaehler et al., 2014) have been found to induce SGs assembly, inhibit cell proliferation and promote apoptosis *via* PKR-mediated eIF2α phosphorylation. Bortezomib, a peptide boronate inhibitor, efficiently induces SGs in many cancer cells and eIF2α phosphorylation.

In addition, PP1 and GADD34 are induced by phosphorylated eIF2α, and GADD34 provides negative feedback on eIF2α phosphorylation (Walter and Ron, 2011). Okadaic acid and salubrinal are well-known PP1 inhibitors (Nakagawa et al., 2018). These two chemicals may interfere with the interaction between PP1 and GADD34 and prevent eIF2α dephosphorylation. Okadaic acid is another well-known PP1 inhibitor (Nakagawa et al., 2018). It has been reported that viruses interfere with SG formation through the dephosphorylation of eIF2α by PP1 and GADD34 (Fusade-Boyer et al., 2019). These two chemicals may interfere with the interaction between PP1 and GADD34 and prevent eIF2α dephosphorylation.

The key eIF4F cap-binding complex components (eIF4A, eIF4E, and eIF4G) also mediate SG formation, which are candidates for coronavirus therapeutic targets. The promotion of G3BP aggregation by eIF4A inhibitors may partly explain their antiviral activities (Gordon et al., 2020a). Pateamine A (PatA) and silvestrol are natural products that disrupt eIF4A function and prevent translation, resulting in SG formation. Studies have shown that inhibition of SGs by Silvestrol affects the synthesis and replication of IAV protein (Slaine et al., 2017). Treatment of early viral infection by PatA and silvestrol will promote SG formation, arrest viral protein synthesis, and lead to failure of viral genome replication. PatA binds irreversibly to eIF4A, blocks IAV replication long-term after discontinuation, and inhibits IAV replication. In contrast, the antiviral effect of silvestrol is fully reversible, leading to rapid SG clearance and recovery of viral protein synthesis upon discontinuation. This study supports the feasibility of targeting the core host protein synthesis machinery to prevent viral replication (Slaine et al., 2017).

4.2.3. Compounds targeted phase two in SG assembly

Targeting SG components may influence the dynamics of SGs. Particularly, G3BP1/2 and TIA-1 are essential for the initiation of SG formation. Small molecules targeting these proteins have the potential for antiviral therapy.

G3BP1/2 contains RNA-binding domains to assist RNA binding. Many viruses affect SG formation through G3BP1/2. Arsenite induces SG formation, probably *via* inducing the dephosphorylation of G3BP1/2 at Ser149 (Gallouzi et al., 1998). CK2 accelerates SG disassembly by promoting G3BP1 phosphorylation (Reineke et al., 2017). Silmitasertib, a CK2 inhibitor, inhibits CK2 and promotes SG formation, showing potent antiviral activity (Ahamad et al., 2020; Gordon et al., 2020a). Clinical trials of silmitasertib as a potential drug for SARS-CoV-2 treatment are currently under consideration (Yadav et al., 2022), suggesting that CK2 plays a role in regulating the SARS-CoV-2 life cycle. Similar to silmitasertib, TMCB also interferes with the disassembly of SGs by targeting CK2 and interacting with the carboxy-terminal domain (Ahamad et al., 2020; Wang F. et al., 2020). Besides, the cells pre-treated with CK2 inhibitor 5-oxo-5,6-dihydroindolo-(1,2-a) quinazoline-7-yl acetic acid (IQA) generates 2.5-fold SG production after Mengo virus with mutant L protein (Mengo-Zn) infection (Langereis et al., 2013) and cannot decompose SGs (Reineke et al., 2015). It is suggested that IQA can inhibit virus-induced SG breakdown (Reineke et al., 2017). Tetrabromocinna mic acid (TBCA) is also a specific CK2 inhibitor. TBCA treatment alone neither alters nor induces SG formation, but residual SGs in cells are increased under arsenite stress (Reineke et al., 2017). This feature has become a new strategy for TBCA to combine other drugs to fight viral infection.

Usually, as a scaffold protein of SG, TIA-1 is an RNA-binding protein and is associated with RNA and other proteins to form SGs *in vivo*. Interaction of TIA-1/TIAR with WNV, ZIKV, TBEV, PV, and DENV products in infected cells interferes with SG formation (Emara and Brinton, 2007; White and Lloyd, 2011; Albornoz et al., 2014; Bonenfant et al., 2019). Boric acid also balances the anti-apoptotic eIF2α-SGs pathway and pro-apoptotic pathway *via* promoting TIA-1 translocation from the nucleus to SGs (Henderson et al., 2015). Moreover, C85 (troxerutin) is very effective for SG formation induced by TIA-1 overexpression or arsenite treatment (Hu et al., 2017). Even more, it has been approved for human therapeutic usage by FDA and found to act as a SARS-CoV-2 main protease inhibitor, representing potential treatment options (Farhat and Khan, 2021). Particularly, C85 could stabilize SGs and perturb the equilibrium between reversible SG assembly and disassembly.

4.2.4. Compounds targeted phase four in SG assembly

Microtubules are intracellular structures involved in the biological processes of cell division, organization of intracellular structures, and intracellular transportation. Microtubule disruption would delay SG formation, in which, as a consequence, SGs are formed smaller in size, greater in number, and variable in distribution (Nadezhdina et al., 2010). Based on enrichment analysis, Bexarotene (also known as targretin) has been found to upregulate the expression of SG proteins

(i.e., DYNC1H1, DCTN1, and LMNA) in rats (Prasad et al., 2021). These proteins are associated with microtubules. Recently, Yuan et al. have shown that Bexarotene effectively inhibited SARS-CoV-2 replication *in vitro* (Yuan et al., 2020). It has been previously shown that AM580 and tamibarotene belong to the same drug class as Bexarotene, showing broad-spectrum antiviral activity against influenza virus, enterovirus A71, Zika virus, adenovirus, MERS-CoV and SARS-CoV (Yuan et al., 2019). Moreover, NDV infection induces canonical SGs and relatively small round granules are formed after treatment with nocodazole (Noc), a microtubule-disrupting drug. Unlike the large and irregular SGs in NDV-infected cells, Noc treatment induces marked microtubule depolymerization, inducing the formation of small, round granules (Sun et al., 2017). Taking current findings together, compounds targeting the protein elements of SGs have the promising potential for antiviral effect on SARS-CoV-2 infection.

5. Conclusion

In this review, we provide an overview of the composition, function, dynamic regulation, and viral-related mechanisms of SGs to help understand the role of SGs in viral infection. We then focus on the regulating function of SGs in the context of viruses, in particular the PKR-elF2α pathway, *via* which many viruses induce or inhibit SG formation by directly affecting elF2α phosphorylation. Specifically, we depict the interaction between SARS-CoV-2 and SG. We believed that several small molecules, including some inhibitors disrupting the interaction of G3BP1/2 with N protein, PRMT inhibitors, and CK2 inhibitors, could be considered as new therapeutic targets against SARS-CoV-2 infection *via* the regulation of SG assembly and dynamics. We also summarize potential antiviral drugs targeting on SGs, including small molecule compounds, such as Salubrinal, Okadaic acid PatA, silvestrol, and Noc. Finally, we describe the mechanism of anti-SARS-CoV-2, including Silmitasertib, TMCB, Bexarotene, and three miRNAs. Overall, our review summarizes the antiviral mechanisms of SGs and provides new insights into the development of SG-targeted antiviral drugs, particularly, the potential drugs against SARS-CoV-2.

Author contributions

LH, YY, and YG conceived, designed, and supervised the research. YG wrote the manuscript and draw the figure. YW wrote the manuscript and categorized the tables. XF, GB, XL, and JM proofread and polished the manuscript. All authors contributed to the article and approved the submitted version.

Funding

This study was financially supported by LH by the grant of the Natural Science Foundation of Zhejiang Province (no. LQ22C070004) and the Administration of Tranditional Chinese Mdeicine of Zhejiang Province (no. GZY-ZJ-KJ-23083).

Acknowledgments

We are extremely grateful to all members of the Hu Lab, past and present, for the interesting discussions and great contributions to the project. We thank the National Clinical Research Center for Child Health for its great support.

Conflict of interest

The authors declare that the research was conducted in the absence of any commercial or financial relationships that could be construed as a potential conflict of interest.

Publisher's note

References

Abdelgalil, A. A., Alkahtani, H. M., and Al-Jenoobi, F. I. (2019). Sorafenib. *Profiles Drug Subst Excip Relat Methodol* 44, 239–266. doi: 10.1016/bs.podrm.2018.11.003

Abrahamyan, L. G., Chatel-Chaix, L., Ajamian, L., Milev, M. P., Monette, A., Clement, J. F., et al. (2010). Novel Staufen1 ribonucleoproteins prevent formation of stress granules but favour encapsidation of HIV-1 genomic RNA. *J. Cell Sci.* 123, 369–383. doi: 10.1242/jcs.055897

Ahamad, S., Gupta, D., and Kumar, V. (2020). Targeting SARS-CoV-2 nucleocapsid oligomerization: insights from molecular docking and molecular dynamics simulations. *J. Biomol. Struct. Dyn.* 40, 1–14. doi: 10.1080/07391102.2020.1839563

Albornoz, A., Carletti, T., Corazza, G., and Marcello, A. (2014). The stress granule component TIA-1 binds tick-borne encephalitis virus RNA and is recruited to perinuclear sites of viral replication to inhibit viral translation. *J. Virol.* 88, 6611–6622. doi: 10.1128/JVI.03736-13

Anderson, P., and Kedersha, N. (2002). Stressful initiations. *J. Cell Sci.* 115, 3227–3234. doi: 10.1242/jcs.115.16.3227

Anderson, P., and Kedersha, N. (2008). Stress granules: the Tao of RNA triage. *Trends Biochem. Sci.* 33, 141–150. doi: 10.1016/j.tibs.2007.12.003

Anderson, P., and Kedersha, N. (2009). Stress granules. *Curr. Biol.* 19, R397–R398. doi: 10.1016/j.cub.2009.03.013

Anderson, P., Kedersha, N., and Ivanov, P. (2015). Stress granules, P-bodies and cancer ☆. *Biochim. Biophys. Acta* 1849, 861–870. doi: 10.1016/j.bbagrm.2014.11.009

Arimoto, K., Fukuda, H., Imajoh-Ohmi, S., Saito, H., and Takekawa, M. (2008). Formation of stress granules inhibits apoptosis by suppressing stress-responsive MAPK pathways. *Nat. Cell Biol.* 10, 1324–1332. doi: 10.1038/ncb1791

Arora, S., Singh, P., Dohare, R., Jha, R., and Ali Syed, M. (2020). Unravelling host-pathogen interactions: ceRNA network in SARS-CoV-2 infection (COVID-19). *Gene* 762:145057. doi: 10.1016/j.gene.2020.145057

Aulas, A., and Vande Velde, C. (2015). Alterations in stress granule dynamics driven by TDP-43 and FUS: a link to pathological inclusions in ALS? *Front. Cell. Neurosci.* 9:423. doi: 10.3339/Fncel.2015.00423

Bonenfant, G., Williams, N., Netzband, R., Schwarz, M. C., Evans, M. J., and Pager, C. T. (2019). Zika virus subverts stress granules to promote and restrict viral gene expression. *J. Virol.* 93:e00520-19. doi: 10.1128/JVI.00520-19

Borghese, F., and Michiels, T. (2011). The leader protein of cardioviruses inhibits stress granule assembly. *J. Virol.* 85, 9614–9622. doi: 10.1128/JVI.00480-11

Bouhaddou, M., Memon, D., Meyer, B., White, K. M., Rezelj, V. V., Correa Marrero, M., et al. (2020). The global phosphorylation landscape of SARS-CoV-2 infection. *Cells* 182, 685–712.e19. doi: 10.1016/j.cell.2020.06.034

Brownsword, M. J., and Locker, N. (2022). A little less aggregation a little more replication: viral manipulation of stress granules. *Wiley Interdiscip Rev RNA* 14:e1741. doi: 10.1002/wrna.1741

Burgess, H. M., and Mohr, I. (2018). Defining the role of stress granules in innate immune suppression by the herpes simplex virus 1 endoribonuclease VHS. *J. Virol.* 92:e00829-18. doi: 10.1128/JVI.00829-18

Cai, H., Liu, X., Zhang, F., Han, Q. Y., Liu, Z. S., Xue, W., et al. (2021). G3BP1 inhibition alleviates intracellular nucleic acid-induced autoimmune responses. *J. Immunol.* 206, 2453–2467. doi: 10.4049/jimmunol.2001111

Cai, T., Yu, Z., Wang, Z., Liang, C., and Richard, S. (2021). Arginine methylation of SARS-Cov-2 nucleocapsid protein regulates RNA binding, its ability to suppress stress granule formation, and viral replication. *J. Biol. Chem.* 297:100821. doi: 10.1016/j.jbc.2021.100821

Carroll, K., Hastings, C., and Miller, C. L. (2014). Amino acids 78 and 79 of mammalian orthoreovirus protein microNS are necessary for stress granule localization, core protein lambda2 interaction, and de novo virus replication. *Virology* 448, 133–145. doi: 10.1016/j.virol.2013.10.009

Chen, L., and Liu, B. (2017). Relationships between stress granules, oxidative stress, and neurodegenerative diseases. *Oxidative Med. Cell. Longev.* 2017:1809592. doi: 10.1155/2017/1809592

Cheng, N., Liu, M., Li, W., Sun, B., Liu, D., Wang, G., et al. (2022). Protein post-translational modification in SARS-CoV-2 and host interaction. *Front. Immunol.* 13:1068449. doi: 10.3389/fimmu.2022.1068449

Choi, S., Choi, S., Choi, Y., Cho, N., Kim, S. Y., Lee, C. H., et al. (2022). Polyhexamethylene guanidine phosphate increases stress granule formation in human 3D lung organoids under respiratory syncytial virus infection. *Ecotoxicol. Environ. Saf.* 229:113094. doi: 10.1016/j.ecoenv.2021.113094

Clavarino, G., Claudio, N., Couderc, T., Dalet, A., Judith, D., Camosseto, V., et al. (2012). Induction of GADD34 is necessary for dsRNA-dependent interferon-beta production and participates in the control of chikungunya virus infection. *PLoS Pathog.* 8:e1002708. doi: 10.1371/journal.ppat.1002708

Courtney, S. C., Scherbik, S. V., Stockman, B. M., and Brinton, M. A. (2012). West nile virus infections suppress early viral RNA synthesis and avoid inducing the cell stress granule response. *J. Virol.* 86, 3647–3657. doi: 10.1128/JVI.06549-11

Dhillon, P., and Rao, C. D. (2018). Rotavirus induces formation of remodeled stress granules and P bodies and their sequestration in Viroplasms to promote progeny virus production. *J. Virol.* 92:e01363-18. doi: 10.1128/JVI.01363-18

Dinh, P. X., Beura, L. K., Das, P. B., Panda, D., Das, A., and Pattnaik, A. K. (2013). Induction of stress granule-like structures in vesicular stomatitis virus-infected cells. *J. Virol.* 87, 372–383. doi: 10.1128/JVI.02305-12

Dolicka, D., Zahoran, S., Correia de Sousa, M., Gjorgjieva, M., Sempoux, C., Fournier, M., et al. (2022). TIA1 loss exacerbates fatty liver disease but exerts a dual role in Hepatocarcinogenesis. *Cancers (Basel)* 14:1704. doi: 10.3390/cancers14071704

Dolliver, S. M., Kleer, M., Bui-Marinos, M. P., Ying, S., Corcoran, J. A., and Khaperskyy, D. A. (2022). Nsp1 proteins of human coronaviruses HCoV-OC43 and SARS-CoV2 inhibit stress granule formation. *PLoS Pathog.* 18:e1011041. doi: 10.1371/journal.ppat.1011041

Dougherty, J. D., Tsai, W. C., and Lloyd, R. E. (2015). Multiple poliovirus proteins repress cytoplasmic RNA granules. *Viruses* 7, 6127–6140. doi: 10.3390/v7122922

Eiermann, N., Haneke, K., Sun, Z., Stoecklin, G., and Ruggieri, A. (2020). Dance with the devil: stress granules and signaling in antiviral responses. *Viruses* 12:984. doi: 10.3390/v12090984

Emara, M. M., and Brinton, M. A. (2007). Interaction of TIA-1/TIAR with West Nile and dengue virus products in infected cells interferes with stress granule formation and processing body assembly. *Proc. Natl. Acad. Sci. U. S. A.* 104, 9041–9046. doi: 10.1073/pnas.0703348104

Fan, A. C., and Leung, A. K. (2016). RNA granules and diseases: a case study of stress granules in ALS and FTLD. *Adv. Exp. Med. Biol.* 907, 263–296. doi: 10.1007/978-3-319-29073-7_11

Farhat, N., and Khan, A. U. (2021). Repurposing drug molecule against SARS-Cov-2 (COVID-19) through molecular docking and dynamics: a quick approach to pick FDA-approved drugs. *J. Mol. Model.* 27:312. doi: 10.1007/s00894-021-04923-w

Finnen, R. L., Hay, T. J., Dauber, B., Smiley, J. R., and Banfield, B. W. (2014). The herpes simplex virus 2 virion-associated ribonuclease vhs interferes with stress granule formation. *J. Virol.* 88, 12727–12739. doi: 10.1128/JVI.01554-14

Finnen, R. L., Zhu, M., Li, J., Romo, D., and Banfield, B. W. (2016). Herpes simplex virus 2 Virion host shutoff endoribonuclease activity is required to disrupt stress granule formation. *J. Virol.* 90, 7943–7955. doi: 10.1128/JVI.00947-16

Fritzlar, S., Aktepe, T. E., Chao, Y. W., Kenney, N. D., McAllaster, M. R., Wilen, C. B., et al. (2019). Mouse norovirus infection arrests host cell translation uncoupled from the stress granule-PKR-eIF2alpha Axis. *mBio* 10:e00960-19. doi: 10.1128/mBio.00960-19

Fung, G., Ng, C. S., Zhang, J., Shi, J., Wong, J., Piesik, P., et al. (2013). Production of a dominant-negative fragment due to G3BP1 cleavage contributes to the disruption of mitochondria-associated protective stress granules during CVB3 infection. *PLoS One* 8:e79546. doi: 10.1371/journal.pone.0079546

Fusade-Boyer, M., Dupre, G., Bessiere, P., Khiar, S., Quentin-Froignant, C., Beck, C., et al. (2019). Evaluation of the antiviral activity of Sephin1 treatment and its consequences on eIF2alpha phosphorylation in response to viral infections. *Front. Immunol.* 10:134. doi: 10.3389/fimmu.2019.00134

Gallouzi, I. E., Parker, F., Chebli, K., Maurier, F., Labourier, E., Barlat, I., et al. (1998). A novel phosphorylation-dependent RNase activity of GAP-SH3 binding protein: a potential link between signal transduction and RNA stability. *Mol. Cell. Biol.* 18, 3956–3965. doi: 10.1128/MCB.18.7.3956

Gao, P., Liu, Y., Wang, H., Chai, Y., Weng, W., Zhang, Y., et al. (2022). Viral evasion of PKR restriction by reprogramming cellular stress granules. *Proc. Natl. Acad. Sci. U. S. A.* 119:e2201169119. doi: 10.1073/pnas.2201169119

Gao, X., Jiang, L., Gong, Y., Chen, X., Ying, M., Zhu, H., et al. (2019). Stress granule: a promising target for cancer treatment. *Br. J. Pharmacol.* 176, 4421–4433. doi: 10.1111/bph.14790

Gordon, D. E., Jang, G. M., Bouhaddou, M., Xu, J., Obernier, K., O'Meara, M. J., et al. (2020a). A SARS-CoV-2-human protein-protein interaction map reveals drug targets and potential drug-repurposing. *bioRxiv*. 583, 459–468. doi: 10.1101/2020.03.22.002386

Gordon, D. E., Jang, G. M., Bouhaddou, M., Xu, J., Obernier, K., White, K. M., et al. (2020b). A SARS-CoV-2 protein interaction map reveals targets for drug repurposing. *Nature* 583, 459–468. doi: 10.1038/s41586-020-2286-9

Guo, X., Yu, K., Xin, Z., Liu, L., Gao, Y., Hu, F., et al. (2022). Porcine epidemic diarrhea virus infection subverts Arsenite-induced stress granules formation. *Front. Microbiol.* 13:931922. doi: 10.3389/fmicb.2022.931922

Heck, M. V., Azizov, M., Stehning, T., Walter, M., Kedersha, N., and Auburger, G. (2014). Dysregulated expression of lipid storage and membrane dynamics factors in Tia1 knockout mouse nervous tissue. *Neurogenetics* 15, 135–144. doi: 10.1007/s10048-014-0397-x

Henderson, K. A., Kobylewski, S. E., Yamada, K. E., and Eckhert, C. D. (2015). Boric acid induces cytoplasmic stress granule formation, eIF2alpha phosphorylation, and ATF4 in prostate DU-145 cells. *Biometals* 28, 133–141. doi: 10.1007/s10534-014-9809-5

Hopkins, K. C., Tartell, M. A., Herrmann, C., Hackett, B. A., Taschuk, F., Panda, D., et al. (2015). Virus-induced translational arrest through 4EBP1/2-dependent decay of 5'-TOP mRNAs restricts viral infection. *Proc. Natl. Acad. Sci. U. S. A.* 112, E2920–E2929. doi: 10.1073/pnas.1418805112

Hou, S., Kumar, A., Xu, Z., Airo, A. M., Stryapunina, I., Wong, C. P., et al. (2017). Zika virus hijacks stress granule proteins and modulates the host stress response. *J. Virol.* 91:e00474-17. doi: 10.1128/JVI.00474-17

Hu, L., Mao, S., Lin, L., Bai, G., Liu, B., and Mao, J. (2022). Stress granules in the spinal muscular atrophy and amyotrophic lateral sclerosis: the correlation and promising therapy. *Neurobiol. Dis.* 170:105749. doi: 10.1016/j.nbd.2022.105749

Hu, L. D., Chen, X. J., Liao, X. Y., and Yan, Y. B. (2017). Screening novel stress granule regulators from a natural compound library. *Protein Cell* 8, 618–622. doi: 10.1007/s13238-017-0430-6

Humoud, M. N., Doyle, N., Royall, E., Willcocks, M. M., Sorgeloos, F., van Kuppeveld, F., et al. (2016). Feline Calicivirus infection disrupts assembly of cytoplasmic stress granules and induces G3BP1 cleavage. *J. Virol.* 90, 6489–6501. doi: 10.1128/JVI.00647-16

Iseni, F., Garcin, D., Nishio, M., Kedersha, N., Anderson, P., and Kolakofsky, D. (2002). Sendai virus trailer RNA binds TIAR, a cellular protein involved in virus-induced apoptosis. *EMBO J.* 21, 5141–5150. doi: 10.1093/emboj/cdf513

Jafarinejad-Farsangi, S., Jazi, M. M., Rostamzadeh, F., and Hadizadeh, M. (2020). High affinity of host human microRNAs to SARS-CoV-2 genome: an in silico analysis. *Noncoding RNA Res* 5, 222–231. doi: 10.1016/j.ncrna.2020.11.005

Jefferson, M., Bone, B., Buck, J. L., and Powell, P. P. (2019). The autophagy protein ATG16L1 is required for Sindbis virus-induced eIF2alpha phosphorylation and stress granule formation. *Viruses* 12:39. doi: 10.3390/v12010039

Kaehler, C., Isensee, J., Hucho, T., Lehrach, H., and Krobitsch, S. (2014). 5-fluorouracil affects assembly of stress granules based on RNA incorporation. *Nucleic Acids Res.* 42, 6436–6447. doi: 10.1093/nar/gku264

Katoh, H., Okamoto, T., Fukuhara, T., Kambara, H., Morita, E., Mori, Y., et al. (2013). Japanese encephalitis virus core protein inhibits stress granule formation through an interaction with Caprin-1 and facilitates viral propagation. *J. Virol.* 87, 489–502. doi: 10.1128/JVI.02186-12

Kedersha, N., Stoecklin, G., Ayodele, M., Yacono, P., Lykke-Andersen, J., Fritzler, M. J., et al. (2005). Stress granules and processing bodies are dynamically linked sites of mRNP remodeling. *J. Cell Biol.* 169, 871–884. doi: 10.1083/jcb.200502088

Kesavardhana, S., Samir, P., Zheng, M., Malireddi, R. K. S., Karki, R., Sharma, B. R., et al. (2021). DDX3X coordinates host defense against influenza virus by activating the NLRP3 inflammasome and type I interferon response. *J. Biol. Chem.* 296:100579. doi: 10.1016/j.jbc.2021.100579

Khaperskyy, D. A., Emara, M. M., Johnston, B. P., Anderson, P., Hatchette, T. F., and McCormick, C. (2014). Influenza a virus host shutoff disables antiviral stress-induced translation arrest. *PLoS Pathog.* 10:e1004217. doi: 10.1371/journal.ppat.1004217

Khaperskyy, D. A., Hatchette, T. F., and McCormick, C. (2012). Influenza a virus inhibits cytoplasmic stress granule formation. *FASEB J.* 26, 1629–1639. doi: 10.1096/fj.11-196915

Kim, D., Maharjan, S., Kang, M., Kim, J., Park, S., Kim, M., et al. (2022). Differential effect of SARS-CoV-2 infection on stress granule formation in Vero and Calu-3 cells. *Front. Microbiol.* 13:997539. doi: 10.3389/fmicb.2022.997539

Kim, D. Y., Reynaud, J. M., Rasalouskaya, A., Akhrymuk, I., Mobley, J. A., Frolov, I., et al. (2016). New World and Old World alphaviruses have evolved to exploit different components of stress granules, FXR and G3BP proteins, for assembly of viral replication complexes. *PLoS Pathog.* 12:e1005810. doi: 10.1371/journal.ppat.1005810

Kim, W. R., Park, E. G., Kang, K. W., Lee, S. M., Kim, B., and Kim, H. S. (2020). Expression analyses of MicroRNAs in hamster lung tissues infected by SARS-CoV-2. *Mol. Cells* 43, 953–963. doi: 10.14348/molcells.2020.0177

Langereis, M. A., Feng, Q., and van Kuppeveld, F. J. (2013). MDA5 localizes to stress granules, but this localization is not required for the induction of type I interferon. *J. Virol.* 87, 6314–6325. doi: 10.1128/JVI.03213-12

Le Sage, V., Cinti, A., McCarthy, S., Amorim, R., Rao, S., Daino, G. L., et al. (2017). Ebola virus VP35 blocks stress granule assembly. *Virology* 502, 73–83. doi: 10.1016/j.virol.2016.12.012

Legros, S., Boxus, M., Gatot, J. S., Van Lint, C., Kruys, V., Kettmann, R., et al. (2011). The HTLV-1 tax protein inhibits formation of stress granules by interacting with histone deacetylase 6. *Oncogene* 30, 4050–4062. doi: 10.1038/onc.2011.120

Li, W., Li, Y., Kedersha, N., Anderson, P., Emara, M., Swiderek, K. M., et al. (2002). Cell proteins TIA-1 and TIAR interact with the 3′ stem-loop of the West Nile virus complementary minus-strand RNA and facilitate virus replication. *J. Virol.* 76, 11989–12000. doi: 10.1128/jvi.76.23.11989-12000.2002

Li, Y. R., King, O. D., Shorter, J., and Gitler, A. D. (2013). Stress granules as crucibles of ALS pathogenesis. *J. Cell Biol.* 201:361. doi: 10.1083/jcb.201302044

Liang, Y., Xie, J., Che, D., Zhang, C., Lin, Y., Feng, L., et al. (2020). MiR-124-3p helps to protect against acute respiratory distress syndrome by targeting p65. *Biosci. Rep.* 40:BSR20192132. doi: 10.1042/BSR20192132

Lindquist, M. E., Mainou, B. A., Dermody, T. S., and Crowe, J. E. Jr. (2011). Activation of protein kinase R is required for induction of stress granules by respiratory syncytial virus but dispensable for viral replication. *Virology* 413, 103–110. doi: 10.1016/j.virol.2011.02.009

Linero, F. N., Thomas, M. G., Boccaccio, G. L., and Scolaro, L. A. (2011). Junin virus infection impairs stress-granule formation in Vero cells treated with arsenite via inhibition of eIF2alpha phosphorylation. *J. Gen. Virol.* 92, 2889–2899. doi: 10.1099/vir.0.033407-0

Liu, W., Liu, L., Kou, G., Zheng, Y., Ding, Y., Ni, W., et al. (2020). Evaluation of Nucleocapsid and spike protein-based enzyme-linked immunosorbent assays for detecting antibodies against SARS-CoV-2. *J. Clin. Microbiol.* 58:e00461-20. doi: 10.1128/JCM.00461-20

Liu, W. J., Yang, Y. T., Zhao, M. Q., Dong, X. Y., Gou, H. C., Pei, J. J., et al. (2015). PKR activation enhances replication of classical swine fever virus in PK-15 cells. *Virus Res.* 204, 47–57. doi: 10.1016/j.virusres.2015.04.012

Liu, Y., Wang, M., Cheng, A., Yang, Q., Wu, Y., Jia, R., et al. (2020). The role of host eIF2alpha in viral infection. *Virol. J.* 17:112. doi: 10.1186/s12985-020-01362-6

Lopez, S., and Arias, C. F. (2012). Rotavirus-host cell interactions: an arms race. *Curr. Opin. Virol.* 2, 389–398. doi: 10.1016/j.coviro.2012.05.001

Mahboubi, H., and Stochaj, U. (2017). Cytoplasmic stress granules: dynamic modulators of cell signaling and disease. *Biochim. Biophys. Acta Mol. basis Dis.* 1863, 884–895. doi: 10.1016/j.bbadis.2016.12.022

Malinowska, M., Niedzwiedzka-Rystwej, P., Tokarz-Deptula, B., and Deptula, W. (2016). Stress granules (SG) and processing bodies (PB) in viral infections. *Acta Biochim. Pol.* 63, 183–188. doi: 10.18388/abp.2015_1060

Martin, S., Zekri, L., Metz, A., Maurice, T., Chebli, K., Vignes, M., et al. (2013). Deficiency of G3BP1, the stress granules assembly factor, results in abnormal synaptic plasticity and calcium homeostasis in neurons. *J. Neurochem.* 125, 175–184. doi: 10.1111/jnc.12189

Matsuki, H., Takahashi, M., Higuchi, M., Makokha, G. N., Oie, M., and Fujii, M. (2013). Both G3BP1 and G3BP2 contribute to stress granule formation. *Genes Cells* 18, 135–146. doi: 10.1111/gtc.12023

McCormick, C., and Khaperskyy, D. A. (2017). Translation inhibition and stress granules in the antiviral immune response. *Nat. Rev. Immunol.* 17, 647–660. doi: 10.1038/nri.2017.63

McInerney, G. M., Kedersha, N. L., Kaufman, R. J., Anderson, P., and Liljestrom, P. (2005). Importance of eIF2alpha phosphorylation and stress granule assembly in alphavirus translation regulation. *Mol. Biol. Cell* 16, 3753–3763. doi: 10.1091/mbc.e05-02-0124

Moeller, B. J., Cao, Y. T., Li, C. Y., and Dewhirst, M. W. (2004). Radiation activates HIF-1 to regulate vascular radiosensitivity in tumors: role of reoxygenation, free radicals, and stress granules. *Cancer Cell* 5, 429–441. doi: 10.1016/S1535-6108(04)00115-1

Montero, H., Rojas, M., Arias, C. F., and Lopez, S. (2008). Rotavirus infection induces the phosphorylation of eIF2alpha but prevents the formation of stress granules. *J. Virol.* 82, 1496–1504. doi: 10.1128/JVI.01779-07

Morimoto, R. I. (2011). The heat shock response: systems biology of proteotoxic stress in aging and disease. *Cold Spring Harb. Symp. Quant. Biol.* 76, 91–99. doi: 10.1101/sqb.2012.76.010637

Moujaber, O., Mahboubi, H., Kodiha, M., Bouttier, M., Bednarz, K., Bakshi, R., et al. (2017). Dissecting the molecular mechanisms that impair stress granule formation in aging cells. *Biochim. Biophys. Acta Mol. Cell Res.* 1864, 475–486. doi: 10.1016/j.bbamcr.2016.12.008

Mukherjee, S., Akbar, I., Bhagat, R., Hazra, B., Bhattacharyya, A., Seth, P., et al. (2019). Identification and classification of hubs in microRNA target gene networks in human neural stem/progenitor cells following Japanese encephalitis virus infection. *mSphere* 4:e00588-19. doi: 10.1128/mSphere.00588-19

Mulvey, M., Arias, C., and Mohr, I. (2007). Maintenance of endoplasmic reticulum (ER) homeostasis in herpes simplex virus type 1-infected cells through the association of a viral glycoprotein with PERK, a cellular ER stress sensor. *J. Virol.* 81, 3377–3390. doi: 10.1128/JVI.02191-06

Nabeel-Shah, S., Lee, H., Ahmed, N., Burke, G. L., Farhangmehr, S., Ashraf, K., et al. (2022). SARS-CoV-2 nucleocapsid protein binds host mRNAs and attenuates stress granules to impair host stress response. *iScience* 25:103562. doi: 10.1016/j.isci.2021.103562

Nadezhdina, E. S., Lomakin, A. J., Shpilman, A. A., Chudinova, E. M., and Ivanov, P. A. (2010). Microtubules govern stress granule mobility and dynamics. *Biochim. Biophys. Acta* 1803, 361–371. doi: 10.1016/j.bbamcr.2009.12.004

Nakagawa, K., Narayanan, K., Wada, M., and Makino, S. (2018). Inhibition of stress granule formation by Middle East respiratory syndrome coronavirus 4a accessory protein facilitates viral translation, leading to efficient virus replication. *J. Virol.* 92:e00902-18. doi: 10.1128/JVI.00902-18

Ng, C. S., Jogi, M., Yoo, J. S., Onomoto, K., Koike, S., Iwasaki, T., et al. (2013). Encephalomyocarditis virus disrupts stress granules, the critical platform for triggering antiviral innate immune responses. *J. Virol.* 87, 9511–9522. doi: 10.1128/JVI.03248-12

Nikolic, J., Civas, A., Lama, Z., Lagaudriere-Gesbert, C., and Blondel, D. (2016). Rabies virus infection induces the formation of stress granules closely connected to the viral factories. *PLoS Pathog.* 12:e1005942. doi: 10.1371/journal.ppat.1005942

Okonski, K. M., and Samuel, C. E. (2013). Stress granule formation induced by measles virus is protein kinase PKR dependent and impaired by RNA adenosine deaminase ADAR1. *J. Virol.* 87, 756–766. doi: 10.1128/JVI.02270-12

Portz, B., Lee, B. L., and Shorter, J. (2021). FUS and TDP-43 phases in health and disease. *Trends Biochem. Sci.* 46, 550–563. doi: 10.1016/j.tibs.2020.12.005

Prasad, K., Alasmari, A. F., Ali, N., Khan, R., Alghamdi, A., and Kumar, V. (2021). Insights into the SARS-CoV-2-mediated alteration in the stress granule protein regulatory networks in humans. *Pathogens* 10:1459. doi: 10.3390/pathogens10111459

Protter, D. S., and Parker, R. (2016). Principles and properties of stress granules. *Trends Cell Biol.* 26, 668–679. doi: 10.1016/j.tcb.2016.05.004

Qin, Q., Carroll, K., Hastings, C., and Miller, C. L. (2011). Mammalian orthoreovirus escape from host translational shutoff correlates with stress granule disruption and is independent of eIF2alpha phosphorylation and PKR. *J. Virol.* 85, 8798–8810. doi: 10.1128/JVI.01831-10

Qin, Q., Hastings, C., and Miller, C. L. (2009). Mammalian orthoreovirus particles induce and are recruited into stress granules at early times postinfection. *J. Virol.* 83, 11090–11101. doi: 10.1128/JVI.01239-09

Raaben, M., Groot Koerkamp, M. J., Rottier, P. J., and de Haan, C. A. (2007). Mouse hepatitis coronavirus replication induces host translational shutoff and mRNA decay, with concomitant formation of stress granules and processing bodies. *Cell. Microbiol.* 9, 2218–2229. doi: 10.1111/j.1462-5822.2007.00951.x

Randall, R. E., and Goodbourn, S. (2008). Interferons and viruses: an interplay between induction, signalling, antiviral responses and virus countermeasures. *J. Gen. Virol.* 89, 1–47. doi: 10.1099/vir.0.83391-0

Reineke, L., and Neilson, J. (2019). Differences between acute and chronic stress granules, and how these differences may impact function in human disease. *Biochem. Pharmacol.* 162, 123–131. doi: 10.1016/j.bcp.2018.10.009

Reineke, L. C., Kedersha, N., Langereis, M. A., van Kuppeveld, F. J., and Lloyd, R. E. (2015). Stress granules regulate double-stranded RNA-dependent protein kinase activation through a complex containing G3BP1 and Caprin1. *MBio* 6:e02486. doi: 10.1128/mBio.02486-14

Reineke, L. C., Tsai, W. C., Jain, A., Kaelber, J. T., Jung, S. Y., and Lloyd, R. E. (2017). Casein kinase 2 is linked to stress granule dynamics through phosphorylation of the stress granule nucleating protein G3BP1. *Mol. Cell. Biol.* 37:e00596-16. doi: 10.1128/MCB.00596-16

Ruggieri, A., Dazert, E., Metz, P., Hofmann, S., Bergeest, J. P., Mazur, J., et al. (2012). Dynamic oscillation of translation and stress granule formation mark the cellular response to virus infection. *Cell Host Microbe* 12, 71–85. doi: 10.1016/j.chom.2012.05.013

Sharma, N. R., Majerciak, V., Kruhlak, M. J., and Zheng, Z. M. (2017). KSHV inhibits stress granule formation by viral ORF57 blocking PKR activation. *PLoS Pathog.* 13:e1006677. doi: 10.1371/journal.ppat.1006677

Sharma, N. R., and Zheng, Z. M. (2021). RNA granules in antiviral innate immunity: a Kaposi's sarcoma-associated herpesvirus journey. *Front. Microbiol.* 12:794431. doi: 10.3389/fmicb.2021.794431

Shi, J., Li, Z., Xu, R., Zhang, J., Zhou, Q., Gao, R., et al. (2022). The PERK/PKR-eIF2alpha pathway negatively regulates porcine Hemagglutinating encephalomyelitis virus replication by attenuating global protein translation and facilitating stress granule formation. *J. Virol.* 96:e0169521. doi: 10.1128/JVI.01695-21

Simpson-Holley, M., Kedersha, N., Dower, K., Rubins, K. H., Anderson, P., Hensley, L. E., et al. (2011). Formation of antiviral cytoplasmic granules during orthopoxvirus infection. *J. Virol.* 85, 1581–1593. doi: 10.1128/JVI.02247-10

Slaine, P. D., Kleer, M., Smith, N. K., Khaperskyy, D. A., and McCormick, C. (2017). Stress granule-inducing eukaryotic translation initiation factor 4A inhibitors block influenza a virus replication. *Viruses* 9:388. doi: 10.3390/v9120388

Sola, I., Galan, C., Mateos-Gomez, P. A., Palacio, L., Zuniga, S., Cruz, J. L., et al. (2011). The polypyrimidine tract-binding protein affects coronavirus RNA accumulation levels and relocalizes viral RNAs to novel cytoplasmic domains different from replication-transcription sites. *J. Virol.* 85, 5136–5149. doi: 10.1128/JVI.00195-11

Somasekharan, S. P., and Gleave, M. (2021). SARS-CoV-2 nucleocapsid protein interacts with immunoregulators and stress granules and phase separates to form liquid droplets. *FEBS Lett.* 595, 2872–2896. doi: 10.1002/1873-3468.14229

Spector, D. L. (2006). SnapShot: cellular bodies. *Cells* 127:1071. doi: 10.1016/j.cell.2006.11.026

Stukalov, A., Girault, V., Grass, V., Karayel, O., Bergant, V., Urban, C., et al. (2021). Multilevel proteomics reveals host perturbations by SARS-CoV-2 and SARS-CoV. *Nature* 594, 246–252. doi: 10.1038/s41586-021-03493-4

Sun, L., Chen, H., Ming, X., Bo, Z., Shin, H. J., Jung, Y. S., et al. (2021). Porcine epidemic diarrhea virus infection induces Caspase-8-mediated G3BP1 cleavage and subverts stress granules to promote viral replication. *J. Virol.* 95:e02344-20. doi: 10.1128/JVI.02344-20

Sun, Y., Dong, L., Yu, S., Wang, X., Zheng, H., Zhang, P., et al. (2017). Newcastle disease virus induces stable formation of bona fide stress granules to facilitate viral replication through manipulating host protein translation. *FASEB J.* 31, 1337–1353. doi: 10.1096/fj.201600980R

Thomas, M. G., Loschi, M., Desbats, M. A., and Boccaccio, G. L. (2011). RNA granules: the good, the bad and the ugly. *Cell. Signal.* 23, 324–334. doi: 10.1016/j.cellsig.2010.08.011

Vincent, H. A., Ziehr, B., and Moorman, N. J. (2017). Mechanism of protein kinase R inhibition by human cytomegalovirus pTRS1. *J. Virol.* 91:e01574-16. doi: 10.1128/JVI.01574-16

Visser, L. J., Medina, G. N., Rabouw, H. H., de Groot, R. J., Langereis, M. A., de Los Santos, T., et al. (2019). Foot-and-mouth disease virus leader protease cleaves G3BP1 and G3BP2 and inhibits stress granule formation. *J. Virol.* 93:e00922-18. doi: 10.1128/JVI.00922-18

Walter, P., and Ron, D. (2011). The unfolded protein response: from stress pathway to homeostatic regulation. *Science* 334, 1081–1086. doi: 10.1126/science.1209038

Wang, F., Li, J., Fan, S., Jin, Z., and Huang, C. (2020). Targeting stress granules: a novel therapeutic strategy for human diseases. *Pharmacol. Res.* 161:105143. doi: 10.1016/j.phrs.2020.105143

Wang, Q., Zhang, Y., Wu, L., Niu, S., Song, C., Zhang, Z., et al. (2020). Structural and functional basis of SARS-CoV-2 entry by using human ACE2. *Cells* 181, 894–904 e899. doi: 10.1016/j.cell.2020.03.045

Wang, W., Chen, J., Yu, X., and Lan, H. Y. (2022). Signaling mechanisms of SARS-CoV-2 Nucleocapsid protein in viral infection, cell death and inflammation. *Int. J. Biol. Sci.* 18, 4704–4713. doi: 10.7150/ijbs.72663

Wang, X., Liao, Y., Yap, P. L., Png, K. J., Tam, J. P., and Liu, D. X. (2009). Inhibition of protein kinase R activation and upregulation of GADD34 expression play a synergistic role in facilitating coronavirus replication by maintaining de novo protein synthesis in virus-infected cells. *J. Virol.* 83, 12462–12472. doi: 10.1128/JVI.01546-09

Wheeler, J. R., Matheny, T., Jain, S., Abrisch, R., and Parker, R. (2016). Distinct stages in stress granule assembly and disassembly. *elife* 5:e18413. doi: 10.7554/eLife.18413

White, J. P., and Lloyd, R. E. (2011). Poliovirus unlinks TIA1 aggregation and mRNA stress granule formation. *J. Virol.* 85, 12442–12454. doi: 10.1128/JVI.05888-11

White, J. P., and Lloyd, R. E. (2012). Regulation of stress granules in virus systems. *Trends Microbiol.* 20, 175–183. doi: 10.1016/j.tim.2012.02.001

Xu, S., Chen, D., Chen, D., Hu, Q., Zhou, L., Ge, X., et al. (2020). Pseudorabies virus infection inhibits stress granules formation via dephosphorylating eIF2alpha. *Vet. Microbiol.* 247:108786. doi: 10.1016/j.vetmic.2020.108786

Yadav, S., Ahamad, S., Gupta, D., and Mathur, P. (2022). Lead optimization, pharmacophore development and scaffold design of protein kinase CK2 inhibitors as potential COVID-19 therapeutics. *J. Biomol. Struct. Dyn.* 41, 1811–1827. doi: 10.1080/07391102.2021.2024449

Yang, W., Ru, Y., Ren, J., Bai, J., Wei, J., Fu, S., et al. (2019). G3BP1 inhibits RNA virus replication by positively regulating RIG-I-mediated cellular antiviral response. *Cell Death Dis.* 10:946. doi: 10.1038/s41419-019-2178-9

Yang, X., Hu, Z., Fan, S., Zhang, Q., Zhong, Y., Guo, D., et al. (2018). Picornavirus 2A protease regulates stress granule formation to facilitate viral translation. *PLoS Pathog.* 14:e1006901. doi: 10.1371/journal.ppat.1006901

Yuan, S., Chan, J. F. W., Chik, K. K. H., Chan, C. C. Y., Tsang, J. O. L., Liang, R., et al. (2020). Discovery of the FDA-approved drugs bexarotene, cetilistat, diiodohydroxyquinoline, and abiraterone as potential COVID-19 treatments with a robust two-tier screening system. *Pharmacol. Res.* 159:104960. doi: 10.1016/j.phrs.2020.104960

Yuan, S., Chu, H., Chan, J. F., Ye, Z. W., Wen, L., Yan, B., et al. (2019). SREBP-dependent lipidomic reprogramming as a broad-spectrum antiviral target. *Nat. Commun.* 10:120. doi: 10.1038/s41467-018-08015-x

Zekri, L., Chebli, K., Tourriere, H., Nielsen, F. C., Hansen, T. V., Rami, A., et al. (2005). Control of fetal growth and neonatal survival by the RasGAP-associated endoribonuclease G3BP. *Mol. Cell. Biol.* 25, 8703–8716. doi: 10.1128/MCB.25.19.8703-8716.2005

Zhang, Q., Sharma, N. R., Zheng, Z. M., and Chen, M. (2019). Viral regulation of RNA granules in infected cells. *Virol. Sin.* 34, 175–191. doi: 10.1007/s12250-019-00122-3

Zhou, P., Yang, X. L., Wang, X. G., Hu, B., Zhang, L., Zhang, W., et al. (2020). Addendum: a pneumonia outbreak associated with a new coronavirus of probable bat origin. *Nature* 588:E6. doi: 10.1038/s41586-020-2951-z

Zhou, Y., Fang, L., Wang, D., Cai, K., Chen, H., and Xiao, S. (2017). Porcine reproductive and respiratory syndrome virus infection induces stress granule formation depending on protein kinase R-like endoplasmic reticulum kinase (PERK) in MARC-145 cells. *Front. Cell. Infect. Microbiol.* 7:111. doi: 10.3389/fcimb.2017.00111

frontiers | Frontiers in Microbiology

TYPE Original Research
PUBLISHED 03 May 2023
DOI 10.3389/fmicb.2023.1185504

OPEN ACCESS

EDITED BY
Gaëtan Ligat,
Université Toulouse III Paul Sabatier, France

REVIEWED BY
Santosh Kumar Karn,
Sardar Bhagwan Singh University, India
Youichi Suzuki,
Osaka Medical and Pharmaceutical University, Japan
Dong Yang,
Tianjin Institute of Environmental and Operational Medicine, China

*CORRESPONDENCE
Sabina Andreu
✉ sandreu@cbm.csic.es

†These authors have contributed equally to this work

RECEIVED 13 March 2023
ACCEPTED 11 April 2023
PUBLISHED 03 May 2023

CITATION
Andreu S, von Kobbe C, Delgado P, Ripa I, Buzón MJ, Genescà M, Gironès N, del Moral-Salmoral J, Ramírez GA, Zúñiga S, Enjuanes L, López-Guerrero JA and Bello-Morales R (2023) Dextran sulfate from *Leuconostoc mesenteroides* B512F exerts potent antiviral activity against SARS-CoV-2 *in vitro* and *in vivo*. *Front. Microbiol.* 14:1185504. doi: 10.3389/fmicb.2023.1185504

Dextran sulfate from *Leuconostoc mesenteroides* B512F exerts potent antiviral activity against SARS-CoV-2 *in vitro* and *in vivo*

Sabina Andreu[1,2]*, Cayetano von Kobbe[2], Pilar Delgado[2], Inés Ripa[1,2], María José Buzón[3], Meritxell Genescà[3], Núria Gironès[2], Javier del Moral-Salmoral[2], Gustavo A. Ramírez[4], Sonia Zúñiga[5], Luis Enjuanes[5], José Antonio López-Guerrero[1,2†] and Raquel Bello-Morales[1,2†]

[1]Department of Molecular Biology, Universidad Autónoma de Madrid, Madrid, Spain, [2]Centro de Biología Molecular Severo Ochoa, Spanish National Research Council—Universidad Autónoma de Madrid (CSIC-UAM), Madrid, Spain, [3]Infectious Diseases Department, Vall d'Hebron Research Institute (VHIR), Hospital Universitari Vall d'Hebron, Universitat Autònoma de Barcelona, VHIR Task Force COVID-19, Barcelona, Spain, [4]Animal Science Department, University of Lleida (UDL), Lleida, Spain, [5]Department of Molecular and Cell Biology, Centro Nacional de Biotecnología-Consejo Superior de Investigaciones Científicas (CNB-CSIC), Madrid, Spain

The emergent human coronavirus SARS-CoV-2 and its resistance to current drugs makes the need for new potent treatments for COVID-19 patients strongly necessary. Dextran sulfate (DS) polysaccharides have long demonstrated antiviral activity against different enveloped viruses *in vitro*. However, their poor bioavailability has led to their abandonment as antiviral candidates. Here, we report for the first time the broad-spectrum antiviral activity of a DS-based extrapolymeric substance produced by the lactic acid bacterium *Leuconostoc mesenteroides* B512F. Time of addition assays with SARS-CoV-2 pseudoviruses in *in vitro* models confirm the inhibitory activity of DSs in the early stages of viral infection (viral entry). In addition, this exopolysaccharide substance also reports broad-spectrum antiviral activity against several enveloped viruses such as SARS-CoV-2, HCoV229E, HSV-1, in *in vitro* models and in human lung tissue. The toxicity and antiviral capacity of DS from *L. mesenteroides* was tested *in vivo* in mouse models which are susceptible to SARS-CoV-2 infection. The described DS, administered by inhalation, a new route of administration for these types of polymers, shows strong inhibition of SARS-CoV-2 infection *in vivo*, significantly reducing animal mortality and morbidity at non-toxic doses. Therefore, we suggest that it may be considered as a potential candidate for antiviral therapy against SARS-CoV-2.

KEYWORDS

virology, SARS–CoV–2, dextran sulfate, antivirals, nebulization

1. Introduction

Several microorganisms, both prokaryotic and eukaryotic, can produce and secrete to the environment extracellular polymeric substances (EPSs) (Bello-Morales et al., 2022), highly heterogeneous and variable polymers composed by carbohydrates, proteins, lipids, nucleic acids and humic substances (More et al., 2014; Bello-Morales et al., 2022). EPSs may perform important adaptive functions, including protection from adverse external conditions and

attachment to surfaces leading to the formation of biofilms (Flemming et al., 2016; Costa et al., 2018). EPSs can also exert antimicrobial activity (Poli et al., 2010; Xiao and Zheng, 2016), and the antiviral effect of these substances against several viruses, including herpes simplex virus type 1 (HSV-1) (Marino-Merlo et al., 2017; Sánchez-León et al., 2020), herpes simplex virus type 2 (HSV-2) (Arena et al., 2005), or influenza virus (Zheng et al., 2006), has been reported.

The antiviral effect of sulfated polysaccharides and other polyanions has been known for decades (Witvrouw et al., 1994). Initially, HSV-1 was inhibited by heparin and other related polyanions (Nahmias and Kibrick, 1964; Nahmias et al., 1964; Takemoto and Fabisch, 1964; Vaheri, 1964). Then, several polysulfates were demonstrated to have a high inhibitory effect against human immunodeficiency virus (HIV) in cell culture (Ito et al., 1987; Baba et al., 1988a; Bagasra and Lischner, 1988; Handa et al., 1991; Witvrouw et al., 1994). Other enveloped viruses, including HSV-2, influenza A virus, respiratory syncytial virus (RSV), cytomegalovirus (CMV), vesicular stomatitis virus (VSV), Sindbis virus, Semliki Forest virus and arenaviruses were also proven to be highly susceptible to polyanions *in vitro* (Baba et al., 1988b; Andrei and De Clercq, 1990; Mastromarino et al., 1991; Lüscher-Mattli et al., 1993; Schols et al., 2016; Sánchez-León et al., 2020; Bello-Morales et al., 2022). Furthermore, a recent study has demonstrated that dextran sulfate (DS), a branched gluocpolysaccharide produced by lactic acid bacteria, inhibits infection of a SARS-CoV-2-pseudotyped HIV-1-based vector *in vitro* (Izumida et al., 2022). These findings generated great initial hope, since, besides their potent antiviral capacity, sulfated polysaccharides were non-toxic in animals and non-specific, so they might be used against different variants or even different viruses.

However, early expectations were followed by wide skepticism when *in vivo* studies showed a poor bioavailability after oral and intravenous administration (Witvrouw et al., 1994). Nevertheless, we still consider that polyanions might be a promising clinical strategy as antivirals against enveloped viruses (Bello-Morales et al., 2022). The key question is how to administer them. Although the poor bioavailability revealed by studies on drug administration led to abandon them as antiviral candidates, we proposed that this difficulty could be overcome by the use of other administration strategies, such as nebulization of aerosols to reach the low respiratory tract (Bello-Morales et al., 2022).

The zoonotic COVID-19 pandemic arisen in late 2019 posed a serious threat to global health and economy. The severe acute respiratory syndrome coronavirus 2 (SARS-CoV-2) (Gorbalenya et al., 2020), the causal agent for this coronavirus disease, has been responsible for millions of infections and deaths. To date, the World Health Organization (WHO), has reported more than 633 million confirmed cases of this disease in the world, including more than 6.6 million deaths [World Health Organization (WHO), 2022]. Two other zoonotic coronaviruses have also caused fatal disease in humans in the last two decades: the severe acute respiratory syndrome coronavirus (SARS-CoV), emerged in China in 2002, and the Middle East respiratory syndrome coronavirus (MERS-CoV), appeared in the Middle East in 2012 (Enjuanes et al., 2016; Choudhary et al., 2021).

Regarding COVID-19 therapeutics, science and technology have come together to produce numerous vaccines in record time (Sarangi et al., 2021). However, besides prevention, the lack of efficient drugs to treat COVID-19 and other respiratory viruses makes imperative to continue the search for useful antiviral agents to treat this kind of viruses. Here we report for the first time the antiviral effect of a dextran sulfate (DS) from *Leuconostoc mesenteroides* B512F against SARS-CoV-2 *in vitro* and *in vivo*. In this work, antiviral assays in mice have been carried out applying the exopolymer by inhalation, a novel administration route for sulfated polyanions. Unlike previous reports using other administration strategies, our results show antiviral effect in mice treated with this inhaled dextran sulfate. This result opens a promising clinical alternative for treatment of infections produced by SARS-CoV-2 and other respiratory viruses.

2. Materials and methods

2.1. Cell lines

The Vero cell line, derived from the kidney of an adult African green monkey, was kindly provided by Dr. Enrique Tabarés (UAM, Madrid, Spain). The Huh-7 cell line (Nakabayashi et al., 1982) was generously provided by Dr. Sonia Zúñiga (CNB-CSIC, Madrid, Spain). HeLa cells (CCL-2) and Vero-E6 cells (CRL-1586) were purchased from the American Tissue Culture Collection (ATCC). Human embryonic kidney HEK293T cells native or expressing human ACE2 were generated by lentiviral transduction with vector CSIB and selection in blasticidin S (Horndler et al., 2021). All cell lines were routinely tested for the absence of mycoplasma.

Cell lines were cultured in low-glucose Dulbecco's modified Eagle medium (DMEM) (Life Technologies) supplemented with 5% fetal bovine serum (FBS), penicillin (50 U/mL) and streptomycin (50 μg/mL) at 37°C in a humidified atmosphere of 5% CO_2.

2.2. Lung tissue

Lung tissues were obtained from patients with no history of COVID-19 and with a recent negative PCR test for SARS-CoV-2 infection undergoing thoracic surgical resection at the Thoracic Surgery Service of the Vall d'Hebron University Hospital (Barcelona, Spain). Cell extraction was performed as described in Grau-Expósito et al. (2022). Briefly, non-neoplastic tissue areas were dissected into small blocks and digested with collagenase IV (Gibco) and DNase I (Roche) for 30 min at 37°C and 400 rpm, and mechanically digested with a pestle. The resulted cellular suspension was subjected to several filtrations and washes with PBS and finally resuspended with RPMI 1640 supplemented with 5% FBS, 100 U/ml penicillin and 100 ug/ml streptomycin. Cell number and viability were evaluated with the LUNA Automated Cell Counter (Logos Biosystems).

2.3. Viruses

HCoV-229E expressing a GFP reporter protein was generously provided by Dr. Volker Thiel, from the University of Bern. This virus was propagated on Huh-7 cells for 5 days at 33°C with 5% CO_2. The infectious titer of the virus stocks was determined according to the Reed and Muench formula (Reed and Muench, 1938) on Huh-7 cell monolayers by the endpoint dilution assay described in Andreu et al. (2021). HSV-1 K26-GFP (a kind gift from. Dr. Prashant Desai; Johns Hopkins University, Baltimore, USA) was obtained by fusion of green fluorescent protein (GFP) with HSV-1 capsid protein VP26 (Desai and Person, 1998). K26-GFP was propagated and titrated in Vero cells. Minute virus of mice (MVM, prototype strain) (Crawford, 1966), which can infect human tumor cells (Riolobos et al., 2010) was kindly provided by Dr. José M. Almendral (CBMSO, Madrid, Spain). SARS-CoV-2 virus (isolate Navarra-2473) was obtained from the nasal sample of a COVID-19 patient admitted to the University of Navarra Clinic (Pamplona, Spain) (Maestro et al., 2021), and was gently provided by Dr. Cristian Smerdou (CIMA, Universidad de Navarra, Spain). The SARS-CoV-2 strain NL/2020 was provided by Pablo Gastaminza (CNB-CSIC, Madrid, Spain).

Lentiviral particles expressing either SARS-CoV-2 spike (St) protein (Wuhan, truncated) or vesicular stomatitis virus (VSV) protein and GFP reporter protein were generated as in Horndler et al. (2021). Briefly, pseudoviruses were obtained by co-transfecting plasmids pCMVA (gag/pol), p-HR-SIN-GFP and either a truncated S envelope (pCR3.1-St) or VSV envelope (pMD2.G) using the JetPEI transfection reagent (Polyplus Transfection). Viral supernatants were obtained after 24 and 48 h of transfection and pooled. Polybrene (4 μg/ml) was added to the viral supernatants before the addition to ACE2+HEK293T cells. Cells were centrifuged for 70 min at 2,100 rpm at 32°C and left in culture for 48 h. Finally, cells were resuspended with 5 mM EDTA and fixed for flow cytometry analysis. Both LV-St and LV-VSV were titrated on ACE2+HEK293T cells by analysis of GFP+ cells on a FACSCanto™ II Flow Cytometer (Becton-Dickinson), and data were processed with FlowJo software (BD, version 10.6.2).

SARS-CoV-2 spike pseudotyped VSV*ΔG(Luc)-S was generated following the protocol previously described in Grau-Expósito et al. (2022).

2.4. Reagents

Chondroitin sulfate sodium salt from shark cartilage (C4384, P1), dextran sulfate sodium salt from *Leuconostoc mesenteroides* B512F M_w >500,000 Da (D8906, P2), dextran sulfate sodium salt M_w 7,000-20,000 Da (D51227, P3), and dextran sulfate sodium salt M_r ~40,000 Da (42867, P4) were purchased from Sigma-Aldrich (Supplementary Figure 1). All were diluted in water to the stock concentrations and stored at 4°C. Such reagents were used in the cytotoxicity and antiviral assays. P2 was the only one that was subjected to SARS-CoV-2 *in vivo* in mouse models.

The different molecular weight polymers were produced by limited hydrolysis and fractionation. The dextran sulfate P2 was obtained from bacterial culture and subsequent chemical transformation. Regarding P2, fractionation of dextran was performed by ethanol, in which the largest molecular weight dextrans precipitate first. Esterification with sulfuric acid was carried out under mild conditions. The dextran sulfate P2 presents an off-white color appearance and comes in powder form. It has a molecular weight >500,000 Da (dextran starting material) and the sulfur content of the polymer is 16.9% (measured by S/C relation analysis), which is equivalent to ~2.3 sulfate groups per glucosyl residue. The pH of the polymer (1% in water at 25°C) is 7.3 and the solubility in water is 100 mg/ml, being purity >95%. When solubilized, its color changes to a very faint yellow.

2.5. Analysis of cell viability

The cytotoxicity of the polymers in Huh-7, ACE2+HEK293T, Vero, Vero E6, and HeLa cell lines was quantified using a CellTiter 96 Aqueous Non-Radioactive Cell Proliferation Assay Kit (Promega) based on MTT reagent. Non-confluent monolayers of cells plated in 96-well tissue culture plates were grown for 24 h before use. Cells were then treated for 48 h with P1, P2, P3, and P4 at concentrations ranging from 0 to 1,000 μg/ml. Four replicates were performed for each concentration. The cells were then incubated as indicated by the manufacturer of the kit, and the resulting colored solution was quantified using the scanning multiwell spectrophotometer iMarkTM Microplate Reader (BioRad), measuring the absorbance at 595 nm. The readouts obtained from the MTT assay were further normalized to the value of untreated cells, and CC_{50} values were calculated.

2.6. Viral assays in cell lines

2.6.1. Time of addition experiments

Time of addition experiments with HSV-1 K26 GFP and pseudoviruses LV-St and LV-VSV were performed to study the phase of infection at which candidate compounds exerted their antiviral activity. Vero and ACE2+HEK293T cell cultures were grown in 48-well culture plates and inoculated at a MOI of 0.1 with HSV-1 K26-GFP or pseudoviruses, respectively for 1 h in the presence or absence of the compounds at a temperature of 37°C. Several protocols were tested in which candidate compounds were added before, during, or/and after viral infection (Figure 2A). After 1 h of adsorption, the virus was washed and replaced with fresh 5% FBS complete medium containing or not the tested compounds. At 24 hours post-infection (h p.i.), cells were fixed for flow cytometry analysis.

2.6.2. Antiviral assays with HCoV-229E, HSV-1 K26 GFP, and MVM

Hereunder, the antiviral activity of the polymers (in contact with cell cultures at all times) was assayed. Cells were seeded in 48-well culture plates and treated for 1 h with either P1, P2, P3, or P4 at a range of concentrations between 0 and 1,000 μg/ml. Then, each cell line was infected with its corresponding virus at a specific MOI in the presence of the candidate compounds. Subsequently, the

virus was removed, and cells were washed with PBS and maintained in a fresh culture medium containing the polymers, in a humidified atmosphere. Cells were fixed for flow cytometry at different h p.i., according to the virus used: (i) HSV-1 K26-GFP infection (MOI 0.1) in Vero cells at 37°C; samples were collected at 24 h p.i; (ii) HCoV-229E infection (MOI 0.5) in Huh-7 cells at 33°C; samples were gathered at 48 h p.i.; (iii) MVM infection (MOI 0.5) in HeLa cells at 37°C; samples were collected at 24 h p.i.

2.6.3. Antiviral assays with LV-St and LV-VSV pseudoviruses

As for pseudoviruses assays, ACE2+HEK293T cells were seeded in 96-well tissue culture plates and infected with either LV-St or LV-VSV (MOI 0.1) previously mixed for 1 h with the compounds at different concentrations, and in the presence of polybrene (4 μg/ml), and transduced as previously described (Section 2). At 48 h p.i., cells were fixed for flow cytometry.

2.6.4. Antiviral assays with SARS-CoV-2

SARS-CoV-2 *in vitro* infection experiments were performed by the CNB Antiviral Screening Platform using the methodology described in Fàbrega-Ferrer et al. (2022). Briefly, Vero-E6 cells were inoculated with SARS-CoV-2 (strain NL/2020) at a MOI of 0.01 in the presence of the P1, P2, P3, and P4. Remdesivir (RMDV) was used as a positive control (Pruijssers et al., 2020). At 48 h p.i., cells were fixed for 20 min at room temperature with a 4% formaldehyde solution in PBS, washed twice with PBS and incubated with incubation buffer (3% BSA; 0.3% Triton X100 in PBS) for 1 h. A monoclonal antibody against the N protein was diluted in the incubation buffer (1:2000, v/v; Genetex HL344) and incubated with the cells for 1 h; after this time, cells were washed with PBS and subsequently incubated with a 1:500 (v/v) dilution of a goat anti-rabbit conjugated to Alexa 488 (Invitrogen). To control for unexpected toxicity of the compounds, nuclei were stained with DAPI (Life Technologies) during the secondary antibody incubation as recommended by the manufacturer. Cells were washed with PBS and imaged using an automated multimode reader (TECAN Spark Cyto) (Fàbrega-Ferrer et al., 2022). All data are referred to controls where infection efficiency was determined in the presence of the vehicle.

2.7. Viral assays in lung tissue

Duplicates of five-fold serial dilutions of the four polymers were tested in human lung tissue (HLT) cells using at least three different donors. HLT cells were added at a density of 300,000 cells/well and incubated with the compounds for 1 h before infection. Then, a MOI of 0.1 of the VSV*ΔG(Luc)-S virus was added to the wells, and plates were spinoculated at 1,200 g and 37°C for 2 h. After the infection, fresh RPMI medium was added to the wells and cell suspensions were transferred into a 96-well flat-bottom plate. Cells were then cultured overnight at 37°C in a 5% CO_2 incubator. Each plate contained the following controls: no cells (background control), cells treated with medium (mock infection), cells infected but untreated (infection control) and cells infected and treated with the drug camostat mesylate (S2874, Sigma) as a positive control (Grau-Expósito et al., 2022). After 20 h, cells were incubated with Britelite plus reagent (Britelite plus kit; PerkinElmer) and then transferred to an opaque black plate. Luminescence was immediately recorded by a luminescence plate reader (LUMIstar Omega). In parallel, drug cytotoxicity was monitored by luminescence. To evaluate cytotoxicity, the CellTiter-Glo Luminescent kit (Promega), was used. Data were normalized to the mock-infected control, after which EC_{50} and CC_{50} values were calculated.

2.8. Immunofluorescence microscopy

After viral assays and infections, cells grown on glass coverslips were fixed in 4% paraformaldehyde for 20 min and rinsed with PBS. All cells were then permeabilized with 0.2% Triton X-100, rinsed, and incubated for 30 min at room temperature with incubation buffer. For MVM infected HeLa cell samples, a rabbit polyclonal antiserum against the VP2 N-terminal domain was used for 1 h of incubation (Maroto et al., 2004). Subsequently, an anti-rabbit antibody conjugated to Alexa 488 (Invitrogen) was added for another 1 h. Nuclei were stained with DAPI for 10 min. After thorough washing, coverslips were mounted in Mowiol and imaged using the LSM 710 Inverted Confocal Microscope (Zeiss). Processing of confocal images was performed using the Fiji-ImageJ software (version Image J 1.53c).

2.9. Flow cytometry analysis

To perform FACS analysis, cells were dissociated by 1 min incubation with 0.05% trypsin/0.1% EDTA (Invitrogen) at room temperature and washed and fixed in 4% paraformaldehyde for 15 min. Finally, cells were rinsed and resuspended in PBS. Cells were analyzed using a FACSCalibur Flow Cytometer (BD). Data were processed with FlowJo software (BD, version 10.6.2).

2.10. *In vivo* toxicity evaluation of polymer 2

To evaluate the toxicity of P2 *in vivo*, C57BL/6J-WT mice were used. 18 mice (8 weeks old) were purchased from Charles River Laboratories Spain and maintained at the Animal Facility of the Centro de Biología Molecular Severo Ochoa (CBMSO, CSIC-UAM, Madrid, Spain). After two weeks of acclimatization, mice were separated into three groups ($n = 6$) and were mock-inoculated (with PBS) or inoculated (with P2 at concentrations 5 and 50 mg/ml diluted in PBS) by inhalation for 30 min for four consecutive days. The inoculation of the animals was performed in a hermetic chamber (35 x 28 x 15 cm). The chamber has a removable perforated partition, so that it can be divided into two compartments of variable size, allowing simultaneous treatment of animals from different sex/bucket. P2 was nebulized using the portable nebulizer device OMRON CompAIR C28P (Omron Healthcare, NE-C28P), which uses air pressure to turn liquids into a mist that can be inhaled. After the exposure to the acute doses of polymer, mice were allowed free access to food and water and monitored daily for morbidity, mortality, and behavioral changes.

On day 15, mice were sacrificed with CO_2 and exsanguinated by cardiac puncture to obtain whole blood for analysis of blood counts and profiles. Several parameters were analyzed to monitor renal, hepatic, and immunological basic profiles. Body weight gain from day 0 (inoculation) to day 15 (sacrifice) was also monitored to exclude weight loss or lack of weight gain that would be indicative of toxicity.

2.11. *In vivo* antiviral evaluation of polymer 2

The antiviral potential of P2 was also evaluated *in vivo*. The mice used in this experiment (Tg-K18hACE2 mice) were obtained from the Jackson Laboratory [SN34860-B6.Cg-Tg (K18-hACE2) 2Prlmn/J.]. The Tg-K18hACE2 transgenic mice express hACE2 under the control of the human cytokeratin 18 promoter in airway epithelial cells (McCray et al., 2007). The original colony was expanded in our facility to produce the experimental cohort. Hemizygous animals were bred with C57BL6/J WT mice and offspring was genotyped according to Jackson's Separated PCR Assay.

Tg-K18hACE2 mice (8 weeks old) were maintained in the Biosafety level 2 Animal Facility of the CBMSO. 12 Tg-K18hACE2 mice were moved to the Biosafety level 3 Animal Facility of the CBMSO, separated into two groups of six individuals each, and after acclimatization, all of them were infected intranasally with a sub-lethal dose of SARS-CoV-2 10^4 PFU/ml of SARS-CoV-2 (Navarra 2473 strain). On days 4, 5, 6, and 7 p.i, mice were mock-inoculated (with PBS) or inoculated (with P2 at 50 mg/ml diluted in PBS) by inhalation for 30 min for four consecutive days. The inoculation of the animals was performed following the same procedure as for the toxicity test (Figure 1). Following acute dose polymer exposure, mice were allowed free access to food and water and were monitored daily for body weight, morbidity, mortality, and behavioral changes (piloerection, lethargy/stagger, eyes closed, hunched posture). Mice were euthanized at 8 d p.i, and lungs were collected from each individual. Lung tissue was processed for biomolecular analysis and histology.

2.12. RNA isolation

Murine lung tissues were collected in 1mL Trizol reagent (TRIReagent®, Sigma) and total RNA was extracted following the manufacturer's protocol. The concentration of RNA was determined by NanoDrop ND-1000 Spectrophotometer (ThermoScientific, Waltham, MA, USA) and its integrity was measured by the Bioanalyzer (Agilent 2100).

The RT-qPCR reactions were provided by the Genomics and NGS Core Facility (GENGS) at the CBMSO. The GENGS facility is part of the PTI+ Global Health (CSIC). The SARS-CoV-2 RT-qPCR assay is based on the "GENGS-3V2F SARS-CoV-2 RT-qPCR assay" [protected by CSIC as trade secret (5723-2020)], replacing the detection of the human gene for a mouse gene. Therefore, the assay detects three viral genes (N1, N2 and ORF1) and one mouse gene. This mouse gene is used as a positive internal control to confirm correct sample collection, correct RNA extraction and the absence of RT-qPCR inhibitors, to avoid false negative results. Viral genes amplifications indicate a SARS-CoV-2 RNA positive sample. Only mouse gene amplification indicates a SARS-CoV-2 RNA negative sample.

RT-qPCR reactions were performed in multiplex in 384-well plates (Shell® 384-Well PCR Plates White Well Clear shell Bio-Rad CN HSP-3805) with a final volume of 10 µl and using a one-step RT-qPCR supermix. Each 10 µl reaction mixture contained 2.5 µl of mastermix, 0.2 µl of primers mix, 0.2 µl of probes and 4 µl of diluted RNA sample. To discard a potential contamination of reagents and/or primer-dimer artifacts a no template control (NTC) reaction was carried out using all the reagents except the sample. RT-qPCR reactions were performed in a CFX Opus 384 Real Time PCR System (Bio-Rad).

To determinate the number of copies of SARS-CoV-2 RNA by absolute quantification, a standard curve of Synthetic SARS-CoV-2 RNA Control 2 (Twist Bioscience, MN908947.3) was performed. This curve was obtained with a qPCR over a five-point 1/10 dilution curve made from the starting SARS-CoV-2 RNA standard concentration (10,000 copies/well). The correlation coefficient obtained for the curve was 0.993.

2.13. Histology and tissue staining

Half of the lung tissue was fixed in 10% formalin for 2 h and then transferred to 30 % sucrose overnight. Subsequently, the tissue was fixed with OCT and stored at −80°C. Lung sections were cut on a cryostat (LEICA CM 1950) in 15 µM slices. Sections were collected on slides (SuperFrost Plus™ Adhesion) and left at room temperature for 2–3 h and then stored at −80°C.

For hematoxylin-eosin (H&E) staining, slides were placed in the hematoxylin cuvette for 20 min (Mayer's hematoxylin solution, Sigma), once thawed at room temperature. Subsequently, they were washed with water for 5 min and briefly shaken to dry them. Then, they were stained with eosin for 2 min (5 ml 1% eosin, 180 ml 70% ethanol, 2 ml acetic acid). The slides were thoroughly washed with 100% ethanol and Neo-Clear (Sigma). Finally, slides were prepared using Neo-Mount (Sigma) as mounting medium. Images were obtained using the CKX41 Inverted Microscope and Digital Camera EP50 (Olympus-Life Science).

For immunohistochemistry analysis, the streptavidin-biotin immunohistochemical (IHC) technique (modified with the use of polymers) was used. Thermal antigen recovery was carried out by heating a pressure cooker with citrate buffer pH 6 with an electric plate, in which the slides were placed in a metal rack at maximum temperature for 3 min. After tempering, the samples were incubated in a 3% hydrogen peroxide solution in methanol and washed in TBS (tris-buffered-saline) buffer pH 7.4. The samples were then incubated in 2.5% horse serum in a humid chamber to prevent drying. Subsequently, the excess serum was removed, and the primary antibody was added: monoclonal antibody against SARS/SARS- COV2 - B46F (MA1-7404, Invitrogen). In negative controls, the primary antibody was replaced by TBS buffer. After the incubation period, the slides were washed in TBS buffer and incubated with polymer (ImmPRESS-VR Polymer Reagent, Vector Laboratories). This was followed by two washes in TBS buffer. Subsequently, development was performed

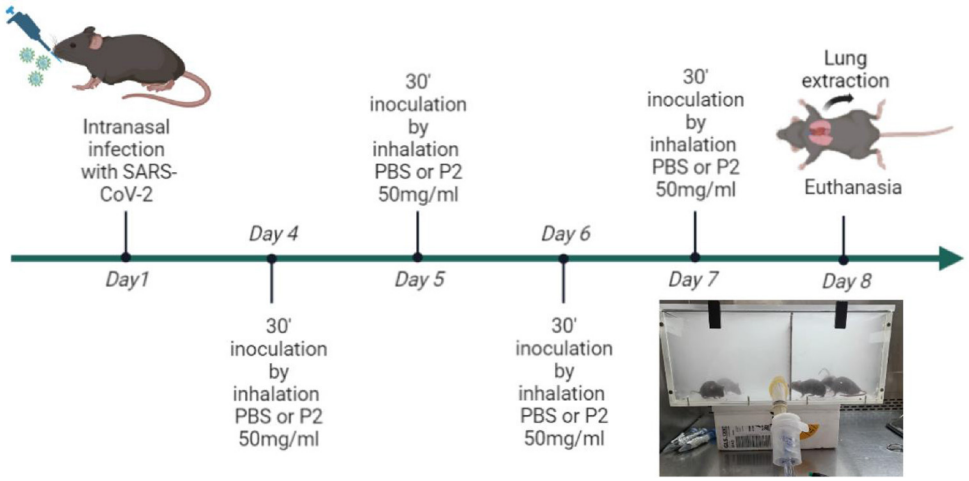

FIGURE 1
Schematic timeline of the antiviral experiments performed with SARS-CoV-2 in the mouse model C57BL6/J-k18-hACE2. The image shows the hermetic chamber where the nebulization of the animals was performed.

(ImmPACT NovaRED Substrate Kit, Peroxidase). After developing, the samples were counterstained with haematoxylin (Gemini AS Automated Slide Stainer, Thermo Fisher Scientific) and, finally, the slides were mounted.

For lung damage semi quantification, tissue sections stained with H&E according to standard procedures for examination by light microscopy were analyzed and scored blindly for lung damage by a board-certified veterinary pathologist. A multiparametric, semiquantitative scoring system was further used to assess the magnitude of histomorphological and histopathological changes in lung tissues based on the following criteria: expansion of parenchymal wall, edema, intra-alveolar hemorrhage, inflammatory cell infiltrates, degeneration of alveolar epithelial cells, bronchiole epithelial cell damage. For each histopathological parameter, a score of 0-3 was ordinally assigned, where 0 indicated normal or no change; 1 indicated less than 10%; 2 indicated 10−50%; and 3 indicated more than 50% of lung regions affected. The cumulative scores of the severity of the three sections provided the total score per animal.

2.14. Ethic statements

This study was carried out in strict accordance with the European Commission legislation for the protection of animals used for scientific purposes (directives 86/609/EEC and 2010/63/EU). Mice were maintained under specific pathogen-free conditions at the CBMSO (CSIC-UAM) animal facility. The protocol for the treatment of the animals was accepted by the "Comité de Ética de la Investigación" of the Universidad Autónoma of Madrid, Spain and approved by the "Consejería General del Medio Ambiente y Ordenación del Territorio de la Comunidad de Madrid" (PROEX 168.6/22). Animals had unlimited access to food and water, and at the conclusion of the studies they were euthanized in a CO_2 chamber, with every effort made to minimize their suffering, followed by lung collection and exsanguination by cardiac puncture to obtain whole blood.

As for human lung tissue cells, the study protocol was approved by the Clinical Research Committee [Institutional Review Board number PR(AG)212/2020] from the Vall d'Hebron University Hospital in Barcelona, Spain. Samples were obtained from adults, all of whom provided their written informed consent.

2.15. Statistics

All statistical analyses were performed using GraphPad Prism (version 8.0.1, GraphPad Software, Inc.). Data were subjected to Mann-Whitney-U tests (non-parametric samples) or two-tailed Student's T-tests (parametric samples) to determine significant differences between groups, and P values < 0.05 were considered statistically significant. For the CC_{50} and EC_{50} values, which indicate the concentration of the compound that leads to a 50% reduction in cell viability and viral infection, respectively, non-linear fit regression models were used (four parameters). For the analysis of the Kaplan-Meier survival curve, the Gehan-Breslow-Wilcoxon tests were performed.

3. Results

3.1. Antiviral assays in cell lines

3.1.1. Time of addition experiments with HSV-1 K26-GFP in Vero cell line

Four different DS polymers were selected for our study: chondroitin sulfate sodium salt from shark cartilage (P1), dextran sulfate sodium salt from *Leuconostoc mesenteroides* B512F M_w >500,000 Da (P2), dextran sulfate sodium salt M_w 7,000-20,000 Da (P3), and dextran sulfate sodium salt M_r ~40,000 Da (P4).

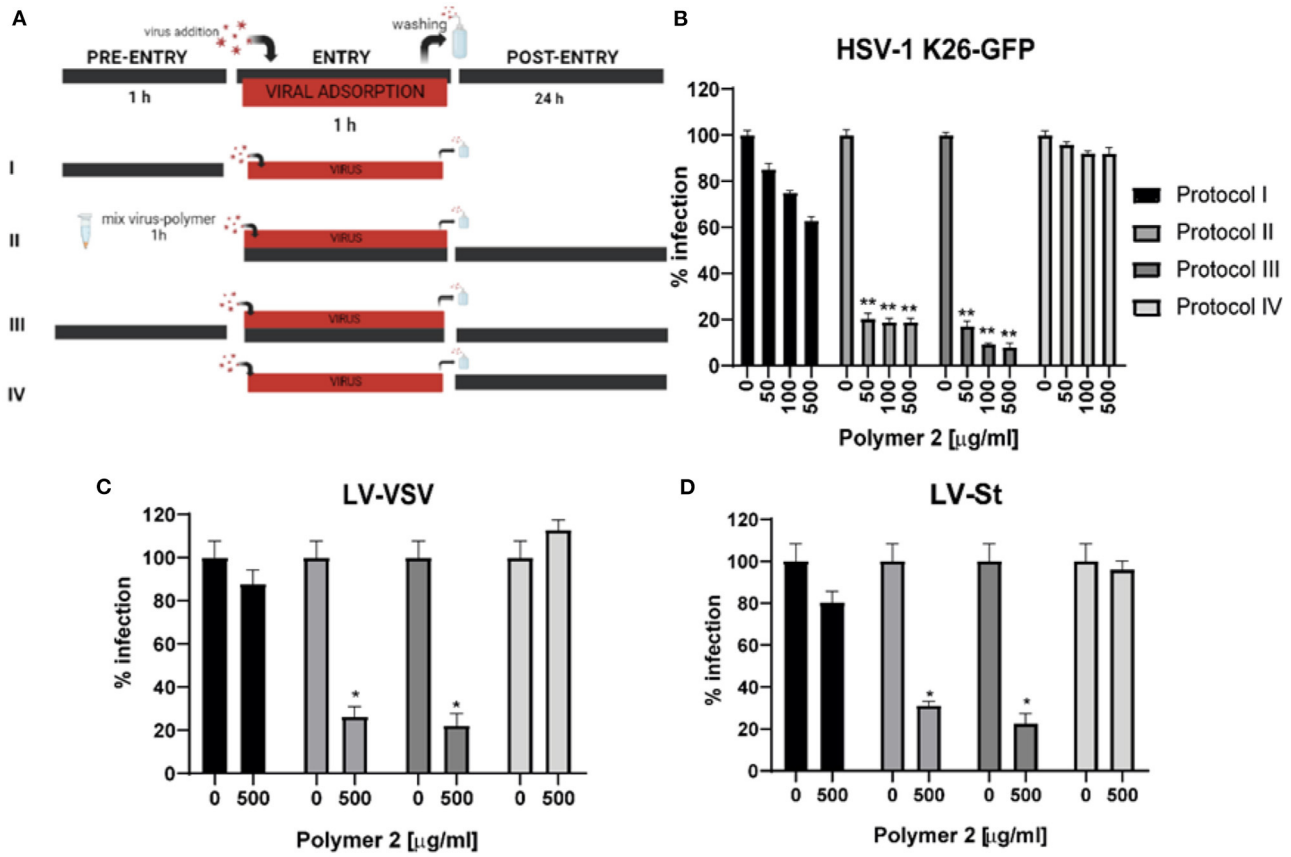

FIGURE 2
Time of addition experiments indicate that P2 interferes with early stages of HSV-1 K26 GFP, LV-VSV and LV-St infection. **(A)** Schematic figure of the times where the compound was present in the assay. Cells were cultured in 48-well plates and subjected to four different protocols: (I) Preincubation of cells with P2 for 1 h; (II) Mix of the virus and P2 for 1h and addition to the cells with post-incubation with P2; (III) Presence of P2 during all steps; (IV) Post-incubation of cells with P2 after viral adsorption. At 24 h, cells were collected for flow cytometry. The red bar represents viral infections; the black bar represents P2. Percentage of infection (+GFP cells) normalized to the non-infected cells for each protocol using **(B)** HSV-1 K26-GFP in Vero cells. **(C)** LV-VSV in ACE2+HEK293T cells. **(D)** LV-St in ACE2+HEK293T cells. Triplicate experiments were performed for each data point ($n = 4$), and the value is presented as mean of the percentage of normalized infection ± S.E.M. *$p < 0.05$ and **$p < 0.0001$ were considered significant as determined using the two-tailed Student's *T*-test.

Regarding time of addition experiments, HSV-1 K26-GFP was selected as the reference virus for this assay, since numerous previous studies have demonstrated the strong inhibitory activity of DSs against this virus *in vitro* (Piret et al., 2000; Witvrouw et al., 2016). Furthermore, the experiment was also assayed with pseudoviruses LV-St and LV-VSV, which enter via the interaction between the protein spike S and the cell receptor ACE2, imitating the way of entry of SARS-CoV-2. These experiments (Figure 2A) were performed in these models to confirm that the inhibitory effects of DS polymers take place on the steps of viral entry (Dyer et al., 1997; Pirrone et al., 2011). When the compounds were added before and/or during viral adsorption, they managed to reduce the viral infection (Figures 2B–D, results of P2 shown). Nonetheless, when they were added just after viral adsorption, no significant decrease in viral particles was detected. The best results were obtained when the compounds were left during all steps (Figure 2, Protocol III), where the infection drastically decreased by more than 90% in HSV-1 infection, and approximately an 80% in both pseudoviruses infections. Therefore, results suggest that the polymers interfere predominantly with the early phase of infection. We selected protocol III as the optimal one to apply in the following trials.

3.1.2. Antiviral assays against enveloped viruses HSV-1, HCoV229E, LV-VSV, and LV-St

First, the cytotoxicity of P1, P2, P3, and P4 at 48 h was evaluated in all cell lines by using an MTT assay. None of them exerted toxic effects at any concentration (EC_{50} values over 1 mg/ml in all cell lines tested). On the contrary, the polymers conserved cellular viability above 80%. In addition, compounds P3 and P4 were able to increase cell viability above 100% on average (Figures 3A–D).

After selecting protocol III as the optimal for the following studies (Figure 3D), different types of cell lines were cultured and infected with their corresponding viruses in the presence of the polymers at different concentrations during all steps. Infection was monitored by the expression of the GFP reporter protein, which was expressed by all viruses used in these assays. Unsurprisingly, all DS polymers (P2, P3, and P4) drastically decreased the infection at concentrations ranging from 10 to 1,000 μg/ml, but chondroitin

10.3389/fmicb.2023.1185504

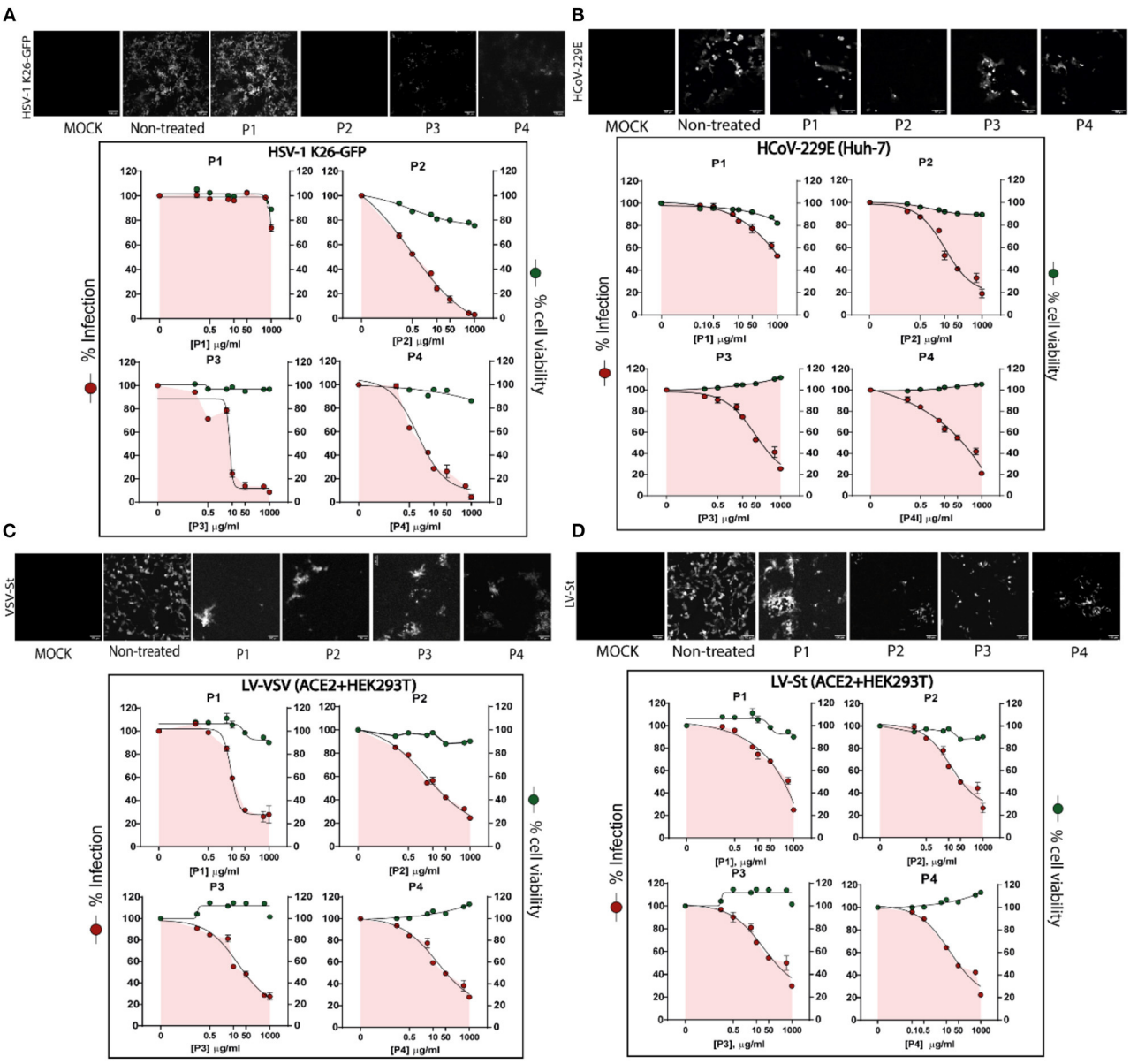

E

EC50 (µg/ml)	P1	P2	P3	P4
HSV-1	>1000	0.42 ± 0.66	7.26 ± 0.04	1.46 ± 0.13
HCoV-229E	>1000	9.60 ± 0.3	87.54 ± 13.99	73.90 ± 2.08
LV-St	45.76 ± 9.02	13.67 ± 3.77	25.67 ± 4.93	16.70 ± 0.63
VSV-St	8.78 ± 7.79	4.84 ± 1.89	18.27 ± 5.51	17.46 ± 4.36

CC50 (µg/ml)	P1	P2	P3	P4
Vero	>1000	>1000	>1000	>1000
Huh-7	>1000	>1000	>1000	>1000
ACE2+HEK293T	>1000	>1000	>1000	>1000

FIGURE 3
Antiviral assays and cytotoxicity of P1, P2, P3, and P4 against enveloped viruses. Results for **(A)** HSV-1 K26 GFP in Vero cell line, **(B)** HCoV-229E in Huh-7 cells, **(C)** LV-VSV in ACE2+HEK293T cells and **(D)** LV-St in ACE2+HEK293T cell line. Each cell line was incubated during all steps with the polymers at concentrations ranging from 0 to 1,000 µg/ml and subsequently infected with its corresponding virus at a specific MOI. Above, fluorescence microscopy images of cells infected with the virus show GFP+ signal corresponding to viral infection. Below, dose-response curves for EC_{50} and CC_{50} values were determined by a non-linear fit model with variable response curve (four parameters); red dots show percentage of infection and green dots represent percentage of viability compared to untreated cells. Triplicate experiments were performed for each data point ($n = 3$), and the value is presented as mean percentage of infection/viability ± S.E.M. For some conditions, S.E.M. values are so small that they are not visible on the plot. **(E)** EC_{50} and CC_{50} values ± S.D for each polymer.

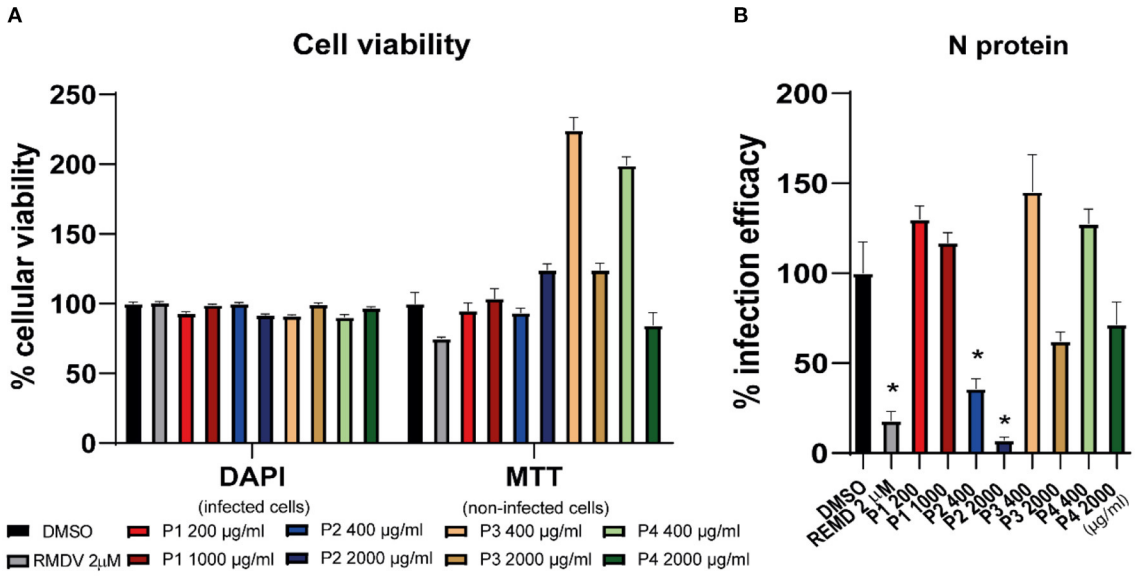

FIGURE 4
P2 decreases the infection of SARS-CoV-2 in Vero-E6 cells *in vitro* at non-cytotoxic concentrations. Vero-E6 cells were inoculated at a MOI of 0.01 with SARS-CoV-2 in the presence of DMSO (vehicle), remdesivir (positive control), and the four polymers. At 48 h post-infection (p.i.), cells were fixed with PFA 4% PBS and processed for immunofluorescence microscopy. Nuclei of infected samples were stained with DAPI. Uninfected cultures were also tested for viability in the presence of the same compound doses using an MTT-based assay. **(A)** Percentage of viability of infected cells (DAPI) and non-infected cells (MTT) in the presence of the compounds for 24 h. Results were normalized to the DMSO-treated cells and are shown as mean ± S.D ($n = 3$). **(B)** Infection efficiency measured as N protein expression reduction and expressed as the percentage of that observed in vehicle DMSO-treated cells and is shown as mean ± S.E.M. ($n = 3$). *$p < 0.01$ was considered significant as determined using the Mann-Whitney-U test.

sulfate sodium salt (P1) had no inhibitory effects on HSV1 K26-GFP infection (Figure 3A).

A similar pattern was observed for the rest of enveloped viruses tested. Fluorescence microscopy images (Figures 3A–D) reported a decrease in GFP+ signal corresponding to viral infection in cells treated with the compounds compared to untreated samples, a decrease that was lower in P1-treated cells. Except for the VSV-St virus, P1 reported the highest EC_{50} values (Figure 3E). In addition, P2 and P4 were the compounds that reported the lowest EC_{50} values in the non-linear fitting regression curves against HSV 1 K26-GFP, HCoV-229E, LV-VSV, and LV-St infections, with a wide protective window in all tested cell lines.

All polymers neutralized the entry of the SARS-CoV-2 S protein-pseudotyped lentivirus LV-St in a dose-dependent manner. This, added to the time-of-addition experiments, suggests that the candidate compounds primarily interfere with early aspects of infection.

3.1.3. Antiviral assays against SARS-CoV-2

To confirm the antiviral potential of the candidate polymers against SARS-CoV-2, they were diluted and mixed with a virus stock to inoculate Vero E6 cells. The antiviral activity was further confirmed by immunofluorescence microscopy, to estimate virus propagation. Cell viability was also evaluated in parallel to infection (DAPI, Figure 4A) and in non-infected cells (MTT, Figure 4A). No cytotoxicity was observed at the assayed doses. In fact, compounds P3 and P4 showed again high viability values in the MTT assay. As for the antiviral assay, DS from *L. mesenteroides* (P2) was highly effective in reducing infection efficiency, as suggested by SARS-CoV-2 N protein staining (Figure 4B). Furthermore, P2 reduced the infection to the same levels as the cells treated with RMDV (positive control), the only clinically approved antiviral for the treatment of COVID-19 patients (National Insitutes of Health Antiviral Therapy, 2022).

3.1.4. Antiviral assays against the non-enveloped minute virus of mice

To assess whether the antiviral activity of the DS polymers was limited to enveloped viruses (Bello-Morales et al., 2022), the compounds were tested against non-enveloped MVM in the HeLa cell line. As expected, none of the polymers were able to reduce the infection of this virus (Figure 5A). Furthermore, none of the compounds exhibited cytotoxic effects (CC_{50} values greater than 1,000 μg/ml) (Figure 5B), but whereas fluorescence microscopy images and flow cytometry data revealed that the percentage of infection remained around 100%.

3.2. Antiviral assays in human lung tissue cells

Following the promising results obtained in cell lines models, the next step was to demonstrate the antiviral activity of DS polymers in models closer to the clinic. A rapid platform for the identification of viral entry inhibitors by using human lung tissue (HLT) was used (Grau-Expósito et al., 2022). Cell suspensions from

10.3389/fmicb.2023.1185504

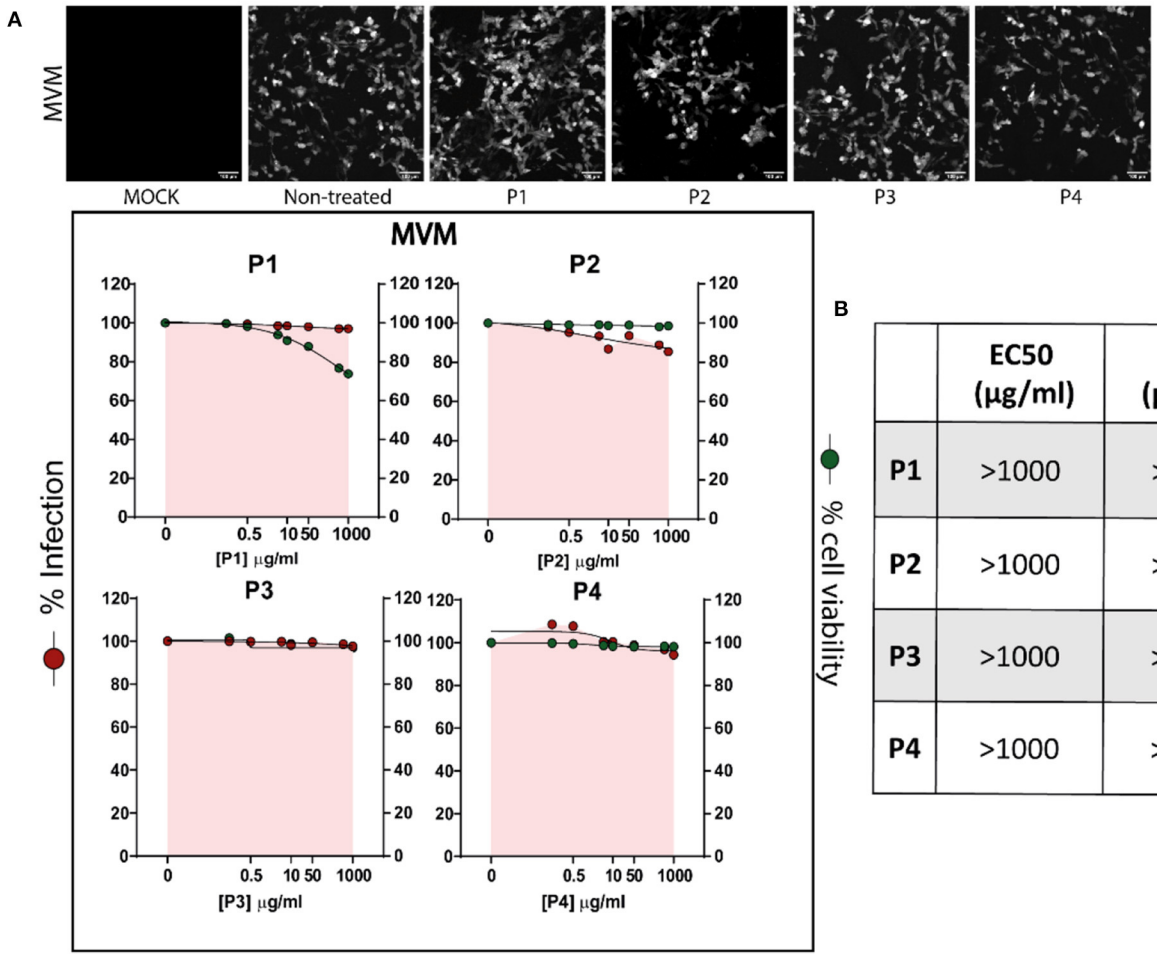

B

	EC50 (µg/ml)	CC50 (µg/ml)
P1	>1000	>1000
P2	>1000	>1000
P3	>1000	>1000
P4	>1000	>1000

FIGURE 5
Polymers P1, P2, P3, and P4 do not exert antiviral activity against non-enveloped virus MVM in the HeLa cell line at non-toxic concentrations. Cells were incubated all the time with the polymers at concentrations ranging from 0 to 1,000 µg/ml, and subsequently infected with MVM at a MOI of 0.5. **(A)** Above, fluorescence microscopy images of cells infected with the virus show GFP+ signal corresponding to viral infection. Below, dose-response curves for EC_{50} and CC_{50} values were determined by a non-linear fit model with variable response curve (four parameters); red dots show percentage of infection and green dots represent percentage of viability compared to untreated cells. Triplicate experiments were performed for each data point ($n = 3$), and the value is presented as mean of the percentage of normalized infection ± S.E.M. For some conditions, S.E.M. values are so small that they are not visible on the plot. **(B)** EC_{50} and CC_{50} values for each polymer in HeLa cells.

primary HLTs were obtained from three different patients with negative PCR tests for SARS-CoV-2, processed, and cultured for the assay. HLT cells were subjected to VSV*ΔG (Luc)-Spike virus in the presence of a 1/5 serial dilution of the different candidates tested. 20 h post-exposure, antiviral activity and cell viability were measured by luminescence. Camostat mesylate was the drug used as a positive control (results not shown) due to previous reports describing high antiviral activity in this HLT model (Grau-Expósito et al., 2022) and in precision-cut lung slices (Hoffmann et al., 2021).

Preliminary assays revealed that the calculated EC_{50} and CC_{50} values in cell line models differed drastically from the values in HLT cells for the same concentration. Therefore, the concentration of polymers was increased, with 25 mg/ml being the maximum concentration tested. Polymers P2 and P3 were the compounds that most effectively inhibited SARS-CoV-2 entry into HLT cells without affecting cell viability (EC_{50} values of 972.7 and 4275.3 µg/ml, respectively). Therefore, the potential benefit of DS from *L. mesenteroides* during the early phase of infection was again demonstrated. Nonetheless, P1 and P4 induced a slight viral entry suppression at high concentrations (Figures 6A, B).

3.3. *In vivo* toxicity evaluation of polymer 2 in mice

After confirming the tolerability and antiviral efficacy of the polymers *in vitro*, with DS from *L. mesenteroides* (P2) standing out as the compound that achieved the lowest EC_{50} values in immortalized cell lines and primary cell cultures, we wanted to evaluate whether inhalation treatment could be effective in protecting mice susceptible to SARS-CoV-2 infection.

First, the toxicity evaluation of the candidate compound was performed. 18 C57BL6/J mice were mock-inoculated or inoculated with different single doses of P2 for four consecutive days (Section 2.10). Several parameters were analyzed, such as body weight

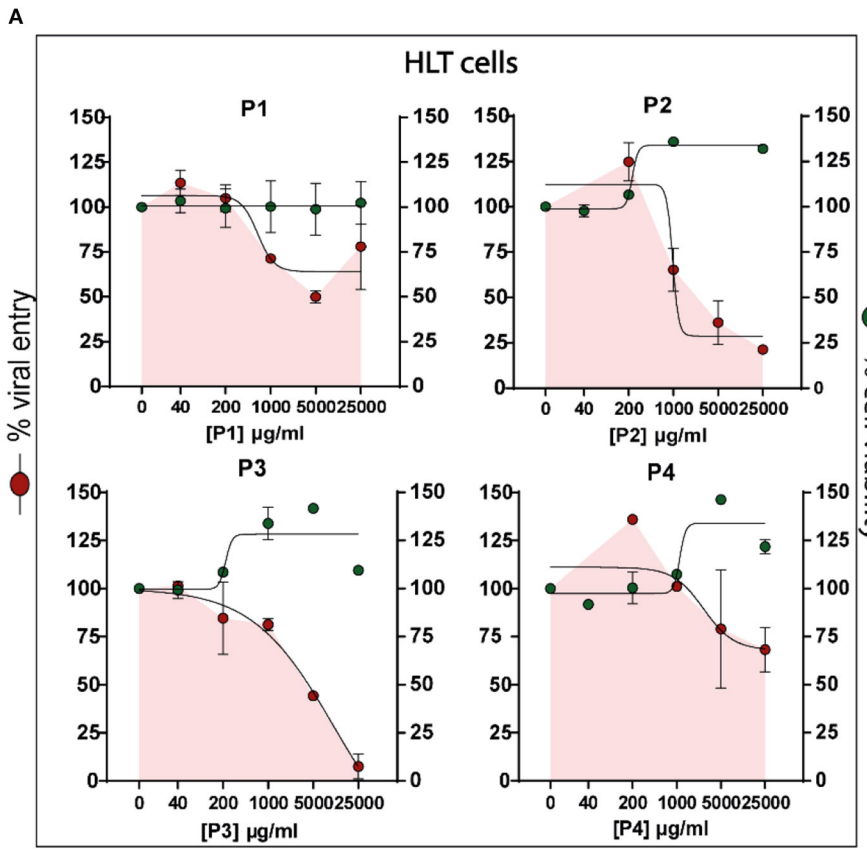

B

	EC50 (µg/ml)	CC50 (µg/ml)
P1	>25000	>25000
P2	957.7 ± 82.32	>25000
P3	4075.3 ± 35.57	>25000
P4	>25000	>25000

FIGURE 6
Percentage of viral entry in HLT cells exposed to VSV*ΔG (Luc)-Spike in the presence of compounds P1, P2, P3, and P4. HLT cells were incubated with VSV*ΔG (Luc)-Spike virus in the presence of a 1/5 serial dilution of the different polymers tested. Antiviral activity and cell viability were measured 20 h p.i by luminescence. **(A)** Non-linear fit model with variable response curve (four parameters) from at least three independent experiments in replicates is shown (red lines). Cytotoxic effect on HLT exposed to drug concentrations in the absence of virus is also shown (green lines). **(B)** CC_{50} and EC_{50} values of each drug for HLT cells. Triplicate experiments were performed for each data point ($n = 3$), and the value is presented as mean of the percentage of viral entry/viability ± S.E.M.

change (Figure 7A). Regarding WBCs count (Figure 7B), liver (Figure 7C), and renal markers (Figure 7D), all data remained within normal parameters established in mice by the clinical laboratory responsible for the biochemical analysis. ALT and AP enzymes in P2-treated mice seemed to decrease, while GOT and Gamma-GT values tended to increase, but without statistical significance. For 15 days there were no significant changes in any of the parameters between the control and experimental groups. No toxic signs such as hypothermia, weakness, diarrhea, or ataxia were observed. Hypochromia and anisocytosis tests were negative. There were also no signs of acute pain, distress, or weight loss. The maximum concentration tested (P2 50 mg/ml) did not show any of these signs and was selected as the dose used for the antiviral assay.

3.4. *In vivo* antiviral activity evaluation of P2 in mice

Being 50 mg/ml the concentration of P2 that exhibited no toxic effects in mice, its antiviral effect against SARS-CoV-2 was tested *in vivo*. Tg-K18hACE2 mice were infected intranasally with 10^4 PFU/ml of SARS-CoV-2, and treated or mock-treated on days 4, 5, 6 and 7 with nebulized P2 50 mg/ml, as previously described. Animals treated with P2 gained weight (Figure 8A), while those treated with PBS started to stop eating and thus their body weight decreased. Kaplan-Meier survival curve (Figure 8B) reports that 50% of the PBS-treated mice died before the end of the experiment, showing a significant mortality kinetic. In contrast, none of the P2-treated individuals died prematurely. Regarding clinical signs (Figure 8C), all PBS-treated mice exhibited piloerection, lethargy, eye closure, and hunched posture on days 7–8 p.i. These results report a significant difference in morbidity, since mice treated with P2 remained clearly asymptomatic.

The viral load in the lungs of the mice was also calculated by quantitative reverse transcription PCR (RT-qPCR). Virus yield in lung tissues was significantly reduced in P2-treated mice, suggesting that viral replication has been suppressed (Figure 9A).

Finally, to evaluate whether treatment with P2 at a concentration of 50 mg/ml caused any significant morphological difference in lung tissue compared to PBS-treated mice, histopathological studies were performed. To assess this, lung tissue was analyzed by histology on day 8 p.i. Lung damage quantification reveals significant differences between treated and

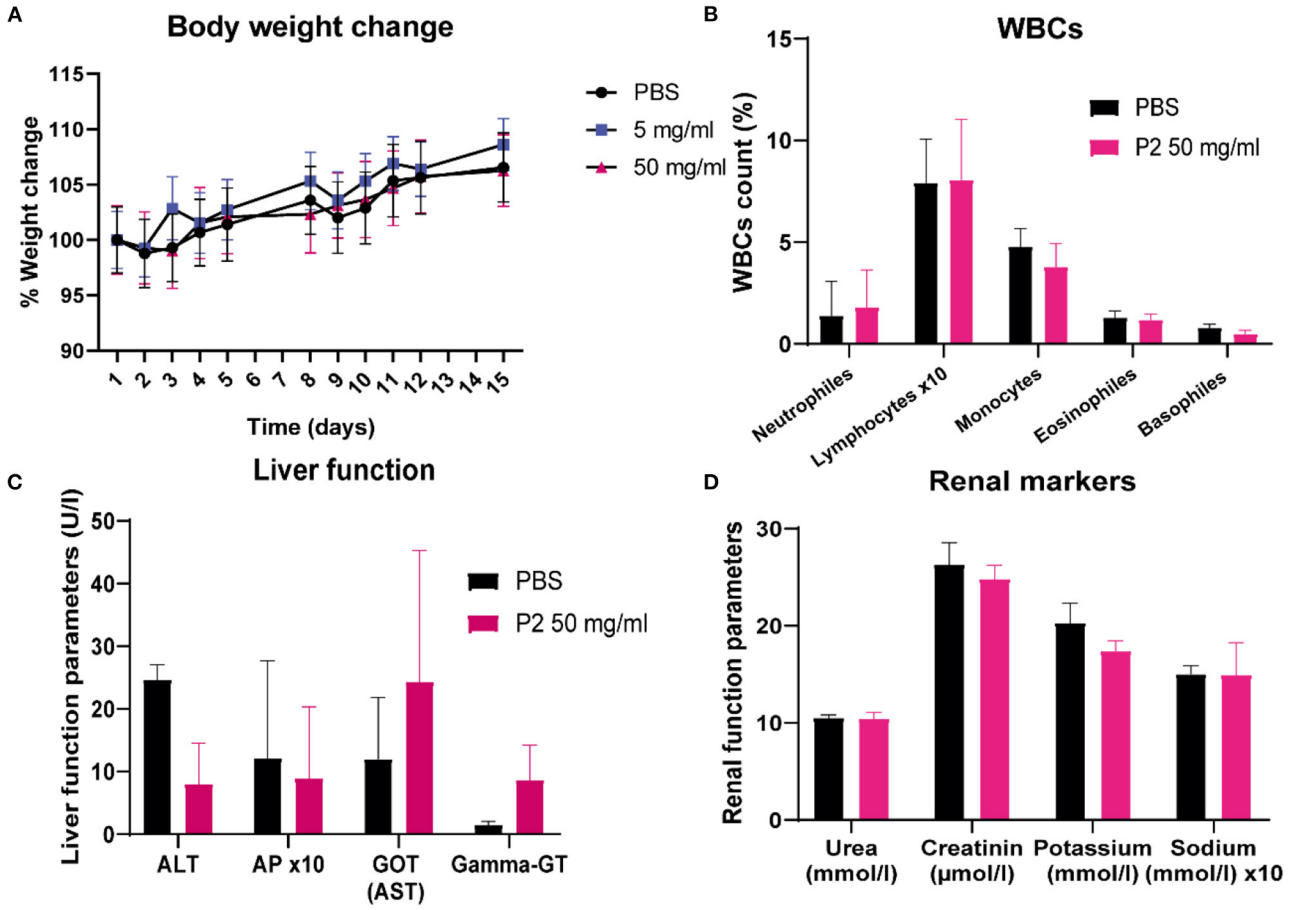

FIGURE 7
Polymer 2 shows no toxic effects in an *in vivo* mouse model. Eighteen C57BL6/J WT mice were distributed in three different groups ($n = 6$) and were mock-inoculated (PBS) or inoculated (P2 at the concentrations of 5 or 50 mg/ml diluted in PBS) by inhalation for 30 min for four consecutive days in a hermetic chamber. On day 15, mice were sacrificed and whole blood was obtained by cardiac puncture. **(A)** Percentage of body weight change, **(B)** WBC count, **(C)** liver markers alanine transaminase (ALT), alkaline phosphatase (AP), aspartate aminotransferase (AST), and Gamma-glutamyl transferase (Gamma-GT), and **(D)** renal markers urea, creatinine, potassium, and sodium levels were analyzed. Mean ($n = 6$) ± S.E.M are shown, and statistical comparisons were performed using the Mann-Whitney-U test.

non-treated animals (Figure 9B). This damage was evaluated by detecting an expansion of the parenchymal wall, desquamation and degeneration of alveolar epithelial cells, edema, and multi-nucleated cell formation, among others. Gross pathology revealed macroscopic manifestations of red lesions and discoloration in lungs of PBS treated mice (Figure 9C, Supplementary Figure 2). In the PBS treatment group, extensive lung epithelial surface disruption and cellular debris are observed; however, no such disruptions were found in the 50 mg/ml P2 group. Such features of diffuse alveolar damage have been described in human lung tissues of patients with positive PCRs for SARS-CoV-2 and COVID-19 symptoms. To support RT-qPCR results, SARS-CoV-2 N protein expression was detected in lung tissue from infected mice by immunohistochemistry (IHC) (Figure 9D). In PBS-treated mice, the staining corresponding to the presence of the virus was more intense compared to the P2-treated ones. These results indicate that P2 is well tolerated by the lung epithelium both *in vitro* and *in vivo* and that this polymer exerts promising antiviral efficacy at the 50 mg/ml concentration *in vivo*.

4. Discussion

Dextrans are high molecular weight branched glucopolysaccharides produced from sucrose by lactic acid bacteria (LAB) belonging to the *Lactobacillaceae* family. The DS P2 used in this work is a dextran derived from *Leuconostoc mesenteroides* strain B512F. It is composed of a linear chain of glucose monomers with approximately 95% α-D-(1,6) linkages, accounting the remaining α-D-(1,3) linkages for the branching of dextran. Regarding the branch lengths, the average branch length is less than three glucose units (Lindberg and Svensson, 1968; Larm et al., 1971), although other methods have indicated branches of greater than 50 glucose units (Senti et al., 1955; Bovey, 1959).

The safety of dextrans is endorsed by the inclusion of dextran 70 in the 22nd (2021) WHO Model List of Essential Medicines [World Health Organization (WHO), 2021]. On the other hand, the toxicity of dextran sulfate sodium (DSS) depends on its molecular weight. DS orally administered to humans did not exert significant side effects or systemic absorption (Abrams et al., 1989). However, administration of 1–5% high molecular weight DSS in drinking

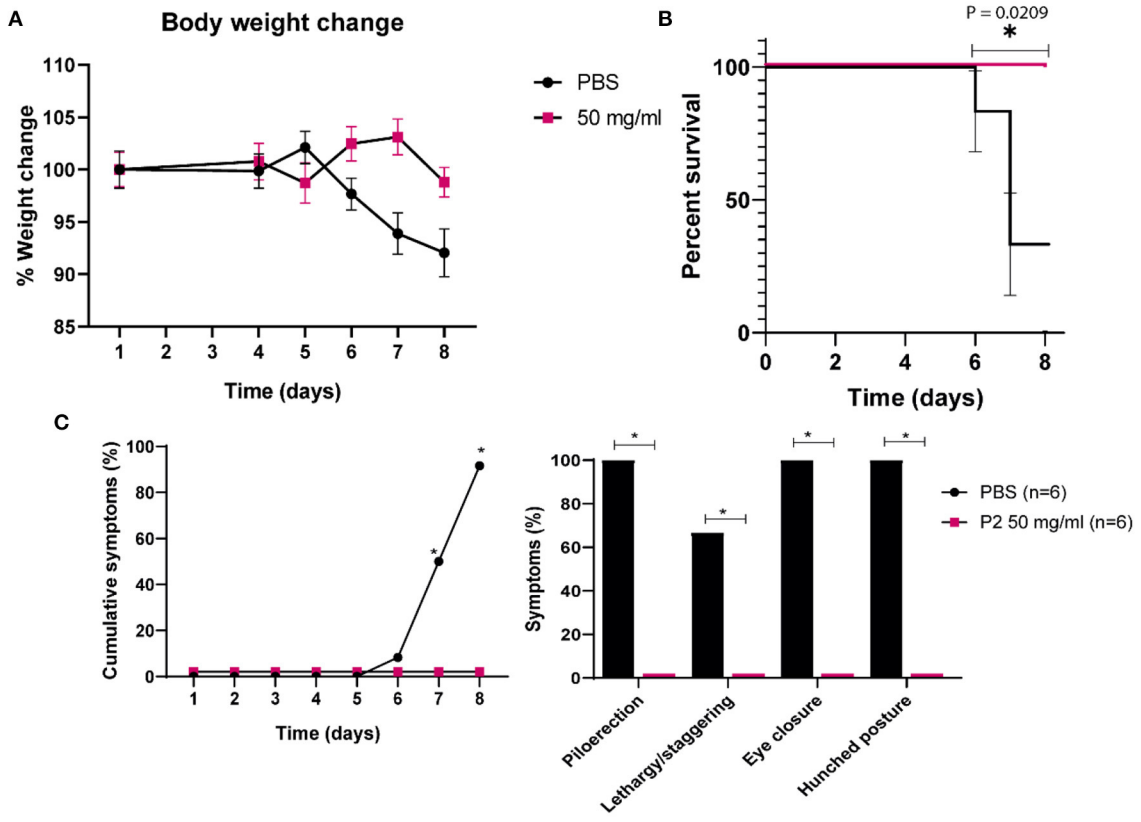

FIGURE 8
Percent survival and clinical signs of Tg-K18hACE2 mice infected with SARS-CoV-2 and treated with P2 by inhalation. Twelve Tg-K18hACE2 mice were distributed into two groups of six individuals each and infected with 10^4 PFU/ml of SARS-CoV-2 (Navarra strain 2473) intranasally. On days 4, 5, 6, and 7 p.i, mice were mock-inoculated (PBS) or inoculated (50 mg/ml P2) by inhalation for 30 min in a hermetic chamber. The mice were euthanized on day 8 p.i. Changes in body weight **(A)**, percent survival **(B)**, and clinical signs **(C)** were monitored daily. The analyzed symptoms (excluding weight loss) consisted of piloerection, lethargy and staggering, eye closure, and hunched posture. Mock-infected mice did not exhibit any symptoms throughout the experiment. The number of cumulative symptoms, exhibiting at least one of the previously described, are represented for each group. The individual symptoms are considered as positive when a mouse showed it at any day during the period 7–8 dpi. Mean ($n = 6$) ± S.E.M. are shown, and statistical comparisons were performed using the Gehan-Breslow-Wilcoxon test; *$p < 0.05$.

water induced acute intestinal injury in mice (Chassaing et al., 2014; Kiesler et al., 2015; Munyaka et al., 2016; Park et al., 2021).

DS is anticoagulant when administered intravenously. When administered by infusion, this polymer has shown to trigger, among other side effects, mild epistaxis, thrombocytopenia or transient elevations in alanine and aspartate aminotransferases (Flexner et al., 1991). However, the effects of DS administered by inhalation in humans or animal models had not been reported before. Here we have demonstrated for the first time the absence of significant side effects of DS after inhalation administration in a mouse model.

Numerous studies have also correlated the molecular weight and degree of sulfation of sulfated polysaccharides with their antiviral activity (Ray et al., 2022). Our *in vitro* assays support this hypothesis since P2 (M_w: 500kDa) reported the lowest EC_{50} values, followed by P4 (M_w: 40 kDa) and finally P3 (M_w: 7–20 kDa) (Witvrouw et al., 2016). However, P1 (chondroitin sulfate from shark cartilage) did not show remarkable antiviral effects. Chondroitin sulfate polymers have been shown to have weaker antiviral effects compared to DS polymers in HSV-1 (Nyberg et al., 2004), and only the chondroitin sulfate type E purified chain from squid cartilage has exhibited potent antiviral activity against HSV-1 (Bergefall et al., 2005). As for SARS-CoV-2, chondroitin sulfates do not show competitive binding to S protein (Kwon et al., 2020), and a recent study reported no activity of chondroitin sulfate against VSV- pseudotyped SARS-CoV-2 vector (Izumida et al., 2022).

The mechanism of action by which DSs exert their antiviral activity depends mainly on non-covalent interactions between the negative charges of the polymers and the positive charges on the virion envelopes (Bello-Morales et al., 2022). This interaction is not specific, as DS polymers have demonstrated antiviral activity against several viruses that use different receptors to enter cells. Furthermore, the polymers tested in our study lack inhibitory activity against the non-enveloped virus MVM, supporting the key role of the interaction between the viral envelope and the compounds. This suggests that their antiviral properties might be a universal phenomenon against enveloped viruses. Not only electrostatic forces, but also van der Waals forces, H-bonds, hydrophobic effects, cation bridging, or steric interactions favor the contact of virions and DSs (Bello-Morales et al., 2022).

Since these polymers have shown low toxicity and potent antiviral activity *in vitro* and *in vivo,* we suggest that they may have promising preventive clinical use, also due to their low

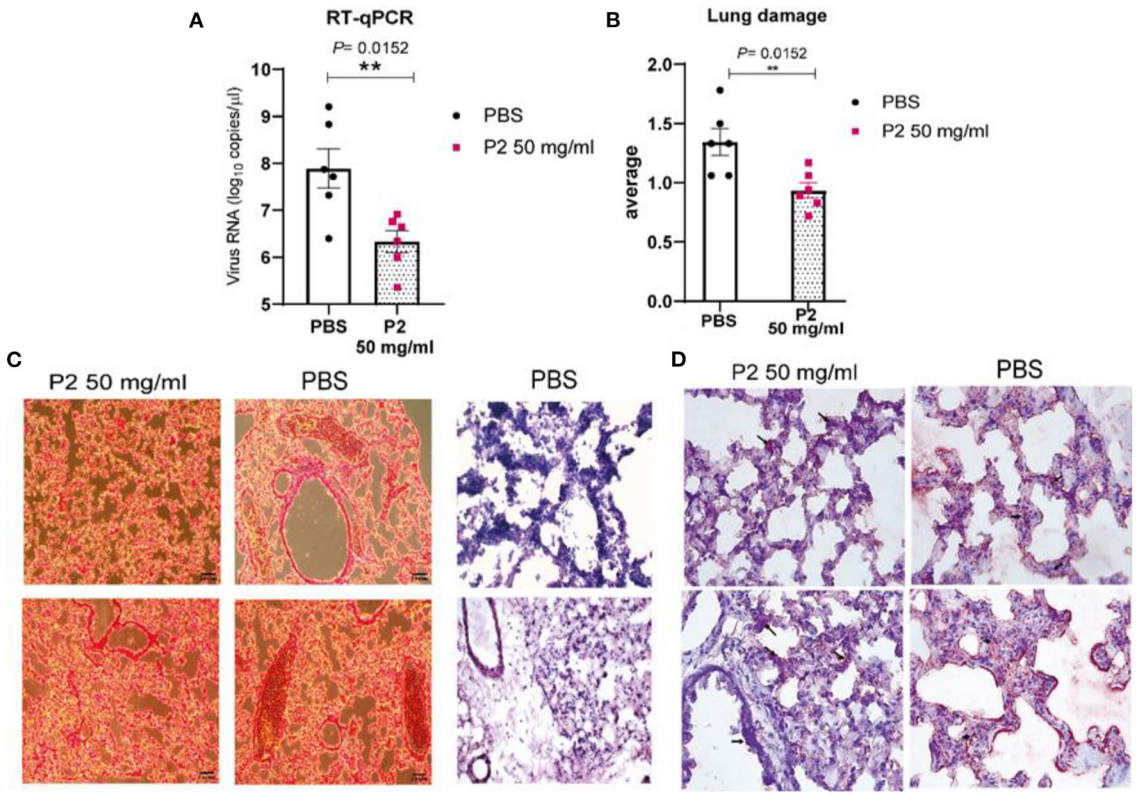

FIGURE 9
Effect of P2 on viral RNA levels and histology of Tg-K18hACE2 mice lung samples. **(A)** Viral genome copies in lung tissue determined by RT-qPCR. **(B)** Semi-quantification of the lung damage. **(C)** Hematoxylin and eosin (H&E) staining and **(D)** immunohistochemistry (IHC) images of N protein of SARS-CoV-2 of infected mice lung tissue 8 days p.i (scale bar, 100 µm, $n = 6$), treated with either PBS or 50 mg/ml P2. Arrows show the presence of cumulative virions. Two representative cryosections from two different mice of the same group are shown. Mean ($n = 6$) ± S.E.M. are shown. Statistical comparisons were made using Mann-Whitney-U tests; $^{**}p = 0.0152$.

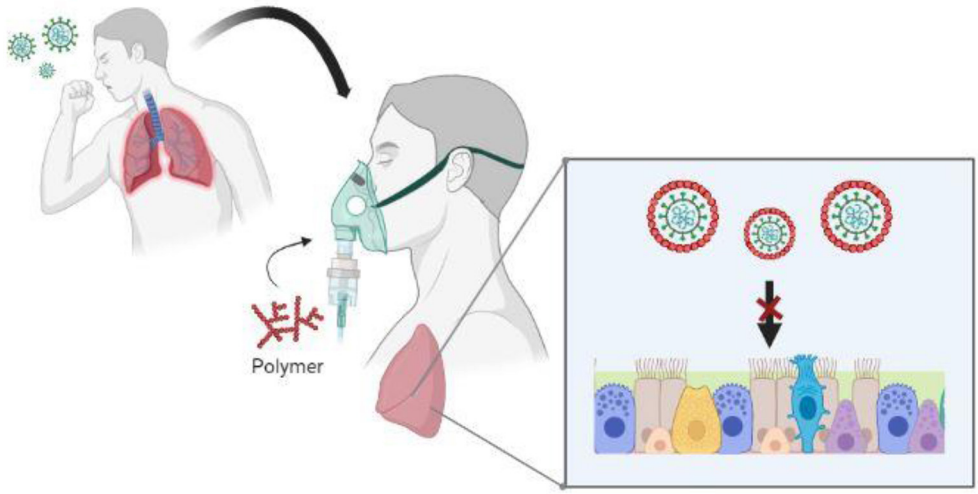

FIGURE 10
Possible strategy of administration of P2. In a patient with suspected SARS-CoV-2 infection, or in early stages of infection, the DS-based polymer is nebulized via aerosols to access the nasal cavity and pulmonary alveoli. Airborne virions can be trapped by the polymer before they attach and enter the respiratory epithelium, thus reducing viral infection.

cost and ease of production. SARS-CoV-2 infection begins via respiratory droplets that are deposited in the nasal, conjunctival, and oral mucosa. Receptors for SARS-CoV-2 are mainly expressed in epithelial cells in the nasal cavity (goblet cells and a subset of ciliated cells), and type II pneumocytes in alveoli (Emrani et al., 2021). Time of addition experiments and testing in HLT

cells have demonstrated that the effect of our polymers takes place mainly in the early steps of the infection. Therefore, we propose the strategy of directly attacking the virus just when it reaches the upper respiratory tract, the lungs, and other target cells present in the airways. This timing is ideal for polysulfates to trap airborne coronaviruses at the respiratory tract level, based on the physical chemistry of polyelectrolyte complexes (Nie et al., 2021; Vert, 2021). Nonetheless, viral replication and shedding could continue for several weeks in the case of severe patients, so repetitive administration should be considered. As part of post COVID-19 syndrome, the persistence of respiratory symptoms, especially dyspnea and cough, beyond four weeks from the outbreak of symptoms appears to be common (Vadász et al., 2020; Montani et al., 2022). Therefore, the precise treatment of respiratory symptoms is important in long-term prospective follow-up studies. The window to treat emerging SARS-CoV-2 infection before its peak is longer in humans compared to the mouse model (Sheahan et al., 2020), and our trials were performed in young mice (disease severity increases with age), so this must be taken into account in treatment design. The main drawback of polyanions is their low bioavailability, which can be avoided by using appropriate administration strategies here proposed, such as gargling, inhalation, and nasal spraying of an aqueous solution to access the oral and nasal cavities, or aerosol nebulization (Figure 10) to access pulmonary alveoli (Bello-Morales et al., 2022). All things considered, we suggest the inhalation with nebulized P2 in combination or not with current antiviral therapies for prevention.

In conclusion, this study highlights the broad-spectrum antiviral properties of exopolymers produced by *L. mesenteroides* B512F against SARS-CoV-2, and it also shows that inhalation is a suitable administration route for treating the infection. *In vivo* assays reported in this work showed no signs of toxicity and demonstrated a drastic inhibition of SARS-CoV-2 infection in mice treated with dextran sulfate 50 mg/ml. In addition, it is broadly active *in vitro* against various enveloped viruses, including the coronavirus HCoV-229E, and HSV-1. The low cost, speed of production, and the ease of application makes this polymer a good alternative for the prevention of COVID-19.

Data availability statement

The data that support the findings of this study are available from the corresponding author, SA, upon reasonable request. Some data are not available due to ethical requirements.

Ethics statement

As for human lung tissue cells, the study protocol was approved by the Clinical Research Committee [Institutional Review Board number PR(AG)212/2020] from the Vall d'Hebron University Hospital in Barcelona, Spain. Samples were obtained from adults, all of whom provided their written informed consent. The patients/participants provided their written informed consent to participate in this study. This study was carried out in strict accordance with the European Commission legislation for the protection of animals used for scientific purposes (directives 86/609/EEC and 2010/63/EU). The protocol for the treatment of the animals was accepted by the Comité de Ética de la Investigación of the Universidad Autónoma of Madrid, Spain and approved by the Consejería General del Medio Ambiente y Ordenación del Territorio de la Comunidad de Madrid (PROEX 168.6/22).

Author contributions

Conceptualization: SA, RB-M, and JL-G. Methodology: SA, RB-M, CK, PD, MB, NG, JM-S, MG, and GR. Formal analysis, investigation, and writing—original draft preparation: SA and RB-M. Writing—review and editing: SA, RB-M, IR, JL-G, PD, SZ, LE, NG, and CK. Supervision: RB-M, JL-G, PD, NG, JM-S, CK, and MB. Funding acquisition: JL-G. All authors have read and agreed to the published version of the manuscript.

Funding

Financial support for the study was provided by the REACT-EU 2021 grant from Comunidad de Madrid to the Project COVTRAVI-19-CM, Plataformas y modelos preclínicos para el abordaje multidisciplinar en COVID-19 y en respuesta a futuras pandemias.

Acknowledgments

We want to thank Cristian Smerdou, Cristina Olagüe, and Gloria González Aseguinolaza from CIMA Universidad de Navara for the SARS-CoV-2 (isolate N-2473) used for the *in vivo* assays. Genomics service at CBMSO is also acknowledged for their technical assistance with RT-qPCRs. We are grateful to the Histology Facility at CNB-CSIC for the histological preparation of biological samples. We also thank Javier Merino and the personnel from the Animal Facilities at CMBSO for their help in the BSL-3 Facilities. We wanted to thank Pablo Gastaminza, co-director of the CNB platform for his help with the *in vitro* SARS-CoV-2 experiments. Finally, we want to thank Dr. Josep Quer for his assistance with the experiments in VHIR, Barcelona, and Dr. García-Sastre for critical review.

Conflict of interest

The authors declare that the research was conducted in the absence of any commercial or financial relationships that could be construed as a potential conflict of interest.

Publisher's note

All claims expressed in this article are solely those of the authors and do not necessarily represent those of

their affiliated organizations, or those of the publisher, the editors and the reviewers. Any product that may be evaluated in this article, or claim that may be made by its manufacturer, is not guaranteed or endorsed by the publisher.

Supplementary material

The Supplementary Material for this article can be found online at: https://www.frontiersin.org/articles/10.3389/fmicb.2023.1185504/full#supplementary-material

References

Abrams, D. I., Kuno, S., Wong, R., Jeffords, K., Nash, M., Molaghan, J. B., et al. (1989). Oral dextran sulfate (UA001) in the treatment of the acquired immunodeficiency syndrome (AIDS) and AIDS-related complex. *Ann. Intern. Med.* 110, 183–188. doi: 10.7326/0003-4819-110-3-183

Andrei, G., and De Clercq, E. (1990). Inhibitory effect of selected antiviral compounds on arenavirus replication in vitro. Antiviral Res. 14, 287–299. doi: 10.1016/0166-3542(90)90009-V

Andreu, S., Ripa, I., Praena, B., López-guerrero, J. A., and Bello-morales, R. (2021). The valproic acid derivative valpromide inhibits pseudorabies virus infection in swine epithelial and mouse neuroblastoma cell lines. *Viruses*. 13, 522. doi: 10.3390/V13122522

Arena, A., Maugeri, T. L., Pavone, B., Iannello, D., Gugliandolo, C., Bisignano, G., et al. (2005). Antiviral and immunoregulatory effect of a novel exopolysaccharide from a marine thermotolerant *Bacillus licheniformis*. *Int. Immunopharmacol.* 6, 8–13. doi: 10.1016/j.intimp.2005.07.004

Baba, M., Pauwels, R., Balzarini, J., Arnout, J., Desmyter, De Clercq, E. et al. (1988a). Mechanism of inhibitory effect of dextran sulfate and heparin on replication of human immunodeficiency virus *in vitro*. *Proc. Natl. Acad Sci. USA*. 85, 6132–6136. doi: 10.1073/PNAS.85.16.6132

Baba, M., Snoeck, R., Pauwels, R., and de Clercq, E. (1988b). Sulfated polysaccharides are potent and selective inhibitors of various enveloped viruses including herpes simplex virus cytomegalovirus, vesicular stomatitis virus and human immunodeficiency virus. *Antimicrob Agents Chemother*. 32, 1742–1745. doi: 10.1128/AAC.32.11.1742

Bagasra, O., and Lischner, H. W. (1988). Activity of dextran sulfate and other polyanionic polysaccharides against human immunodeficiency Virus. *J. Infect. Dis*. 158, 1084–1087. doi: 10.1093/INFDIS/158.5.1084

Bello-Morales, R., Andreu, S., Ruiz-Carpio, V., Ripa, I., and López-Guerrero, J. A. (2022). Extracellular polymeric substances: still promising antivirals. *Viruses*.14, 1337. doi: 10.3390/V14061337

Bergefall, K., Trybala, E., Johansson, M., Uyama, T., Naito, S., Yamada, S., et al. (2005). Chondroitin sulfate characterized by the e-disaccharide unit is a potent inhibitor of herpes simplex virus infectivity and provides the virus binding sites on Gro2C Cells. *J. Biol. Chem*. 280, 32193–32199. doi: 10.1074/JBC.M503645200

Bovey, F. A. (1959). Enzymatic polymerization I molecular weight and branching during the formation of dextran. *J. Polymer Sci*. 35, 167–182. doi: 10.1002/POL.1959.1203512813

Chassaing, B., Aitken, J. D., Malleshappa, M., and Vijay-Kumar, M. (2014). Dextran sulfate sodium (DSS)-induced colitis in mice. *Curr. Protoc. Immunol.* 3, 104. doi: 10.1002./0471142735.IM1525S104

Choudhary, J., Dheeman, S., Sharma, V., Katiyar, P., Karn, S. K., Sarangi, M. K., et al. (2021). Insights of severe acute respiratory syndrome coronavirus (SARS-CoV-2) pandemic: a current review. *Biol. Proced. Online*. 23, 5. doi: 10.1186./S12575-020-00141-5

Costa, O. Y. A., Raaijmakers, J. M., and Kuramae, E. E. (2018). Microbial extracellular polymeric substances: ecological function and impact on soil aggregation. *Front. Microbiol*. 9, 1636. doi: 10.3389/FMICB.2018.01636

Crawford, L. V. A. (1966). Minute virus of mice. *Virology* 29, 605–612. doi: 10.1016/0042-6822(66)90284-4

Desai, P., and Person, S. (1998). Incorporation of the green fluorescent protein into the herpes simplex virus type 1 capsid. *J. Virol.* 72, 7563–7568. doi: 10.1128/jvi.72.9.7563-7568.1998

Dyer, A. P., Banfield, B. W., Martindale, D., Spannier, D. M., and Tufaro, F. (1997). Dextran sulfate can act as an artificial receptor to mediate a type-specific herpes simplex virus infection *via* glycoprotein. *BJ. Virol.* 71, 191–198. doi: 10.1128/JVI.71.1.191-198.1997

Emrani, J., Ahmed, M., Jeffers-Francis, L., Teleha, J. C., Mowa, N., Newman, R. H., et al. (2021). SARS-COV-2 Infection transmission transcription translation proteins, and treatment: a review. Int. J. Biol. Macromol. 193, 1249. doi: 10.1016/j.ijbiomac.2021.10.172

Enjuanes, L., Zuñiga, S., Castaño-Rodriguez, C., Gutierrez-Alvarez, J., Canton, J., Sola, I., et al. (2016). Molecular basis of coronavirus virulence and vaccine development. *Adv. Virus Res*. 96, 245–286. doi: 10.1016/BS.AIVIR.08003

Fàbrega-Ferrer, M., Herrera-Morandé, A., Muriel-Goñi, S., Pérez-Saavedra, J., Bueno, P., Castro, V., et al. (2022). Structure and inhibition of SARS-Co V-1 and SARS-CoV main proteases by oral antiviral compound AG7404. *Antiviral Res*. 208, 105458. doi: 10.1016/J.ANTIVIRAL.2022.105458

Flemming, H. C., Wingender, J., Szewzyk, U., Steinberg, P., Rice, S. A., Kjelleberg, S., et al. (2016). Biofilms: an emergent form of bacterial life. *Nat. Rev. Microbiol.* 14, 563–575. doi: 10.1038/NRMICRO.2016.94

Flexner, C., Barditch-Crovo, P. A., Kornhauser, D. M., Farzadegan, H., Nerhood, L. J., Chaisson, R. E., et al. (1991). Pharmacokinetics toxicity and activity of intravenous dextran sulfate in human immunodeficiency virus infection. *Antimicrob.* Agents Chemother. 35, 2544–2550. doi: 10.1128/AAC.35.12.2544

Gorbalenya, A. E., Baker, S. C., Baric, R. S., Groot, d. e., Drosten, R. J., Gulyaeva, C., et al. (2020). B. W., et al. The species severe acute respiratory syndrome-related coronavirus: classifying 2019-NCoV and naming it SARS-CoV-2. *Nat. Microbiol.* 5, 536–544. doi: 10.1038/S41564-020-0695-Z

Grau-Expósito, J., Perea, D., Suppi, M., Massana, N., Vergara, A., Soler, M. J., et al. (2022). Evaluation of SARS-CoV-2 entry inflammation and new therapeutics in human lung tissue cells. *PLoS Pathog*. 18, e1010171. doi: 10.1371/JOURNAL.PPAT.1010171

Handa, A., Hoshino, H., Nakajima, K., Adachi, M., Ikeda, K., Achiwa, K., et al. (1991). Inhibition of infection with human immunodeficiency virus type 1 by sulfated gangliosides. *Biochem Biophys Res. Commun*. 175, 1–9. doi: 10.1016/S0006-291X(05)81191-X

Hoffmann, M., Hofmann-Winkler, H., Smith, J. C., Krüger, N., Arora, P., Sørensen, L. K., et al. (2021). Camostat mesylate inhibits SARS-CoV-2 ACTIVATION by tmprss2-related proteases and its metabolite GBPA exerts antiviral activity. *EBioMedicine* 65, 103255. doi: 10.1016/J.EBIOM.2021.103255

Horndler, L., Delgado, P., Abia, D., alabanov, I. Martínez-Fleta, P., Cornish, G., et al. (2021). Flow cytometry multiplexed method for the detection of neutralizing human antibodies to the native SARS-CoV-2 spike protein EMBO. *Mol. Med*. 13, e13549. doi: 10.15252/EMMM.202013549

Ito, M., Baba, M., Sato, A., Pauwels, R., Clercq, De., Shigeta, E., et al. (1987). *Inhibitory effect of dextran sulfate and heparin on the replication of human immunodeficiency virus (HIV) in vitro. Antiviral. Res*. 7, 361–367. doi: 10.1016/0166-3542(87)90018-0

Izumida, M., Kotani, O., Hayashi, H., Smith, C., Fukuda, T., Suga, K., et al. (2022). Unique mode of antiviral action of a marine alkaloid against ebola virus and SARS-CoV-2. *Viruses*. 14, 816. doi: 10.3390/V14040816/S1

Kiesler, P., Fuss, I. J., and Strober, W. (2015). Experimental models of inflammatory bowel diseases. *Cell Mol. Gastroenterol. Hepatol.* 1, 241–248. doi: 10.1016/J.JCMGH.01006

Kwon, P. S., Oh, H., Kwon, S. J., Jin, W., Zhang, F., Fraser, K., et al. (2020). Sulfated polysaccharides effectively inhibit SARS-CoV-2 *in vitro*. *Cell Discov*. 6, 50. doi: 10.1038/S41421-020-00192-8

Larm, O., Lindberg, B., and Svensson, S. (1971). Studies on the length of the side chains of the dextran elaborated by leuconostoc mesenteroides, *NRRLB-512. Carbohydr. Res*. 20, 39–48.

Lindberg, B., and Svensson, S. (1968). Structural studies on dextran from leuconostoc mesenteroides NRRLB-512. *Acta Chem. Scand*. 22, 33.

Lüscher-Mattli, M., Glück, R., Kempf, C., and Zanoni-Grassi, M. A. (1993). Comparative study of the effect of dextran sulfate on the fusion and the in vitro replication of influenza A and B. Semliki forest, vesicular stomatitis, rabies, sendai, and mumps virus. *Arch. Virol*. 130, 317–326. doi: 10.1007/BF01309663

Maestro, S., Córdoba, K. M., Olague, C., Argemi, J., Ávila, M. A., González-Aseguinolaza, G., et al. (2021). Heme oxygenase-, inducer hemin does not inhibit SARS-CoV-2 virus infection. *Biomed. Pharmacotherapy* 137, 111384. doi: 10.1016/J.BIOPHA.2021.111384

Marino-Merlo, F., Papaianni, E., Maugeri, T. L., Zammuto, V., Spanò, A., Nicolaus, B., et al. (2017). Anti-Herpes simplex virus 1 and immunomodulatory activities of a poly-γ- glutamic acid from bacillus horneckiae strain APA of shallow vent origin. *Appl. Microbiol. Biotechnol.* 101, 7487–7496. doi: 10.1007/S00253-017-8472-5

Maroto, B., Valle, N., Saffrich, R., and Almendral, J. M. (2004). Nuclear export of the nonenveloped parvovirus virion is directed by an unordered protein signal exposed on the capsid surface. *J. Virol.* 78, 10685–10694. doi: 10.1128/JVI.78.19.10685-10694.2004

Mastromarino, P., Conti, C., Petruzziello, R., Lapadula, R., and Orsi, N. (1991). Effect of polyions on the early events of sindbis virus infection of vero cells. *Arch. Virol.* 121, 19–27. doi: 10.1007/BF01316741

McCray, P. B., Pewe, L., Wohlford-Lenane, C., Hickey, M., Manzel, L., Shi, L., et al. (2007). Lethal infection of K18-HACE2 mice infected with severe acute respiratory syndrome coronavirus. *J. Virol.* 81, 813–821. doi: 10.1128/JVI.02012-06

Montani, D., Savale, L., Noel, N., Meyrignac, O., Colle, R., Gasnier, M., et al. (2022). Post-acute COVID-19 syndrome. *Eur.* Resp. Rev. 31, 21. doi: 10.1183./16000617.0185-2021

More, T. T., Yadav, J. S. S., Yan, S., Tyagi, R. D., and Surampalli, R. Y. (2014). Extracellular polymeric substances of bacteria and their potential environmental applications. *J. Environ. Manage.* 144, 1–25. doi: 10.1016/J.JENVMAN.05010

Munyaka, P. M., Rabbi, M. F., Khafipour, E., and Ghia, J. E. (2016). Acute dextran sulfate sodium (DSS)-induced colitis promotes gut microbial dysbiosis in mice. *J. Basi. Microbiol.* 56, 986–998. doi: 10.1002/JOBM.201500726

Nahmias, A. J., and Kibrick, S. (1964). Inhibitory effect of heparin on herpes simplex virus. *J. Bacteriol.* 87, 1060–1066. doi: 10.1128/JB.87.5.1060-1066.1964

Nahmias, A. J., Kibrick, S., and Bernfeld, P. (1964). Effect of synthetic and biological polyanions on herpes simplex virus. *Proc. Soc. Exp. Biol. Med.* 115, 993–996. doi: 10.3181/00379727-115-29098

Nakabayashi, H., Miyano, K., Sato, J., Yamane, T., and Taketa, K. (1982). Growth of human hepatoma cells lines with differentiated functions in chemically defined medium. *Cancer Res.* 42, 3858–3863.

National Institutes of Health (NIH). (2022). *Antiviral Therapy | Coronavirus Disease 2019 (COVID-19) Treatment Guidelines*. Available online at: https://www.covid19treatmentguidelines.nih.gov/ (accessed November 21, 2022).

Nie, C., Pouyan, P., Lauster, D., Trimpert, J., Kerkhoff, Y., Szekeres, G. P., et al. (2021). Polysulfates block SARS-CoV-2 uptake through electrostatic interactions. *Angew. Chem. Int. Ed. Engl.* 60, 15870. doi: 10.1002/ANIE.202102717

Nyberg, K., Ekblad, M., Bergström, T., Freeman, C., Parish, C. R., Ferro, V., et al. (2004). The low molecular weight heparan sulfate-mimetic, pi-88, inhibits cell-to-cell spread of herpes simplex virus. *Antiviral. Res.* 63, 15–24. doi: 10.1016/J.ANTIVIRAL.01001

Park, H., Yeo, S., Kang, S., and Huh, C. S. (2021). Longitudinal microbiome analysis in a dextran sulfate sodium-induced colitis mouse model. *Microorganisms* 9, 1–18. doi: 10.3390/MICROORGANISMS9020370

Piret, J., Lamontagne, J., Bestman-Smith, J., Roy, S., Gourde, P., Désormeaux, A., et al. (2000). *In vitro* and *in vivo* evaluations of sodium lauryl sulfate and dextran sulfate as microbicides against herpes, simplex and human immunodeficiency viruses. J. *Clin. Microbiol.* 38, 110–119. doi: 10.1128/JCM.38.1.110-119.2000

Pirrone, V., Wigdahl, B., and Krebs, F. C. (2011). The rise and fall of polyanionic inhibitors of the human immunodeficiency virus type 1. *Antiviral. Res.* 90, 168–182. doi: 10.1016/J.ANTIVIRAL.03, 176.

Poli, A., Anzelmo, G., and Nicolaus, B. (2010). Bacterial exopolysaccharides from extreme marine habitats: production characterization and biological activities. *Mar. Drugs.* 8, 1779–1802. doi: 10.3390/MD8061779

Pruijssers, A. J., George, A. S., Schäfer, A., Leist, S. R., Gralinksi, L. E., Dinnon, K. H., et al. (2020). Remdesivir inhibits SARS-Co V-2 in human lung cells and chimeric SARS-CoV expressing the SARS-CoV-2 RNA polymerase in mice. *Cell Rep.* 32, 107940. doi: 10.1016/J.CELREP.2020.107940

Ray, B., Ali, I., Jana, S., Mukherjee, S., Pal, S., Ray, S. (2022). Antiviral strategies using natural source-derived sulfated polysaccharides in the light of the COVID-19 pandemic major human pathogenic viruses. *Viruses* 14, 35. doi: 10.3390./v14010035

Reed, L. J., and Muench, H. A. (1938). Simple method of estimating fifty per cent endpoints. *Am. J. Epidemiol.* 27, 493–497. doi: 10.1093/oxfordjournals.aje.a118408

Riolobos, L., Valle, N., Hernando, E., Maroto, B., Kann, M., Almendral, J. M., et al. (2010). Viral oncolysis that targets Raf-1 signaling control of nuclear transport. J. *Virol.* 84, 2090. doi: 10.1128/JVI.01550-09

Sánchez-León, E., Bello-Morales, R., López-Guerrero, J. A., Poveda, A., Jiménez-Barbero, J., Gironès, N., et al. (2020). Isolation and characterization of an exopolymer produced by bacillus licheniformis: in vitro antiviral activity against enveloped viruses. Carbohydr. Polym. 248, 116737. doi: 10.1016/J.CARBPOL.2020.116737

Sarangi, M. K., Padhi, S., Dheeman, S., Karn, S. K., Patel, L. D., Yi, D. K., et al. (2021). Diagnosis prevention and treatment of coronavirus disease: a review. *Antiviral Chem. Chemoth.* 20, 243–266. doi: 10.1080/14787210.2021.1944103

Schols, D., Clercq, E, De. Balzarini, J., Baba, M., Witvrouw, M., Hosoya, M., et al. (2016). Sulphated polymers are potent and selective inhibitors of various enveloped viruses including herpes simplex virus cytomegalovirus, vesicular stomatitis virus respiratory syncytial virus and toga- arena- and retroviruses. *Antiviral Chem. Chemoth.* 1, 233–240. doi: 10.1177/095632029000100402

Senti, F. R., Hellman, N. N., Ludwig, N. H., Babcock, G. E., Tobin, R., Glass, C. A., et al. (1955). Viscosity sedimentation and light-scattering properties of fraction of an acid-hydrolyzed dextran. *J. Polymer Sci.* 17, 527–546. doi: 10.1002/POL.1955.120178605

Sheahan, T. P., Sims, A. C., Zhou, S., Graham, R. L., Pruijssers, A. J., Agostini, M. L., et al. (2020). An orally bioavailable broad-spectrum antiviral inhibits SARS-CoV-2 in human airway epithelial cell cultures and multiple coronaviruses in mice. *Sci. Transl. Med.* 12, eabb5883. doi: 10.1126./scitranslmed.abb5883

Takemoto, K. K., and Fabisch, P. (1964). Inhibition of herpes virus by natural and synthetic acid polysaccharides. *Proc. Soc. Exp. Biol. Med.* 116, 140–144. doi: 10.3181/00379727-116-29183

Vadász, I., Husain-Syed, F., Dorfmüller, P., Roller, F. C., Tello, K., Hecker, M., et al. (2020). Severe organising pneumonia following COVID-19. *Thorax.* 76, 201–204. doi: 10.1136/THORAXJNL-2020-216088

Vaheri, A. (1964). Heparin and related polyionic substances as virus inhibitors. *Acta Pathol. Microbiol. Scand. Suppl.* 171, 171–198.

Vert, M. (2021). The non-specific antiviral activity of polysulfates to fight SARS-CoV-2, its mutants and viruses with cationic spikes. *J. Biomater Sci Polym. Ed.* 32, 1466–1471. doi: 10.1080/09205063.2021.1925391

Witvrouw, M., Desmyter, J., and De Clercq, E. (1994). 4 Antiviral portrait series: 4. Polysulfates as inhibitors of HIV and other enveloped viruses. *Antivir. Chem. Chemother.* 5, 345–359. doi: 10.1177/095632029400500601

Witvrouw, M., Schols, D., Andrei, G., Snoeck, R., Hosoya, M., Pauwels, R., et al. (2016). Antiviral activity of low-MW dextran sulphate (Derived from Dextran MW 1,000) compared to dextran sulphate samples of higher MW. *Antivir. Chem. Chemother.* 2, 171–179. doi: 10.1177/095632029100200307

World Health Organization (WHO) (2021). WHO Model List of Essential Medicines - 22nd List Available online at: https://www.who.int/publications/i/item/WHO-MHP-HPS-EML-202102

World Health Organization (WHO) (2022). Coronavirus (COVID-19) Dashboard. Available online at: https://covid19.who.int/ (accessed February 14, 2022).

Xiao, R., and Zheng, Y. (2016). Overview of microalgal extracellular polymeric substances (EPS) and their applications. *Biotechnol. Adv.* 34, 1225–1244. doi: 10.1016/J.BIOTECHADV.08004

Zheng, W., Chen, C., Cheng, Q., Wang, Y., and Chu, C. (2006). Oral administration of exopolysaccharide from aphanothece halophytica (Chroococcales) significantly inhibits influenza virus (H1N1)-induced pneumonia in mice. *Int. Immunopharmacol.* 6, 1093–1099. doi: 10.1016/J.INTIMP.01020

frontiers | Frontiers in Microbiology

TYPE Original Research
PUBLISHED 05 May 2023
DOI 10.3389/fmicb.2023.1173061

OPEN ACCESS

EDITED BY
Gaëtan Ligat,
Université Toulouse III Paul Sabatier, France

REVIEWED BY
Md. Golzar Hossain,
Bangladesh Agricultural University, Bangladesh
Valerio Taverniti,
INSERM UMR_S1110 Institute de Recherche sur les Maladies Virales et Hepatiques, France

*CORRESPONDENCE
Yingbin Wang
✉ ybwang@xmu.edu.cn
Tianying Zhang
✉ zhangtianying@xmu.edu.cn
Quan Yuan
✉ yuanquan@xmu.edu.cn

†These authors have contributed equally to this work and share first authorship

RECEIVED 24 February 2023
ACCEPTED 11 April 2023
PUBLISHED 05 May 2023

CITATION
Qi R, Cao J, Wu Y, Lei X, He J, Zhang L, Fu R, Chen F, Wang Y, Zhang T, Xia N and Yuan Q (2023) Combination therapy of therapeutic antibody and vaccine or entecavir in HBV carrier mice.
Front. Microbiol. 14:1173061.
doi: 10.3389/fmicb.2023.1173061

Combination therapy of therapeutic antibody and vaccine or entecavir in HBV carrier mice

Ruoyao Qi[1,2†], Jiali Cao[3†], Yangtao Wu[1,2†], Xing Lei[1,2], Jinhang He[1,2], Liang Zhang[1,2], Rao Fu[1,2], Feng Chen[1,2], Yingbin Wang[1,2*], Tianying Zhang[1,2*], Ningshao Xia[1,2] and Quan Yuan[1*]

[1]State Key Laboratory of Molecular Vaccinology and Molecular Diagnostics, School of Life Sciences & School of Public Health, Xiamen University, Xiamen, Fujian, China, [2]National Institute of Diagnostics and Vaccine Development in Infectious Diseases, Xiamen University, Xiamen, Fujian, China, [3]Department of Clinical Laboratory, Women and Children's Hospital, School of Medicine, Xiamen University, Xiamen, Fujian, China

Chronic infection with the hepatitis B virus (HBV) is a leading causes of liver cirrhosis and hepatocellular carcinoma. However, managing HBV treatments is challenging due to the lack of effective monotherapy. Here, we present two combination approaches, both of which aim to target and enhance the clearance of HBsAg and HBV-DNA. The first approach involves the use of antibodies to continuously suppress HBsAg, followed by the administration of a therapeutic vaccine in a sequential manner. This approach results in better therapeutic outcomes compared to the use of these treatments individually. The second approach involves combining antibodies with ETV, which effectively overcomes the limitations of ETV in suppressing HBsAg. Thus, the combination of therapeutic antibodies, therapeutic vaccines, and other existing drugs is a promising strategy for the development of novel strategies to treat hepatitis B.

KEYWORDS

HBV, therapeutic antibodies, therapeutic vaccine, nucleotid analogs, combination (combined) therapy

1. Introduction

Since the discovery of the Australia antigen by Blumberg et al. in 1965, chronic hepatitis B (CHB) has been considered a neglectable public health concern for almost 60 years (Blumberg et al., 1965). However, the fact remains that 296 million people with CHB urgently require effective eradication therapeutics, as CHB is a leading cause of liver cirrhosis and hepatocellular carcinoma (Jeng et al., 2023). Currently, interferon-based therapies and nucleos(t)ide analogs (NAs) are the only two primary treatment options available for hepatitis B virus. Interferon-α and its pegylated version offered long-lasting virologic response with restricted effectiveness and frequent adverse effects (Ye and Chen, 2021). NAs are an effective treatment for reducing the levels of HBV-DNA in patients and are generally well tolerated. However, achieving functional cure of HBV, as indicated by HBsAg seroconversion, is rare achieved with NAs (Broquetas and Carrion, 2022). Collectively, development of effective therapeutics for CHB is still in urgent need.

As our understanding of chronic HBV infection deepens, it becomes clear that the primary obstacle to achieving a functional cure for HBV is the high level of peripheral HBsAg, which acts as a brilliant decoy to evade the immune system. During the past few decades, various monotherapies targeting HBsAg through distinct pathways have demonstrated promising but

limited outcomes in both preclinical and clinical studies. Therapeutic vaccine, antibody and siRNA are the most commonly used types of monotherapies for treating CHB. In terms of HBV therapeutic vaccines, a minor decline of HBsAg has been observed in clinical trials of TG1050, BRII-179 and NASVAC (Zoulim et al., 2020; Akbar et al., 2021; Ma et al., 2021). Clinical trials of therapeutic antibodies such as HH-003, BRII-877, and VIR-3434 have been reported to transiently induce HBsAg loss by 1–2 log IU/mL. Similarly, comparable reduction of HBsAg has also been observed in clinical trials of siRNA such as JNJ-3989, arc-521, and VIR-2218 (van den Berg et al., 2020). While all the aforementioned monotherapies have shown inspiring outcomes, achieving the functional cure of HBV remains rare.

In addition to monotherapy, emerging combination strategies have demonstrated remarkable therapeutic efficacy. The effectiveness of therapeutic vaccines has been shown to increase through the knockdown of virus antigen expression *via* siRNA in preclinical studies (Michler et al., 2020). Moreover, effective inhibition of HBV expression has been reported through a combination of HBV targeted therapy and PD-1 immune checkpoint blockade (Zhen et al., 2021). Furthermore, treatment of HBV infection with nucleic acid polymers and peg-IFN has resulted in functional cure in 35% of participants (Bazinet et al., 2021). Thus, the strategic design of various monotherapy combinations may effectively attain functional cure for HBV.

In our preview studies, we reported several HBV therapeutic antibodies that target different domains of HBsAg. Among these mAbs, the E6F6 mAb binds to a linear epitope (aa 119–125 of HBsAg), while the 129G1 mAb recognizes the 'second loop' linear epitope (aa 137–151 of HBsAg; Zhang et al., 2016). Additionally, a bat HBV core antigen derived therapeutic vaccine presenting HBsAg-aa113-135(SEQ13) has been designated as a therapeutic vaccine (Zhang et al., 2020). Administration of all three of these interventions demonstrates substantial HBsAg and HBV-DNA loss in HBV-carrier mouse. Here, to assess the potential synergy effect of HBV therapeutic antibodies with other interventions, we evaluated the extent of HBsAg and HBV-DNA loss through the administration of mouse-originated and humanized HBV therapeutic antibodies in multiple mouse models.

2. Materials and methods

2.1. Mouse

For AAV-HBV mouse model, based on C57BL/6 strain, was developed using rAAV8-1.3HBV (ayw) purchased from Beijing FivePlus Molecular Medicine Institute Co. Ltd. Each mouse was intravenously injected with 2.5×10^{10} vg AAV-HBV. Assessments were conducted 4 weeks after AAV-HBV infection to establish immune tolerance. To facilitate the following assessments, a serum HBsAg titer ranging from 1×10^3–2×10^4 IU/mL was selected. To ensure that each group of AAV-HBV mice had the same baseline level of HBsAg, mice of the same age were divided into groups based on their serum HBsAg titer.

The HBV-transgenic (HBV-Tg) mouse, aged between 10 and 12 weeks, were kindly provided by Pei-Jer Chen (NTU, Taiwan; Wu et al., 2010). To enable the subsequent assessments, a serum HBsAg titer ranging from 1×10^3–2×10^4 IU/mL was selected. To ensure that each group of HBV-tg mice had a consistent baseline level of HBsAg, mice of the same age were divided into groups based on their serum HBsAg titer.

2.2. Antibodies

The 129G1 mAb were produced using hybridoma technology and characterized as previously described (Huang et al., 2012). Babl/c F1 Mice were subjected to intraperitoneal injections of paraffin oil to saturate peritoneal macrophages and prevent phagocytosis of antibody-secreting cells. After a 3-day incubation period, E6F6 hybridoma cells were administered intraperitoneally, and ascites were collected 3 to 7 days thereafter. The collected ascites was then subjected to centrifugation at 12,000 revolutions per minute for a duration of 10 min, followed by a 1:1 blending of the ascites supernatant with saturated ammonium sulfate. The mixture was allowed to precipitate on ice for a duration of 30 min before the precipitate was re-suspended in System A liquid of the Protein A column purification system. Subsequent centrifugation at 12,000 revolutions per minute for 10 min resulted in the discarding of the supernatant. The remaining solution was filtered and applied to a Protein A column for purification. The 162 and rc162 mAb used in this study were provided by our partner, Yangsheng TANG Co., Ltd.

2.3. Vaccines

The CRT3-SEQ13 gene fragment was synthesized by GENEWIZ, Inc. (Suzhou, China), and subsequently cloned into the pTO-T7 expression vector, which had been previously constructed in our lab (Luo et al., 2000). Following transfection of correct plasmids expressing CR-T3-SEQ13 into *Escherichia coli* strain ER2566 (Yang et al., 2005). The transfected ER2566 were cultured in an Erlenmeyer flask at 37°C for 4 h. Subsequently, IPTG was added, and the culture was incubated overnight at 16°C. The resulting precipitation was resuspended in lysis buffer containing 20 mM PB pH 6.0, 150 mM NaCl, and 5 mM EDTA. Sonication was performed for 3–4 min per bottle of bacteria, followed by centrifugation at 25,000 g for 20 min to collect the supernatant. The supernatant was heat-treated at 60°C for 20 min in a water bath, followed by another round of centrifugation at 25,000 g for 20 min to collect the supernatant. Saturated ammonium sulfate was slowly added to the supernatant in a 10:3 ratio (supernatant: ammonium sulfate) while stirring, and the mixture was left at 4°C for 2 h (or overnight). The mixture was then centrifuged, and the supernatant was discarded. The resulting precipitate was dissolved in PBS. If the precipitate did not dissolve after 10 min, DTT was added in a 5 mM concentration gradient up to a maximum of 20 mM. The solution was then filtered through a 0.22um filter and purified through ultracentrifugation using a sucrose density gradient (20, 40, 60, 80%) at 23,000 rpm for 10 h at 4°C. The desired protein was dialyzed in PBS, and the buffer was changed at least three times. The antigens were mixed with alum adjuvant using the protocol previously described (Zhang et al., 2015). The CR-T3-SEQ13 protein and vaccine formulation used in this study were kindly provided by our partner, Xiamen Innovax Biotech Co., Ltd.

To prepare the sample for electron microscopy, the protein was diluted in PBS at a 2x gradient. Negative staining of the protein

solution was performed by placing a drop on a copper grid and staining with 1–2% phosphotungstic acid (PTA) at pH 6.5–7.0 for 5–10 s, followed by drying for observation under a transmission electron microscope.

2.4. Virological indicators

The HBV DNA levels in the mouse serum specimens were measured using a real-time qPCR assay from Premix Ex Taq™ (Takara, Dalian, China). The primer sequences were as follows: 5′-TTTCACCTCTGCCTAATCAT-3′ and 5′-TCAGAAGGCAAAAAAGAGAGTAACTC-3′. The probe sequence was 5′-HexCCTTGGGTGGCTTTGGGGCATGGA-1-3′.

The HBsAg chemiluminescent quantitation kit and HBeAg quantitation ELISA kit were obtained from Beijing Wantai Biological Pharmacy Enterprise Co., Ltd. The mouse serum was diluted at a ratio of 1:1000 using ED11. The chemiluminescence plate was equilibrated to room temperature, and 20 μL of the sample dilution was added. Following this, 100 μL of the sample and 5 standard samples (45, 9, 1.8, 0.36, and 0.072) were added and incubated at 37°C for 1 h. Subsequently, 50 μL of the enzyme-labeled secondary antibody was added and incubated at 37°C for 1 h. The plate was washed five times to remove any excess liquid, and any residual moisture was removed by shaking the plate dry. Finally, 100 μL of the color developing solution (A + B) was added, and the third reading was recorded. The actual IU value of the sample was calculated based on the standard samples.

The anti-SEQ13 and anti-CRT3-SEQ13 titers were detected using indirect ELISA kits developed by Beijing Wantai Biological Pharmacy Enterprise Co., Ltd. The anti-162 mAb titer was detected using indirect ELISA kits developed by Yangsheng TANG Co., Ltd. The recombinant HBsAg protein (CHO cell-derived, Wantai Biological Pharmacy Enterprise Co., Ltd., Beijing, China) or synthesized SEQ13 peptide (Jingju, Xiamen, China) was added at a concentration of 200 ng per well to coat the wells. Nonspecific binding was prevented by blocking with a solution of 2% bovine serum albumin (BSA) and 10% sucrose in phosphate-buffered saline (PBS). A series of sample dilutions ranging from 10 to 10,000 were prepared. During the assay, 100 μL of the specimens were added to the reaction well and incubated at 37°C for 60 min. Antibody titers was detected through horseradish peroxidase (HRP)-conjugated anti-mouse/human pAb (Thermo Scientific, Rockford, United States). Following the reaction of the chromogenic substrate and the stop solution, measure the absorbance of each well at 450 nm and 630 nm. The maximum dilution fold that yielded an OD450 nm- 630 nm value greater than 0.1 was used to calculate the antibody titer as follows: titer = (OD450 nm- 630 nm) /0.1 × dilution fold.

2.5. Quantification and statistical analysis

Statistical analyses were conducted using Prism 8 software (GraphPad). The bars rep-resent the mean. For datasets containing more than two groups, both normality and homogeneity of variance tests were performed. If these tests were passed, an ordinary one-way ANOVA with Tukey's post-hoc test was performed to compare the means of each group. If only the normality test was passed, Brown-Forsythe and Welch ANOVA tests were used, followed by the Kruskal–Wallis test and Dunnett T3 test for post-hoc comparisons. If neither test was passed, the Kruskal–Wallis test and Dunn's method were employed to compare the mean rank of each group. For datasets containing only two groups, an unpaired t-test was performed if both normality and homogeneity of variance tests were passed. If only the normality test was passed, an unpaired t-test with Welch's correction was used. If neither test was passed, the Mann–Whitney test was performed to compare the mean rank of each group.

3. Results

3.1. Manufacturing and characterization of therapeutic agents for hepatitis B virus

The current investigation focuses on exploring the potential of the therapeutic vaccine CRT3-SEQ13 and therapeutic anti-HBV antibodies 129G1, E6F6, and 162 for managing hepatitis B virus (HBV) infection. These agents are promising candidates for treating chronic HBV infection, as they have exhibited significant inhibitory effects on HBV in various HBV-carrying mouse models and have induced high levels of anti-HBV humoral immune response (Zhang et al., 2016, 2020).

CRT3-SEQ13 exists as polymeric particles with 180 or 240 copies in PBS buffer. The protein purity of the four proteins was assessed using SDS-PAGE (Figure 1A), and their degree of polymerization was evaluated using HPLC (Figure 1B). The results showed that the protein purity was optimal, and the degree of polymerization met the expected standard. Since CRT3-SEQ13 is a virus-like particle (VLP), particle formation was assessed by transmission electron microscopy negative staining, and the results confirmed the expected particle formation (Figures 1C,D). To verify the immunogenicity of CRT3-SEQ13, wildtype C57BL/6 mice were administered intramuscularly. The serum anti-immunogen assessment demonstrated that two injections of CRT3-SEQ13 on day 0 and day 14 induced potent and sustained humoral response (Figures 1E,F). The HBV therapeutic antibodies, 129G1, and E6F6, were produced and characterized as reported (Zhang et al., 2016).

3.2. Administration of therapeutic antibodies over the long-term promotes functional cure

In our previous research on HBV therapeutic antibodies, we demonstrated that administration of antibodies can lead to prolonged suppression of HBV. However, it is unclear whether long-term antibody administration can promote functional cure of HBV.

To address this question, we assessed short-term (Figure 2A) and long-term (Figure 2C) therapeutic antibody administration in an AAV-HBV mouse model. Short-term administration of E6F6 maintained mouse serum HBsAg at baseline levels during treatment, but HBsAg levels rebounded rapidly 12 days after the end of treatment and returned to baseline levels in 30 days (Figure 2B).

In contrast, long-term therapeutic antibody administration was highly effective, with sustained suppression of serum HBsAg over a monitoring period of 171 days (Figure 2D). The absence of rebound in serum HBsAg levels for 71 days after treatment suggests that these AAV-HBV mice may have achieved functional cure.

These results demonstrate that long-term administration of therapeutic antibodies can effectively eradicate HBV infection, while

10.3389/fmicb.2023.1173061

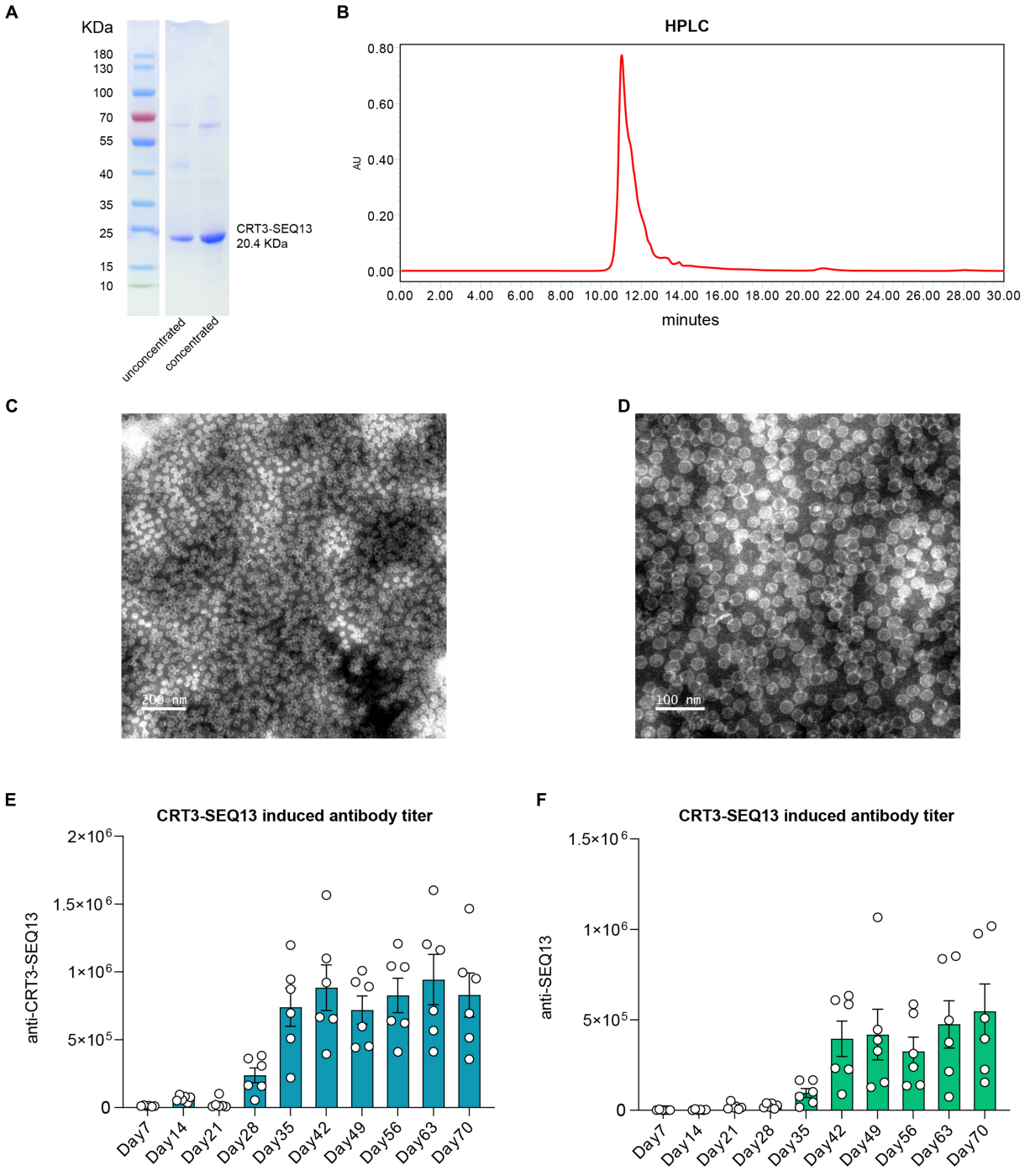

FIGURE 1
Characteristics of HBV therapeutic vaccine CRT3-SEQ13. **(A)** Western blot shown the purity and molecular weight of CRT3-SEQ13. **(B)** High performance liquid chromatography demonstrated the purity of CRT3-SEQ13. Electron microscope photo of CRT3-SEQ13 at **(C)** 200nm and **(D)** 100nm scale. 12μg CRT3-SEQ13 was administrated at day 0, and day14 intramuscularly, **(E)** anti-CRT3-SEQ13, and **(F)** anti-SEQ13 titer were shown in wildtype mouse serum.

short-term administration is insufficient to achieve eradication. These findings are promising for the treatment of HBV in preclinical studies. However, frequent antibody injections may pose challenges for patient compliance during clinical practice. Therefore, multiple HBV combination interventions have been evaluated to facilitate HBV eradication and improve patient compliance.

3.3. Sustained suppression of HBsAg ameliorates therapeutic vaccine efficacy in central tolerance mouse model

In order to assess the potential synergy effect of HBV therapeutic vaccine and antibody, we conducted a sequential administration of

10.3389/fmicb.2023.1173061

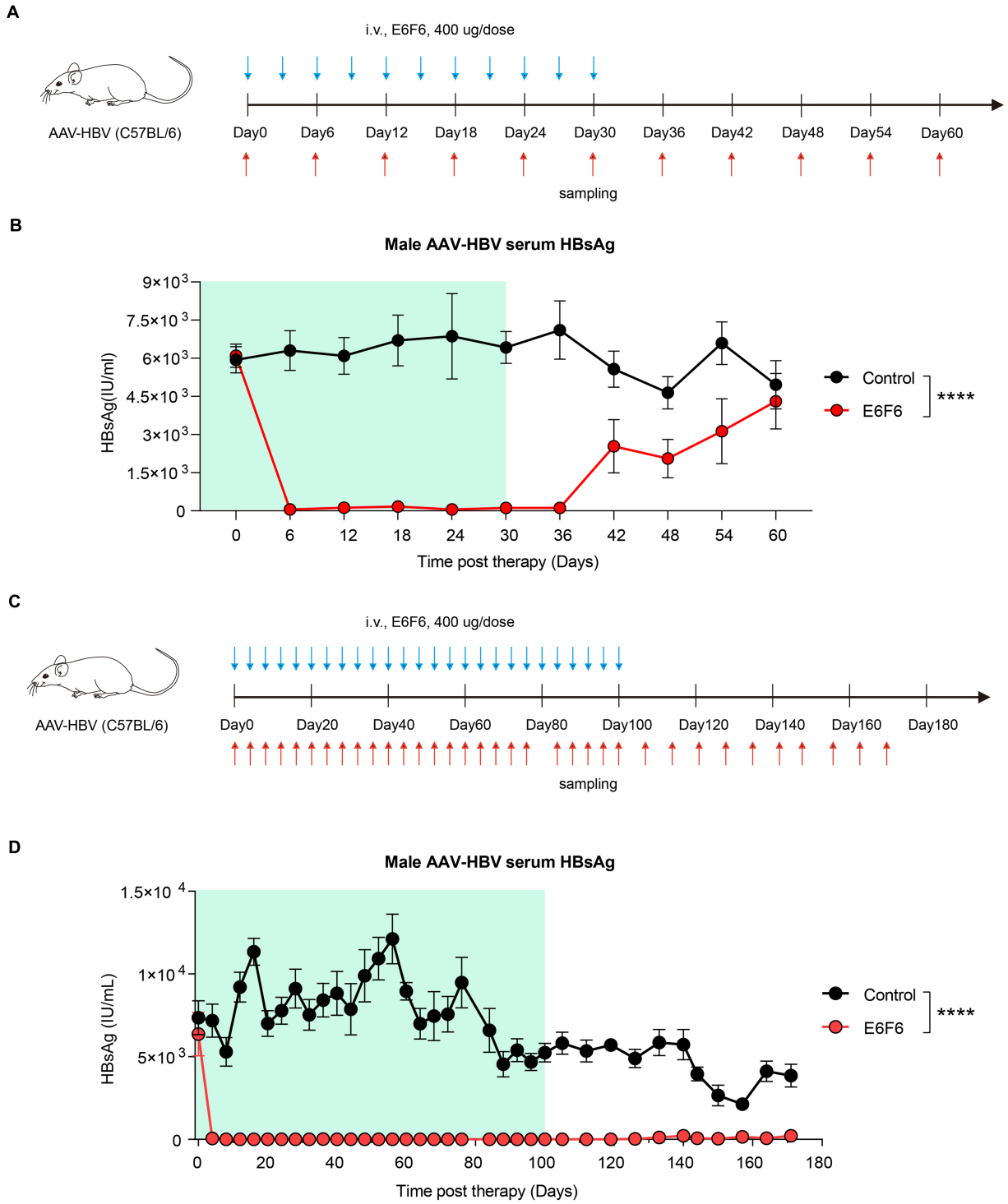

FIGURE 2
Sustained E6F6 administration eradicate HBV infection efficiently. **(A)** AAV-HBV mice (n=8/group; HBsAg: 1×10^3–2×10^4IU/mL) were administrated with E6F6 intravenously as indicated by blue arrows, the time of blood sampling was indicated by red arrows. Vehicle was injected intravenously as control. Schematic representation of the short-term E6F6 therapy procedure. **(B)** Time kinetic of HBsAg in male AAV-HBV mice during short-term E6F6 administration. **(C)** AAV-HBV mice (n=4/group; HBsAg: 1×10^3–2×10^4IU/mL) were administrated with E6F6 intravenously. Schematic representation of the long-term E6F6 therapy procedure. **(D)** Time kinetic of HBsAg in male AAV-HBV mice during long-term E6F6 administration. Results were representative of three independent experiments. Statistical analyses were performed between red line and black line. *p<0.05; **p<0.01; ***p<0.001; ****p<0.0001.

CRT3-SEQ13 and 129G1 in HBV-transgenic (HBV-tg) mouse model. HBV-tg mice were carefully selected based on their serum HBsAg levels, ranging from 1×10^3IU/mL to 2×10^4IU/mL, which corresponds to the typical HBsAg titer observed in the majority of CHB patients. To ensure a thorough evaluation, the mice were subjected to a rigorous injection schedule: 17 injections of 129G1

monoclonal antibody at three-day intervals over a 48-day period, as depicted in Figure 3A, followed by six administrations of CRT3-SEQ13 on days 30, 44, 51, 58, 65, and 72. To account for the gender-related nature of HBV infection, we used both male and female HBV-tg mice to assess the therapeutic potential of this combination therapy.

Remarkably, in the female HBV-tg mouse, circulating HBsAg levels were maintained below 10 IU/mL following 129G1 administration in both the monotherapy and combination therapy groups (Figures 3B,E). As anticipated, serum HBsAg titers returned to baseline level after 129G1 was discontinued in 129G1 monotherapy group. It is noteworthy that the administration of CRT3-SEQ13 monotherapy resulted in a significant reduction of serum HBsAg levels from 5,500 IU/mL to 300 IU/mL in the female HBV-tg mouse model (Figure 3B). While both CRT3-SEQ13 monotherapy and combination therapy produced similar results in suppressing serum HBsAg at the endpoint of assessment, the combination therapy displayed superior efficacy in maintaining serum HBsAg levels throughout the 107-day study period. Moreover, there were no significant differences observed in epitope-specific (SEQ13) and vaccine-specific (CRT3-SEQ13) antibody levels between the CRT3-SEQ13 monotherapy group and combination therapy group in the female HBV-tg mouse (Figures 3C,D).

In male HBV-tg mouse, the administration of CRT3-SEQ13 monotherapy led to a significant decrease in serum HBsAg levels from 17,000 IU/mL to 6,000 IU/mL (Figure 3E). Furthermore, the combination therapy group achieved a much more substantial reduction in serum HBsAg levels, plummeting from 17,000 IU/mL to 1,200 IU/mL in the male HBV-tg mouse. This impressive decline was made possible by the efficient facilitation of HBsAg clearance through the administration of 129G1 mAb in combination therapy. Still, epitope-specific (SEQ13) and vaccine-specific (CRT3-SEQ13) antibodies did not show significant difference in CRT3-SEQ13 monotherapy group and combination therapy group in male HBV-tg mouse (Figures 3F,G).

These results indicate that HBV therapeutic antibody monotherapy is insufficient in sustaining the restraint of circulating HBsAg in a high HBsAg load scenario, but the administration of 129G1 monoclonal antibody over a period of 48 days significantly improves the efficacy of CRT3-SEQ13.

3.4. Prolonged repression of HBsAg promotes therapeutic vaccine efficacy in peripheral tolerance mouse model

In order to further validate the synergistic effect of HBV therapeutic vaccine and antibody, CRT3-SEQ13 and 129G1 were administrated sequentially in AAV-HBV mouse model (Figure 4A). The results showed that circulating HBsAg level in AAV-HBV was maintained below 10 IU/mL in both monotherapy and combination therapy groups upon 129G1 administration (Figure 4B). However, it was observed that serum HBsAg levels in the 129G1 monotherapy group quickly rebounded to baseline levels following the discontinuation of the 129G1 treatment on day 48. In contrast, the CRT3-SEQ13 monotherapy group did not display a significant decline in serum HBsAg titer in the AAV-HBV mouse model when compared to the control group. Interestingly, the combination therapy group exhibited a notable reduction in HBsAg levels, remaining under 2,000 IU/mL upon CRT3-SEQ13 administration, with two out of five mice exhibiting HBsAg levels under 100 IU/mL at the endpoint of assessment. Moreover, the immunogen-specific antibody titers in the AAV-HBV mouse model were found to rise rapidly within 7 days of CRT3-SEQ13 administration. Besides, both epitope-specific (SEQ13) and vaccine-specific (CRT3-SEQ13) antibody titers did not exhibit any significant differences between the CRT3-SEQ13 monotherapy group and combination therapy group (Figures 4C,D).

Collectively, these results demonstrate that the administration of 129G1 enhances the efficacy of CRT3-SEQ13 in the peripheral tolerance mouse model, showcasing the potential of this combination therapy in treating chronic hepatitis B infections.

3.5. Preclinical evaluation of humanized HBV therapeutic antibody

In order to fully explore the therapeutic potential of therapeutic antibody and entecavir (ETV), we conducted a series of preclinical experiments using both the AAV-HBV and HBV-tg mouse models. A single shot of humanized 162 mAb was administrated, experimental design is shown in Figure 5A. Specifically, different dosages of 162 mAb were administered, including 1 mg/kg (1mpk), 5 mg/kg (5mpk), and 30 mg/kg (30mpk), along with Entecavir (ETV) which was given *via* drinking to assess the synergy potential of 162 mAb and ETV. We also included a vehicle group which received the solvent of 162 mAb as control.

In the AAV-HBV mouse model, we observed a remarkable decrease in serum HBsAg levels from 6,600 IU/mL to 700 IU/mL, 300 IU/mL and 100 IU/mL in the 1mpk group, 5 mpk group and 30 mpk group, respectively, on day 2 post 162 mAb administration (Figure 5B). Similarly, in the HBV-tg mouse model, we observed a significant reduction in serum HBsAg levels from 4,100 IU/mL to 1,500 IU/mL, 500 IU/mL and 200 IU/mL in the 1mpk group, 5 mpk group and 30 mpk group, respectively, on day 2 post 162 mAb administration (Figure 5C). In both AAV-HBV and HBV-tg mouse model, ETV monotherapy did not affect HBsAg level, as expected.

We also assessed the HBV-DNA level of both the AAV-HBV and HBV-tg mouse models, as ETV mainly interferes with HBV reverse transcription. In the AAV-HBV mouse model, we observed a significant reduction in serum HBV-DNA levels from 4×10^7 IU/mL to 1.8×10^5 IU/mL, 3.4×10^4 IU/mL, and 5.8×10^4 IU/mL in the 1mpk group, 5 mpk group, and 30 mpk group, respectively, on day 2 post 162 mAb administration (Figure 5D). Similarly, in the HBV-tg mouse model, we observed a significant reduction in serum HBV-DNA levels from 4.1×10^6 IU/mL to 2.3×10^6 IU/mL, 1×10^6 IU/mL and 6.6×10^5 IU/mL in the 1mpk group, 5 mpk group and 30 mpk group, respectively, on day 2 post 162 mAb administration (Figure 5E). ETV monotherapy was effective in reducing serum HBV-DNA levels in both models, and the combination therapy of 162 mAb and ETV did not interfere with the therapeutic effect of each other.

Taken together, our findings suggest that the humanized 162 mAb demonstrated a promising therapeutic potential in both AAV-HBV and HBV-tg mouse models, and the combination therapy of 162 mAb and ETV might work in synergy to overcome the limitations of both monotherapies.

10.3389/fmicb.2023.1173061

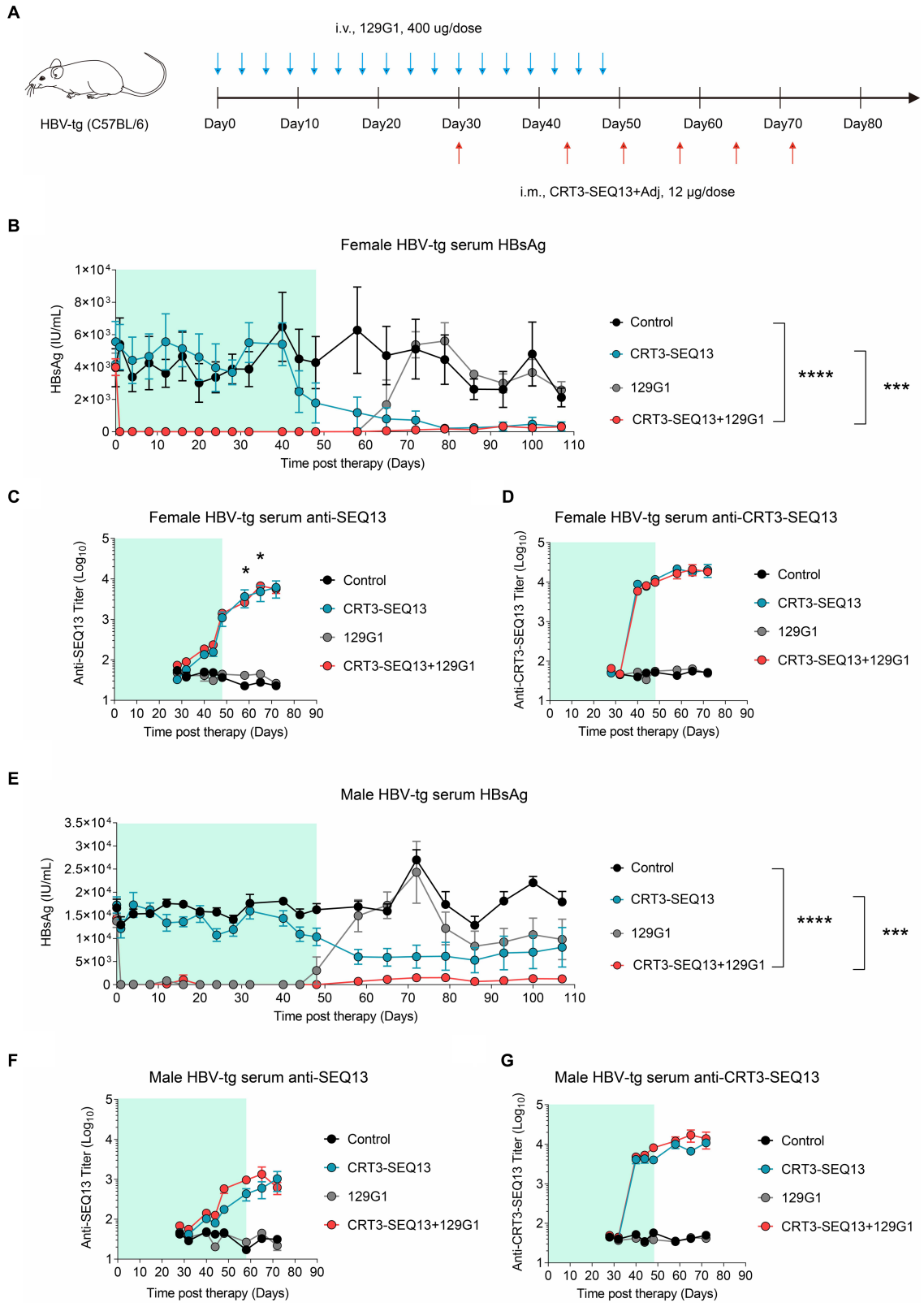

FIGURE 3
The combination of therapeutic antibody and vaccine breaks central immune tolerance in HBV-tg. **(A–G)** Central tolerance, HBV-transgenic mice (*n*=4/group; HBsAg: $1x10^3$–$2x10^4$IU/mL) were administrated with 400μg 129G1 intravenously every 3days as indicated by blue arrows, 12μg CRT3-SEQ13 was administrated at day 30, day 44, day 51, day 58, day 65, and day 72 intramuscularly as indicated by red arrows. Start of vaccination was day30. PBS was injected intravenously as control. **(A)** Schematic representation of the combination therapy procedure used for **(B–G)**. **(B–D)** Time kinetic of virological indicators in male HBV-tg mice. Serum levels of **(B)** HBsAg, **(C)** An-ti-SEQ13 antibodies, and **(D)** Anti-CRT3-SEQ13 antibodies. **(E–G)** Time kinetic of virological indicators in female HBV-tg mice. Serum levels of **(E)** HBsAg, **(F)** Anti-SEQ13 antibodies, and **(G)** Anti-CRT3-SEQ13 antibodies. Results were representative of three independent experiments. Statistical analyses were performed between red line and black line. *p<0.05; **p<0.01; ***p<0.001; ****p<0.0001.

10.3389/fmicb.2023.1173061

3.6. Maximum suppression of HBsAg achieved through reverse chimeric HBV therapeutic antibody administration weekly

To further investigate the pharmacodynamics (PD) and pharmacokinetics (PK) of 162 mAb in mouse, we designed a reverse chimeric 162(rc162) mAb, which was composed of mouse Fc and humanized Fab. We then administered four doses of rc162 mAb to AAV-HBV mouse models to assess its ability to retain serum HBsAg titer over time (Figure 6A). The results showed that serum HBsAg was significantly reduced from 4,500 IU/mL to 50 IU/mL, 20 IU/mL and 10 IU/mL in the 1mpk, 5 mpk, and 30 mpk groups, respectively, on day 2 post rc162 mAb administration (Figure 6B). Furthermore, the administration of rc162 mAb also led to a reduction in serum HBV-DNA levels from 1.4×10^7 IU/mL to 3.5×10^5 IU/mL, 3×10^4 IU/mL, and 3×10^4 IU/mL in the 1mpk, 5 mpk, and 30 mpk groups, respectively (Figure 6C). Besides, serum HBeAg levels did not show any significant difference after four doses of rc162 mAb administration over 29 days (Figure 6D). In terms of pharmacokinetics, the analysis of rc162 mAb showed a consistent antibody titer during the 29-day time course, which was almost the opposite trend of the HBsAg titer (Figure 6E).

All in all, these findings suggest that weekly administration of rc162 mAb can persistently suppress serum HBsAg and HBV-DNA, which makes the combination therapy of rc162 mAb and therapeutic vaccine a promising future prospect.

4. Discussion

Numerous preclinical and clinical trials for CHB indicated that monotherapy alone may be insufficient to achieve functional cure effectively. Previews studies have shown that several therapeutic

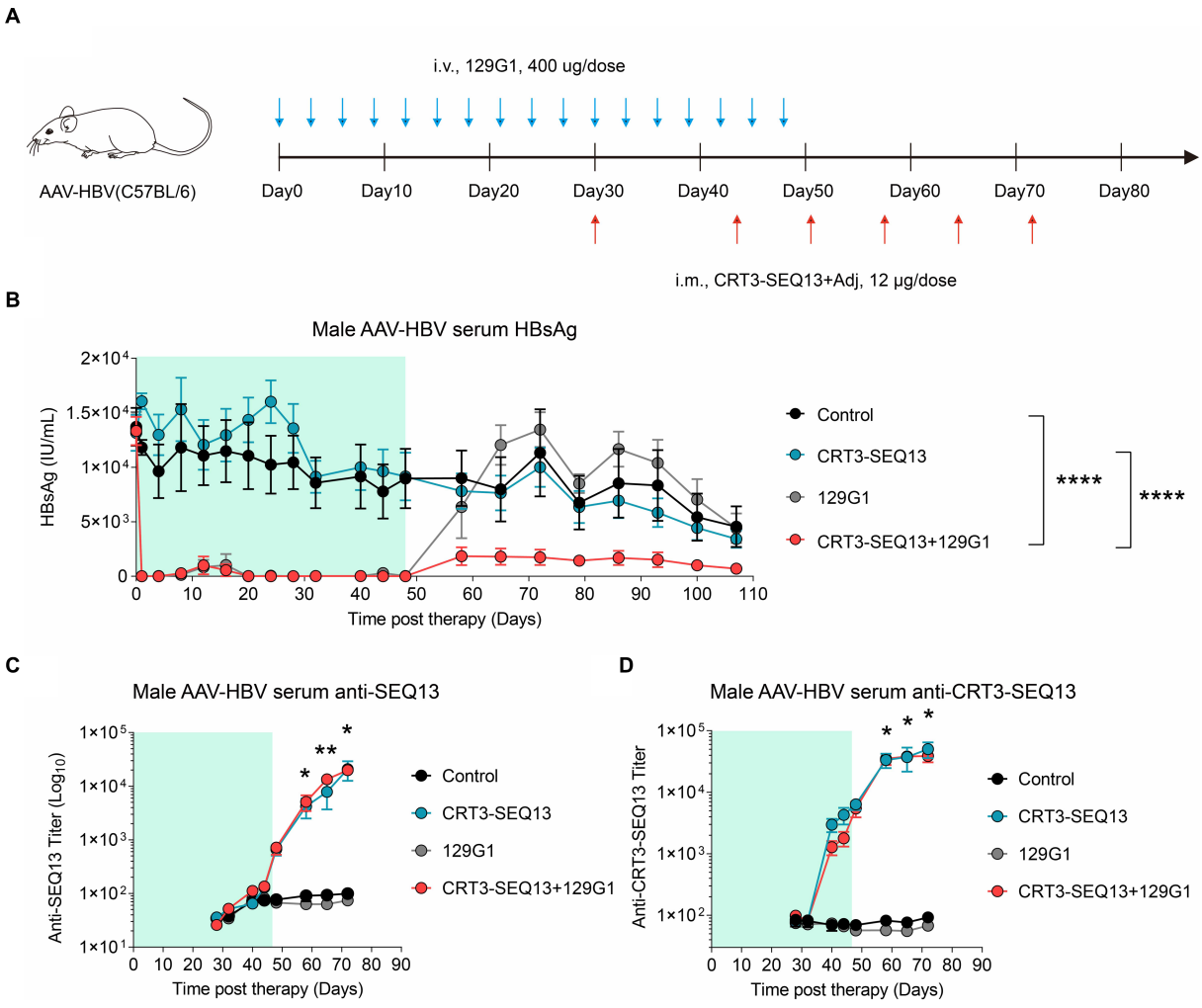

FIGURE 4
The combination of therapeutic antibody and vaccine facilitate serum HBsAg clearance in AAV-HBV **(A–D)** Peripheral tolerance, AAV-HBV mice (n=5/group; HBsAg: 1×10^3–2×10^4IU/mL) were administrated with 400μg 129G1 intravenously every 3days as indicated by blue arrows, 12μg CRT3-SEQ13 was administrated intramuscularly at day 30, day 44, day 51, day 58, day 65, and day 72 as indicated by red arrows. Start of vaccination was day 30. PBS was injected intravenously as control. **(A)** Schematic representation of the combination therapy procedure used for **(B–D)**. **(B-D)** Time kinetic of virological indicators in AAV-HBV. Serum levels of **(B)** HBsAg, **(C)** anti-SEQ13 antibodies and **(D)** anti-CRT3-SEQ13 antibodies. Results were representative of three independent experiments. Statistical analyses were performed between red line and black line. *p<0.05; **p<0.01; ***p<0.001; ****p<0.0001.

10.3389/fmicb.2023.1173061

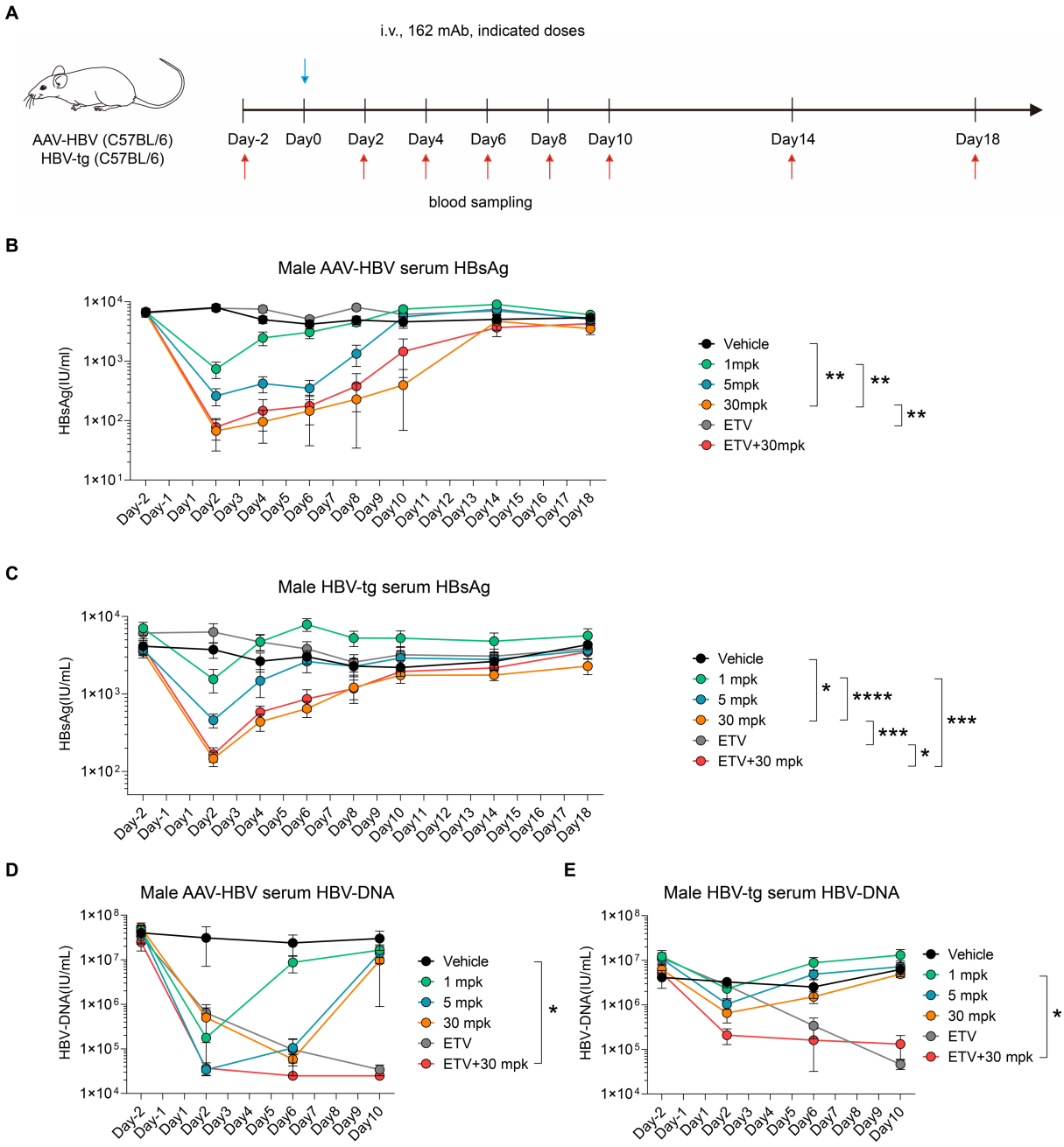

FIGURE 5
Humanized therapeutic antibody eradicate HBV in synergistic combination with ETV. **(A–E)** AAV-HBV and HBV-transgenic mice (n=8/group; HBsAg: 1×10^3–2×10^4IU/mL) were administrated with 162 intravenously as indicated by blue arrows, the time of blood sampling was indicated by red arrows. Vehicle was injected intravenously as control. **(A)** Schematic representation of the combination therapy procedure used for **(B–E)**. **(B,D)** Time kinetic of virological indicators in male AAV-HBV mice. Serum levels of **(B)** HBsAg, **(D)** HBV-DNA. **(C,E)** Time kinetic of virological indicators in male HBV-tg mice. Serum levels of **(C)** HBsAg, **(E)** HBV-DNA. Results were representative of three independent experiments. *p<0.05; **p<0.01; ***p<0.001; ****p<0.0001.

antibodies against HBV results in significant decline in HBsAg levels upon administration. However, the suppression effect of HBsAg cannot be sustained as antibody administration stops. Therefore, it is crucial to reinvigorate host adaptive immunity to achieve functional cure effectively. Base on this theory, we have designed a combination strategy of HBV therapeutic antibody and vaccine to facilitate HBsAg clearance. The 129G1 mAb, which targets HBsAg, was administrated first to eliminate HBV-expressing cells and control circulating HBsAg. After 30 days of passive immunization, CRT3-SEQ13 was introduced to induce host active immunity. In male mouse model with high viremia and high antigenemia, our combination therapy demonstrated striking therapeutic efficacy compared to monotherapy. These promising results have given us the confidence to assess HBV therapeutic antibody in clinical trials. In order to do so, humanized and reverse chimeric forms of E6F6 mAb were generated and evaluated in HBV carrier mouse. Similar therapeutic effects were verified through pharmacodynamics and pharmacokinetics analysis. A randomized, double-blind, placebo-controlled phase I clinical study

10.3389/fmicb.2023.1173061

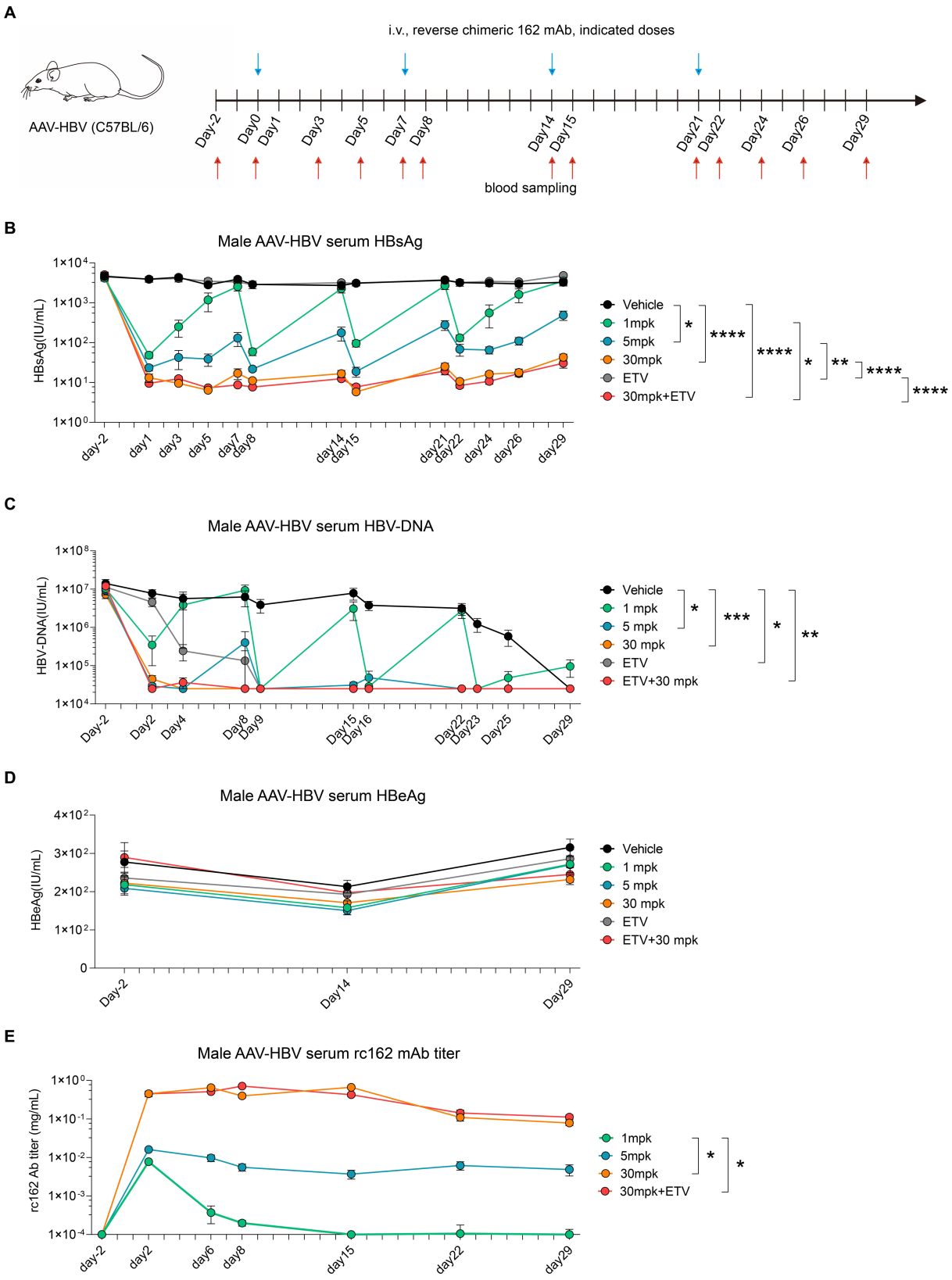

FIGURE 6
Sequential administration of reverse chimeric HBV therapeutic antibody suppresses HBsAg persistently **(A–E)** AAV-HBV mice (n=8/group; HBsAg: 1×10^3–2×10^4IU/mL) were administrated with rc162 mAb intravenously every 7days as indicated by blue arrows, the time of blood sampling was indicated by red arrows. Vehicle was injected intravenously as control. **(A)** Schematic representation of the combination therapy procedure used for **(B–E)**. **(B, D)** Time kinetic of virological indicators in male AAV-HBV mice. Serum levels of **(B)** HBsAg, **(C)** HBV-DNA, **(D)** HBeAg, **(E)** 162 mAb. Results were representative of three independent experiments. *p<0.05; **p<0.01; ***p<0.001; ****p<0.0001.

to evaluate the safety, tolerability, pharmacokinetics of 162 mAb with a single ascending dose in healthy adult subjects is currently active in Australia (NCT05310487). All in all, we demonstrated that prolonged administration of an HBsAg targeting antibody promotes therapeutic vaccine efficacy and is well-tolerated in human.

To assess the synergy effect of HBV therapeutic vaccine and antibody in the HBV carrier mouse, we evaluated the combination of CRT3-SEQ13 and 129G1 mAb due to the fact that E6F6 mAb directly binds CRT3-SEQ13. We assessed multiple combination strategies of E6F6 mAb and CRT3-SEQ13 in our pilot experiment. However, neither the administration of E6F6 mAb first in combination with CRT3-SEQ13 nor the administration of both E6F6 mAb and CRT3-SEQ13 at the same time showed a synergistic effect. Based on this observation, we selected the 129G1 mAb, which recognized HBsAg but did not bind to CRT3-SEQ13. In the second part, the humanized 162 mAb was constructed using the Fab of E6F6 mAb, as the E6F6 mAb demonstrated the most striking therapeutic effect among all candidates (Zhang et al., 2016). Moreover, the E6F6 mAb recognizes an evolutionarily conserved epitope (GPCK(R)TCT) of HBsAg and only forms a smaller immune complex. This unique binding characteristic of E6F6 mAb is important for HBsAg clearance through opsonophagocytosis *in vivo*.

In regard to the induced vaccine-specific antibody titer by CRT3-SEQ13, little difference was detected regardless of the administration of 129G1 mAb. These results may be perplexing as serum HBsAg titer did make a difference. Two possible explanations exist for this issue: First, the administration of the HBsAg therapeutic antibody is capable of eradicating HBV-expressing cells as we have previously demonstrated (Zhang et al., 2016). Second, we hypothesized that the quality of antibodies induced by CRT3-SEQ13 or the immune suppressive environment might be important for HBsAg clearance.

During the preclinical experiments of the humanized therapeutic antibody 162 mAb, only one shot was administrated due to host rejection. In our pilot experiments, significant anti-drug antibodies were developed when multiple shots of 162 mAb were administered to the subjects. The production of anti-drug antibodies might neutralize the therapeutic efficacy of 162 mAb and induce health problems in mice. To circumvent this issue, rc162 mAb consisting of a mouse Fc and humanized E6F6 Fab. Without the antigenicity from human Fc, rc162 can be administrated at multiple times without causing side effects. Furthermore, sustained HBsAg decline can be achieved through weekly administration of rc162 mAb.

As a sexually related disease, many studies suggest that males may exhibit certain symptoms of hepatitis B virus (HBV) infection more frequently than females. Specifically, males may exhibit higher HBsAg levels, more severe liver damage, cirrhosis, and a higher incidence of liver cancer resulting from chronic HBV infection when compared to females. This may be attributed to the fact that male hormones (such as testosterone) can contribute to liver damage. Sexual differences have also been observed in mouse models, with female mice displaying lower levels of HBsAg and HBV-DNA, making them more responsive to treatment. This explains why therapeutic vaccine administration alone is capable of eradicating HBV in female mice. Most of the assessments in this manuscript were conducted on male mouse models, which is a more stringent model, intended to emphasize the differences between the treatments.

In this study, we have evaluated the potential for synergistic effects of therapeutic antibody, therapeutic vaccine, and nucleoside analogs. In addition to the interventions mentioned above, several other HBV interventions could be considered as potential candidates in combination with E6F6 or CRT3-SEQ13. These include IFN-a (interferon-alpha), another drug marketed for the treatment of HBV, aside from NAs. Although the synergy effect of IFN-a and E6F6 or CRT3-SEQ13 has been assessed, little to no synergy effect has been observed. Another intervention is siRNA (small interfering RNA), which targets and degrades HBV mRNA. A combination strategy of siRNA administration followed by treatment with E6F6 or CRT3-SEQ13 demonstrated robust therapeutic efficacy. However, due to non-disclosure agreements, we are unable to present the data at this time. In summary, we believe that our therapeutic antibody and vaccine, in combination with other targeted therapies, may demonstrate similar synergy effects.

In the present study, we opted to conduct a 5-week monitoring period for assessing the therapeutic effect of E6F6 and CRT3-SEQ13 based on our pilot experiments. Previous studies have reported that the duration of therapeutic effect induced by these antibodies may range from 2 to 10 months (Zhang et al., 2020). However, in cases where the HBV infection is not completely eliminated, a rapid rebound of mouse serum HBsAg has been observed after the end of treatment. Considering the practical constraints of time and resources, we deemed it appropriate to limit the monitoring period to 5 weeks post-treatment. While we did not present data to support sustained loss of HBsAg for several months (3 to 6 months) after the end of treatment, the fact that CRT3-SEQ13 demonstrated sustained therapeutic effect for at least 40 weeks (Zhang et al., 2020) leads us to speculate that this combination therapy may show a similar sustained effect.

In conclusion, our data suggest that 162 mAb is an outstanding candidate for the treatment of CHB in combination with therapeutic antibody or nucleos(t)ide analogs. Our findings provide new insights into the design of a therapeutic strategy against persistent viral infection based on combination therapy of antibody and vaccine. With numerous promising HBV monotherapies currently under development, combining other anti-HBV candidates with 162 mAb may further facilitate the achievement of the global hepatitis elimination targets under the Sustainable Development Agenda 2030.

Data availability statement

The original contributions presented in the study are included in the article/Supplementary material, further inquiries can be directed to the corresponding author.

Ethics statement

The animal study was reviewed and approved by Ethics Committee of Xiamen University 32,170,943.

Author contributions

RQ: conceptualization, investigation, and writing—original draft preparation. JC: methodology, data curation, and funding acquisition. YW (Yangtao Wu): resources and visualization. XL, LZ, and RF: validation. JH: software. FC: formal analysis. YW (Yingbin Wang): project administration. TZ: conceptualization, funding acquisition. NX: supervision and funding acquisition. QY: writing—review and editing. All authors contributed to the article and approved the submitted version.

Funding

This research was funded by National Natural Science Foundation of China grants 32170943 (to TZ), 82102379 (to JC), and 31730029 (to NX); Natural Science Foundation of Fujian Province 2020J06007 (to TZ); Fujian provincial health technology project 2021QNB025 (to JC, suported by Xiamen Municipal Health Commission); and Xiamen Youth Innovation Fund Project 3502Z20206060 (to TZ).

Conflict of interest

The authors declare that the research was conducted in the absence of any commercial or financial relationships that could be construed as a potential conflict of interest.

Publisher's note

Supplementary material

The Supplementary material for this article can be found online at: https://www.frontiersin.org/articles/10.3389/fmicb.2023.1173061/full#supplementary-material

References

Akbar, S. M. F., Al Mahtab, M., Aguilar, J. C., Yoshida, O., Penton, E., Gerardo, G. N., et al. (2021). Sustained antiviral and liver protection by a nasal therapeutic vaccine (NASVAC, containing both HBsAg and HBcAg) in patients with chronic hepatitis B: 2-year follow-up of phase III clinical trial. *Pathogens* 10:1440. doi: 10.3390/pathogens10111440

Bazinet, M., Pantea, V., Placinta, G., Moscalu, I., Cebotarescu, V., Cojuhari, L., et al. (2021). Benefit of transaminase elevations in establishing functional cure of HBV infection during nap-based combination therapy. *J. Viral Hepat.* 28, 817–825. doi: 10.1111/jvh.13483

Blumberg, B. S., Alter, H. J., and Visnich, S. (1965). A "New" Antigen in Leukemia Sera. *JAMA* 191, 541–546. doi: 10.1001/jama.1965.03080070025007

Broquetas, T., and Carrion, J. A. (2022). Current perspectives on Nucleos(t)ide analogue therapy for the long-term treatment of hepatitis B virus. *Hepat. Med.* 14, 87–100. doi: 10.2147/HMER.S291976

Huang, C. H., Yuan, Q., Chen, P. J., Zhang, Y. L., Chen, C. R., Zheng, Q. B., et al. (2012). Influence of mutations in hepatitis B virus surface protein on viral antigenicity and phenotype in occult HBV strains from blood donors. *J. Hepatol.* 57, 720–729. doi: 10.1016/j.jhep.2012.05.009

Jeng, W. J., Papatheodoridis, G. V., and Lok, A. S. F. (2023). Hepatitis B. *Lancet* 401, 1039–1052. doi: 10.1016/S0140-6736(22)01468-4

Luo, W. X., Zhang, J., Yang, H. J., Li, S. W., Xie, X. Y., Pang, S. Q., et al. (2000). Construction and application of an *Escherichia coli* high effective expression vector with an enhancer. *Sheng Wu Gong Cheng Xue Bao* 16, 578–581.

Ma, H., Lim, T. H., Leerapun, A., Weltman, M., Jia, J., Lim, Y. S., et al. (2021). Therapeutic vaccine BRII-179 restores HBV-specific immune responses in patients with chronic HBV in a phase Ib/IIa study. *JHEP Rep.* 3:100361. doi: 10.1016/j.jhepr.2021.100361

Michler, T., Kosinska, A. D., Festag, J., Bunse, T., Su, J., Ringelhan, M., et al. (2020). Knockdown of virus antigen expression increases therapeutic vaccine efficacy in high-titer hepatitis B virus carrier mice. *Gastroenterology* 158:e1769, 1762–1775.e9. doi: 10.1053/j.gastro.2020.01.032

van den Berg, F., Limani, S. W., Mnyandu, N., Maepa, M. B., Ely, A., and Arbuthnot, P. (2020). Advances with RNAi-based therapy for hepatitis B virus infection. *Viruses* 12:851. doi: 10.3390/v12080851

Wu, M. H., Ma, W. L., Hsu, C. L., Chen, Y. L., Ou, J. H., Ryan, C. K., et al. (2010). Androgen receptor promotes hepatitis B virus-induced hepatocarcinogenesis through modulation of hepatitis B virus RNA transcription. *Sci. Transl. Med.* 2:32ra35. doi: 10.1126/scitranslmed.3001143

Yang, H. J., Chen, M., Cheng, T., He, S. Z., Li, S. W., Guan, B. Q., et al. (2005). Expression and immunoactivity of chimeric particulate antigens of receptor binding site-core antigen of hepatitis B virus. *World J. Gastroenterol.* 11, 492–497. doi: 10.3748/wjg.v11.i4.492

Ye, J., and Chen, J. (2021). Interferon and hepatitis B: current and future perspectives. *Front. Immunol.* 12:733364. doi: 10.3389/fimmu.2021.733364

Zhang, T. Y., Guo, X. R., Wu, Y. T., Kang, X. Z., Zheng, Q. B., Qi, R. Y., et al. (2020). A unique B cell epitope-based particulate vaccine shows effective suppression of hepatitis B surface antigen in mice. *Gut* 69, 343–354. doi: 10.1136/gutjnl-2018-317725

Zhang, Y., Li, M., Yang, F., Li, Y., Zheng, Z., Zhang, X., et al. (2015). Comparable quality attributes of hepatitis E vaccine antigen with and without adjuvant adsorption-dissolution treatment. *Hum. Vaccin. Immunother.* 11, 1129–1139. doi: 10.1080/21645515.2015.1009343

Zhang, T. Y., Yuan, Q., Zhao, J. H., Zhang, Y. L., Yuan, L. Z., Lan, Y., et al. (2016). Prolonged suppression of HBV in mice by a novel antibody that targets a unique epitope on hepatitis B surface antigen. *Gut* 65, 658–671. doi: 10.1136/gutjnl-2014-308964

Zhen, S., Qiang, R., Lu, J., Tuo, X., Yang, X., and Li, X. (2021). Enhanced antiviral benefit of combination therapy with anti-HBV and anti-PD1 gRNA/cas9 produces a synergistic antiviral effect in HBV infection. *Mol. Immunol.* 130, 7–13. doi: 10.1016/j.molimm.2020.12.004

Zoulim, F., Fournier, C., Habersetzer, F., Sprinzl, M., Pol, S., Coffin, C. S., et al. (2020). Safety and immunogenicity of the therapeutic vaccine TG1050 in chronic hepatitis B patients: a phase 1b placebo-controlled trial. *Hum. Vaccin. Immunother.* 16, 388–399. doi: 10.1080/21645515.2019.1651141

frontiers | Frontiers in Microbiology

TYPE Original Research
PUBLISHED 29 August 2023
DOI 10.3389/fmicb.2023.1206951

OPEN ACCESS

EDITED BY
Franck Touret,
Aix-Marseille Université, France

REVIEWED BY
Saumya Anang,
Dana–Farber Cancer Institute, United States
Ashley N. Brown,
University of Florida, United States

*CORRESPONDENCE
M. Gabriella Santoro
✉ santoro@uniroma2.it

†These authors have contributed equally to this work and share first authorship

RECEIVED 16 April 2023
ACCEPTED 07 August 2023
PUBLISHED 29 August 2023

CITATION
Piacentini S, Riccio A, Santopolo S, Pauciullo S, La Frazia S, Rossi A, Rossignol J-F and Santoro MG (2023) The FDA-approved drug nitazoxanide is a potent inhibitor of human seasonal coronaviruses acting at postentry level: effect on the viral spike glycoprotein. *Front. Microbiol.* 14:1206951. doi: 10.3389/fmicb.2023.1206951

The FDA-approved drug nitazoxanide is a potent inhibitor of human seasonal coronaviruses acting at postentry level: effect on the viral spike glycoprotein

Sara Piacentini[1†], Anna Riccio[1†], Silvia Santopolo[1], Silvia Pauciullo[1], Simone La Frazia[1], Antonio Rossi[2], Jean-Francois Rossignol[3] and M. Gabriella Santoro[1,2*]

[1]Department of Biology, University of Rome Tor Vergata, Rome, Italy, [2]Institute of Translational Pharmacology, CNR, Rome, Italy, [3]Romark Institute of Medical Research, Tampa, FL, United States

Coronaviridae is recognized as one of the most rapidly evolving virus family as a consequence of the high genomic nucleotide substitution rates and recombination. The family comprises a large number of enveloped, positive-sense single-stranded RNA viruses, causing an array of diseases of varying severity in animals and humans. To date, seven human coronaviruses (HCoV) have been identified, namely HCoV-229E, HCoV-NL63, HCoV-OC43 and HCoV-HKU1, which are globally circulating in the human population (seasonal HCoV, sHCoV), and the highly pathogenic SARS-CoV, MERS-CoV and SARS-CoV-2. Seasonal HCoV are estimated to contribute to 15–30% of common cold cases in humans; although diseases are generally self-limiting, sHCoV can sometimes cause severe lower respiratory infections and life-threatening diseases in a subset of patients. No specific treatment is presently available for sHCoV infections. Herein we show that the anti-infective drug nitazoxanide has a potent antiviral activity against three human endemic coronaviruses, the Alpha-coronaviruses HCoV-229E and HCoV-NL63, and the Beta-coronavirus HCoV-OC43 in cell culture with IC_{50} ranging between 0.05 and 0.15 μg/mL and high selectivity indexes. We found that nitazoxanide does not affect HCoV adsorption, entry or uncoating, but acts at postentry level and interferes with the spike glycoprotein maturation, hampering its terminal glycosylation at an endoglycosidase H-sensitive stage. Altogether the results indicate that nitazoxanide, due to its broad-spectrum anti-coronavirus activity, may represent a readily available useful tool in the treatment of seasonal coronavirus infections.

KEYWORDS

antiviral, HCoV-229E, HCoV-OC43, HCoV-NL63, nitazoxanide, spike glycoprotein

1. Introduction

Coronaviruses (CoV), members of the family *Coronaviridae* (order *Nidovirales*), comprise a large number of enveloped, positive-sense single-stranded RNA viruses causing respiratory, enteric, hepatic and neurological diseases of varying severity in animals and humans (Cui et al., 2019; Fung and Liu, 2019). Coronaviruses have the largest identified RNA genomes (typically

ranging from 27 to 32 kb) containing multiple open reading frames with an invariant gene order [a large replicase-transcriptase gene preceding structural (S-E-M-N) and accessory genes] (Fung and Liu, 2019). On the basis of their phylogenetic relationships and genomic structures, CoV are subdivided in four genera: Alpha-, Beta-, Gamma- and Delta-coronavirus; among these Alpha- and Beta-CoVs infect only mammals, whereas Gamma- and Delta-CoVs infect birds, and only occasionally can infect mammals (Cui et al., 2019). Human coronaviruses (HCoV) were discovered in the 1960s and were originally thought to cause only mild disease in humans (Cui et al., 2019; Fung and Liu, 2019). This view changed in 2002 with the SARS (Severe Acute Respiratory Syndrome) epidemic and in 2012 with the MERS (Middle East Respiratory Syndrome) outbreak, two zoonotic infections that resulted in mortality rates greater than 10 and 35%, respectively (Cui et al., 2019; Fung and Liu, 2019). Near the end of 2019, the seventh coronavirus known to infect humans, SARS-CoV-2, phylogenetically in the SARS-CoV clade, emerged in Wuhan, China. SARS-CoV-2 turned out to be a far more serious threat to public health than SARS-CoV and MERS-CoV because of its ability to spread more efficiently, making it difficult to contain worldwide with more than 768 million confirmed cases and over 6.9 million deaths reported worldwide, as of July 23rd, 2023.[1] The clinical features of COVID-19, the disease associated with SARS-CoV-2, vary ranging from asymptomatic state to respiratory symptoms that, in a subset of patients, may progress to pneumonia, acute respiratory distress syndrome (ARDS), multi organ dysfunction and death (Tang et al., 2020; Lamers and Haagmans, 2022).

Only two HCoV, HCoV-OC43 and HCoV-229E, were known prior to the emergence of SARS-CoV (Tyrrell and Bynoe, 1965; Hamre and Procknow, 1966), while two more, HCoV-NL63 and HCoV-HKU1, were identified between 2004 and 2005 (van der Hoek et al., 2004; Woo et al., 2005). HCoV-OC43 and HCoV-HKU1 likely originated in rodents, while HCoV-229E and HCoV-NL63, similarly to SARS-CoV and MERS-CoV, originated in bats (Fung and Liu, 2019).

These four HCoV (seasonal HCoV, sHCoV) are globally distributed and are estimated to contribute to 15–30% of cases of common cold in humans (Lim et al., 2016; Liu et al., 2021). Although diseases are generally self-limiting, sHCoV can sometimes cause severe lower respiratory infections, including life-threatening pneumonia and bronchiolitis especially in infants, elderly people, or immunocompromised patients (Pene et al., 2003; Chiu et al., 2005; Gorse et al., 2009; Zhang et al., 2022); in addition, besides respiratory illnesses, sHCoV may cause enteric and neurological diseases (Arbour et al., 2000; Jacomy et al., 2006; Risku et al., 2010; Morfopoulou et al., 2016), while a possible involvement of HCoV-229E in the development of Kawasaki disease was suggested (Esper et al., 2005; Shirato et al., 2014).

Whereas all seasonal coronaviruses cause respiratory tract infections, HCoV-OC43, HCoV-229E, HCoV-NL63 and HCoV-HKU1 are genetically dissimilar (Figure 1A), belonging to two distinct taxonomic genera (Alpha and Beta), and use different receptors that represent the major determinants of tissue tropism and host range (Fung and Liu, 2019). HCoV-229E and HCoV-NL63 have adopted cell surface enzymes as receptors, such as aminopeptidase N (APN) for HCoV-229E and angiotensin converting enzyme 2 (ACE2) for HCoV-NL63, while HCoV-OC43 and HCoV-HKU1 use 9-*O*-acetylated sialic acid as a receptor (Lim et al., 2016; Fung and Liu, 2019). In all cases, sHCoV infection is initiated by the binding of the spike (S) glycoprotein, anchored into the viral envelope, to the host receptor (Fung and Liu, 2019).

The coronavirus spike protein is a trimeric class-I fusion glycoprotein (Li, 2016); each monomer, with a molecular weight of 150–200 kDa after N-linked glycosylation (Lim et al., 2016), is synthesized as a fusogenically-inactive precursor that assembles into an inactive homotrimer, which is endoproteolytically cleaved by cellular proteases giving rise to a metastable complex of two functional subunits: S1 (bulb) containing the receptor-binding domain responsible for recognition and attachment to the host receptor, and the membrane-anchored S2 (stalk) that contains the fusion machinery (Li, 2016; Santopolo et al., 2021a). During synthesis in the infected cell, the nascent spike is imported into the endoplasmic reticulum (ER), where the protein is glycosylated (Sicari et al., 2020; Santopolo et al., 2021a). S glycoproteins passing the quality control mechanisms of the ER are transported to the ER/Golgi intermediate compartment (ERGIC), the presumed site of viral budding (Li, 2016; Fung and Liu, 2019).

Despite the fact that endemic seasonal coronaviruses may cause severe, life-threatening diseases in a subset of patients, no specific treatment is available for sHCoV infections.

Nitazoxanide, a thiazolide originally developed as an antiprotozoal agent and used in clinical practice for the treatment of infectious gastroenteritis (Rossignol et al., 2001, 2006b), and second-generation thiazolides have emerged as a new class of broad-spectrum antiviral drugs (Rossignol, 2014). Herein we investigated the antiviral activity of nitazoxanide against three human endemic coronaviruses belonging to two different genera: the Alpha-coronaviruses HCoV-229E and HCoV-NL63, and the Beta-coronavirus HCoV-OC43. We report that nitazoxanide is a potent inhibitor of HCoV replication acting at postentry level and interfering with Alpha- and Beta- sHCoV spike glycoprotein maturation.

2. Materials and methods

2.1. Cell culture and treatments

Human normal lung MRC-5 fibroblasts (American Type Culture Collection, ATCC, CCL-171) and rhesus monkey kidney LLC-MK2 cells (a kind gift from Lia van der Hoek, Academic Medical Center, University of Amsterdam) were grown at 37°C in a 5% CO_2 atmosphere in minimal essential medium (MEM, Gibco 32360–026) for LLC-MK2 cells or EMEM (ATCC 30–2003) for MRC-5 cells, supplemented with 10% fetal calf serum (FCS), 2 mM glutamine and antibiotics. Nitazoxanide [2-acetyloxy-*N*-(5-nitro-2-thiazolyl) benzamide, Alinia] (NTZ) and tizoxanide (TIZ; Romark Laboratories, L.C.), remdesivir (MedChemExpress), ribavirin and chloroquine (Sigma-Aldrich), dissolved, respectively, in DMSO stock solution (NTZ, TIZ, remdesivir) or water (ribavirin, chloroquine), were diluted in culture medium, added to infected cells after the virus adsorption period, and maintained in the medium for the duration of the experiment, unless differently specified. Controls received equal

1 https://covid19.who.int/

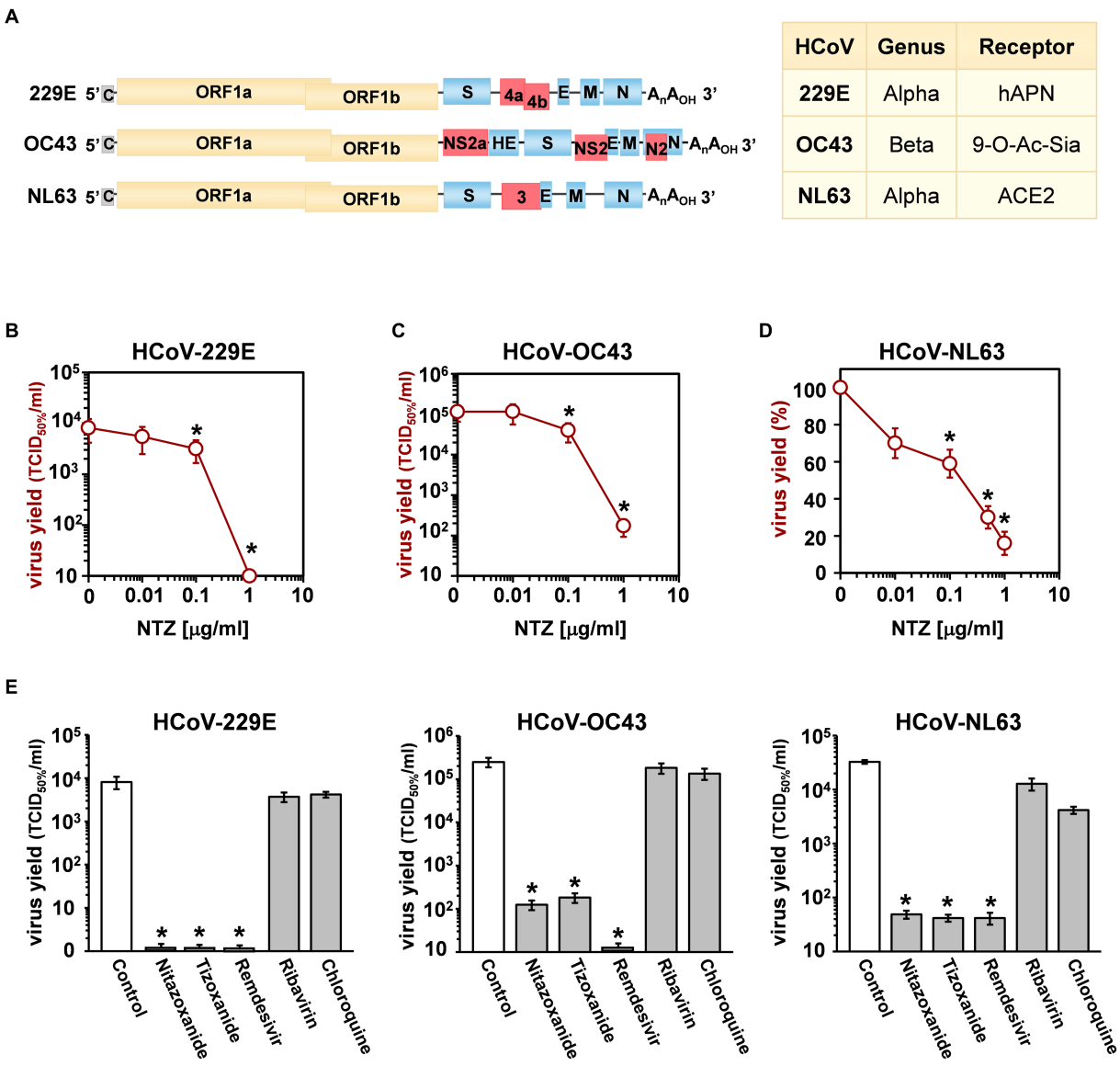

FIGURE 1
Antiviral activity of nitazoxanide against human seasonal coronaviruses. **(A)** Schematic representation of genome structure, classification and receptors of the human coronaviruses HCoV-229E, HCoV-OC43 and HCoV-NL63. ORF1a and ORF1b are represented as yellow boxes; genes encoding structural proteins spike (S), nucleocapsid (N), envelope (E), membrane (M), and hemagglutinin-esterase (HE) are shown as blue boxes, and genes encoding accessory proteins are shown as red boxes. hAPN, human aminopeptidase N; 9-O-Ac-Sia, N-acetyl-9-O-acetylneuraminic acid; ACE2, angiotensin-converting enzyme 2. **(B–D)** MRC-5 **(B,C)** and LLC-MK2 **(D)** cells mock-infected or infected with HCoV-229E **(B)**, HCoV-OC43 **(C)** or HCoV-NL63 **(D)** at an MOI of 0.1 $TCID_{50}$/cell were treated with different concentrations of NTZ or vehicle immediately after the adsorption period. In the case of HCoV-NL63, NTZ was removed at 48 h after infection. Virus yield in cell supernatants was determined at 48 **(B)**, 96 **(C)** or 120 **(D)** hours p.i. by infectivity assay **(B,C)** or RNA quantification by qRT-PCR **(D)**. Data, expressed as $TCID_{50}$/ml **(B,C)** or percent of untreated control **(D)**, represent the mean ± S.D. of duplicate samples. **(E)** MRC-5 cells infected with HCoV-229E or HCoV-OC43 and LLC-MK2 cells infected with HCoV-NL63 (0.1 $TCID_{50}$/cell) were treated with 3 μM nitazoxanide, the NTZ active metabolite tizoxanide, remdesivir, chloroquine and ribavirin after virus adsorption. In the case of HCoV-NL63, NTZ and tizoxanide were removed at 48 h after infection. Virus yields were determined at 48 (HCoV-229E), 72 (HCoV-OC43) or 120 (HCoV-NL63) hours p.i. by infectivity assay. Data, expressed as $TCID_{50}$/ml, represent the mean ± S.D. of duplicate samples. *$p < 0.05$; ANOVA test.

amounts of DMSO vehicle, which did not affect cell viability or virus replication. Cell viability was determined by the 3-(4,5-dimethylthiazol-2-yl)-2,5-diphenyltetrazolium bromide (MTT) to MTT formazan conversion assay (Sigma-Aldrich), as described (Pizzato Scomazzon et al., 2019). The 50% lethal dose (LD_{50}) was calculated using Prism 5.0 software (Graph-Pad Software Inc.). Microscopical examination of mock-infected or virus-infected cells was performed daily to detect virus-induced cytopathic effect and possible morphological changes and/or cytoprotection induced by the drug. Microscopy studies were performed using a Leica DM-IL microscope and images were captured on a Leica DC 300 camera using Leica Image-Manager500 software.

2.2. Coronavirus infection and titration

Human coronaviruses HCoV-229E (ATCC), HCoV-OC43 (ATCC) and HCoV-NL63 (strain Amsterdam-1, a kind gift from

Lia van der Hoek, University of Amsterdam), were used for this study. Due to its poor ability to grow in cell culture the fourth known seasonal HCoV, HKU1, was not investigated. For HCoV-229E and HCoV-OC43 infection, confluent MRC-5 cell monolayers were infected for 1 h at 33°C at a multiplicity of infection (MOI) of 0.1 or 0.5 $TCID_{50}$ (50% tissue culture infectious dose)/cell. For HCoV-NL63 infection, confluent LLC-MK2 cell monolayers were infected at 33°C for 2 h, as previously described (Milewska et al., 2014), at a MOI of 0.1 $TCID_{50}$/cell. After the adsorption period, the viral inoculum was removed, and cell monolayers were washed three times with phosphate-buffered saline (PBS). Cells were maintained at 33°C in growth medium containing 2% FCS. For HCoV-229E and HCoV-OC43 infections, virus yield was determined in the supernatants collected from infected cells at different times after infection (p.i.) by $TCID_{50}$ infectivity assay, as described previously (Santoro et al., 1988), using confluent MRC-5 cells in 96-well plates. In the case of HCoV-NL63, which requires 5 to 6 days for infectious progeny production and is characterized by a weak and transient cytopathic effect, virus yield was determined in the supernatant collected from infected cells at 120 h p.i. by viral RNA quantification, as previously reported (Castillo et al., 2022). Quantification of viral RNA in the supernatants of infected cells is described below. $TCID_{50}$ infectivity assay in confluent LLC-MK2 cell monolayers in 96-well plates was also utilized in some experiments. The IC_{50} (50% inhibitory concentration) of the compounds tested was calculated using Prism 5.0 software.

2.3. HCoV RNA extraction and quantification

Measurement of sHCoV genomic RNA was performed by real-time quantitative reverse transcription-PCR (qRT-PCR), as described (Coccia et al., 2017). Briefly, total RNA from mock-infected or HCoV-infected cells was prepared using ReliaPrep RNA Cell Miniprep System (Promega) and reverse transcription was performed with PrimeScript RT Reagent Kit (Takara) in 20 µL final reaction volume (37°C for 15 min, 85°C for 5 s) according to the manufacturer's protocol. Extracellular viral RNA was extracted from 200 µL of the supernatant of mock-infected or sHCoV-infected cell cultures with Viral Nucleic Acid Extraction Kit II (Geneaid) and 10 µL were subjected to reverse transcription using SuperScript™ VILO™ cDNA Synthesis Kit (Life Technologies) (25°C for 10 min, 42°C for 60 min and 85°C for 5 min), as described in the manufacturer's protocol. Real-time PCR analysis was performed with CFX-96 (Bio-Rad) using SensiFAST SYBR® kit (Bioline) and primers specific for the membrane protein gene of HCoV-OC43 and HCoV-229E (Vijgen et al., 2005) or for the nucleoprotein gene of HCoV-NL63 (Pyrc et al., 2006). Relative quantities of selected mRNAs were normalized to ribosomal L34 RNA levels in the same sample. The sequences of the L34 primers were as follows: sense 5′-GGCCCTGCTGACATG TTTCTT-3′, antisense 5′-GTCCCGAACCCCTGGTAATAGA-3′. All reactions were made in triplicate using samples derived from three biological repeats with a negative control (mock-infected sample) and a "no template" control (NTC) included in each run. Subsequently the data were exported to Microsoft Excel and GraphPad Prism software for further analysis.

2.4. HCoV genomic RNA transfection

For sHCoV genomic RNA transfection experiments, MRC-5 cell monolayers were infected with HCoV-OC43 or HCoV-229E for 1 h at 33°C at an MOI of 0.1 $TCID_{50}$/cell and sHCoV genomic RNA was extracted from the supernatants at 24 h p.i. using TRIzol-LS reagent (Life Technologies) as described in the manufacturer's protocol. MRC-5 cell monolayers were mock-transfected or transfected with sHCoV genomic RNA (1 µg/mL) using TransIT-mRNA Transfection Kit (Mirus Bio) at 33°C. After 4 h, transfection medium was removed and cells were treated with NTZ or vehicle and maintained at 33°C in growth medium containing 2% FCS. At 24 h after treatment, culture supernatants were collected for virus progeny titer determination, and cell monolayers were processed for viral proteins detection.

2.5. Protein analysis, western blot and endoglycosidase digestion

For analysis of proteins whole-cell extracts (WCE) were prepared after lysis in High Salt Buffer (HSB; Santopolo et al., 2021b). Briefly, cells were washed twice with ice-cold PBS and then lysed in HSB (40 µL). After one cycle of freeze and thaw, and centrifugation at 16,000 ×*g* (10 min at 4°C), supernatant and pellet fractions were collected (Santoro et al., 1982). For Western blot analysis, cell extracts (20 µg/sample) were separated by SDS-PAGE under reducing conditions and blotted to a nitrocellulose membrane. Membranes were incubated with rabbit polyclonal anti-HCoV-OC43 spike (CSB-PA336163EA01HIY, Cusabio) or nucleocapsid (40643-T62, Sino Biological) antibodies, anti-HCoV-229E spike (PAB21477-100, LGC NAC Company) or nucleocapsid (40640-T62, Sino Biological) antibodies, anti β-actin (A2066, Sigma-Aldrich) antibodies, and monoclonal α-tubulin (T5168, Sigma-Aldrich) antibodies, followed by decoration with peroxidase-labeled anti-rabbit or anti-mouse IgG (Super-Signal detection kit, Pierce). Spike proteins densitometric and molecular weight analysis were performed with Image Lab Software 6.1, after acquisition on a ChemiDoc XRS+ (Bio-Rad).

For endoglycosidase digestion experiments, MRC-5 cells were mock-infected or infected with HCoV-OC43 or HCoV-229E at an MOI of 0.5 $TCID_{50}$/cell and treated with NTZ (1 µg/mL) or vehicle immediately after the virus adsorption period. At 24 h p.i., cell monolayers were lysed in HSB buffer. After centrifugation at 16,000 ×*g* (10 min at 4°C), samples containing the same amount of protein (20 µg/sample) were processed for endoglycosidase-H (Endo-H, NEB) digestion using 5 milliunits Endo-H for 16 h at 37°C, according to the manufacturer's protocol (Riccio et al., 2022). Digestions were terminated with the addition of Laemmli sample buffer (La Frazia et al., 2018). Samples were heated at 95°C for 5 min, separated by SDS-PAGE and processed for Western blot as described above. Quantitative evaluation of proteins was determined as described (Santoro et al., 1989; Amici et al., 2015). All results shown are representative of at least three independent experiments.

2.6. Immunofluorescence microscopy

MRC-5 cells infected with HCoV-OC43 or HCoV-229E were grown in 8-well chamber slides (Lab-Tek II) and, after the adsorption

period, were treated with NTZ, or vehicle for 24 h. Cells were fixed, permeabilized and processed for immunofluorescence as described (Riccio et al., 2022) using anti-HCoV-OC43 or anti-HCoV-229E spike antibodies, followed by decoration with Alexa Fluor 555-conjugated antibodies (Molecular Probes, Invitrogen). Nuclei were stained with Hoechst 33342 (Molecular Probes, Invitrogen). Images were captured using a ZEISS Axio Observer Inverted Microscope and analyzed using ZEN 3.1 (blue edition) software. For confocal microscopy, images were acquired on Olympus FluoView FV-1000 confocal laser scanning system (Olympus America Inc., Center Valley, PA) and analyzed using Imaris (v6.2) software (Bitplane, Zurich, Switzerland). Images shown in all figures are representative of at least three random fields (scale-bars are indicated).

2.7. Statistical analysis

Statistical analyses were performed using Prism 5.0 software (GraphPad Software). Comparisons between two groups were made using Student's *t*-test; comparisons among groups were performed by one-way ANOVA with Bonferroni adjustments. $p \leq 0.05$ were considered significant. Data are expressed as the means ± standard deviations (SD) of results from duplicate or quadruplicate samples. Each experiment (in duplicate) was repeated at least twice.

3. Results

3.1. Antiviral activity of nitazoxanide against human seasonal coronaviruses

Three different human globally distributed coronaviruses, HCoV-229E, HCoV-OC43, and HCoV-NL63, were utilized for the current study. The genomic structure, classification, and receptors of these HCoVs are summarized in Figure 1A.

Nitazoxanide antiviral activity was first investigated in human lung MRC-5 and monkey kidney LLC-MK2 cells infected with HCoVs 229E (Figure 1B), OC43 (Figure 1C) and NL63 (Figure 1D) at the MOI of 0.1 $TCID_{50}$/cell, and treated with different concentrations of the drug starting after the virus adsorption period. In the case of HCoV-NL63, which required 120 h for infectious progeny production, nitazoxanide was removed at 48 h after infection to avoid possible cytostatic/cytotoxic effects due to prolonged NTZ treatment *in vitro* (Wang et al., 2018). It should also be noted that, as previously reported in different cell lines (Loo et al., 2020), HCoV-OC43 and HCoV-229E display distinct replication kinetics, with HCoV-229E replicating more rapidly than HCoV-OC43, and viral loads peaking at 48 h and 96 h p.i. respectively under the conditions described.

At 48 (229E), 96 (OC43) and 120 (NL63) hours after infection, viral titers were determined in the supernatant of infected cells by $TCID_{50}$ assay (Figures 1B,C) or viral RNA quantification (Figure 1D; Supplementary Figures S1A,B). Nitazoxanide showed a remarkable antiviral activity against all three HCoVs, reducing virus yield dose-dependently with IC_{50} values in the submicromolar range.

To compare the effect of nitazoxanide with other antiviral drugs, MRC-5 and LLC-MK2 cells were infected with the different HCoVs at the MOI of 0.1 $TCID_{50}$/cell and treated with nitazoxanide, the NTZ bioactive metabolite tizoxanide, the antiviral drugs remdesivir and ribavirin, or chloroquine at the same concentration (3 μM) starting after virus adsorption. In the case of HCoV-NL63, NTZ and tizoxanide were removed at 48 h after infection. Virus yields were determined at 48 (HCoV-229E), 72 (HCoV-OC43) or 120 (HCoV-NL63) hours after infection by $TCID_{50}$ assay. Nitazoxanide, tizoxanide and remdesivir showed comparable antiviral activity against all three HCoV, whereas chloroquine and ribavirin were not found to be effective when treatment was started after infection (Figure 1E).

Next, the effect of short-treatment with nitazoxanide was investigated in MRC-5 cells infected with HCoV-OC43 and HCoV-229E. MRC-5 cells were infected with the OC43 or 229E HCoV strains at the MOI of 0.5 $TCID_{50}$/cell and treated with different concentrations of the drug starting after the virus adsorption period. At 24 h after infection, viral titers were determined in the supernatant of infected cells by $TCID_{50}$ assay (Figure 2A) and viral RNA level quantification (Supplementary Figures S1C,D); in parallel, the effect of nitazoxanide on mock-infected cell viability was determined by MTT assay. The results, shown in Figures 2A,B, confirmed a potent antiviral activity of nitazoxanide, with IC_{50} values of 0.15 μg/mL and 0.05 μg/mL and selectivity indexes higher than 330 and 1,000 for HCoV-OC43 and HCoV-229E, respectively.

3.2. Nitazoxanide acts at postentry level

To determine the effect of NTZ treatment before virus infection, MRC-5 cells were treated with NTZ (1 or 2.5 μg/mL) or vehicle for 2 h and the drug was removed before infection with OC43 or 229E HCoVs (0.5 $TCID_{50}$/cell). In parallel, MRC-5 cells were infected with OC43 or 229E HCoVs (0.5 $TCID_{50}$/cell) in the absence of the drug, and treated with 1 or 2.5 μg/mL NTZ or vehicle starting immediately after the adsorption period for the duration of the experiment. Alternatively, MRC-5 cells were treated 2 h before infection and treatment was continued during and after the adsorption period. Virus yield was determined at 24 h p.i. by $TCID_{50}$ assay. As shown in Figures 3A,B, NTZ pretreatment did not significantly affect HCoV replication when the drug was removed before infection; on the other hand, treatment started after infection was effective in reducing infectious progeny production by approximately 3-fold in both HCoV models, without affecting cell viability ($LD_{50} > 50$ μg/mL).

In a different experiment, MRC-5 cells were infected with OC43 or 229E HCoV (0.5 $TCID_{50}$/cell) and treated with NTZ (1 μg/mL) or vehicle only during the 1 h adsorption period, after which time the drug was removed. Virus yield was determined at 24 h p.i. by $TCID_{50}$ assay. As shown in Figure 3C, NTZ treatment during virus adsorption did not affect HCoV replication. These results suggest that nitazoxanide acts at postentry level.

In order to rule out any effect of the drug on virus adsorption, entry or uncoating, OC43 and 229E HCoV genomic RNA was extracted and transfected into MRC-5 monolayers, as described in Materials and Methods, and schematically represented in Figure 3D. After 4 h, the transfection medium was removed and cells were treated with NTZ (2.5 μg/mL) or vehicle for 24 h. Virus yield was determined at 24 h after treatment in the supernatant of transfected cells. As shown in Figure 3E, genomic RNA transfection resulted in the production of infectious viral progeny (10^2–10^3 $TCID_{50}$/ml) already at 24 h after transfection. Higher virus titers were detected at later times after transfection (data not shown). NTZ treatment greatly

A

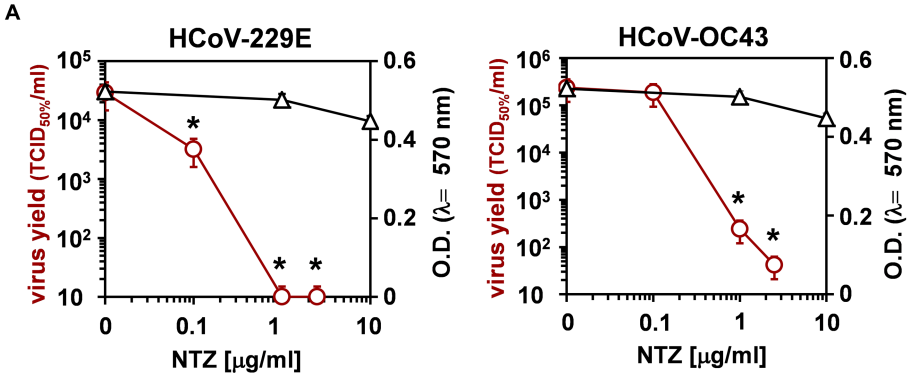

B

HCoV	IC_{50}	LD_{50}	SI
229E	0.05	>50	>1000
OC43	0.15	>50	>333

FIGURE 2
Effect of short treatment with nitazoxanide in OC43 and 229E HCoV-infected human lung cells. **(A,B)** MRC-5 cell monolayers mock-infected or infected with HCoV-229E and HCoV-OC43 (0.5 $TCID_{50}$/cell) were treated with different concentrations of NTZ or vehicle immediately after the adsorption period. Virus yield (O, red line) was determined at 24 h p.i. by infectivity assay. In parallel, cell viability (△, black line) was determined by MTT assay in mock-infected cells **(A)**. Absorbance (O.D.) of converted dye was measured at λ = 570 nm. IC_{50} and LD_{50} in μg/ml **(B)** were calculated using Prism 5.0 software. Data represent the mean ± S.D. of duplicate samples. Selectivity indexes (SI) are indicated. *$p < 0.05$; ANOVA test.

reduced the production of both HCoV-OC43 and HCoV-229E infectious particles after RNA transfection. Altogether, these results demonstrate that nitazoxanide is not acting on HCoV adsorption, entry or uncoating.

3.3. Nitazoxanide treatment impairs HCoV-OC43 and HCoV-229E spike maturation

Interestingly, NTZ-treatment initiated between 0 and 6 h p.i. was equally effective in inhibiting HCoV-OC43 virus replication, whereas the antiviral activity was impaired when treatment was started as late as 12 h p.i. (Figure 3F). Similar results were obtained after HCoV-229E infection (Supplementary Figure S2).

To investigate whether NTZ may affect human coronavirus structural proteins expression, MRC-5 cells were infected with HCoV-OC43 (0.5 $TCID_{50}$/cell) and treated with 0.1, 1 or 2.5 μg/mL NTZ or vehicle starting immediately after the adsorption period. At 24 h p.i., levels of the viral nucleocapsid (N) and spike (S) proteins were determined in the infected cells by immunoblot analysis using specific antibodies, and virus yield was determined in the culture supernatants by infectivity assay. As shown in Figure 4A, no significant differences in N and S protein levels were detected in NTZ-treated cells, as compared to control, at concentrations that caused a > 99% reduction in viral yield in the same samples (Figure 4B). Comparable levels of S-protein were also detected by confocal microscopy in MRC-5 cells infected with OC43 or 229E HCoVs (0.5 $TCID_{50}$/cell) and treated with NTZ (1 μg/mL) or vehicle after the adsorption period for 24 h (Figure 4C; Supplementary Figure S3). Interestingly, treatment with NTZ at concentrations higher than 0.1 μg/mL caused an evident alteration in the electrophoretic mobility pattern of the spike glycoprotein (Figure 4A). An alteration in the molecular mass of the HCoV-OC43 spike protein of approximately 5.8 kDa was in fact detected in MRC-5 cells treated with 2.5 μg/mL NTZ (Figures 5A,C). In a parallel experiment, a similar alteration in the HCoV-229E spike molecular mass (8.3 kDa) was detected in MRC-5 cells treated with 2.5 μg/mL NTZ (Figures 5B,D), indicating an effect of the drug in the glycoprotein maturation process. These results are in line with our previous observation that the thiazolide affects the maturation of the SARS-CoV-2 S glycoprotein in human cells transfected with plasmids encoding different SARS-CoV-2 spike variants (Riccio et al., 2022). In this case, we have found that nitazoxanide blocks the maturation of the SARS-CoV-2 S glycoprotein at a stage preceding resistance to digestion by endoglycosidase-H (Endo-H), an enzyme that removes *N*-linked carbohydrate chains that have not been terminally glycosylated (Figure 5E; Ohuchi et al., 1997), thus impairing SARS-CoV-2 S intracellular trafficking and infectivity.

As indicated in the Introduction, glycosylation of coronavirus S proteins, like other cell surface glycoproteins, is initiated in the endoplasmic reticulum, adding the "high mannose" oligosaccharides; the mannose-rich sugar component is processed in the Golgi apparatus, and terminal glycosylation occurs in the *trans* cisternae of the Golgi apparatus (Xu and Ng, 2015).

To obtain insights on the effect of NTZ on HCoV S maturation, we therefore investigated whether nitazoxanide could affect HCoV-OC43 and HCoV-229E spike proteins terminal glycosylation. MRC-5 cells were infected with HCoV-OC43 or HCoV-229E (0.5 $TCID_{50}$/cell)

10.3389/fmicb.2023.1206951

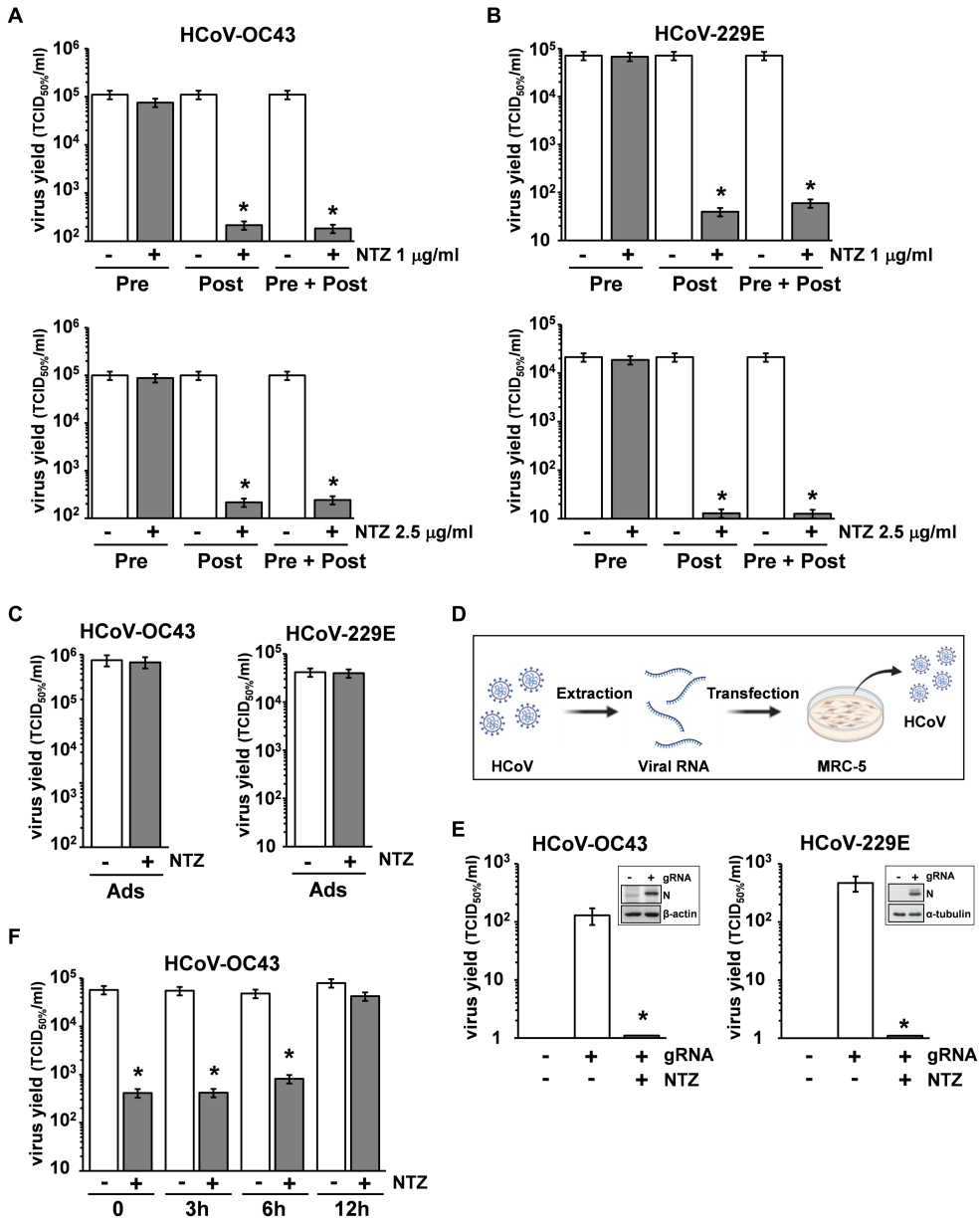

FIGURE 3
Nitazoxanide acts at postentry level. **(A,B)** MRC-5 cells mock-infected or infected with HCoV-OC43 **(A)** or HCoV-229E **(B)** (0.5 $TCID_{50}$/cell) were treated with NTZ 1 μg/mL [**(A,B)** top; filled bars], NTZ 2.5 μg/mL [**(A,B)** bottom; filled bars] or vehicle (empty bars) 2 h before infection (Pre), after the adsorption period (Post), or 2 h before infection and treatment was continued during and after the adsorption period (Pre + Post). Virus yield was determined at 24 h p.i. by $TCID_{50}$ infectivity assay. **(C)** MRC-5 cells mock-infected or infected with HCoV-OC43 or HCoV-229E were treated with NTZ (1 μg/mL) or vehicle only during the adsorption period (Ads). Virus yield was determined at 24 h p.i. by infectivity assay. **(A–C)** Data represent the mean ± S.D. of duplicate samples. *$p < 0.01$; Student's *t*-test. **(D)** Schematic representation of HCoV genomic RNA transfection assay. **(E)** MRC-5 cells were transfected with HCoV-OC43 or HCoV-229E genomic RNA for 4 h and treated with NTZ (2.5 μg/mL) or vehicle for 24 h. Virus yield was determined at 24 h after treatment in the supernatant of transfected cells by $TCID_{50}$ infectivity assay. Nucleocapsid (N) protein levels in HCoV-OC43 or HCoV-229E RNA-transfected cells are shown (insets). **(F)** MRC-5 cells infected with HCoV-OC43 were treated with NTZ (1 μg/mL) or vehicle at the indicated times after infection. Virus yield was determined at 24 h p.i. by infectivity assay. **(E,F)** Data represent the mean ± S.D. of duplicate samples. *$p < 0.01$; Student's *t*-test.

and treated with 1 μg/mL NTZ or vehicle starting immediately after the adsorption period. At 24 h p.i., protein aliquots (20 μg) from NTZ-treated or control cells were subjected to digestion with Endo-H and then analyzed by immunoblot. The results, shown in Figures 5F,G, indicate that, at this time, a fraction (approximately 40% in the case of HCoV-OC43, and 30% for HCoV-229E) of the spike proteins was found to be terminally glycosylated becoming Endo-H-resistant in control cells under the conditions described; notably, the spike proteins from NTZ-treated cells remained instead sensitive to digestion with the glycosidase up to 24 h after synthesis. Because acquisition of Endo-H resistance is a marker for transport into the *cis* and *middle* Golgi compartments (Ohuchi et al., 1997), these results indicate that nitazoxanide may impair S protein trafficking between the ER and the Golgi complex.

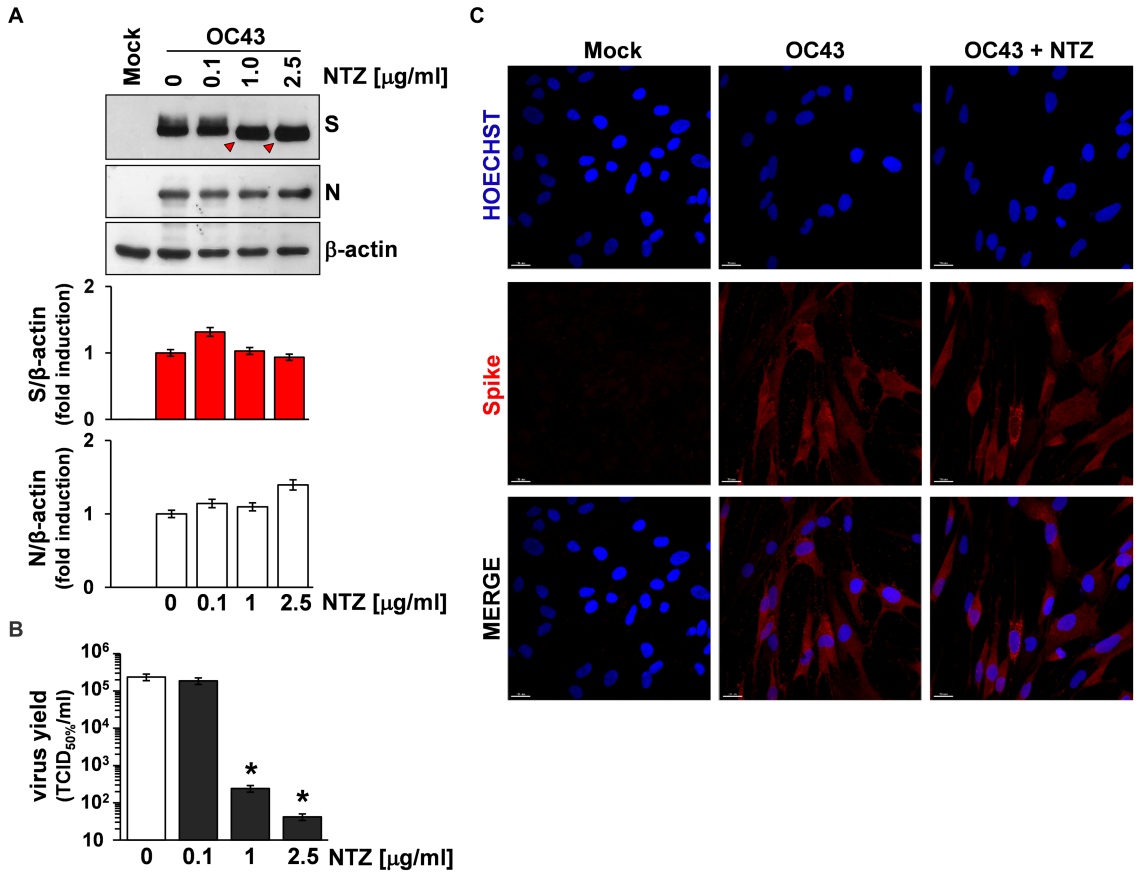

FIGURE 4
Effect of Nitazoxanide on HCoV-OC43 spike expression. **(A,B)** MRC-5 cells were mock-infected or infected with HCoV-OC43 at an MOI of 0.5 $TCID_{50}$/cell and treated with different concentrations of NTZ or vehicle immediately after the virus adsorption period. After 24 h, whole cell extracts (WCE) were analyzed for levels of viral S and N proteins by IB using anti-spike and anti-N HCoV-OC43 antibodies [**(A)** top], and quantitated by scanning densitometry. Relative amounts of S and N proteins were determined after normalizing to β-actin [**(A)** bottom]. The faster-migrating form of the S protein in NTZ-treated cells is indicated by red arrowheads. In the same experiment virus yield was determined at 24 h p.i. in the supernatant of infected cells by $TCID_{50}$ infectivity assay **(B)**. Data represent the mean ± S.D. of duplicate samples. *$p < 0.01$; ANOVA test. **(C)** Confocal images of HCoV-OC43 spike glycoprotein (red) in MRC-5 cells mock-infected or infected with HCoV-OC43 at an MOI of 0.5 $TCID_{50}$/cell and treated with NTZ (1 μg/mL) or vehicle for 24 h. Nuclei are stained with Hoechst (blue). Merge images are shown. Scale bar, 20 μm.

4. Discussion

Coronaviridae is recognized as one of the most rapidly evolving virus family as a consequence of the high genomic nucleotide substitution rates and recombination (Cui et al., 2019). As indicated in the Introduction, to date, seven human CoVs have been identified, namely HCoV-229E, HCoV-NL63, HCoV-OC43 and HCoV-HKU1, globally circulating in the human population, and the highly pathogenic SARS-CoV, MERS-CoV and SARS-CoV-2. Among these, SARS-CoV-2 is responsible for a devastating pandemic that is causing unprecedented public health interventions (COVID-19 Excess Mortality Collaborators, 2022). Given the proportion of the COVID-19 pandemic, major efforts have been directed over the past months towards a global vaccination plan.[2] At the same time, the emergence of several SARS-CoV-2 spike variants that facilitate virus spread and may affect the efficacy of recently developed vaccines (Dong et al., 2021; Harvey et al., 2021; Planas et al., 2021; Carabelli et al., 2023), together with the short-lasting protective immunity typical of HCoV (Edridge et al., 2020), creates great concern and highlights the importance of identifying antiviral drugs to reduce coronavirus-related morbidity and mortality. So far, for SARS-CoV-2, two different RNA-dependent RNA polymerase (RdRp) inhibitors remdesivir (Santoro and Carafoli, 2020) and molnupiravir (Wahl et al., 2021; Jayk Bernal et al., 2022), and a viral protease inhibitor, Paxlovid (SARS-CoV-2 3CL protease inhibitor nirmatrelvir co-packaged with ritonavir), have been approved by health authorities in different countries (Hammond et al., 2022; Wen et al., 2022). On the other hand, no specific antiviral drug or vaccine are presently available for seasonal coronavirus infections.

Nitazoxanide has been proven to have a broad-spectrum antiviral activity (Rossignol, 2014; Li and De Clercq, 2020). In particular, nitazoxanide, its active metabolite tizoxanide and second generation thiazolides were found to be effective against several widespread RNA pathogens, including rotavirus, hepatitis C, and influenza and

2 https://cdn.who.int/media/docs/default-source/immunization/covid-19/strategy-to-achieve-global-covid-19-vaccination-by-mid-2022.pdf?sfvrsn=5a68433c_5

10.3389/fmicb.2023.1206951

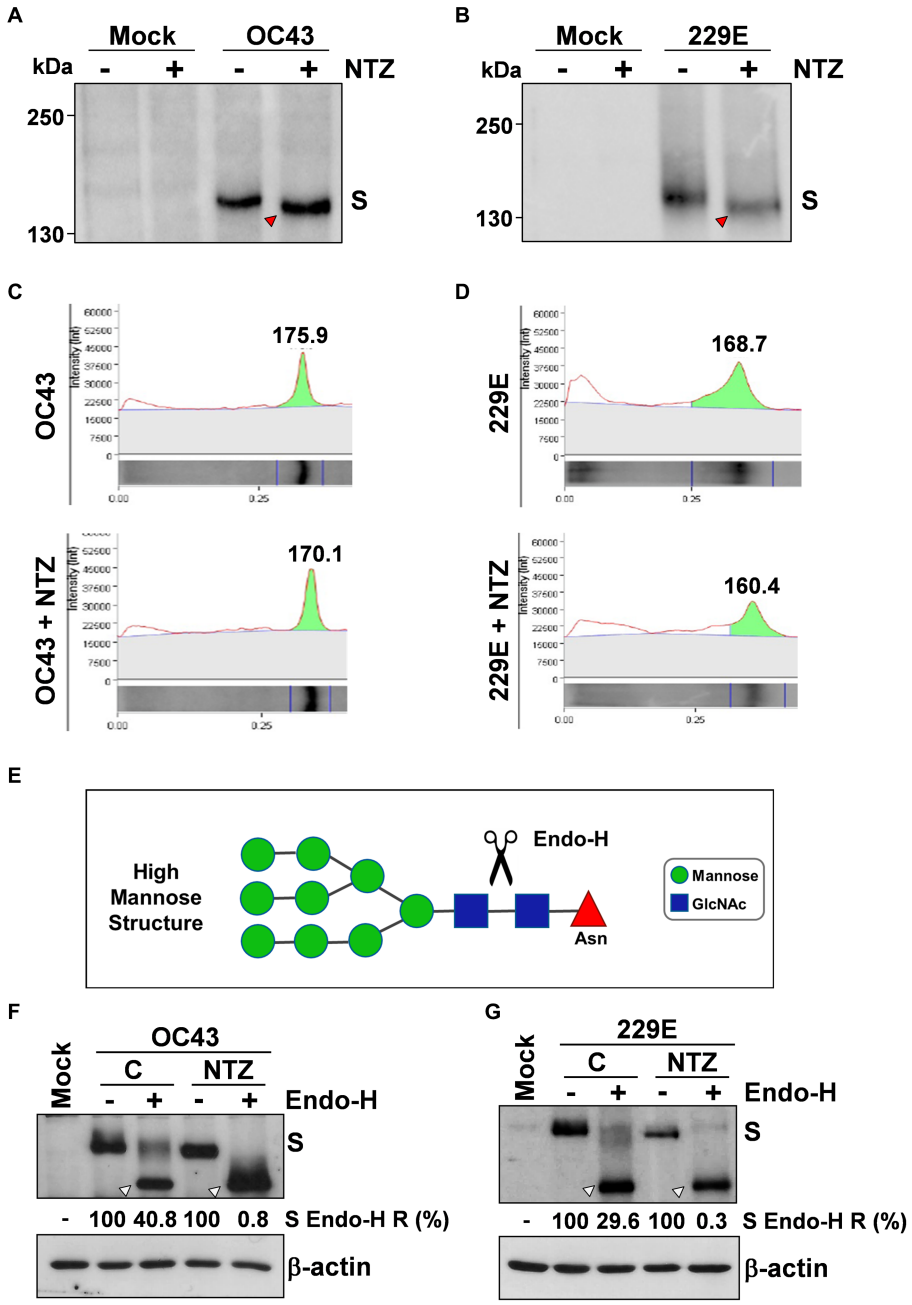

FIGURE 5
Nitazoxanide impairs HCoV-OC43 and HCoV-229E spike maturation at an Endo-H sensitive stage. **(A–D)** MRC-5 cells were mock-infected or infected with HCoV-OC43 **(A,C)** or HCoV-229E **(B,D)** at an MOI of 0.5 $TCID_{50}$/cell and treated with NTZ (2.5 μg/mL) or vehicle immediately after the virus adsorption period. After 24 h, WCE were analyzed for levels of S protein by IB using anti-S HCoV-OC43 **(A,C)** or anti-S HCoV-229E **(B,D)** antibodies. Red arrowheads indicate the faster-migrating forms of the HCoV-OC43 **(A)** and HCoV-229E **(B)** spike proteins in NTZ-treated cells. Spike proteins densitometric and molecular weight analysis **(C,D)** are shown. (**E**) Diagram of substrate specificity of endoglycosidase-H (Endo-H). Mannose (green circles), *N*-acetylglucosamine (GlcNAc, blue squares) and asparagine (Asn, red triangle) residues are shown. Scissors represent the cleavage site of Endo-H. **(F,G)** MRC-5 cells were mock-infected or infected with HCoV-OC43 **(F)** or HCoV-229E **(G)** at an MOI of 0.5 $TCID_{50}$/cell and treated with NTZ (1 μg/mL) or vehicle immediately after the virus adsorption period. After 24 h proteins were digested with Endo-H (+) or left untreated (–) and processed for IB analysis using anti-S HCoV-OC43 **(F)** or anti-S HCoV-229E **(G)** antibodies, and quantitated by scanning densitometry. The Endo-H-cleaved faster-migrating S forms are indicated by white arrowheads. The percentage of Endo-H-resistant (Endo-H R) S protein in the different samples is indicated.

parainfluenza viruses in laboratory settings (Korba et al., 2008; Rossignol et al., 2009b; La Frazia et al., 2013, 2018; Belardo et al., 2015; Piacentini et al., 2018; Stachulski et al., 2021), as well as in clinical studies (Rossignol et al., 2006a, 2009a; Haffizulla et al., 2014). In the case of *Coronaviridae*, we first reported the effect of the drug against a canine strain of the virus (CCoV S-378) in canine A72 cells in 2007 (Santoro et al., 2007). Cao et al. (2015) showed that among 727 compounds tested against various strains of coronavirus, nitazoxanide

was among the three most effective compounds tested (Cao et al., 2015). Nitazoxanide and tizoxanide were also found to be effective against MERS-CoV in LLC-MK2 cells with IC_{50}s of 0.92 and 0.83 μg/mL, respectively, (Rossignol, 2016). As for SARS-CoV-2, at an early stage of the pandemic, Wang et al. reported that nitazoxanide inhibits SARS-CoV-2 replication in Vero E6 cells at low μM concentrations (EC_{50} = 2.12 μM; Wang et al., 2020); these observations were recently confirmed in different types of cells, including human lung-derived Calu-3 cells (Rocco et al., 2021; Son et al., 2022), as well as in animal models (Miorin et al., 2022). Tizoxanide was also recently found to be effective against SARS-CoV-2 in Vero E6 cells with an EC_{50} of 0.8 μg/mL (Riccio et al., 2022). More importantly several studies have recently shown an antiviral activity and clinical benefits of nitazoxanide in COVID-19 patients (Blum et al., 2021; Rocco et al., 2021, 2022; Silva et al., 2021; Rossignol et al., 2022a). It should be mentioned that no significant effect of nitazoxanide in the prevention or outcome of SARS-CoV-2 infections was reported in some studies (Fowotade et al., 2022; Sokhela et al., 2022). A recent study, while confirming the *in vitro* efficacy of nitazoxanide and tizoxanide against SARS-CoV-2, found that, in a SARS-CoV-2 virus challenge model in hamsters, oral and intranasal treatment with nitazoxanide failed to impair viral replication in affected organs, due to insufficient diffusion of the drug into the lungs and in the upper respiratory tract (Driouich et al., 2022), suggesting that the different results reported could depend on the dosage used, and that optimization of the NTZ formulation may be required to improve clinical efficacy of the drug.

In the case of seasonal HCoVs, it should be pointed out that treatment of subjects with laboratory-confirmed sHCoV infection with nitazoxanide administered orally twice daily for 5 days was associated with improvement in time to return to usual health and time until subjects are able to perform normal activities (Rossignol et al., unpublished results). However, the mechanism at the basis of the antiviral activity of nitazoxanide against coronaviruses is not yet understood.

We now show that nitazoxanide has a potent antiviral activity against three human endemic coronaviruses, the Alpha-coronaviruses HCoV-229E and HCoV-NL63, and the Beta-coronavirus HCoV-OC43 in cell culture with IC_{50} ranging between 0.05 and 0.15 μg/mL and high (>330) selectivity indexes. The fourth known seasonal HCoV, HKU1, was not investigated because of its poor ability to grow in cell culture.

We found that nitazoxanide does not affect virus adsorption, entry or uncoating of HCoVs, but acts at postentry level, interfering with the spike S-glycoprotein maturation at concentrations that do not inhibit S and N protein expression in the infected cell. These results confirm in two different actively-replicating HCoV models our previous observation that nitazoxanide affects the maturation of the SARS-CoV-2 S glycoprotein in human cells transfected with plasmids encoding different SARS-CoV-2 spike variants (Riccio et al., 2022). The results are also in line with our previous studies on influenza and parainfluenza viruses, where nitazoxanide was shown to impair terminal glycosylation and intracellular trafficking of the class-I viral fusion glycoproteins influenza hemagglutinin and paramyxovirus fusion proteins (Rossignol et al., 2009b; La Frazia et al., 2018; Piacentini et al., 2018).

As previously observed in the case of the hemagglutinin protein during human and avian influenza virus infection (Rossignol et al., 2009b; La Frazia et al., 2018), and of exogenously expressed SARS-CoV-2 S protein in human cells (Riccio et al., 2022), nitazoxanide was found to hamper the spike protein maturation at an Endo-H-sensitive stage, thus preventing its final processing. This effect has been previously associated to the drug-mediated inhibition of ERp57, an ER-resident glycoprotein-specific thiol-oxidoreductase which is essential for correct disulfide-bond architecture of selected viral proteins (Piacentini et al., 2018).

Because of the critical role of the spike protein in coronavirus assembly (Fung and Liu, 2019; Santopolo et al., 2021a), hampering S maturation may result in hindering progeny virus particle formation; however, we cannot exclude the existence of additional mechanisms that may contribute to the antiviral activity of thiazolides. Multiple mechanisms have in fact been implicated in the host-directed antiviral activity of nitazoxanide depending on the type of viral pathogen, including: interfering with the host cell energy metabolism and decreasing cellular ATP levels by mild uncoupling of mitochondrial oxidative phosphorylation (OXPHOS; Hammad et al., 2022; Rossignol et al., 2022b), and regulating the redox state of infected cells (Huang et al., 2023); induction of autophagy by inhibiting the Akt/mTOR/ULK1 signaling pathway in different types of cells (Lam et al., 2012; Shou et al., 2020); induction of PKR activation and subsequent phosphorylation of eIF2-α (Elazar et al., 2009; Ashiru et al., 2014); amplification of the host innate immune response, via an increase in RIG-I-like receptor activation, enhanced mitochondrial antiviral signaling protein and interferon regulatory factor 3 activities (Jasenosky et al., 2019); induction or enhancement of interferon (IFN)-stimulated gene expression (Gekonge et al., 2015; Petersen et al., 2016; Trabattoni et al., 2016; Jasenosky et al., 2019).

Interestingly, the antiviral activity of nitazoxanide and its bioactive metabolite tizoxanide against all sHCoV strains tested was found to be comparable to the direct-acting antiviral (DAA), potent RdRp inhibitor remdesivir (Santoro and Carafoli, 2020). It should be noted that, as in the case of other DAA, remdesivir may loose its efficacy due to the emergence of drug-resistant mutations in the target protein. This is in fact been already reported for use of remdesivir in SARS-CoV-2 infections *in vitro* after prolonged exposure to the drug, as well as in COVID-19 patients (Gandhi et al., 2022; Stevens et al., 2022). On the other hand nitazoxanide, being a host-directed antiviral (Rossignol, 2014; Li and De Clercq, 2020), it is unlikely to give rise to resistance.

In addition, remdesivir requires intravenous administration,[3] whereas nitazoxanide is an oral drug with a well-established safety profile (Rossignol, 2014). Finally, due to their different mechanism of action, a possible use of combination of the two drugs could be hypothesized.

As indicated in the Introduction, HCoV-229E, HCoV-OC43 and HCoV-NL63, as well as HCoV-HKU1, are distributed globally, and generally cause mild upper respiratory tract diseases in adults; however, they may sometimes cause life-threatening diseases in a subset of patients (Arbour et al., 2000; Pene et al., 2003; Chiu et al., 2005; Jacomy et al., 2006; Gorse et al., 2009; Risku et al., 2010; Lim

3 https://www.covid19treatmentguidelines.nih.gov/therapies/antivirals-including-antibody-products/remdesivir/

et al., 2016; Morfopoulou et al., 2016; Liu et al., 2021; Zhang et al., 2022). Interestingly, whereas HCoV-229E was suggested to be involved in the development of Kawasaki disease (Esper et al., 2005; Shirato et al., 2014), HCoV-OC43 has been shown to have neuroinvasive properties and to cause encephalitis in animal models (reviewed in Bergmann et al., 2006; Cheng et al., 2020). Moreover, both HCoV-OC43 and HCoV-229E were shown to establish persistent infections in cell cultures (Arbour et al., 1999a,b), while the presence of HCoV-OC43 RNA was detected in human brain autopsy samples from multiple sclerosis patients (Arbour et al., 2000; Cheng et al., 2020).

These observations, together with the knowledge that HCoV infection does not induce long-lasting protective immunity (Edridge et al., 2020), highlight the need for broad-spectrum anti-coronavirus drugs. The results described in the present study indicate that nitazoxanide, which has been used for decades in medical practice as a safe and effective antiprotozoal drug (Rossignol et al., 2001, 2006b; Rossignol, 2014), due to its broad-spectrum anti-coronavirus activity, may represent a readily available useful tool in the treatment of seasonal coronavirus infections.

Data availability statement

The raw data supporting the conclusions of this article will be made available by the authors, without undue reservation.

Ethics statement

Ethical approval was not required for the studies on humans in accordance with the local legislation and institutional requirements because only commercially available established cell lines were used.

Author contributions

SPi, ARi, SS, and SPa performed the study on the antiviral activity and the transfection experiments. SPi, ARi, ARo, and SL performed the analysis of protein synthesis and maturation. MS and J-FR designed the study. MS, SPi, and ARi wrote the manuscript. All authors contributed to the article and approved the submitted version.

Funding

This research was supported by Romark Laboratories LC, Tampa, Florida, and by a grant from the Italian Ministry of University and Scientific Research (PRIN project N 2010PHT9NF-006).

Acknowledgments

The authors thank Lia van der Hoek (Academic Medical Center, University of Amsterdam) for providing the HCoV-NL63 Amsterdam-1 strain and the LLC-MK2 cell line. We also thank Elena Romano (University of Rome Tor Vergata) for assistance with confocal microscopy. SPa is enrolled in the PhD Program in Cellular and Molecular Biology, Department of Biology, University of Rome Tor Vergata, Rome, Italy.

Conflict of interest

Financial support for this study was in part provided by Romark Laboratories LC, the company that owns the intellectual property rights related to nitazoxanide. J-FR is an employee and stockholder of Romark Laboratories, LC.

The remaining authors declare that the research was conducted in the absence of any commercial or financial relationships that could be construed as a potential conflict of interest.

Publisher's note

All claims expressed in this article are solely those of the authors and do not necessarily represent those of their affiliated organizations, or those of the publisher, the editors and the reviewers. Any product that may be evaluated in this article, or claim that may be made by its manufacturer, is not guaranteed or endorsed by the publisher.

Supplementary material

The Supplementary material for this article can be found online at: https://www.frontiersin.org/articles/10.3389/fmicb.2023.1206951/full#supplementary-material

References

Amici, C., La Frazia, S., Brunelli, C., Balsamo, M., Angelini, M., and Santoro, M. G. (2015). Inhibition of viral protein translation by indomethacin in vesicular stomatitis virus infection: role of eIF2α kinase PKR. *Cell. Microbiol.* 17, 1391–1404. doi: 10.1111/cmi.12446

Arbour, N., Côté, G., Lachance, C., Tardieu, M., Cashman, N. R., and Talbot, P. J. (1999a). Acute and persistent infection of human neural cell lines by human coronavirus OC43. *J. Virol.* 73, 3338–3350. doi: 10.1128/JVI.73.4.3338-3350.1999

Arbour, N., Day, R., Newcombe, J., and Talbot, P. J. (2000). Neuroinvasion by human respiratory coronaviruses. *J. Virol.* 74, 8913–8921. doi: 10.1128/JVI.74.19.8913-8921.2000

Arbour, N., Ekandé, S., Côté, G., Lachance, C., Chagnon, F., Tardieu, M., et al. (1999b). Persistent infection of human oligodendrocytic and neuroglial cell lines by human coronavirus 229E. *J. Virol.* 73, 3326–3337. doi: 10.1128/JVI.73.4.3326-3337.1999

Ashiru, O., Howe, J. D., and Butters, T. D. (2014). Nitazoxanide, an antiviral thiazolide, depletes ATP-sensitive intracellular Ca(2+) stores. *Virology* 462-463, 135–148. doi: 10.1016/j.virol.2014.05.015

Belardo, G., Cenciarelli, O., La Frazia, S., Rossignol, J. F., and Santoro, M. G. (2015). Synergistic effect of nitazoxanide with neuraminidase inhibitors against influenza A viruses in vitro. *Antimicrob. Agents Chemother.* 59, 1061–1069. doi: 10.1128/AAC.03947-14

Bergmann, C. C., Lane, T. E., and Stohlman, S. A. (2006). Coronavirus infection of the central nervous system: host-virus stand-off. *Nat. Rev. Microbiol.* 4, 121–132. doi: 10.1038/nrmicro1343

Blum, V. F., Cimerman, S., Hunter, J. R., Tierno, P., Lacerda, A., Soeiro, A., et al. (2021). Nitazoxanide superiority to placebo to treat moderate COVID-19 – a pilot prove of concept randomized double-blind clinical trial. *EClinicalMedicine* 37:100981. doi: 10.1016/j.eclinm.2021.100981

Cao, J., Forrest, J. C., and Zhang, X. (2015). A screen of the NIH clinical collection small molecule library identifies potential anti-coronavirus drugs. *Antivir. Res.* 114, 1–10. doi: 10.1016/j.antiviral.2014.11.010

Carabelli, A. M., Peacock, T. P., Thorne, L. G., Harvey, W. T., Hughes, J., COVID-19 Genomics UK Consortium et al. (2023). SARS-CoV-2 variant biology: immune escape,

transmission and fitness. *Nat. Rev. Microbiol.* 21, 162–177. doi: 10.1038/s41579-022-00841-7

Castillo, G., Mora-Díaz, J. C., Nelli, R. K., and Giménez-Lirola, L. G. (2022). Human air-liquid-interface organotypic airway cultures express significantly more ACE2 receptor protein and are more susceptible to HCoV-NL63 infection than monolayer cultures of primary respiratory epithelial cells. *Microbiol. Spectr.* 10:e0163922. doi: 10.1128/spectrum.01639-22

Cheng, Q., Yang, Y., and Gao, J. (2020). Infectivity of human coronavirus in the brain. *EBioMedicine* 56:102799. doi: 10.1016/j.ebiom.2020.102799

Chiu, S. S., Hung Chan, K., Wing Chu, K., Kwan, S. W., Guan, Y., Man Poon, L. L., et al. (2005). Human coronavirus NL63 infection and other coronavirus infections in children hospitalized with acute respiratory disease in Hong Kong, China. *Rev. Infect. Dis.* 40, 1721–1729. doi: 10.1086/430301

Coccia, M., Rossi, A., Riccio, A., Trotta, E., and Santoro, M. G. (2017). Human NF-κB repressing factor acts as a stress-regulated switch for ribosomal RNA processing and nucleolar homeostasis surveillance. *Proc. Natl. Acad. Sci. U. S. A.* 114, 1045–1050. doi: 10.1073/pnas.1616112114

COVID-19 Excess Mortality Collaborators (2022). Estimating excess mortality due to the COVID-19 pandemic: a systematic analysis of COVID-19-related mortality, 2020-21. *Lancet* 399, 1513–1536. doi: 10.1016/S0140-6736(21)02796-3

Cui, J., Li, F., and Shi, Z. (2019). Origin and evolution of pathogenic coronaviruses. *Nat. Rev. Microbiol.* 17, 181–192. doi: 10.1038/s41579-018-0118-9

Dong, Y., Dai, T., Wang, B., Zhang, L., Zeng, L. H., Huang, J., et al. (2021). The way of SARS-CoV-2 vaccine development: success and challenges. *Signal Transduct. Target. Ther.* 6:387. doi: 10.1038/s41392-021-00796-w

Driouich, J. S., Cochin, M., Touret, F., Petit, P. R., Gilles, M., Moureau, G., et al. (2022). Pre-clinical evaluation of antiviral activity of nitazoxanide against SARS-CoV-2. *EBioMedicine* 82:104148. doi: 10.1016/j.ebiom.2022.104148

Edridge, A. W. D., Kaczorowska, J., Hoste, A. C. R., Bakker, M., Klein, M., Loens, K., et al. (2020). Seasonal coronavirus protective immunity is short-lasting. *Nat. Med.* 26, 1691–1693. doi: 10.1038/s41591-020-1083-1

Elazar, M., Liu, M., McKenna, S. A., Liu, P., Gehrig, E. A., Puglisi, J. D., et al. (2009). The anti-hepatitis C agent nitazoxanide induces phosphorylation of eukaryotic initiation factor 2alpha via protein kinase activated by double-stranded RNA activation. *Gastroenterology* 137, 1827–1835. doi: 10.1053/j.gastro.2009.07.056

Esper, F., Shapiro, E. D., Weibel, C., Ferguson, D., Landry, M. L., and Kahn, J. S. (2005). Association between a novel human coronavirus and Kawasaki disease. *J. Infect. Dis.* 191, 499–502. doi: 10.1086/428291

Fowotade, A., Bamidele, F., Egbetola, B., Fagbamigbe, A. F., Adeagbo, B. A., Adefuye, B. O., et al. (2022). A randomized, open-label trial of combined nitazoxanide and atazanavir/ritonavir for mild to moderate COVID-19. *Front. Med.* 9:956123. doi: 10.3389/fmed.2022.956123

Fung, T. S., and Liu, D. X. (2019). Human coronavirus: host-pathogen interaction. *Annu. Rev. Microbiol.* 73, 529–557. doi: 10.1146/annurev-micro-020518-115759

Gandhi, S., Klein, J., Robertson, A. J., Peña-Hernández, M. A., Lin, M. J., Roychoudhury, P., et al. (2022). De novo emergence of a remdesivir resistance mutation during treatment of persistent SARS-CoV-2 infection in an immunocompromised patient: a case report. *Nat. Commun.* 13:1547. doi: 10.1038/s41467-022-29104-y

Gekonge, B., Bardin, M. C., and Montaner, L. J. (2015). Short communication: Nitazoxanide inhibits HIV viral replication in monocyte-derived macrophages. *AIDS Res. Hum. Retrovir.* 31, 237–241. doi: 10.1089/aid.2014.0015

Gorse, G. J., O'Connor, T. Z., Hall, S. L., Vitale, J. N., and Nichol, K. L. (2009). Human coronavirus and acute respiratory illness in older adults with chronic obstructive pulmonary disease. *J. Infect. Dis.* 199, 847–857. doi: 10.1086/597122

Haffizulla, J., Hartman, A., Hoppers, M., Resnick, H., Samudrala, S., Ginocchio, C., et al. (2014). Effect of nitazoxanide in adults and adolescents with acute uncomplicated influenza: a double-blind, randomised, placebo-controlled, phase 2b/3 trial. *Lancet Infect. Dis.* 14, 609–618. doi: 10.1016/S1473-3099(14)70717-0

Hammad, N., Ransy, C., Pinson, B., Talmasson, J., Bréchot, C., Bouillaud, F., et al. (2022). Antiviral effect of thiazolides relies on mitochondrial mild uncoupling. *bioRxiv*. doi: 10.1101/2022.09.16.508272

Hammond, J., Leister-Tebbe, H., Gardner, A., Abreu, P., Bao, W., Wisemandle, W., et al. (2022). Oral nirmatrelvir for high-risk, nonhospitalized adults with Covid-19. *N. Engl. J. Med.* 386, 1397–1408. doi: 10.1056/NEJMoa2118542

Hamre, D., and Procknow, J. J. (1966). A new virus isolated from the human respiratory tract. *Proc. Soc. Exp. Biol. Med.* 121, 190–193. doi: 10.3181/00379727-121-30734

Harvey, W. T., Carabelli, A. M., Jackson, B., Gupta, R. K., Thomson, E. C., Harrison, E. M., et al. (2021). SARS-CoV-2 variants, spike mutations and immune escape. *Nat. Rev. Microbiol.* 19, 409–424. doi: 10.1038/s41579-021-00573-0

Huang, Z., Zheng, H., Wang, Y., Wang, X., Wang, C., Liu, Y., et al. (2023). The modulation of metabolomics and antioxidant stress is involved in the effect of nitazoxanide against influenza a virus *in vitro*. *Acta Virol.* 67:11612. doi: 10.3389/av.2023.11612

Jacomy, H., Fragoso, G., Almazan, G., Mushynski, W. E., and Talbot, P. J. (2006). Human coronavirus OC43 infection induces chronic encephalitis leading to disabilities in BALB/C mice. *Virology* 349, 335–346. doi: 10.1016/j.virol.2006.01.049

Jasenosky, L. D., Cadena, C., Mire, C. E., Borisevich, V., Haridas, V., Ranjbar, S., et al. (2019). The FDA-approved oral drug nitazoxanide amplifies host antiviral responses and inhibits Ebola virus. *iScience.* 19, 1279–1290. doi: 10.1016/j.isci.2019.07.003

Jayk Bernal, A., Gomes da Silva, M. M., Musungaie, D. B., Kovalchuk, E., Gonzalez, A., Delos Reyes, V., et al. (2022). Molnupiravir for oral treatment of Covid-19 in nonhospitalized patients. *N. Engl. J. Med.* 386, 509–520. doi: 10.1056/NEJMoa2116044

Korba, B. E., Montero, A. B., Farrar, K., Gaye, K., Mukerjee, S., Ayers, M. S., et al. (2008). Nitazoxanide, tizoxanide and other thiazolides are potent inhibitors of hepatitis B virus and hepatitis C virus replication. *Antivir. Res.* 77, 56–63. doi: 10.1016/j.antiviral.2007.08.005

La Frazia, S., Ciucci, A., Arnoldi, F., Coira, M., Gianferretti, P., Angelini, M., et al. (2013). Thiazolides, a new class of antiviral agents effective against rotavirus infection, target viral morphogenesis, inhibiting viroplasm formation. *J. Virol.* 87, 11096–11106. doi: 10.1128/JVI.01213-13

La Frazia, S., Piacentini, S., Riccio, A., Rossignol, J. F., and Santoro, M. G. (2018). The second-generation thiazolide haloxanide is a potent inhibitor of avian influenza virus replication. *Antivir. Res.* 157, 159–168. doi: 10.1016/j.antiviral.2018.06.008

Lam, K. K., Zheng, X., Forestieri, R., Balgi, A. D., Nodwell, M., Vollett, S., et al. (2012). Nitazoxanide stimulates autophagy and inhibits mTORC1 signaling and intracellular proliferation of *Mycobacterium tuberculosis*. *PLoS Pathog.* 8:e1002691. doi: 10.1371/journal.ppat.1002691

Lamers, M. M., and Haagmans, B. L. (2022). SARS-CoV-2 pathogenesis. *Nat. Rev. Microbiol.* 20, 270–284. doi: 10.1038/s41579-022-00713-0

Li, F. (2016). Structure, function, and evolution of coronavirus spike proteins. *Annu. Rev. Virol.* 3, 237–261. doi: 10.1146/annurev-virology-110615-042301

Li, G., and De Clercq, E. (2020). Therapeutic options for the 2019 novel coronavirus (2019-nCoV). *Nat. Rev. Drug Discov.* 19, 149–150. doi: 10.1038/d41573-020-00016-0

Lim, Y. X., Ng, Y. L., Tam, J. P., and Liu, D. (2016). Human coronaviruses: a review of virus–host interactions. *Diseases* 4:26. doi: 10.3390/diseases4030026

Liu, D. X., Liang, J. Q., and Fung, T. S. (2021). "Human coronavirus-229E, -OC43, -NL63, and -HKU1 (Coronaviridae)" in *Encyclopedia of Virology*. eds. D. Bamford and M. Zuckerman. Elsevier Ltd., Academic Press, 4th ed, 428–440. doi: 10.1016/B978-0-12-809633-8.21501-X

Loo, S. L., Wark, P. A. B., Esneau, C., Nichol, K. S., Hsu, A. C. Y., and Bartlett, N. W. (2020). Human coronaviruses 229E and OC43 replicate and induce distinct antiviral responses in differentiated primary human bronchial epithelial cells. *Am. J. Physiol. Lung Cell. Mol. Physiol.* 319, L926–L931. doi: 10.1152/ajplung.00374.2020

Milewska, A., Zarebski, M., Nowak, P., Stozek, K., Potempa, J., and Pyrc, K. (2014). Human coronavirus NL63 utilizes heparan sulfate proteoglycans for attachment to target cells. *J. Virol.* 88, 13221–13230. doi: 10.1128/JVI.02078-14

Miorin, L., Mire, C. E., Ranjbar, S., Hume, A. J., Huang, J., Crossland, N. A., et al. (2022). The oral drug nitazoxanide restricts SARS-CoV-2 infection and attenuates disease pathogenesis in Syrian hamsters. *bioRxiv*. doi: 10.1101/2022.02.08.479634

Morfopoulou, S., Brown, J. R., Davies, E. G., Anderson, G., Virasami, A., Qasim, W., et al. (2016). Human coronavirus OC43 associated with fatal encephalitis. *N. Engl. J. Med.* 375, 497–498. doi: 10.1056/NEJMc1509458

Ohuchi, R., Ohuchi, M., Garten, W., and Klenk, H. D. (1997). Oligosaccharides in the stem region maintain the influenza virus hemagglutinin in the metastable form required for fusion activity. *J. Virol.* 71, 3719–3725. doi: 10.1128/jvi.71.5.3719-3725.1997

Pene, F., Merlat, A., Vabret, A., Rozenberg, F., Buzyn, A., Dreyfus, F., et al. (2003). Coronavirus 229E-related pneumonia in immunocompromised patients. *Clin. Infect. Dis.* 37, 929–932. doi: 10.1086/377612

Petersen, T., Lee, Y. J., Osinusi, A., Amorosa, V. K., Wang, C., Kang, M., et al. (2016). Interferon stimulated gene expression in HIV/HCV coinfected patients treated with nitazoxanide/peginterferon-alfa-2a and ribavirin. *AIDS Res. Hum. Retrovir.* 32, 660–667. doi: 10.1089/aid.2015.0236

Piacentini, S., la Frazia, S., Riccio, A., Pedersen, J. Z., Topai, A., Nicolotti, O., et al. (2018). Nitazoxanide inhibits paramyxovirus replication by targeting the fusion protein folding: role of glycoprotein-specific thiol oxidoreductase ERp57. *Sci. Rep.* 8:10425. doi: 10.1038/s41598-018-28172-9

Pizzato Scomazzon, S., Riccio, A., Santopolo, S., Lanzilli, G., Coccia, M., Rossi, A., et al. (2019). The zinc-finger AN1-type domain 2a gene acts as a regulator of cell survival in human melanoma: role of E3-ligase cIAP2. *Mol. Cancer Res.* 17, 2444–2456. doi: 10.1158/1541-7786.MCR-19-0243

Planas, D., Bruel, T., Grzelak, L., Guivel-Benhassine, F., Staropoli, I., Porrot, F., et al. (2021). Sensitivity of infectious SARS-CoV-2 B.1.1.7 and B.1.351 variants to neutralizing antibodies. *Nat. Med.* 27, 917–924. doi: 10.1038/s41591-021-01318-5

Pyrc, K., Bosch, B. J., Berkhout, B., Jebbink, M. F., Dijkman, R., Rottier, P., et al. (2006). Inhibition of human coronavirus NL63 infection at early stages of the replication cycle. *Antimicrob. Agents Chemother.* 50, 2000–2008. doi: 10.1128/AAC.01598-05

Riccio, A., Santopolo, S., Rossi, A., Piacentini, S., Rossignol, J. F., and Santoro, M. G. (2022). Impairment of SARS-CoV-2 spike glycoprotein maturation and fusion activity by nitazoxanide: an effect independent of spike variants emergence. *Cell. Mol. Life Sci.* 79:227. doi: 10.1007/s00018-022-04246-w

Risku, M., Lappalainen, S., Räsänen, S., and Vesikari, T. (2010). Detection of human coronaviruses in children with acute gastroenteritis. *J. Clin. Virol.* 48, 27–30. doi: 10.1016/j.jcv.2010.02.013

Rocco, P. R. M., Silva, P. L., Cruz, F. F., Melo-Junior, M. A. C., Tierno, P. F. G. M. M., Moura, M. A., et al. (2021). Early use of nitazoxanide in mild Covid-19 disease: randomised, placebo-controlled trial. *Eur. Respir. J.* 58:2003725. doi: 10.1183/13993003.03725-2020

Rocco, P. R. M., Silva, P. L., Cruz, F. F., Tierno, P. F. G. M. M., Rabello, E., Junior, J. C., et al. (2022). Nitazoxanide in patients hospitalized with covid-19 pneumonia: a multicentre, randomized, double-blind, placebo-controlled trial. *Front. Med.* 9:844728. doi: 10.3389/fmed.2022.844728

Rossignol, J. F. (2014). Nitazoxanide: a first-in-class broad-spectrum antiviral agent. *Antivir. Res.* 110, 94–103. doi: 10.1016/j.antiviral.2014.07.014

Rossignol, J. F. (2016). Nitazoxanide, a new drug candidate for the treatment of Middle East respiratory syndrome coronavirus. *J. Infect. Public Health* 9, 227–230. doi: 10.1016/j.jiph.2016.04.001

Rossignol, J. F., Abu-Zekry, M., Hussein, A., and Santoro, M. G. (2006a). Effect of nitazoxanide for treatment of severe rotavirus diarrhoea: randomised double-blind placebo-controlled trial. *Lancet* 368, 124–129. doi: 10.1016/S0140-6736(06)68852-1

Rossignol, J. F., Ayoub, A., and Ayers, M. S. (2001). Treatment of diarrhea caused by Giardia intestinalis and *Entamoeba histolytica* or *E. dispar*: a randomized, double-blind, placebo-controlled study of nitazoxanide. *J. Infect. Dis.* 184, 381–384. doi: 10.1086/322038

Rossignol, J. F., Bardin, M. C., Fulgencio, J., Mogelnicki, D., and Bréchot, C. (2022a). A randomized double-blind placebo-controlled clinical trial of nitazoxanide for treatment of mild or moderate COVID-19. *eClinicalMedicine.* 45:101310. doi: 10.1016/j.eclinm.2022.101310

Rossignol, J. F., Elfert, A., el–Gohary, Y., and Keeffe, E. B. (2009a). Improved virologic response in chronic hepatitis C genotype 4 treated with nitazoxanide, peginterferon, and ribavirin. *Gastroenterology* 136, 856–862. doi: 10.1053/j.gastro.2008.11.037

Rossignol, J. F., Kabil, S. M., el–Gohary, Y., and Younis, A. M. (2006b). Effect of nitazoxanide in diarrhea and enteritis caused by Cryptosporidium species. *Clin. Gastroenterol. Hepatol.* 4, 320–324. doi: 10.1016/j.cgh.2005.12.020

Rossignol, J. F., La Frazia, S., Chiappa, L., Ciucci, A., and Santoro, M. G. (2009b). Thiazolides, a new class of anti-influenza molecules targeting viral hemagglutinin at the post-translational level. *J. Biol. Chem.* 284, 29798–29808. doi: 10.1074/jbc.M109.029470

Rossignol, J. F., Tijsma, A. S. L., and van Baalen, C. A. (2022b). Mechanism of antiviral activity of Nitazoxanide: effect on adenosine triphosphate in influenza-virus infected Madin Darby canine kidney cells. *J. Infect. Dis. Preve. Med.* 10:262. doi: 10.35841/2329-8731.22.10.262

Santopolo, S., Riccio, A., Rossi, A., and Santoro, M. G. (2021b). The proteostasis guardian HSF1 directs the transcription of its paralog and interactor HSF2 during proteasome dysfunction. *Cell. Mol. Life Sci.* 78, 1113–1129. doi: 10.1007/s00018-020-03568-x

Santopolo, S., Riccio, A., and Santoro, M. G. (2021a). The biogenesis of SARS-CoV-2 spike glycoprotein: multiple targets for host-directed antiviral therapy. *Biochem. Biophys. Res. Commun.* 538, 80–87. doi: 10.1016/j.bbrc.2020.10.080

Santoro, M. G., Amici, C., Elia, G., Benedetto, A., and Garaci, E. (1989). Inhibition of virus protein glycosylation as the mechanism of the antiviral action of prostaglandin A in Sendai virus-infected cells. *J. Gen. Virol.* 70, 789–800. doi: 10.1099/0022-1317-70-4-789

Santoro, M. G., and Carafoli, E. (2020). Remdesivir: from Ebola to COVID-19. *Biochem. Biophys. Res. Commun.* 538, 145–150. doi: 10.1016/j.bbrc.2020.11.043

Santoro, M. G., Ciucci, A., Gianferretti, P., Belardo, G., La Frazia, S., Carta, S., et al. (2007). Thiazolides: a new class of broad-spectrum antiviral drugs targeting virus maturation. *Antivir. Res.* 74:A31. doi: 10.1016/j.antiviral.2007.01.019

Santoro, M. G., Favalli, C., Mastino, A., Jaffe, B. M., Esteban, M., and Garaci, E. (1988). Antiviral activity of a synthetic analog of prostaglandin A in mice infected with influenza A virus. *Arch. Virol.* 99, 89–100. doi: 10.1007/BF01311026

Santoro, M. G., Jaffe, B. M., Garaci, E., and Esteban, M. (1982). Antiviral effect of prostaglandins of the A series: inhibition of vaccinia virus replication in cultured cells. *J. Gen. Virol.* 63, 435–440. doi: 10.1099/0022-1317-63-2-435

Shirato, K., Imada, Y., Kawase, M., Nakagaki, K., Matsuyama, S., and Taguchi, F. (2014). Possible involvement of infection with human coronavirus 229E, but not NL63, in Kawasaki disease. *J. Med. Virol.* 86, 2146–2153. doi: 10.1002/jmv.23950

Shou, J., Wang, M., Cheng, X., Wang, X., Zhang, L., Liu, Y., et al. (2020). Tizoxanide induces autophagy by inhibiting PI3K/Akt/mTOR pathway in RAW264.7 macrophage cells. *Arch. Pharm. Res.* 43, 257–270. doi: 10.1007/s12272-019-01202-4

Sicari, D., Chatziioannou, A., Koutsandreas, T., Sitia, R., and Chevet, E. (2020). Role of the early secretory pathway in SARS-CoV-2 infection. *J. Cell Biol.* 219:e202006005. doi: 10.1083/jcb.202006005

Silva, M., Espejo, A., Pereyra, M. L., Lynch, M., Thompson, M., Taconelli, H., et al. (2021). Efficacy of Nitazoxanide in reducing the viral load in COVID-19 patients. Randomized, placebo-controlled, single-blinded, parallel group, pilot study. *medRxiv*. doi: 10.1101/2021.03.03.21252509

Sokhela, S., Bosch, B., Hill, A., Simmons, B., Woods, J., Johnstone, H., et al. (2022). Randomized clinical trial of nitazoxanide or sofosbuvir/daclatasvir for the prevention of SARS-CoV-2 infection. *J. Antimicrob. Chemother.* 77, 2706–2712. doi: 10.1093/jac/dkac266

Son, J., Huang, S., Zeng, Q., Bricker, T. L., Case, J. B., Zhou, J., et al. (2022). JIB-04 has broad-spectrum antiviral activity and inhibits d3SARS-CoV-2 replication and coronavirus pathogenesis. *MBio* 13:e0337721. doi: 10.1128/mbio.03377-21

Stachulski, A. V., Rossignol, J. F., Pate, S., Taujanskas, J., Robertson, C. M., Aerts, R., et al. (2021). Synthesis, antiviral activity, preliminary pharmacokinetics and structural parameters of thiazolide amine salts. *Future Med. Chem.* 13, 1731–1741. doi: 10.4155/fmc-2021-0055

Stevens, L. J., Pruijssers, A. J., Lee, H. W., Gordon, C. J., Tchesnokov, E. P., Gribble, J., et al. (2022). Mutations in the SARS-CoV-2 RNA-dependent RNA polymerase confer resistance to remdesivir by distinct mechanisms. *Sci. Transl. Med.* 14:eabo0718. doi: 10.1126/scitranslmed.abo0718

Tang, X., Wu, C., Li, X., Song, Y., Yao, X., Wu, X., et al. (2020). On the origin and continuing evolution of SARS-CoV-2. *Natl. Sci. Rev.* 7, 1012–1023. doi: 10.1093/nsr/nwaa036

Trabattoni, D., Gnudi, F., Ibba, S. V., Saulle, I., Agostini, S., Masetti, M., et al. (2016). Thiazolides elicit anti-viral innate immunity and reduce HIV replication. *Sci. Rep.* 6:27148. doi: 10.1038/srep27148

Tyrrell, D. A. J., and Bynoe, M. L. (1965). Cultivation of a novel type of common cold virus in organ culture. *Br. Med. J.* 1, 1467–1470. doi: 10.1136/bmj.1.5448.1467

van der Hoek, L., Pyrc, K., Jebbink, M. F., Vermeulen-Oost, W., Berkhout, R. J. M., Wolthers, K. C., et al. (2004). Identification of a new human coronavirus. *Nat. Med.* 10, 368–373. doi: 10.1038/nm1024

Vijgen, L., Keyaerts, E., Moës, E., Maes, P., Duson, G., and van Ranst, M. (2005). Development of one-step, real-time, quantitative reverse transcriptase PCR assays for absolute quantitation of human coronaviruses OC43 and 229E. *J. Clin. Microbiol.* 43, 5452–5456. doi: 10.1128/JCM.43.11.5452-5456.2005

Wahl, A., Gralinski, L. E., Johnson, C. E., Yao, W., Kovarova, M., Dinnon, K. H. III, et al. (2021). SARS-CoV-2 infection is effectively treated and prevented by EIDD-2801. *Nature* 591, 451–457. doi: 10.1038/s41586-021-03312-w

Wang, M., Cao, R., Zhang, L., Yang, X., Liu, J., Xu, M., et al. (2020). Remdesivir and chloroquine effectively inhibit the recently emerged novel coronavirus (2019-nCoV) in vitro. *Cell Res.* 30, 269–271. doi: 10.1038/s41422-020-0282-0

Wang, X., Shen, C., Liu, Z., Peng, F., Chen, X., Yang, G., et al. (2018). Nitazoxanide, an antiprotozoal drug, inhibits late-stage autophagy and promotes ING1-induced cell cycle arrest in glioblastoma. *Cell Death Dis.* 9:1032. doi: 10.1038/s41419-018-1058-z

Wen, W., Chen, C., Tang, J., Wang, C., Zhou, M., Cheng, Y., et al. (2022). Efficacy and safety of three new oral antiviral treatment (molnupiravir, fluvoxamine and Paxlovid) for COVID-19: a meta-analysis. *Ann. Med.* 54, 516–523. doi: 10.1080/07853890.2022.2034936

Woo, P. C. Y., Lau, S. K. P., Chu, C., Chan, K. H., Tsoi, H. W., Huang, Y., et al. (2005). Characterization and complete genome sequence of a novel coronavirus, coronavirus HKU1, from patients with pneumonia. *J. Virol.* 79, 884–895. doi: 10.1128/JVI.79.2.884-895.2005

Xu, C., and Ng, D. T. W. (2015). Glycosylation-directed quality control of protein folding. *Nat. Rev. Mol. Cell Biol.* 16, 742–752. doi: 10.1038/nrm4073

Zhang, Z., Liu, W., Zhang, S., Wei, P., Zhang, L., Chen, D., et al. (2022). Two novel human coronavirus OC43 genotypes circulating in hospitalized children with pneumonia in China. *Emerg. Microbes Infect.* 11, 168–171. doi: 10.1080/22221751.2021.2019560

frontiers | Frontiers in Microbiology

TYPE Original Research
PUBLISHED 26 September 2023
DOI 10.3389/fmicb.2023.1251275

OPEN ACCESS

EDITED BY
Gaëtan Ligat,
Université Toulouse III Paul Sabatier, France

REVIEWED BY
Carlos Minahk,
CCT CONICET Tucuman, Argentina
Pamela Del Carmen Mancha-Agresti,
Federal University of Minas Gerais, Brazil
Mindy Engevik,
Medical University of South Carolina,
United States

*CORRESPONDENCE
Xingcui Zhang
✉ zhangxc923@163.com
Zhenhui Song
✉ szh7678@126.com

†These authors have contributed equally to this work

RECEIVED 01 July 2023
ACCEPTED 05 September 2023
PUBLISHED 26 September 2023

CITATION
Kan Z, Zhang S, Liao G, Niu Z, Liu X, Sun Z, Hu X, Zhang Y, Xu S, Zhang J, Zou H, Zhang X and Song Z (2023) Mechanism of *Lactiplantibacillus plantarum* regulating Ca^{2+} affecting the replication of PEDV in small intestinal epithelial cells.
Front. Microbiol. 14:1251275.
doi: 10.3389/fmicb.2023.1251275

Mechanism of *Lactiplantibacillus plantarum* regulating Ca^{2+} affecting the replication of PEDV in small intestinal epithelial cells

Zifei Kan[1,2†], Shujuan Zhang[1†], Guisong Liao[1†], Zheng Niu[1,3], Xiangyang Liu[1,4], Zhiwei Sun[1], Xia Hu[1], Yiling Zhang[1,5], Shasha Xu[1], Jingyi Zhang[1], Hong Zou[1], Xingcui Zhang[1*] and Zhenhui Song[1,6*]

[1]College of Veterinary Medicine, Southwest University, Chongqing, China, [2]School of Medicine, University of Electronic Science and Technology of China, Chengdu, China, [3]College of Veterinary Medicine, Northwest A and F University, Shanxi, China, [4]College of Veterinary Medicine, Xinjiang Agricultural University, Ürümqi, China, [5]College of Animal Scienceand Technology, Chongqing Three Gorges Vocational College, Chongqing, China, [6]Immunology Research Center, Medical Research Institute, Southwest University, Chongqing, China

Porcine epidemic diarrhea virus (PEDV) mainly invades the small intestine and promotes an inflammatory response, eventually leading to severe diarrhea, vomiting, dehydration, and even death of piglets, which seriously threatens the economic development of pig farming. In recent years, researchers have found that probiotics can improve the intestinal microenvironment and reduce diarrhea. At the same time, certain probiotics have been shown to have antiviral effects; however, their mechanisms are different. Herein, we aimed to investigate the inhibitory effect of *Lactiplantibacillus plantarum* supernatant (LP-1S) on PEDV and its mechanism. We used IPEC-J2 cells as a model to assess the inhibitory effect of LP-1S on PEDV and to further investigate the relationship between LP-1S, Ca^{2+}, and PEDV. The results showed that a divalent cation chelating agent (EGTA) and calcium channel inhibitors (Bepridil hydrochloride and BAPTA-acetoxymethylate) could inhibit PEDV proliferation while effectively reducing the intracellular Ca^{2+} concentration. Furthermore, LP-1S could reduce PEDV-induced loss of calcium channel proteins (TRPV6 and PMCA1b), alleviate intracellular Ca^{2+} accumulation caused by PEDV infection, and promote the balance of intra- and extracellular Ca^{2+} concentrations, thereby inhibiting PEDV proliferation. In summary, we found that LP-1S has potential therapeutic value against PEDV, which is realized by modulating Ca^{2+}. This provides a potential new drug to treat PEDV infection.

KEYWORDS

***Lactiplantibacillus plantarum*, LP-1S, PEDV, Ca^{2+}, intestinal epithelial cells**

1. Introduction

Porcine epidemic diarrhea (PED) is an acute, highly contagious intestinal disease of pigs caused by Porcine epidemic diarrhea virus (PEDV) (Cao et al., 2015). The virus mainly colonizes the intestinal mucosa of the host, with the largest amount of virus found in the small intestine mucosa, but can also be detected in the lung, heart, and liver (Narayanan et al., 2012). The clinical signs of the disease are vomiting and watery diarrhea, which consequently lead dehydration in newborn piglets, eventually leading to their death (Ding et al., 2014). PED is

more frequent in winter when it is cold, and has a very high mortality rate for piglets within 2 weeks of age, causing serious economic losses to the pig industry (Wu et al., 2020). PED outbreaks caused by highly virulent PEDV variants are still occurring in pig farms in several countries or regions, and existing vaccines or drugs cannot achieve the desired control of PED. Moreover, the continuous detoxification of sick pigs poses additional challenges to the prevention and control of this disease (Jang et al., 2022; Yao et al., 2023). Therefore, there is an urgent need to develop new drugs for this infectious disease.

Ca^{2+} acts as an important second messenger in intracellular signal transduction processes. Ca^{2+} is essential for the transmembrane transmission of biological signals, the regulation of glandular secretion, and the maintenance of acid-base homeostasis in the body (Seo et al., 2015; Hussey et al., 2023). The maintenance of calcium homeostasis depends on various calcium channel proteins [e.g., transient receptor potential cation channel subfamily V member 6 (TRPV6) and stromal interaction molecule (STIM)] in the membranes of the endoplasmic reticulum, Golgi apparatus, mitochondria, and other cellular organelles (Liou et al., 2005; Bibollet et al., 2023), transporters [sodium-calcium exchanger Na(+)/Ca(2+)-Exchange Protein 1 (NCX-1) (Tarifa et al., 2022)], and ion pumps [e.g., the cell membrane calcium pump, plasma membrane calcium-transporting ATPase 1 (PMCA1b)] (Rodrat et al., 2022; Dai et al., 2023). Disruption of any of these components can affect calcium homeostasis. Under normal conditions, the concentration of free intracellular Ca^{2+} is much lower than the concentration of Ca^{2+} in other calcium pools, such as the endoplasmic reticulum and outside the cell (Peng et al., 2001). In general, the transcellular pathway for intestinal Ca^{2+} uptake consists of three steps (Guo et al., 2016): (i) Crossing the brush border membrane (BBM) of the intestinal cells via the epithelial Ca^{2+} channel (TRPV6); (ii) binding to proteins with high Ca^{2+} affinity to form calcium-binding protein-D9k (CaBPD9k), which in turn moves from the BBM to the basolateral membrane (BLM); and (iii) extracellular excretion via the plasma membrane Ca^{2+}-ATPase (PMCA1b/Ca^{2+} pump) and Na^{+}/Ca^{2+} exchanger (NCX1). Among them, TRPV6 and PMCA1b, as calcium channel proteins, have received much research attention because they are the major Ca^{2+} transport proteins in the intestinal epithelium and have important roles in maintaining intra- and extracellular homeostasis and controlling ions entering and leaving the cell (Zhao et al., 2022).

In recent years, research has shown that a variety of probiotics can maintain microbial homeostasis in the intestinal environment and prevent diarrhea (Hu et al., 2022; Liang et al., 2023). Antiviral research into probiotics and their metabolites has also become a hot topic (Leblanc et al., 2022; Liu et al., 2022) *Lactiplantibacillus plantarum* (Lp) significantly reduced the cytopathic effects of respiratory syncytial virus (RSV), influenza B virus, and HCoV-229E coronavirus (Spacova et al., 2023). Lp is a gram-positive facultative anaerobic bacterium that is widely found in nature, is commonly found in various fermented foods, and is one of the important flora of the gut microbiota. Its optimum growth temperature is 30 ~ 37°C, its optimum pH is about 7.0, and the colony growth shape is white opaque dots on MRS (De Man, Rogosa and Sharpe) solid medium. A strain of *Lactobacillus plantarum* was successfully isolated from the cecum of piglets in a pig farm in Rongchang, Chongqing, China, and named LP-1 (GenBank accession no. MH727586.1). Its main metabolites were found to include acids (33.96%), amino acids (and their derivatives) (32.08%), and polysaccharides (15.1%) through the pristine analysis using gas chromatography–mass spectrometry (GC–MS) (Huang et al., 2021) LP, as a probiotic, also has the role of promoting intestinal health. Consequently, the present study aimed to investigate the inhibitory effect of *Lactiplantibacillus plantarum* supernatant (LP-1S) on PEDV and its mechanism.

2. Materials and methods

2.1. Cells, viruses, bacteria, reagents, and antibodies

African green monkey kidney cells (Vero, used at 10th generation) and porcine small intestinal epithelial cells (IPEC-J2, used at 10th generations) were purchased from Suer Biotech (Shanghai, China) and were cultured in Dulbecco's modified Eagle's medium (DMEM) medium with 10% fetal bovine serum, at 37°C, in a 5% CO_2 cell incubator. PEDV-LJX strain and PEDV N mouse-derived monoclonal antibodies were kindly donated by GuangLiang Liu, Researcher, Lanzhou Veterinary Research Institute, Chinese Academy of Agricultural Sciences. *Lactiplantibacillus plantarum* LP-1 was obtained by pre-laboratory isolation. TRPV6 polyclonal rabbit antibodies (Vol: 50 μL, Cat No: 13411-1AP, Dilution: 1:4,000), horseradish peroxidase (HRP)-goat anti-mouse IgG (H + L) (Vol: 100 μL, Cat No: D110087-0100, Dilution: 1:4,000) and β-actin goat anti-rabbit antibody (Vol: 500 μL, Cat No: SA00001-2, Dilution: 1:5,000) were purchased from Proteintech. PMCA1b Polyclonal Rabbit Antibodies (Vol: 100 μL, Cat No: GR3312280-1, Dilution: 1:2,000) were purchased from Abcam (Cambridge, MA, United States). Fura-2-acetoxymethyl ester (Fura-2 AM) and $CaCl_2$ were purchased from Beyotime Biotechnology Co. (Shanghai, China). EGTA, Fluo3-AM, and BAPTA-AM were purchased from Solarbio (Beijing, China). Bepridil hydrochloride (BP) was purchased from MCE (Monmouth junction, NJ, United States). Ca^{2+} standard solution (1,000 μg/mL) was purchased from National Research Center for Reference Materials, Beijing, China.

2.2. Preparation of LP-1S

Lactiplantibacillus plantarum LP-1 was inoculated onto MRS solid medium and incubated at 37°C. After 24 h, single colonies were picked, inoculated in MRS liquid medium, incubated at 37°C with shaking 180 rpm for 12 h until they reached a measured OD_{595} value between 0.8 ~ 0.9, and centrifuged at 3,000 × *g* for 10 min. The supernatant was retained and filtered using a 0.44 μm–0.22 μm microporous filter membrane gradient. The filtered supernatant (LP-S1) was stored at −20°C for a short time.

2.3. 3-(4,5-dimethylthiazol-2-yl)-2,5-diphenyltetrazolium bromide (MTT) assay

Firstly, LP-1S was diluted with DMEM basal medium to 0, 1/2, 1/4, 1/8, 1/16, 1/32, and 1/64 times the original concentration.

Different dilutions of LP-1S were added to each well of a microtiter plate, containing 3.6×10^6 cells per well. A positive control group (PEDV-infected group) and a negative control were set, and the adsorption culture was replaced with DMEM maintenance solution after 90 min. When the cytopathic effect (CPE) of the PEDV-infected group reached 70%, the maintenance solution was discarded, the wells were washed three times with 0.01 M phosphate-buffered saline (PBS), 5 mg/mL MTT reagent was added to each well, the plate was incubated at 37°C for 4 h to allow the formation of formazan crystals, and the OD_{575} values were then measured. Cell viability was calculated, and the IC50 of LP-S1 was calculated: lgIC50 = Xm-I (P-(3-Pm-Pn)/4) [in which Xm: lg maximum dose, I: lg (maximum dose/adjacent dose), P: sum of positive response rates, Pm: maximum positive response rate, Pn: minimum positive response rate].

2.4. $TCID_{50}$ PEDV virulence assay

Cell samples from LP-1S pretreated PEDV-infected, PEDV-infected, and negative control cell groups were collected at different time points and centrifuged to collect supernatants. Vero cells in 96-well plates were grown to 90%, and different dilution gradients of LP-1S were inoculated into 96-well plates containing DMEM basal medium, and after the viruses were incubated separately for 1.5 h, the DMEM basal medium was replaced and the CPE was observed daily. Finally, the $TCID_{50}$ of each PEDV group was measured according to the Reed-Muench method (Zhang et al., 2012).

2.5. Western blotting assay

Quantified protein samples were subjected to sodium dodecyl sulfate-polyacrylamide gel electrophoresis, then the separated proteins were transferred to polyvinylidene fluoride membranes (Merck Millipore, Billerica, MA, United States), which were blocked in 5% skim milk for 1.5 h, followed by incubation with the corresponding primary antibodies overnight at 4°C. Next day, the membranes were incubated with the corresponding secondary antibodies for 90 min at 37°C. The immunoreactive protein bands were visualized using the FX5 imaging system (VILBER, Marne-la-vallée, Ile-de-France, France), and the grayscale values were analyzed.

2.6. Quantitative real-time reverse transcription PCR

2.6.1. RNA extraction and reverse transcription

Total RNA was extracted from cells and reverse transcribed to cDNA using RNAiso plus (Invitrogen, Waltham, MA, United States) and 5×PrimeScript RT Master Mix (Promega, Madison, WI, United States).

2.6.2. Relative fluorescence quantitative PCR

The full sequences of *TRPV6*, *PMCA1b*, and *ACTB* (β-actin genes) were downloaded from GenBank. Primers were designed against the sequences using Primer Premier 5.0 software (Premier Biosoft, San Francisco, CA, United States). The primer sequences are shown in Table 1. The cDNA was amplified using quantitative real-time PCR (qPCR) using ACTB as an internal reference by Biotech Co. Ltd., Shanghai, China. The reaction system comprised: 10 μL SYBR PreMix ExTaq II (Takara, Shiga, Japan), 0.5 μL forward primer, 0.5 μL reverse primer, 2 μL cDNA, and 7 μL H2O, in a 20 μL reaction. The reaction conditions were: 95°C for 30 s; followed by 40 cycles of 95°C for 5 s and 60°C for 15 s. Each sample was repeated three times. The primers are shown in in Table 1. The $2^{-\Delta\Delta Ct}$ method was used to analyze the expression of the corresponding mRNAs (Livak and Schmittgen, 2001).

2.6.3. Absolute fluorescence quantitative PCR

The PEDV-M primer sequences were downloaded from GenBank (Table 2). The PEDV gene copy number was detected using absolute fluorescence quantitative PCR. The reaction parameters were: pre-denaturation at 95°C for 30 s; followed by 40 cycles of denaturation at 95°C for 5 s, annealing at 54°C for 30 s, and 40 cycles. The linear relationship between cycle threshold (CT) values and copy number was analyzed using the Bio-Rad CFX Manager software random matrix method to calculate the copy number of the *PEDV M* gene.

2.6.4. Transfection with TRPV6 and PMCA1b interference plasmids

The shRNA sequence was designed and synthesized by Wuhan Jinkairui Biotechnology Co. (Figure 1) and then ligated with the interference vector pLVX-shRNA2Puro. 3.6×106 cells were inoculated in each well, and the cells were removed from the incubator when they reached 90% confluence at the time of transfection. Add 0.8 μg of plasmid DNA into 50 μL Opti-MEM medium and mix gently. Add 1.6 μL of TransIntroM EL into the diluted plasmid DNA, mix gently, and let it stand at room temperature for 15 min. Add the plasmid DNA-TransIntromM EL complex into the cells and incubate at 37°C CO2 for 6 h. After transfection, remove the cells from the incubator. The cells were incubated at 37°C in a CO2 incubator, and after 6 h of transfection, the medium was changed and the culture was continued for 36 h.

2.7. Calcium ion fluorescent probe (Fluo3-Am) analysis

Fluo3-AM was diluted to a 2 mM Fluo3-AM stock solution using dimethyl sulfoxide and stored at −20°C for later use. The preserved

TABLE 1 Primer sequences for *TRPV6*, *PMCA1b*, and *ACTB* (β-actin).

Gene	GenBank accession	Sequences (5′–3′)
TRPV6	CP071569.1	F: CCTGCTGGAACTTCTTGTCACCTC
		R: AAGTACCGCCGCCCGTATCTC
PMCA1b	X53456.1	F: CCTGCTGGAACTTCTTGTCACCTC
		R: CTGCTCCTGCTCAATTCGACTCTG
ACTB	XM_003124280.5	F: CTCTTCCAGCCCTCCTTCC
		R: GGTCCTTGCGGATGTCG

TABLE 2 Primer sequences for the *PEDV M* gene.

Gene	GenBank accession	Sequences (5′–3′)
PEDV M	AF353511.1	F: AGGTTGCTACTGGCGTACAG
		R: GAGTAGTCGCCGTGTTTGGA

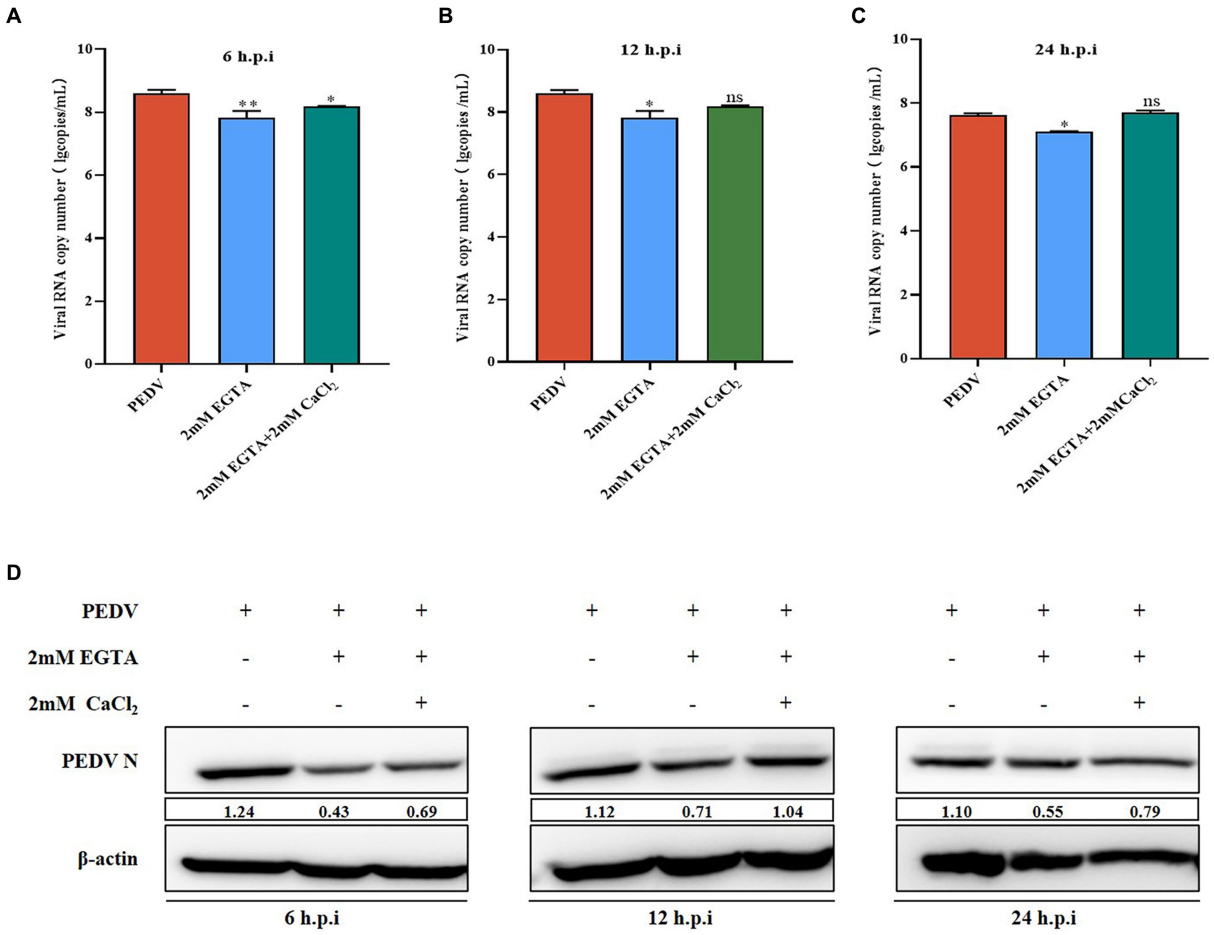

FIGURE 1
Effect of EGTA and $CaCl_2$ pretreatment on PEDV. **(A)** PEDV-M mRNA levels at 6 h after EGTA and $CaCl_2$ pretreatment in PEDV-infected cells; **(B)** PEDV-M mRNA levels at 12 h after EGTA and $CaCl_2$ pretreatment in PEDV-infected cells; **(C)** PEDV-M mRNA levels at 24 h after EGTA and $CaCl_2$ pretreatment in PEDV-infected cells; **(D)** PEDV-N protein levels at different time points after EGTA and $CaCl_2$ pretreatment in PEDV-infected cells.

Fluo3-AM stock solution was diluted with 0.1 M Hanks' Balanced Salt Solution (HBSS; Beyotime Biotechnology Co.), added to cells in a microtiter plate (3.6×10^6 cells per well) and incubated for 60 min at 37°C with 5% CO_2. The wells were washed using 0.1 M HEPES (Amphoteric buffer, Beyotime Biotechnology Co.) buffered saline three times, added with HBSS containing 1% fetal bovine serum, and incubated for 30 min. Changes in intracellular calcium ion content were observed using fluorescence microscopy.

2.8. Flame atomic absorption analysis

0.25 mL, 0.5 mL, 1 mL, 1.5 mL, and 2 mL of a Ca standard solution (10 μg/mL) were added to a 50 mL volumetric flask and added with 50 mL with medium solution (0.5% HNO_3 + 2 mg/mL K^+). Then, the standard concentration was measured and the standard curve was plotted. Finally, the collected cell supernatant and intracellular fluid were diluted 5,000 times with medium solution and then assayed on the flame atomic absorption spectrophotometer. The absorbance and concentration values of each sample were recorded. Changes in extracellular calcium ion content were then analyzed with reference to the standard curve.

2.9. Statistical analysis

All results were subjected toa *t*-test and one-way analysis of variance (ANOVA) using the statistical software GraphPad Prism 8.0 (GraphPad Inc., La Jolla, CA, United States) and IBM SPSS Statistics 23 to determine statistical differences between multiple groups. A p-value > 0.05 (ns) indicates a non-significant difference, a p-value < 0.05 indicates a significant difference (*), a p-value < 0.01 expresses a highly significant difference (**), and a p-value < 0.001 expresses a very significant difference (***).

3. Results

3.1. PEDV infection affects changes in intra- and extracellular Ca^{2+} concentrations

Several viruses have been shown to promote their replication and infection by modulating cellular calcium ion levels; however, the effect of PEDV infection on intra- and extracellular Ca^{2+} concentrations is unknown. We used the calcium ion fluorescence

probe Fluo-3 AM to detect the intracellular Ca^{2+} concentration under PEDV infection, which showed that the intracellular Ca^{2+} fluorescence intensity after 2 h, 8 h, 24 h, and 48 h of PEDV infection was extremely significantly higher than that in the negative control group, under fluorescence microscopy (Figures 2A,B). The changes in the extracellular Ca^{2+} concentration under PEDV infection were detected using the flame atomic absorption method. A Ca^{2+} standard curve was first established (Figure 2C). The results of sample detection showed that the Ca^{2+} concentration in the extracellular fluid was significantly lower after PEDV infection (at 2 h, 8 h, 24 h, and 48 h) compared with that in the negative control group, in which the calcium ion concentration in the extracellular fluid was significantly lower in the 2 h, 8 h, and 24 h infection groups compared with that in the negative control group (Figure 2D). These results showed that PEDV infection causes a significant difference in the intra- and extracellular Ca^{2+} concentrations, i.e., PEDV infection causes a significant increase in the flow of Ca^{2+} from the extracellular space into the cells.

3.2. Inhibition of PEDV replication by the divalent cation chelating agent EGTA

We observed that PEDV infection can cause significant changes in intra- and extracellular Ca^{2+} concentrations. To further elucidate the relationship between Ca^{2+} and PEDV, we treated the cells with the specific Ca^{2+} chelator, EGTA, to detect the effect of Ca^{2+} on PEDV replication. First, the toxicity of EGTA toward IPEC-J2 cells was examined using the MTT assay, which showed that an EGTA concentration below 2 mM was not toxic to IPEC-J2 cells (Figure 3A). qRT-PCR and western blotting were used to detect the effect on PEDV replication after pretreatment of IPEC-J2 cells with different concentrations of EGTA. The results showed that after pretreatment with 1 mM and 2 mM EGTA, the PEDV M gene copy number decreased significantly at 6 h, 12 h, and 24 h post-infection compared with that in the untreated group, and the effect of 2 mM EGTA was more obvious (Figure 3B). The results of western blotting also showed that the PEDV-N protein level decreased at 6 h, 12 h, and 24 h after 1 mM and 2 mM EGTA pretreatment compared with the PEDV-infected only group, and the effect of 2 mM EGTA pretreatment at 6 h and 24 h was more obvious (Figure 3C). This demonstrated that EGTA pretreatment had an inhibitory effect on PEDV in a concentration-dependent manner. However, since EGTA can also chelate other divalent cations in the cell, whether the inhibition of PEDV replication in this process is dependent on Ca^{2+} chelation needs to be further investigated.

3.3. Supplementation of extracellular Ca^{2+} concentration to promote PEDV infection

In Section 3.2, we demonstrated that EGTA pretreatment inhibited PEDV replication. To confirm that EGTA exerts its effect by chelating Ca^{2+}, we first added $CaCl_2$ solution after EGTA pretreatment and examined the changes of PEDV after Ca^{2+} concentration backfill. The results showed that the PEDV-M copy number was significantly lower than that of the PEDV-infected only group after 6, 12, and 24 h after 2 mM EGTA pretreatment, while the PEDV-M copy number increased significantly after pretreatment in the 2 mM EGTA+$CaCl_2$ group compared with that

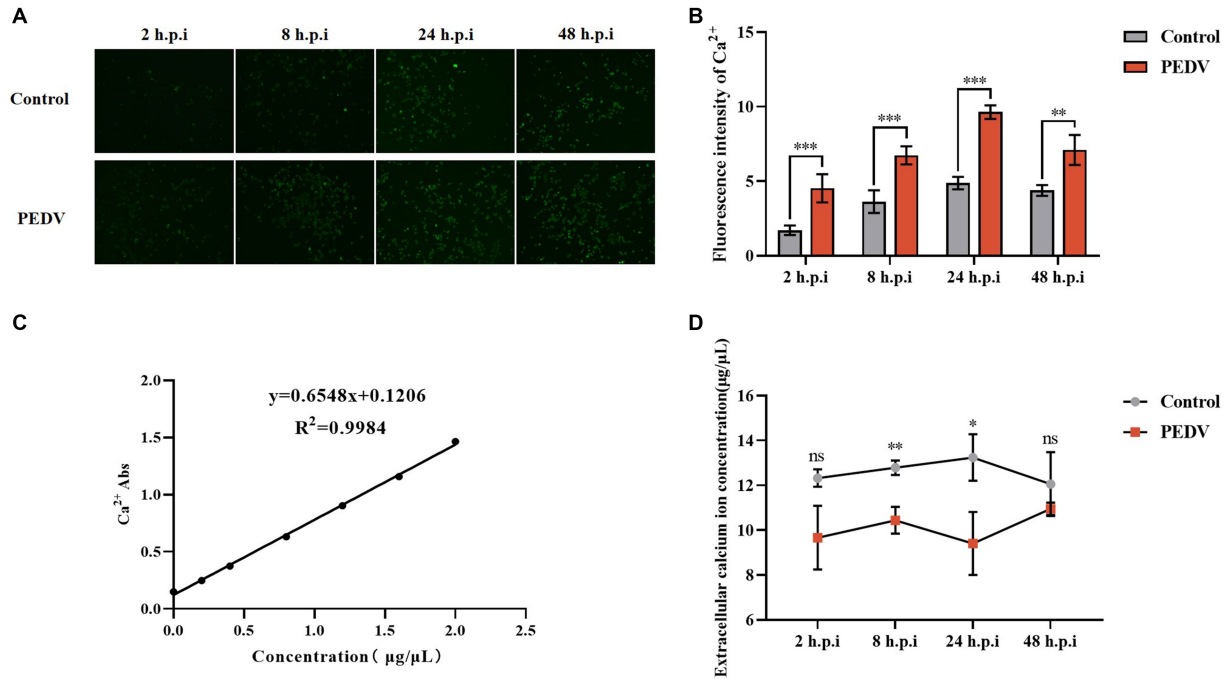

FIGURE 2
Changes in intra- and extracellular Ca^{2+} concentrations after PEDV infection. **(A)** intracellular Ca^{2+} fluorescence intensity graph (10×); **(B)** fluorescence intensity statistics graph; **(C)** Ca^{2+} standard curve; **(D)** extracellular Ca^{2+} concentration measurement.

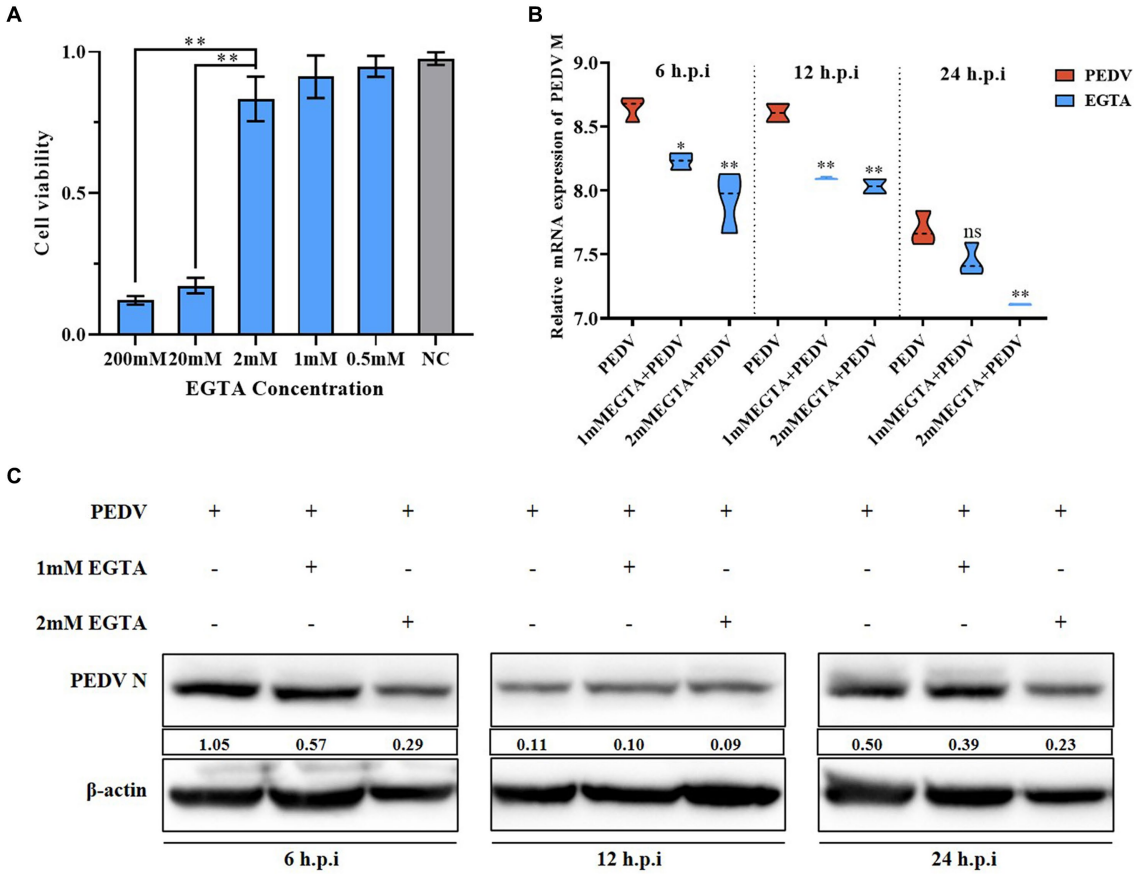

FIGURE 3
Effect of different concentrations of EGTA on PEDV. **(A)** EGTA toxicity assay in IPEC-J2 cells; **(B)** PEDV M gene copy number at 6 h, 12 h, and 24 h after pretreatment of cells with different concentrations of EGTA followed by PEDV infection; **(C)** PEDV-N protein levels at 6 h, 12 h, and 24 h after pretreatment of cells with different concentrations of EGTA followed by PEDV infection.

in the 2 mM EGTA pretreatment only group (Figure 1A). The PEDV-N protein level was also detected and found to be significantly lower in the 2 mM EGTA pretreatment group than in the PEDV-infected only group; while the PEDV-N level in the 2 mM EGTA+$CaCl_2$ group was significantly higher than that in the EGTA group (Figure 1B).

3.4. Ca^{2+} channel inhibitors promote PEDV infection

To further investigate the specific role played by calcium channels during viral infection, we chose a long-acting calcium channel inhibitor (BP) and the Ca^{2+} complexing agent BAPTA-AM to investigate the role of calcium channels in PEDV infection. BP inhibits cellular Ca^{2+} inward flow. BAPTA is released from BAPTA-AM by the action of a lipase upon entry into the cell. The released BAPTA can rapidly complex with Ca^{2+}, thus controlling the intracellular calcium ion levels. We detected no cytotoxicity of BP on IPEC-J2 cells at less than 2 μM using the MTT assay (Figure 4A). IPEC-J2 cells pretreated with 2 μM BP and then infected with PEDV infected were examined for PEDV-M gene copy number as well as PEDV N protein expression levels. The results showed that after 6–24 h of infection, the PEDV-M copy number was lower than that of the PEDV-infected only group, which was more significant at 6 h and 12 h (Figure 4B); the PEDV-N protein level was also reduced in the BP pretreated group, and the reduction was more significant after 12 h (Figure 4C). Thus, BP significantly inhibited PEDV M gene expression from 6 to 24 h, and the inhibitory effect on the PEDV-N protein level was more pronounced with extended time. In addition, we similarly observed a significantly lower PEDV-M gene copy number than that in the PEDV-infected alone group from 6 to 24 h after pretreatment with 20 μM BAPTA-AM (Figure 4D); the PEDV-N protein levels also decreased more significantly after 12 h (Figure 4E).

3.5. Important role of channel proteins in the regulation of intra- and extracellular Ca^{2+}

Intracellular and extracellular Ca^{2+} transmembrane transport mainly involves membrane transporter proteins, carrier proteins, and channel proteins. To further investigate the role played by calcium channel proteins during PEDV infection, we selected two typical Ca^{2+} transport channels, TRPV6 and PMCA1b, as the subjects of our study. Firstly, we constructed vectors for RNA interference of *TRPV6* and *PMCA1b* (shTRPV6/shPMCA1b)

10.3389/fmicb.2023.1251275

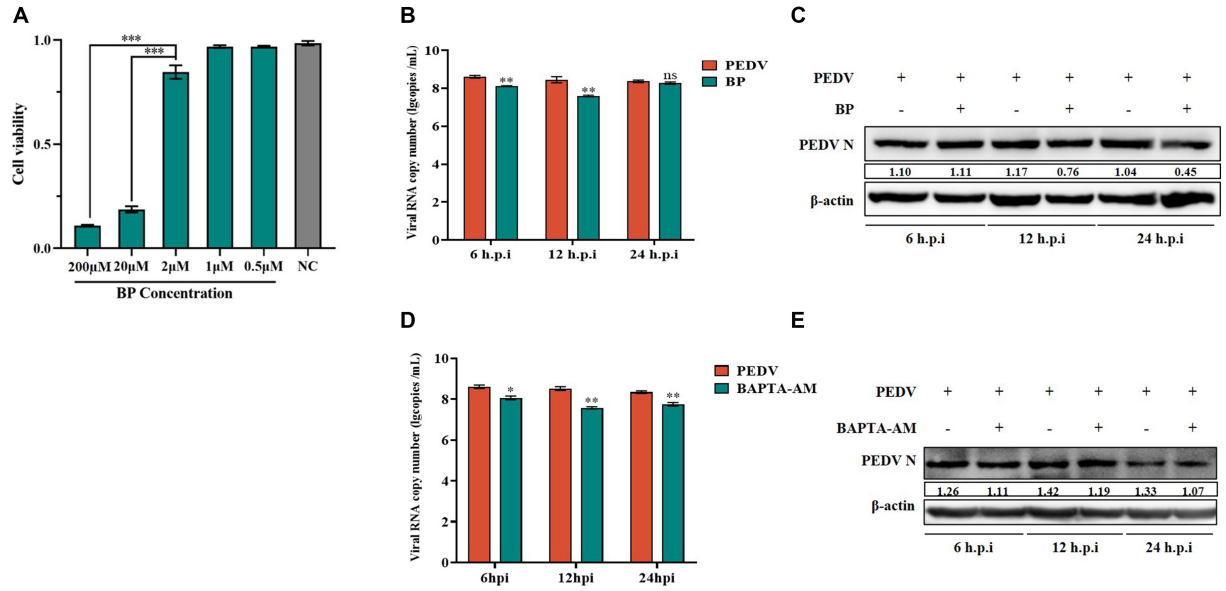

FIGURE 4
Effect of BP and BAPTA-AM on PEDV. **(A)** Cytotoxicity assay of BP; **(B)** PEDV M gene copy number in BP pretreated cells infected with PEDV at 6 h, 12 h, and 24 h; **(C)** PEDV N protein levels in the PEDV group after BP treatment; **(D)** PEDV M gene copy number in BAPTA-AM pretreated cells infected with PEDV at 6 h, 12 h, and 24 h; **(E)** PEDV N protein levels in the PEDV group after BAPTA-AM treatment.

separately to determine the association between TRPV6/PMCA1b and PEDV. The results showed that both interfering vectors were stably expressed in IPEC-J2 cells and significantly reduced the protein levels of TRPV6 and PMCA1b (Figures 5A,B). The fluorescence from the interference vector would have an effect on the detection of Fluo-3 AM; therefore, another calcium probe, Fura-2 AM, was chosen to detect the intracellular Ca^{2+} concentration. As shown in Figure 5C, the intracellular Ca^{2+} concentration was elevated after interfering with *TRPV6* and *PMCA1b* compared with that in the blank group, and the addition of 6 mM $CaCl_2$ at 120 s showed a more pronounced upregulation of the Ca^{2+} concentration in the *PMCA1b* interference group (Table 3).

3.6. Ca^{2+} channel proteins inhibit PEDV infection

Under normal physiological conditions, TRPV6 mediates Ca^{2+} inward flow and PMCA1b promotes intracellular Ca^{2+} flow to the extracellular space. After 6 h and 12 h post-PEDV infection, the PEDV-M copy number and PEDV-N protein levels were significantly upregulated in the shTRPV6 group, and the viral titer was also significantly increased (Figures 6A–C). Similarly, the PEDV-M gene copy number, PEDV-N protein level, and the viral titer were significantly increased in the shPMCA1b group (Figures 6D–F).

3.7. LP-1S can effectively inhibit PEDV replication

Lactobacillus, as a probiotic flora, is highly effective against intestinal diarrheal diseases. Probiotics are present in the intestinal tract of animals and have a protective effect on intestinal health. Our laboratory previously isolated a strain of *Lactiplantibacillus plantarum*, LP-1, and we sought to verify whether the metabolites of this bacterium have an anti-PEDV effect. We first measured its growth curve, and the results showed that LP-1 entered the logarithmic growth phase after 6 h and reached the end of logarithmic growth phase (maximum growth value) at 12 h (Figure 7A); therefore, we chose 12 h as the best time to obtain the *Lactiplantibacillus plantarum* supernatant, LP-S1. Subsequently, the toxicity of LP-S1 toward IPEC-J2 cells was determined using the MTT assay, and the LP-1S 1/4-fold dilution was found to be the optimal treatment concentration dose for IPEC-J2 cells (Figure 7B). The 1/4-fold dilution of LP-1S was used to pretreat the cells in the PEDV-infected group, and the proteins were collected at 2 h, 8 h, 12 h, and 24 h. Western blotting showed that the PEDV-N protein level in the LP-1S pretreatment group decreased gradually and significantly with increasing time (Figure 7C). The viral solution collected at different time points after LP-1S pretreatment was used to detect the viral titer, and the TCID50 data showed that the viral titer at 12 h, 24 h, and 48 h showed a decreasing trend, with a more significant decrease at 24 h (Figure 7D).

3.8. LP-1S upregulates the Ca^{2+} channel protein

We showed that PEDV infection caused elevated intracellular Ca^{2+} and was associated with two Ca^{2+} channel proteins, TRPV6 and PMCA1b. LP-1S has an anti-PEDV effect; however, whether it affects Ca^{2+} is unknown. TRPV6 and PMCA1b are calcium channel proteins mainly expressed in the gastrointestinal tract and have high permeability to Ca^{2+}. To further verify whether LP-1S is associated with Ca^{2+} channel proteins, we examined the mRNA and protein expression levels of TRPV6 and PMCA1b in the PEDV infection

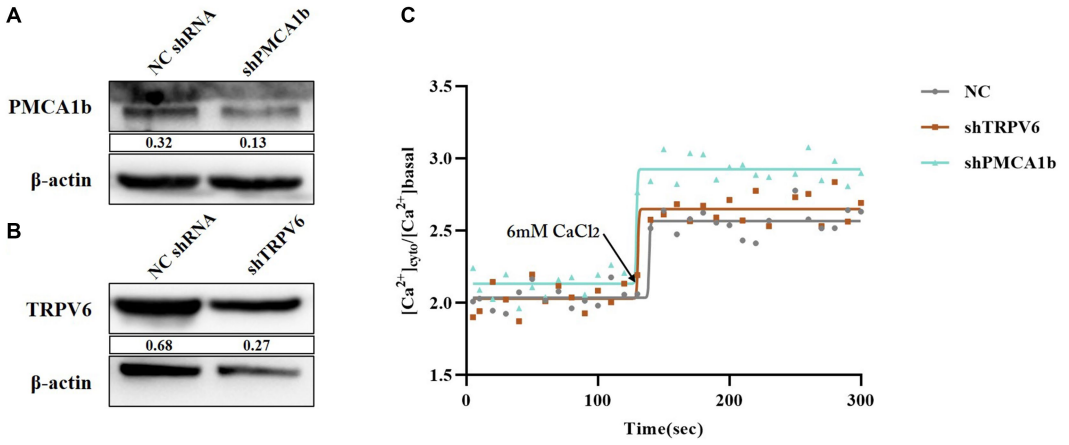

FIGURE 5
Validation of the effect of *TRPV6*/*PMCA1b* interference and its impact on intracellular Ca^{2+}. **(A)** PMCA1b protein levels after shPMCA1b expression in IPEC-J2 cells; **(B)** TRPV6 protein levels after shTRPV6 expression in IPEC-J2 cells; **(C)** Effect of shTRPV6/shPMCA1b treatment on intracellular Ca^{2+}.

TABLE 3 Sequence of *TRPV6* and *PMCA1b* shRNA interference fragments.

Gene	Sequences (5′–3′)
TRPV6	F: 5′-GGTGGAAGACAGACAGGATAT-3′
PMCA1b	F: 5′-GGGCGCCTGTATTACTCAAGA-3′

group and after LP-1S pretreatment. The results showed that the mRNA level of *TRPV6* significantly increased at 12 h after LP-1S pretreatment compared with that in the PEDV-infected only group (Figure 8A), and the protein level likewise significantly increased at 12 h (Figure 8B). Similarly, the mRNA and protein levels of PMCA1b increased after LP-1S pretreatment compared with those in the PEDV-infected group, with mRNA levels at 6 h and 12 h (Figure 8C) and protein levels at 6 h (Figure 8D) being the most significant.

3.9. LP-1S affects changes in intra- and extracellular Ca^{2+} concentrations

It was previously verified that Ca^{2+} endocytosis contributes to PEDV infection, and TRPV6 and PMCA1b are key channel proteins that regulate Ca^{2+}. LP-1S pretreatment significantly reduced the extent of PEDV infection and increased the levels of TRPV6 and PMCA1b. To further investigate the relationship between LP-1S and Ca^{2+}, we examined the changes induced by LP-1S on intra- and extracellular Ca^{2+} concentrations using the calcium fluorescent probe Fluo-3 AM and flame atomic absorption, respectively. According to the intracellular Ca^{2+} concentration, the intensity of intracellular Ca^{2+} fluorescence was significantly weaker in the negative control group, the LP-1S pre-treatment group, and the LP-1S group than in the PEDV-infected group, and the intracellular Ca^{2+} concentration was significantly lower than that of the PEDV-infected group at 2 h, 8 h, 24 h, and 48 h (Figures 9A,B). In terms of the extracellular Ca^{2+} concentration, the extracellular Ca^{2+} concentration after LP-1S pretreatment was higher than that of the PEDV-infected group at 2 h, 8 h, 24 h, and 48 h, with 2–24 h being the most significant period (Figure 9C).

4. Discussion

In recent years, despite the increased research on PEDV in various countries, the incidence of PEDV-induced diarrhea in piglets remains high in clinical practice; therefore, the search for effective anti-PEDV drugs is still a top priority for PEDV prevention and control. Calcium ion imbalance is a hallmark of viral infection (Kumar et al., 2022). Several studies have shown that different viral infections lead to an imbalance of calcium ions inside and outside the cell. For example, the mRNA encoding the calbindin D-28 K and calretinin has an important role in the early stages of rabies infection (Korie et al., 2023). SARS-CoV-2 ORF 3a interferes with calcium homeostasis and induces autophagy to enhance viral infection (Garrido-Huarte et al., 2023). Calcium imbalance triggers the mitochondrial apoptotic pathway to promote infection by chicken anemia virus (Yu et al., 2023). Herpes simplex virus (HSV) infection induces a rapid increase in the intracellular calcium ion concentration, which plays a key role in facilitating virus entry (Jiang et al., 2023). Rotavirus disrupts calcium homeostasis by NSP4 viroporin activity, directly or indirectly, in response to elevated cytoplasmic calcium levels and regulates rotavirus replication and virion assembly (Hyser et al., 2010). Dengue virus (DENV) infection disrupts intracellular calcium homeostasis causing an increase in intracellular calcium levels (Dionicio et al., 2018).

We found that PEDV infection activates plasma membrane Ca^{2+} channels, leading to a large accumulation of intracellular calcium ions, and that this Ca^{2+} imbalance leads to changes in intracellular gene expression, energy metabolism, and other functions, which in turn promotes viral replication (Figure 6). We then further verified the link between PEDV and Ca^{2+} using a divalent cation chelating agent (EGTA), calcium channel inhibitors (BP and BAPTA-AM), and calcium channel proteins (TRPV6 and PMCA1b). Pretreatment with 2 mM EGTA significantly inhibited PEDV M expression, and PEDV expression M was significantly increased when the cells were supplemented with Ca^{2+}, suggesting that EGTA effectively reduced the inward flow of extracellular free Ca^{2+} by chelating it, thereby inhibiting PEDV proliferation. In contrast, $CaCl_2$ supplementation induced an increase in intracellular Ca^{2+} flow, leading to an increase in PEDV expression (Figure 1). Similarly, PEDV infection was

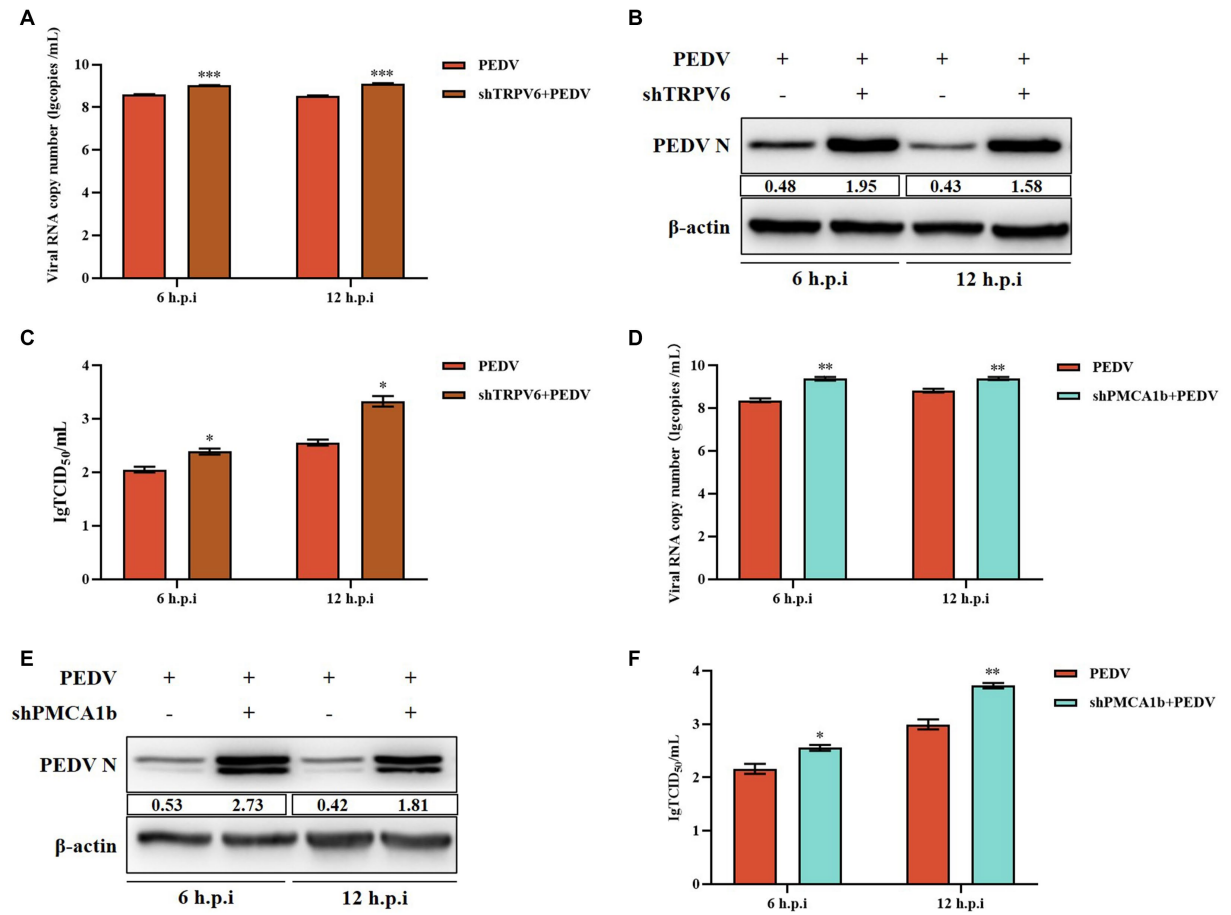

FIGURE 6
Effect of interfering with *TRPV6* and *PMCA1b* on PEDV. **(A)** PEDV-M gene copy number in IPEC-J2 cells after shTRPV6 treatment; **(B)** PEDV-N protein levels in IPEC-J2 cells after shTRPV6 treatment; **(C)** PEDV infection of IPEC-J2 after shTRPV6 pretreatment cells; **(D)** PEDV-M gene copy number in IPEC-J2 cells after shPMCA1b treatment; **(E)** PEDV protein levels in IPEC-J2 cells after shPMCA1b treatment; **(F)** change in the viral titer in IPEC-J2 cells infected with PEDV after shPMCA1b pretreatment.

significantly reduced when Ca^{2+} endocytosis was blocked using BAPTA-AM. In addition, the calcium channel protein TRPV6, which strictly regulates Ca^{2+} influx, is necessary to avoid Ca^{2+} overload (McGoldrick et al., 2018). When we interfered with *TRPV6* expression, PEDV invasion was significantly enhanced, which might have been caused by the disruption of Ca^{2+} channel function, resulting in intracellular Ca^{2+} overload, thus facilitating the viral invasion. By contrast, interfering with P*MCA1b* significantly inhibited its associated channels, reducing the flow of intracellular Ca^{2+} into the extracellular compartment, thereby exacerbating PEDV invasion. Therefore, we concluded that PEDV infection can be significantly reduced by inhibiting calcium channels, and this effect gradually increases with time (Figure 6).

Probiotics are now considered as an effective alternative to antibiotics, and can colonize the intestinal tract. Probiotics function by reducing inflammatory response, protecting the intestinal structure, maintaining intestinal microbial homeostasis, and improving the immunity of the body (Thomas and Versalovic, 2010). The metabolites in LP-1S inhibited PEDV proliferation in a time- and concentration-dependent manner; however, whether this effect correlated with Ca^{2+} concentration has not been reported. To further reveal whether LP-1S has the ability to modulate Ca^{2+} concentration and thus exert antiviral effects, we conducted a follow-up study. The results showed that LP-1S could significantly reduce the intracellular Ca^{2+} concentration. A low intracellular Ca^{2+} concentration is a prerequisite to ensure normal cell function therefore, this might be an important method by which LP-1S inhibits the proliferation of PEDV. Further study revealed that under PEDV infection conditions, LP-1S pretreatment affected intestinal Ca^{2+} channel proteins (TRPV6, PMCA1b), among which PMCA1b was more sensitive to PEDV infection than TRPV6. LP-1S might precisely enhance the regulation of Ca^{2+} by PMCA1b and TRPV6 to reduce the intracellular Ca^{2+} concentration and maintain an intracellular low calcium state, thus exerting an anti-PEDV effect (Figure 10). Therefore, intracellular calcium homeostasis is particularly important to maintain normal cellular physiological functions and resistance to viral infection (Klapczyńska et al., 2023; Sørensen et al., 2023). Overall, LP-1S significantly reduced the intracellular Ca^{2+} concentration, whereas the increase in the extracellular Ca^{2+} concentration suggested that LP-1S might exert its anti-PEDV effects mainly through Ca^{2+} channel proteins that inhibit intracellular Ca^{2+} in-flow and promote Ca^{2+} out-flow (Figure 9).

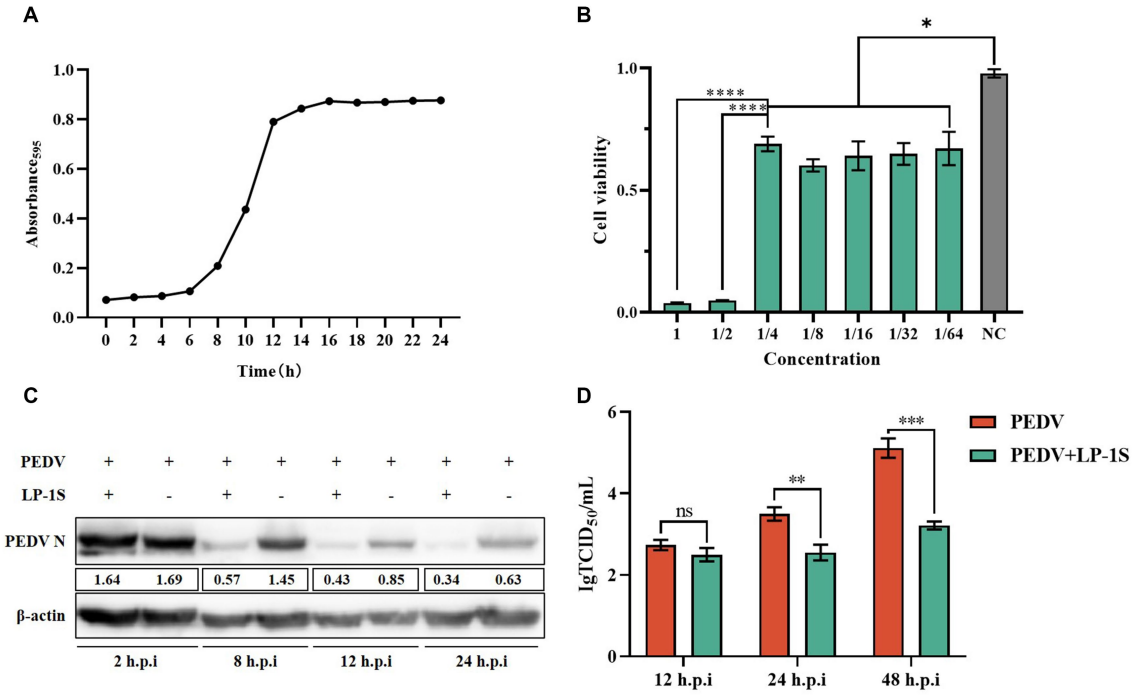

FIGURE 7
LP-1S can effectively inhibit PEDV replication **(A)** Growth curve of *Lactiplantibacillus plantarum* under LP-1S treatment. **(B)** MTT assay detection of the toxicity of LP-1S toward IPEC-J2 cells; **(C)** PEDV-N levels after treatment with 1/4 times dilution of LP-1S; **(D)** TCID50 results after LP-1S pretreatment.

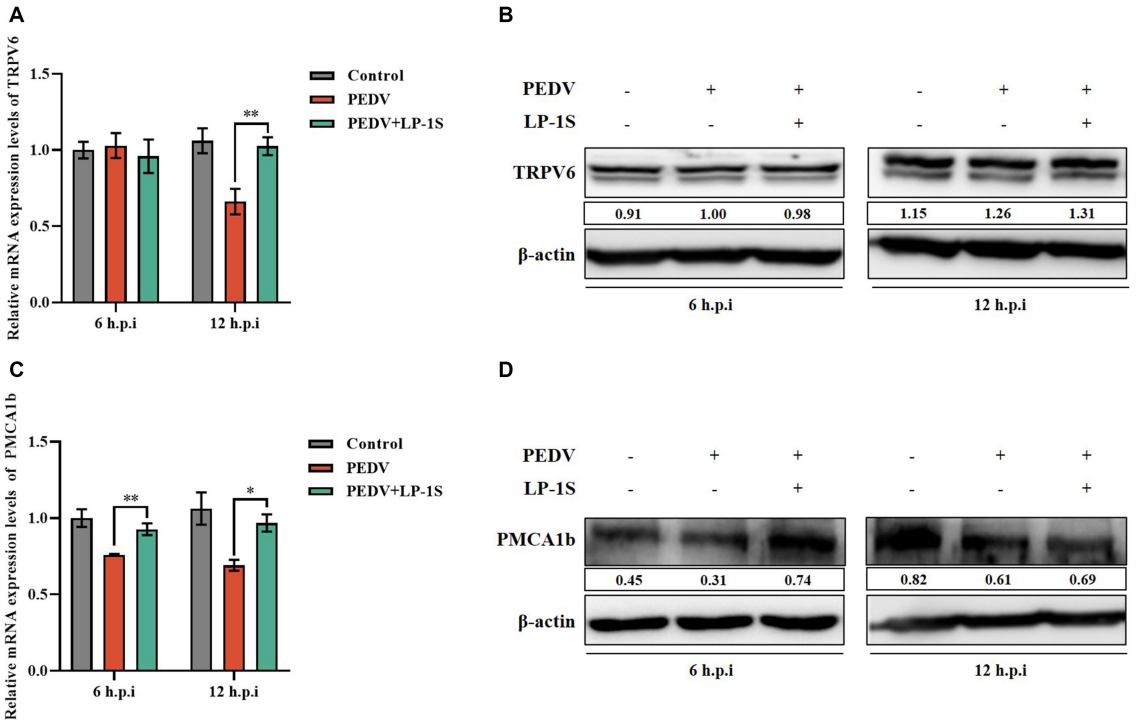

FIGURE 8
The level of expression of TRPV6 and PMCA1b after LP-1S treatment. **(A)** *TRPV6* mRNA statistics after attack following LP-1S treatment; **(B)** TRPV6 protein expression levels after attack following by LP-1S treatment; **(C)** *PMCA1b* mRNA statistics after attack followingLP-1S treatment; **(D)** PMCA1b protein levels after attack following LP-1S treatment.

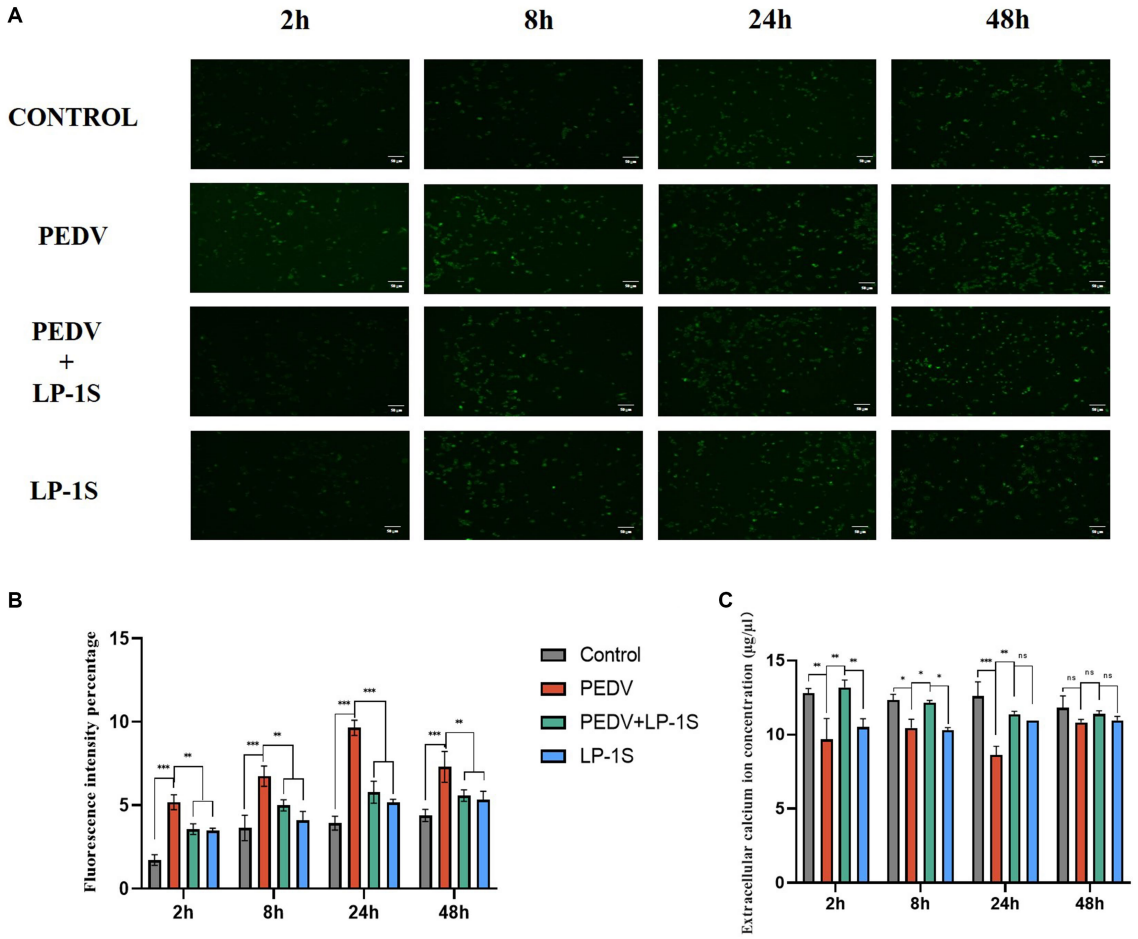

FIGURE 9
Effect of tapping on intra- and extracellular calcium ions after LP-1S treatment. **(A)** Fluorescence plot of intracellular calcium ions; **(B)** fluorescence statistics of intracellular calcium ions; **(C)** Changes in extracellular Ca^{2+}.

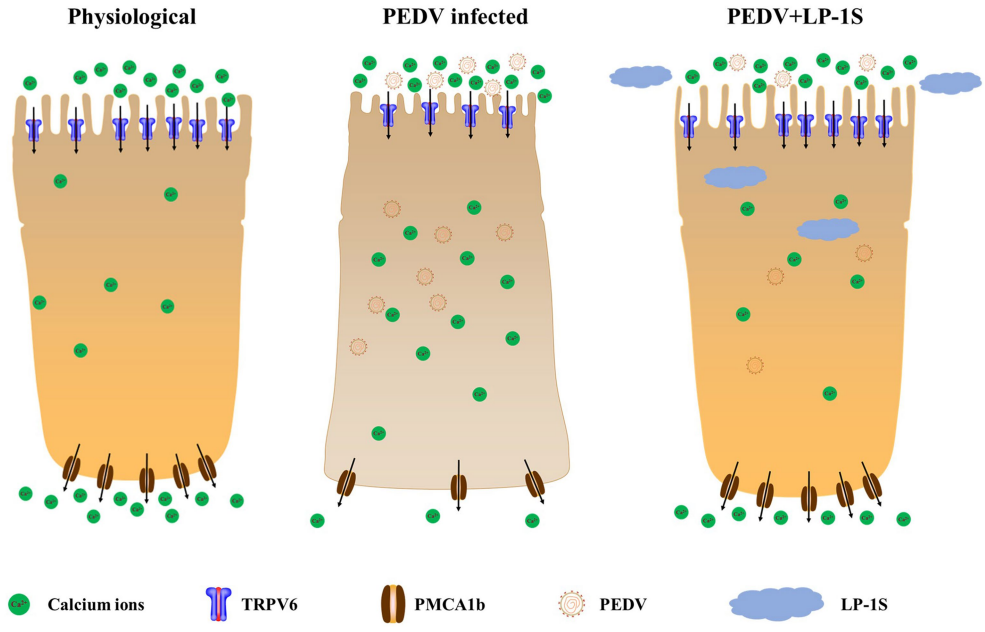

FIGURE 10
The mechanism by which LP-1S regulates Ca^{2+}.

In this study, we used calcium ion modulators to determine that an intra- and extracellular Ca^{2+} imbalance promotes PEDV infection. Using western blotting and qRT-PCR, LP-1S was observed to significantly inhibit PEDV replication. Finally, using Ca^{2+} fluorescent probes and flame atomic absorption, we demonstrated that LP-1S ameliorates the PEDV-induced Ca^{2+} imbalance. These result provides a possible treatment strategy for PEDV and could from the basis for the development of effective drugs.

Data availability statement

The datasets presented in this study can be found in online repositories. The names of the repository/repositories and accession number(s) can be found in the article/supplementary material.

Ethics statement

Ethical approval was not required for the studies on animals in accordance with the local legislation and institutional requirements because only commercially available established cell lines were used.

Author contributions

ZK, SZ, and GL: conceptualization. ZK: methodology. ZN: software. ZK, SZ, and ZN: validation. ZSu and XL: formal analysis. XH: investigation. ZSo: resources, supervision, project administration, and funding acquisition. YZ: data curation. SZ: writing—original draft preparation. ZN: writing—review and editing. SX, JZ, and HZ: visualization. All authors contributed to the article and approved the submitted version.

Funding

This work was supported by grants from the Central University Basic Research Fund of China [grant number XDJK2020RC001] and the Venture and Innovation Support Program for Chongqing Overseas Returnees [grant number cx2019097] and 2020 Chongqing Rongchang Agricultural and Animal Hi-Tech Specialization.

Acknowledgments

We are grateful to GuangLiang Liu and YuGuang Fu (Lanzhou Veterinary Research Institute of Chinese Academy of Agricultural Sciences) for their support and comments on the manuscript. We also thank them for kindly providing the antibodies used in this study. We thank the staff of the Southwest University for their generous support and valuable advice.

Conflict of interest

The authors declare that the research was conducted in the absence of any commercial or financial relationships that could be construed as a potential conflict of interest.

Publisher's note

References

Bibollet, H., Kramer, A., Bannister, R. A., and Hernández-Ochoa, E. O. (2023). Advances in $Ca_V1.1$ gating: new insights into permeation and voltage-sensing mechanisms. *Channels (Austin)* 17:2167569. doi: 10.1080/19336950.2023.2167569

Cao, L., Ge, X., Gao, Y., Herrler, G., Ren, Y., Ren, X., et al. (2015). Porcine epidemic diarrhea virus inhibits dsRNA-induced interferon-β production in porcine intestinal epithelial cells by blockade of the RIG-I-mediated pathway. *Virol. J.* 12:127. doi: 10.1186/s12985-015-0345-x

Dai, C., Tan, M., Meng, X., Dong, J., and Zhang, Y. (2023). Effects of potassium channel knockdown on peripheral blood T lymphocytes and NFAT signaling pathway in Xinjiang Kazak patients with hypertension. *Clin. Exp. Hyperten. New York, N.Y.: 1993* 45:2169449. doi: 10.1080/10641963.2023.2169449

Ding, Z., Fang, L., Jing, H., Zeng, S., Wang, D., Liu, L., et al. (2014). Porcine epidemic diarrhea virus nucleocapsid protein antagonizes beta interferon production by sequestering the interaction between IRF3 and TBK1. *J. Virol.* 88, 8936–8945. doi: 10.1128/JVI.00700-14

Dionicio, C. L., Peña, F., Constantino-Jonapa, L. A., Vazquez, C., Yocupicio-Monroy, M., Rosales, R., et al. (2018). Dengue virus induced changes in Ca^{2+} homeostasis in human hepatic cells that favor the viral replicative cycle. *Virus Res.* 245, 17–28. doi: 10.1016/j.virusres.2017.11.029

Garrido-Huarte, J. L., Fita-Torró, J., Viana, R., Pascual-Ahuir, A., and Proft, M. (2023). Severe acute respiratory syndrome coronavirus-2 accessory proteins ORF3a and ORF7a modulate autophagic flux and Ca^{2+} homeostasis in yeast. *Front. Microbiol.* 14:1152249. doi: 10.3389/fmicb.2023.1152249

Guo, D., Hou, T., and He, H. (2016). Bioactive peptides promoting calcium absorption mechanism and calcium ion channels. *J. Food Safe. Qual. Test.* 11, 4531–4535. doi: 10.19812/j.cnki.jfsq11-5956/ts.2016.11.052

Hu, T. Y., Lian, Y. B., Qian, J. H., Yang, Y. L., Ata, E. B., Zhang, R. R., et al. (2022). Immunogenicity of engineered probiotics expressing conserved antigens of influenza virus and FLIC flagellin against H9N2 AIVinfection in mice. *Res. Vet. Sci.* 153, 115–126. Advance online publication. doi: 10.1016/j.rvsc.2022.10.024

Huang, S., Yu, Q., Xie, L., Ran, L., Wang, K., Yang, Y., et al. (2021). Inhibitory effects of *Lactobacillus plantarum* metabolites on porcine epidemic diarrhea virus replication. *Res. Vet. Sci.* 139, 32–42. doi: 10.1016/j.rvsc.2021.07.002

Hussey, J. W., Limpitikul, W. B., and Dick, I. E. (2023). Calmodulin mutations in human disease. *Channels (Austin, Tex.)* 17:2165278. doi: 10.1080/19336950.2023.2165278

Hyser, J. M., Collinson-Pautz, M. R., Utama, B., and Estes, M. K. (2010). Rotavirus disrupts calcium homeostasis by NSP4 viroporin activity. *MBio* 1, e00265–e00210. doi: 10.1128/mBio.00265-10

Jang, G., Lee, D., and Lee, C. (2022). Development of a next-generation vaccineplatform for porcine epidemic diarrhea virus using a reverse genetics system. *Viruses* 14:2319. doi: 10.3390/v14112319

Jiang, P., Li, S. S., Xu, X. F., Yang, C., Cheng, C., Wang, J. S., et al. (2023). TRPV4 channel is involved in HSV-2 infection in human vaginal epithelial cells through triggering Ca^{2+} oscillation. *Acta Pharmacol. Sin.* 44, 811–821. doi: 10.1038/s41401-022-00975-7

Klapczyńska, K., Aleksandrowicz, M., and Koźniewska, E. (2023). Role of the endothelial reverse mode sodium-calcium exchanger in the dilation of the rat middle cerebral artery during hypoosmotic hyponatremia. *Pflug. Archiv. Eur. J. Physiol.* 475, 381–390. doi: 10.1007/s00424-022-02770-z

Korie, G. C., Sallau, A. B., Kanu, B., Kia, G. S. N., and Kwaga, J. K. P. (2023). Rabies virus infection is associated with variations in calbindin D-28K and calretinin mRNA expression levels in mouse brain tissue. *Arch. Virol.* 168:143. doi: 10.1007/s00705-023-05753-2

Kumar, P. S., Radhakrishnan, A., Mukherjee, T., Khamaru, S., Chattopadhyay, S., and Chattopadhyay, S. (2022). Understanding the role of Ca^{2+} via transient receptor potential

(TRP) channel in viral infection: implications in developing future antiviral strategies. *Virus Res.* 323:198992. Advance online publication. doi: 10.1016/j.virusres.2022.198992

Leblanc, D., Raymond, Y., Lemay, M. J., Champagne, C. P., and Brassard, J. (2022). Effect of probiotic bacteria on porcine rotavirus OSU infection of porcine intestinal epithelial IPEC-J2 cells. *Arch. Virol.* 167, 1999–2010. doi: 10.1007/s00705-022-05510-x

Liang, T., Xie, X., Wu, L., Li, L., Yang, L., Jiang, T., et al. (2023). Metabolism of resistant starch RS3 administered in combination with Lactiplantibacillus plantarum strain 84-3 by human gut microbiota in simulated fermentation experiments *in vitro* and in a rat model. *Food Chem.* 411:135412. doi: 10.1016/j.foodchem.2023.135412

Liou, J., Kim, M. L., Heo, W. D., Jones, J. T., Myers, J. W., Ferrell, J. E. Jr., et al. (2005). STIM is a Ca2+ sensor essential for Ca2+-store-depletion-triggered Ca2+ influx. *Curr. Biol.* 15, 1235–1241. doi: 10.1016/j.cub.2005.05.055

Liu, J., Gao, K., Li, D., Zeng, Y., Chen, X., Liang, X., et al. (2022). Recombinant invasive *Lactobacillus plantarum* expressing the J subgroup avian leukosis virus Gp85 protein induces protection against avian leukosis in chickens. *Appl. Microbiol. Biotechnol.* 106, 729–742. doi: 10.1007/s00253-021-11699-9

Livak, K. J., and Schmittgen, T. D. (2001). Analysis of relative gene expression data using real-time quantitative PCR and the 2(-Delta Delta C(T)) method. *Methods (San Diego, Calif.)* 25, 402–408. doi: 10.1006/meth.2001.1262

McGoldrick, L. L., Singh, A. K., Saotome, K., Yelshanskaya, M. V., Twomey, E. C., Grassucci, R. A., et al. (2018). Opening of the human epithelial calcium channel TRPV6. *Nature* 553, 233–237. doi: 10.1038/nature25182

Narayanan, A., Kehn-Hall, K., Senina, S., Lundberg, L., Van Duyne, R., Guendel, I., et al. (2012). Curcumin inhibits Rift Valley fever virus replication in human cells. *J. Biol. Chem.* 287, 33198–33214. doi: 10.1074/jbc.M112.356535

Peng, J. B., Brown, E. M., and Hediger, M. A. (2001). Structural conservation of the genes encoding CaT1, CaT2, and related cation channels. *Genomics* 76, 99–109. doi: 10.1006/geno.2001.6606

Rodrat, M., Wongdee, K., Teerapornpuntakit, J., Thongbunchoo, J., Tanramluk, D., Aeimlapa, R., et al. (2022). Vasoactive intestinal peptide and cystic fibrosis transmembrane conductance regulator contribute to the transepithelial calcium transport across intestinal epithelium-like Caco-2 monolayer. *PLoS One* 17:e0277096. doi: 10.1371/journal.pone.0277096

Seo, M. D., Enomoto, M., Ishiyama, N., Stathopulos, P. B., and Ikura, M. (2015). Structural insights into endoplasmic reticulum stored calcium regulation by inositol 1,4,5-trisphosphate and ryanodine receptors. *Biochim. Biophys. Acta* 1853, 1980–1991. doi: 10.1016/j.bbamcr.2014.11.023

Sørensen, C. E., Trauzold, A., Christensen, N. M., Tawfik, D., Szczepanowski, M., and Novak, I. (2023). Synergistic effects of agonists and two-pore-domain potassium channels on secretory responses of human pancreatic duct cells Capan-1. *Pflug. Archiv. Eur. J. Physiol.* 475, 361–379. doi: 10.1007/s00424-022-02782-9

Spacova, I., De Boeck, I., Cauwenberghs, E., Delanghe, L., Bron, P. A., Henkens, T., et al. (2023). Development of a live biotherapeutic throat spray with lactobacilli targeting respiratory viral infections. *Microb. Biotechnol.* 16, 99–115. doi: 10.1111/1751-7915.14189

Tarifa, C., Vallmitjana, A., Jiménez-Sábado, V., Marchena, M., Llach, A., Herraiz-Martínez, A., et al. (2022). Spatial distribution of calcium Sparks determines their ability to induce afterdepolarizations in human atrial myocytes. *JACC Basic Transl. Sci.* 8, 1–15. doi: 10.1016/j.jacbts.2022.07.013

Thomas, C. M., and Versalovic, J. (2010). Probiotics-host communication: modulation of signaling pathways in the intestine. *Gut Microbes* 1, 148–163. doi: 10.4161/gmic.1.3.11712

Wu, Y., Zhang, H., Shi, Z., Chen, J., Li, M., Shi, H., et al. (2020). Porcine epidemic diarrhea virus nsp15 antagonizes interferon signaling by RNA degradation of TBK1 and IRF3. *Viruses* 12:599. doi: 10.3390/v12060599

Yao, X., Qiao, W. T., Zhang, Y. Q., Lu, W. H., Wang, Z. W., Li, H. X., et al. (2023). A new PEDV strain CH/HLJJS/2022 can challenge current detection methods and vaccines. *Virol. J.* 20:13. doi: 10.1186/s12985-023-01961-z

Yu, X., Wang, T., Li, Y., Li, Y., Bai, B., Fang, J., et al. (2023). Apoptin causes apoptosis in HepG-2 cells via Ca^{2+} imbalance and activation of the mitochondrial apoptotic pathway. *Cancer Med.* 12, 8306–8318. doi: 10.1002/cam4.5528

Zhang, H., Gao, S., Lercher, M. J., Hu, S., and Chen, W. H. (2012). EvolView, an online tool for visualizing, annotating and managing phylogenetic trees. *Nucleic Acids Res.* 40, W569–W572. doi: 10.1093/nar/gks576

Zhao, Y., Huang, J., and Tang, F. (2022). Progress of TRPV6 ion channel structure and post-translational modification of the protein. *Biotechnology* 32, 642–648+669.

frontiers | Frontiers in Microbiology

TYPE Review
PUBLISHED 12 October 2023
DOI 10.3389/fmicb.2023.1233433

OPEN ACCESS

EDITED BY
Gaëtan Ligat,
Université Toulouse III Paul Sabatier, France

REVIEWED BY
Manoj Baranwal,
Thapar Institute of Engineering and Technology,
India
Wei Ye,
Air Force Medical University, China

*CORRESPONDENCE
Liaqat Ali
✉ liaqatbiotech@gmail.com
Jing Yang
✉ WIBPJYang@126.com

RECEIVED 02 June 2023
ACCEPTED 25 September 2023
PUBLISHED 12 October 2023

CITATION
Afzal S, Ali L, Batool A, Afzal M, Kanwal N, Hassan M, Safdar M, Ahmad A and Yang J (2023) Hantavirus: an overview and advancements in therapeutic approaches for infection.
Front. Microbiol. 14:1233433.
doi: 10.3389/fmicb.2023.1233433

Hantavirus: an overview and advancements in therapeutic approaches for infection

Samia Afzal[1], Liaqat Ali[2]*, Anum Batool[2], Momina Afzal[1], Nida Kanwal[2], Muhammad Hassan[1], Muhammad Safdar[1], Atif Ahmad[1] and Jing Yang[3]*

[1]CEMB, University of the Punjab, Lahore, Pakistan, [2]Department of Biological Sciences, National University of Medical Sciences (NUMS), Rawalpindi, Pakistan, [3]Wuhan Institute of Biological Products Co., Ltd., Wuhan, Hubei, China

Hantaviruses are a significant and emerging global public health threat, impacting more than 200,000 individuals worldwide each year. The single-stranded RNA viruses belong to the *Hantaviridae* family and are responsible for causing two acute febrile diseases in humans: Hantavirus pulmonary syndrome (HPS) and hemorrhagic fever with renal syndrome (HFRS). Currently, there are no licensed treatments or vaccines available globally for HTNV infection. Various candidate drugs have shown efficacy in increasing survival rates during the early stages of HTNV infection. Some of these drugs include lactoferrin, ribavirin, ETAR, favipiravir and vandetanib. Immunotherapy utilizing neutralizing antibodies (NAbs) generated from Hantavirus convalescent patients show efficacy against HTNV. Monoclonal antibodies such as MIB22 and JL16 have demonstrated effectiveness in protecting against HTNV infection. The development of vaccines and antivirals, used independently and/or in combination, is critical for elucidating hantaviral infections and the impact on public health. RNA interference (RNAi) arised as an emerging antiviral therapy, is a highly specific degrades RNA, with post-transcriptional mechanism using eukaryotic cells platform. That has demonstrated efficacy against a wide range of viruses, both *in vitro* and *in vivo*. Recent antiviral methods involve using small interfering RNA (siRNA) and other, immune-based therapies to target specific gene segments (S, M, or L) of the Hantavirus. This therapeutic approach enhances viral RNA clearance through the RNA interference process in Vero E6 cells or human lung microvascular endothelial cells. However, the use of siRNAs faces challenges due to their low biological stability and limited *in vivo* targeting ability. Despite their successful inhibition of Hantavirus replication in host cells, their antiviral efficacy may be hindered. In the current review, we focus on advances in therapeutic strategies, as antiviral medications, immune-based therapies and vaccine candidates aimed at enhancing the body's ability to control the progression of Hantavirus infections, with the potential to reduce the risk of severe disease.

KEYWORDS

Hantavirus, HFRS, HPS, immunotherapy, siRNA

1. Introduction

Hantaviruses are negative-sense, single-stranded tri-segmented RNA viruses that belong to the order *Bunyavirales*, family *Hantaviridae* and genus *Orthohantavirus* (Kuhn and Schmaljohn, 2023). They exclusively maintain themselves in the population of their natural host and produce a persistent viral infection in them and make a continuous shedding in rodent excreta. They

cause two acute febrile diseases in humans: Hantavirus pulmonary syndrome (HPS) and hemorrhagic fever with renal syndrome (HFRS) (Khaiboullina et al., 2005). Hantaviruses pose an emerging global threat to public health causing a devastating effect on human lives, affecting more than 200,000 individuals worldwide annually (Bi et al., 2008). Moreover, the number of cases is significantly increasing day by day in different parts of the world (Watson et al., 2014). Two major outbreaks of Hantavirus disease, reported in the last century, were the first to catch global attention. The first, HFRS outbreak, occurred during the Korean War (1950–1953), affected more than 3,000 US troops (Tian and Stenseth, 2019). The second, HPS outbreak, was documented in the southwestern regions of the US in 1993 (Mills et al., 1999). Pathophysiological studies have revealed that Hantavirus transmits by rodents, mainly through contaminated saliva, feces, urine, and aerosols. It can also be transmitted by bites of affected animals, though it is rarely reported (Brocato and Hooper, 2019). Although the Hantaviruses transmit from natural hosts to humans through a natural ecological process, the outbreak is accelerated by rodent animals like striped field mice and seasonal climatic fluctuations (Tian and Stenseth, 2019).

The clinical presentations of the disease depend on the geographic distribution of the viral strains around the world. In Asia, Hantavirus (HNTV) and Seoul virus (SEOV) primarily infect the human kidney and cause hemorrhagic fever with renal syndrome (HFRS). In North America, Andes virus (ANDV) and Sin Nombre virus (SNV) target the lungs and cause Hantavirus cardiopulmonary syndrome (HCPS) or Hantavirus pulmonary syndrome (HPS), with a high rate of mortality. While in Europe, Puumala virus (PUUV) and Dobrava-Belgarde virus (DOBV) cause a milder form of HFRS, the nephropathia epidemica (Echterdiek et al., 2019). These viruses, like any other enveloped virus, get inactivated when exposed to detergents, UV radiations, hypochlorite solutions, organic solvents, and high temperature (60°C for 30 min). They attach to the host cell surface receptors by glycoprotein and infect a number of cells including dendritic, lymphocyte, and epithelial cells. It has been revealed that integrins, the transmembrane proteins of the host cell, play a pivotal role in viral attachment and entry into the cell. Two types of integrin, β_1 and β_3-integrin interact with G_n of apathogenic Hantaviruses and glycoprotein of pathogenic Hantaviruses, respectively (Gavrilovskaya et al., 1998; Mackow and Gavrilovskaya, 2009).

2. Hantavirus genome organization

The genome of Hantaviruses contains three segments of single stranded, negative ribonucleic acid (RNA) molecules with a terminal sequence at their 3`end (Avšič-Županc et al., 2019) as shown in Figure 1. These genome segments are named according to their nucleotide sequence length as small (S), medium (M), and large (L) as shown in Figure 1 (Singh et al., 2022). Hantaviruses are enveloped viruses with a spherical structure of about 80 to 120 nm length in diameter. The envelope membrane is composed of bilayer of exterior lipids secreted from Golgi complex (Hepojoki et al., 2012). The lipid bilayer is lined with spikes (viral proteins) that protrude from the layer around 10 nm. These spikes appear as heterodimers of Gn and Gc glycoproteins and show a significant binding affinity with oligomers (Huiskonen et al., 2010). The complex and unusual symmetry of the spikes is considered rarely common in enveloped viruses (Huiskonen et al., 2010). The S segment comprises 1,700 to 2,100 bp nucleotides encoding N protein that synthesizes the nucleocapsid of the virion. The M segment containing 3,613–3,707 bp nucleotides encodes the envelop protein of 1,150 amino acids for glycoprotein. It carries a conserved pentapeptide motif "WAASA" at its N-terminus that acts as a target site for co-translational cleavage by the cellular peptidase complex (Löber et al., 2001). The L segment is 6,500 nucleotides wide and encodes about 2,160 amino acids for the biosynthesis of RNA-dependent RNA polymerase and other viral proteins like reverse transcriptase that converts the negative sense RNA into positive sense mRNA for protein synthesis and multiple genome copies. Variation and genetic alterations in M and S segments can disturb the virulence and antigenicity of virus (Du et al., 2014).

3. Prevalence

In humans Hantaviruses can cause serious fatal diseases such as hemorrhagic fever renal syndrome (HFRS) in Asia, HFRS and nephropathia epidemica (NE) in Europe and Hantavirus cardiopulmonary syndrome (HCPS) in North and South Americas. In recent years, almost 200,000 people around the world are affected by Hantaviruses annually, with a case fatality of 1–15% for HFRS, 0.1–1% for NE and up to 40–60% for HCPS. Bi et al. (2008) and Singh et al., (2022) two significant outbreaks were documented in the last century which brought Hantavirus disease to worldwide attention. More than 3,000 United Nations forces contracted the HFRS during the Korean War (1950–1953), which was the first time it happened and the second was the outbreak of HCPS in 1993 in the Four Corners area of the United States (Tian and Stenseth, 2019).

3.1. Asia

90% of all the documented cases worldwide are from China, which has the greatest frequency of HFRS, mainly caused by HTNV and SEOV. One of the key HFRS hotspots is the populous central Chinese province of Shaanxi (Yu et al., 2015). According to Chinese Center for Disease Control and Prevention (China CDC) a total of 77,558 cases and 866 fatalities were reported from 2006–2012 possessing a case fatality rate of 1.13%, death rate of 0.01 per 100,000 and a yearly incidence rate of 0.83 per 100,000 cases. HFRS cases have been documented in 30 out of 32 provinces in China as of yet (Zhang et al., 2014). HFRS cases have been mainly documented in autumn-winter and spring seasons (Ke et al., 2016). The incidence of HFRS in China remained low nationwide as compared to the previous five years. As of 18 December 2021, 29 provincial-level administrative divisions (PLDAs) reported 8,502 cases with 54 (0.63%) deaths which was 9.10 and 17.39% more than the 7,793 cases and 46 deaths in 2020 (Aitichou et al., 2005; Wei et al., 2021). Epidemiology of HTNV across asia is shown in Figure 2. The Khabarovsk region reported the first HFRS case in 1934 in Asian Russia. From 1978–1995 a total of 3,145 cases of HFRS in Asian Russia occurred, with a 1.7% morbidity rate (Onishchenko and Ezhlova, 2013). HTNV was first isolated in Korea and an average of 1% mortality rate is recorded for the 300–500 cases reported annually (Lee et al., 2013). A few HFRS have been reported in Vietnam (Huong et al., 2010), Thailand (Suputthamongkol et al., 2005), Singapore (Wong et al., 1985), Sri Lanka (Vitarana et al., 1988),

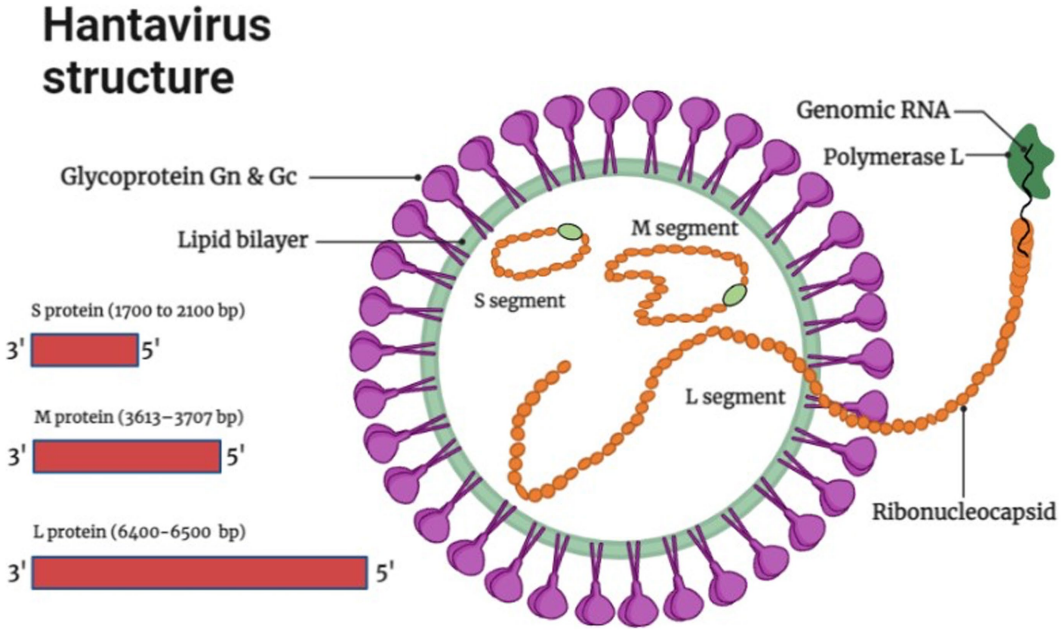

FIGURE 1
Hantavirus structure and genome organization (Image generated: www.biorender.com).

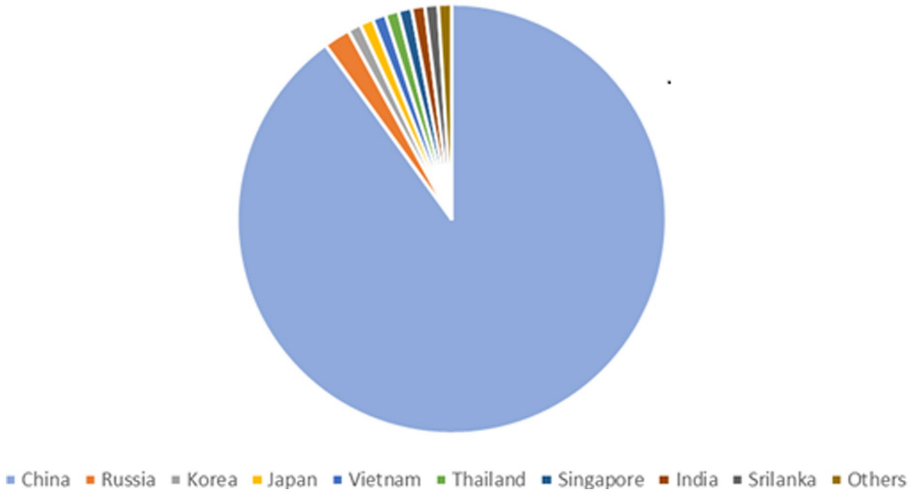

FIGURE 2
Epidemiology of Hantavirus cases across Asia, showing 90% infections in China, 2% in Russia and 1% in Korea, Japan, Vietnam, Thailand, Singapore, India, Srilanka, Others.

India (Chandy et al., 2009) and Japan (Lokugamage et al., 2004) but more data needs to be recorded from these and other regions in Asia (Heyman et al., 2011).

3.2. Europe

Greater than 10,000 HFRS and thousands of NE (nephropathia epidemica) cases are identified on an annual basis all over Europe and are primarily caused by PUUV, DOBV, and SAAV (Vaheri et al., 2013) and (Jiang H. et al., 2017). HFRS cases have been recorded in Finland, Germany, Belgium, France, UK, Poland, the Balkans but in many other areas very few cases are recorded even though the sero-positive prevalence is high in them, which is why more data needs to be documented in Europe because Hantavirus associate infections are high in these areas but remain undocumented (Heyman et al., 2011). Greater than 2,800 cases of Hantavirus caused HFRS were reported in Germany in 2012 (Krüger et al., 2013). In UK SEOV virus associated with acute kidney injury (AKI) in rats was first isolated in Scotland in 1977 and only caused AKI in 1 of 15 rats (Duggan, 2019). Figure 3 No. of HTNV cases across Europe from 2016–2020.

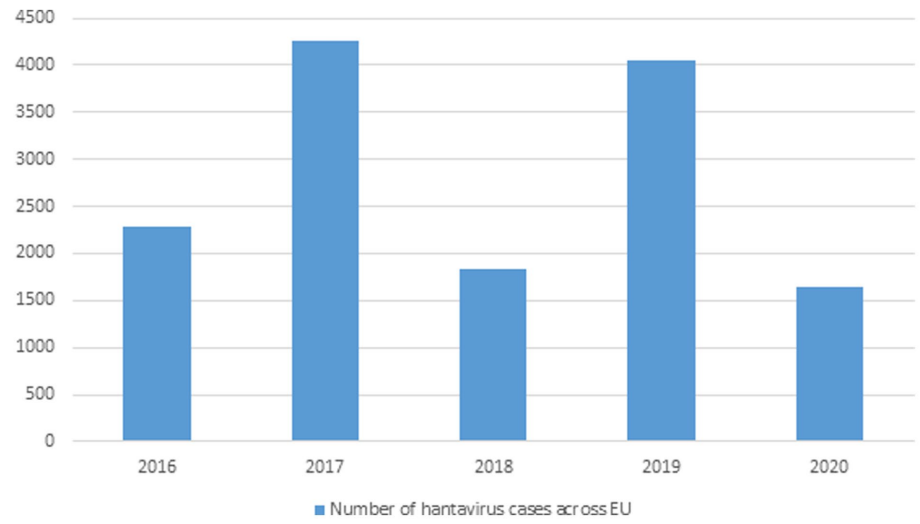

FIGURE 3
Data showing Hantavirus cases in the EU from 2016–2020 (This data was published by the European Center for Disease Control and Prevention).

3.3. Americas

In 1993, HCPS was initially identified as a hantaviral illness during the Four Corners outbreak in the USA. In North and South Americas almost 200 cases are documented annually. HCPS in Americas is primarily caused by ANDV and SNV. HCPS cases have also been reported in Bolivia, Paraguay, Uruguay, Brazil, Argentina, Panama, Chile, and Canada (Jonsson et al., 2010). In Canada 143 confirmed HCPS cases have been recorded as of 2020 (Warner et al., 2020). Each year between 100 and 200 cases of HCPS are recorded in Argentina, mostly in spring and summer (Jiang H. et al., 2017). Chile has the annual mortality rate of 32–35% for HCPS (Martinez-Valdebenito et al., 2014). Brazil recorded 2032 HCPS cases as of 2017. Table 1 shows the Hantavirus reported cases across North and South America (Warner et al., 2020; Armién et al., 2023).

3.4. Africa

No indigenous Hantavirus was recognized in Africa 15 years ago (Kruger et al., 2015). Since then, only a few studies have examined SEOV and other hantaviruses in Africa and their effects on human health. Due to the lack of regionally specific SEOV testing in human blood samples and the paucity of investigations, it appears that SEOV is not a significant public health hazard on the continent (Heyman et al., 2004). However, there are substantial indications that humans and wild rats in 17 different African nations may be infected with organisms similar to SEOV (Clement et al., 2019). In Africa, the SEOV is not seen as a serious hazard to the general population.

3.5. Pathogenesis

Hantaviruses infections cause HFRS, NE, and HCPS in humans, the symptoms associated with them and their mode of transmission is discussed below.

3.6. Symptoms associated with HFRS and NE

Kidneys are primarily affected in both HFRS and NE. NE is a relatively mild version of HFRS. Symptoms include thrombocytopenia, fever, differing degrees of acute renal failure, myalgia some cases have also reported symptoms related to ocular and central nervous systems. Both of them have five clinical phases febrile, hypotensive, oliguric, polyuric and convalescent. Complications can include multiorgan failure, bleedings, severe encephalomyelitis, pituitary hemorrhage, pulmonary edema, shock and fatal outcome in case of NC and all the aforementioned complications in addition to glomerulonephritis, respiratory distress syndrome and disseminated intravascular congestion can occur in HFRS as shown in Table 2 (Jiang et al., 2016; Jiang H. et al., 2017; Hautala et al., 2021).

3.7. Symptoms associated with HCPS

Lungs are mainly affected in HCPS. Three phases are associated with HCPS they are prodromal, cardiopulmonary, convalescent phases. Prodromal phase lasts 1–5 days and symptoms include malaise, fever, gastrointestinal distress and headaches. Cardiopulmonary phase symptoms include cardiopulmonary malfunction, pulmonary edema, cough, dyspnea and hypoxia. Convalescent phase is the recovery phase where all previous symptoms subside except for dyspnea, which can persist up to 1–2 years (Llah et al., 2018).

3.8. Spread of hantaviruses

Hantaviruses basically infect rodents and are also found in small insectivorous mammals and bats. They cause asymptomatic infections in rodents, and are transmitted to humans through rodent bite, inhalation of aerosolized virus particles and via inhalation of dried

TABLE 1 Reported HTNV cases across North, Central, and South America.

Country	Cases	Year	Source
USA	850	1993–2021	CDC
Canada	143	As of 2020	Warner et al. (2020)
Panama	712	1999–2019	Armién et al. (2023)
Costa Rica	3	Till 2016	PAHO
Argentina	1,350	As 2016	PAHO
Chile	1,028	As of 2016	PAHO
Brazil	2032	Till 2017	PAHO
Paraguay	319	Till 2016	PAHO
Uruguay	169	Till 2016	PAHO
Bolivia	300	Till 2016	PAHO
Ecuador	73	As of 2016	PAHO
Peru	6	As of 2016	PAHO
French Guiana	3	Till 2016	PAHO

TABLE 2 Depicts five phases of HFRS and NE and the main associated features.

Phase	Time of occurrence	Main features
Febrile	1–7 days	Myalgia, fever
Hypo-tensive	1–3 days	Hypo-tension
Oliguric	2–6 days	Decreased urine level
Polyuric	2 weeks	Increased urine level
Convalescent	3–6 months	Frailty, lethargy

feces, urine and saliva of rodents. Hantavirus infection in humans mainly affects the endothelial cells in lungs and kidneys and leads to HCPS, NE, and HFRS (Ermonval et al., 2016). Environmental factors such as availability of food, climate change, geographical location also contributes to Hantavirus infection (Guterres and de Lemos, 2018).

3.9. Proposed mechanism of Hantavirus pathogenesis

The infection begins with contact of Gn and Gc surface proteins with β-integrin receptors, yet how hantaviruses spread in the human body is still not fully known. Given that they express 3-integrin receptors and are found close to epithelial cells, immature dendritic cells likely play a crucial role (Gavrilovskaya et al., 1999, 2002). Platelet dysfunction, immunological responses, and the disruption of endothelial cell barrier capabilities likely have a role in the pathological process of Hantavirus (Mackow and Gavrilovskaya, 2009). DCs in humans are extremely mobile, they link innate and adaptive immunity and reside in pathogen-host interface in the respiratory mucosa and lung alveoli. They have the ability to "snorkel" through the epithelial-tight junctions by introducing their dendritic projections into the airway lumen (Jahnsen et al., 2006) and contract Hantavirus in the lungs (Raftery et al., 2002; Marsac et al., 2011). Additionally, monocytes exposed to HTNV transform into cells that resemble DCs (Markotić et al., 2007; Schönrich et al., 2008) that might serve as Trojan horse, assisting viruses to spread across the human body and eventually infect endothelial cells in numerous organs. It has been seen in various studies that EC become stimulated during PUUV infection, increasing the production of chemokines and adhesion molecules such as E-Selectin, intercellular adhesion molecule 1 (ICAM-1) and VCAM-1 (Temonen et al., 1996). Stimulated chemokines include a neutrophil activator and recruiter called IL-8 (interleukin 8) (Klingström et al., 2008; Sadeghi et al., 2011; Libraty et al., 2012; Kyriakidis and Papa, 2013). Production of human leucocyte antigen mainly HLA-E is elevated on EC, which in turn activates nature killer (NK) cells (Kraus et al., 2004; Björkström et al., 2011). Hantavirus-infected EC may be removed by activated immune cell's cytotoxic action, which could lead to vascular leakage (Hayasaka et al., 2007). HTNV infected EC are somewhat defended from cytotoxic T cells and NK cells (Gupta et al., 2013) uninfected EC's are however, vulnerable to cytotoxic assault and bystander killing. According to recent studies, neutrophils can generally contribute to the immunopathogenesis (Gupta et al., 2010; Saffarzadeh et al., 2012) by interacting with active EC they go through 2 mechanisms of programmed cell death. Virus-induced 2 integrin signaling causes neutrophils to become activated, which then leads to either NETosis or the production of inflammatory cytokines like TNF-α or VEGF, depending on the 2 integrin ligands involved and possibly additional micro-environmental stimuli, resulting in increase in the vascular leakage, though through different processes (Schönrich et al., 2015). Pentraxin-related protein 3 (PTX3), a humoral pattern-recognizing receptor, activates complement during acute HFRS (Outinen et al., 2012). PTX3 is kept in neutrophil granules and released *via* integrins in response to signals (Jaillon et al., 2007; Razvina et al., 2015). In addition to cytoskeletal rearrangements in EC, the soluble complement components C3a and C5a produced after complement activation by antibodies and PTX3 also causes IL-8 production (Monsinjon et al., 2003). As a result, PTX3 draws additional neutrophils to the endothelium barrier, escalating the inflammation in the vessels. TNF alpha a pro-inflammatory cytokine is released by Hantavirus-infected macrophages, DC as well as NK cells, neutrophils and CD8+ T cells that have been activated (Raftery et al., 2002; Marsac et al., 2011; Shin et al., 2012). TNF-α (Tumor necrosis factor alpha) eliminates the virus from infected cells by non-cytolytic processes, it may, on the one hand, aid in the control of hantaviral propagation (Khaiboullina et al., 2000; Guidotti and Chisari, 2001). On the other hand, vascular leakage and breathing problems are generated if it is given externally in proportions that are encountered during Hantavirus infection (Tracey and Cerami, 1994; Wimer, 1998). Both direct and indirect methods may cause localized TNF-local release at the EC contact to promote vascular permeability(Schönrich et al., 2015). Figure 4 illustrates the proposed immunological mechanisms that result in endothelial barrier breakdown by the Hantavirus.

3.10. Replication cycle of hantaviruses

Macrophages and vascular endothelial cells, particularly those in the lungs and kidneys, are targeted by the Hantavirus (Yanagihara and Silverman, 1990). In order to facilitate binding, Gn protein of the virus engages with integrin receptors that reside on the outer layer of the

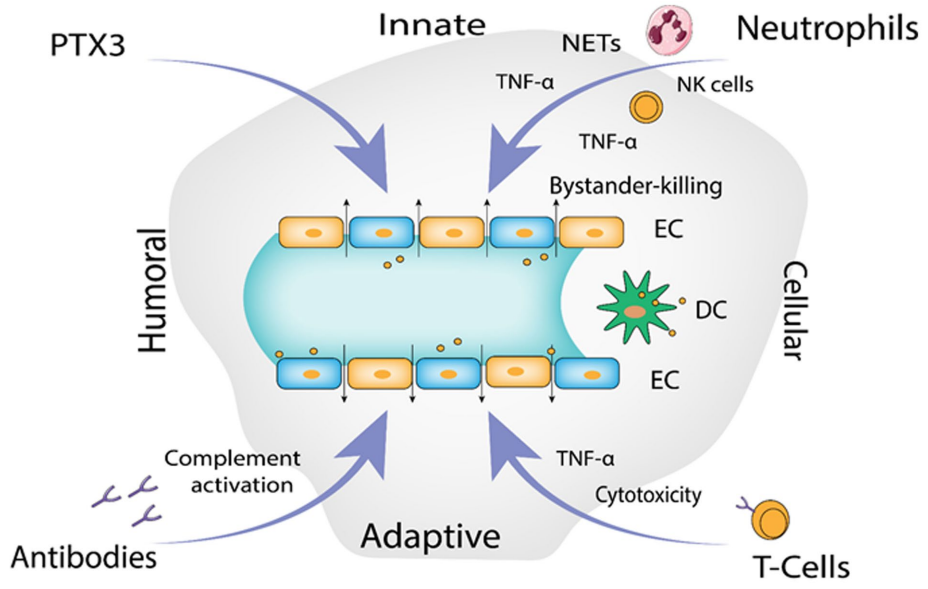

FIGURE 4
The proposed immunological mechanisms leading to endothelial barrier breakdown by the Hantavirus (Image generated: www.biorender.com).

cell it invades, according to a number of findings (Mir and Panganiban, 2010). A family of heterodimeric proteins called integrins include both alpha and beta chains. Both cell to extracellular matrix and cell to cell interactions are facilitated by it (Takagi and Springer, 2002; Campbell and Humphries, 2011). Virons are eventually carried to lysosomes after binding, which is accomplished *via* clathrin-coated pits. In the endolysosomal compartment, virions uncoat, releasing three viral nucleocapsids into the cytoplasm (Jin et al., 2002). The virus is engulfed by clathrin-coated vesicle (CCV), which is composed of clathrin-coated cellular membrane (Ramanathan and Jonsson, 2008). Three mRNAs transcribed by RdRp, one from the S, M, and L sections of the viral RNA. Free ribosomes are locations for the translation of the S and L derived mRNAs. Whereas, (RER) rough endoplasmic reticulum is where M-specific mRNAs are converted into proteins. Two glycoproteins, Gn and Gc, are produced as a result of the glycoprotein precursor's intrinsic cleavage at a highly conserved amino acid sequence (Spiropoulou, 2001). For glycosylation, the Golgi complex receives the glycoproteins Gn and Gc, where hanta virions are thought to develop as illustrated in Figure 5. Followed by exocytosis, migration to the golgi cisternae, then to the outer membrane of secretory vesicles and finally egression through exocytosis. The details of virion egress, however, are mostly unclear (Szabo, 2017). Other possible mechanisms for virus entry include caveola, macropinocytosis, cholesterol-dependent endocytosis, clathrin-independent endocytosis-mediated receptor and micropinocytosis (Ramanathan et al., 2007).

4. Diagnosis

Initial diagnosis can be performed by observing the symptoms associated with HCPS, HFRS, and NE. Since Hantaviruses are rodent transmitted viruses so clues can be obtained for diagnosis at the time of taking patient's history by asking if a patient recently traveled to areas infested with rodents or came in contact with rodents or their excretions. Screening tests such as Complete Blood Count (CBC) and peripheral smear can also be used (Dvorscak and Czuchlewski, 2014).

Serological methods available for definite diagnosis of infection caused by Hantaviruses. Serology is used to detect IgG and IgM anti-hantaviral antibodies in the blood of the patient. The IgM antibodies appear extremely early during the course of the infection, whereas IgG antibodies appear later in the process. Enzyme Linked Immunosorbent Assay (ELISA) and the strip immunoblot detects viral antibodies, only disadvantage is the potential for cross reacting with other viral antigens, but are still extremely useful and important for diagnosis purposes. Indirect Immunofluorescence assay is more specific than Elisa but it is laborious. Neutralization tests are the most specific serological tests but are costly, laborious and require BSL-3 conditions. Immunochromatographic tests are readily performed and are cheap but cross reactivity minimizes precision of results obtained (Schubert et al., 2001; Meisel et al., 2006; Navarrete et al., 2007).

Molecular methods include Real Time RT PCR, an important, sensitive and fast technique for detecting viral RNA in blood, blood clots or tissues, its only disadvantage includes that it only yields results during the viremic phase of the Hantavirus caused infection (Aitichou et al., 2005). Microarray technique is fast, sensitive and allows simultaneous detection of thousands of viruses but is costly and the data analysis is complex. Next Generation Sequencing (NGS) is also used for virus detection and complete sequencing but it is expensive and requires complex bioinformatics tools.

Virological methods include isolation in cell cultures which allows extensive functional and virological studies but is laborious and requires specially trained personnel and BSL-3 conditions. Immunohistochemistry by enzyme immunoassay and immunofluorescent test allows diagnosis from infected tissues of organs but laborious preparations are required (Kruger et al., 2015).

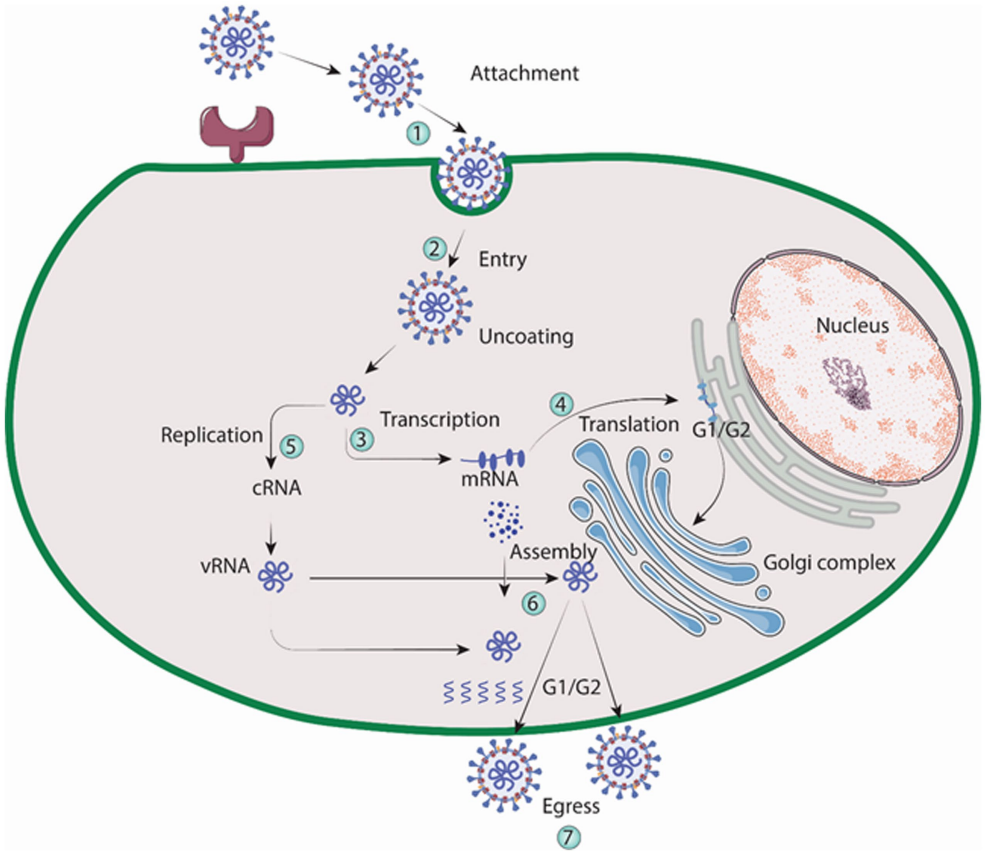

FIGURE 5
Replication cycle of Hantavirus (Image generated: www.biorender.com).

5. Treatment and management

Hantavirus infections are managed mostly by managing the symptoms, providing supporting care and admitting patients to the Intensive Care Unit (ICU), providing patients with oxygen therapy, by administrating an antiviral ribavirin, which has showed reduction in death rate of patients still in their initial stages of infection. Treatment for HCPS patients includes respiratory and cardiac monitoring and support which includes mechanical ventilation, hemofiltration and membrane oxygenation. Supportive treatment for HRFS includes electrolyte infusion and hydration to stabilize blood pressure, acute thrombocytopenia is managed with transfusing platelets, uremia is managed with intermittent hemodialysis and continuous renal replacement therapy is given to manage multi-organ pulmonary edema (Sargianou et al., 2012; Liu et al., 2020).

6. Recent therapeutic advances against Hantavirus

6.1. Blocking viral entry

The following candidate drugs have been shown to increase survival rate only in the initial stages of HTNV infection, but are ineffective in later stages.

6.1.1. Griffithsin

A protein called griffithsin (GRFT), which was first discovered from red algae, has demonstrated potential as a multifunctional antiviral agent. Its capacity to prevent the invasion of several viruses, including HIV and SARS-CoV, has been researched (O'Keefe et al., 2010; Lusvarghi and Bewley, 2016). The spikes of the Hantavirus consist of tetramers formed by Gn-Gc heterodimers, which envelop the entire surface of the virus particle. Gn, one of the viral envelope glycoproteins, contains several N-linked glycosylation sites and is positioned on the virus surface, making it a potential primary target for GRFT. A high-mannose oligosaccharide-binding lectin called Griffithsin (GRFT) is now being tested in phase I clinical trials as a topical microbicide for the defense against several viruses. It is a powerful inhibitor of ANDV infection. The fact that GRFT prevented the entry of pseudo-particles containing ANDV envelope glycoprotein into host cells suggests that it prevents the function of viral envelope protein during entry. To combat ANDV and SNV infection, 3mGRFT (trimeric synthetic tandemer of GRFT) is more effective than GRFT (Shrivastava-Ranjan et al., 2020). In a recent study GFRT prevented the entry and HTNV infection of recombinant vesicular stomatitis virus (VSV) containing HTNV glycoproteins into host cells *in vitro* by attaching to the viral N-glycans. It also shielded the suckling mice from death brought on by cerebral exposure to HTNV, according to *in vivo* tests. These findings highlighted the importance of GRFT as a potential HTNV infection inhibitor (Zhao et al., 2022).

6.1.2. Coumarin

Coumarin and its derivatives have been found to have antiviral activity against a variety of viruses, including human immunodeficiency virus (HIV), hepatitis virus, herpes simplex virus, CHIKV, and enterovirus 71. Coumarin derivative's potential use is as antiviral medicines. The diverse chemical makeup of coumarin derivatives however, meant that these substances had an impact on the many stages of a virus life cycle. Tricyclic coumarin GUT-70 inhibited HIV's ability to attach and fuse to cellular walls and plasma membranes, while dipyranocoumarin (+)-calanolide A could block reverse transcription (Xu et al., 2021). Coumarin dimmer analogs could also block HIV integrase, and amide coumarin derivatives could affect how HIV was put together. On the basis of molecular structure of coumarin, two of the most common coumarin derivatives, dicoumarin and pyrone-coumarin, were synthesized. It was demonstrated that the tri-fluoro substituent on the benzene ring of the dicoumarin derivatives N6 and N7 had a strong anti-HTNV action (Li et al., 2022a). Dicoumarin demonstrated increased anti-HTNV activity, and adding Cl or CF3 might increase the inhibitory activity and selectivity to the HTNV, according to the structure activity relationship (SAR). To clarify the connection between the chemical structure and the biological action against the HTNV, more research is necessary. N6, a derivative of coumarin, showed both *in vivo* and *in vitro* action against HTNV, and AKT1 may have played a role in the molecular mechanism by which N6 combats viral infection (Reguera et al., 2010; Li et al., 2021, 2022b). Therefore, finding novel coumarin compounds that could fight viral infection has significant significance for creating potent drugs.

6.1.3. Lactoferrin

Lactoferrin (LF), a glycoprotein that binds to iron and has been shown to have broad antibacterial, antifungal and antiviral properties, inhibited hantaviral attachment, adsorption (Masson et al., 1969; Buys et al., 2011). Both *in vitro* and *in vivo* studies have demonstrated that LF guards against Hantavirus infection (Murphy et al., 2001). Lactoferrin was found partially effective in preventing HFRS by restricting focus formation in suckling mice, but when used *in-vivo* in combinations with ribavirin, it prevented focus development entirely (Murphy et al., 2001).

In a study, Seoul virus (SEOV) was used to infect Vero E6 cells in order to test the antiviral potency of LF against hantaviruses. The objective of the study was to contrast LF's antiviral activity with that of Rbv.100 μg/mL of RBV administered after infection reduced the number of foci by 97.5%. Vero E6 cells treated with 400 μg/mL of LF showed a significant 85% decrease in the number of foci as compared to the control group. However, in LF-pretreated cells, the number of foci began to increase by 24 h post-infection (hpi). At 24 hpi LF prevented viral shedding, but not after 48 hpi (Murphy et al., 2001). As shown by another supporting study, the findings suggested that LF may attach to cell surfaces and prevent SEOV from adhering to host cells in the early stages of infection (Murphy et al., 2000). It is interesting to note that, LF improved cell survival rates following hantaviral amplification despite not inhibiting the formation of NP or Gc. This is due to the ability of LF to increase the cytocidal activity of NK cells (Murphy et al., 2001). However, the specific method through which LF block SEOV absorption, affect host immune responses and has an effect on other Hantavirus species are still unknown.

6.1.4. Virus fusion inhibitors (domain III and stem peptides)

Several processes are thought to be involved in virus-cell membrane fusion (Kielian and Rey, 2006; Harrison, 2015). During viral fusion, fusion proteins become activated and insert a fusion peptide or loop into the target membrane. As a result, an intermediate phase is generated in which one end of the fusion protein can join to the viral envelope *via* transmembrane region, linking the viral and cellular membranes together. The fusion protein undergoes conformational changes which can draw both anchors together, achieving a hairpin-like structure where both domains gather at one end. After that, the outer leaflets of membranes fuse to form a hemi-fusion intermediate, followed by complete membrane fusion once the opposed membranes have been brought together with the help of local membrane curvature. A pore is formed as a result of the fusion, allowing the virus to inject its ribonucleocapsids into the cytoplasm of the cell and begin replication.

On the basis of molecular structures, viral fusion proteins are categorized into three classes: I, II, and III. Alpha helices make up the majority of class I fusion proteins, while beta sheets make up the majority of class II proteins. Class III fusion proteins exhibit characteristics from both class I and class II (Kielian, 2014; Modis, 2014; Harrison, 2015). *In silico* and *in vitro* investigations reveal that Hantavirus Gc glycoprotein resembles class II fusion proteins (Cifuentes-Munoz et al., 2011). Three domains (I-III) and a stem connecting the ectodomain to the transmembrane region make up class II fusion proteins (Rey et al., 1995; Kielian, 2006). During fusion, DIII advances toward the fusion loop to adopt a hairpin-like structure (Bressanelli et al., 2004; Gibbons et al., 2004). This movement is followed by stem region which folds against the trimeric core created by the fusion protein (Roman-Sosa and Kielian, 2011; DuBois et al., 2013; Klein et al., 2013). It is possible to intervene and stop the fusion process as a result of these significant conformational changes, thereby inhibiting viral infection. It is possible to delay or block viral entry by selectively binding ligands to a fusion protein's intermediate form before it assumes its post-fusion conformation (Barriga et al., 2016). It has been demonstrated that protein fragments spanning the stem region and domain III (DIII) are capable of inhibiting these fusion proteins. Due to this, to block viral fusion and entrance into the cell, recombinant ANDV DIII and stem peptides were developed. A 60% reduction in Vero E6 infection by ANDV *via* the endosomal pathway was achieved by combining DIII with the C-terminal of stem region. Over 95% infection was prevented when ANDV fused at the plasma membrane. These findings indicated that a stem fragment method used against Hantavirus may obviously block the fusion of related viruses belonging to the same genus (Barriga et al., 2016).

6.1.5. Hantavirus-binding receptor inhibitors (cyclic nonapeptides)

Hantaviruses have two transmembrane glycoproteins, Gn and Gc, derived from a single glycoprotein precursor through proteolytic cleavage that occurs during post-translational modifications (Jonsson and Schmaljohn, 2001). The entry of hantaviruses into human endothelial cells is facilitated by the interaction of viral surface glycoproteins with αvβ3 integrins present on the host cell surface (Gavrilovskaya et al., 1999; Raymond et al., 2005). Both Gn and Gc may play a role in the entry of viruses, Gn is involved in the viral

attachment process while Gc is thought to drive membrane fusion (Mackow and Gavrilovskaya, 2001; Tischler et al., 2005).

Small molecules like peptide ligands have potential therapeutic applications as they can bind to specific proteins and interfere with particular protein–protein interactions (Mayor et al., 2021). For this purpose, particular peptides can be synthesized either by imitating one of the binding partners or by creating new binding interactions. Novel peptide ligands were created with the ability to block SNV infection. SNV, the causative agent of HCPS, is classified as a category A pathogen by the NIAID. Currently, there is no specific treatment for HCPS and its fatality rate remains high reaching approximately 40%.

Therapeutics that target SNV particularly are still lacking. To tackle this issue, researchers are utilizing phage display technique to discover cyclic nonapeptides that can bind to the cellular receptor αvβ3. By identifying these peptides, they aim to prevent Hantavirus entry including SNV into the human endothelial cells particularly during *in vitro* experiments with Vero E6 cells (Larson et al., 2005; Hall et al., 2007). These peptides offer therapeutic promise while avoiding the potential adverse effects often associated with conventional mAbs employed as therapeutic agents to inhibit such interaction (Baudouin et al., 2003; Gauvreau et al., 2003). Cyclic nonapeptides were created using peptide sequences from phage that displayed the most potent infection inhibition. However, when tested, the isolated peptides showed lower effectiveness in blocking infection (ranging from 9.0 to 27.6% inhibition) compared to the phage-presented peptides, which achieved inhibition levels of 74.0 to 82.6%. As the phage displayed pentavalent peptides, the focus was on exploring whether presenting the identified peptides in a multivalent manner would lead to enhance inhibition. In order to do this, certain cyclic peptides were bound to multivalent nanoparticles using carboxyl linkages and their ability to suppress infection was examined (Hall et al., 2008).

With a 4:1 nanoparticle-to-virus ratio, SNV infection was reported to be inhibited *in vitro* by two of the synthetic cyclic nonapeptides CLVRNLAWC and CQATTARNC. CLVRNLAWC inhibited the infection by 9–32.5% while CQATTARNC inhibited it by 27.6–37.6%. At a 20:1 ratio, CQATTARNC decreased infection by 50% (Hall et al., 2008). These findings demonstrate the potential therapeutic value of multivalent inhibitors in the disruption of interactions between proteins, particularly those critical for host cell viral infection. Based on molecular makeup and potential capacity to engage the αvβ3 cell receptor, further peptidomimetic compounds were selected. In the first round of screening, 49 peptidomimetic compounds and in the second round, 68 compounds were found having an anti-Hantavirus action in lower 2,000 μM range. Due to this, a special collection of chemicals were acquired for the subsequent phases of drug development. The antiviral potential of these chemical compounds requires improvement and *in vivo* research to support it (Hall et al., 2010).

6.2. Blocking viral replication

6.2.1. Ribavirin

When used both *in vitro* and *in vivo*, the purine nucleoside analog ribavirin exhibits a wide range of antiviral effects against numerous different RNA, DNA viruses and it works by blocking viral replication. However, its pleiotropic effects, make it difficult to understand how it works (Fernandez-Larsson and Patterson, 1990; Graci and Cameron, 2006). These contain both direct mechanisms, like interfering with RNA capping, inhibiting polymerase activity, and inducing lethal mutagenesis, as well as indirect mechanisms, such as inhibiting inosine monophosphate dehydrogenase and exerting immunomodulatory effects (see Figure 6). The first specialized phase in the cellular production of guanine nucleotides, involves the catalytic activity of enzyme IMPDH. This process relies on NAD^+ and involves the transformation of inosine monophosphate to xanthosine monophosphate. Because Ribavirin 5′-monophosphate (RMP) bears structural resemblance to GMP, It serves as a highly effective competitive inhibitor of IMP dehydrogenase (Streeter et al., 1973). Human IMP dehydrogenase (IMPDH) type I and type II isoforms are both potently inhibited by RMP, which reduces *de novo* GTP production. Because of this disturbance, viral RdRp (RNA-dependent RNA polymerase) cannot function properly. The antiviral effects of ribavirin are assumed to be related to its ability to inhibit IMP dehydrogenase (IMPDH) (Graci and Cameron, 2006).

Moreover, RBV was found to control host immunological responses by inhibiting the production of interleukin-10 by regulatory T cells (Kobayashi et al., 2012). The blocking mechanism of ribavirin is believed to target the capping (Goswami et al., 1979) and translation efficiency (Toltzis and Huang, 1986) of viral mRNA, along with the direct reduction of the viral polymerase's activity (Wray et al., 1985; Fernandez-Larsson and Patterson, 1989). Ribavirin acts by interfering with the accuracy and effectiveness of polymerase replication. As a result, it may induce chain termination more frequently or improper nucleotide insertion, which could result in error catastrophe. Recent investigation showed that ribavirin rises the chances of error made by the Hantavirus polymerase within a cell culture model (Severson et al., 2003). We assumed that this elevated error rate is because of the integration of ribavirin into the viral RNAs *via* RNA-dependent RNA polymerase. It has been shown that ribavirin causes hantaviruses to replicate in an error-prone manner, which lowers the viral titer (Severson et al., 2003).

Although more investigation is required to completely understand how ribavirin inhibits Hantavirus, the findings of Severson et al. (2003) indicated that ribavirin may function as a mutagen *via* directly integrating into the S-segment of cRNA or mRNA through the viral RdRp. The amount of error-free mRNA falls when ribavirin is integrated into mRNA, which might lower the amount of viral proteins required to construct infectious viral particles. The amount of mRNA was, however, significantly decreased in these experiments. This finding implies that the ribavirin integration may reduce mRNA stability. This theory appears to be a logical and convincing explanation given the virus life cycle. As a result, the integration of ribavirin could accelerate viral mRNA to become more unstable and break down more quickly within the host cell (Jonsson et al., 2005).

6.2.2. ETAR

ETAR, also known as (1-beta-d-ribofuranosyl-3-ethynyl-[1,2,4] triazole), functions as a nucleoside analog and is similar to ribavirin in that it prevents HV replication by lowering the levels of GTP. Notably, ETAR showed superior efficacy to ribavirin as a therapeutic option in trials on suckling mice infected with HTNV. Due to the absence of pseudo base pairs, ETAR is unlikely to cause mutations (Chung et al., 2008). Furthermore, there is no proof that ETAR has any immunoregulatory effects (Szabo, 2017).

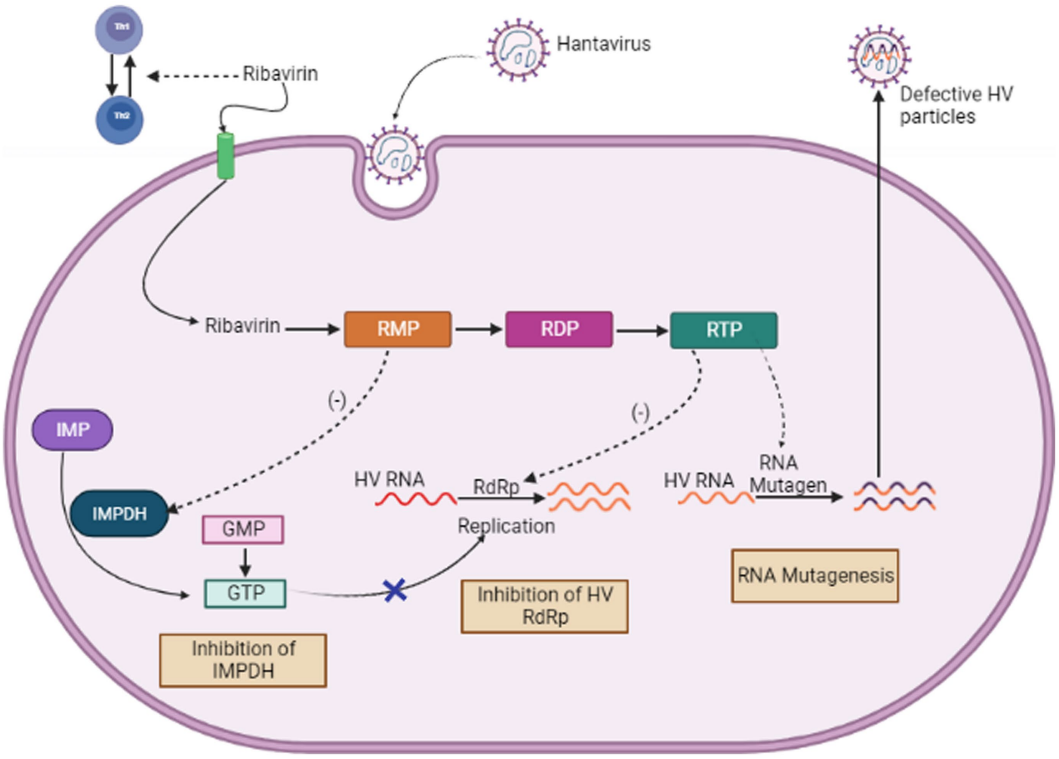

FIGURE 6
Mechanism of Action of Ribavirin (Image generated: www.biorender.com).

6.2.3. Favipiravir

T-705 is a pyrazine derivative also referred to as favipiravir or 6-fluoro-3-hydroxy-2-pyrazinecarboxamide. It was initially known for its ability to combat influenza, but it is now thought to have antiviral capabilities against a number of other viruses that rely on RdRp for replication (Furuta et al., 2009). Flaviviruses, noroviruses, arenaviruses, and bunyaviruses (Gowen et al., 2007) are some of these viruses. T-705 works as a prodrug that is transformed into T-705-4-ribofuranosyl-5-triphosphate with the help of several intracellular enzymes. When T-705-4-ribofuranosyl-5-triphosphate is created, it functions as a purine nucleotide analog, it is incorporated into the newly synthesized RNA chain, selectively inhibiting RdRp (Furuta et al., 2005). Favipiravir causes the production of non-infectious viral particles when it is employed by the viral polymerase as an alternative nucleoside substrate.

Favipiravir was investigated in both non-fatal and fatal SNV/ANDV hamster models, and the outcome showed a reduction in viral load in hamster serum and different organs. Furthermore, in the lethal ANDV infection model, the use of Favipiravir led to 100% survival (Safronetz et al., 2013). Other studies have shown that after viremia has started, the ANDV/hamster model did not offer protection against delayed antiviral treatment (Munir et al., 2021).

6.2.4. Baloxavir acid

Small molecules also gained importance for their antiviral potential (Deng et al., 2020). Baloxavir, a recently licensed influenza medication derived from BXM, is an endonuclease-targeting small molecule that prevents the translation of the influenza virus and also prevents the virus from replicating. Since the mRNA produced by the viral RdRp lacks a 5′ cap and both hantaviruses and influenza viruses fall within the category of negative-sense RNA viruses, these viruses must acquire a host mRNA cap and apply it to their mRNA (Reguera et al., 2010). BXA specifically targets the PA-PB1-PB2 trimer belonging to the endonuclease domain of the influenza virus. The structures of the RdRp molecules of VSV, a mononegavirus, and another bunyavirus, La Crosse virus (LACV), among others, suggest that the RdRp molecules of negative-sense viruses share certain fundamental characteristics. Particularly within the order *Bunyavirales*, the endonuclease domain of RdRp appears to be more conserved than the other domains. BXA was incorporated into the active center of the RNA endonuclease domain by utilizing the well-known ANDV LP RNA endonuclease domain structure and computationally modeling the HTNV domain. This novel method revealed a previously unknown relationship with Influenza B virus (IBV), illuminating the potential fitness implications. Modeling outcomes might explain why BXA inhibits Hantavirus replication. Additionally, because of the structural closeness of the endonucleases in these viruses, this approach may also apply to arenaviruses (Ye et al., 2019).

6.2.5. siRNA-based therapy

RNA interference (RNAi) has emerged as a new exciting frontier for antiviral therapies. RNAi is a post-transcriptional, and highly specific cellular mechanism in eukaryotic cells where small non-coding RNA molecules (typically 21–25 nucleotides long) bind to specific mRNA molecules and degrade them, thereby inhibiting the expression of specific genes (Ambesajir et al., 2012). For the degradation and cleavage of the mRNA before translation, the siRNA duplexes are integrated into an RNA-induced silencing complex (RISC) (Fire et al., 1998; Elbashir et al., 2001; MacRae et al., 2006). The siRNAs possess complementary sequences that bind to the target mRNA after

transcription and inhibit its translation, as illustrated in Figure 7. The precision and accuracy of RNAi make it an accessible option for gene silencing (Tian et al., 2021). Since the discovery of RNAi in 1900, RNAi technologies have developed rapidly to suppress rogue viruses. So, there is a wide range of viruses that can be inhibited by RNAi-based methods, both *in vivo* and *in vitro* (Weinberg and Arbuthnot, 2010).

Research has shown that HIV-1, polioviruses, nairoviruses, and Lassa viruses can be eradicated using RNAi as a strategy *in vitro* by inhibiting viral replication (Flusin et al., 2011). Researchers found that RNAi can be used to inhibit SARS-CoV-2 replication (Ricci et al., 2020). For some other viruses that affect humans and animals, RNAi-based therapies effectively reduce viral loads and increase the chances of survival (DeVincenzo et al., 2010). But the problem with RNAi technology is its delivery and most of the studies are only limited to *in vitro*. Scientists are working to find carriers to safely deliver the siRNA (Bobbin and Rossi, 2016). In this way, RNAi combinations can avoid problems associated with multidrug sensitivities and toxicity. By targeting rapidly evolving viral sequences, RNAi-based therapies prevent the emergence of drug-resistant viruses (Chen et al., 2018). It is also possible for RNAi-based drugs to produce a sustained therapeutic response since genes can be introduced.

Hantaviral replication can be prevented most directly and effectively by targeting viral RNAs. A prospective antiviral method has been evaluated using siRNA against targeted hantaviral genes, which may enhance virus RNA clearance based on RNA interfering (RNAi) processes. In Vero E6 cells or human lung microvascular endothelial cells, it has been demonstrated that siRNAs targeting the S, M, or L segments of the ANDV may decrease viral replication. In Vero E6 cells, an S-targeted siRNA pool appeared to be more efficient in inhibiting viral transcription and replication than an M- or L-targeted siRNA pool (Chiang et al., 2014). Significantly, even if administered after infection, these siRNAs may prevent ANDV replication.

However, since siRNAs are low in biological stability and *in vivo* targeting ability, their antiviral efficacy may be severely hindered despite their successful inhibition of Hantavirus amplification in host cells. One method of treating in a mouse model of HTNV-induced encephalitis is intraperitoneal administration of recombinant antibodies that recognize HTNV Gc (3G1-Ck-tP). These antibodies were combined with siRNAs that target the encoding regions of the HTNV genome. This resulted in siRNAs being delivered precisely to HTNV-infected brain cells and HTNV intracranial infection being prevented (Yang et al., 2017). Moreover, the shRNA expression showed promising results by

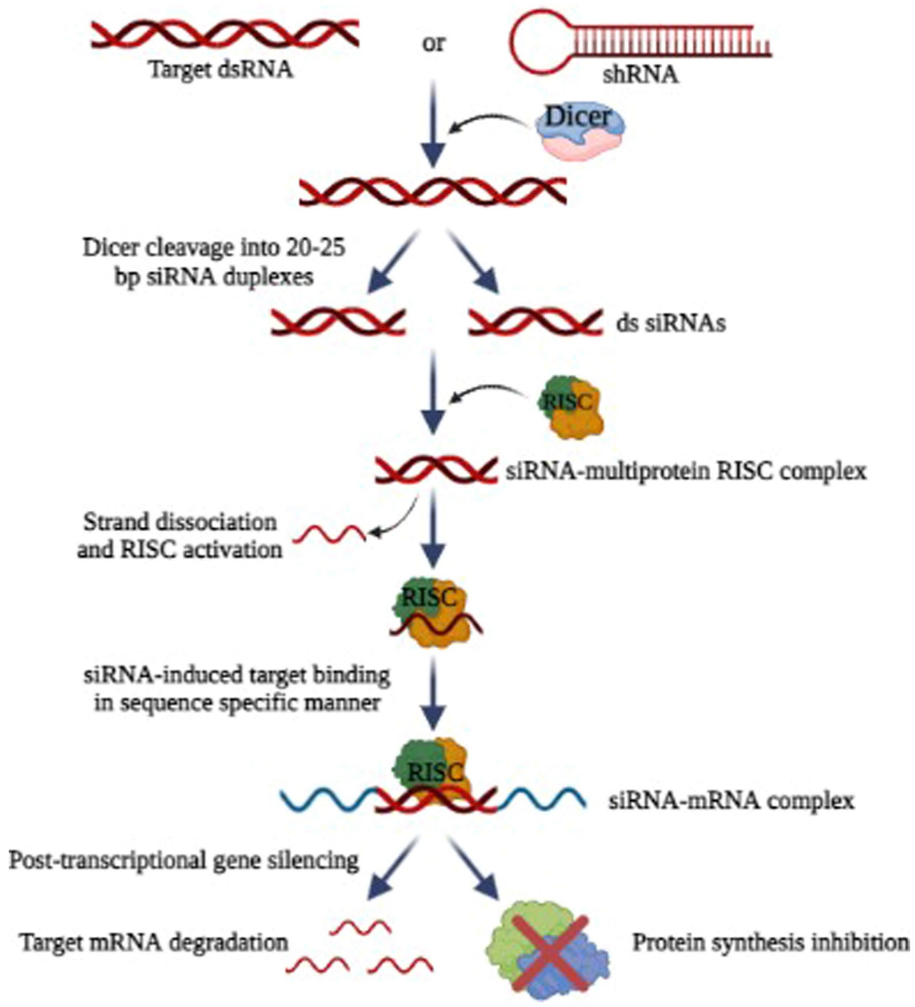

FIGURE 7
Mechanism of RNA interference (Image generated: www.biorender.com).

inhibiting HTNV infection in both *in vitro* and *in vivo* (Liu et al., 2016). To ensure the stability and selectivity of siRNAs, innovative delivery mechanisms should be created; however, it is yet unknown how effective and safe these systems will be in the treatment of HFRS or HCPS.

6.3. Host-targeting antiviral

6.3.1. Vandetanib

Hantavirus-induced increased endothelial microvascular cell permeability was checked through *in-vitro* techniques. The expression of the cellular adhesion molecules including VE-cadherin and VEGF were both increased and decreased as a result of ANDV infection, which also increased the phosphorylation of the VEGF-receptor 2 (VEGFR2) (Gorbunova et al., 2010; Bird et al., 2016). As a result of ANDV infection, the VEGF-A expression was shown to be enhanced in the 3D model of human lungs tissue (Sundström et al., 2016).

The activation of SFK (Src family kinases) signaling may result from the binding of VEGF to VEGFR2, which has the ability to cause the dissociation, internalization, and destruction of VE-cadherin. The structural integrity of adherent junctions was damaged as a result of changes in VE-cadherin expression and localization, which led to an increase in cellular permeability (Jiang et al., 2016). According to studies, the connection between β3 integrin and VEGFR2 can be disrupted by HTNV or ANDV infection, which causes excessive phosphorylation of VEGFR2. Because of this disturbance, infected endothelium cells may become more permeable by becoming more VEGF-responsive (Wang et al., 2012).

In one investigation, it was discovered that the use of a VEGFR2 kinase inhibitor and SFK inhibitors significantly reduced the increased endovascular permeability brought on by ANDV. Particularly successful were the SFK inhibitors dasatinib and pazopanib, which prevented VE-cadherin separation by more than 90% (Gorbunova et al., 2011). Another study demonstrated that Vandetanib, a tyrosine kinase inhibitor specifically target VEGFR2, has a capacity to inhibit *in vitro* phosphorylation of VEGFR2, leading to the reduction of VE cadherin degradation (Bird et al., 2016). However, Vandetanib showed signs of potential side effects during human studies, including hypertension, dermatologic responses, and other cardiorespiratory consequences (Grande et al., 2013).

In the ANDV/hamster model, giving the therapy at doses of 10, 25 and 50 mg/kg/day, beginning 5 days prior the ANDV threat, resulted in a slowed mortality and raised overall survival rate by 23%. The same tiny therapeutic molecules, however, failed to protect the hamsters from a lethal ANDV challenge when given once viremia had started in the hamster model infected with ANDV (Munir et al., 2021).

6.3.2. Bradykinin B2 receptor antagonists

Using bradykinin receptor antagonists as a treatment for Hantavirus infections is another interesting strategy. All Hantavirus infections commonly cause vascular leakage and increased capillary permeability. The underlying mechanisms that result in alterations in vascular permeability following Hantavirus infection are yet unknown. Hantaviruses have been reported to be the cause of enhanced stimulation of kinin-kallikrein system following endothelial cells infection, which leads to release of bradykinin (Golias et al., 2007). Bradykinin is a nonapeptide-binding bradykinin B2 receptor that functions as an inflammatory mediator that causes vessels to dilate, increases vascular leakage and lowers blood pressure in Hantavirus infection.

It is acknowledged as the main facilitator of vascular leakage by destroying inter-endothelial connections. Additionally, the synthesis of interleukin-1 and tumor necrosis factor alpha is also induced (Maurer et al., 2011). Icatibant, a synthetic polypeptide that resembles bradykinin structurally, works as a strong, focused, and aggressive antagonist of the bradykinin B2 receptor. Icatibant binds to the bradykinin B2 receptor, preventing bradykinin from attaching to this receptor (Taylor et al., 2013). It stops vasodilatation brought on by bradykinin in humans and in C1 esterase inhibitor-knockout animals, it reverses enhanced vascular permeability, as well as inhibiting bradykinin-induced effects *in vivo* with dose- and time-dependent inhibition (Cockcroft et al., 1994; Cicardi et al., 2010). Following subcutaneous injection, Icatibant is almost completely bioavailable. Many people just need a single 30-mg dose because the drug is well tolerated (Cicardi et al., 2010; Deeks, 2010).

6.4. Corticosteroid therapy/ anti-inflammatory agents

As discussed already, Hantavirus affects endothelium cells and causes the host to produce pro-inflammatory cytokines especially TNF-α during the course of infection. Although not categorized as an antiviral, restricting this aspect of the immunological response to virus infection was hypothesized to offer potential clinical advantages. An immunomodulatory treatment was firstly performed in which only intramuscular injection or oral administration of cortisone was permitted. Although there was no reduction in mortality with this therapeutic approach, fatality was decreased to shock. An additional method to administer methylprednisolone for the treatment of HCPS was used but the outcome offered no clinical advantages (Priya and Priya, 2020).

6.5. Immunotherapy

Immunotherapy could be done against HTNV by utilizing neutralizing antibodies (NAbs) generated as a result of Hantavirus infection. It has been established that human convalescent plasma offers protective benefits to animals in both infection and lethal disease models of SNV/mouse (Medina et al., 2007) and ANDV/hamster (Brocato et al., 2012), respectively. These findings determine the sufficiency of neutralizing antibodies in preventing infection and disease (Brocato and Hooper, 2019).

Studies have only been done with animal models (suckling mice, hamsters, infant rats) where antibody efficacy was measured at cellular level using focus reduction neutralization test (FRNT) and hemagglutination test (HI) (Manigold and Vial, 2014). Although presently no particular effective treatment has been found against hantaviruses that cause HPS, according to numerous studies neutralizing antibodies can block HPS *in vivo*. An open trial has been carried out in Chile to assess the effectiveness of using human immunological sera as an HPS therapy (Vial et al., 2015). When compared to the 32% case fatality rates in the rest of the nation over the course of the study, the results showed a borderline statistical significance (Vial et al., 2015; Dheerasekara et al., 2020).

It was hypothesized that treatment at an earlier stage of HTNV infection could further enhance results. However, the practical implementation of immunotherapy is restricted by the requirement

for ABO blood typing of convalescent plasma and the absence of a standardized product, which prevents its widespread use (Brocato and Hooper, 2019).

6.5.1. Monoclonal antibodies

Antibodies have been employed on a global scale to prevent and treat viral infectious diseases (Casadevall, 1999). Researchers are currently working on generating antibodies targeting various viruses responsible for causing hemorrhagic fevers. One instance involves the development of a group of engineered human monoclonal antibodies (MAbs) designed to combat the Ebola virus (Maruyama et al., 1999). These specialized antibodies have shown efficacy not only in treating infections but also in providing protection before and after exposure to various viruses, including cytomegalovirus (CMV) (Aulitzky et al., 1991) and respiratory syncytial virus (RSV) (Malley et al., 1998). Up until now, there has not been a successful therapeutic antibody available for clinical use in treating and preventing Hantavirus infection. As a result, the development of Hantavirus-neutralizing MAbs is of utmost importance to establish effective immunotherapy and prophylaxis against Hantavirus infection (Xu et al., 2002).

During the 1980s, researchers extensively studied monoclonal antibodies targeting HTNV, detailing their interactions with the glycoproteins, Gn and Gc, and identifying specific neutralization sites (Arikawa et al., 1989). In an attempt to establish a link between particular viral epitopes and protection against HTNV infection, researchers conducted assessments on monoclonal antibodies using passive transfer techniques (Schmaljohn et al., 1990). This significant experiment provided compelling evidence that out of the 15 tested monoclonal antibodies, a neutralizing immune response to either Gn or Gc alone is adequate to prevent HTNV infection in hamsters. Following the HTNV/hamster experiment, the effectiveness of the recombinant Human GP monoclonal antibody HCO2 in providing protection was verified (Liang et al., 1996). This protective potential of neutralizing monoclonal antibodies was further validated in a later study utilizing a suckling mouse/HTNV model (Arikawa et al., 1992).

In a recent development, two genetically engineered monoclonal antibodies demonstrated their ability to protect hamsters from fatal ANDV-HPS (Garrido et al., 2018). One source patient with high antibody titers was chosen after screening 27 ANDV convalescent HCPS sera. Utilizing recombinant DNA technology, researchers generated recombinant monoclonal antibodies from memory B cells specific to the ANDV glycoprotein. The resulting candidates, JL16 and MIB22, displayed effective neutralization of ANDV *in vitro* (Garrido et al., 2018; Dheerasekara et al., 2020). When passively transferred antibodies on days 3 and 8 after infection, the administered antibodies successfully prevented lethality in hamsters infected with ANDV via intranasal exposure, whether given individually or in combination (Brocato and Hooper, 2019).

In another investigation, researchers produced and analyzed 18 murine monoclonal antibodies (MAbs) targeting HTNV strain Chen. Out of these, 13 MAbs were directed at the viral nucleocapsid protein (NP), four identified the viral envelope glycoprotein G2, and one MAb responded with both NP and G2. Only the monoclonal antibodies (MAbs) that specifically targeted epitopes on G2 exhibited positive results in the hemagglutination inhibition (HI) test. Additionally, these MAbs demonstrated *in vitro* virus-neutralizing activity and provided *in vivo* protection against HTNV infection in susceptible mice. Because the mice received virus-neutralizing MAbs one day before and two days after being exposed to HTNV, all of them were protected. This suggests that these particular neutralizing MAbs could be helpful for both pre- and post-exposure preventive measures, as well as potential immunotherapy against HTNV infection. In endemic regions of China, Phase II clinical trials are being conducted to evaluate the efficacy of these neutralizing MAbs as an emergent treatment for patients in the early stages of HRFS (Xu et al., 2002).

Anti-Hantaan Virus murine monoclonal antibody was developed for treating HFRS and a single dose of 2.5-20 mg was administered to healthy Chinese volunteers intravenously and the results indicated that it was nicely received (Xu et al., 2009). The cross-reactivity of novel and previously created MAbs effective against N protein of TULV, TMPV, DOBV and PUUV were assessed contrary to N proteins of fifteen shrew and rodent borne hantaviruses using various immunological techniques in order to have a large collection of well-described Hantavirus-specific MAbs. The results indicated that all MAbs, with the exception of those that are exclusive to TPMV, displayed various cross-reactivity patterns with Hantavirus N proteins and recognized native viral antigens in infected mammalian cells (Avižinienė et al., 2023). A recently discovered widely neutralizing antibody was structurally analyzed by Mittler et al. (2023) on a patient who had recovered from Puumala virus (Old world Hantavirus) infection. The authors created an improved variant of this patient-extracted antibody that could defend against Andes (New world Hantavirus) and Puumala virus, in rodent models using functional research, structural data along with complementary binding and neutralization. The therapeutic candidate ADI-65534, which is a broadly neutralizing antibody possesses a potential to treat Hantavirus infections.

6.5.2. Polyclonal antibodies

In a recent study, polyclonal immunotherapy in which purified IgG polyclonal antibodies produced in DNA immunized alpacas (ANDV M/SNV M) were given to Syrian hamsters, which protected them completely against HPS (Sroga et al., 2021). Studies have demonstrated the immunogenicity of Hantavirus DNA vaccines in various animal species, such as geese, rabbits and ducks (Hooper et al., 1999; Brocato et al., 2012, 2013). A substantial step forward was recently achieved with the development of a fully human polyclonal antibody using trans-chromosomal bovine that had received ANDV and SNV DNA vaccines. This product has demonstrated positive protection against two deadly HPS animal models (Hooper et al., 2014). Presently, researchers are actively working to broaden their investigation and develop a standardized polyclonal antibody capable of targeting a variety of Hantaviruses, including HTNV, ANDV, SNV, and PUUV. The objective is to advance this product through preclinical testing and ultimately carry out a Phase 1 clinical study, paving the path for potential therapeutic applications. Table 3 (Vilcek, 1991; Murphy et al., 2000, 2001; Sundstrom et al., 2001; Glass et al., 2003; Maes et al., 2004; Chung et al., 2008, 2013; Hall et al., 2008; Antonen et al., 2013; Ogg et al., 2013; Safronetz et al., 2013; Vial et al., 2013, 2015; Laine et al., 2015; Barriga et al., 2016; Bird et al., 2016; Garrido et al., 2018; Brocato and Hooper, 2019).

7. Vaccines and immunotherapy

As viruses are constantly emerging from zoonotic origin, vaccines seem to be the most effective therapeutic option to reduce the incidence of disease (Ahmed et al., 2022). Different vaccines are under development against hantaviruses to improve protective efficacy and

safety profiles (Saavedra et al., 2021). Attenuated and killed vaccines are the most common and primitive method of vaccine development that is injected into the animal or human body to elicit a protective immune response (Naeem et al., 2021). These vaccines are prepared by growing the isolated viral strain on the Vero cell line followed by inactivation through physical and chemical means. Similarly, the formalin-inactivated vaccine, Hantavax, was the first developed vaccine to prevent hantaviral infection in South Korea, it was developed using the HTNV strain ROK 84/105, which multiplies in lactating mice's brains. Its clinical trial proved that it was well endured in human volunteers and successfully lowered the incidence of HFRS patients (Cho et al., 2002; Dheerasekara et al., 2020). However, the neutralizing antibody response was poor after two doses, therefore 3rd dose was injected to attain protective immune response in the host that lasts for 3–4 year (Dheerasekara et al., 2020). A bivalent inactivated vaccine against infection caused by SEOV and HTNV was developed in 1994 and was approved for use in China in 2005. It was found effective against HTNV and SEOV infections (Cho et al., 2002).

The success achieved by Hantavax is to decrease the incidence of hantaviral infection (Munir et al., 2021) but still needs a more effective and safe vaccine against Hantavirus which becomes possible to improve through modernization in virology and molecular biology with the development of more applied biological techniques. Hantavax is less efficient for long-term immunity and negligible cell-mediated immunity which can be overcome by immunizing the individual multiple times. Therefore, a vaccine is required that induces more effective and long-lasting immunity against the Hantavirus (Mohsen et al., 2017). Virus-Like Particles are considered efficient with better safety profiles, and prolonged immunity with the production of high titers of antibodies in humans (Mohsen and Bachmann, 2022). VLPs of Hantavirus are constructed using the M and S gene segment or only the M segment that interacts with each other to form virus-like particles *in vitro* similar to Hantavirus virion (Acuña et al., 2014; Brocato and Hooper, 2019) along with the incorporation of CD40L or GMCSF gene segment in vectors that stimulates activation of macrophages and dendritic cells (Ying et al., 2016; Dong et al., 2019). CD40L or GMCSF decorated VLPs provide prolonged immunity with elevated humoral and cell-mediated immune response than undecorated VLPs (Ying et al., 2016; Dong et al., 2019). Another approach involves the insertion of gene segments from nucleocapsid protein from DOBV, HTNV, and PUUV into HBV core particles, it is shown to be highly immunogenic with or without adjuvant that stimulates the generation of all classes of IgG antibodies (Brocato and Hooper, 2019).

Recombinant vaccines are constructed using Glycoprotein C (Gc), Glycoprotein N (Gn), or Nucleocapsid protein that shows high immunogenicity and antigenicity, bearing the ability to induce protection against Hantavirus (Dheerasekara et al., 2020). The baculovirus expression system was used to develop the more efficient recombinant vaccines using Gc, Gn, or N protein (Dheerasekara et al., 2020) followed by immunization in hamsters which develop partial protection from infection when used solely either Gc or Gn and complete protection when Gc/Gn used in combination or immunized with N protein (Brocato and Hooper, 2019). The nucleocapsid protein is more conserved among different hantaviral species, therefore, the immune response produced against N protein induces highly cross-reactive antibody responses to PUUV, DOBV, and ANDV produced by *E. coli* (Krüger et al., 2011). Moreover, the use of adjuvants enhances the immunogenicity and protective efficacy of the vaccine in humans (Porter et al., 2012).

TABLE 3 Lists some examples of potential antiviral therapies against Hantavirus.

Antiviral therapy	Type	Function	Target	Disease	References
Lactoferrin	Lactoferrin	Block viral entry	Viral GP	HFRS	Murphy et al. (2000, 2001)
Ribavirin	Nucleoside analogs	Inhibit viral replication	RdRp	HCPS and HFRS	Chung et al. (2013) and Ogg et al. (2013)
Favipiravir	Pyrazine derivatives	Block viral entry	RdRp	HCPS	Safronetz et al. (2013)
Vandetanib	Tyrosine kinase inhibitor	Improve vascular function	VEGF/Vascular function	HCPS	Bird et al. (2016)
ETAR	Nucleoside analog	Inhibit viral entry	RdRp	HCPS and HFRS	Chung et al. (2008)
Corticosteroids	Hormone	Rebuild immune homeostasis	Immunotherapy	HCPS and HFRS	Vial et al. (2013) and Brocato and Hooper (2019)
Human Immune Sera	Human pAbs	Block viral entry	Viral GP	HCPS	Vial et al. (2015)
JL16 and MIB22	Human mAbs	Block viral entry	Viral GP	HCPS	Garrido et al. (2018)
Domain III and stem peptides	Peptides	Block viral entry	Gc glycoprotein	HCPS and HFRS	Barriga et al. (2016)
CLVRNLAWC and CQATTARNC	Cyclic nonapeptides	Block viral entry	Host receptor	HCPS	Hall et al. (2008)
Icatibant	Small molecule	Improve vascular function	BK type 2 receptor	HFRS	Antonen et al. (2013) and Laine et al. (2015)
TNF-α	Small proteins/Pro-inflammatory cytokines	Increase systemic toxicity	Vascular function	HCPS and HFRS	Vilcek (1991), Sundstrom et al. (2001) and Maes et al. (2004)
RANTES/IP- 10/MCP-1	Small proteins/Pro-inflammatory chemokines	Immunomodu lators/ Inhibit viral infection	Microvascular endothelium	HFRS	Sundstrom et al. (2001) and Glass et al. (2003)

The S and M cDNA segment of HTNV was inserted into the vaccinia virus to develop a molecular virus vector-based vaccine (Brocato and Hooper, 2019). Protective efficacy was evaluated in Syrian hamsters by inoculating two doses of VACV-vectored HTNV vaccine which resulted in protection from HTNV or SEOV but not PUUV (Munir et al., 2021). Cross-reactive antibodies of HTNV protected against SEOV but were unable to protect from PUUV (Malinin and Platonov, 2017). Clinical trials were conducted to further evaluate the vaccine efficacy (McClain et al., 2000; Brocato and Hooper, 2019) and it was confirmed that the vaccine was safe to inoculate and resulted in the production of neutralizing antibodies against both VACV and HTNV, and the subcutaneous route was preferred to administer the vaccine (Perley et al., 2020). The efficacy of the vaccine was also evaluated in vaccinated and non-vaccinated individuals and 72% efficacy was observed in non-vaccinated and 26% in vaccinated individuals (Dheerasekara et al., 2020). Moreover, non-replicating adenovirus vectors were used to provoke vigorous cytolytic response when ANDV N protein, Gn, Gc, or Gc and Gn in combination was expressed (Safronetz et al., 2009). Similarly, the Vesicular stomatitis virus (VSV) pseudo-type virus containing Gn and Gc of Hantavirus and ANDV glycoprotein precursor (GPC)was separately inoculated in mice and hamsters and it produced robust neutralizing antibody response (Saavedra et al., 2021). However, it required 3 doses to produce long-term immunity in an individual (Brocato and Hooper, 2019; Saavedra et al., 2021).

All vaccines have shown their efficacy against hantaviruses but the safety and efficacy was varied between primitive and modern-generation vaccines. DNA vaccine encoding the HTNV Gn and lysosomal-associated membrane protein 1 which directed to major histocompatibility complex II (MHC) and processed as an exogenous antigen resulting in robust humoral and cell-mediated immune response (Jiang D.-B. et al., 2017). Normally, inactivated vaccines have poor immunological memory but DNA vaccines have much-improved memory profiles. The S and M segments of SEOV were cloned into an expression vector pWRG7077 or Sindbis replicon vector (Munir et al., 2021). The results depicted that the M segment had shown improved protection from SEOV infection in Syrian hamsters (Brocato et al., 2021). Therefore, the M segment of HTNV, PUUV, ANDV, SNV, SEOV, and DOBV is used for vaccination in non-human primates that elicits an elevated level of antibody response (Liu et al., 2020). Several DNA vaccines against HTNV associated infections are currently undergoing clinical trials. Hopper's group have developed several vaccines against the envelope glycoprotein gene of hantaviruses and further studies have confirmed the ability of these vaccines to produce neutralizing antibodies against HFRS in multiple animal species and even protected hamsters against HFRS (Schmaljohn et al., 2014). Apart from vaccine development, delivery methods and routes are much more significant to achieve desired efficacy. Multiple administration routes are studied and found gene gun inoculation is more effective than any other route (Dheerasekara et al., 2020). Moreover, a combination of different DNA vaccines of hantaviruses is much more efficient to provoke an immune response rather than a single vaccine administration (Brocato et al., 2013). Currently no FDA approved treatment and vaccines are available against HTNV worldwide. There are still many unresolved issues regarding mass production, safety and efficacy and no significant effect in lowering the severity of the disease. However, more research is required in vaccine delivery routes to improve the immunogenicity of the vaccine.

Apart from vaccines, monoclonal and polyclonal antibodies are used to eliminate hantaviral pathogens in the human or animal body against Gc and Gn (Duehr et al., 2020). Furthermore, DNA vaccination of ANDV, SNV, HTNV, and PUUV in bovines produces purified polyclonal human IgG antibodies exhibiting high neutralization activity and provided effective protection against lethal HCPS (Liu et al., 2020). Therefore, it is worldwide tested and used as a promising prophylactic therapy. The administration of neutralizing antibodies during the acute phase of HPS is considered an effective treatment for hantaviral infection (Iglesias et al., 2022). The patients with low titers of neutralizing antibodies often had a severe disease while mild disease cases were present in individuals with higher antibody titers (Iglesias et al., 2022; Iheozor-Ejiofor et al., 2022). Therefore, different clinicians and scientists speculated that a strong neutralizing antibody response or passive immunization can efficiently reduce the severity of the disease by reducing viremia (Shah et al., 2020).

8. Future therapeutic developments

8.1. Hantavirus-induced cytokine and chemokine response

One of the main contributors to HPS and HFRS symptoms during the course of Hantavirus infection may be the cytokine production. Cytokines, particularly TNF-α, IL-1, and IL-6 play a vital role in inducing fever and septic shock. TNF-α is produced by Hantavirus infected neutrophils, NK cells, CD8+ T cells, DC and macrophages (Schönrich et al., 2015). The excessive production of TNF-α may cause systemic toxicity (Maes et al., 2004). Although the precise mechanism is yet unknown, these cytokines also play a significant part in the vascular permeability seen in HPS and HFRS (Sundstrom et al., 2001). One of the most significant pro-inflammatory cytokines is TNF-α. Monocytes and macrophages infiltrate the area of inflammation and release TNF-α (Vilcek, 1991). Patients with severe NE were found to have significantly higher plasma levels of TNF-α (Linderholm et al., 1996). The kidney biopsies from NE patients revealed that TNF-α expression was elevated in the peritubular regions (Temonen et al., 1996). Patients with HTNV infection have higher serum levels of soluble IL-2 receptor (sIL-2R) and soluble IL-6 receptor (sIL-6R). sIL-2R and sIL-6R serum levels increased two days and six days after the onset of HFRS, respectively (Markotic et al., 2002). The infected monolayers of endothelial cells remained irreversibly permeable while uninfected monolayers fully restored their function (Niikura et al., 2004). Chemokines serve as inflammatory mediators and are responsible for the regulation of viral infections. HTNV infected endothelial cells *in vitro*, resulted in the production of significant amount of interferon-inducible protein (IP-10) and regulated upon activation, normal T cell expressed and secreted (RANTES), also called CCL5 (Sundstrom et al., 2001). Another study showed production of chemokines like RANTES, IP-10, IL-6, and IL-8 by HTNV but NYV failed to generate the majority of these cellular chemokines (Geimonen et al., 2002). Inflammatory chemokines like RANTES and monocyte chemotactic protein-1 (MCP-1), usually produced by acute respiratory viruses, can increase inflammatory responses giving rise to virus immunopathology (Glass et al., 2003). All supernatant cell lines harboring hantaviruses have a substantial increase in RANTES mRNA

TABLE 4 Describing evaluation of Hantavirus vaccines in various animal models and some vaccines currently undergoing clinical trials.

Vaccine type	Antigen	Animal model	Immunogenicity evaluation	References
Inactivated vaccine	Formalin inactivated HNTV	Humans	Humoral response Neutralizing antibodies	Khan et al. (2019)
Virus-like particles	HTNV-VLP with CD40L or GM-CSF	Mice	Cytotoxic response Neutralization antibody Cytolytic activity	Dong et al. (2019)
	M	DHFR-deficient CHO cells	Antigen-specific IFN-γ production Effective against HTNV Still in developing phases	Dong et al. (2019)
Virus-vector vaccines	Replication-competent VSV-vectored SNV or ANDV glycoproteins	Syrian Hamster	Cross-reactive IgG antibodies Neutralizing antibodies	Warner et al. (2019)
	Replication-competent VSV-vectored ANDV glycoproteins	Syrian Hamsters	Neutralizing antibodies	Prescott et al. (2014)
	Non-replicating Ad vector expressing N, Gn, Gc, or Gn/Gc	Syrian Hamsters	CD8+ cell response Neutralizing antibodies	Safronetz et al. (2009)
Recombinant vaccines	Yeast-expressed DOBV nucleoprotein	Mice	NP-specific IgG response Th1/Th2 response Cross-reactivity with HTNV and PUUV	Geldmacher et al. (2004)
	Nucleoproteins from ANDV, TOPV, DOBV or PUUV	Bank voles	Specific CD8+ cell production Cross-reactive response against PUUV	de Carvalho et al. (2002)
	Truncated recombinant PUUV nucleoprotein linked to bacterial membrane protein	Mice	CD8+ T-cell response NP IgG response	Maes et al. (2006)
DNA vaccines	HTNV/PUUV/SNV/ANDV M gene segment mix	Rabbits	Neutralizing antibodies	Hooper et al. (2013)
	HTNV M segment	Rhesus macaques	Neutralizing antibodies Cross-reactivity with SEOV and DOBV	Hooper et al. (2001)
	ANDV and HNTV M gene segments	Rhesus macaques	Neutralizing antibodies	Hooper et al. (2006)
	SNV M gene segment	Syrian hamsters	Neutralizing antibodies	Hooper et al. (2013)
	PUUV M gene segment	Syrian hamsters	Protection against lethal ANDV infection, without nAbs Neutralizing antibodies	Brocato et al. (2013)
	Gn glycoprotein	BALB/c mice	Effective against HTNV Still in developing phases	Jiang D.-B. et al. (2017)
Subunit vaccines	NP (nucleocapsid protein)	E.coli mutant ICONE NMRI mice	Effective against PUUV In developing Phases	Maes et al. (2008)

(Khaiboullina and St. Jeor, 2002). The conclusion that chemokines play a significant role in virus pathogenesis, which has been drawn for other viruses, is supported by this data. Due to the dual functions that these chemokines play in viral infections, inhibiting them or using them as immunomodulators may be important strategies to treat or reduce viral illness, depending on the type of virus. During HTNV infection, production of IP-10 and RANTES can lead to an increased effector immune response directed against the infected vascular endothelial cells (Sundstrom et al., 2001). Consideration should be given to a general therapeutic strategy for Hantavirus infections that combine antiviral and anti-chemokine therapy.

8.2. Potential vaccines undergoing development against Hantavirus

Hantaviruses enter human societies by zoonotic transmission *via* inhaling contaminated aerosols. Normally, half a million people are infected worldwide annually with a mortality rate of up to 40%. The HFRS and HPS seem to be serious health threats in endemic areas due to their cryptic transmission and unpredictable nature of disease occurrence in healthy adults with elevated case fatality rates. The inappropriate commercialization of therapeutics in endemic areas constantly increases the prevalence of the disease. Moreover, no special antiviral drugs were found efficient to be used in hantaviral infection except ribavirin. However, during HPS and HFRS cases, the ribavirin had been found effective but its efficacy could not prevent the severity of the disease.

Since there are so many cases of hantaviral infection each year, medicinal countermeasures to prevent infection from these viruses must be developed. Animal models have repeatedly shown that antivirals are not effective if administered after the onset of viremia. Therefore, the development of vaccination and an antiviral that can be used separately or in combination is much necessary for public health. Immunization may provide long-lasting immunity while an antiviral, such as polyclonal antibody treatment, would provide immediate immunity. So, vaccines and passive immunotherapy can effectively prevent and treat hantaviral infections in endemic regions of the world. The transmission from person to person becomes limited by vaccination and some vaccines are currently undergoing clinical trials (see Table 4) (Hooper et al., 2001, 2006, 2013; de Carvalho et al., 2002; Geldmacher et al., 2004; Maes et al., 2006, 2008; Safronetz et al., 2009; Brocato et al., 2013; Prescott et al., 2014; Jiang D.-B. et al., 2017; Dong et al., 2019; Khan et al., 2019; Warner et al., 2019).

Author contributions

LA and SA conceived the study. LA, MA, MH, MS, AA, AB, JY, and NK searched the literature and drafted the manuscript. LA, SA, AB, NK, and JY critically reviewed the manuscript. All authors contributed to the article and approved the submitted version.

Conflict of interest

JY was employed by Wuhan Institute of Biological Products Co., Ltd.

The remaining authors declare that the research was conducted in the absence of any commercial or financial relationships that could be construed as a potential conflict of interest.

Publisher's note

All claims expressed in this article are solely those of the authors and do not necessarily represent those of their affiliated organizations, or those of the publisher, the editors and the reviewers. Any product that may be evaluated in this article, or claim that may be made by its manufacturer, is not guaranteed or endorsed by the publisher.

References

Acuña, R., Cifuentes-Muñoz, N., Márquez, C. L., Bulling, M., Klingström, J., Mancini, R., et al. (2014). Hantavirus gn and gc glycoproteins self-assemble into virus-like particles. *J. Virol.* 88, 2344–2348. doi: 10.1128/JVI.03118-13

Ahmed, A., Safdar, M., Sardar, S., Yousaf, S., Farooq, F., Raza, A., et al. (2022). Modern vaccine strategies for emerging zoonotic viruses. *Expert Rev. Vaccines* 21, 1711–1725. doi: 10.1080/14760584.2022.2148660

Aitichou, M., Saleh, S. S., McElroy, A. K., Schmaljohn, C., and Ibrahim, M. S. (2005). Identification of Dobrava, Hantaan, Seoul, and Puumala viruses by one-step real-time RT-PCR. *J. Virol. Methods* 124, 21–26. doi: 10.1016/j.jviromet.2004.10.004

Ambesajir, A., Kaushik, A., Kaushik, J. J., and Petros, S. T. (2012). RNA interference: a futuristic tool and its therapeutic applications. *Saudi J. Biol. Sci.* 19, 395–403. doi: 10.1016/j.sjbs.2012.08.001

Antonen, J., Leppänen, I., Tenhunen, J., Arvola, P., Mäkelä, S., Vaheri, A., et al. (2013). A severe case of Puumala Hantavirus infection successfully treated with bradykinin receptor antagonist icatibant. *Scand. J. Infect. Dis.* 45, 494–496. doi: 10.3109/00365548.2012.755268

Arikawa, J., Schmaljohn, A. L., Dalrymple, J. M., and Schmaljohn, C. S. (1989). Characterization of Hantaan virus envelope glycoprotein antigenic determinants defined by monoclonal antibodies. *J. Gen. Virol.* 70, 615–624. doi: 10.1099/0022-1317-70-3-615

Arikawa, J., Yao, J.-S., Yoshimatsu, K., Takashima, I., and Hashimoto, N. (1992). Protective role of antigenic sites on the envelope protein of Hantaan virus defined by monoclonal antibodies. *Arch. Virol.* 126, 271–281. doi: 10.1007/BF01309700

Armién, B., Muñoz, C., Cedeño, H., Salazar, J. R., Salinas, T. P., González, P., et al. (2023). Hantavirus in Panama: twenty years of epidemiological surveillance experience. *Viruses* 15:1395. doi: 10.3390/v15061395

Aulitzky, W., Schulz, T., Tilg, H., Niederwieser, D., Larcher, K., Ostberg, L., et al. (1991). Human monoclonal antibodies neutralizing cytomegalovirus (CMV) for prophylaxis of CMV disease: report of a phase I trial in bone marrow transplant recipients. *J. Infect. Dis.* 163, 1344–1347. doi: 10.1093/infdis/163.6.1344

Avižinienė, A., Kučinskaitė-Kodzė, I., Petraitytė-Burneikienė, R., Žvirblienė, A., Mertens, M. L., Schmidt, S., et al. (2023). Characterization of a panel of cross-reactive Hantavirus Nucleocapsid protein-specific monoclonal antibodies. *Viruses* 15:532. doi: 10.3390/v15020532

Avšič-Županc, T., Saksida, A., and Korva, M. (2019). Hantavirus infections. *Clin. Microbiol. Infect.* 21s, e6–e16. doi: 10.1111/1469-0691.12291

Barriga, G. P., Villalón-Letelier, F., Márquez, C. L., Bignon, E. A., Acuña, R., Ross, B. H., et al. (2016). Inhibition of the Hantavirus fusion process by predicted domain III and stem peptides from glycoprotein Gc. *PLoS Negl. Trop. Dis.* 10:e0004799. doi: 10.1371/journal.pntd.0004799

Baudouin, V., Crusiaux, A., Haddad, E., Schandene, L., Goldman, M., Loirat, C., et al. (2003). Anaphylactic shock caused by immunoglobulin E sensitization after retreatment with the chimeric anti-interleukin-2 receptor monoclonal antibody basiliximab. *Transplantation* 76, 459–463. doi: 10.1097/01.TP.0000073809.65502.8F

Bi, Z., Formenty, P. B., and Roth, C. E. (2008). Hantavirus infection: a review and global update. *J. Infect. Dev. Countries* 2, 003–023. doi: 10.3855/jidc.317

Bird, B. H., Shrivastava-Ranjan, P., Dodd, K. A., Erickson, B. R., and Spiropoulou, C. F. (2016). Effect of Vandetanib on Andes virus survival in the hamster model of Hantavirus pulmonary syndrome. *Antivir. Res.* 132, 66–69. doi: 10.1016/j.antiviral.2016.05.014

Björkström, N. K., Lindgren, T., Stoltz, M., Fauriat, C., Braun, M., Evander, M., et al. (2011). Rapid expansion and long-term persistence of elevated NK cell numbers in humans infected with Hantavirus. *J. Exp. Med.* 208, 13–21. doi: 10.1084/jem.20100762

Bobbin, M. L., and Rossi, J. J. (2016). RNA interference (RNAi)-based therapeutics: delivering on the promise? *Annu. Rev. Pharmacol. Toxicol.* 56, 103–122. doi: 10.1146/annurev-pharmtox-010715-103633

Bressanelli, S., Stiasny, K., Allison, S. L., Stura, E. A., Duquerroy, S., Lescar, J., et al. (2004). Structure of a flavivirus envelope glycoprotein in its low-pH-induced membrane fusion conformation. *EMBO J.* 23, 728–738. doi: 10.1038/sj.emboj.7600064

Brocato, R. L., and Hooper, J. W. (2019). Progress on the prevention and treatment of Hantavirus disease. *Viruses* 11:610. doi: 10.3390/v11070610

Brocato, R., Josleyn, M., Ballantyne, J., Vial, P., and Hooper, J. W. (2012). DNA vaccine-generated duck polyclonal antibodies as a postexposure prophylactic to prevent Hantavirus pulmonary syndrome (HPS). *PLoS One* 7:e35996. doi: 10.1371/journal.pone.0035996

Brocato, R., Josleyn, M., Wahl-Jensen, V., Schmaljohn, C., and Hooper, J. (2013). Construction and nonclinical testing of a Puumala virus synthetic M gene-based DNA vaccine. *Clin. Vaccine Immunol.* 20, 218–226. doi: 10.1128/CVI.00546-12

Brocato, R. L., Kwilas, S. A., Josleyn, M. D., Long, S., Zeng, X., Perley, C. C., et al. (2021). Small animal jet injection technique results in enhanced immunogenicity of Hantavirus DNA vaccines. *Vaccine* 39, 1101–1110. doi: 10.1016/j.vaccine.2021.01.002

Buys, K. K., Jung, K.-H., Smee, D. F., Furuta, Y., and Gowen, B. B. (2011). Maporal virus as a surrogate for pathogenic New World hantaviruses and its inhibition by favipiravir. *Antivir. Chem. Chemother.* 21, 193–200. doi: 10.3851/IMP1729

Campbell, I. D., and Humphries, M. J. (2011). Integrin structure, activation, and interactions. *Cold Spring Harb. Perspect. Biol.* 3:a004994. doi: 10.1101/cshperspect.a004994

Casadevall, A. (1999). Passive antibody therapies: progress and continuing challenges. *Clin. Immunol.* 93, 5–15. doi: 10.1006/clim.1999.4768

Chandy, S., Boorugu, H., Chrispal, A., Thomas, K., Abraham, P., and Sridharan, G. (2009). Hantavirus infection: a case report from India. *Indian J. Med. Microbiol.* 27:267. doi: 10.4103/0255-0857.53215

Chen, X., Mangala, L. S., Rodriguez-Aguayo, C., Kong, X., Lopez-Berestein, G., and Sood, A. K. (2018). RNA interference-based therapy and its delivery systems. *Cancer Metastasis Rev.* 37, 107–124. doi: 10.1007/s10555-017-9717-6

Chiang, C.-F., Albariño, C. G., Lo, M. K., and Spiropoulou, C. F. (2014). Small interfering RNA inhibition of Andes virus replication. *PLoS One* 9:e99764. doi: 10.1371/journal.pone.0099764

Cho, H.-W., Howard, C. R., and Lee, H.-W. (2002). Review of an inactivated vaccine against hantaviruses. *Intervirology* 45, 328–333. doi: 10.1159/000067925

Chung, D.-H., Kumarapperuma, S. C., Sun, Y., Li, Q., Chu, Y.-K., Arterburn, J. B., et al. (2008). Synthesis of 1-β-d-ribofuranosyl-3-ethynyl-[1, 2, 4] triazole and its *in vitro* and *in vivo* efficacy against Hantavirus. *Antivir. Res.* 79, 19–27. doi: 10.1016/j.antiviral.2008.02.003

Chung, D.-H., Västermark, Å., Camp, J. V., McAllister, R., Remold, S. K., Chu, Y.-K., et al. (2013). The murine model for Hantaan virus-induced lethal disease shows two distinct paths in viral evolutionary trajectory with and without ribavirin treatment. *J. Virol.* 87, 10997–11007. doi: 10.1128/JVI.01394-13

Cicardi, M., Banerji, A., Bracho, F., Malbrán, A., Rosenkranz, B., Riedl, M., et al. (2010). Icatibant, a new bradykinin-receptor antagonist, in hereditary angioedema. *N. Engl. J. Med.* 363, 532–541. doi: 10.1056/NEJMoa0906393

Cifuentes-Munoz, N., Barriga, G. P., Valenzuela, P. D., and Tischler, N. D. (2011). Aromatic and polar residues spanning the candidate fusion peptide of the Andes virus Gc protein are essential for membrane fusion and infection. *J. Gen. Virol.* 92, 552–563. doi: 10.1099/vir.0.027235-0

Clement, J., LeDuc, J. W., Lloyd, G., Reynes, J.-M., McElhinney, L., Van Ranst, M., et al. (2019). Wild rats, laboratory rats, pet rats: global Seoul Hantavirus disease revisited. *Viruses* 11:652. doi: 10.3390/v11070652

Cockcroft, J., Chowienczyk, P., Brett, S., Bender, N., and Ritter, J. (1994). Inhibition of bradykinin-induced vasodilation in human forearm vasculature by icatibant, a potent

B2-receptor antagonist. *Br. J. Clin. Pharmacol.* 38, 317–321. doi: 10.1111/j.1365-2125.1994.tb04360.x

de Carvalho, N., Gonzalez Delia Valle, M., Padula, P., Bjorling, E., Plyusnin, A., and Lundkvist, A. (2002). Cross-protection against challenge with Puumala virus after immunization with nucleocapsid proteins from different hantaviruses. *J. Virol.* 76, 6669–6677. doi: 10.1128/jvi.76.13.6669-6677.2002

Deeks, E. D. (2010). Icatibant. *Drugs* 70, 73–81. doi: 10.2165/11204500-000000000-00000

Deng, X., Tian, S., Yu, Z., Wang, L., Liang, R., Li, Y., et al. (2020). Development of small-molecule inhibitors against hantaviruses. *Microbes Infect.* 22, 272–277. doi: 10.1016/j.micinf.2020.05.011

DeVincenzo, J., Lambkin-Williams, R., Wilkinson, T., Cehelsky, J., Nochur, S., Walsh, E., et al. (2010). A randomized, double-blind, placebo-controlled study of an RNAi-based therapy directed against respiratory syncytial virus. *Proc. Natl. Acad. Sci.* 107, 8800–8805. doi: 10.1073/pnas.0912186107

Dheerasekara, K., Sumathipala, S., and Muthugala, R. (2020). Hantavirus infections—treatment and prevention. *Curr. Treat. Options Infect. Dis.* 12, 410–421. doi: 10.1007/s40506-020-00236-3

Dong, Y., Ma, T., Zhang, X., Ying, Q., Han, M., Zhang, M., et al. (2019). Incorporation of CD40 ligand or granulocyte-macrophage colony stimulating factor into Hantaan virus (HTNV) virus-like particles significantly enhances the long-term immunity potency against HTNV infection. *J. Med. Microbiol.* 68, 480–492. doi: 10.1099/jmm.0.000897

Du, H., Li, J., Yu, H.-T., Jiang, W., Zhang, Y., Wang, J.-N., et al. (2014). Early indicators of severity and construction of a risk model for prognosis based upon laboratory parameters in patients with hemorrhagic fever with renal syndrome. *Clin. Chem. Lab. Med.* 52, 1667–1675. doi: 10.1515/cclm-2014-0016

DuBois, R. M., Vaney, M.-C., Tortorici, M. A., Kurdi, R. A., Barba-Spaeth, G., Krey, T., et al. (2013). Functional and evolutionary insight from the crystal structure of rubella virus protein E1. *Nature* 493, 552–556. doi: 10.1038/nature11741

Duehr, J., McMahon, M., Williamson, B., Amanat, F., Durbin, A., Hawman, D. W., et al. (2020). Neutralizing monoclonal antibodies against the Gn and the Gc of the Andes virus glycoprotein spike complex protect from virus challenge in a preclinical hamster model. *MBio* 11, e00028–e00020. doi: 10.1128/mBio.00028-20

Duggan, J. M. (2019). Prevalence of Seoul Hantavirus in UK wild rats: an emerging public health problem? *Vet. Rec.* 184:523. doi: 10.1136/vr.l1163

Dvorscak, L., and Czuchlewski, D. R. (2014). Successful triage of suspected Hantavirus cardiopulmonary syndrome by peripheral blood smear review. *Am. J. Clin. Pathol.* 142, 196–201. doi: 10.1309/AJCPNFVWG46NUHED

Echterdiek, F., Kitterer, D., Alscher, M. D., Schwenger, V., Ruckenbrod, B., Bald, M., et al. (2019). Clinical course of Hantavirus-induced nephropathia epidemica in children compared to adults in Germany—analysis of 317 patients. *Pediatr. Nephrol.* 34, 1247–1252. doi: 10.1007/s00467-019-04215-9

Elbashir, S. M., Harborth, J., Lendeckel, W., Yalcin, A., Weber, K., and Tuschl, T. (2001). Duplexes of 21-nucleotide RNAs mediate RNA interference in cultured mammalian cells. *Nature* 411, 494–498. doi: 10.1038/35078107

Ermonval, M., Baychelier, F., and Tordo, N. (2016). What do we know about how hantaviruses interact with their different hosts? *Viruses* 8:223. doi: 10.3390/v8080223

Fernandez-Larsson, R., and Patterson, J. L. (1989). Altered ATP function of a vesicular stomatitis virus mutant detected by kinetic analysis of the transcriptase using phosphorylated ribavirin. *J. Gen. Virol.* 70, 2791–2797. doi: 10.1099/0022-1317-70-10-2791

Fernandez-Larsson, R., and Patterson, J. L. (1990). Ribavirin is an inhibitor of human immunodeficiency virus reverse transcriptase. *Mol. Pharmacol.* 38, 766–770.

Fire, A., Xu, S., Montgomery, M. K., Kostas, S. A., Driver, S. E., and Mello, C. C. (1998). Potent and specific genetic interference by double-stranded RNA in *Caenorhabditis elegans*. *Nature* 391, 806–811. doi: 10.1038/35888

Flusin, O., Vigne, S., Peyrefitte, C. N., Bouloy, M., Crance, J.-M., and Iseni, F. (2011). Inhibition of Hazara nairovirus replication by small interfering RNAs and their combination with ribavirin. *Virol. J.* 8, 1–11. doi: 10.1186/1743-422X-8-249

Furuta, Y., Takahashi, K., Kuno-Maekawa, M., Sangawa, H., Uehara, S., Kozaki, K., et al. (2005). Mechanism of action of T-705 against influenza virus. *Antimicrob. Agents Chemother.* 49, 981–986. doi: 10.1128/AAC.49.3.981-986.2005

Furuta, Y., Takahashi, K., Shiraki, K., Sakamoto, K., Smee, D. F., Barnard, D. L., et al. (2009). T-705 (favipiravir) and related compounds: novel broad-spectrum inhibitors of RNA viral infections. *Antivir. Res.* 82, 95–102. doi: 10.1016/j.antiviral.2009.02.198

Garrido, J. L., Prescott, J., Calvo, M., Bravo, F., Alvarez, R., Salas, A., et al. (2018). Two recombinant human monoclonal antibodies that protect against lethal Andes Hantavirus infection *in vivo*. *Sci. Transl. Med.* 10:eaat6420. doi: 10.1126/scitranslmed.aat6420

Gauvreau, G. M., Becker, A. B., Boulet, L. P., Chakir, J., Fick, R. B., Greene, W. L., et al. (2003). The effects of an anti-CD11a mAb, efalizumab, on allergen-induced airway responses and airway inflammation in subjects with atopic asthma. *J. Allergy Clin. Immunol.* 112, 331–338. doi: 10.1067/mai.2003.1689

Gavrilovskaya, I. N., Brown, E. J., Ginsberg, M. H., and Mackow, E. R. (1999). Cellular entry of hantaviruses which cause hemorrhagic fever with renal syndrome is mediated by β3 integrins. *J. Virol.* 73, 3951–3959. doi: 10.1128/JVI.73.5.3951-3959.1999

Gavrilovskaya, I. N., Peresleni, T., Geimonen, E., and Mackow, E. R. (2002). Pathogenic hantaviruses selectively inhibit β 3 integrin directed endothelial cell migration. *Arch. Virol.* 147, 1913–1931. doi: 10.1007/s00705-002-0852-0

Gavrilovskaya, I. N., Shepley, M., Shaw, R., Ginsberg, M. H., and Mackow, E. R. (1998). β3 integrins mediate the cellular entry of hantaviruses that cause respiratory failure. *Proc. Natl. Acad. Sci.* 95, 7074–7079. doi: 10.1073/pnas.95.12.7074

Geimonen, E., Neff, S., Raymond, T., Kocer, S. S., Gavrilovskaya, I. N., and Mackow, E. R. (2002). Pathogenic and nonpathogenic hantaviruses differentially regulate endothelial cell responses. *Proc. Natl. Acad. Sci.* 99, 13837–13842. doi: 10.1073/pnas.192298899

Geldmacher, A., Skrastina, D., Petrovskis, I., Borisova, G., Berriman, J. A., Roseman, A. M., et al. (2004). An amino-terminal segment of Hantavirus nucleocapsid protein presented on hepatitis B virus core particles induces a strong and highly cross-reactive antibody response in mice. *Virology* 323, 108–119. doi: 10.1016/j.virol.2004.02.022

Gibbons, D. L., Vaney, M.-C., Roussel, A., Vigouroux, A., Reilly, B., Lepault, J., et al. (2004). Conformational change and protein–protein interactions of the fusion protein of Semliki Forest virus. *Nature* 427, 320–325. doi: 10.1038/nature02239

Glass, W. G., Rosenberg, H. F., and Murphy, P. M. (2003). Chemokine regulation of inflammation during acute viral infection. *Curr. Opin. Allergy Clin. Immunol.* 3, 467–473. doi: 10.1097/00130832-200312000-00008

Golias, C., Charalabopoulos, A., Stagikas, D., Charalabopoulos, K., and Batistatou, A. (2007). The kinin system-bradykinin: biological effects and clinical implications. Multiple role of the kinin system-bradykinin. *Hippokratia* 11, 124–128.

Gorbunova, E., Gavrilovskaya, I. N., and Mackow, E. R. (2010). Pathogenic hantaviruses Andes virus and Hantaan virus induce adherens junction disassembly by directing vascular endothelial cadherin internalization in human endothelial cells. *J. Virol.* 84, 7405–7411. doi: 10.1128/JVI.00576-10

Gorbunova, E. E., Gavrilovskaya, I. N., Pepini, T., and Mackow, E. R. (2011). VEGFR2 and Src kinase inhibitors suppress Andes virus-induced endothelial cell permeability. *J. Virol.* 85, 2296–2303. doi: 10.1128/JVI.02319-10

Goswami, B. B., Borek, E., Sharma, O. K., Fujitaki, J., and Smith, R. A. (1979). The broad spectrum antiviral agent ribavirin inhibits capping of mRNA. *Biochem. Biophys. Res. Commun.* 89, 830–836. doi: 10.1016/0006-291X(79)91853-9

Gowen, B. B., Wong, M.-H., Jung, K.-H., Sanders, A. B., Mendenhall, M., Bailey, K. W., et al. (2007). *In vitro* and *in vivo* activities of T-705 against arenavirus and bunyavirus infections. *Antimicrob. Agents Chemother.* 51, 3168–3176. doi: 10.1128/AAC.00356-07

Graci, J., and Cameron, C. E. (2006). Mechanisms of action of ribavirin against distinct viruses. *Rev. Med. Virol.* 16, 37–48. doi: 10.1002/rmv.483

Grande, E., Kreissl, M. C., Filetti, S., Newbold, K., Reinisch, W., Robert, C., et al. (2013). Vandetanib in advanced medullary thyroid cancer: review of adverse event management strategies. *Adv. Ther.* 30, 945–966. doi: 10.1007/s12325-013-0069-5

Guidotti, L. G., and Chisari, F. V. (2001). Noncytolytic control of viral infections by the innate and adaptive immuneresponse. *Annu. Rev. Immunol.* 19, 65–91. doi: 10.1146/annurev.immunol.19.1.65

Gupta, S., Braun, M., Tischler, N. D., Stoltz, M., Sundström, K. B., Björkström, N. K., et al. (2013). Hantavirus-infection confers resistance to cytotoxic lymphocyte-mediated apoptosis. *PLoS Pathog.* 9:e1003272. doi: 10.1371/journal.ppat.1003272

Gupta, A. K., Joshi, M. B., Philippova, M., Erne, P., Hasler, P., Hahn, S., et al. (2010). Activated endothelial cells induce neutrophil extracellular traps and are susceptible to NETosis-mediated cell death. *FEBS Lett.* 584, 3193–3197. doi: 10.1016/j.febslet.2010.06.006

Guterres, A., and de Lemos, E. R. S. (2018). Hantaviruses and a neglected environmental determinant. *One Health* 5, 27–33. doi: 10.1016/j.onehlt.2017.12.002

Hall, P. R., Hjelle, B., Brown, D. C., Ye, C., Bondu-Hawkins, V., Kilpatrick, K. A., et al. (2008). Multivalent presentation of antihantavirus peptides on nanoparticles enhances infection blockade. *Antimicrob. Agents Chemother.* 52, 2079–2088. doi: 10.1128/AAC.01415-07

Hall, P. R., Leitão, A., Ye, C., Kilpatrick, K., Hjelle, B., Oprea, T. I., et al. (2010). Small molecule inhibitors of Hantavirus infection. *Bioorg. Med. Chem. Lett.* 20, 7085–7091. doi: 10.1016/j.bmcl.2010.09.092

Hall, P. R., Malone, L., Sillerud, L. O., Ye, C., Hjelle, B. L., and Larson, R. S. (2007). Characterization and NMR solution structure of a novel cyclic pentapeptide inhibitor of pathogenic hantaviruses. *Chem. Biol. Drug Des.* 69, 180–190. doi: 10.1111/j.1747-0285.2007.00489.x

Harrison, S. C. (2015). Viral membrane fusion. *Virology* 479, 498–507. doi: 10.1016/j.virol.2015.03.043

Hautala, N., Partanen, T., Kubin, A.-M., Kauma, H., and Hautala, T. (2021). Central nervous system and ocular manifestations in Puumala Hantavirus infection. *Viruses* 13:1040. doi: 10.3390/v13061040

Hayasaka, D., Maeda, K., Ennis, F. A., and Terajima, M. (2007). Increased permeability of human endothelial cell line EA. hy926 induced by Hantavirus-specific cytotoxic T lymphocytes. *Virus Res.* 123, 120–127. doi: 10.1016/j.virusres.2006.08.006

Hepojoki, J., Strandin, T., Lankinen, H., and Vaheri, A. (2012). Hantavirus structure–molecular interactions behind the scene. *J. Gen. Virol.* 93, 1631–1644. doi: 10.1099/vir.0.042218-0

Heyman, P., Ceianu, C., Christova, I., Tordo, N., Beersma, M., Alves, M. J., et al. (2011). A five-year perspective on the situation of haemorrhagic fever with renal syndrome and status of the Hantavirus reservoirs in Europe, 2005-2010. *Eur. Secur.* 16:19961. doi: 10.2807/ese.16.36.19961-en

Heyman, P., Plyusnina, A., Berny, P., Cochez, C., Artois, M., Zizi, M., et al. (2004). Seoul Hantavirus in Europe: first demonstration of the virus genome in wild *Rattus norvegicus* captured in France. *Eur. J. Clin. Microbiol. Infect. Dis.* 23, 711–717. doi: 10.1007/s10096-004-1196-3

Hooper, J. W., Brocato, R. L., Kwilas, S. A., Hammerbeck, C. D., Josleyn, M. D., Royals, M., et al. (2014). DNA vaccine–derived human IgG produced in transchromosomal bovines protect in lethal models of Hantavirus pulmonary syndrome. *Sci. Transl. Med.* 6:264ra162. doi: 10.1126/scitranslmed.3010082

Hooper, J. W., Custer, D. M., Smith, J., and Wahl-Jensen, V. (2006). Hantaan/Andes virus DNA vaccine elicits a broadly cross-reactive neutralizing antibody response in nonhuman primates. *Virology* 347, 208–216. doi: 10.1016/j.virol.2005.11.035

Hooper, J., Custer, D., Thompson, E., and Schmaljohn, C. (2001). DNA vaccination with the Hantaan virus M gene protects hamsters against three of four HFRS hantaviruses and elicits a high-titer neutralizing antibody response in Rhesus monkeys. *J. Virol.* 75, 8469–8477. doi: 10.1128/JVI.75.18.8469-8477.2001

Hooper, J. W., Josleyn, M., Ballantyne, J., and Brocato, R. (2013). A novel sin Nombre virus DNA vaccine and its inclusion in a candidate pan-Hantavirus vaccine against Hantavirus pulmonary syndrome (HPS) and hemorrhagic fever with renal syndrome (HFRS). *Vaccine* 31, 4314–4321. doi: 10.1016/j.vaccine.2013.07.025

Hooper, J., Kamrud, K., Elgh, F., Custer, D., and Schmaljohn, C. (1999). DNA vaccination with Hantavirus M segment elicits neutralizing antibodies and protects against Seoul virus infection. *Virology* 255, 269–278. doi: 10.1006/viro.1998.9586

Huiskonen, J. T., Hepojoki, J., Laurinmaki, P., Vaheri, A., Lankinen, H., Butcher, S. J., et al. (2010). Electron cryotomography of Tula Hantavirus suggests a unique assembly paradigm for enveloped viruses. *J. Virol.* 84, 4889–4897. doi: 10.1128/JVI.00057-10

Huong, V. T. Q., Yoshimatsu, K., Luan, V. D., Nhi, L., Arikawa, J., and Nguyen, T. M. N. (2010). Hemorrhagic fever with renal syndrome, Vietnam. *Emerg. Infect. Dis.* 16:363. doi: 10.3201/eid1602.091204

Iglesias, A. A., Períolo, N., Bellomo, C. M., Lewis, L. C., Olivera, C. P., Anselmo, C. R., et al. (2022). Delayed viral clearance despite high number of activated T cells during the acute phase in Argentinean patients with Hantavirus pulmonary syndrome. *EBioMedicine* 75:103765. doi: 10.1016/j.ebiom.2021.103765

Iheozor-Ejiofor, R., Vapalahti, K., Sironen, T., Levanov, L., Hepojoki, J., Lundkvist, Å., et al. (2022). Neutralizing antibody titers in hospitalized patients with acute Puumala Orthohantavirus infection do not associate with disease severity. *Viruses* 14:901. doi: 10.3390/v14050901

Jahnsen, F. L., Strickland, D. H., Thomas, J. A., Tobagus, I. T., Napoli, S., Zosky, G. R., et al. (2006). Accelerated antigen sampling and transport by airway mucosal dendritic cells following inhalation of a bacterial stimulus. *J. Immunol.* 177, 5861–5867. doi: 10.4049/jimmunol.177.9.5861

Jaillon, S., Peri, G., Delneste, Y., Frémaux, I., Doni, A., Moalli, F., et al. (2007). The humoral pattern recognition receptor PTX3 is stored in neutrophil granules and localizes in extracellular traps. *J. Exp. Med.* 204, 793–804. doi: 10.1084/jem.20061301

Jiang, H., Du, H., Wang, L. M., Wang, P. Z., and Bai, X. F. (2016). Hemorrhagic fever with renal syndrome: pathogenesis and clinical picture. *Front. Cell. Infect. Microbiol.* 6:1. doi: 10.3389/fcimb.2016.00001

Jiang, D.-B., Sun, L.-J., Cheng, L.-F., Zhang, J.-P., Xiao, S.-B., Sun, Y.-J., et al. (2017). Recombinant DNA vaccine of Hantavirus Gn and LAMP1 induced long-term immune protection in mice. *Antivir. Res.* 138, 32–39. doi: 10.1016/j.antiviral.2016.12.001

Jiang, H., Zheng, X., Wang, L., Du, H., Wang, P., and Bai, X. (2017). Hantavirus infection: a global zoonotic challenge. *Virol. Sin.* 32, 32–43. doi: 10.1007/s12250-016-3899-x

Jin, M., Park, J., Lee, S., Park, B., Shin, J., Song, K.-J., et al. (2002). Hantaan virus enters cells by clathrin-dependent receptor-mediated endocytosis. *Virology* 294, 60–69. doi: 10.1006/viro.2001.1303

Jonsson, C. B., Figueiredo, L. T. M., and Vapalahti, O. (2010). A global perspective on Hantavirus ecology, epidemiology, and disease. *Clin. Microbiol. Rev.* 23, 412–441. doi: 10.1128/CMR.00062-09

Jonsson, C. B., Milligan, B. G., and Arterburn, J. B. (2005). Potential importance of error catastrophe to the development of antiviral strategies for hantaviruses. *Virus Res.* 107, 195–205. doi: 10.1016/j.virusres.2004.11.009

Jonsson, C. B., and Schmaljohn, C. S. (2001). Replication of hantaviruses. *Curr. Top. Microbiol. Immunol.* 256, 15–32. doi: 10.1007/978-3-642-56753-7_2

Ke, G., Hu, Y., Huang, X., Peng, X., Lei, M., Huang, C., et al. (2016). Epidemiological analysis of hemorrhagic fever with renal syndrome in China with the seasonal-trend decomposition method and the exponential smoothing model. *Sci. Rep.* 6, 1–7. doi: 10.1038/srep39350

Khaiboullina, S. F., Morzunov, S., and St Jeor, S. C. (2005). Hantaviruses: molecular biology, evolution and pathogenesis. *Curr. Mol. Med.* 5, 773–790. doi: 10.2174/156652405774962317

Khaiboullina, S. F., Netski, D. M., Krumpe, P., and St. Jeor, S. C. (2000). Effects of tumor necrosis factor alpha on sin Nombre virus infection *in vitro*. *J. Virol.* 74, 11966–11971. doi: 10.1128/JVI.74.24.11966-11971.2000

Khaiboullina, S. F., and St. Jeor, S. C. (2002). Hantavirus immunology. *Viral Immunol.* 15, 609–625. doi: 10.1089/088282402320914548

Khan, A., Shin, O. S., Na, J., Kim, J. K., Seong, R.-K., Park, M.-S., et al. (2019). A systems vaccinology approach reveals the mechanisms of immunogenic responses to hantavax vaccination in humans. *Sci. Rep.* 9:4760. doi: 10.1038/s41598-019-41205-1

Kielian, M. (2006). Class II virus membrane fusion proteins. *Virology* 344, 38–47. doi: 10.1016/j.virol.2005.09.036

Kielian, M. (2014). Mechanisms of virus membrane fusion proteins. *Ann. Rev. Virol.* 1, 171–189. doi: 10.1146/annurev-virology-031413-085521

Kielian, M., and Rey, F. A. (2006). Virus membrane-fusion proteins: more than one way to make a hairpin. *Nat. Rev. Microbiol.* 4, 67–76. doi: 10.1038/nrmicro1326

Klein, D. E., Choi, J. L., and Harrison, S. C. (2013). Structure of a dengue virus envelope protein late-stage fusion intermediate. *J. Virol.* 87, 2287–2293. doi: 10.1128/JVI.02957-12

Klingström, J., Lindgren, T., and Ahlm, C. (2008). Sex-dependent differences in plasma cytokine responses to Hantavirus infection. *Clin. Vaccine Immunol.* 15, 885–887. doi: 10.1128/CVI.00035-08

Kobayashi, T., Nakatsuka, K., Shimizu, M., Tamura, H., Shinya, E., Atsukawa, M., et al. (2012). Ribavirin modulates the conversion of human CD 4+ CD 25− T cell to CD 4+ CD 25+ FOXP 3+ T cell via suppressing interleukin-10-producing regulatory T cell. *Immunology* 137, 259–270. doi: 10.1111/imm.12005

Kraus, A. A., Raftery, M. J., Giese, T., Ulrich, R., Zawatzky, R., Hippenstiel, S., et al. (2004). Differential antiviral response of endothelial cells after infection with pathogenic and nonpathogenic hantaviruses. *J. Virol.* 78, 6143–6150. doi: 10.1128/JVI.78.12.6143-6150.2004

Kruger, D. H., Figueiredo, L. T. M., Song, J.-W., and Klempa, B. (2015). Hantaviruses—globally emerging pathogens. *J. Clin. Virol.* 64, 128–136. doi: 10.1016/j.jcv.2014.08.033

Krüger, D. H., Schönrich, G., and Klempa, B. (2011). Human pathogenic hantaviruses and prevention of infection. *Hum. Vaccin.* 7, 685–693. doi: 10.4161/hv.7.6.15197

Krüger, D. H., Ulrich, R. G., and Hofmann, J. (2013). Hantaviruses as zoonotic pathogens in Germany. *Dtsch. Arztebl. Int.* 110:461. doi: 10.3238/arztebl.2013.0461

Kuhn, J. H., and Schmaljohn, C. S. (2023). A brief history of bunyaviral family Hantaviridae. *Diseases* 11:38. doi: 10.3390/diseases11010038

Kyriakidis, I., and Papa, A. (2013). Serum TNF-α, sTNFR1, IL-6, IL-8 and IL-10 levels in hemorrhagic fever with renal syndrome. *Virus Res.* 175, 91–94. doi: 10.1016/j.virusres.2013.03.020

Laine, O., Leppänen, I., Koskela, S., Antonen, J., Mäkelä, S., Sinisalo, M., et al. (2015). Severe Puumala virus infection in a patient with a lymphoproliferative disease treated with icatibant. *Infect. Dis.* 47, 107–111. doi: 10.3109/00365548.2014.969304

Larson, R. S., Brown, D. C., Ye, C., and Hjelle, B. (2005). Peptide antagonists that inhibit sin Nombre virus and hantaan virus entry through the beta3-integrin receptor. *J. Virol.* 79, 7319–7326. doi: 10.1128/JVI.79.12.7319-7326.2005

Lee, S.-H., Chung, B.-H., Lee, W.-C., and Choi, I.-S. (2013). Epidemiology of hemorrhagic fever with renal syndrome in Korea, 2001–2010. *J. Korean Med. Sci.* 28, 1552–1554. doi: 10.3346/jkms.2013.28.10.1552

Li, Z., Kong, D., Liu, Y., and Li, M. (2022a). Pharmacological perspectives and molecular mechanisms of coumarin derivatives against virus disease. *Genes Dis.* 9, 80–94. doi: 10.1016/j.gendis.2021.03.007

Li, Z., Wang, F., Liu, Y., Zhai, D., Zhang, X., Ying, Q., et al. (2021). Coumarin derivative N6 as a novel anti-Hantavirus infection agent targeting Akt. *Front. Pharmacol.* 12:745646. doi: 10.3389/fphar.2021.745646

Li, Z., Wang, F., Ying, Q., Kong, D., Zhang, X., Dong, Y., et al. (2022b). *In vitro* anti-Hantavirus activity of protein kinase inhibitor 8G1 targeting AKT/mTOR/eIF4E signaling pathway. *Front. Microbiol.* 13:880258. doi: 10.3389/fmicb.2022.1086239

Liang, M., Chu, Y.-K., and Schmaljohn, C. (1996). Bacterial expression of neutralizing mouse monoclonal antibody fab fragments to Hantaan virus. *Virology* 217, 262–271. doi: 10.1006/viro.1996.0113

Libraty, D. H., Mäkelä, S., Vlk, J., Hurme, M., Vaheri, A., Ennis, F. A., et al. (2012). The degree of leukocytosis and urine GATA-3 mRNA levels are risk factors for severe acute kidney injury in Puumala virus nephropathia epidemica. *PLoS One* 7:e35402. doi: 10.1371/journal.pone.0035402

Linderholm, M., Ahlm, C., Settergren, B., Waage, A., and Tärnvik, A. (1996). Elevated plasma levels of tumor necrosis factor (TNF)-α, soluble TNF receptors, interleukin (IL)-6, and IL-IO in patients with hemorrhagic fever with renal syndrome. *J. Infect. Dis.* 173, 38–43. doi: 10.1093/infdis/173.1.38

Liu, Y.-y., Chen, L.-j., Zhong, Y., Shen, M.-x., Ma, N., Liu, B.-y., et al. (2016). Specific interference shRNA-expressing plasmids inhibit Hantaan virus infection *in vitro* and *in vivo*. *Acta Pharmacol. Sin.* 37, 497–504. doi: 10.1038/aps.2015.165

Liu, R., Ma, H., Shu, J., Zhang, Q., Han, M., Liu, Z., et al. (2020). Vaccines and therapeutics against hantaviruses. *Front. Microbiol.* 10:2989. doi: 10.3389/fmicb.2019.02989

Llah, S. T., Mir, S., Sharif, S., Khan, S., and Mir, M. A. (2018). Hantavirus induced cardiopulmonary syndrome: a public health concern. *J. Med. Virol.* 90, 1003–1009. doi: 10.1002/jmv.25054

Löber, C., Anheier, B., Lindow, S., Klenk, H.-D., and Feldmann, H. (2001). The Hantaan virus glycoprotein precursor is cleaved at the conserved pentapeptide WAASA. *Virology* 289, 224–229. doi: 10.1006/viro.2001.1171

Lokugamage, N., Kariwa, H., Lokugamage, K., Iwasa, M. A., Hagiya, T., Yoshii, K., et al. (2004). Epizootiological and epidemiological study of Hantavirus infection in Japan. *Microbiol. Immunol.* 48, 843–851. doi: 10.1111/j.1348-0421.2004.tb03616.x

Lusvarghi, S., and Bewley, C. A. (2016). Griffithsin: an antiviral lectin with outstanding therapeutic potential. *Viruses* 8:296. doi: 10.3390/v8100296

Mackow, E. R., and Gavrilovskaya, I. N. (2001). Cellular receptors and Hantavirus pathogenesis. *Curr. Top. Microbiol. Immunol.* 256, 91–115. doi: 10.1007/978-3-642-56753-7_6

Mackow, E. R., and Gavrilovskaya, I. N. (2009). Hantavirus regulation of endothelial cell functions. *Thromb. Haemost.* 102, 1030–1041. doi: 10.1160/TH09-09-0640

MacRae, I. J., Zhou, K., Li, F., Repic, A., Brooks, A. N., Cande, W. Z., et al. (2006). Structural basis for double-stranded RNA processing by dicer. *Science* 311, 195–198. doi: 10.1126/science.1121638

Maes, P., Clement, J., Cauwe, B., Bonnet, V., Keyaerts, E., Robert, A., et al. (2008). Truncated recombinant puumala virus nucleocapsid proteins protect mice against challenge *in vivo*. *Viral Immunol.* 21, 49–60. doi: 10.1089/vim.2007.0059

Maes, P., Clement, J., Gavrilovskaya, I., and Van Ranst, M. (2004). Hantaviruses: immunology, treatment, and prevention. *Viral Immunol.* 17, 481–497. doi: 10.1089/vim.2004.17.481

Maes, P., Keyaerts, E., Bonnet, V., Clement, J., Avsic-Zupanc, T., Robert, A., et al. (2006). Truncated recombinant Dobrava Hantavirus nucleocapsid proteins induce strong, long-lasting immune responses in mice. *Intervirology* 49, 253–260. doi: 10.1159/000093454

Malinin, O. V., and Platonov, A. E. (2017). Insufficient efficacy and safety of intravenous ribavirin in treatment of haemorrhagic fever with renal syndrome caused by Puumala virus. *Infect. Dis.* 49, 514–520. doi: 10.1080/23744235.2017.1293841

Malley, R., DeVincenzo, J., Ramilo, O., Dennehy, P. H., Meissner, H. C., Gruber, W. C., et al. (1998). Reduction of respiratory syncytial virus (RSV) in tracheal aspirates in intubated infants by use of humanized monoclonal antibody to RSV F protein. *J. Infect. Dis.* 178, 1555–1561. doi: 10.1086/314523

Manigold, T., and Vial, P. (2014). Human Hantavirus infections: epidemiology, clinical features, pathogenesis and immunology. *Swiss Med. Wkly.* 144, w13937–w. doi: 10.4414/smw.2014.13937

Markotic, A., Gagro, A., Dasic, G., Kuzman, I., Lukas, D., Nichol, S., et al. (2002). Immune parameters in hemorrhagic fever with renal syndrome during the incubation and acute disease: case report. *Croat. Med. J.* 43, 587–590.

Markotić, A., Hensley, L., Daddario, K., Spik, K., Anderson, K., and Schmaljohn, C. (2007). Pathogenic hantaviruses elicit different immunoreactions in THP-1 cells and primary monocytes and induce differentiation of human monocytes to dendritic-like cells. *Coll. Antropol.* 31, 1159–1167.

Marsac, D., García, S., Fournet, A., Aguirre, A., Pino, K., Ferres, M., et al. (2011). Infection of human monocyte-derived dendritic cells by ANDES Hantavirus enhances pro-inflammatory state, the secretion of active MMP-9 and indirectly enhances endothelial permeability. *Virol. J.* 8, 1–9. doi: 10.1186/1743-422X-8-223

Martinez-Valdebenito, C., Calvo, M., Vial, C., Mansilla, R., Marco, C., Palma, R. E., et al. (2014). Person-to-person household and nosocomial transmission of Andes Hantavirus, southern Chile, 2011. *Emerg. Infect. Dis.* 20:1629. doi: 10.3201/eid2010.140353

Maruyama, T., Rodriguez, L. L., Jahrling, P. B., Sanchez, A., Khan, A. S., Nichol, S. T., et al. (1999). Ebola virus can be effectively neutralized by antibody produced in natural human infection. *J. Virol.* 73, 6024–6030. doi: 10.1128/JVI.73.7.6024-6030.1999

Masson, P., Heremans, J., and Schonne, E. (1969). Lactoferrin, an iron-binbing protein Ni neutrophilic leukocytes. *J. Exp. Med.* 130, 643–658. doi: 10.1084/jem.130.3.643

Maurer, M., Bader, M., Bas, M., Bossi, F., Cicardi, M., Cugno, M., et al. (2011). New topics in bradykinin research. *Allergy* 66, 1397–1406. doi: 10.1111/j.1398-9995.2011.02686.x

Mayor, J., Torriani, G., Engler, O., and Rothenberger, S. (2021). Identification of novel antiviral compounds targeting entry of hantaviruses. *Viruses* 13:685. doi: 10.3390/v13040685

McClain, D. J., Summers, P. L., Harrison, S. A., Schmaljohn, A. L., and Schmaljohn, C. S. (2000). Clinical evaluation of a vaccinia-vectored Hantaan virus vaccine. *J. Med. Virol.* 60, 77–85. doi: 10.1002/(SICI)1096-9071(200001)60:1<77::AID-JMV13>3.0.CO;2-S

Medina, R. A., Mirowsky-Garcia, K., Hutt, J., and Hjelle, B. (2007). Ribavirin, human convalescent plasma and anti-β 3 integrin antibody inhibit infection by sin Nombre virus in the deer mouse model. *J. Gen. Virol.* 88, 493–505. doi: 10.1099/vir.0.82459-0

Meisel, H., Wolbert, A., Razanskiene, A., Marg, A., Kazaks, A., Sasnauskas, K., et al. (2006). Development of novel immunoglobulin G (IgG), IgA, and IgM enzyme immunoassays based on recombinant Puumala and Dobrava Hantavirus nucleocapsid proteins. *Clin. Vaccine Immunol.* 13, 1349–1357. doi: 10.1128/CVI.00208-06

Mills, J. N., Ksiazek, T. G., Peters, C., and Childs, J. E. (1999). Long-term studies of Hantavirus reservoir populations in the southwestern United States: a synthesis. *Emerg. Infect. Dis.* 5:135. doi: 10.3201/eid0501.990116

Mir, M. A., and Panganiban, A. T. (2010). The triplet repeats of the sin Nombre Hantavirus 5′ untranslated region are sufficient in cis for nucleocapsid-mediated translation initiation. *J. Virol.* 84, 8937–8944. doi: 10.1128/JVI.02720-09

Mittler, E., Serris, A., Esterman, E. S., Florez, C., Polanco, L. C., O'Brien, C. M., et al. (2023). Structural and mechanistic basis of neutralization by a pan-Hantavirus protective antibody. *Sci. Transl. Med.* 15:eadg1855. doi: 10.1126/scitranslmed.adg1855

Modis, Y. (2014). Relating structure to evolution in class II viral membrane fusion proteins. *Curr. Opin. Virol.* 5, 34–41. doi: 10.1016/j.coviro.2014.01.009

Mohsen, M. O., and Bachmann, M. F. (2022). Virus-like particle vaccinology, from bench to bedside. *Cell. Mol. Immunol.* 19, 993–1011. doi: 10.1038/s41423-022-00897-8

Mohsen, M. O., Zha, L., Cabral-Miranda, G., and Bachmann, M. F.. *Major findings and recent advances in virus–like particle (VLP)-based vaccines. Seminars in immunology*. (2017). Amsterdam: Elsevier.

Monsinjon, T., Gasque, P., Chan, P., Ischenko, A., Brady, J. J., and Fontaine, M. (2003). Regulation by complement C3a and C5a anaphylatoxins of cytokine production in human umbilical vein endothelial cells. *FASEB J.* 17, 1003–1014. doi: 10.1096/fj.02-0737com

Munir, N., Jahangeer, M., Hussain, S., Mahmood, Z., Ashiq, M., Ehsan, F., et al. (2021). Hantavirus diseases pathophysiology, their diagnostic strategies and therapeutic approaches: a review. *Clin. Exp. Pharmacol. Physiol.* 48, 20–34. doi: 10.1111/1440-1681.13403

Murphy, M. E., Kariwa, H., Mizutani, T., Tanabe, H., Yoshimatsu, K., Arikawa, J., et al. (2001). Characterization of *in vitro* and *in vivo* antiviral activity of lactoferrin and ribavirin upon Hantavirus. *J. Vet. Med. Sci.* 63, 637–645. doi: 10.1292/jvms.63.637

Murphy, M., Kariwa, H., Mizutani, T., Yoshimatsu, K., Arikawa, J., and Takashima, I. (2000). *In vitro* antiviral activity of lactoferrin and ribavirin upon Hantavirus. *Arch. Virol.* 145, 1571–1582. doi: 10.1007/s007050070077

Naeem, M. A., Adeel, M. M., Kanwal, A., Ahmad, S., Ahmad, W., Akram, Q., et al. (2021). Reconnoitering *Mycobacterium tuberculosis* lipoproteins to design subunit vaccine by immunoinformatics approach. *Adv. Life Sci.* 8, 300–306.

Navarrete, M., Barrera, C., Zaror, L., and Otth, C. (2007). Rapid immunochromatographic test for Hantavirus Andes contrasted with capture-IgM ELISA for detection of Andes-specific IgM antibodies. *J. Med. Virol.* 79, 41–44. doi: 10.1002/jmv.20759

Niikura, M., Maeda, A., Ikegami, T., Saijo, M., Kurane, I., and Morikawa, S. (2004). Modification of endothelial cell functions by Hantaan virus infection: prolonged hyper-permeability induced by TNF-alpha of hantaan virus-infected endothelial cell monolayers. *Arch. Virol.* 149, 1279–1292. doi: 10.1007/s00705-004-0306-y

Ogg, M., Jonsson, C. B., Camp, J. V., and Hooper, J. W. (2013). Ribavirin protects Syrian hamsters against lethal Hantavirus pulmonary syndrome—after intranasal exposure to Andes virus. *Viruses* 5, 2704–2720. doi: 10.3390/v5112704

O'Keefe, B. R., Giomarelli, B., Barnard, D. L., Shenoy, S. R., Chan, P. K., McMahon, J. B., et al. (2010). Broad-spectrum *in vitro* activity and *in vivo* efficacy of the antiviral protein griffithsin against emerging viruses of the family Coronaviridae. *J. Virol.* 84, 2511–2521. doi: 10.1128/JVI.02322-09

Onishchenko, G., and Ezhlova, E. (2013). Epidemiologic surveillance and prophylaxis of hemorrhagic fever with renal syndrome in Russian Federation. *Zh. Mikrobiol. Epidemiol. Immunobiol.* 4, 23–32.

Outinen, T., Mäkelä, S., Huhtala, H., Hurme, M., Meri, S., Pörsti, I., et al. (2012). High pentraxin-3 plasma levels associate with thrombocytopenia in acute Puumala Hantavirus-induced nephropathia epidemica. *Eur. J. Clin. Microbiol. Infect. Dis.* 31, 957–963. doi: 10.1007/s10096-011-1392-x

Perley, C. C., Brocato, R. L., Wu, H., Bausch, C., Karmali, P. P., Vega, J. B., et al. (2020). Anti-HFRS human IgG produced in transchromosomic bovines has potent Hantavirus neutralizing activity and is protective in animal models. *Front. Microbiol.* 11:832. doi: 10.3389/fmicb.2020.00832

Porter, K. R., Ewing, D., Chen, L., Wu, S.-J., Hayes, C. G., Ferrari, M., et al. (2012). Immunogenicity and protective efficacy of a vaxfectin-adjuvanted tetravalent dengue DNA vaccine. *Vaccine* 30, 336–341. doi: 10.1016/j.vaccine.2011.10.085

Prescott, J., DeBuysscher, B. L., Brown, K. S., and Feldmann, H. (2014). Long-term single-dose efficacy of a vesicular stomatitis virus-based Andes virus vaccine in Syrian hamsters. *Viruses* 6, 516–523. doi: 10.3390/v6020516

Priya, A. J., and Priya, V. V. (2020). Drug therapy of Hantavirus-a review. *PalArch's J. Archaeol. Egypt* 17, 345–354.

Raftery, M. J., Kraus, A. A., Ulrich, R., Krüger, D. H., and Schönrich, G. N. (2002). Hantavirus infection of dendritic cells. *J. Virol.* 76, 10724–10733. doi: 10.1128/JVI.76.21.10724-10733.2002

Ramanathan, H. N., Chung, D.-H., Plane, S. J., Sztul, E., Chu, Y.-k., Guttieri, M. C., et al. (2007). Dynein-dependent transport of the hantaan virus nucleocapsid protein to the endoplasmic reticulum-Golgi intermediate compartment. *J. Virol.* 81, 8634–8647. doi: 10.1128/JVI.00418-07

Ramanathan, H. N., and Jonsson, C. B. (2008). New and Old World hantaviruses differentially utilize host cytoskeletal components during their life cycles. *Virology* 374, 138–150. doi: 10.1016/j.virol.2007.12.030

Raymond, T., Gorbunova, E., Gavrilovskaya, I. N., and Mackow, E. R. (2005). Pathogenic hantaviruses bind plexin-semaphorin-integrin domains present at the apex of inactive, bent alphavbeta3 integrin conformers. *Proc. Natl. Acad. Sci. U. S. A.* 102, 1163–1168. Epub 20050118. doi: 10.1073/pnas.0406743102

Razvina, O., Jiang, S., Matsubara, K., Ohashi, R., Hasegawa, G., Aoyama, T., et al. (2015). Differential expression of pentraxin 3 in neutrophils. *Exp. Mol. Pathol.* 98, 33–40. doi: 10.1016/j.yexmp.2014.11.009

Reguera, J., Weber, F., and Cusack, S. (2010). Bunyaviridae RNA polymerases (L-protein) have an N-terminal, influenza-like endonuclease domain, essential for viral cap-dependent transcription. *PLoS Pathog.* 6:e1001101. doi: 10.1371/journal.ppat.1001101

Rey, F. A., Heinz, F. X., Mandl, C., Kunz, C., and Harrison, S. C. (1995). The envelope glycoprotein from tick-borne encephalitis virus at 2 Å resolution. *Nature* 375, 291–298. doi: 10.1038/375291a0

Ricci, F., Izzicupo, P., Moscucci, F., Sciomer, S., Maffei, S., Di Baldassarre, A., et al. (2020). Recommendations for physical inactivity and sedentary behavior during the coronavirus disease (COVID-19) pandemic. *Front. Public Health* 8:199. doi: 10.3389/fpubh.2020.00199

Roman-Sosa, G., and Kielian, M. (2011). The interaction of alphavirus E1 protein with exogenous domain III defines stages in virus-membrane fusion. *J. Virol.* 85, 12271–12279. doi: 10.1128/JVI.05902-11

Saavedra, F., Diaz, F. E., Retamal-Díaz, A., Covian, C., González, P. A., and Kalergis, A. M. (2021). Immune response during Hantavirus diseases: implications for immunotherapies and vaccine design. *Immunology* 163, 262–277. doi: 10.1111/imm.13322

Sadeghi, M., Eckerle, I., Daniel, V., Burkhardt, U., Opelz, G., and Schnitzler, P. (2011). Cytokine expression during early and late phase of acute Puumala Hantavirus infection. *BMC Immunol.* 12, 1–10. doi: 10.1186/1471-2172-12-65

Saffarzadeh, M., Juenemann, C., Queisser, M. A., Lochnit, G., Barreto, G., Galuska, S. P., et al. (2012). Neutrophil extracellular traps directly induce epithelial and endothelial cell death: a predominant role of histones. *PLoS One* 7:e32366. doi: 10.1371/journal.pone.0032366

Safronetz, D., Falzarano, D., Scott, D. P., Furuta, Y., Feldmann, H., and Gowen, B. B. (2013). Antiviral efficacy of favipiravir against two prominent etiological agents of Hantavirus pulmonary syndrome. *Antimicrob. Agents Chemother.* 57, 4673–4680. doi: 10.1128/AAC.00886-13

Safronetz, D., Hegde, N. R., Ebihara, H., Denton, M., Kobinger, G. P., St. Jeor, S., et al. (2009). Adenovirus vectors expressing Hantavirus proteins protect hamsters against lethal challenge with Andes virus. *J. Virol.* 83, 7285–7295. doi: 10.1128/JVI.00373-09

Sargianou, M., Watson, D. C., Chra, P., Papa, A., Starakis, I., Gogos, C., et al. (2012). Hantavirus infections for the clinician: from case presentation to diagnosis and treatment. *Crit. Rev. Microbiol.* 38, 317–329. doi: 10.3109/1040841X.2012.673553

Schmaljohn, C. S., Chu, Y.-K., Schmaljohn, A. L., and Dalrymple, J. M. (1990). Antigenic subunits of Hantaan virus expressed by baculovirus and vaccinia virus recombinants. *J. Virol.* 64, 3162–3170. doi: 10.1128/jvi.64.7.3162-3170.1990

Schmaljohn, C. S., Spik, K. W., and Hooper, J. W. (2014). DNA vaccines for HFRS: laboratory and clinical studies. *Virus Res.* 187, 91–96. doi: 10.1016/j.virusres.2013.12.020

Schönrich, G., Krüger, D. H., and Raftery, M. J. (2015). Hantavirus-induced disruption of the endothelial barrier: neutrophils are on the payroll. *Front. Microbiol.* 6:222. doi: 10.3389/fmicb.2015.00222

Schönrich, G., Rang, A., Lütteke, N., Raftery, M. J., Charbonnel, N., and Ulrich, R. G. (2008). Hantavirus-induced immunity in rodent reservoirs and humans. *Immunol. Rev.* 225, 163–189. doi: 10.1111/j.1600-065X.2008.00694.x

Schubert, J., Tollmann, F., and Weissbrich, B. (2001). Evaluation of a pan-reactive Hantavirus enzyme immunoassay and of a Hantavirus immunoblot for the diagnosis of nephropathia epidemica. *J. Clin. Virol.* 21, 63–74. doi: 10.1016/S1386-6532(00)00187-6

Severson, W. E., Schmaljohn, C. S., Javadian, A., and Jonsson, C. B. (2003). Ribavirin causes error catastrophe during Hantaan virus replication. *J. Virol.* 77, 481–488. doi: 10.1128/JVI.77.1.481-488.2003

Shah, V., Firmal, P., Alam, A., Ganguly, D., and Chattopadhyay, S. (2020). Overview of immune response during SARS-CoV-2 infection: lessons from the past. *Front. Immunol.* 11:1949. doi: 10.3389/fimmu.2020.01949

Shin, O. S., Yanagihara, R., and Song, J.-W. (2012). Distinct innate immune responses in human macrophages and endothelial cells infected with shrew-borne hantaviruses. *Virology* 434, 43–49. doi: 10.1016/j.virol.2012.08.004

Shrivastava-Ranjan, P., Lo, M. K., Chatterjee, P., Flint, M., Nichol, S. T., Montgomery, J. M., et al. (2020). Hantavirus infection is inhibited by griffithsin in cell culture. *Front. Cell. Infect. Microbiol.* 10:561502. doi: 10.3389/fcimb.2020.561502

Singh, S., Numan, A., Sharma, D., Shukla, R., Alexander, A., Jain, G. K., et al. (2022). Epidemiology, virology and clinical aspects of Hantavirus infections: an overview. *Int. J. Environ. Health Res.* 32, 1815–1826. doi: 10.1080/09603123.2021.1917527

Spiropoulou, C. (2001). Hantavirus maturation. *Hantaviruses*, 256, 33–46. doi: 10.1007/978-3-642-56753-7_3

Sroga, P., Sloan, A., Warner, B. M., Tierney, K., Lew, J., Liu, G., et al. (2021). Polyclonal alpaca antibodies protect against Hantavirus pulmonary syndrome in a lethal Syrian hamster model. *Sci. Rep.* 11:17440. doi: 10.1038/s41598-021-96884-6

Streeter, D. G., Witkowski, J., Khare, G. P., Sidwell, R. W., Bauer, R. J., Robins, R. K., et al. (1973). Mechanism of action of 1-β-D-ribofuranosyl-1, 2, 4-triazole-3-carboxamide (Virazole), a new broad-spectrum antiviral agent. *Proc. Natl. Acad. Sci.* 70, 1174–1178. doi: 10.1073/pnas.70.4.1174

Sundstrom, J. B., McMullan, L. K., Spiropoulou, C. F., Hooper, W. C., Ansari, A. A., Peters, C. J., et al. (2001). Hantavirus infection induces the expression of RANTES and IP-10 without causing increased permeability in human lung microvascular endothelial cells. *J. Virol.* 75, 6070–6085. doi: 10.1128/JVI.75.13.6070-6085.2001

Sundström, K. B., Nguyen Hoang, A. T., Gupta, S., Ahlm, C., Svensson, M., and Klingström, J. (2016). Andes Hantavirus-infection of a 3D human lung tissue model reveals a late peak in progeny virus production followed by increased levels of proinflammatory cytokines and VEGF-A. *PLoS One* 11:e0149354. doi: 10.1371/journal.pone.0149354

Suputthamongkol, Y., Nitatpattana, N., Chayakulkeeree, M., and Palabodeewat, S. (2005). Hantavirus infection in Thailand: first clinical case report. *Southeast Asian J. Trop. Med. Public Health* 36, 700–703.

Szabo, R. (2017). Antiviral therapy and prevention against Hantavirus infections. *Acta Virol.* 61, 3–12. doi: 10.4149/av_2017_01_3

Takagi, J., and Springer, T. A. (2002). Integrin activation and structural rearrangement. *Immunol. Rev.* 186, 141–163. doi: 10.1034/j.1600-065X.2002.18613.x

Taylor, S. L., Wahl-Jensen, V., Copeland, A. M., Jahrling, P. B., and Schmaljohn, C. S. (2013). Endothelial cell permeability during Hantavirus infection involves factor XII-dependent increased activation of the kallikrein-kinin system. *PLoS Pathog.* 9:e1003470. doi: 10.1371/journal.ppat.1003470

Temonen, M., Mustonen, J., Helin, H., Pasternack, A., Vaheri, A., and Holthöfer, H. (1996). Cytokines, adhesion molecules, and cellular infiltration in nephropathia epidemica kidneys: an immunohistochemical study. *Clin. Immunol. Immunopathol.* 78, 47–55. doi: 10.1006/clin.1996.0007

Tian, Z., Liang, G., Cui, K., Liang, Y., Wang, Q., Lv, S., et al. (2021). Insight into the prospects for RNAi therapy of cancer. *Front. Pharmacol.* 12:644718. doi: 10.3389/fphar.2021.644718

Tian, H., and Stenseth, N. C. (2019). The ecological dynamics of Hantavirus diseases: from environmental variability to disease prevention largely based on data from China. *PLoS Negl. Trop. Dis.* 13:e0006901. doi: 10.1371/journal.pntd.0006901

Tischler, N. D., Gonzalez, A., Perez-Acle, T., Rosemblatt, M., and Valenzuela, P. D. T. (2005). Hantavirus Gc glycoprotein: evidence for a class II fusion protein. *J. Gen. Virol.* 86, 2937–2947. doi: 10.1099/vir.0.81083-0

Toltzis, P., and Huang, A. (1986). Effect of ribavirin on macromolecular synthesis in vesicular stomatitis virus-infected cells. *Antimicrob. Agents Chemother.* 29, 1010–1016. doi: 10.1128/AAC.29.6.1010

Tracey, K. J., and Cerami, A. (1994). Tumor necrosis factor: a pleiotropic cytokine and therapuetic target. *Annu. Rev. Med.* 45, 491–503. doi: 10.1146/annurev.med.45.1.491

Vaheri, A., Henttonen, H., Voutilainen, L., Mustonen, J., Sironen, T., and Vapalahti, O. (2013). Hantavirus infections in Europe and their impact on public health. *Rev. Med. Virol.* 23, 35–49. doi: 10.1002/rmv.1722

Vial, P. A., Valdivieso, F., Calvo, M., Rioseco, M. L., Riquelme, R., Araneda, A., et al. (2015). A non-randomized multicentre trial of human immune plasma for treatment of Hantavirus cardiopulmonary syndrome caused by Andes virus. *Antivir. Ther.* 20, 377–386. doi: 10.3851/IMP2875

Vial, P., Valdivieso, F., Ferres, M., Riquelme, R., Rioseco, M., Calvo, M., et al. (2013). Hantavirus study Group in Chile High-dose intravenous methylprednisolone for Hantavirus cardiopulmonary syndrome in Chile: a double-blind, randomized controlled clinical trial. *Clin. Infect. Dis.* 57, 943–951. doi: 10.1093/cid/cit394

Vilcek, J. (1991). Tumor necrosis factor-new insights into the molecular mechanisms of its multiple actions. *J. Biol. Chem.* 266:7313. doi: 10.1016/S0021-9258(20)89445-9

Vitarana, T., Colombage, G., Bandaranayake, V., and Lee, H. (1988). Hantavirus disease in Sri Lanka. *Lancet (London, England)* 2:1263.

Wang, W., Zhang, Y., Li, Y., Pan, L., Bai, L., Zhuang, Y., et al. (2012). Dysregulation of the β3 integrin-VEGFR2 complex in Hantaan virus–directed hyperpermeability upon treatment with VEGF. *Arch. Virol.* 157, 1051–1061. doi: 10.1007/s00705-012-1245-7

Warner, B. M., Dowhanik, S., Audet, J., Grolla, A., Dick, D., Strong, J. E., et al. (2020). Hantavirus cardiopulmonary syndrome in Canada. *Emerg. Infect. Dis.* 26:3020. doi: 10.3201/eid2612.202808

Warner, B. M., Stein, D. R., Jangra, R. K., Slough, M. M., Sroga, P., Sloan, A., et al. (2019). Vesicular stomatitis virus-based vaccines provide cross-protection against Andes and sin nombre viruses. *Viruses* 11:645. doi: 10.3390/v11070645

Watson, D. C., Sargianou, M., Papa, A., Chra, P., Starakis, I., and Panos, G. (2014). Epidemiology of Hantavirus infections in humans: a comprehensive, global overview. *Crit. Rev. Microbiol.* 40, 261–272. doi: 10.3109/1040841X.2013.783555

Wei, J., Huang, X., Li, S., Du, S., Yu, P., and Li, J. (2021). A Total of 2,657 reported cases and 14 deaths due to hemorrhagic fever with renal syndrome—Shaanxi Province, China, January 1–December 19, 2021. *China CDC Weekly* 3:1143. doi: 10.46234/ccdcw2021.272

Weinberg, M. S., and Arbuthnot, P. (2010). Progress in the use of RNA interference as a therapy for chronic hepatitis B virus infection. *Genome Med.* 2, 1–7.

Wimer, B. M. (1998). Implications of the analogy between recombinant cytokine toxicities and manifestations of Hantavirus infections. *Cancer Biother. Radiopharm.* 13, 193–207. doi: 10.1089/cbr.1998.13.193

Wong, T., Chan, Y., and Lee, H. (1985). Haemorrhagic fever with renal syndrome in Singapore: a case report. *Southeast Asian J. Trop. Med. Public Health* 16, 525–527.

Wray, S. K., Gilbert, B. E., Noall, M. W., and Knight, V. (1985). Mode of action of ribavirin: effect of nucleotide pool alterations on influenza virus ribonucleoprotein synthesis. *Antivir. Res.* 5, 29–37. doi: 10.1016/0166-3542(85)90012-9

Xu, Z., Chen, Q., Zhang, Y., and Liang, C. (2021). Coumarin-based derivatives with potential anti-HIV activity. *Fitoterapia* 150:104863. doi: 10.1016/j.fitote.2021.104863

Xu, Z., Wei, L., Wang, L., Wang, H., and Jiang, S. (2002). The *in vitro* and *in vivo* protective activity of monoclonal antibodies directed against Hantaan virus: potential application for immunotherapy and passive immunization. *Biochem. Biophys. Res. Commun.* 298, 552–558. doi: 10.1016/S0006-291X(02)02491-9

Xu, R., Yang, X. Y., Yang, D. F., Zou, C. Y., Gong, P. L., and Zeng, F. D. (2009). Phase I evaluation of the safety and pharmacokinetics of a single-dose intravenous injection of a murine monoclonal antibody against Hantaan virus in healthy volunteers. *Antimicrob. Agents Chemother.* 53, 5055–5059. doi: 10.1128/AAC.00728-09

Yanagihara, R., and Silverman, D. J. (1990). Experimental infection of human vascular endothelial cells by pathogenic and nonpathogenic hantaviruses. *Arch. Virol.* 111, 281–286. doi: 10.1007/BF01311063

Yang, J., Sun, J.-F., Wang, T.-T., Guo, X.-H., Wei, J.-X., Jia, L.-T., et al. (2017). Targeted inhibition of Hantavirus replication and intracranial pathogenesis by a chimeric protein-delivered siRNA. *Antivir. Res.* 147, 107–115. doi: 10.1016/j.antiviral.2017.10.005

Ye, C., Wang, D., Liu, H., Ma, H., Dong, Y., Yao, M., et al. (2019). An improved enzyme-linked focus formation assay revealed baloxavir acid as a potential antiviral therapeutic against Hantavirus infection. *Front. Pharmacol.* 10:1203. doi: 10.3389/fphar.2019.01203

Ying, Q., Ma, T., Cheng, L., Zhang, X., Truax, A. D., Ma, R., et al. (2016). Construction and immunological characterization of CD40L or GM-CSF incorporated Hantaan virus like particle. *Oncotarget* 7:63488. doi: 10.18632/oncotarget.11329

Yu, P., Tian, H., Ma, C., Ma, C., Wei, J., Lu, X., et al. (2015). Hantavirus infection in rodents and haemorrhagic fever with renal syndrome in Shaanxi province, China, 1984–2012. *Epidemiol. Infect.* 143, 405–411. doi: 10.1017/S0950268814001009

Zhang, S., Wang, S., Yin, W., Liang, M., Li, J., Zhang, Q., et al. (2014). Epidemic characteristics of hemorrhagic fever with renal syndrome in China, 2006–2012. *BMC Infect. Dis.* 14, 1–10. doi: 10.1186/1471-2334-14-384

Zhao, Y., Zhao, N., Cai, Y., Zhang, H., Li, J., Liu, J., et al. (2022). An algal lectin griffithsin inhibits Hantaan virus infection *in vitro* and *in vivo*. *Front. Cell. Infect. Microbiol.* 12:1813. doi: 10.3389/fcimb.2022.881083

frontiers | Frontiers in Microbiology

TYPE Correction
PUBLISHED 12 December 2023
DOI 10.3389/fmicb.2023.1343080

OPEN ACCESS

APPROVED BY
Frontiers Editorial Office,
Frontiers Media SA, Switzerland

*CORRESPONDENCE
Liaqat Ali
✉ liaqatbiotech@gmail.com
Jing Yang
✉ WIBPJYang@126.com

RECEIVED 22 November 2023
ACCEPTED 23 November 2023
PUBLISHED 12 December 2023

CITATION
Afzal S, Ali L, Batool A, Afzal M, Kanwal N, Hassan M, Safdar M, Ahmad A and Yang J (2023) Corrigendum: Hantavirus: an overview and advancements in therapeutic approaches for infection. *Front. Microbiol.* 14:1343080. doi: 10.3389/fmicb.2023.1343080

Corrigendum: Hantavirus: an overview and advancements in therapeutic approaches for infection

Samia Afzal[1], Liaqat Ali[2]*, Anum Batool[2], Momina Afzal[1], Nida Kanwal[2], Muhammad Hassan[1], Muhammad Safdar[1], Atif Ahmad[1] and Jing Yang[3]*

[1]CEMB, University of the Punjab, Lahore, Pakistan, [2]Department of Biological Sciences, National University of Medical Sciences (NUMS), Rawalpindi, Pakistan, [3]Wuhan Institute of Biological Products Co., Ltd., Wuhan, Hubei, China

KEYWORDS

hantavirus, HFRS, HPS, immunotherapy, siRNA

A corrigendum on

Hantavirus: an overview and advancements in therapeutic approaches for infection

by Afzal, S., Ali, L., Batool, A., Afzal, M., Kanwal, N., Hassan, M., Safdar, M., Ahmad, A., and Yang, J. (2023). *Front. Microbiol.* 14:1233433. doi: 10.3389/fmicb.2023.1233433

In the published article, there were errors in Table 1, Table 3, and Table 4.

The caption for Table 1 only listed North and South America, but Table 1 contains countries from North, Central, and South America.

In Table 1, the reference for the row "Canada" was incorrectly listed as "Jonsson et al. (2010)". The correct reference is "Warner et al. (2020)".

In Table 1, the reference for the row "Panama" was incorrectly listed as "Martinez-Valdebenito et al. (2014)". The correct reference is "Armién et al. (2023)". The corrected Table 1 and its caption "Reported HTNV cases across North, Central, and South America." appear below.

In Table 3, the reference for the row "Lactoferrin" was incorrectly listed as "Gorbunova et al. (2010) and Arikawa et al. (1989)". The correct reference is "Murphy et al. (2000, 2001)".

In Table 3, the reference for the row "Ribavirin" was incorrectly listed as "Schmaljohn et al. (1990) and Liang et al. (1996)". The correct reference is "Chung et al. (2013) and Ogg et al. (2013)".

In Table 3, the reference for the row "Favipiravir" was incorrectly listed as "Arikawa et al. (1992)". The correct reference is "Safronetz et al. (2013)".

In Table 3, the reference for the row "Vandenatib" was incorrectly listed as "Garrido et al. (2018)". The correct reference is "Bird et al. (2016)".

In Table 3, the reference for the row "ETAR" was incorrectly listed as "Golias et al. (2007)". The correct reference is "Chung et al. (2008)".

In Table 3, the reference for the row "Coritcosteroids" was incorrectly listed as "Mills et al. (1999) and Xu et al. (2009)". The correct reference is "Vial et al. (2013) and Brocato and Hooper (2019)".

In Table 3, the reference for the row "Human Immune Sera" was incorrectly listed as "Tian et al. (2021)". The correct reference is "Vial et al. (2015)".

In Table 3, the reference for the row "JL16 and MIB22" was incorrectly listed as "Weinberg and Arbuthnot (2010)". The correct reference is "Garrido et al. (2018)".

In Table 3, the reference for the row "Domain III and Stem Peptides" was incorrectly listed as "Taylor et al. (2013)". The correct reference is "Barriga et al. (2016)".

In Table 3, the reference for the row "CLVRNLAWC and CQATTARNC" was incorrectly listed as "Cicardi et al. (2010)". The correct reference is "Hall et al. (2008)".

In Table 3, the reference for the row "Incatibant" was incorrectly listed as "Avižiniene et al. (2023) and Mittler et al. (2023)". The correct reference is "Antonen et al. (2013) and Laine et al. (2015)".

In Table 3, the reference for the row "TNF-α" was incorrectly listed as "Brocato et al. (2012), Manigold and Vial (2014), and Vial et al. (2015)". The correct reference is "Vilcek (1991), Sundstrom et al. (2001), and Maes et al. (2004)".

In Table 3, the reference for the row "RANTES/IP-10/MCP-1" was incorrectly listed as "Manigold and Vial (2014), and Malley et al. (2004)". The correct reference is "Sundstrom et al. (2001) and Glass et al. (2003)". The corrected Table 3 and its caption "Lists some examples of potential antiviral therapies against Hantavirus." appear below.

In Table 4, the reference for the row "Inactivated Vaccine" was incorrectly listed as "Sroga et al. (2021)". The correct reference is "Khan et al. (2019)".

In Table 4, the reference for the row "Virus-like Particles 1" was incorrectly listed as "Jonsson et al. (2005)". The correct reference is "Dong et al. (2019)".

In Table 4, the reference for the row "Virus-like Particles 2" was incorrectly listed as "Wray et al. (1985)". The correct reference is "Dong et al. (2019)".

In Table 4, the reference for the row "Virus-Vector Vaccines 1" was incorrectly listed as "Hopper et al. (1999)". The correct reference is "Warner et al. (2019)".

In Table 4, the reference for the row "Virus-Vector Vaccines 2" was incorrectly listed as "Brocato et al. (2013)". The correct reference is "Prescott et al. (2014)".

In Table 4, the reference for the row "Virus-Vector Vaccines 3" was incorrectly listed as "Deng et al. (2020)". The correct reference is "Safronetz et al. (2009)".

In Table 4, the reference for the row "Recombinant Vaccines 1" was incorrectly listed as "Hopper et al. (2014)". The correct reference is "Geldmacher et al. (2004)".

In Table 4, the reference for the row "Recombinant Vaccines 2" was incorrectly listed as "Ogg et al. (2013)". The correct reference is "de Carvalho et al. (2002)".

In Table 4, the reference for the row "Recombinant Vaccines 3" was incorrectly listed as "Ogg et al. (2013)". The correct reference is "Maes et al. (2006)".

In Table 4, the reference for the row "DNA Vaccines 1" was incorrectly listed as "Vial et al. (2013)". The correct reference is "Hooper et al. (2013)".

In Table 4, the reference for the row "DNA Vaccines 2" was incorrectly listed as "Antonen et al. (2013)". The correct reference is "Hooper et al. (2001)".

In Table 4, the reference for the row "DNA Vaccines 3" was incorrectly listed as "Laine et al. (2015)". The correct reference is "Hooper et al. (2006)".

In Table 4, the reference for the row "DNA Vaccines 4" was incorrectly listed as "Vial et al. (2013)". The correct reference is "Hooper et al. (2013)".

In Table 4, the reference for the row "DNA Vaccines 5" was incorrectly listed as "Fire et al. (1998)". The correct reference is "Brocato et al. (2013)".

In Table 4, the reference for the row "DNA Vaccines 6" was incorrectly listed as "Safronetz et al. (2013)". The correct reference is "Jiang et al. (2017)".

In Table 4, the reference for the row "Subunit Vaccines" was incorrectly listed as "Ye et al. (2019)". The correct reference is "Maes et al. (2008)". The corrected Table 4 and its caption "Describing evaluation of Hantavirus vaccines in various animal models and some vaccines currently undergoing clinical trials." appear below.

The authors apologize for these errors and state that they do not change the scientific conclusions of the article in any way. The original article has been updated.

Publisher's note

References

Antonen, J., Leppänen, I., Tenhunen, J., Arvola, P., Mäkelä, S., Vaheri, A., et al. (2013). A severe case of Puumala Hantavirus infection successfully treated with bradykinin receptor antagonist icatibant. *Scand. J. Infect. Dis.* 45, 494–496. doi: 10.3109/00365548.2012.755268

Armién, B., Muñoz, C., Cedeño, H., Salazar, J. R., Salinas, T. P., González, P., et al. (2023). Hantavirus in Panama: twenty years of epidemiological surveillance experience. *Viruses* 15:1395. doi: 10.3390/v15061395

Barriga, G. P., Villalón-Letelier, F., Márquez, C. L., Bignon, E. A., Acuña, R., Ross, B. H., et al. (2016). Inhibition of the Hantavirus fusion process by predicted domain III and stem peptides from glycoprotein Gc. *PLoS Negl. Trop. Dis.* 10:e0004799. doi: 10.1371/journal.pntd.0004799

Bird, B. H., Shrivastava-Ranjan, P., Dodd, K. A., Erickson, B. R., and Spiropoulou, C. F. (2016). Effect of Vandetanib on Andes virus survival in the

hamster model of Hantavirus pulmonary syndrome. *Antivir. Res.* 132, 66–69. doi: 10.1016/j.antiviral.2016.05.014

Brocato, R., Josleyn, M., Wahl-Jensen, V., Schmaljohn, C., and Hooper, J. (2013). Construction and nonclinical testing of a Puumala virus synthetic M gene-based DNA vaccine. *Clin. Vaccine Immunol.* 20, 218–226. doi: 10.1128/CVI.00546-12

Brocato, R. L., and Hooper, J. W. (2019). Progress on the prevention and treatment of Hantavirus disease. *Viruses* 11:610. doi: 10.3390/v11070610

Chung, D.-H., Kumarapperuma, S. C., Sun, Y., Li, Q., Chu, Y.-K., Arterburn, J. B., et al. (2008). Synthesis of 1-β-d-ribofuranosyl-3-ethynyl-[1, 2, 4] triazole and its *in vitro* and *in vivo* efficacy against Hantavirus. *Antivir. Res.* 79, 19–27. doi: 10.1016/j.antiviral.2008.02.003

Chung, D.-H., Västermark, Å., Camp, J. V., McAllister, R., Remold, S. K., Chu, Y.-K., et al. (2013). The murine model for Hantaan virus-induced lethal disease shows two distinct paths in viral evolutionary trajectory with and without ribavirin treatment. *J. Virol.* 87, 10997–11007. doi: 10.1128/JVI.01394-13

de Carvalho, N., Gonzalez Delia Valle, M., Padula, P., Bjorling, E., Plyusnin, A., and Lundkvist, A. (2002). Cross-protection against challenge with Puumala virus after immunization with nucleocapsid proteins from different hantaviruses. *J. Virol.* 76, 6669–6677. doi: 10.1128/jvi.76.13.6669-6677.2002

Dong, Y., Ma, T., Zhang, X., Ying, Q., Han, M., Zhang, M., et al. (2019). Incorporation of CD40 ligand or granulocyte-macrophage colony stimulating factor into Hantaan virus (HTNV) virus-like particles significantly enhances the long-term immunity potency against HTNV infection. *J. Med. Microbiol.* 68, 480–492. doi: 10.1099/jmm.0.000897

Garrido, J. L., Prescott, J., Calvo, M., Bravo, F., Alvarez, R., Salas, A., et al. (2018). Two recombinant human monoclonal antibodies that protect against lethal Andes Hantavirus infection *in vivo*. *Sci. Transl. Med.* 10:eaat6420. doi: 10.1126/scitranslmed.aat6420

Geldmacher, A., Skrastina, D., Petrovskis, I., Borisova, G., Berriman, J. A., Roseman, A. M., et al. (2004). An amino-terminal segment of Hantavirus nucleocapsid protein presented on hepatitis B virus core particles induces a strong and highly cross-reactive antibody response in mice. *Virology* 323, 108–119. doi: 10.1016/j.virol.2004.02.022

Glass, W. G., Rosenberg, H. F., and Murphy, P. M. (2003). Chemokine regulation of inflammation during acute viral infection. *Curr. Opin. Allergy Clin. Immunol.* 3, 467–473. doi: 10.1097/00130832-200312000-00008

Hall, P. R., Hjelle, B., Brown, D. C., Ye, C., Bondu-Hawkins, V., Kilpatrick, K. A., et al. (2008). Multivalent presentation of antihantavirus peptides on nanoparticles enhances infection blockade. *Antimicrob. Agents Chemother.* 52, 2079–2088. doi: 10.1128/AAC.01415-07

Hooper, J., Custer, D., Thompson, E., and Schmaljohn, C. (2001). DNA vaccination with the Hantaan virus M gene protects hamsters against three of four HFRS hantaviruses and elicits a high-titer neutralizing antibody response in Rhesus monkeys. *J. Virol.* 75, 8469–8477. doi: 10.1128/JVI.75.18.8469-8477.2001

Hooper, J. W., Custer, D. M., Smith, J., and Wahl-Jensen, V. (2006). Hantaan/Andes virus DNA vaccine elicits a broadly cross-reactive neutralizing antibody response in nonhuman primates. *Virology* 347, 208–216. doi: 10.1016/j.virol.2005.11.035

Hooper, J. W., Josleyn, M., Ballantyne, J., and Brocato, R. (2013). A novel sin Nombre virus DNA vaccine and its inclusion in a candidate pan-Hantavirus vaccine against Hantavirus pulmonary syndrome (HPS) and hemorrhagic fever with renal syndrome (HFRS). *Vaccine* 31, 4314–4321. doi: 10.1016/j.vaccine.2013.07.025

Jiang, D.-B., Sun, L.-J., Cheng, L.-F., Zhang, J.-P., Xiao, S.-B., Sun, Y.-J., et al. (2017). Recombinant DNA vaccine of Hantavirus Gn and LAMP1 induced long-term immune protection in mice. *Antivir. Res.* 138, 32–39. doi: 10.1016/j.antiviral.2016.12.001

Khan, A., Shin, O. S., Na, J., Kim, J. K., Seong, R.-K., Park, M.-S., et al. (2019). A systems vaccinology approach reveals the mechanisms of immunogenic responses to hantavax vaccination in humans. *Sci. Rep.* 9:4760. doi: 10.1038/s41598-019-41205-1

Laine, O., Leppänen, I., Koskela, S., Antonen, J., Mäkelä, S., Sinisalo, M., et al. (2015). Severe Puumala virus infection in a patient with a lymphoproliferative disease treated with icatibant. *Infect. Dis.* 47, 107–111. doi: 10.3109/00365548.2014.969304

Maes, P., Clement, J., Cauwe, B., Bonnet, V., Keyaerts, E., Robert, A., et al. (2008). Truncated recombinant puumala virus nucleocapsid proteins protect mice against challenge *in vivo*. *Viral Immunol.* 21, 49–60. doi: 10.1089/vim.2007.0059

Maes, P., Clement, J., Gavrilovskaya, I., and Van Ranst, M. (2004). Hantaviruses: immunology, treatment, and prevention. *Viral Immunol.* 17, 481–497. doi: 10.1089/vim.2004.17.481

Maes, P., Keyaerts, E., Bonnet, V., Clement, J., Avsic-Zupanc, T., Robert, A., et al. (2006). Truncated recombinant Dobrava Hantavirus nucleocapsid proteins induce strong, long-lasting immune responses in mice. *Intervirology* 49, 253–260. doi: 10.1159/00009 3454

Murphy, M., Kariwa, H., Mizutani, T., Yoshimatsu, K., Arikawa, J., and Takashima, I. (2000). *In vitro* antiviral activity of lactoferrin and ribavirin upon Hantavirus. *Arch. Virol.* 145, 1571–1582. doi: 10.1007/s007050070077

Murphy, M. E., Kariwa, H., Mizutani, T., Tanabe, H., Yoshimatsu, K., Arikawa, J., et al. (2001). Characterization of *in vitro* and *in vivo* antiviral activity of lactoferrin and ribavirin upon Hantavirus. *J. Vet. Med. Sci.* 63, 637–645. doi: 10.1292/jvms.63.637

Ogg, M., Jonsson, C. B., Camp, J. V., and Hooper, J. W. (2013). Ribavirin protects Syrian hamsters against lethal Hantavirus pulmonary syndrome—after intranasal exposure to Andes virus. *Viruses* 5, 2704–2720. doi: 10.3390/v5112704

Prescott, J., DeBuysscher, B. L., Brown, K. S., and Feldmann, H. (2014). Long-term single-dose efficacy of a vesicular stomatitis virus-based Andes virus vaccine in Syrian hamsters. *Viruses* 6, 516–523. doi: 10.3390/v6020516

Safronetz, D., Falzarano, D., Scott, D. P., Furuta, Y., Feldmann, H., and Gowen, B. B. (2013). Antiviral efficacy of favipiravir against two prominent etiological agents of Hantavirus pulmonary syndrome. *Antimicrob. Agents Chemother.* 57, 4673–4680. doi: 10.1128/AAC.00886-13

Safronetz, D., Hegde, N. R., Ebihara, H., Denton, M., Kobinger, G. P., St. Jeor, S., et al. (2009). Adenovirus vectors expressing Hantavirus proteins protect hamsters against lethal challenge with Andes virus. *J. Virol.* 83, 7285–7295. doi: 10.1128/JVI.00373-09

Sundstrom, J. B., McMullan, L. K., Spiropoulou, C. F., Hooper, W. C., Ansari, A. A., Peters, C. J., et al. (2001). Hantavirus infection induces the expression of RANTES and IP-10 without causing increased permeability in human lung microvascular endothelial cells. *J. Virol.* 75, 6070–6085. doi: 10.1128/JVI.75.13.6070-6085.2001

Vial, P., Valdivieso, F., Ferres, M., Riquelme, R., Rioseco, M., Calvo, M., et al. (2013). Hantavirus study Group in Chile High-dose intravenous methylprednisolone for Hantavirus cardiopulmonary syndrome in Chile: a double-blind, randomized controlled clinical trial. *Clin. Infect. Dis.* 57, 943–951. doi: 10.1093/cid/cit394

Vial, P. A., Valdivieso, F., Calvo, M., Rioseco, M. L., Riquelme, R., Araneda, A., et al. (2015). A non-randomized multicentre trial of human immune plasma for treatment of Hantavirus cardiopulmonary syndrome caused by Andes virus. *Antivir. Ther.* 20, 377–386. doi: 10.3851/IMP2875

Vilcek, J. (1991). Tumor necrosis factor-new insights into the molecular mechanisms of its multiple actions. *J. Biol. Chem.* 266:7313. doi: 10.1016/S0021-9258(20)89445-9

Warner, B. M., Dowhanik, S., Audet, J., Grolla, A., Dick, D., Strong, J. E., et al. (2020). Hantavirus cardiopulmonary syndrome in Canada. *Emerg. Infect. Dis.* 26:3020. doi: 10.3201/eid2612.202808

Warner, B. M., Stein, D. R., Jangra, R. K., Slough, M. M., Sroga, P., Sloan, A., et al. (2019). Vesicular stomatitis virus-based vaccines provide cross-protection against Andes and sin nombre viruses. *Viruses* 11:645. doi: 10.3390/v11070645

10.3389/fmicb.2023.1343080

TABLE 1 Reported HTNV cases across North, Central, and South America.

Country	Cases	Year	Source
USA	850	1993–2021	CDC
Canada	143	As of 2020	Warner et al. (2020)
Panama	712	1999–2019	Armién et al. (2023)
Costa Rica	3	Till 2016	PAHO
Argentina	1,350	As 2016	PAHO
Chile	1,028	As of 2016	PAHO
Brazil	2,032	Till 2017	PAHO
Paraguay	319	Till 2016	PAHO
Uruguay	169	Till 2016	PAHO
Bolivia	300	Till 2016	PAHO
Ecuador	73	As of 2016	PAHO
Peru	6	As of 2016	PAHO
French Guiana	3	Till 2016	PAHO

10.3389/fmicb.2023.1343080

TABLE 3 Lists some examples of potential antiviral therapies against Hantavirus.

Antiviral therapy	Type	Function	Target	Disease	References
Lactoferrin	Lactoferrin	Block viral entry	Viral GP	HFRS	Murphy et al. (2000, 2001)
Ribavirin	Nucleoside analogs	Inhibit viral replication	RdRp	HCPS and HFRS	Chung et al. (2013) and Ogg et al. (2013)
Favipiravir	Pyrazine derivatives	Block viral entry	RdRp	HCPS	Safronetz et al. (2013)
Vandetanib	Tyrosine kinase inhibitor	Improve vascular function	VEGF/Vascular function	HCPS	Bird et al. (2016)
ETAR	Nucleoside analog	Inhibit viral entry	RdRp	HCPS and HFRS	Chung et al. (2008)
Corticosteroids	Hormone	Rebuild immune homeostasis	Immunotherapy	HCPS and HFRS	Vial et al. (2013) and Brocato and Hooper (2019)
Human Immune Sera	Human pAbs	Block viral entry	Viral GP	HCPS	Vial et al. (2015)
JL16 and MIB22	Human mAbs	Block viral entry	Viral GP	HCPS	Garrido et al. (2018)
Domain III and stem peptides	Peptides	Block viral entry	Gc glycoprotein	HCPS and HFRS	Barriga et al. (2016)
CLVRNLAWC and CQATTARNC	Cyclic nonapeptides	Block viral entry	Host receptor	HCPS	Hall et al. (2008)
Icatibant	Small molecule	Improve vascular function	BK type 2 receptor	HFRS	Antonen et al. (2013) and Laine et al. (2015)
TNF-α	Small proteins/Pro-inflammatory cytokines	Increase systemic toxicity	Vascular function	HCPS and HFRS	Vilcek (1991), Sundstrom et al. (2001) and Maes et al. (2004)
RANTES/IP- 10/MCP-1	Small proteins/ Pro-inflammatory chemokines	Immunomodulators/ Inhibit viral infection	Microvascular endothelium	HFRS	Sundstrom et al. (2001) and Glass et al. (2003)

TABLE 4 Describing evaluation of Hantavirus vaccines in various animal models and some vaccines currently undergoing clinical trials.

Vaccine type	Antigen	Animal model	Immunogenicity evaluation	References
Inactivated vaccine	Formalin inactivated HNTV	Humans	Humoral response Neutralizing antibodies	Khan et al. (2019)
Virus-like particles	HTNV-VLP with CD40L or GM-CSF	Mice	Cytotoxic response Neutralization antibody Cytolytic activity	Dong et al. (2019)
	M	DHFR-deficient CHO cells	Antigen-specific IFN-γ production Effective against HTNV Still in developing phases	Dong et al. (2019)
Virus-vector vaccines	Replication-competent VSV-vectored SNV or ANDV glycoproteins	Syrian Hamster	Cross-reactive IgG antibodies Neutralizing antibodies	Warner et al. (2019)
	Replication-competent VSV-vectored ANDV glycoproteins	Syrian Hamsters	Neutralizing antibodies	Prescott et al. (2014)
	Non-replicating Ad vector expressing N, Gn, Gc, or Gn/Gc	Syrian Hamsters	CD8+ cell response Neutralizing antibodies	Safronetz et al. (2009)
Recombinant vaccines	Yeast-expressed DOBV nucleoprotein	Mice	NP-specific IgG response Th1/Th2 response Cross-reactivity with HTNV and PUUV	Geldmacher et al. (2004)
	Nucleoproteins from ANDV, TOPV, DOBV or PUUV	Bank voles	Specific CD8+ cell production Cross-reactive response against PUUV	de Carvalho et al. (2002)
	Truncated recombinant PUUV nucleoprotein linked to bacterial membrane protein	Mice	CD8+ T-cell response NP IgG response	Maes et al. (2006)
DNA vaccines	HTNV/PUUV/SNV/ANDV M gene segment mix	Rabbits	Neutralizing antibodies	Hooper et al. (2013)
	HTNV M segment	Rhesus macaques	Neutralizing antibodies Cross-reactivity with SEOV and DOBV	Hooper et al. (2001)
	ANDV and HNTV M gene segments	Rhesus macaques	Neutralizing antibodies	Hooper et al. (2006)
	SNV M gene segment	Syrian hamsters	Neutralizing antibodies	Hooper et al. (2013)
	PUUV M gene segment	Syrian hamsters	Protection against lethal ANDV infection, without nAbs Neutralizing antibodies	Brocato et al. (2013)
	Gn glycoprotein	BALB/c mice	Effective against HTNV Still in developing phases	Jiang et al. (2017)
Subunit vaccines	NP (nucleocapsid protein)	*E. coli* mutant ICONE NMRI mice	Effective against PUUV In developing Phases	Maes et al. (2008)

frontiers | Frontiers in Microbiology

TYPE Review
PUBLISHED 16 October 2023
DOI 10.3389/fmicb.2023.1218654

OPEN ACCESS

EDITED BY
Cécile E. Malnou,
Université Toulouse III Paul Sabatier, France

REVIEWED BY
Perumal Vivekanandan,
Indian Institute of Technology Delhi, India
Sabine Chapuy-Regaud,
Institut National de la Santé et de la Recherche Médicale (INSERM), France

*CORRESPONDENCE
Milan Surjit
✉ milan@thsti.res.in

RECEIVED 07 May 2023
ACCEPTED 28 September 2023
PUBLISHED 16 October 2023

CITATION
Kumar S, Ansari S, Narayanan S, Ranjith-Kumar CT and Surjit M (2023) Antiviral activity of zinc against hepatitis viruses: current status and future prospects.
Front. Microbiol. 14:1218654.
doi: 10.3389/fmicb.2023.1218654

Antiviral activity of zinc against hepatitis viruses: current status and future prospects

Shiv Kumar[1], Shabnam Ansari[1], Sriram Narayanan[2], C. T. Ranjith-Kumar[2] and Milan Surjit[1]*

[1]Virology Laboratory, Centre for Virus Research, Therapeutics and Vaccines, Translational Health Science and Technology Institute, NCR Biotech Science Cluster, Faridabad, Haryana, India, [2]University School of Biotechnology, Guru Gobind Singh Indraprastha University, New Delhi, India

Viral hepatitis is a major public health concern globally. World health organization aims at eliminating viral hepatitis as a public health threat by 2030. Among the hepatitis causing viruses, hepatitis B and C are primarily transmitted via contaminated blood. Hepatitis A and E, which gets transmitted primarily via the feco-oral route, are the leading cause of acute viral hepatitis. Although vaccines are available against some of these viruses, new cases continue to be reported. There is an urgent need to devise a potent yet economical antiviral strategy against the hepatitis-causing viruses (denoted as hepatitis viruses) for achieving global elimination of viral hepatitis. Although zinc was known to mankind for a long time (since before Christ era), it was identified as an element in 1746 and its importance for human health was discovered in 1963 by the pioneering work of Dr. Ananda S. Prasad. A series of follow up studies involving zinc supplementation as a therapy demonstrated zinc as an essential element for humans, leading to establishment of a recommended dietary allowance (RDA) of 15 milligram zinc [United States RDA for zinc]. Being an essential component of many cellular enzymes and transcription factors, zinc is vital for growth and homeostasis of most living organisms, including human. Importantly, several studies indicate potent antiviral activity of zinc. Multiple studies have demonstrated antiviral activity of zinc against viruses that cause hepatitis. This article provides a comprehensive overview of the findings on antiviral activity of zinc against hepatitis viruses, discusses the mechanisms underlying the antiviral properties of zinc and summarizes the prospects of harnessing the therapeutic benefit of zinc supplementation therapy in reducing the disease burden due to viral hepatitis.

KEYWORDS

zinc, viral hepatitis, hepatitis A virus, hepatitis B virus, hepatitis C, hepatitis E virus

1. Introduction

Zinc is the second most abundant trace element found in humans. A healthy adult body contains 2–4 grams of zinc. Zinc is involved in several biological functions including growth, development, maintenance of immune system and disease resistance. It shows broad anti-inflammatory and anti-oxidant properties. At molecular level, many enzymes and proteins that regulate DNA replication, transcription, signal transduction and apoptosis require zinc for their activities (Maret and Sandstead, 2006; John et al., 2010; Ryu et al., 2020).

Plasma or serum zinc levels between 0.8 and 1.20 μg/ml is considered normal in a healthy individual. Zinc is absorbed in the small intestine by a carrier-mediated mechanism in a concentration dependent manner and increases with increasing dietary zinc (Roohani et al., 2013; Ryu et al., 2020). The portal system delivers absorbed zinc directly to the liver, which directs its circulation for delivery to the other tissues. About 70% of the zinc in circulation is bound to albumin, and any condition that alters serum albumin concentration can have a secondary effect on serum zinc levels (Roohani et al., 2013).

Zinc level gets affected by many conditions such as infections, changes in steroid hormone levels, and muscle catabolism during weight loss or illness (Roohani et al., 2013; Ryu et al., 2020). Around 2 billion people are suggested to have prolonged zinc deficiency worldwide, majority of which includes population from economically weaker countries (Prasad, 2013). Zinc deficiency enhances vulnerability to many viral infections and increasing number of studies support the therapeutic benefit of zinc supplementation in alleviating several viral diseases (Sadeghsoltani et al., 2021). This review provides a comprehensive summary of the antiviral effect of zinc in viral hepatitis and discusses the possible scope of better management of viral hepatitis cases using more potent zinc formulations.

2. Antiviral effect of zinc on hepatitis viruses

Majority of viral hepatitis is caused by the Hepatitis A virus (HAV), Hepatitis B virus (HBV), Hepatitis C virus (HCV), Hepatitis D virus (HDV) and Hepatitis E virus (HEV; Myers et al., 2002). In addition, Herpes viruses such as Epstein–Barr virus (EBV), Cytomegalo virus (CMV), Adenovirus and Varicella zoster virus (VZV) also induce hepatic injury (Lalazar and Ilan, 2014). Herpes simplex virus (HSV) induced hepatitis is a rare cause of acute liver failure (Chaudhary et al., 2017).

2.1. Hepatitis A virus

HAV is a positive stranded nonenveloped RNA virus that is transmitted via the fecal-oral route (Martin and Lemon, 2006; Traore et al., 2012). It is the most common cause of acute viral hepatitis globally (Hauri et al., 2006). It does not cause chronic hepatitis but it adds to further deterioration of liver infected with other hepatotropic viruses (Keeffe, 1995; Vento et al., 1998). A vaccine is available against it (Hauri et al., 2006). No specific treatment is available against it but the disease is self-limiting and there is no lasting injury.

2.2. Hepatitis B virus

HBV is transmitted through exposure to contaminated blood products and body fluids (Myers et al., 2002). It is a DNA virus. Chronic infection with hepatitis B virus (HBV) is estimated to affect 400 million individuals globally, and it is the leading cause of HCC (Lok et al., 2001). Vaccines and antiviral therapies are available against HBV (Das et al., 2019; Zhu et al., 2022).

2.3. Hepatitis C virus

HCV is transmitted through exposure to contaminated blood products (Myers et al., 2002). HCV affects more than 170 million people worldwide (Bhatia et al., 2014; Manns et al., 2017). Coinfections of hepatitis viruses are frequently observed in clinical setting. Furthermore, their propensity for chronicity sets the stage for superinfection with other viruses (Myers et al., 2002). It frequently causes chronic infection, leading to hepatocellular carcinoma (HCC; Vento et al., 1998; Manns et al., 2017). No vaccine is available against it. Treatment options for HCV cases include a combination of broadly-acting antivirals (such as peg-interferon, ribavirin) and specific direct-acting antiviral (Sofosbuvir; Bhatia et al., 2014).

2.4. Hepatitis D virus

HDV is transmitted through exposure to contaminated blood products and body fluids (Myers et al., 2002). It requires the HBV surface antigen (HBsAg) to replicate and is dependent on the latter (Huang and Lo, 2014). Around 5% of HBV carriers (approximately 20 million individuals) are coinfected with the HDV (Myers et al., 2002). No vaccine is available against HDV but HBV vaccinated people are protected from it as it is a significant threat only in HBV infected individuals. Recently, Bulevirtide was shown to be a potential treatment option against HDV (Dietz-Fricke et al., 2023).

2.5. Hepatitis E virus

HEV is a positive stranded quasi-enveloped RNA virus (Nimgaonkar et al., 2018). It is transmitted via the fecal-oral route. It can also get transmitted via blood transfusion. Zoonotic transmission of HEV from animals to human is also reported. It is a major cause of acute viral hepatitis globally (Primadharsini et al., 2021). HAV and HEV are major cause of community level outbreaks and epidemics in areas with poor sanitary conditions (Wu et al., 2016; Primadharsini et al., 2021). It may cause chronic infection in immune compromised individuals. At present, a vaccine against HEV is available in China (Wu et al., 2016). HEV cases are self-limiting in otherwise healthy individuals. A combination of broadly-acting antivirals are the option for off-label therapy in severe HEV cases (Netzler et al., 2019).

There is a need to formulate more potent, side-effect free therapeutics for treatment of viral hepatitis cases (Cowan et al., 2011). Controlled zinc supplementation is known to be a safe, side effect free therapy against Wilson's disease (Brewer et al., 2000). Zinc is widely used as an antimicrobial agent, without any side effect (Wessels et al., 2022). Zinc supplementation is a part of standard care in the treatment of diarrhea in infants (Bajait and Thawani, 2011). Multiple laboratories have independently evaluated the antiviral potential of zinc against hepatitis viruses using diverse experimental approaches. Compilation and careful interpretation of the available data will be useful in evaluating the therapeutic potential of zinc in the treatment of viral

hepatitis cases. Below sections compile majority of the available data on antiviral activity of zinc *in vivo* and *in vitro*.

2.6. Clinical trials on evaluation of therapeutic benefit of zinc compounds in viral hepatitis patients

Multiple clinical trials have been performed to determine the therapeutic benefit of zinc supplementation in viral hepatitis patients (Table 1). Majority of the trials involved HCV patients (10 trials), one trial involved HBV patients and one trial involved HEV patients. In some studies, serum zinc level was measured in the patients before and after the treatment regimen and compared to that of the placebo group. Pre-existing zinc deficiency was observed in 4 trials while normal zinc level was observed in 3 trials and zinc level was not measured in 5 trials. Zinc supplementation increased the serum zinc level in three of the four zinc deficient groups tested. Effect of zinc supplementation on disease outcome was evaluated by measuring the levels of serum albumin, ALT (alanine aminotransferase), AST (aspartate aminotransferase) and viral load [sustained viral response (SVR)]. In trials involving only zinc supplementation or zinc supplementation in addition to the standard antiviral therapeutics, there was an increased therapeutic response, compared to the placebo group. However, there was lack of positive clinical outcome with Zinc supplementation in four trials of chronic HCV cases (Table 1). In summary, these studies support the therapeutic benefit of zinc supplementation in a subset of viral hepatitis patients.

Serum zinc levels are decreased in HCV patients and the underlying mechanism is proposed to be due to the requirement of zinc binding by the viral non-structural proteins NS3 and NS5A (Love et al., 1996; Stempniak et al., 1997; Tellinghuisen et al., 2004). Comparison of serum zinc levels in chronic hepatitis C patients before and after treatment with Direct acting antivirals (DAAs) revealed an increase in the serum zinc level after DAA treatment (Suda et al., 2019). Importantly, they showed that the increased zinc level was not attributed to an increase in the albumin level, but it was a direct outcome of the viral RNA clearance (Suda et al., 2019).

Chronic hepatitis due to HCV infection is a known risk factor of HCC. In an interesting study, Hosui et al. evaluated the effect of oral zinc supplementation on the risk of HCC development in DAA treatment-cured chronic hepatitis C suffering individuals (Hosui et al., 2021). One year and three year follow up study after the end of DAA therapy showed cumulative incidence rates of 1.8 and 5.6%, respectively in the no zinc supplemented (control) group. None from the zinc supplemented group developed HCC. Moreover, serum zinc concentration was significantly higher in the no HCC group than the HCC group (Hosui et al., 2021). These data suggest the therapeutic benefit of zinc supplementation in reducing the risk of HCC development in individuals recovered from chronic hepatitis C.

In addition to viral infections, there are other inducers of hepatic dysfunction such as alcohol consumption. Multiple independent clinical trials have been carried out to assess the therapeutic benefit of zinc supplementation in non-viral hepatitis patients with liver cirrhosis (Overbeck et al., 2008; Diglio et al., 2020). Zinc supplementation significantly increased the serum zinc level, reduced the serum albumin level and improved the overall disease condition in those patients, further attesting the therapeutic benefit of zinc in hepatitis patients (Overbeck et al., 2008; Diglio et al., 2020).

2.7. Antiviral effect of zinc compounds in cell culture-based infection/replicon models of hepatitis viruses.

Several independent studies support the antiviral role of zinc on replication and survival of HAV, HCV and HEV (Table 2; Figure 1). All studies used safe dose of zinc, which did not affect the viability of the cells that were used in the experiment. Zinc sulphate partially inhibited the replication of HAV in Huh7 (human hepatoma) cells (Ogawa et al., 2019). Zinc sulphate and zinc chloride inhibit replication of the genomic length HCV RNA at a concentration of 100 μM, with maximum effect at 48 h of treatment (Yuasa et al., 2006). Another study by Gupta et al. compared the HCV inhibitory effect of zinc oxide nanoparticles [ZnO(NP)] and tetrapods [ZnO(TP)] with conventional zinc salts such as $ZnSO_4$, which revealed the superior antiviral potency of the ZnO(TP) against HCV (Gupta et al., 2022). Zinc salts, ZnO(NP) and ZnO(TP) also show antiviral activity against HEV, latter being the most potent (Gupta et al., 2022). ZnO(NP) and ZnO(TP) are nanoparticle conjugated variants of ZnO, which is better absorbed in the intestine, possess better bioavailability and reduced undesirable side effect characteristics (Sirelkhatim et al., 2015; Jiang et al., 2018). Therefore, ZnO(NP) and ZnO(TP) are safer alternatives to the conventional zinc salts for therapeutic use. Inhibitory effect of ZnO(TP) was comparable to that of sofosbuvir, a well-known DAA used in the treatment of HCV cases, further testifying the antiviral potential of ZnO(TP) against HCV (Yuasa et al., 2006; Gupta et al., 2022).

3. Broad-spectrum antiviral effect of zinc: insight from studies on other viruses

Antiviral effect of zinc have been demonstrated *in vivo* and *in vitro* in several viruses, including corona viruses, picornaviruses, papilloma viruses, metapneumoviruses, rhinoviruses, herpes simplex viruses, varicella-zoster viruses, respiratory syncytial viruses, retroviruses, SARS-CoV and SARS-CoV-2 etc. (Bracha and Schlesinger, 1976; Gupta and Rapp, 1976; Polatnick and Bachrach, 1978; Katz and Margalith, 1981; Kümel et al., 1990; Hulisz, 2004; Krenn et al., 2009; Te Velthuis et al., 2010; Liu and Kielian, 2012; Wei et al., 2012; Antoine et al., 2016; Liu et al., 2021; Samad et al., 2021). Based on the available literature, mechanism underlying the antiviral properties of zinc may be broadly classified into two categories: (a) direct inhibitory effect on the different stages of the life cycle of the virus and (b) indirect effect of zinc attributed to its ability to modulate various host cellular processes and immune response. Zinc shows direct inhibitory action against several viruses. It acts by interfering with different steps of the viral life cycle, it inhibits the activity of key viral proteins and competes with other bivalent ions such as manganese, magnesium or calcium to interrupt the function of viral proteins. Direct antiviral activity of zinc against viruses is schematically illustrated in Figures 2, 3.

TABLE 1 Clinical trials on evaluation of therapeutic benefit of zinc compounds in viral hepatitis patients.

Disease etiology	Number of participants (NT_{Zn} vs. $NT_{placebo}$)	Zinc dosage, treatment duration	Effect of zinc supplementation					Effect of Zinc Supplementation	Reference
			Serum Zinc levels Pre/Post (μg/dl; m ± SD)	SVR % (Np/NT)	Serum Albumin Pre/Post (g/dl; m ± SD)	ALT (IU/ml)	AST (IU/ml)		
A. Positive clinical outcome in viral hepatitis patients with zinc supplementation									
(IFN + RBV + Zinc) vs. (IFN + RBV + Placebo)									
HCV	$NT_{(VitC/E + Polaprezinc)} = 9$ $NT_{Placebo} = 12$	Polaprezinc: 75 mg/2× day (17 mg zinc), 48 weeks	IGpre/post: 63.7 ± 4.4/68.1 ± 5.3 CGpre/post: 62.9 ± 3.1/62.6 ± 2.7	IG: NR CG: NR	IGpre/post: 3.9 ± 0.1/3.8 ± 0.2 CGpre/post: 3.8 ± 0.2/3.9 ± 0.1	IGpre/post: 47 ± 6/23 ± 3 CGpre/post: 61 ± 6/38 ± 3	IGpre/post: 53 ± 13/30 ± 4 CGpre/post: 50 ± 8/37 ± 5	Polaprezinc induces antioxidative functions in the liver resulting in reduced hepatocyte injury during PEG-IFN α-2b plus ribavirin therapy	Murakami et al. (2007)
(IFN + Zinc) vs. (IFN + Placebo)									
HCV	$NT_{polaprezinc} = 15$ $NT_{Zinc\ Sulphate} = 9$ $NT_{placebo} = 10$	Polaprezinc: 75 mg/2× day (34 mg zinc) Zinc Sulphate: 150 mg/2× day (34 mg zinc), 20 weeks	IG:NR CG:NR	IG: 9/24 (37.5%) CG: 2/10 (20.0%)	IG: NR CG: NR	IGpost:97 ± 16 CGpost:101 ± 20	NR	Polaprezinc works better than Zinc Sulphate in increasing the therapeutic response of IFN-α against chronic hepatitis C	Nagamine et al. (2000)
HCV	$NT_{Polaprezinc} = 35$ $NT_{placebo} = 40$	IFN: 106 units/day Polaprezinc: 75 mg/x2 day (34 mg Zn), 25.7 weeks	IGpost: 75.4 ± 21.3 CGpost: 84.1 ± 19.8	IG: 18/32 (56.3%) CG: 8/36 (22.2%)	IG: NR CG: NR	IGpost:79.0 ± 76.6 CGpost:66.4 ± 31.7	IGpost:76.5 ± 65.9 CGpost 65.9 ± 40.3	Zinc supplementation enhances the response to interferon therapy in patients with intractable chronic HCV infections	Takagi et al. (2001)
(RBV + Zinc) vs. (RBV)									
HEV	$NT_{(RBV + Zinc\ Acetate\ dehydrate)} = 3$ $NT_{(Zinc\ Acetate\ dehydrate)} = 5$	NR	IGpre/post: NR CGpre/post: NR	IG: 2/3 (67%) CG: 0/5 (0%)	IG: NR CG: NR	NR	NR	Zinc supplementation increases serum zinc level and reduces HEV load and AST/ALT levels in HEV patients who do not respond to ribavirin therapy	Horvatits et al. (2023)
(BCAA + Zn) vs. (BCAA + Placebo)									
HBV	$NT_{(BCAA + ZnSO4)} = 19$ $NT_{BCAA} = 21$	BCAA: 4 g/day Zinc Sulfate: 200–600 mg/day (variable), 25.7 weeks	IGpre/post: 58.4 ± 9.2/59.7 ± 0.27 CGpre/post: 60.2 ± 9.0/61.1 ± 0.15	IG: NR CG: NR	IGpre/post: 3.3 ± 0.2/2.2 ± 0.07 CGpre/post: 3.3 ± 0.2/2.0 ± 0.08	NR	NR	Zinc supplementation along with branched-chain amino acid improves disorders of nitrogen metabolism in liver cirrhosis in HBV patients	Hayashi et al. (2007)
(Zn) vs. (Placebo) in Viral cirrhosis									
HCV	$NT_{Polaprezinc} = 32$ $NT_{placebo} = 30$	Polaprezinc: 1 g/ day, 5 years	IGpre: NR CGpre: NR	IG: 499.6 (8.4–850) CG: 576.0 (7.4–850)	IGpre: NR CGpre: NR	IGpost: 86.3 (41–231) CGpost: 93.39 (45–201)	IGpost: 61 (40–118) CGpost: 82.1 (46–138)	Polaprezinc supplementation reduced AST level, ALT level and incidence of HCC.	Matsuoka et al. (2009)

(Continued)

10.3389/fmicb.2023.1218654

TABLE 1 (Continued)

Disease etiology	Number of participants (NT_{Zn} vs. $NT_{placebo}$)	Zinc dosage, treatment duration	Effect of zinc supplementation					Effect of Zinc Supplementation	Reference
			Serum Zinc levels Pre/Post (μg/dl; m ± SD)	SVR % (Np/NT)	Serum Albumin Pre/Post (g/dl; m ± SD)	ALT (IU/ml)	AST (IU/ml)		
HCV	$NT_{Polaprezinc}$ = 14 (comparison of parameters pre- and post-zinc treatment)	Polaprezinc: 75 mg/x3 day (51 mg Zinc), 25.7 weeks	IGpre/post: 64 ± 15/78 ± 26	IG: NR	IG: NR	IGpre/post: 106 ± 33/65 ± 23	IGpre/post: 92 ± 33/63 ± 23	Polaprezinc exerts an anti-inflammatory effect on the liver in patients with HCV-related CLD by reducing iron overload	Himoto et al. (2007)
HCV	$NT_{Zinc\ Sulphate}$ = 9 (comparison of parameters pre- and post-zinc treatment)	Zinc sulfate 200 mg/day (136 mg zinc), 10.7 weeks	IGpre/post: 74.2 ± 12.4/125 ± 25.0	IG: NR	IGpre/post: 33 ± 4.8/34.5 ± 4.4	IGpre/post: 83/61	NR	Zinc supplementation is beneficial in zinc deficient patients with cirrhosis	Bianchi et al. (2000)
B. Lack of positive clinical outcome in viral hepatitis patients with Zinc supplementation									
(IFN + RBV + Zn) vs. (IFN + RBV + Placebo)									
HCV	$NT_{Zinc\ gluconate}$ = 18 $NT_{Placebo}$ = 20	Zinc Gluconate: 78 mg/5× day (50 mg zinc), 24 weeks	IG Pre:56.9 ± 16.9 CG Pre: 60.6 ± 10.8	IG: 9/18 (50%) CG: 10/20 (50%)	IG pre: 3.6 ± 0.3 CG pre:3.7 ± 0.4	IGpost: 170 ± 145 CGpost: 146 ± 96	IGpost:135 ± 102 CGpost: 96 ± 86	Zinc supplementation may be a complementary therapy in chronic hepatitis C patients to increase the tolerance to IFN-alpha-2a and ribavirin	Ko et al. (2005)
HCV	$NT_{Polaprezinc}$ = 39 $NT_{placebo}$ = 39	Polaprezinc: 75 mg/2× day (17 mg zinc), 24 weeks	IG Pre:73.3 ± 20.3 CG Pre: 69.8 ± 17.2	IG: 13/39(33.3%) CG:13/39(33.3%)	IG: NR CG: NR	IGpost: 95.6 ± 61.1 CGpost:97.4 ± 59.8	IG: NR CG: NR	Polaprezinc did not show any additional therapeutic benefit in HCV patients treated with IFN and ribavirin	Suzuki et al. (2006)
HCV	$NT_{Zinc\ gluconate}$ = 16 $NT_{Placebo}$ = 16	Zinc Gluconate: 30 mg zinc/day, 24 weeks	IG Pre/post: 75 ± 19/84 ± 28 CG Pre/post: 62.9 ± 3.1/62.6 ± 2.7	IG: 13/16(81.2%) CG:14/16(87.5%)	IG: NR CG: NR	IGpost: 78 ± 52 CGpost: 65 ± 71	IGpost: 85 ± 75 CGpost: 69 ± 59	30 mg/day zinc gluconate did not significantly improve the outcome of treatment in thalassemia patients with chronic hepatitis C	Abbasinazari et al. (2014)
HCV	$NT_{Polaprezinc}$ = 16 $NT_{placebo}$ = 16	polaprezinc:75 mg (17 mg zinc)x2 day, 48 weeks	IG Post:69.4 ± 6.5 CG Post: 73.9 ± 7.5	IG: 8/16(50%) CG:7/16(43.8%)	IG: NR CG: NR	IG: NR CG: NR	IGpost: 45.6 ± 39.3 CGpost: 48.2 ± 26.9	Polaprezinc did not further improve hematologic side effects, liver function in chronic HCV patients treated with PEG-IFN-α2b and ribavirin.	Kim et al. (2008)

10.3389/fmicb.2023.1218654

TABLE 2 Anti-viral effect of zinc on hepatitis viruses in respective cell culture-based infection models/replicon models.

Disease Etiology	Model system	Zinc species and dosage (μM)	Percentage reduction in viral RNA level	Affected stage of the viral life cycle	Reduction in viral load	Reference
HAV	Huh7, infectious HAV	Zinc Sulphate: 100	55	Replication	Yes	Ogawa et al. (2019)
HCV	Huh7, HCV replicon	Zinc Sulphate: 100 Zinc Chloride: 100	60	Replication	Yes	Yuasa et al. (2006)
HCV	Huh7 cells, HCV replicon	Zinc Oxide (NP*): 200 Zinc Oxide (TP*): 200 Zinc Sulphate: 200	90	Replication	Yes	Gupta et al. (2022)
HEV	Huh7 cells, infectious HEV	Zinc Sulphate: 200 Zinc Acetate: 200	90	Replication	Yes	Kaushik et al. (2017)
HEV	Huh 7.5, HEV replicon	Zinc salt#: 115	95	Replication	Yes	Horvatits et al. (2023)
HEV	Huh7, HEV replicon	Zinc Oxide (NP*): 100 Zinc Oxide (TP*): 100 Zinc Sulphate: 100	90	Replication	Yes	Gupta et al. (2022)

*NP, Nanoparticle; TP, Tetrapod.#Full name not reported.

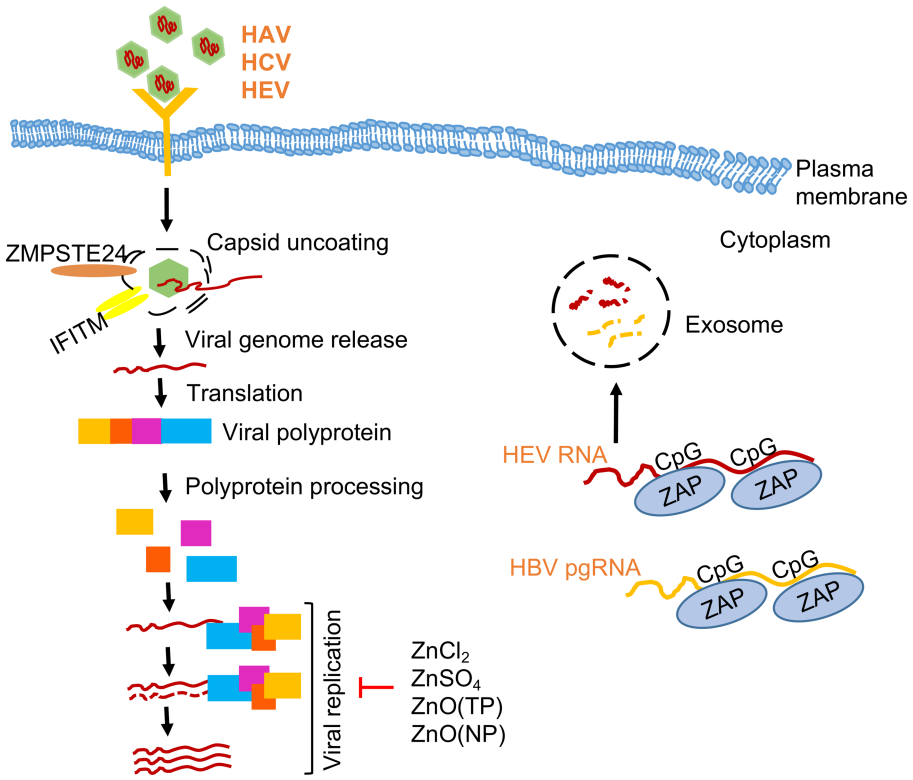

FIGURE 1
Effect of zinc on hepatitis viruses. A simplified scheme of life cycle of HAV, HCV and HEV is shown. Note that HAV and HEV are quasi-enveloped whereas HCV is an enveloped virus. Zinc salts ($ZnCl_2$, $ZnSO_4$), ZnO nanoparticles (NP) and ZnO tetrapod-shaped nanoparticles (TP) inhibits the replication of Hepatitis A (HAV), Hepatitis C (HCV) and Hepatitis E viruses (HEV). Zinc finger antiviral protein (ZAP) binds to CpG motifs in HEV RNA and HBV pre-genomic (pg) RNA and targets them for degradation.

3.1. Effect of zinc on infectivity of the virus and target cell entry

Zinc may directly accumulate on the virus and inactivate it or interfere with its entry into the target cell. Zinc application leads to its deposition on HSV thereby inactivating the virus and inhibiting its cellular entry (Kümel et al., 1990). Recently zinc Oxide tetrapod nanoparticles with engineered oxygen vacancies (Zoten) were shown to possess potent therapeutic benefit in HSV-2 (Herpes simplex virus-2) mediated genital herpes (Antoine et al., 2016). Zoten blocks cellular entry of HSV-2 by efficiently trapping and inactivating the virus, thereby preventing the disease (Figure 2). It

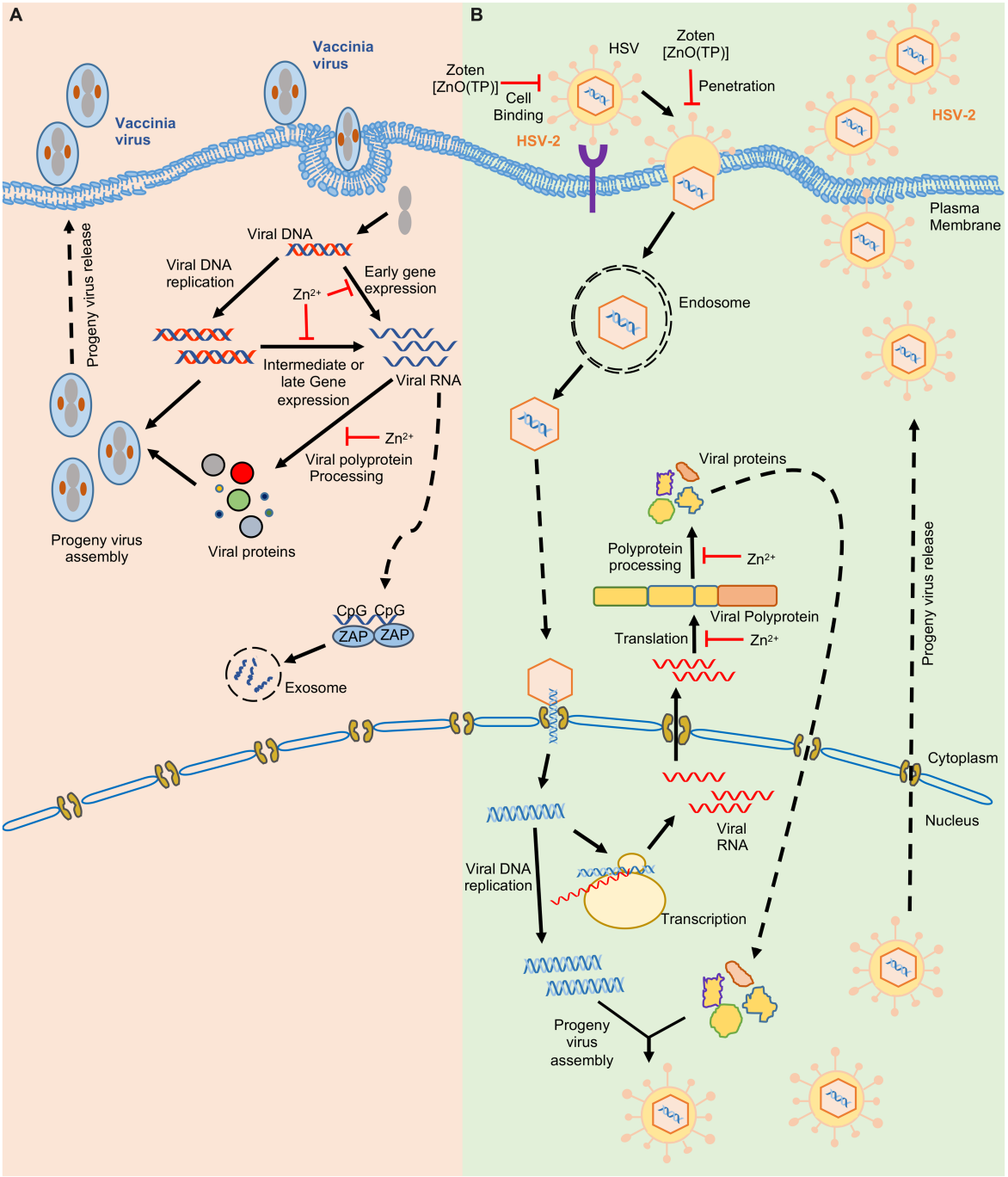

FIGURE 2
Effect of zinc on Vaccinia and Herpes simplex virus-2. Schematic showing the life cycle of Vaccinia virus **(A)** Herpes Simplex virus-2 **(B)**. '' indicates the steps inhibited by zinc.

also enhances T cell and antibody mediated immunity in mice, have adjuvant like properties and thus reduces chances of reinfection (Antoine et al., 2016; Samad et al., 2021). Zinc treatment was shown to moderately inhibit enterovirus D68 attachment and entry into target cells (Figure 3; Liu et al., 2021). In the case of Rhinovirus, zinc may act as a competitive inhibitor of virus binding to the ICAM1 (intercellular adhesion molecule 1) on the host cell surface, which is the receptor for virus entry (Hulisz, 2004; Figure 3). Zinc and Nickel inhibit membrane fusion of SFV (Semliki forest virus) by targeting the viral transmembrane E1 protein (Figure 3; Liu and Kielian, 2012).

3.2. Effect of zinc on viral protein translation and polyprotein processing

Zinc inhibits proteolytic processing of nonstructural polyproteins of several viruses such as rhinovirus and Picornavirus (Krenn et al.,

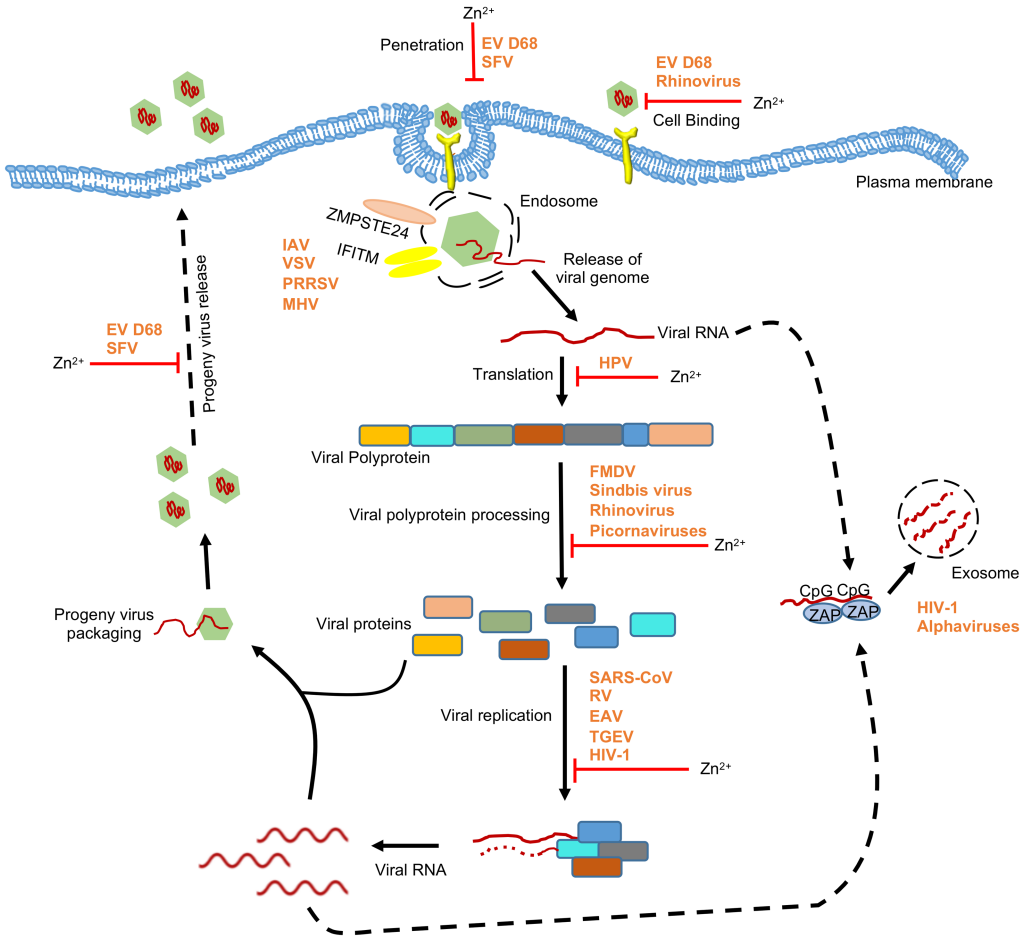

FIGURE 3
Effect of zinc on RNA viruses. Schematic showing the effect of zinc on life cycle of RNA viruses. Apart from directly inhibiting different stages of viral life cycle, zinc mediates its antiviral activity through zinc-containing proteins such as ZAP and ZMPSTE24. ZAP binds to CpG motif in viral RNA and targets them for exosomal degradation. ZMPSTE24 and IFITM complex interferes with entry of viruses. EV D68, enterovirus D68; HPV, human papilloma virus; RSV, respiratory syncytial virus; TGEV, transmissible gastroenteritis virus; SFV, Semliki forest virus; SARS-CoV, severe acute respiratory syndrome coronavirus; FMDV, foot and mouth disease virus; HIV-1, human immunodeficiency virus-1; IAV, influenza A virus; VSV, vesicular stomatitis virus; PRRSV, porcien reproductive and respiratory syndrome virus; MHV, mouse hepatitis virus. " indicates the steps inhibited by zinc.

2009). Zinc ionophores such as Pyrithione and Hinokitol also demonstrate antiviral activity by inhibiting the processing of picornavirus nonstructural polyprotein (Krenn et al., 2009). Zinc treatment inhibits HSV-2, Sindbis, FMDV (Foot and mouth disease virus) and Vaccinia virus growth in infected cells by blocking their polypeptide processing (Figures 2, 3; Bracha and Schlesinger, 1976; Gupta and Rapp, 1976; Polatnick and Bachrach, 1978; Katz and Margalith, 1981).

3.3. Effect of zinc on viral replication and transcription

Replication of viral genome is an essential step for proliferation and maintenance of genomic integrity of the virus. RNA dependent RNA polymerase (RdRp) produced by proteolytic processing of the viral nonstructural proteins plays the central role in the viral replication process. Zinc inhibits RdRp activity of many viruses, including TGEV (Transmissible gastroenteritis virus), SARS-CoV (Severe acute respiratory syndrome coronavirus), EAV (Equine arteritis virus), Rhinovirus and HEV (Hepatitis E virus; Korant et al., 1974; Hung et al., 2002; Te Velthuis et al., 2010; Wei et al., 2012; Kaushik et al., 2017). Different steps in the replication process have been shown to be targeted by zinc for inhibiting RdRp activity. In case of SARS-CoV, zinc treatment reduced template binding and elongation by the RdRp whereas in case of EAV, initiation step of RNA synthesis was inhibited (Te Velthuis et al., 2010). Zinc also inhibits Rhinovirus RdRp activity *in vitro* although the mechanism remains to be understood (Korant et al., 1974; Hung et al., 2002). Clinical trials have shown the therapeutic benefit of zinc in alleviating rhinovirus induced common cold symptoms (Eby et al., 1984; Hulisz, 2004; Kurugöl et al., 2006). Zinc inhibits HIV-1 (Human immunodeficiency virus-1) protease and reverse transcriptase activity (Zhang et al., 1991; Haraguchi et al., 1999; Fenstermacher and DeStefano, 2011). Some other HIV-1 encoded proteins are dependent on zinc to carry out their function (Zheng et al., 1996). Effect of zinc supplementation in HIV infected patients have been investigated in clinical trials (Mocchegiani and Muzzioli, 2000; Bobat et al., 2005; Baum et al., 2010). HIV infected

children showed a significant decrease in the frequency of watery diarrhea after 3 months of zinc supplementation. However, neither viral load was altered nor $CD4^+$ T lymphocytes level was improved (Bobat et al., 2005). Similar effect of zinc supplementation was observed in HIV infected patients having pneumocystis carinii and candida (Mocchegiani et al., 1995). Another study has shown potent antiviral activity of PEGylated ZnO nanoparticle against H1N1 influenza virus (Ghaffari et al., 2019). Recently, polyamide fibers with embedded zinc ions (zinc oxide) were shown to prevent and deactivate Influenza A virus H1N1 and SARS-CoV-2 (Gopal et al., 2021). Further, higher zinc intake was found to reduce the severity of disease in COVID-19 patients (Asoudeh et al., 2023). In addition, many clinical trials have attempted to evaluate the therapeutic benefit of zinc in COVID-19 patients (Carlucci et al., 2020; Chinni et al., 2021; Gordon and Hardigan, 2021; Thomas et al., 2021; Beran et al., 2022; Tabatabaeizadeh, 2022). Though some studies reported a positive outcome, further investigation is warranted to draw a clear conclusion.

Zinc is also reported to act by inhibiting viral particle production and inhibit viral topoisomerase activity in vaccinia virus, inhibit endosomal membrane fusion in Semliki Forest virus and inhibit viral protein E6 and E7 synthesis (thereby stimulating apoptosis) in Human papilloma virus infected cells (Read et al., 2019).

4. Antiviral function of zinc-containing host proteins

Zinc finger antiviral protein (ZAP) is a well characterized host protein that recognizes the CpG dinucleotide present in RNA and targets them for degradation through exosome (Guo et al., 2007; Gonçalves-Carneiro et al., 2022). Since CpG containing RNA is not produced in human, ZAP efficiently targets viral RNA, justifying its antiviral property. Human ZAP contains four zinc finger motifs, located at the N-terminus. Zinc finger motifs mediate its interaction with CpG RNA and mutation of some cysteine residues in the zinc finger motif of ZAP result in loss of its antiviral activity (Guo et al., 2004). Structural studies have clearly demonstrated the role of zinc finger motif of ZAP in mediating its antiviral function (Chen et al., 2012). ZAP also associates with triphosphate motif-containing protein 25 (TRIM25, an E3 ubiquitin ligase), which acts as a co-factor of ZAP and supports its antiviral function (Zheng et al., 2017). P72 RNA helicase (a DEAD box family RNA helicase) also associates with ZAP and helps in its antiviral function (Chen et al., 2008).

ZAP has been shown to inhibit HIV-I by targeting multiple viral mRNA for degradation (Zhu et al., 2011). ZAP inhibits alphaviruses by targeting the CpG dinucleotides in the NSP2 region containing RNA (Nguyen et al., 2023). ZAP inhibits human cytomegalovirus by targeting its UL4/UL5 transcripts (Gonzalez-Perez et al., 2021). In a recent study, Yu et al. demonstrated that expression of ZAP and IFN-β was significantly reduced upon HEV infection (Yu et al., 2021). ZAP was shown to interact with the 5'UTR region of the HEV genome. Knockdown of ZAP decreased phosphorylation of IRF3, thus limiting host innate immune system, while poly(I:C) induction in cells upregulated IRF3 phosphorylation and ZAP, thus inhibiting HEV replication (Yu et al., 2021). Hence ZAP shows antiviral activity against HEV. ZAP also shows antiviral activity against HBV by interacting with the HBV pgRNA (pre-genomic RNA) and targeting it for degradation (Mao et al., 2013).

Considering the pattern and specificity of ZAP binding to CpG RNA, it is expected that ZAP acts as a broad spectrum antiviral factor that acts by targeting the virus while retaining resistance to evolving mutations in the viral genome. Unless the virus encodes a specific mechanism to antagonize CpG RNA binding property of ZAP or deplete ZAP or its cofactors, it is unlikely to escape the antiviral activity of the ZAP. On top of that ZAP is also reported to stimulate the RIG-I signaling pathway, which is a major antiviral response mechanism of the host (Hayakawa et al., 2011).

ZMPSTE24 is another host zinc finger motif containing protein, which shows antiviral activity against many enveloped viruses, including influenza virus, Vesicular stomatitis virus (VSV), Vaccinia virus, Porcine reproductive and respiratory syndrome virus (PRRSV) and arenaviruses (Fu et al., 2017; Katwal et al., 2022; Stott-Marshall and Foster, 2022). A recent report demonstrates that ZMPSTE24 inhibits infection of SARS-CoV-2-spike pseudotyped lentivirus, suggesting its antiviral function against the SARS-CoV-2. A similar phenomenon was also observed in the case of the mouse hepatitis virus (MHV; Shilagardi et al., 2022). ZMPSTE24 acts by interacting with interferon-inducible membrane proteins (IFITM) and preventing fusion of the viral envelope (Fu et al., 2017; Li et al., 2017).

5. Effect of zinc on host

5.1. Maintenance of zinc homeostasis by metallothioneins and zinc transporters

Metallothionein (MT) is a cysteine rich low molecular weight protein, which binds to zinc and copper to regulate their homeostasis in cells and also sequester heavy metals such as cadmium and mercury to alleviate heavy metal poisoning and superoxide stress. There are four MT isoforms in mice (MT1-4) and several isoform/variants in human (Vašák, 2005). MT1 and MT2 are expressed in all organs, while MT3 is expressed in brain and MT4 in stratified tissues. About 10% of human genome encode zinc binding proteins which play crucial biological functions. The availability of zinc is regulated by MT and zinc transporters. MTs sense the intracellular zinc level and modulate zinc through sequestration, distribution and release. Promoter region for MT1 and MT2 contains several metal and glucocorticoid regulatory elements (MREs and GREs). Metal responsive transcription factor 1 (MTF-1) regulates the transcription of MTs (Figure 4; Vašák, 2005). MTF-1 contains six zinc fingers which is responsible for DNA binding, and thus binds to the promoter proximal MREs. Increased Zinc concentration mediate efficient DNA binding of MTF1 (Grzywacz et al., 2015). Another study has shown that during cellular stress, Nitric Oxide (NO) produced by immune cells induce MT1 and MT2 to release zinc and these free zinc ions bind to MTF1, leading to its activation (Stitt et al., 2006). MTs mobilize zinc to nucleus, cytoplasm, golgi and endoplasmic reticulum. MTs also interact with proteins such as GTP, ATP, Gluthatione and these interactions enable their localization in extracellular milieu (Maret, 1994; Jiang et al., 1998; Subramanian Vignesh and Deepe, 2017).

It has been postulated that MTs deliver zinc to the thymulin, which is important for the function of the latter and that aberrant MT regulation can have direct effect on downstream functions of thymulin such as T cell selection, differentiation and function (Subramanian Vignesh and Deepe, 2017). Zinc also regulates the expression of MHC

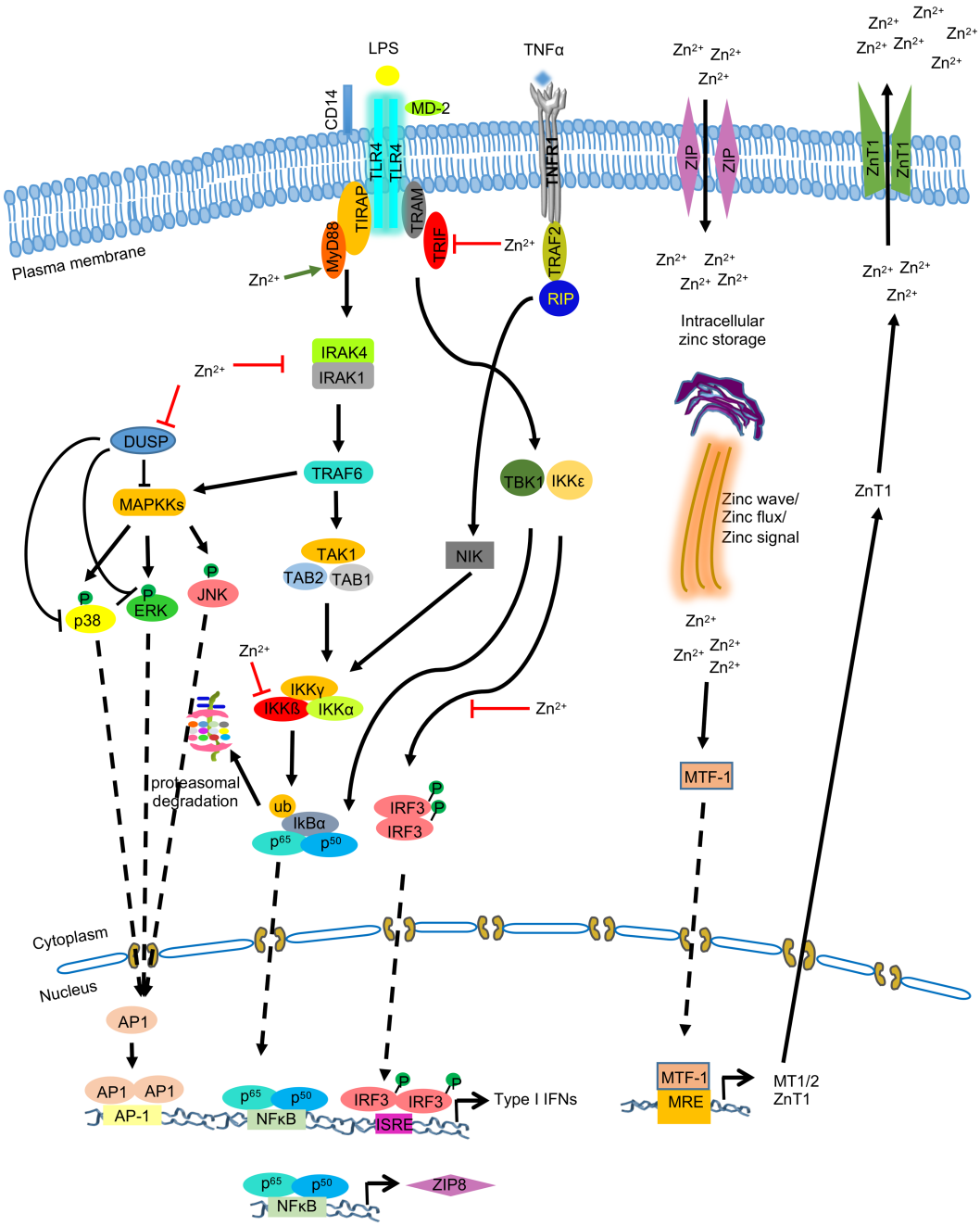

FIGURE 4
Zinc-Metallothionein homeostasis and zinc signaling in monocytes, macrophages and dendritic cells. LPS mediated stimulation of TLR4 leads to activation of NFκB, IRF3, and MAPK signaling pathways, resulting in production of type I IFNs and ZIP8. Zinc mobilization via ZIP8 increases intracellular zinc level, which acts on MAPK, NFκB, and IRF3 signaling pathways by inhibiting dual specificity phosphatase (DUSP) and by inhibiting IKKβ and IRF3 phosphorylation. Metal Responsive element-binding transcription factor-1 (MTF-1) promotes the synthesis of metallothioneins (MT), which in turn binds to and translocates zinc into organelles. MTF-1 also activates the synthesis of ZnT1, which exports zinc out of the cell. " indicates the steps inhibited by zinc.

II on dendritic cell (DC) surface. Excess zinc reduces MHC II expression while zinc deficiency elevates MHC II expression on DCs. Thus, it has been proposed that MT-Zn sequestration regulates MHC II expression in DCs, further influencing thymic T cell selection (Kitamura et al., 2006; George et al., 2016).

Several studies also suggest that MT-Zn homeostasis regulates immunological function of bone marrow. Reports have shown that either deficiency of dietary zinc and chronic zinc exposure leads to B-cell and T-cell apoptosis (King et al., 1995; Fraker and King, 2004). Thus, absence of MT expression in bone marrow diminishes zinc homeostasis unless compensatory zinc transporters and MTs are provided. MTs transfer zinc to other metalloproteins including the zinc-dependent transcription factor which regulates the differentiation of precursor cells in bone marrow. For example, Early growth

response-1 (Egr-1), a zinc-dependent transcription factor promotes differentiation of monocyte into macrophage (Krishnaraju et al., 1995), while another zinc dependent transcription factor growth factor independent-1 (Gif-1) antagonizes monocyte to macrophage differentiation and rather promotes neutrophil differentiation (Hock et al., 2003). Studies have also shown that exogenously added Zn-MT binds to unknown MT receptor on T-Cell membrane and reduces surface thiol expression. This enhances IL-2 release which promotes T-Cell survival and proliferation (Subramanian Vignesh and Deepe Jr., 2017).

Dendritic cells express MTs in response to thermal stress, which then mediate zinc distribution to regulate intracellular redox environment in DCs. MT1 expressed in DCs induces tolerogenic potential of DCs by promoting differentiation of naïve T cell into FOXP3 expressing Treg cells (Reis e Sousa, 2006; Maldonado and von Andrian, 2010). During inflammation and changed redox state of cells, MTs release zinc. These free zinc ions activate MTs, stimulate MTF-1 and downregulates pro-inflammatory cytokines such as IL6, TNF-α, interleukin IL-1 and also suppresses transcription factor NF-kB. NF-kB induces the expression of pro-inflammatory cytokines 1 L-1, IL-6, TNF- α, which activates MTF-1 transcription factor. MTF-1 upregulates the expression of MTs, and zinc efflux transporter ZnT-1, which helps in maintaining Zn-MT homeostasis and helps recover cells from redox state (Figure 4; Grzywacz et al., 2015).

Zinc transporters play important roles in Zn^{2+} transport, distribution and homeostasis (Lazarczyk and Favre, 2008; Lichten and Cousins, 2009). Zinc transporters belong to two families: 10 SLC30s/ZnTs and 14 SLC39s/ZIPs. ZIPs mediate influx of Zn^{2+} from extracellular space to intracellular cytoplasm via diffusion, symporter or secondary active transporter. ZnTs export Zn^{2+} from cytoplasmic space to extracellular space (Andrews et al., 2004; Lichten and Cousins, 2009). The ZnTs and the ZIPs with their expression and distribution in the different tissues are listed in the Table 3. Inside the cell, specific set of ZnTs and ZIPs are involved in storage of Zn^{2+} in organelles or its release into cytosol, depending on the state of the cell. Intracellular distribution of ZnTs and ZIPs is schematically shown in Figure 5.

Through sequence analysis it was observed that the ZIP family of transporters contains 8 transmembrane domains (TMDs-1-8). These 8 transmembrane domains are responsible for the zinc transport. A cytoplasmic segment lies between the 3rd and 4th TMD (Taylor and Nicholson, 2003; Bin et al., 2011). These proteins are further divided into four subfamilies- I, II, gufA, and LIV-1 (Taylor and Nicholson, 2003). Amongst these, the LIV-1 sub family members contain a HEXXH motif within TM5 (transmembrane domain 5) and varying lengths of the N-terminal extracellular domain (ECD; Taylor and Nicholson, 2003). Out of the 14 ZIPs identified in mammals, ZIP1, ZIP2, ZIP3 belong to the ZIP II subfamily. ZIP 9 is a member of the ZIP I subfamily and ZIP 11 is of the gufA subfamily (Yu et al., 2013). The remaining 9 ZIPs belong to LIV-1 subfamily (Ryu et al., 2020). The functional roles of LIV-1 subfamily proteins are predominantly due to their ECDs. The role of the ZIP-CTD present between TM3 and TM4 remains unknown (Bin et al., 2018).

The transport mechanisms being used by ZIPs is not yet clearly elucidated and requires further study, but the cell-based assays done using isotopes suggest that ZIP2 controls the zinc flux through a time, temperature and concentration dependent manner as seen in erythroleukemia cells (Gaither and Eide, 2000). It was further seen that ZIP2 was stimulated only by HCO_3-, with a high affinity to zinc, suggesting a Zinc- HCO_3- symporter mechanism (Gaither and Eide, 2000). ZIP8 has also been shown to act as a Zn- HCO_3^- symporter in complementary RNA injected Xenopus oocytes (Liu et al., 2008).

TABLE 3 Expression and distribution of ZnTs and ZIPs.

Name of the protein	Expression and tissue distribution	Reference
A. Expression and distribution of ZnTs		
ZnT1	Ubiquitous	Andrews et al. (2004)
ZnT2	Widely distributed	Itsumura et al. (2013)
ZnT3	Brain	Hildebrand et al. (2015)
ZnT4	Ubiquitous	Huang and Gitschier (1997)
ZnT5	Ubiquitous	Inoue et al. (2002)
ZnT6	Widely distributed	Huang et al. (2007)
ZnT7	Widely distributed	Huang et al. (2007)
ZnT8	Pancreas	Wenzlau et al. (2007)
ZnT9	ubiquitous	Myers et al. (2012)
ZnT10	Small intestine, Liver, Brain	Bosomworth et al. (2012)
B. Expression and distribution of ZIPs		
ZIP1	Ubiquitous	Dufner-Beattie et al. (2006)
ZIP2	Liver, ovary, skin, dendritic cell	Peters et al. (2007)
ZIP3	Widely distributed	Dufner-Beattie et al. (2006)
ZIP4	Small intestine	Andrews (2008)
ZIP5	Small intestine, kidney, pancreas	Guo et al. (2014)
ZIP6	Widely distributed	Mathews et al. (2006)
ZIP7	Widely distributed, Colon	Groth et al. (2013)
ZIP 8	Widely distributed	Li et al. (2016)
ZIP9	Widely distributed	Hara et al. (2017)
ZIP 10	Widely distributed, Renal cell	Hara et al. (2017)
ZIP 13	Hard and connective tissues	Hara et al. (2017)
ZIP14	Widely distributed	Hara et al. (2017)

ZnTs are part of a superfamily of cation diffusion facilitators. Mammalian ZnTs are predicted to have at least 6 TMDs (Fukada and Kambe, 2011). The ZnTs possess a histidine/serine rich loop of differing lengths between the 4th and 5th TMDs (Fukada and Kambe, 2011). Further ZnTs contain a large cytoplasmic domain at the C-terminus (CTD) with a copper chaperone like architecture (Lu and Fu, 2007). This domain has an important role in diabetes research as mutations in the CTD of ZnT8 increases the risk of developing diabetes (Parsons et al., 2018). The transport mechanism utilized by ZnTs is not clearly understood in the mammalian system, but studies done on *E. coli* Zinc transporter YiiP suggests that ZnTs control the zinc efflux through a Zn^{2+}/H^+ antiporter (Lu and Fu, 2007).

Zinc is an essential component of several cellular processes in the host. It is also essential for normal development and functioning of the innate and adaptive immune systems. The diverse functional properties help in further strengthening the antiviral action of zinc, either by stimulating a better immune response in the host and/or by

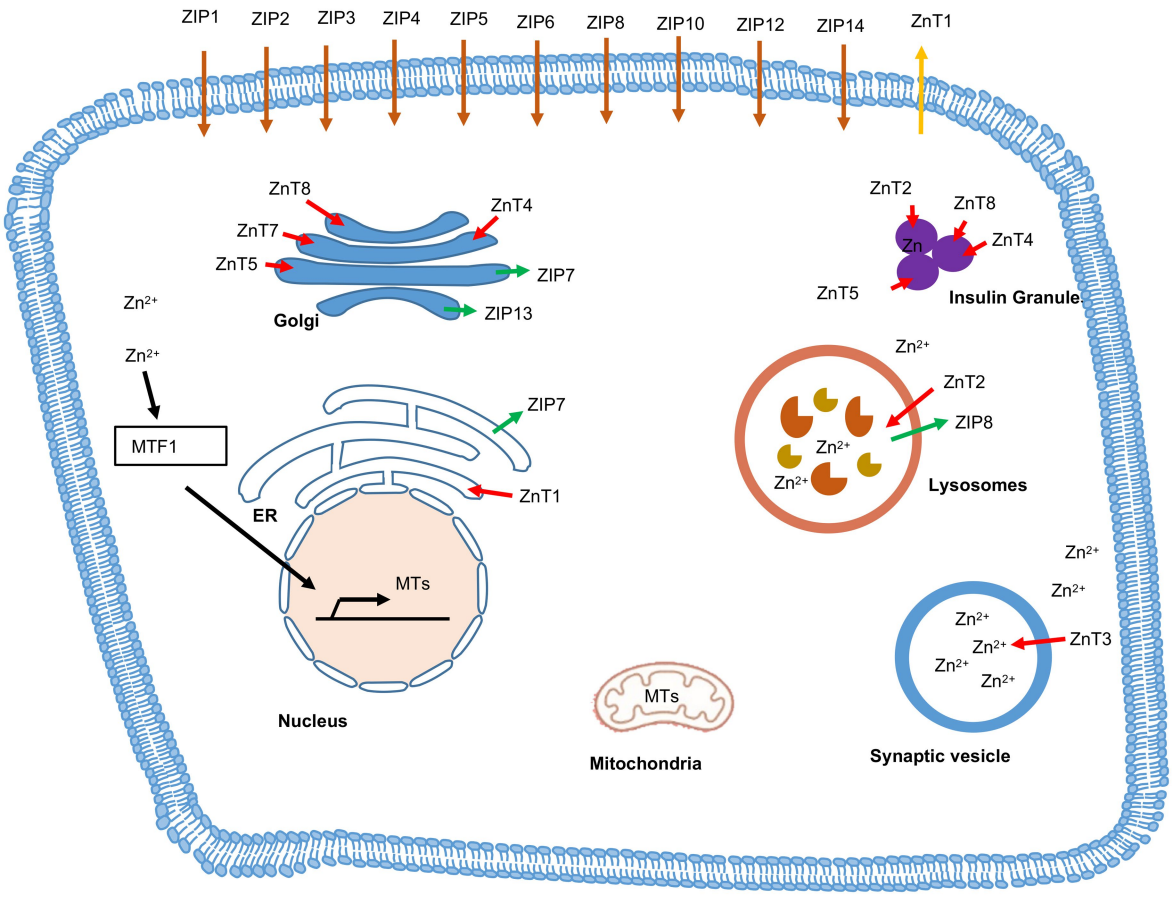

FIGURE 5
Subcellular localization of Zinc transporters (ZnTs), Zrt- and Irt- like proteins (ZIPs) and Metallothionein (MT). Red arrow indicates the flow of Zn^{2+} from cytosol to cellular organelles via ZnTs and green arrow indicates the flow of Zn^{2+} from cellular organelles to cytosol via ZIPs. Brown arrow indicates the ZIPs located on plasma membrane, which transports zinc inside the cytosol. Orange arrow indicates the ZnTs located on plasma membrane, which transports zinc outside the cell. MTs translocate zinc into nucleus, golgi, endoplasmic reticulum (ER), mitochondria and lysosomes.

promoting the synthesis/activation of antiviral factors/pathways, as described in the following sections.

5.2. Modulation of host immune system by zinc

5.2.1. Zinc signaling in monocytes, macrophages, and dendritic cells

There is a reduction in phagocytosis of macrophages, decrease in chemotaxis of polymorphonuclear cells and decrease in the production of proinflammatory cytokines upon zinc deficiency (Rink and Kirchner, 2000; Bonaventura et al., 2015). Upon entering the host, pathogens are recognized by the pattern recognitions receptors (PRRs) such as Toll-like receptors (TLRs), which initiate different signaling cascades, leading to production of host factors essential for survival.

Except TLR3, activation of all other TLRs by various ligands increases intracellular Zn^{2+} level, which inhibits the phosphorylation of IRF3 in murine macrophages, leading to reduced production of type I interferons such as IFNβ. Conversely, zinc deficiency increases the level of LPS-induced IFNβ (Haase et al., 2008; Brieger et al., 2013; Figure 4). Thus, increased Zn^{2+} level negatively regulates TRIF/TRAM-dependent signaling pathway (Figure 4). Increased Zn^{2+} level also activates MAP kinases (mitogen activated protein kinases) in LPS-treated macrophages in a IRAK-TRAF-dependent manner, leading to production of proinflammatory cytokines. Zinc mediated inhibition of MAPK phosphatases such as the dual-specificity phosphatases (DUSPs) and degradation of IRAK1 is proposed to control the effect of zinc on MAPKs (Haase et al., 2008; Wan et al., 2014; Figure 4). Further, zinc modulates MyD88-dependent activity of the transcription factor NFκB. Hasse et al. reported that zinc depeletion reduced LPS-induced phosphorylation of IKKβ in monocytes and reduced DNA binding by NFκB (Haase et al., 2008). However, few other studies reported inhibition of NFκB activity by zinc (Von Bülow et al., 2007; Haase and Rink, 2009; Prasad et al., 2011). Subsequently, it was found that zinc transporter ZIP8 was a target of NFκB (Liu et al., 2013). NFκB mediated upregulation of ZIP8 levels further increases intracellular Zn^{2+} level, which in turn inhibits IKKβ phosphorylation, leading to the inhibition of NFκB activity. Zinc also inhibits the activity of phosphodiesterase (PDE) in monocytes, leading to the inhibition of NFκB activity (Von Bülow et al., 2007).

5.2.2. Zinc signaling in T cells

Multiple studies have investigated the effect of zinc on T cells, which has been elegantly reviewed by Kim and Woo Lee (Kim et al., 2021). In brief, intracellular Zn^{2+} level is high in activated T cells. ZIP6 and ZIP8 are the predominant zinc transporters present in T cells. Upon TCR stimulation, ZIP6 mediates Zn^{2+} influx and loss of ZIP6 impairs T cell activation (Colomar-Carando et al., 2019). Subsequently it was found that Src and/or Syk family kinase ZAP70 mediated phosphorylation of ZIP6 was essential for localization of the latter to the immunological synapse and Zn^{2+} influx upon TCR stimulation (Kim et al., 2021). Zn^{2+} influx also inhibits SHP-1 mediated dephosphorylation of the LCK, enabling increased phosphorylation of ZAP70 kinase by LCK at the immunological synapse (Chiang and Sefton, 2001; Štefanová et al., 2003; Figure 6). Note that Zn^{2+} also facilitates the binding of LCK to CD4 and CD8α, which is important for TCR signaling (Lin et al., 1998).

On the other hand, ZIP8 is predominantly localized to the lysosome and it mobilizes lysosomal Zn^{2+} to cytoplasm. ZIP8 expression is increased upon TCR stimulation, leading to increased translocation of Zn^{2+} from lysosome to cytoplasm, which inhibits the phosphatase activity of Calcineurin. This leads to CREB (cyclic AMP response element-binding protein) mediated transcriptional upregulation of IFNγ and perforin gene expression, which are key antiviral effectors of the host (Aydemir et al., 2009; Figure 6). Besides, Zn^{2+} is also known to modulate the activity of ERK, PI3K and STAT3 signaling pathways in T cells, thereby influencing production of proinflammatory cytokines and differentiation of Th17 cells (Kaltenberg et al., 2010; Kitabayashi et al., 2010; Plum et al., 2014).

5.2.3. Zinc signaling in other immune cells

Zinc deficiency reduces natural killer cell cytotoxic activity and impairs host immune response against foreign pathogens, while zinc supplementation can reverse this effect (Fernandes et al., 1979; Fraker et al., 1982). Role of ZnTs in mast cell activation and mast cell mediated allergic reaction has been reported, indicating that ZnT5 mediates FcεRI signaling which leads to activation and translocation of PKC to plasma membrane. PKC stimulates nuclear translocation of NF-κB and cytokine production in mast cells (Nishida et al., 2009). Zinc has also been shown to increase the production of IFNα in leucocytes (Samad et al., 2021). Zinc transporters ZIP7 and ZIP 10 are essential for B cell development and BCR-induced B cell proliferation (Hojyo et al., 2014; Anzilotti et al., 2019).

6. Possible mechanism (s) controlling the antiviral function of zinc in hepatitis viruses

Exact molecular mechanism of antiviral function of zinc against any particular hepatitis virus has not been conclusively demonstrated. Nevertheless, information obtained from several independent studies strongly support the benefit of zinc action against HAV, HBV, HCV, HEV and provide a scientific basis for further investigation. Here, we attempt to extrapolate the possible mechanism (s) (based on information obtained from studies on direct and/or indirect antiviral effect of zinc on all viruses), which enable zinc to antagonize HAV, HBV, HCV and HEV infection and suggest future directions for experimental validation of those possibilities. It is important to obtain clear mechanistic understanding of zinc action in order to harness its complete therapeutic potential for management of viral hepatitis.

As mentioned in previous sections, antiviral effect of zinc against HCV has been evaluated in multiple clinical trials, which provides an overall conclusion that zinc supplementation have therapeutic benefit when taken along with standard antiviral therapy. *In vitro*, zinc shows potent inhibitory effect on HCV RdRp, although its mechanism of action remains to be explored (Yuasa et al., 2006; Gupta et al., 2022). Recently, our laboratory showed antiviral activity of ZnO nanoparticles [ZnO(NP)] and tetrapods [ZnO(TP)] against genotype 3a-HCV replicon (Gupta et al., 2022). It is possible that zinc acts by chelating magnesium ions, which is required for HCV RdRp activity or acts through other steps in controlling RdRp function (Ouirane et al., 2019).

Zinc was also shown to prevent with IFN-λ3 binding to its receptor IFNLR1, resulting in inhibition of IFN-λ3 signaling, consequently leading to an increase in HCV replication. Single nucleotide polymorphisms rs12979860 and rs809917 in IFNL gene locus clears HCV as well as inflammation and fibrosis progression in viral and non-viral liver disease (Read et al., 2017). Further studies on HCV patients with rs12979860 and rs809917 SNPs should clarify the therapeutic benefit of zinc supplementation in HCV patients.

Previous studies done in our laboratory showed the antiviral activity of zinc against genotypes 1 (g1) and 3 (g3) of HEV, which are major cause of HEV-induced hepatitis in human. Zinc inhibits the activity of HEV RNA-dependent RNA polymerase (RdRp), *in vitro* (Kaushik et al., 2017). Similar antiviral activity was also observed in cell-based models of g1- and g3-HEV, upon treatment with ZnO nanoparticles [ZnO(NP)] and tetrapods [ZnO(TP)] (Gupta et al., 2022). In agreement with the *in vitro* data, a recent report demonstrated the anti-HEV activity of zinc in ribavirin nonresponsive HEV patients (Horvatits et al., 2023).

A recent report suggests that the anti-HEV activity of zinc is mediated by its effect on host. Overexpression of Zinc-finger antiviral protein (ZAP), an interferon (IFN)-stimulated gene, inhibits HEV replication, while its knockdown by RNA interference significantly increases HEV RNA level. Silencing of ZAP also decreases interferon regulatory factor 3 (IRF3) phosphorylation in HEV infected cells. Thus, ZAP is an anti-HEV host factor, which blocks viral replication in cooperation with IFN-β (Yu et al., 2021).

An analysis of the protein–protein interactions between human and HEV proteins revealed enrichment of proteins linked to the mitochondrial oxidative phosphorylation pathway (Chandru et al., 2018). It is known that zinc wave results in production of the mitochondrial reactive oxygen species (ROS; Slepchenko et al., 2016). Future study should clarify the involvement, if any, of mitochondrial oxidative phosphorylation pathway in modulating the anti-HEV activity of zinc. Additionally, it has been shown that HEV encoded proteins have an impact on a number of cellular pathways, which may be crucial for survival of the virus inside infected cells (Wißing et al., 2021). Zinc may exert its antiviral effects by interfering with the interplay between HEV and the host signaling pathways.

HEV infection also triggers neuronal disorders such as neurological amyotrophy and Guillain-Barrre syndrome (Jha et al.,

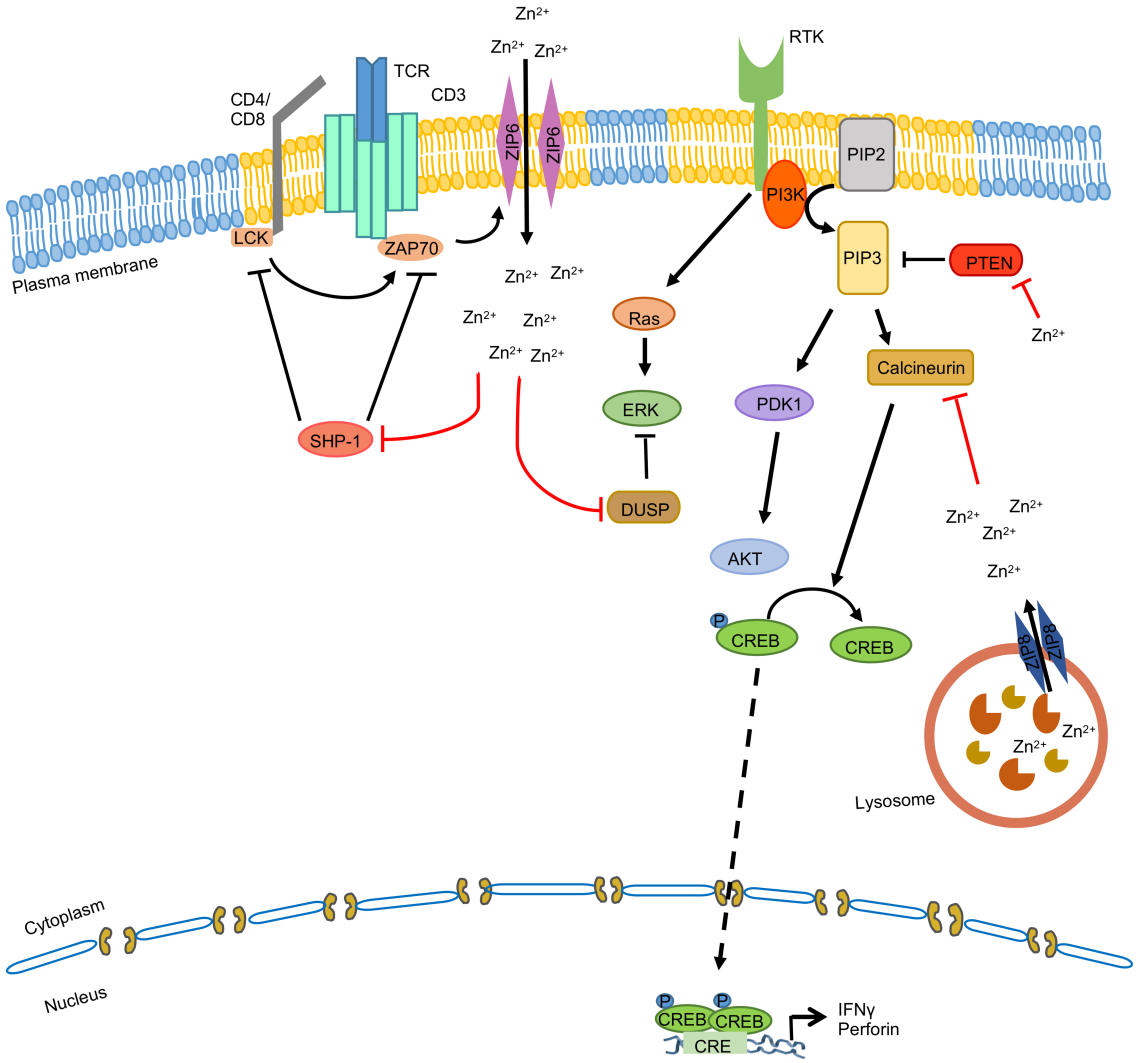

FIGURE 6
Zinc signaling in T cells. TCR stimulation induces ZAP70 mediated phosphorylation of ZIP6, leading to its localization to the immunological synapse in lipid rafts (yellow). ZIP6 mediates Zn^{2+} influx, which inhibits SHP-1 mediated dephosphorylation of the LCK and DUSP mediated dephosphorylation of the MAPKs. ZIP8 is present on the lysosome and it mobilizes lysosomal Zn^{2+} to cytoplasm, which inhibits Calcineurin mediated dephosphorylation of CREB, leading to CREB mediated transcriptional upregulation of IFNγ and perforin. '' indicates the steps inhibited by zinc.

2021). HEV infects neuronal cells in culture (Drave et al., 2016). Zinc acts as a neurotransmitter, modulates intracellular and extracellular signaling, which is essential for maintaining normal neuronal physiology (Frederickson et al., 2000). Variations in intracellular level of free zinc decide between survival or death of neurons during ischemic injury (Aras and Aizenman, 2011; Slepchenko et al., 2017). Thus, zinc supplementation might act in a different manner in HEV infected neurons than hepatocytes.

Two studies reported inhibition of HAV replication upon treatment with zinc sulphate and zinc chloride (Ogawa et al., 2019; Kanda et al., 2020). Zinc chloride showed more potent anti-HAV effect than zinc sulphate. It enhanced the antiviral effect of interferon-alpha-2a against HAV (Kanda et al., 2020). Level of mitogen-activated protein kinase 12 (MAPK12) upregulated and six related genes baculoviral IAP repeat containing 3 (BIRC3), interleukin 1 beta (IL1β), proline-serine–threonine phosphatase interacting protein 1 (PSTPIP1), prostaglandin-endoperoxide synthase 2 (PTGS2), PYD and CARD domain containing (PYCARD), and tumor necrosis factor alpha (TNFα) were downregulated in zinc chloride treated cells (Kanda et al., 2020). Further investigations are warranted to uncover the possible direct/indirect role of zinc against HAV.

Limited information exists regarding direct antiviral effect of zinc against HBV to draw any mechanistic insight. One clinical trial evaluated the therapeutic benefit of zinc supplementation in HBV patients, indicating some improvement in liver function (Hayashi et al., 2007; Himoto et al., 2007). It is noteworthy that zinc binding is essential for function of the HBX protein, which is a key protein encoded by HBV (Ramakrishnan et al., 2019). Further, many host antiviral proteins and ISGs inhibit HBV replication either by targeting protein viral proteins and/or RNA. For example, host antiviral factor ZAP inhibits HBV replication (Mao et al., 2013). ISG20 selectively degrades HBV RNA (Liu et al., 2017; Imam et al., 2020). Myeloid differentiation primary response 88 (MYD88) inhibits HBV replication by promoting viral pregenomic RNA degradation and

retention of viral preS/S RNA in the nucleus (Li et al., 2010). Myxovirus Resistance Gene A (MxA), an ISG, interacts with viral core protein and inhibits HBV replication (Gordien et al., 2001; Li et al., 2012). Since zinc is known to influence the activity of these genes/pathways under different conditions, additional studies involving suitable model systems are required to assess the possible therapeutic benefit of zinc in HBV cases. Knowledge obtained from our understanding of the mechanism of zinc action in other viruses should be the guiding criteria for designing experiments in HBV cases.

7. Challenges associated with zinc supplementation therapy

7.1. Rigorous cellular zinc homeostasis

Zinc homeostasis in the cell is a multistep process constituting three main stages, namely the zinc influx into the cells, zinc efflux from the cells and the storage within the cells. As described earlier, this process is realized through zinc transporters and the zinc binding proteins. In normal conditions, zinc homeostasis is tightly and neatly controlled, but while considering zinc supplementation, the dosage and the amount need to be judiciously and carefully curated. Any imbalance of zinc levels due to supplementation might cause disruption of zinc transport, leading to zinc accumulation in the cells causing toxicity. One of the major challenges to zinc supplementation is that zinc is needed in a large number of cellular processes and therefore interacts with a large number of proteins. It is really difficult to keep track of the effect of zinc supplementation on all these proteins.

7.2. Expression of zinc transporters in target cells and their effects

A number of reports suggest that differential expression and activity of ZIP and ZnTs are responsible for the pathogenesis and progression of chronic diseases. ZIP transporters are known to promote the invasive activity of cancers. Reduced expression in ZIPs has been seen in prostate cancer, where the cellular zinc is reduced, which accelerates the disease progression. ZIP4 is known to get atypically overexpressed in case of "acrodermatitis enteropathica." ZIPs are known to play roles in epithelial–mesenchymal transition, anoikis resistance, and metastasis. In such cases, abnormal expression of ZIPs elevates the cytosolic zinc levels, which may extend the zinc dependent growth factor signaling and cause aberrant activation of cellular signaling pathways (Kagara et al., 2007). A myriad of secretory and membrane-bound enzymes which need zinc like matrix metalloproteinases are involved in cancer metastasis, and capture zinc in the early secretory pathway. Thus, ZnT transporters like ZnT5, ZnT6, and ZnT7 might be facilitating zinc uptake by these enzymes and their activation (Kambe, 2012). These examples merely illustrate that abnormal dysregulation of the zinc transporters have been observed in various disease and zinc supplementation could have a similar effect on these transporters and could lead to deleterious effects if not administered correctly.

Zinc interferes with the copper absorption in the body, even at a very little dose above the RDA (Recommended Dietary Allowance). Actually, higher concentration of zinc induces more expression of metallothioneins in the lumen to absorb more amount of zinc. However, this protein also has a high affinity for copper, resulting in a copper deficiency, and may cause anemia, neutropenia and myelopathy (Francis et al., 2022).

7.3. Zinc toxicity

Zinc is known to have many beneficial functions and has seen to play a role in protection in various infectious diseases, but excess zinc can cause zinc toxicity or side effects. Most often the zinc toxicity depends on the route of exposure to zinc or on the dosage. Zinc toxicity can be divided into two types- (a) acute and (b) chronic toxicity. Acute toxicity is caused by ingestion of salts of zinc such as zinc sulphate and zinc chloride which manifests into gastrointestinal symptoms like diarrhea, renal injury, acute respiratory distress syndrome (ARDS), liver necrosis, thrombocytopenia, coagulopathy and might lead to death in extreme cases (Barceloux, 1999). Chronic toxicity causes bone marrow damage and neurological symptoms. One of the major causes of concern in case of chronic toxicity is that if zinc is chronically ingested it can result in copper deficiency can lead to sideroblastic anemia, granulocytopenia, and myelodysplastic syndrome (Irving et al., 2003; Sheqwara and Alkhatib, 2013). Orally consumed zinc is absorbed by the jejunum of the small intestine. This process is facilitated by the metallothionein complex in the enterocyte villi (Ruttkay-Nedecky et al., 2013). Zinc binds to the metallothionine, which is known to be involved in the regulation of other metals as well, especially copper having the highest affinity to it (Ruttkay-Nedecky et al., 2013). To remove the excess zinc, the human body produces more metallothionein to prevent excess free zinc but in turn also decreases copper levels, thus, forming a dynamic antagonistic relationship. Here, the zinc homeostasis can only be maintained by the excretion of the metallothionein-zinc complex via bile and faeces. In case of zinc overdose, excretion of zinc will not be fast enough and thus it will get accumulated and cause clinical complications (Agnew and Slesinger, 2020).

8. Advances in zinc supplementation strategy and future perspectives

8.1. Zinc derivatives

Due to the advancement in nanotechnology, biomedical nanoparticles have gained considerable attention due to their prominence in biomedical applications and are being explored for molecular diagnostics, drug delivery, gene therapy. In case of Zinc based nanotechnology, zinc oxide-based nanoparticles have taken the center stage (Zhang and Xiong, 2015; Bashandy et al., 2018).

Zinc oxide nanoparticles (ZnO NPs) are important and are used in a variety of fields due to their unusual properties. ZnO nanoparticles have a small particle size which helps in the easier absorption of zinc by the body and are used as food additives and the US FDA has classified it as a GRAS (Jiang et al., 2018). In addition to this ZnO NPs are relatively inexpensive and less toxic. These properties make ZnOs an excellent candidate for biomedical applications. ZnOs have been used in anti-cancer treatment, drug delivery, antibacterial, diabetes treatment, anti-inflammation, wound healing and bioimaging (Zhang

and Xiong, 2015; Mishra et al., 2017). In recent years nanoparticles of gold and silver have been predominantly studied and deployed against viral diseases. However, Zn nanoparticles might be relatively less toxic than silver and gold nanoparticles and more cost efficient. ZnO nanoparticles have proven to be successful as a therapeutic strategy for various viral diseases, although they have not been very extensively studied in animal as well as human models, but promising results have been obtained in various cell-based models (Aderibigbe, 2017). Zinc oxide nanoparticles have been shown to have a virostatic effect against HSV-1 and were able to efficiently trap virions from entering the human corneal fibroblasts (Mishra et al., 2011). Surface modified zinc oxide nanoparticles have been shown to alter the infection of Herpes simplex virus -I by neutralizing the virus by utilizing the electrostatic interference caused by the hydrophobic zinc nanoparticles (Farouk and Shebl, 2018). PEGylated zinc oxide nanoparticles have been shown to be successful in inhibiting H1N1 viral infection and there was a 1.2 log10 TCID50 decrease in the viral titer (Ghaffari et al., 2019). Further ZnO nanoparticles suppressed replication in case of nidovirus and also have been shown to disrupt the replication of a range of RNA viruses (Gurunathan et al., 2020). In MA104 cells (African green monkey fetal kidney), ZnO nanoparticles led to a 10-fold decrease in the chikungunya viral load (Kumar et al., 2018).

In addition to this, ZnO tetrapods have also been used as an alternative for the traditional nanoparticles (Mishra and Adelung, 2018). The unique 3D structure gives them a higher flexibility as a biomedical engineering tool than traditional spherical or 1D nanoparticles as tetrapods avoid the agglomeration issues faced by the other two. The first use of ZnO nano tetrapods was for the efficient delivery of plasmid DNA (Nie et al., 2006). Furthermore, zinc tetrapods have been used to trap virus particles using oxygen vacancies on the synthesized ZnO tetrapods. Polar surfaces were created in the tetrapods due to the oxide, which helped in trapping the negatively charged functional glycoprotein groups present on the virion surface (Mishra et al., 2011). Dendritic cells could easily take up such entrapped virus particles and neutralize them. This success of this strategy has been shown in humans and mice in the cases of HPV, ZIKA, HIV and Dengue. Apart from this ZnO nanoparticles and tetrapods have been shown to have an antiviral role in HSV, HEV and HCV by suppressing the viral replication (Mishra et al., 2011; Gupta et al., 2022).

Although zinc based nanoparticles have been shown to play antiviral roles they need to be further characterized to be successfully established as a commercially available therapeutic for viral diseases.

8.2. Modulators of zinc transporter

Zinc transport can be modulated by zinc ionophores. Zinc ionophores have been shown to inhibit replication of many viruses *in vitro*. Four zinc ionophores have shown to have antiviral roles which are Pyrithione, Hinokitiol, PDTC and Chloroquine. Pyrithione, Hinokitiol and PDTC inhibit the replication of the following viruses *in vitro*: coxsackievirus, equine arteritis virus, SARS-CoV, HSV, mengovirus and rhinovirus (Lanke et al., 2007; Krenn et al., 2009; Te Velthuis et al., 2010; Qiu et al., 2013). Chloroquine inhibits the replication of the following viruses: HCV, HCoV-229E, MERS-CoV, SARS-CoV, HIV-1 and Zika virus (Romanelli et al., 2004; Delvecchio et al., 2016; Read et al., 2017; Chandru et al., 2018). In addition to this, another zinc ionophore, Quercetin is known to inhibit replication of Influenza A virus and Rhino virus (Wu et al., 2016; Mehrbod et al., 2021). These studies indicate that zinc ionophores may be used as antivirals and since zinc has a significant role to play in liver homeostasis, the use of these ionophores is likely be an excellent antiviral strategy against hepatitis causing viruses.

8.3. Future perspectives

ZnO NPs have shown promise in biomedical applications due to their anti-viral, anti-bacterial and anti-diabetic roles. Inherently toxic, the ZnO NPs inhibit cancerous cells as well as bacteria by generating intracellular ROS generation. This activates the apoptotic signaling pathway making these nanoparticles excellent anticancer and anti-bacterial agents. Furthermore, Zinc nanoparticles and tetrapods have shown significant antiviral activities ranging from affecting replication, to neutralizing viruses and influencing viral entry. As drug carriers, ZnO NPs enhance therapeutic efficiency by promoting the bioavailability of the drugs or biomolecules.

The FDA has listed ZnO NPs as a safe substance. However, they should be further explored and studied as there are no comparative analysis of the biological advantages of Zinc nanoparticles over other metal nanoparticles. Further, there is lack of information on evidence based randomized trials and animal studies emphasizing their therapeutic roles. Focused studies on these aspects would help us better understand their diagnostic and therapeutic potential.

It is also important to be cautious and careful while interpreting and extrapolating the data obtained from cell-based experiments to patient studies. Generally zinc compounds are used in micromolar (μM)-millimolar (mM) concentration in the cell-based studies to evaluate their antiviral potential whereas plasma zinc concentration ranges between 10 and 18 μM in human (Rükgauer et al., 1997). On top of that free zinc levels are very tightly controlled *in vivo*. Although intracellular level of zinc maybe in micromolar concentration, most of it is bound to metallothioneins, thereby reducing the free zinc concentration to nanomolar scale (Krężel and Maret, 2006; Zheng et al., 2017). Such complex regulation makes it difficult to fully harness the therapeutic benefit of zinc based on the data obtained in cell-based experiments. Therefore, even though a zinc compound may exhibit very potent antiviral effect in laboratory condition, it needs stringent evaluation in the clinic.

The treatment of viral hepatitis has evolved rapidly over the last few years especially with the introduction of curated therapies for Hepatitis C. In addition to this the improvement in HAV, HBV and HEV vaccination has also led to a significant advance in viral hepatitis management. Viral hepatitis treatment is still dependent on a few drugs like Ribavirin and PEGylated Interferon but none of these are known to specifically target these viruses. Thus, targeted therapies can be further explored; one such strategy could be the use of zinc salt, zinc nanoparticles and zinc ionophore based therapies. We have recently shown the antiviral activity of zinc oxide nanoparticles and tetrapods against HEV and HCV, which could pave the way for the development of new therapeutic strategies against these viruses (Gupta et al., 2022).

Zinc oxide nanoparticles have shown promising antiviral effects on various viruses, but further research needs to be performed to explore and understand the underlying mechanism of zinc

nanoparticles dependent antiviral activities. Zinc seems to inhibit the enzyme activities of viral protease and polymerases and is also involved in the physical processes of viral attachment and uncoating (Mishra et al., 2011). However, it is important to study these in clinical scenarios as zinc could become a viable supplement to the traditional viral treatments. A number of *in vitro* studies have demonstrated that free zinc possesses a strong antiviral effect through the trials with creams and tablets containing higher amounts of zinc (Mishra et al., 2011). These studies also tell us that when zinc is used at therapeutic doses and in the right form could improve viral clearance in case of acute and chronic infections. Zinc supplementation can be successful in two ways: it can be either be administered to improve the systemic immunity and the antiviral response in zinc deficient patients or can be used to specifically target viral replication and the symptoms of infection (Mishra et al., 2011). Although zinc-based strategies have been shown to have various roles in inhibiting the viral replication, there is a lack of information on whether these zinc-based strategies are sufficient as a standalone treatment or in enhancement of the effect of other antiviral treatments. Zinc supplementation with Ribavirin or PEGylated IFN-α reduced the side effects of Ribavirin/PEGylated IFN-α in case of HCV and HEV chronic patients but had no additive effect on these treatments (Farouk and Shebl, 2018; Suda et al., 2019). It has also been proven that in chronic patients of HCV and HBV zinc supplementation induces anti oxidative functioning of the liver preventing further liver damage during the treatment with Ribavirin and PEGylated IFN-α (Murakami et al., 2007). Zinc supplementation has also been shown to reduce inflammation and production of cytokines like NF-κB in chronic HCV and HBV patients (Nagamine et al., 2000). Accumulating data, through both *in vitro* and clinical studies, suggest that zinc supplementation in addition to other antiviral therapy is a viable treatment regimen for viral hepatitis. Although this needs to be further elucidated through large cohort based clinical studies.

Author contributions

SK, SA, SN, CR-K, and MS wrote the manuscript. MS and CR-K edited the manuscript draft. MS conceptualized the review. All authors contributed to the article and approved the submitted version.

Conflict of interest

The authors declare that the research was conducted in the absence of any commercial or financial relationships that could be construed as a potential conflict of interest.

Publisher's note

References

Abbasinazari, M., Alavian, S. M., Behnava, B., Asgharinia, M., Salimi, S., Keshvari, M., et al. (2014). Effect of zinc supplementation on viral response in patients with chronic hepatitis C and Beta thalassemia major, a pilot study. *J. Clin. Diagn. Res.* 8, HC16–HC19. doi: 10.7860/JCDR/2014/10403.5305

Aderibigbe, B. A. (2017). Metal-based nanoparticles for the treatment of infectious diseases. *Molecules* 22:1370. doi: 10.3390/molecules22081370

Agnew, U. M., and Slesinger, T. L. (2020). *Zinc toxicity* Florida, United States: Stat Pearls Publishing.

Andrews, G. K. (2008). Regulation and function of Zip 4, the acrodermatitis enteropathica gene. *Biochem. Soc. Trans.* 36, 1242–1246. doi: 10.1042/BST0361242

Andrews, G. K., Wang, H., Dey, S. K., and Palmiter, R. D. (2004). Mouse zinc transporter 1 gene provides an essential function during early embryonic development. *Genesis* 40, 74–81. doi: 10.1002/gene.20067

Antoine, T. E., Hadigal, S. R., Yakoub, A. M., Mishra, Y. K., Bhattacharya, P., Haddad, C., et al. (2016). Intravaginal zinc oxide tetrapod nanoparticles as novel immunoprotective agents against genital herpes. *J. Immunol.* 196, 4566–4575. doi: 10.4049/jimmunol.1502373

Anzilotti, C., Swan, D. J., Boisson, B., Deobagkar-Lele, M., Oliveira, C., Chabosseau, P., et al. (2019). An essential role for the Zn2+ transporter ZIP7 in B cell development. *Nat. Immunol.* 20, 350–361. doi: 10.1038/s41590-018-0295-8

Aras, M. A., and Aizenman, E. (2011). Redox regulation of intracellular zinc: molecular signalling in the life and death of neurons. *Antioxid. Redox Signal.* 15, 2249–2263. doi: 10.1089/ars.2010.3607

Asoudeh, F., Ebrahimzadeh, A., Ghoreishy, S. M., Imani, H., Mousavi, S. M., Zargarzadeh, N., et al. (2023). The association between dietary intakes of zinc, vitamin C and COVID-19 severity and related symptoms: A cross-sectional study. *Clin. Nut. ESPEN* 55, 244–250. doi: 10.1016/j.clnesp.2023.03.013

Aydemir, T. B., Liuzzi, J. P., McClellan, S., and Cousins, R. J. (2009). Zinc transporter ZIP8 (SLC39A8) and zinc influence IFN-γ expression in activated human T cells. *J. Leukoc. Biol.* 86, 337–348. doi: 10.1189/jlb.1208759

Bajait, C., and Thawani, V. (2011). Role of zinc in pediatric diarrhea. *Indian J. Pharm.* 43, 232–235. doi: 10.4103/0253-7613.81495

Barceloux, D. G. (1999). Zinc. *J. Toxicol. Clin. Toxicol.* 37, 279–292. doi: 10.1081/clt-100102426

Bashandy, S. A., Alaamer, A., Moussa, S. A. A., and Omara, E. A. (2018). Role of zinc oxide nanoparticles in alleviating hepatic fibrosis and nephrotoxicity induced by thioacetamide in rats. *Can. J. Physiol. Pharmacol.* 96, 337–344. doi: 10.1139/cjpp-2017-0247

Baum, M. K., Lai, S., Sales, S., Page, J. B., and Campa, A. (2010). Randomized, controlled clinical trial of zinc supplementation to prevent immunological failure in HIV-infected adults. *Clin. Infect. Dis.* 50, 1653–1660. doi: 10.1086/652864

Beran, A., Mhanna, M., Srour, O., Ayesh, H., Stewart, J. M., Hjouj, M., et al. (2022). Clinical significance of micronutrient supplements in patients with coronavirus disease 2019: a comprehensive systematic review and meta-analysis. *Clin. Nut. ESPEN* 48, 167–177. doi: 10.1016/j.clnesp.2021.12.033

Bhatia, H. K., Singh, H., Grewal, N., and Natt, N. K. (2014). Sofosbuvir: a novel treatment option for chronic hepatitis C infection. *J. Pharmacol. Pharmacother.* 5, 278–284. doi: 10.4103/0976-500X.142464

Bianchi, G. P., Marchesini, G., Brizi, M., Rossi, B., Forlani, G., Boni, P., et al. (2000). Nutritional effects of oral zinc supplementation in cirrhosis. *Nutr. Res.* 20, 1079–1089. doi: 10.1016/S0271-5317(00)00194-9

Bin, B. H., Fukada, T., Hosaka, T., Yamasaki, S., Ohashi, W., Hojyo, S., et al. (2011). Biochemical characterization of human ZIP13 protein: a homo-dimerized zinc transporter involved in the spondylocheiro dysplastic Ehlers-Danlos syndrome. *J. Biol. Chem.* 286, 40255–40265. doi: 10.1074/jbc.M111.256784

Bin, B. H., Seo, J., and Kim, S. T. (2018). Function, structure, and transport aspects of ZIP and ZnT zinc transporters in immune cells. *J Immunol Res* 2018, 1–9. doi: 10.1155/2018/9365747

Bobat, R., Coovadia, H., Stephen, C., Naidoo, K. L., McKerrow, N., Black, R. E., et al. (2005). Safety and efficacy of zinc supplementation for children with HIV-1 infection in South Africa: a randomised double-blind placebo-controlled trial. *Lancet* 366, 1862–1867. doi: 10.1016/S0140-6736(05)67756-2

Bonaventura, P., Benedetti, G., Albarède, F., and Miossec, P. (2015). Zinc and its role in immunity and inflammation. *Autoimmun. Rev.* 14, 277–285. doi: 10.1016/j.autrev.2014.11.008

Bosomworth, H. J., Thornton, J. K., Coneyworth, L. J., Ford, D., and Valentine, R. A. (2012). Efflux function, tissue-specific expression and intracellular trafficking of the Zn transporter ZnT10 indicate roles in adult Zn homeostasis. *Metallomics* 4, 771–779. doi: 10.1039/c2mt20088k

Bracha, M., and Schlesinger, M. J. (1976). Inhibition of Sindbis virus replication by zinc lons. *Virology* 72, 272–277. doi: 10.1016/0042-6822(76)90330-5

Brewer, G. J., Johnson, V. D., Dick, R. D., Hedera, P., Fink, J. K., and Kluin, K. J. (2000). Treatment of Wilson's disease with zinc. XVII: treatment during pregnancy. *Hepatology* 31, 364–370. doi: 10.1002/hep.510310216

Brieger, A., Rink, L., and Haase, H. (2013). Differential regulation of TLR-dependent MyD88 and TRIF signaling pathways by free zinc ions. *J. Immunol.* 191, 1808–1817. doi: 10.4049/jimmunol.1301261

Carlucci, P. M., Ahuja, T., Petrilli, C., Rajagopalan, H., Jones, S., and Rahimian, J. (2020). Zinc sulfate in combination with a zinc ionophore may improve outcomes in hospitalized COVID-19 patients. *J. Med. Microbiol.* 69, 1228–1234. doi: 10.1099/jmm.0.001250

Chandru, S., Nair, V. P., Saumya, A., Das, M. S., Madhu, P., Nidhi, K., et al. (2018). Host-virus protein interaction network reveals the involvement of multiple host processes in the life cycle of hepatitis E virus. *mSystems* 3, 1–21. doi: 10.1128/mSystems.00135-17

Chaudhary, D., Ahmed, S., Liu, N., and Marsano-Obando, L. (2017). Acute liver failure from herpes simplex virus in an immunocompetent patient due to direct inoculation of the peritoneum. *ACG Case Rep. J.* 4:e23. doi: 10.14309/crj.2017.23

Chen, G., Guo, X., Lv, F., Xu, Y., and Gao, G. (2008). P 72 DEAD box RNA helicase is required for optimal function of the zinc-finger antiviral protein. *Proc. Natl. Acad. Sci.* 105, 4352–4357. doi: 10.1073/pnas.0712276105

Chen, S., Xu, Y., Zhang, K., Wang, X., Sun, J., Gao, G., et al. (2012). Structure of N-terminal domain of ZAP indicates how a zinc-finger protein recognizes complex RNA. *Nat. Struct. Mol. Biol.* 19, 430–435. doi: 10.1038/nsmb.2243

Chiang, G. G., and Sefton, B. M. (2001). Specific dephosphorylation of the Lck tyrosine protein kinase at Tyr-394 by the SHP-1 protein-tyrosine phosphatase. *J. Biol. Chem.* 276, 23173–23178. doi: 10.1074/jbc.M101219200

Chinni, V., El-Khoury, J., Perera, M., Bellomo, R., Jones, D., Bolton, D., et al. (2021). Zinc supplementation as an adjunct therapy for COVID-19: challenges and opportunities. *Br. J. Clin. Pharmacol.* 87, 3737–3746. doi: 10.1111/bcp.14826

Colomar-Carando, N., Meseguer, A., Jutz, S., Herrera-Fernández, V., Olvera, A., Kiefer, K., et al. (2019). Zip 6 transporter is an essential component of the lymphocyte activation machinery. *J. Immunol.* 202, 441–450. doi: 10.4049/jimmunol.1800689

Cowan, M. L., Thomas, H. C., and Foster, G. R. (2011). Therapy for chronic viral hepatitis: current indications, optimal therapies and delivery of care. *Clin. Med.* 11, 184–189. doi: 10.7861/clinmedicine.11-2-184

Das, S., Ramakrishnan, K., Behera, S. K., Ganesapandian, M., Xavier, A. S., and Selvarajan, S. (2019). Hepatitis B vaccine and immunoglobulin: key concepts. *J. Clin. Transl. Hepatol.* 7, 165–171. doi: 10.14218/JCTH.2018.00037

Delvecchio, R., Higa, L. M., Pezzuto, P., Valadão, A. L., Garcez, P. P., Monteiro, F. L., et al. (2016). Chloroquine, an endocytosis blocking agent, inhibits Zika virus infection in different cell models. *Viruses* 8:322. doi: 10.3390/v8120322

Dietz-Fricke, C., Tacke, F., Zöllner, C., Demir, M., Schmidt, H. H., Schramm, C., et al. (2023). Treating hepatitis D with bulevirtide–real-world experience from 114 patients. *JHEP Rep.* 5:100686. doi: 10.1016/j.jhepr.2023.100686

Diglio, D. C., Fernandes, S. A., Stein, J., Azeredo-da-Silva, A., de Mattos, A. A., and Tovo, C. V. (2020). Role of zinc supplementation in the management of chronic liver diseases: a systematic review and meta-analysis. *Ann. Hepatol.* 19, 190–196. doi: 10.1016/j.aohep.2019.08.011

Drave, S. A., Debing, Y., Walter, S., Todt, D., Engelmann, M., Friesland, M., et al. (2016). Extra-hepatic replication and infection of hepatitis E virus in neuronal-derived cells. *J. Viral Hepat.* 23, 512–521. doi: 10.1111/jvh.12515

Dufner-Beattie, J., Huang, Z. L., and Geiser, J. (2006). Mouse ZIP1 and ZIP3 genes together are essential for adaptation to dietary zinc deficiency during pregnancy. *Genesis* 44, 239–251. doi: 10.1002/dvg.20211

Eby, G. A., Davis, D. R., and Halcomb, W. W. (1984). Reduction in duration of common colds by zinc gluconate lozenges in a double-blind study. *Antimicrob. Agents Chemother.* 25, 20–24. doi: 10.1128/AAC.25.1.20

Farouk, F., and Shebl, R. I. (2018). Comparing surface chemical modifications of zinc oxide nanoparticles for modulating their antiviral activity against herpes simplex virus type-1. *Int. J. Nanopart. Nanotechnol.* 4:21. doi: 10.35840/2631-5084/5521

Fenstermacher, K. J., and DeStefano, J. J. (2011). Mechanism of HIV reverse transcriptase inhibition by zinc: formation of a highly stable enzyme-(primer-template) complex with profoundly diminished catalytic activity. *J. Biol. Chem.* 286, 40433–40442. doi: 10.1074/jbc.M111.289850

Fernandes, G., Nair, M., Onoe, K., Tanaka, T., Floyd, R., and Good, R. A. (1979). Impairment of cell-mediated immunity functions by dietary zinc deficiency in mice. *Proc. Natl. Acad. Sci.* 76, 457–461. doi: 10.1073/pnas.76.1.457

Fraker, P. J., Caruso, R., and Kierszenbaum, F. (1982). Alteration of the immune and nutritional status of mice by synergy between zinc deficiency and infection with Trypanosoma cruzi. *J. Nutr.* 112, 1224–1229. doi: 10.1093/jn/112.6.1224

Fraker, P. J., and King, L. E. (2004). Reprogramming of the immune system during zinc deficiency. *Annu. Rev. Nutr.* 24, 277–298. doi: 10.1146/annurev.nutr.24.012003.132454

Francis, Z., Book, G., Litvin, C., and Kalivas, B. (2022). The COVID-19 pandemic and zinc-induced copper deficiency: an important link. *Am. J. Med.* 135, e290–e291. doi: 10.1016/j.amjmed.2022.03.008

Frederickson, C. J., Suh, S. W., Silva, D., Frederickson, C. J., and Thompson, R. B. (2000). Importance of zinc in the central nervous system: the zinc-containing neuron. *J. Nutr.* 130, 1471S–1483S. doi: 10.1093/jn/130.5.1471S

Fu, B., Wang, L., Li, S., and Dorf, M. E. (2017). ZMPSTE24 defends against influenza and other pathogenic viruses. *J. Exp. Med.* 214, 919–929. doi: 10.1084/jem.20161270

Fukada, T., and Kambe, T. (2011). Molecular and genetic features of zinc transporters in physiology and pathogenesis. *Metallomics* 3, 662–674. doi: 10.1039/c1mt00011j

Gaither, L. A., and Eide, D. J. (2000). Functional expression of the human hZIP2 zinc transporter. *J. Biol. Chem.* 275, 5560–5564. doi: 10.1074/jbc.275.8.5560

George, M. M., Vignesh, K. S., Figueroa, J. A. L., Caruso, J. A., and Deepe, G. S. (2016). Zinc induces dendritic cell tolerogenic phenotype and skews regulatory T cell–Th17 balance. *J. Immunol.* 197, 1864–1876. doi: 10.4049/jimmunol.1600410

Ghaffari, H., Tavakoli, A., Moradi, A., Tabarraei, A., Bokharaei-Salim, F., Zahmatkeshan, M., et al. (2019). Inhibition of H1N1 influenza virus infection by zinc oxide nanoparticles: another emerging application of nanomedicine. *J. Biomed. Sci.* 26, 70–10. doi: 10.1186/s12929-019-0563-4

Gonçalves-Carneiro, D., Mastrocola, E., Lei, X., DaSilva, J., Chan, Y. F., and Bieniasz, P. D. (2022). Rational attenuation of RNA viruses with zinc finger antiviral protein. *Nat. Microbiol.* 7, 1558–1567. doi: 10.1038/s41564-022-01223-8

Gonzalez-Perez, A. C., Stempel, M., Wyler, E., Urban, C., Piras, A., Hennig, T., et al. (2021). The zinc finger antiviral protein ZAP restricts human cytomegalovirus and selectively binds and destabilizes viral UL4/UL5 transcripts. *MBio* 12, 10–1128. doi: 10.1128/mBio.02683-20

Gopal, V., Nilsson-Payant, B. E., French, H., Siegers, J. Y., Yung, W. S., Hardwick, M., et al. (2021). Zinc-embedded polyamide fabrics inactivate SARS-CoV-2 and influenza A virus. *ACS Appl. Mater. Interfaces* 13, 30317–30325. doi: 10.1021/acsami.1c04412

Gordien, E., Rosmorduc, O., Peltekian, C., Garreau, F., Bréchot, C., and Kremsdorf, D. (2001). Inhibition of hepatitis B virus replication by the interferon-inducible MxA protein. *J. Virol.* 75, 2684–2691. doi: 10.1128/JVI.75.6.2684-2691.2001

Gordon, A. M., and Hardigan, P. C. (2021). A case-control study for the effectiveness of oral zinc in the prevention and mitigation of COVID-19. *Front. Med.* 8:756707. doi: 10.3389/fmed.2021.756707

Groth, C., Sasamura, T., Khanna, M. R., Whitley, M., and Fortini, M. E. (2013). Protein trafficking abnormalities in Drosophila tissues with impaired activity of the ZIP7 zinc transporter catsup. *Development* 140, 3018–3027. doi: 10.1242/dev.088336

Grzywacz, A., Gdula-Argasińska, J., Muszyńska, B., Tyszka-Czochara, M., Librowski, T., and Opoka, W. (2015). Metal responsive transcription factor 1 (MTF-1) regulates zinc dependent cellular processes at the molecular level. *Acta Biochim. Pol.* 62, 491–498. doi: 10.18388/abp.2015_1038

Guo, X., Carroll, J. W. N., Mac Donald, M. R., Goff, S. P., and Gao, G. (2004). The zinc finger antiviral protein directly binds to specific viral mRNAs through the CCCH zinc finger motifs. *J. Virol.* 78, 12781–12787. doi: 10.1128/JVI.78.23.12781-12787.2004

Guo, H., Jin, X., and Zhu, T. (2014). SLC39A5 mutations interfering with the BMP/TGF-b pathway in non-syndromic high myopia. *J. Med. Genet.* 51, 518–525. doi: 10.1136/jmedgenet-2014-102351

Guo, X., Ma, J., Sun, J., and Gao, G. (2007). The zinc-finger antiviral protein recruits the RNA processing exosome to degrade the target mRNA. *Proc. Natl. Acad. Sci.* 104, 151–156. doi: 10.1073/pnas.0607063104

Gupta, J., Irfan, M., Ramgir, N., Muthe, K. P., Debnath, A. K., Ansari, S., et al. (2022). Antiviral activity of zinc oxide nanoparticles and Tetrapods against the hepatitis E and hepatitis C viruses. *Front. Microbiol.* 13:881595. doi: 10.3389/fmicb.2022.881595

Gupta, P., and Rapp, F. (1976). Effect of zinc ions on synthesis of herpes simplex virus type 2-induced polypeptides. *Proc. Soc. Exp. Biol. Med.* 152, 455–458. doi: 10.3181/00379727-152-39417

Gurunathan, S., Qasim, M., Choi, Y., Do, J. T., Park, C., Hong, K., et al. (2020). Antiviral potential of nanoparticles—can nanoparticles fight against coronaviruses? *Nano* 10:1645. doi: 10.3390/nano10091645

Haase, H., Ober-Blöbaum, J. L., Engelhardt, G., Hebel, S., Heit, A., Heine, H., et al. (2008). Zinc signals are essential for lipopolysaccharide-induced signal transduction in monocytes. *J. Immunol.* 181, 6491–6502. doi: 10.4049/jimmunol.181.9.6491

Haase, H., and Rink, L. (2009). Functional significance of zinc-related signaling pathways in immune cells. *Annu. Rev. Nutr.* 29, 133–152. doi: 10.1146/annurev-nutr-080508-141119

Hara, T., Takeda, T. A., Takagishi, T., Fukue, K., Kambe, T., and Fukada, T. (2017). Physiological roles of zinc transporters: molecular and genetic importance in zinc homeostasis. *J. Physiol. Sci.* 67, 283–301. doi: 10.1007/s12576-017-0521-4

Haraguchi, Y., Sakurai, H., Hussain, S., Anner, B. M., and Hoshino, H. (1999). Inhibition of HIV-1 infection by zinc group metal compounds. *Antivir. Res.* 43, 123–133. doi: 10.1016/s0166-3542(99)00040-6

Hauri, A. M., Fischer, E., Fitzenberger, J., Uphoff, H., and Koenig, C. (2006). Active immunisation during an outbreak of hepatitis a in a German day-care Centre. *Vaccine* 24, 5684–5689. doi: 10.1016/j.vaccine.2006.04.053

Hayakawa, S., Shiratori, S., Yamato, H., Kameyama, T., Kitatsuji, C., Kashigi, F., et al. (2011). ZAPS is a potent stimulator of signaling mediated by the RNA helicase RIG-I during antiviral responses. *Nat. Immunol.* 12, 37–44. doi: 10.1038/ni.1963

Hayashi, M., Ikezawa, K., Ono, A., Okabayashi, S., Hayashi, Y., Shimizu, S., et al. (2007). Evaluation of the effects of combination therapy with branched-chain amino acid and zinc supplements on nitrogen metabolism in liver cirrhosis. *Hepatol. Res.* 37, 615–619. doi: 10.1111/j.1872-034X.2007.00095.x

Hildebrand, M. S., Phillips, A. M., and Mullen, S. A. (2015). Loss of synaptic Zn2? Transporter function increases risk of febrile seizures. *Sci. Rep.* 5:17816. doi: 10.1038/srep17816

Himoto, T., Hosomi, N., Nakai, S., Deguchi, A., Kinekawa, F., Matsuki, M., et al. (2007). Efficacy of zinc administration in patients with hepatitis C virus-related chronic liver disease. *Scand. J. Gastroenterol.* 42, 1078–1087. doi: 10.1080/00365520701272409

Hock, H., Hamblen, M. J., Rooke, H. M., Traver, D., Bronson, R. T., Cameron, S., et al. (2003). Intrinsic requirement for zinc finger transcription factor Gfi-1 in neutrophil differentiation. *Immunity* 18, 109–120. doi: 10.1016/s1074-7613(02)00501-0

Hojyo, S., Miyai, T., Fujishiro, H., Kawamura, M., Yasuda, T., Hijikata, A., et al. (2014). Zinc transporter SLC39A10/ZIP10 controls humoral immunity by modulating B-cell receptor signal strength. *Proc. Natl. Acad. Sci.* 111, 11786–11791. doi: 10.1073/pnas.1323557111

Horvatits, T., Behrendt, P., Schuebel, N., Guthoff, M., Wiegand, J., Harth, A., et al. (2023). Oral zinc supplementation in chronically HEV-infected patients not responding to ribavirin monotherapy. *Hepat. Mon.* 23:e130865. doi: 10.5812/hepatmon-130865

Hosui, A., Tanimoto, T., Okahara, T., Ashida, M., Ohnishi, K., Wakahara, Y., et al. (2021). Oral zinc supplementation decreases the risk of HCC development in patients with HCV eradicated by DAA. *Hepatol. Commun.* 5, 2001–2008. doi: 10.1002/hep4.1782

Huang, L., and Gitschier, J. (1997). A novel gene involved in zinc transport is deficient in the lethal milk mouse. *Nat. Genet.* 17, 292–297. doi: 10.1038/ng1197-292

Huang, C. R., and Lo, S. J. (2014). Hepatitis D virus infection, replication and cross-talk with the hepatitis B virus. *WJG* 20, 14589–14597. doi: 10.3748/wjg.v20.i40.14589

Huang, L., Yu, Y. Y., and Kirschke, C. P. (2007). Znt 7 (Slc 30a7)- deficient mice display reduced body zinc status and body fat accumulation. *J. Biol. Chem.* 282, 37053–37063. doi: 10.1074/jbc.M706631200

Hulisz, D. (2004). Efficacy of zinc against common cold viruses: an overview. *J. Am. Pharm. Assoc.* 44, 594–603. doi: 10.1331/1544-3191.44.5.594.Hulisz

Hung, M., Gibbs, C. S., and Tsiang, M. (2002). Biochemical characterization of rhinovirus RNA-dependent RNA polymerase. *Antivir. Res.* 56, 99–114. doi: 10.1016/s0166-3542(02)00101-8

Imam, H., Kim, G. W., Mir, S. A., Khan, M., and Siddiqui, A. (2020). Interferon-stimulated gene 20 (ISG20) selectively degrades N6-methyladenosine modified hepatitis B virus transcripts. *PLoS Pathog.* 16:e1008338. doi: 10.1371/journal.ppat.1008338

Inoue, K., Matsuda, K., and Itoh, M. (2002). Osteopenia and male specific sudden cardiac death in mice lacking a zinc transporter gene, Znt 5. *Hum. Mol. Genet.* 11, 1775–1784. doi: 10.1093/hmg/11.15.1775

Irving, J. A., Mattman, A., Lockitch, G., Farrell, K., and Wadsworth, L. D. (2003). Element of caution: a case of reversible cytopenias associated with excessive zinc supplementation. *CMAJ* 169, 129–131.

Itsumura, N., Inamo, Y., and Okazaki, F. (2013). Compound heterozygous mutations in SLC30A2/ZnT2 results in low milk zinc concentrations: a novel mechanism for zinc deficiency in a breast-fed infant. *PLoS One* 8:e64045. doi: 10.1371/journal.pone.0064045

Jha, A. K., Kumar, G., Dayal, V. M., Ranjan, A., and Suchismita, A. (2021). Neurological manifestations of hepatitis E virus infection: an overview. *World J. Gastroenterol.* 27, 2090–2104. doi: 10.3748/wjg.v27.i18.2090

Jiang, J., Jiang, P., and Jiye, C. (2018). The advancing of zinc oxide nanoparticles for biomedical applications. *Bioinorg. Chem. Appl.* 2018, 1–18. doi: 10.1155/2018/1062562

Jiang, L. J., Maret, W., and Vallee, B. L. (1998). The ATP–metallothionein complex. *Proc. Natl. Acad. Sci.* 95, 9146–9149. doi: 10.1073/pnas.95.16.9146

John, E., Laskow, T. C., Buchser, W. J., Pitt, B. R., Basse, P. H., Butterfield, L. H., et al. (2010). Zinc in innate and adaptive tumor immunity. *J. Transl. Med.* 8:118. doi: 10.1186/1479-5876-8-118

Kagara, N., Tanaka, N., Noguchi, S., and Hirano, T. (2007). Zinc and its transporter ZIP10 are involved in invasive behaviour of breast cancer cells. *Cancer Sci.* 98, 692–697. doi: 10.1111/j.1349-7006.2007.00446.x

Kaltenberg, J., Plum, L. M., Ober-Blöbaum, J. L., Hönscheid, A., Rink, L., and Haase, H. (2010). Zinc signals promote IL-2-dependent proliferation of T cells. *Eur. J. Immunol.* 40, 1496–1503. doi: 10.1002/eji.200939574

Kambe, T. (2012). Molecular architecture and function of ZnT transporters. *Curr. Top. Membr.* 69, 199–220. doi: 10.1016/B978-0-12-394390-3.00008-2

Kanda, T., Sasaki, R., Masuzaki, R., Takahashi, H., Fujisawa, M., Matsumoto, N., et al. (2020). Additive effects of zinc chloride on the suppression of hepatitis A virus replication by interferon in human hepatoma huh 7 cells. *In Vivo* 34, 3301–3308. doi: 10.21873/invivo.12168

Katwal, P., Aftab, S., Nelson, E., Hildreth, M., Li, S., and Wang, X. (2022). Role of zinc metalloprotease (ZMPSTE24) in porcine reproductive and respiratory syndrome virus (PRRSV) replication in vitro. *Arch. Virol.* 167, 2281–2286. doi: 10.1007/s00705-022-05529-0

Katz, E. H. U. D., and Margalith, E. (1981). Inhibition of vaccinia virus maturation by zinc chloride. *Antimicrob. Agents Chemother.* 19, 213–217. doi: 10.1128/aac.19.2.213

Kaushik, N., Subramani, C., Anang, S., Muthumohan, R., Shalimar, , Nayak, B., et al. (2017). Zinc salts block hepatitis E virus replication by inhibiting the activity of viral RNA-dependent RNA polymerase. *J. Virol.* 91, e00754–e00717. doi: 10.1128/JVI.00754-17

Keeffe, E. B. (1995). Is hepatitis a more severe in patients with chronic hepatitis B and other chronic liver diseases? *Am. J. Gastroenterol.* 90, 201–205.

Kim, B., Kim, H. Y., and Lee, W. W. (2021). Zap 70 regulates TCR-mediated zip 6 activation at the immunological synapse. *Front. Immunol.* 12:687367. doi: 10.3389/fimmu.2021.687367

Kim, K. I., Kim, S. R., Sasase, N., Akimoto, Y., Shikata, M., Ohtani, A., et al. (2008). Blood cell, liver function, and response changes by PEG-interferon-α2b plus ribavirin with polaprezinc therapy in patients with chronic hepatitis C. *Hepatol. Int.* 2, 111–115. doi: 10.1007/s12072-007-9029-y

King, L. E., Osati-Ashtiani, F., and Fraker, P. J. (1995). Depletion of cells of the B lineage in the bone marrow of zinc-deficient mice. *Immunology* 85, 69–73.

Kitabayashi, C., Fukada, T., Kanamoto, M., Ohashi, W., Hojyo, S., Atsumi, T., et al. (2010). Zinc suppresses Th17 development via inhibition of STAT3 activation. *Int. Immunol.* 22, 375–386. doi: 10.1093/intimm/dxq017

Kitamura, H., Morikawa, H., Kamon, H., Iguchi, M., Hojyo, S., Fukada, T., et al. (2006). Toll-like receptor–mediated regulation of zinc homeostasis influences dendritic cell function. *Nat. Immunol.* 7, 971–977. doi: 10.1038/ni1373

Ko, W. S., Guo, C. H., Hsu, G. S. W., Chiou, Y. L., Yeh, M. S., and Yaun, S. R. (2005). The effect of zinc supplementation on the treatment of chronic hepatitis C patients with interferon and ribavirin. *Clin. Biochem.* 38, 614–620. doi: 10.1016/j.clinbiochem.2005.04.003

Korant, B. D., Kauer, J. C., and Butterworth, B. E. (1974). Zinc ions inhibit replication of rhinoviruses. *Nature* 248, 588–590. doi: 10.1038/248588a0

Krenn, B. M., Gaudernak, E., Holzer, B., Lanke, K., Van Kuppeveld, F. J. M., and Seipelt, J. (2009). Antiviral activity of the zinc ionophores pyrithione and hinokitiol against picornavirus infections. *J. Virol.* 83, 58–64. doi: 10.1128/JVI.01543-08

Krężel, A., and Maret, W. (2006). Zinc-buffering capacity of a eukaryotic cell at physiological pZn. *JBIC J. Biol. Inorgan. Chem.* 11, 1049–1062. doi: 10.1007/s00775-006-0150-5

Krishnaraju, K., Nguyen, H. Q., Liebermann, D. A., and Hoffman, B. (1995). The zinc finger transcription factor Egr-1 potentiates macrophage differentiation of hematopoietic cells. *Mol. Cell. Biol.* 15, 5499–5507. doi: 10.1128/MCB.15.10.5499

Kumar, R., Sahoo, G., Pandey, K., Nayak, M. K., Topno, R., Rabidas, V., et al. (2018). Virostatic potential of zinc oxide (ZnO) nanoparticles on capsid protein of cytoplasmic side of chikungunya virus. *Int. J. Infect. Dis.* 73:368. doi: 10.1016/j.ijid.2018.04.4247

Kümel, G., Schrader, S., Zentgraf, H., Daus, H., and Brendel, M. (1990). The mechanism of the antiherpetic activity of zinc sulphate. *J. Gen. Virol.* 71, 2989–2997. doi: 10.1099/0022-1317-71-12-2989

Kurugöl, Z., Akilli, M., Bayram, N., and Koturoglu, G. (2006). The prophylactic and therapeutic effectiveness of zinc sulphate on common cold in children. *Acta Paediatr.* 95, 1175–1181. doi: 10.1080/08035250600603024

Lalazar, G., and Ilan, Y. (2014). Viral diseases of the liver. Liver Immunology: Principles and Practice, 159–171.

Lanke, K., Krenn, B. M., Melchers, W. J. G., Seipelt, J., and Van Kuppeveld, F. J. M. (2007). PDTC inhibits picornavirus polyprotein processing and RNA replication by transporting zinc ions into cells. *J. Gen. Virol.* 88, 1206–1217. doi: 10.1099/vir.0.82634-0

Lazarczyk, M., and Favre, M. (2008). Role of Zn2+ ions in host-virus interactions. *J. Virol.* 82, 11486–11494. doi: 10.1128/JVI.01314-08

Li, D., Achkar, J.-P., and Haritunians, T. (2016). A pleiotropic missense variant in SLC39A8 is associated with Crohn's disease and human gut microbiome composition. *Gastroenterology* 151, 724–732. doi: 10.1053/j.gastro.2016.06.051

Li, S., Fu, B., Wang, L., and Dorf, M. E. (2017). ZMPSTE24 is downstream effector of interferon-induced transmembrane antiviral activity. *DNA Cell Biol.* 36, 513–517. doi: 10.1089/dna.2017.3791

Li, J., Lin, S., Chen, Q., Peng, L., Zhai, J., Liu, Y., et al. (2010). Inhibition of hepatitis B virus replication by MyD88 involves accelerated degradation of pregenomic RNA and nuclear retention of pre-S/S RNAs. *J. Virol.* 84, 6387–6399. doi: 10.1128/JVI.00236-10

Li, N., Zhang, L., Chen, L., Feng, W., Xu, Y., Chen, F., et al. (2012). MxA inhibits hepatitis B virus replication by interaction with hepatitis B core antigen. *Hepatology* 56, 803–811. doi: 10.1002/hep.25608

Lichten, L. A., and Cousins, R. J. (2009). Mammalian zinc transporters: nutritional and physiologic regulation. *Annu. Rev. Nutr.* 29, 153–176. doi: 10.1146/annurev-nutr-033009-083312

Lin, R. S., Rodriguez, C., Veillette, A., and Lodish, H. F. (1998). Zinc is essential for binding of p56lck to CD4 and CD8α. *J. Biol. Chem.* 273, 32878–32882. doi: 10.1074/jbc.273.49.32878

Liu, M. J., Bao, S., Gálvez-Peralta, M., Pyle, C. J., Rudawsky, A. C., Pavlovicz, R. E., et al. (2013). ZIP8 regulates host defense through zinc-mediated inhibition of NF-κB. *Cell Rep.* 3, 386–400. doi: 10.1016/j.celrep.2013.01.009

Liu, S., Cao, X., Guo, H., and Wei, W. (2021). Zinc influx restricts enterovirus D68 replication. *Front. Microbiol.* 12:748546. doi: 10.3389/fmicb.2021.748546

Liu, C. Y., and Kielian, M. (2012). Identification of a specific region in the e1 fusion protein involved in zinc inhibition of semliki forest virus fusion. *J. Virol.* 86, 3588–3594. doi: 10.1128/JVI.07115-11

Liu, Z., Li, H., Soleimani, M., Girijashanker, K., Reed, J. M., He, L., et al. (2008). Cd^{2+} versus Zn^{2+} uptake by the ZIP8 HCO3--dependent symporter: kinetics, electrogenicity and trafficking. *Biochem. Biophys. Res. Commun.* 365, 814–820. doi: 10.1016/j.bbrc.2007.11.067

Liu, Y., Nie, H., Mao, R., Mitra, B., Cai, D., Yan, R., et al. (2017). Interferon-inducible ribonuclease ISG20 inhibits hepatitis B virus replication through directly binding to the epsilon stem-loop structure of viral RNA. *PLoS Pathog.* 13:e1006296. doi: 10.1371/journal.ppat.1006296

Lok, A. S., Heathcote, E. J., and Hoofnagle, J. H. (2001). Management of hepatitis B: 2000—summary of a workshop. *Gastroenterology* 120, 1828–1853. doi: 10.1053/gast.2001.24839

Love, R. A., Parge, H. E., Wickersham, J. A., Hostomsky, Z., Habuka, N., Moomaw, E. W., et al. (1996). The crystal structure of hepatitis C virus NS3 proteinase reveals a trypsin-like fold and a structural zinc binding site. *Cells* 87, 331–342. doi: 10.1016/S0092-8674(00)81350-1

Lu, M., and Fu, D. (2007). Structure of the zinc transporter Yii P. *Science* 317, 1746–1748. doi: 10.1126/science.1143748

Maldonado, R. A., and von Andrian, U. H. (2010). How tolerogenic dendritic cells induce regulatory T cells. *Adv. Immunol.* 108, 111–165. doi: 10.1016/B978-0-12-380995-7.00004-5

Manns, M. P., Buti, M., Gane, E. D., Pawlotsky, J. M., Razavi, H., Terrault, N., et al. (2017). Hepatitis C virus infection. *Nat. Rev. Dis. Primers* 3, 1–19. doi: 10.1038/nrdp.2017.6

Mao, R., Nie, H., Cai, D., Zhang, J., Liu, H., Yan, R., et al. (2013). Inhibition of hepatitis B virus replication by the host zinc finger antiviral protein. *PLoS Pathog.* 9:e1003494. doi: 10.1371/journal.ppat.1003494

Maret, W. (1994). Oxidative metal release from metallothionein via zinc-thiol/disulfide interchange. *Proc. Natl. Acad. Sci.* 91, 237–241. doi: 10.1073/pnas.91.1.237

Maret, W., and Sandstead, H. H. (2006). Zinc requirements and the risks and benefits of zinc supplementation. *J. Trace Elem. Med. Biol.* 20, 3–18. doi: 10.1016/j.jtemb.2006.01.006

Martin, A., and Lemon, S. M. (2006). Hepatitis a virus: from discovery to vaccines. *Hepatology* 43, S164–S172. doi: 10.1002/hep.21052

Mathews, W. R., Ong, D., Milutinovich, A. B., and Van Doren, M. (2006). Zinc transport activity of fear of intimacy is essential for proper gonad morphogenesis and DE-cadherin expression. *J. Embryol. Exp. Morpholog.* 133, 1143–1153. doi: 10.1242/dev.02256

Matsuoka, S., Matsumura, H., Nakamura, H., Oshiro, S., Arakawa, Y., Hayashi, J., et al. (2009). Zinc supplementation improves the outcome of chronic hepatitis C and liver cirrhosis. *J. Clin. Biochem. Nutr.* 45, 292–303. doi: 10.3164/jcbn.jcbn08-246

Mehrbod, P., Hudy, D., Shyntum, D., Markowski, J., Łos, M. J., and Ghavami, S. (2021). Quercetin as a natural therapeutic candidate for the treatment of influenza virus. *Biomol. Ther.* 11:10. doi: 10.3390/biom11010010

Mishra, Y. K., and Adelung, R. (2018). ZnO tetrapod materials for functional applications. *Mater. Today* 21, 631–651. doi: 10.1016/j.mattod.2017.11.003

Mishra, Y. K., Adelung, R., Röhl, C., Shukla, D., Spors, F., and Tiwari, V. (2011). Virostatic potential of micro–nano filopodia-like ZnO structures against herpes simplex virus-1. *Antivir. Res.* 92, 305–312. doi: 10.1016/j.antiviral.2011.08.017

Mishra, P. K., Mishra, H., Ekielski, A., Talegaonkar, S., and Vaidya, B. (2017). Zinc oxide nanoparticles: a promising nanomaterial for biomedical applications. *Drug Discov. Today* 22, 1825–1834. doi: 10.1016/j.drudis.2017.08.006

Mocchegiani, E., and Muzzioli, M. (2000). Therapeutic application of zinc in human immunodeficiency virus against opportunistic infections. *J. Nutr.* 130, 1424S–1431S. doi: 10.1093/jn/130.5.1424S

Mocchegiani, E., Veccia, S., Ancarani, F., Scalise, G., and Fabris, N. (1995). Benefit of oral zinc supplementation as an adjunct to zidovudine (AZT) therapy against opportunistic infections in AIDS. *Int. J. Immunopharmacol.* 17, 719–727. doi: 10.1016/0192-0561(95)00060-f

Murakami, Y., Koyabu, T., Kawashima, A., Kakibuchi, N., Kawakami, T., Takaguchi, K., et al. (2007). Zinc supplementation prevents the increase of transaminase in chronic hepatitis C patients during combination therapy with pegylated interferon α-2b and ribavirin. *J. Nutr. Sci. Vitaminol.* 53, 213–218. doi: 10.3177/jnsv.53.213

Myers, S. A., Nield, A., and Myers, M. (2012). Zinc transporters, mechanisms of action and therapeutic utility: implications for type 2 diabetes mellitus. *J. Nut. Metabol.* 2012, 1–13. doi: 10.1155/2012/173712

Myers, R. P., Ratziu, V., Benhamou, Y., Di Martino, V., Moussalli, J., Hélène Tainturier, M., et al. (2002). Infections with multiple hepatotropic viruses. *Polymicro. Dis.*, 51–73. doi: 10.1128/9781555817947.ch4

Nagamine, T., Takagi, H., Takayama, H., Kojima, A., Kakizaki, S., Mori, M., et al. (2000). Preliminary study of combination therapy with interferon-α and zinc in chronic hepatitis C patients with genotype 1b. *Biol. Trace Elem. Res.* 75, 53–63. doi: 10.1385/BTER:75:1-3:53

Netzler, N. E., Enosi Tuipulotu, D., Vasudevan, S. G., Mackenzie, J. M., and White, P. A. (2019). Antiviral candidates for treating hepatitis E virus infection. *Antimicrob. Agents Chemother.* 63, e00003–e00019. doi: 10.1128/aac.00003-19

Nguyen, L. P., Aldana, K. S., Yang, E., Yao, Z., and Li, M. M. (2023). Alphavirus evasion of zinc finger antiviral protein (ZAP) correlates with CpG suppression in a specific viral ns P 2 gene sequence. *Viruses* 15:830. doi: 10.3390/v15040830

Nie, L., Gao, L., Feng, P., Zhang, J., Fu, X., Liu, Y., et al. (2006). Three-dimensional functionalized tetrapod-like ZnO nanostructures for plasmid DNA delivery. *Small* 2, 621–625. doi: 10.1002/smll.200500193

Nimgaonkar, I., Ding, Q., Schwartz, R. E., and Ploss, A. (2018). Hepatitis E virus: advances and challenges. *Nat. Rev. Gastroenterol. Hepatol.* 15, 96–110. doi: 10.1038/nrgastro.2017.150

Nishida, K., Hasegawa, A., Nakae, S., Oboki, K., Saito, H., Yamasaki, S., et al. (2009). Zinc transporter Znt 5/Slc 30a5 is required for the mast cell–mediated delayed-type allergic reaction but not the immediate-type reaction. *J. Exp. Med.* 206, 1351–1364. doi: 10.1084/jem.20082533

Ogawa, M., Kanda, T., Suganami, A., Nakamoto, S., Win, N. N., Tamura, Y., et al. (2019). Antiviral activity of zinc sulfate against hepatitis A virus replication. *Futur. Virol.* 14, 399–406. doi: 10.2217/fvl-2019-0031

Ouirane, K. B., Boulard, Y., and Bressanelli, S. (2019). The hepatitis C virus RNA-dependent RNA polymerase directs incoming nucleotides to its active site through magnesium-dependent dynamics within its F motif. *J. Biol. Chem.* 294, 7573–7587. doi: 10.1074/jbc.RA118.005209

Overbeck, S., Rink, L., and Haase, H. (2008). Modulating the immune response by oral zinc supplementation: a single approach for multiple diseases. *Arch. Immunol. Ther. Exp.* 56, 15–30. doi: 10.1007/s00005-008-0003-8

Parsons, D. S., Hogstrand, C., and Maret, W. (2018). The C-terminal cytosolic domain of the human zinc transporter ZnT8 and its diabetes risk variant. *FEBS J.* 285, 1237–1250. doi: 10.1111/febs.14402

Peters, J. L., Dufner-Beattie, J., and Xu, W. (2007). Targeting of the mouse Slc 39a2 (Zip 2) gene reveals highly cell-specific patterns of expression, and unique functions in zinc, iron, and calcium homeostasis. *Genesis* 45, 339–352. doi: 10.1002/dvg.20297

Plum, L. M., Brieger, A., Engelhardt, G., Hebel, S., Nessel, A., Arlt, M., et al. (2014). PTEN-inhibition by zinc ions augments interleukin-2-mediated Akt phosphorylation. *Metallomics* 6, 1277–1287. doi: 10.1039/c3mt00197k

Polatnick, J., and Bachrach, H. L. (1978). Effect of zinc and other chemical agents on foot-and-mouth disease virus replication. *Antimicrob. Agents Chemother.* 13, 731–734. doi: 10.1128/AAC.13.5.731

Prasad, A. S. (2013). Discovery of human zinc deficiency: its impact on human health and disease. *Adv. Nutr.* 4, 176–190. doi: 10.3945/an.112.003210

Prasad, A. S., Bao, B., Beck, F. W., and Sarkar, F. H. (2011). Zinc-suppressed inflammatory cytokines by induction of A20-mediated inhibition of nuclear factor-κB. *Nutrition* 27, 816–823. doi: 10.1016/j.nut.2010.08.010

Primadharsini, P. P., Nagashima, S., and Okamoto, H. (2021). Mechanism of cross-species transmission, adaptive evolution and pathogenesis of hepatitis E virus. *Viruses* 13:909. doi: 10.3390/v13050909

Qiu, M., Chen, Y. U., Chu, Y., Song, S., Yang, N. A., Gao, J., et al. (2013). Zinc ionophores pyrithione inhibits herpes simplex virus replication through interfering with proteasome function and NF-κB activation. *Antivir. Res.* 100, 44–53. doi: 10.1016/j.antiviral.2013.07.001

Ramakrishnan, D., Xing, W., Beran, R. K., Chemuru, S., Rohrs, H., Niedziela-Majka, A., et al. (2019). Hepatitis B virus X protein function requires zinc binding. *J. Virol.* 93, e00250–e00219. doi: 10.1128/JVI.00250-19

Read, S. A., O'Connor, K. S., Suppiah, V., Ahlenstiel, C. L., Obeid, S., Cook, K. M., et al. (2017). Zinc is a potent and specific inhibitor of IFN-λ3 signalling. *Nat. Commun.* 8, 1–15. doi: 10.1038/ncomms15245

Read, S. A., Obeid, S., Ahlenstiel, C., and Ahlenstiel, G. (2019). The role of zinc in antiviral immunity. *Adv. Nutr.* 10, 696–710. doi: 10.1093/advances/nmz013

Reis e Sousa, C. (2006). Dendritic cells in a mature age. *Nat. Rev. Immunol.* 6, 476–483. doi: 10.1038/nri1845

Rink, L., and Kirchner, H. (2000). Zinc-altered immune function and cytokine production. *J. Nutr.* 130:1407S. doi: 10.1093/jn/130.5.1407S

Romanelli, F., Smith, K. M., and Hoven, A. D. (2004). Chloroquine and hydroxychloroquine as inhibitors of human immunodeficiency virus (HIV-1) activity. *Curr. Pharm. Des.* 10, 2643–2648. doi: 10.2174/1381612043383791

Roohani, N., Hurrell, R., Kelishadi, R., and Schulin, R. (2013). Zinc and its importance for human health: an integrative review. *J. Res. Med. Sci.* 18, 144–157.

Rükgauer, M., Klein, J., and Kruse-Jarres, J. D. (1997). Reference values for the trace elements copper, manganese, selenium, and zinc in the serum/plasma of children, adolescents, and adults. *J. Trace Elem. Med. Biol.* 11, 92–98. doi: 10.1016/S0946-672X(97)80032-6

Ruttkay-Nedecky, B., Nejdl, L., Gumulec, J., Zitka, O., Masarik, M., Eckschlager, T., et al. (2013). The role of metallothionein in oxidative stress. *Int. J. Mol. Sci.* 14, 6044–6066. doi: 10.3390/ijms14036044

Ryu, M. S., Aydemir, T.B., Marriott, B.P., Birt, D.F., Stallings, V.A., and Yates, A.A. (2020). *Present knowledge in nutrition.11th ed.* Cambridge, Massachusetts: Wiley-Blackwell. 393–408.

Sadeghsoltani, F., Mohammadzadeh, I., Safari, M. M., Hassanpour, P., Izadpanah, M., Qujeq, D., et al. (2021). Zinc and respiratory viral infections: important trace element in anti-viral response and immune regulation. *Biol. Trace Elem. Res.* 200, 2556–2571. doi: 10.1007/s12011-021-02859-z

Samad, N., Sodunke, T. E., Abubakar, A. R., Jahan, I., Sharma, P., Islam, S., et al. (2021). The implications of zinc therapy in combating the COVID-19 global pandemic. *J. Inflamm. Res.* 14, 527–550. doi: 10.2147/JIR.S295377

Sheqwara, J., and Alkhatib, Y. (2013). Sideroblastic anemia secondary to zinc toxicity. *Blood* 122:311. doi: 10.1182/blood-2012-12-469239

Shilagardi, K., Spear, E. D., Abraham, R., Griffin, D. E., and Michaelis, S. (2022). The integral membrane protein ZMPSTE24 protects cells from SARS-CoV-2 spike-mediated pseudovirus infection and syncytia formation. *MBio* 13:e0254322. doi: 10.1128/mbio.02543-22

Sirelkhatim, A., Mahmud, S., Seeni, A., Kaus, N. H. M., Ann, L. C., Bakhori, S. K. M., et al. (2015). Review on zinc oxide nanoparticles: antibacterial activity and toxicity mechanism. *Nano Lett.* 7, 219–242. doi: 10.1007/s40820-015-0040-x

Slepchenko, K. G., Lu, Q., and Li, Y. V. (2016). Zinc wave during the treatment of hypoxia is required for initial reactive oxygen species activation in mitochondria. *Int. J. Physiol. Pathophysiol. Pharmacol.* 8, 44–51.

Slepchenko, K. G., Lu, Q., and Li, Y. V. (2017). Cross talk between increased intracellular zinc (Zn^{2+}) and accumulation of reactive oxygen species in chemical ischemia. *Am. J. Phys. Cell Phys.* 313, C448–C459. doi: 10.1152/ajpcell.00048.2017

Štefanová, I., Hemmer, B., Vergelli, M., Martin, R., Biddison, W. E., and Germain, R. N. (2003). TCR ligand discrimination is enforced by competing ERK positive and SHP-1 negative feedback pathways. *Nat. Immunol.* 4, 248–254. doi: 10.1038/ni895

Stempniak, M., Hostomska, Z., Nodes, B. R., and Hostomsky, Z. (1997). The NS3 proteinase domain of hepatitis C virus is a zinc-containing enzyme. *J. Virol.* 71, 2881–2886. doi: 10.1128/jvi.71.4.2881-2886.1997

Stitt, M. S., Wasserloos, K. J., Tang, X., Liu, X., Pitt, B. R., and Croix, C. M. S. (2006). Nitric oxide-induced nuclear translocation of the metal responsive transcription factor, MTF-1 is mediated by zinc release from metallothionein. *Vasc. Pharmacol.* 44, 149–155. doi: 10.1016/j.vph.2005.10.004

Stott-Marshall, R. J., and Foster, T. L. (2022). Inhibition of arenavirus entry and replication by the cell-intrinsic restriction factor ZMPSTE24 is enhanced by IFITM antiviral activity. *Front. Microbiol.* 13:840885. doi: 10.3389/fmicb.2022.840885

Subramanian Vignesh, K., and Deepe, G. S. Jr. (2017). Metallothioneins: emerging modulators in immunity and infection. *Int. J. Mol. Sci.* 18:2197. doi: 10.3390/ijms18102197

Suda, T., Okawa, O., Shirahashi, R., Tokutomi, N., and Tamano, M. (2019). Changes in serum zinc levels in hepatitis C patients before and after treatment with direct-acting antiviral agents. *Hepatol. Res.* 49, 1353–1356. doi: 10.1111/hepr.13409

Suzuki, H., Takagi, H., Sohara, N., Kanda, D., Kakizaki, S., Sato, K., et al. (2006). Gunma liver study group triple therapy of interferon and ribavirin with zinc supplementation for patients with chronic hepatitis C: a randomized controlled clinical trial. *World J. Gastroenterol.* 12, 1265–1269. doi: 10.3748/wjg.v12.i8.1265

Tabatabaeizadeh, S. A. (2022). Zinc supplementation and COVID-19 mortality: a meta-analysis. *Eur. J. Med. Res.* 27, 70–76. doi: 10.1186/s40001-022-00694-z

Takagi, H., Nagamine, T., Abe, T., Takayama, H., Sato, K., Otsuka, T., et al. (2001). Zinc supplementation enhances the response to interferon therapy in patients with chronic hepatitis C. *J. Viral Hepat.* 8, 367–371. doi: 10.1046/j.1365-2893.2001.00311.x

Taylor, K. M., and Nicholson, R. I. (2003). The LZT proteins; the LIV-1 subfamily of zinc transporters. *Biochim. Biophys. Acta - Biomembr.* 1611, 16–30. doi: 10.1016/s0005-2736(03)00048-8

Te Velthuis, A. J., van den Worm, S. H., Sims, A. C., Baric, R. S., Snijder, E. J., and van Hemert, M. J. (2010). Zn2+ inhibits coronavirus and arterivirus RNA polymerase activity in vitro and zinc ionophores block the replication of these viruses in cell culture. *PLoS Pathog.* 6:e1001176. doi: 10.1371/journal.ppat.1001176

Tellinghuisen, T. L., Marcotrigiano, J., Gorbalenya, A. E., and Rice, C. M. (2004). The NS5A protein of hepatitis C virus is a zinc metalloprotein. *J. Biol. Chem.* 279, 48576–48587. doi: 10.1074/jbc.M407787200

Thomas, S., Patel, D., Bittel, B., Wolski, K., Wang, Q., Kumar, A., et al. (2021). Effect of high-dose zinc and ascorbic acid supplementation vs usual care on symptom length and reduction among ambulatory patients with SARS-CoV-2 infection: the COVID A to Z randomized clinical trial. *JAMA Netw. Open* 4:e210369. doi: 10.1001/jamanetworkopen.2021.0369

Traore, K. A., Rouamba, H., Nebie, Y., Sanou, M., Traore, A. S., Barro, N., et al. (2012). Seroprevalence of fecal-oral transmitted hepatitis A and E virus antibodies in Burkina Faso. *PLoS One* 7:e48125. doi: 10.1371/journal.pone.0048125

Vašák, M. (2005). Advances in metallothionein structure and functions. *J. Trace Elem. Med. Biol.* 19, 13–17. doi: 10.1016/j.jtemb.2005.03.003

Vento, S., Garofano, T., Renzini, C., Cainelli, F., Casali, F., Ghironzi, G., et al. (1998). Fulminant hepatitis associated with hepatitis a virus superinfection in patients with chronic hepatitis C. *N. Engl. J. Med.* 338, 286–290. doi: 10.1056/NEJM199801293380503

Von Bülow, V., Dubben, S., Engelhardt, G., Hebel, S., Plümäkers, B., Heine, H., et al. (2007). Zinc-dependent suppression of TNF-α production is mediated by protein kinase A-induced inhibition of Raf-1, IκB kinase β, and NF-κB. *J. Immunol.* 179, 4180–4186. doi: 10.4049/jimmunol.179.6.4180

Wan, Y., Petris, M. J., and Peck, S. C. (2014). Separation of zinc-dependent and zinc-independent events during early LPS-stimulated TLR4 signaling in macrophage cells. *FEBS Lett.* 588, 2928–2935. doi: 10.1016/j.febslet.2014.05.043

Wei, Z., Burwinkel, M., Palissa, C., Ephraim, E., and Schmidt, M. F. (2012). Antiviral activity of zinc salts against transmissible gastroenteritis virus in vitro. *Vet. Microbiol.* 160, 468–472. doi: 10.1016/j.vetmic.2012.06.019

Wenzlau, J. M., Juhl, K., and Yu, L. (2007). The cation efflux transporter ZnT8 (Slc 30A8) is a major autoantigen in human type 1 diabetes. *Proc. Natl. Acad. Sci. U. S. A.* 104, 17040–17045. doi: 10.1073/pnas.0705894104

Wessels, I., Rolles, B., Slusarenko, A. J., and Rink, L. (2022). Zinc deficiency as a possible risk factor for increased susceptibility and severe progression of Corona virus disease 19. *Br. J. Nutr.* 127, 214–232. doi: 10.1017/S0007114521000738

Wißing, M. H., Brüggemann, Y., Steinmann, E., and Todt, D. (2021). Virus–host cell interplay during hepatitis E virus infection. *Trends Microbiol.* 29, 309–319. doi: 10.1016/j.tim.2020.07.002

Wu, X., Chen, P., Lin, H., Hao, X., and Liang, Z. (2016). Hepatitis E virus: current epidemiology and vaccine. *Hum. Vaccin. Immunother.* 12, 2603–2610. doi: 10.1080/21645515.2016.1184806

Wu, W., Li, R., Li, X., He, J., Jiang, S., Liu, S., et al. (2016). Quercetin as an antiviral agent inhibits influenza A virus (IAV) entry. *Viruses* 8:6. doi: 10.3390/v8010006

Yu, W., Ji, H., Long, F., Chen, S., He, Q., Xia, Y., et al. (2021). Inhibition of hepatitis E virus replication by zinc-finger antiviral protein synergizes with IFN-β. *J. Viral Hepat.* 28, 1219–1229. doi: 10.1111/jvh.13522

Yu, Y., Wu, A., Zhang, Z., Yan, G., Zhang, F., Zhang, L., et al. (2013). Characterization of the Guf a subfamily member SLC39A11/Zip 11 as a zinc transporter. *J. Nutr. Biochem.* 24, 1697–1708. doi: 10.1016/j.jnutbio.2013.02.010

Yuasa, K., Naganuma, A., Sato, K., Ikeda, M., Kato, N., Takagi, H., et al. (2006). Zinc is a negative regulator of hepatitis C virus RNA replication. *Liver Int.* 26, 1111–1118. doi: 10.1111/j.1478-3231.2006.01352.x

Zhang, Z. Y., Reardon, I. M., Hui, J. O., O'Connell, K. L., Poorman, R. A., Tomasselli, A. G., et al. (1991). Zinc inhibition of renin and the protease from human immunodeficiency virus type 1. *Biochemistry* 30, 8717–8721. doi: 10.1021/bi00100a001

Zhang, Z. Y., and Xiong, H. M. (2015). Photoluminescent ZnO nanoparticles and their biological applications. *Materials* 8, 3101–3127. doi: 10.3390/ma8063101

Zheng, R., Jenkins, T. M., and Craigie, R. (1996). Zinc folds the N-terminal domain of HIV-1 integrase, promotes multimerization, and enhances catalytic activity. *Proc. Natl. Acad. Sci.* 93, 13659–13664. doi: 10.1073/pnas.93.24.13659

Zheng, X., Wang, X., Tu, F., Wang, Q., Fan, Z., and Gao, G. (2017). TRIM25 is required for the antiviral activity of zinc finger antiviral protein. *PLoS Pathog.* 13, e1006145–e1001128. doi: 10.1371/journal.ppat.1006145

Zhu, Y., Chen, G., Lv, F., Wang, X., Ji, X., Xu, Y., et al. (2011). Zinc-finger antiviral protein inhibits HIV-1 infection by selectively targeting multiply spliced viral mRNAs for degradation. *Proc. Natl. Acad. Sci.* 108, 15834–15839. doi: 10.1073/pnas.1101676108

Zhu, M., Wang, H., Lou, T., Xiong, P., Zhang, J., Li, L., et al. (2022). Current treatment of chronic hepatitis B: clinical aspects and future directions. *Front. Microbiol.* 13:975584. doi: 10.3389/fmicb.2022.975584

frontiers | Frontiers in Microbiology

TYPE Review
PUBLISHED 25 October 2023
DOI 10.3389/fmicb.2023.1255935

OPEN ACCESS

EDITED BY
Cécile E. Malnou,
Université Toulouse III Paul Sabatier, France

REVIEWED BY
Brian Ward,
University of Rochester Medical Center, United States
Yuxiang Wang,
National Institutes of Health, United States

*CORRESPONDENCE
Jiannan Feng
✉ fengjiannan1970@qq.com
Chunxia Qiao
✉ bioqcx@126.com

RECEIVED 10 July 2023
ACCEPTED 13 October 2023
PUBLISHED 25 October 2023

CITATION
Peng F, Hu N, Liu Y, Xing C, Luo L, Li X, Wang J, Chen G, Xiao H, Liu C, Shen B, Feng J and Qiao C (2023) Functional epitopes and neutralizing antibodies of vaccinia virus. *Front. Microbiol.* 14:1255935. doi: 10.3389/fmicb.2023.1255935

Functional epitopes and neutralizing antibodies of vaccinia virus

Fenghao Peng[1], Naijing Hu[1], Yingjun Liu[2], Cong Xing[3], Longlong Luo[1], Xinying Li[1], Jing Wang[1], Guojiang Chen[1], He Xiao[1], Chenghua Liu[1], Beifen Shen[1], Jiannan Feng[1]* and Chunxia Qiao[1]*

[1]State Key Laboratory of Toxicology and Medical Countermeasures, Institute of Pharmacology and Toxicology, Beijing, China, [2]School of Medicine and Holistic Integrative Medicine, Nanjing University of Chinese Medicine, Nanjing, China, [3]Joint National Laboratory for Antibody Drug Engineering, The First Affiliated Hospital, School of Medicine, Henan University, Kaifeng, China

Smallpox is an infectious disease caused by the variola virus, and it has a high mortality rate. Historically it has broken out in many countries and it was a great threat to human health. Smallpox was declared eradicated in 1980, and Many countries stopped nation-wide smallpox vaccinations at that time. In recent years the potential threat of bioterrorism using smallpox has led to resumed research on the treatment and prevention of smallpox. Effective ways of preventing and treating smallpox infection have been reported, including vaccination, chemical drugs, neutralizing antibodies, and clinical symptomatic therapies. Antibody treatments include anti-sera, murine monoclonal antibodies, and engineered humanized or human antibodies. Engineered antibodies are homologous, safe, and effective. The development of humanized and genetically engineered antibodies against variola virus via molecular biology and bioinformatics is therefore a potentially fruitful prospect with respect to field application. Natural smallpox virus is inaccessible, therefore most research about prevention and/or treatment of smallpox were done using vaccinia virus, which is much safer and highly homologous to smallpox. Herein we summarize vaccinia virus epitope information reported to date, and discuss neutralizing antibodies with potential value for field application.

KEYWORDS

vaccinia virus, variola virus, epitope, neutralizing antibody, engineered antibody

1. Introduction

Variola virus (the smallpox virus) is one of the largest and most complex viruses in the world. It is a member of the genus *Orthopoxvirus* of the *Chordopoxvirinae* subfamily of the *Poxviridae* family (Theves et al., 2016). Smallpox is a highly contagious virus that only infects humans. There are two forms of infectious viral particles; mature virions (MV) and enveloped virions (EV). MVs are the main form, and they play a major role in the spread of the virus between hosts. EV is formed by an MV and an extracellular enveloped membrane. By experimental operation, the enveloped membrane of EV is easy to be destroyed (Condit et al., 2006; Roberts and Smith, 2008). EV facilitates infection between cells (Roberts and Smith, 2008).

Poxviruses include a large family of viruses characterized by large linear dsDNA genomes, cytoplasmic replication sites, and complex virion morphology (Lefkowitz et al., 2005; Condit

et al., 2006). The prototype laboratory virus used for poxvirus research was vaccinia virus, which was used as a live, naturally attenuated vaccine to eradicate smallpox (Roberts and Smith, 2008). Members of the poxvirus family are very similar, so lessons learned from vaccinia can easily be applied to other poxviruses. Vaccinia virus particles are "brick-like" or "ovoid" membrane-bound particles with a complex internal structure characterized by a walled, double-concave core flanked by "lateral bodies." VACV produces two different forms of infectious virion, both of which are targets of antibody responses to smallpox vaccine. Most infectious VACVs are intracellular MV, which remain inside the cell until cell lysis. MV has a membrane that is associated with at least 19 different viral proteins. A27, L1, D8, H3, and A28 are known targets of neutralizing antibodies. A small portion of the MV in the cell gains additional membrane by being wrapped in the Golgi cisternae. They are eventually released as EV through exocytosis and are responsible for the virus's long-distance transmission within the host. EV has an additional outer membrane than MV and is associated with at least six different viral proteins, with B5 being the primary target for neutralizing antibodies and A33 triggering a protective antibody response. For optimal smallpox immune protection, antibodies against both smallpox virus MV and EV are required (Roberts and Smith, 2008). Antibodies block the transmission of the virus between and within individuals by recognizing epitopes of MV and EV.

The mortality rate of smallpox is >50% (Fulginiti et al., 2003; Nafziger, 2005). Starting in the 17th century smallpox caused a worldwide pandemic that killed approximately 400,000 people every year in Europe, and blinded one third of those it infected. In the 20th century smallpox killed at least 300 million people worldwide. From 1967 to the end of the 1970s a widespread campaign aimed at elimination via vaccination was implemented, resulting in the eradication of smallpox. In 1980 the World Health Organization (WHO) announced the eradication of smallpox, and ceased worldwide vaccination against the disease. Currently only two secure laboratories, one in Russia and one in the US, are authorized to store live smallpox virus.

Historically smallpox has never been used as a weapon in wars because of its high infectivity and lethality. Now, the smallpox virus has become one of the best materials for use in biological warfare or bioterrorism (Pennington, 2003). After the 9/11 attack in the US the smallpox virus was listed as one of the most important biological agents with potential use for terrorist attacks in that country. The cessation of smallpox immunization means a large number of people today have no resistance against smallpox. Other *Orthopoxvirus* spp. and their possible mutation or recombination in nature may also threaten human health. Thus, it is necessary to research potential antagonists against smallpox.

Vaccination is a simple and effective means of preventing smallpox before or after exposure to the virus (Mayr, 2003; Meyer et al., 2020). Expanding the reserves of smallpox vaccines has become a global need. Although the efficacy of traditional smallpox vaccines has been fully verified they sometimes did cause side effects (Parrino and Graham, 2006), which necessitates the development of a safer and more effective smallpox vaccine. Several different types of smallpox vaccines have been developed, including cell-cultured live virus vaccines, replicating and non-replicating attenuated live virus vaccines, protein-based subunit vaccines, DNA-based subunit vaccines, and vector-based subunit vaccines (Addeo et al., 2021). Dryvax (Amanna et al., 2006) is a traditional smallpox vaccine that is no longer stored in the United States. Currently the two main vaccines are ACAM2000 (Beachkofsky et al., 2010; Nalca and Zumbrun, 2010) and Jynneos (Kennedy and Greenberg, 2009; Rao et al., 2022). In the event of a smallpox outbreak, antiviral drugs such as cidofovir, ribavirin, and tecovirimat (TPOXX®; ST-246) (Russo et al., 2021) could be used for emergency treatment. Tecovirimat is a potent antiviral that was approved for the treatment of symptomatic smallpox by the US Food and Drug Administration in July 2018, and it has been stockpiled by the US government for use in a smallpox outbreak.

Antibodies have been used as therapeutic agents for hundreds of years, including antiserum, mouse monoclonal antibodies, and human/humanized antibodies. In individuals for whom smallpox vaccination is contraindicated, specific vaccinia immunoglobulin (VIG) or monoclonal antibodies (mAbs) are alternative strategies for preventive or post-infection treatment. The indications that grant the use of VIG include generalized vaccinia, progressive vaccinia, eczema vaccinatum, and certain accidental implantations. Data suggest VIG efficacy for prophylaxis of vaccinial superinfection of eczema, burns, chickenpox, immunosuppression, pregnancy, or certain skin conditions (Hopkins and Lane, 2004). There is limited potential for the broadscale use of VIG extracted from the serum of vaccine recipients however (Hopkins and Lane, 2004), and VIG obtained from animals such as mice or rabbits tends to cause side effects. Murine mAbs also have several disadvantages in humans, including a lack of antibody-dependent cell-mediated cytotoxicity, complement-dependent cytotoxicity, a short half-life, and human anti-mouse antibody reactions, which reduce efficacy and can cause allergic reactions (Hansel et al., 2010). Therefore the development of humanized and genetically engineered antibodies against smallpox virus via molecular biology, immunology, and bioinformatic methods is a worthwhile prospect. Such endeavors require an understanding of the antigenic epitopes of smallpox viral proteins (e.g., A27, B5, D8) to facilitate the generation of neutralizing antibodies.

Because the smallpox virus is dangerous and currently stored under highly regulated conditions, the effects of anti-smallpox antibodies are estimated using the vaccinia virus (VACV). Most research about prevention and/or treatment of smallpox were done using vaccinia virus, which is much safer and highly homologous to smallpox. At least 20 proteins have been identified on the surface of smallpox MVs, and 6 have been identified on EV. Rodriguez et al. (1985) isolated a series of monoclonal antibodies against VACV, including anti-B5 monoclonal antibody MAb20 and anti-A27 monoclonal antibody C3. In 2011 Meng et al. (2011) immunized BALB/c mice with VACV, and after fusion and clone screening 66 mAbs were obtained. Their epitopes were identified on 11 proteins; D8, A14, wRl48, D13, H3, A56, A33, C3, B5, A10, and F13. The proteins recognized by neutralizing antibodies include A33 (Fogg et al., 2004; Fang et al., 2006), B5 (Fogg et al., 2004; Aldaz-Carroll et al., 2007), L1 (Wolffe et al., 1995; Ichihashi and Oie, 1996; Fogg et al., 2004), H3 (Lin et al., 2000; Davies et al., 2005), A27, D8 (Sakhatskyy et al., 2006), A28 (Nelson et al., 2008), A17 (Wallengren et al., 2001), A30, B7, and F8. Among them, L1 (Bisht et al., 2008), H3 (Lin et al., 2000), A27 (Chung et al., 1998; Vázquez and Esteban, 1999), D8 (Hsiao et al., 1999), and A28 (Senkevich et al., 2004) are related to virus adsorption, membrane fusion, and virus entry. B5 is involved in virus packaging, particle release, virus morphology, plaque formation, and intercellular infection (Aldaz-Carroll et al., 2005). A33

is related to virus transmission between cells. Proteins with neutralizing epitopes include the EV proteins B5, A33 (Breiman and Smith, 2010; Breiman et al., 2013; Monticelli et al., 2020), and the MV proteins H3, L1, D8, A13, A27, A17, and A28. Those proteins and their monoclonal antibodies are reviewed below.

2. Viral proteins and protective mAbs

2.1. B5

B5 is an EV protein that is highly conserved among orthopoxviruses (Engelstad and Smith, 1993). It is a glycosylated type I membrane protein with a relative molecular weight of 4.2×10^4 Da. The extracellular domain of B5 contains four short repeat domains similar to complement regulatory proteins, but it has no notable complementary function. B5 is necessary for virus packaging, and it contains epitopes that are recognized by neutralizing antibodies which block virus infection (Bell et al., 2004; Aldaz-Carroll et al., 2007; Benhnia et al., 2009), providing a protective effect both *in vitro* and *in vivo*. The localization of B5 to the surface of intracellular EV and its transport from the endoplasmic reticulum to the Golgi network is dependent on its interaction with A33 and A34. A33, A34, and B5 form a trimeric protein complex that is vital for their endoplasmic reticulum exit and Golgi transportation. The three glycoproteins efficiently localize and become incorporated into the outer extracellular virion membrane, and directly influence the release of infectious poxvirions (Monticelli et al., 2020).

Chen et al. (2006) generated two human anti-B5 mAbs via phage display technology, 8AH7AL and 8AH8AL. The two mAbs displayed high binding affinities to B5. In a mouse lung infection model administration of 22.5 μg 8AH8AL 24 h prior to infection provided complete protection, and 5 mg VIG provided similar protection against intranasal inoculation with 10^5 plaque-forming units (PFU) of VACV (WR strain). Administration of 90 μg 8AH8AL 48 h post-infection also completely protected mice. The mAb 8AH8AL inhibited the spread of vaccinia virus *in vitro*, protected mice from subsequent intranasal challenge with virulent vaccinia virus. However, 5 mg VIG sometimes led to death, indicating a worse therapeutic effect than that of 8AH8AL. Froude et al. (2011) generated a humanized anti-B5 hB5R mAb whose maternal antibody was isolated from immunized rats. In a murine model where mice were infected with 10^7 VACV PFU intranasally and given 10 μg of antibody intraperitoneally 5 h later, body weight loss was reduced relative to the control group.

2.2. A33

A33 is a specific EV type II membrane glycoprotein involved in the efficient formation of endocellular enveloped virus, and transmission of the virus in the host (Matho et al., 2015). It has strong immunogenicity and effectively induces protective antibodies *in vivo*. Pre-immunization with vaccines containing the A33 subunit or post-treatment with anti-A33 antibodies may help protect animals infected with a lethal dose of VACV (Galmiche et al., 1999; Zajonc, 2017). In *in vitro* models anti-A33 antibodies inhibited comet formation, suggesting they can block intercellular transmission (Galmiche et al., 1999).

Three fragment antigen-binding (Fab) regions that recognize overlapped epitopes of A33 glycoprotein have been isolated from simians; 6C, 12F, and 12C (Chen et al., 2007). The corresponding genes were fused with the human heavy chain constant region to form full antibodies. Their affinities were 20 nmol/L (6C), 0.14 nmol/L (12F), and 0.46 nmol/L (12C). The affinity of 6C was approximately 140 times weaker than that of 12F, but its neutralizing effects were similar to those of 12F both *in vitro* and *in vivo*. In a mouse model of intranasally introduced infection, injection of 6C 24 h before infection completely protected mice from death and minimized weight loss, and weight loss recovery was observed within 15 d post-infection. As little as 22.5 μg of 6C could completely protect mice to a similar degree as 5 mg of VIG. In addition, whether mice were injected 24 h before or 48 h after infection, 90 μg 6C or the anti-B5 mAb 8AH8AL—or a combination of both (45 μg each)—completely protected mice from death. Anti-B5 mAb-treated mice exhibited less weight loss during 15 d of treatment, particularly in the post-infection administration experiment, amounting to better efficacy than that demonstrated by 6C. The efficacy of the combination group was between that of the two single antibody groups.

Matho et al. (2015) generated seven mouse anti-A33 mAbs that bind to conformational epitopes on A33 rather than linear epitopes, five of which neutralized endocellular enveloped virus in the presence of complement. The authors elucidated the crystal structures of three representative neutralizing mAbs (A2C7, A20G2, and A27D7), then estimated the binding kinetics of each to wild-type A33 and to an engineered A33 protein containing a single alanine substitution in the epitope area. A2C7 and A20G2 are bound to a single A33 subunit, whereas A27D7 is bound to both A33 subunits. Alanine substitution did not affect the binding of A27D7, which also showed high affinity binding to the recombinant A33 protein. A27D7 was an effective cross-neutralizer against orthopoxvirus strains such as agamia virus, monkeypox virus, and VACV, and it protected mice from lethal challenge with agamia virus (Matho et al., 2015).

Paran et al. (2013) reported that a single dose of Sindbis VACV A33 (a recombinant vaccinia virus protein A33 using Sindbis virus-expressing System) did not protect mice from cowpox virus infection, but effectively protected mice from VACV-WR and ectromelia virus challenges. Homologous vaccination with cowpox virus A33 also failed to protect mice from cowpox challenge, and provided only partial protection against VACV-WR. A single protective region located in residues 104–120 of VACV A33 was identified that carries the H2Kd $CD8^+$ T cell epitope and the B cell epitope, recognized by the neutralizing antibody mAb 1G10, which effectively blocks extracellular virion transmission (Paran et al., 2013).

Mucker et al. (2020) evaluated the ability of the anti-A33 humanized monoclonal antibody C6C to affect VACV infection *in vitro*. Enveloped virions released from infected cells were either sensitive or resistant to C6C, suggesting that different types of biologically distinct extracellular virions particles exist, including extracellular enveloped virions and cell-associated released virions. In addition, mAb C6C bound to the recombinant A33 homolog of the Zaire strain of the monkeypox virus (Mucker et al., 2020).

2.3. L1

L1 is an MV membrane protein with a relative molecular mass of 2.9×10^4 Da that is highly conserved among all sequenced poxviruses.

It has a transmembrane domain at the C-terminus, and no signal peptide at the N-terminus, but it is myristoylated and can attach to the membrane easily. The L1 protein is required for the virus to enter host cells, and is an important target recognized by neutralizing antibodies. It was originally identified using the neutralizing antibody 7D11 (Wolffe et al., 1995). L1 is comprised of three pairs of disulfide bonds, two of which are necessary for the production of infectious virions (Blouch et al., 2005). Once the disulfide bonds are broken, L1 is not recognized by neutralizing antibodies (Wolffe et al., 1995; Ichihashi and Oie, 1996). Ichihashi et al. (1994) produced the anti-L1 neutralizing antibodies 2D5 and 8C2, which block viral cell plaque formation. Su et al. (2007) investigated the neutralizing effects of the mouse anti-L1 monoclonal antibody 7D11, including its Fab, F (ab'), and full IgG using plaque formation assays, and reported that the neutralizing effects of Fab were weaker. X-ray diffraction techniques revealed the crystal structure of 7D11 interacting with the L1 protein. Based on the contact area and inter-molecular distance, 7D11 bound to the L1 antigen mainly via its heavy chain, and the effect of the light chain was very weak. 7D11 also formed hydrogen bonds and van der Waals interactions with loop l and loop 2 of L1. 7D11 binding sites are conserved among VACV, smallpox virus, and monkeypox virus suggesting that 7D11 may exhibit cross-protective effects. Kaever et al. (2014) generated five mouse anti-L1 mAbs, which can be categorized into three groups based on their epitopes. At a concentration of 20 g/mL three mAbs (M12B9, M2E9, and M7B6) neutralized more than 70% of VACV, but the other two did not neutralize the virus. The neutralizing antibodies have a higher affinity for the recombinant L1 protein than the non-neutralizing antibodies, and they also bind to viral particles. The epitopes of the neutralizing antibodies were mapped to a conformational epitope with Asp35 as the key residue, and the epitope was similar to that of 7D11 (Kaever et al., 2014). By immunizing two alpacas Walper et al. (2014) generated multiple specific single-domain antibodies with affinities ranging from 4×10^{-9} M to 7×10^{-10} M. The single-domain antibodies, as capture and tracer agents, reduced the detection limit to 4×10^{5} PFU/mL in a sandwich assay–a four-fold improvement over conventional antibodies. This demonstrates the development of single-domain antibodies and the ability to detect viruses in sandwich assays (Walper et al., 2014).

2.4. D8

Matho et al. (2014) described the crystal structure of the adhesion protein D8. Its N-terminal domain contains a carbonic anhydrase fold region (CAH; residues 1–234) followed by a smaller domain (residues 235–273). The remainder of the protein consists of a transmembrane domain (274–294) and a small tail (295–304) within the virion. The CAH domain can bind to glycosaminoglycans and chondroitin sulfate (CS) in host cells because it has a central positively charged gap that complements the negative charge of CS. The optimal ligand for D8 is CS-E, which is characterized as a disaccharide moiety with two sulfate hydroxyl groups at the 4′ and 6′ positions of GalNAc (Matho et al., 2014). Hsiao et al. (1999) constructed A27 and D8 single null, and A27-D8 double-null virus strains based on the WR32-7/Indl4K virus strain. The A27-null virus was amplified in BSC40 cells, but the infectivity of the D8 null and A27-D8 double null strains was significantly lower than that of the wild-type virus, with virulence of only 10%. This indicates that D8 is key for virus infection and endocytosis, and that the A27 protein cannot compensate for loss of D8 function.

Sakhatskyy et al. (2006) constructed a DNA vaccine encoding D8 and immunized BALB/c mice, which induced neutralizing antiserum and protected mice against a lethal dose of VACV. Addition of the D8 protein to the existing subunit vaccine induced antibodies with better neutralizing activity. Based on this, they proposed that D8 was a satisfactory recognition target for neutralizing antibodies. Matho et al. (2012) generated the anti-D8 monoclonal antibody LA5, which is capable of neutralizing VACV in the presence of complement. They described the D8 and LA5 Fab structures to respective resolutions of 0.142 and 0.16 nm, and the crystal structure of the LA5 Fab-D8 complex to 0.21 nm. Based on these structures they predicted that the binding site of CS is located in the central positively charged gap of the D8 molecule. The structure of the gap is highly conserved across several poxviruses. The D8 epitope recognized by LA5 consists of 23 discrete residues scattered across 80% of the D8 sequence. Interestingly LA5 binds to the region above the gap with high affinity, and the antigen–antibody interaction area is unusually large, covering the 243.4 nm protein surface.

Matho et al. tested the capacity of a panel of mouse monoclonal antibodies to compete with CS-E for D8 binding. CS-E binding was only completely abolished by LA5. D8 forms a hexameric arrangement via the self-association of its C-terminal domain. Oligomerization of D8 allows VACV to adhere to multiple CS variants, including CS-C and potentially CS-A, thus improving overall binding efficiency to CS-E (Matho et al., 2014). Matho et al. characterized several epitopes of human D8 antibodies (VACV66, VACV-138, and VACV-304) and determined the first crystal structures of human antibodies that bind to D8. The epitopes are located in the CAH domain, which possesses moderate neutralizing activity in the presence of complement. The crystal structures of VACV-66, VACV-138, and VACV-304 bound to the D8 CAH domain have respective resolutions of 2.23, 2.90, and 2.90 Å. VACV-138 and VACV-304 completely block the binding of D8 to CS-A, whereas VACV-304 only partially blocks binding of D8 to the high-affinity ligand CS-E, indicating the presence of both a high-affinity and a low-affinity CS binding region in the D8 gap. VACV-66 laterally binds to D8 far away from the CS-binding gap, explaining why VACV-66 does not interfere with D8 binding to CS-E (Matho et al., 2018).

2.5. A13

The theoretical molecular weight of A13 is 8×10^{3} Da, but some studies show that A13 migrates to 1.2×10^{4} Da in SDS-PAGE analysis. A13 is an antigenic molecule recognized by neutralizing antibodies. Xu et al. (2011) described the mAb 11F7 (IgG2a), which bound to A13 with an affinity of 3.4 nM/L and neutralized MVs. The antibody recognizes the 10-amino acid epitope ISSLYNLVKSS which is highly conserved among *Orthopoxvirus* species, including VACV and monkeypox virus, indicating its potential to exert a wide range of protective effects. BALB/c mice were injected intraperitoneally with 2 mg of the antibody 24 h before intranasal challenge with VACV WR virus, and changes in body weight and mortality rate were observed. After challenged with VACV WR, all mice lost significant body weight, but mice that received either 11F7 or anti-H3 #41 lost less

weight on average than mice that received PBS. mice that received anti-B5 antibody B126 lost less weight on average than mice that received 11F7. In addition, more mice that received B126 (100%), 11F7 (80%) or anti-H3 (80%) survived the challenge than mice that received PBS (40%). Anti-A13 antibody had good protective effects, and the efficacy of anti-A13 antibody alone was similar to that of anti-H3 antibody #41. The therapeutic effect of the anti-A13 antibody is evidently weaker than that of the anti-B5 antibody B126 (IgG2a) (Benhnia et al., 2009) administered orally. Mice administered B126 alone and in combination with anti-A13 survived and maintained body weight, and body weight in the combined group was greater than that in the B126 alone group.

2.6. H3

H3 is the envelope protein of MV and has a relative molecular mass of 3.5×10^4 Da. The gene encoding H3 is a late gene in the MV virus, and its sequence is highly conserved among members of the poxvirus family. H3 can bind to heparan sulfate on the cell surface, which is related to the adsorption of MV to cells. Lin et al. (2000) constructed an H3-deficient virus that had a smaller plaque size, a virulence one tenth that of the wild-type virus, and a modified morphology. Notably however, H3 is not involved in cell fusion. In a mouse model involving intranasal virus inoculation, mice inoculated with wild-type virus had higher mortality and greater weight loss than mice infected with the H3-deficient virus, which exhibited a higher survival rate and faster recovery. These observations indicated that the H3 protein is related to virus infection, and that the toxicity of H3-deficient virus *in vivo* is reduced. The H3 protein evidently also plays a role in the assembly of virus particles. Davies et al. (2005) reported that H3-specific antibodies are detectable in most people vaccinated with the Dryvax vaccine, especially after a second vaccination. Anti-H3 polyclonal antibody purified from human serum was able to reduce plaque formation by 50% at a dose of 44 μg/mL. After mice were immunized with Dryvax, anti-H3 antibodies were detected in serum via protein microarray technology. Mice further immunized with H3 had serum neutralizing activity higher than that obtained with the VV_{NYBOH} vaccine strain (anti-H3 antiserum had a functional titer of 1:3760, whereas anti-vaccine antiserum had a functional titer of 1:172). Moreover, immunized mice resisted challenges with intranasally administered VACV WR as high as $5 \times LD_{50}$. In passive transfer experiments using anti-H3 antiserum some mice were able to resist a challenge with $3 \times LD_{50}$ VACV WR (survival rates were 5/10 in the antiserum group and 0/10 in the control group, $p < 0.05$).

2.7. A27

A27 is another MV membrane protein that can bind glycosaminoglycans on the cell surface and mediate the fusion of virus and cell. The A27 protein is a trimer containing two parallel α-helices and one antiparallel α-helix (Wang et al., 2014). The structure of A27 is similar to that of influenza hemagglutinin or HIV gp41, except A27 has no membrane-anchoring sequence. Instead it has a domain that interacts with the A17 protein, thus A17 is considered to be a membrane-anchoring helper for A27. The C-terminus of A27 interacts specifically with the N-terminus of A17 via a parallel, cooperative binding mechanism at the F1 and F2 binding sites. Thr88-Lys99 of A27 interacts with Ser32-Lys36 of A17 at the F1 binding site, and Phe80-Glu87 of A27 binds to Leu20-Gln29 of A17 at the F2 binding site (Wang et al., 2014). A27 and A26 form a stable complex, and this helps A17 to bind to the surface of MV particles (Howard et al., 2008).

He et al. (2007) tested the neutralizing titer of anti-A27 antibodies in antiserum after Dryvax vaccination. Antibodies binding to recombinant A27 protein were detected in the antiserum, but neutralizing capacity was not significantly weakened after removal of A27 antibodies. Antibodies against recombinant A27 protein were used in passive transfer experiments, and they enhanced the neutralizing capacity of VIG, indicating that A27 is a neutralizing epitope. A27 is not the main epitope recognized by VIG however, at least in Dryvax vaccine antiserum. Fogg et al. (2008) reported that the antibodies produced by A27-immunized and L1-immunized mice were comparable. In an intranasal virus mouse model however, the anti-A27 antibody was less effective than the anti-L1 antibody. In addition, the ability of mice immunized with both L1 and A33 to resist virus infection was worse than that of animals immunized with A27 and A33. In cytological experiments rabbit anti-L1 polyclonal antibody had a comparable neutralizing effect to anti-A27 polyclonal antibody in both human and mouse cell lines, and in glycosaminoglycan-deficient cell lines, irrespective of whether the antibody was given before or after virus adsorption. This suggests that early identification of neutralizing antibodies is necessary in animal models, at least for the identification of A27 and L1 antibodies.

Thomas et al. produced and characterized three groups of mAbs. All group I mAbs (1G6, 12G2, and 8H10) bound to a linear peptide spanning residues 21–40, located near the glycosaminoglycan binding site of A27. These mAbs could neutralize MV and resist VACV attack in a complement-dependent manner. This suggests that the group I mAbs may interfere with A27 cell adhesion. The crystal structures of 1G6 and the non-neutralizing mAb 8E3 bound to the corresponding linear epitope-containing peptides indicate that both the light and heavy chains of the antibody are important for binding to the antigen. For both antibodies, the L1 loop is important for the overall polar interaction with the antigen, whereas for 8E3 the light chain was more important for contact with the antigen. mAbs that bound to the functional region of antigens (e.g., mAb 1G6) provided greater protection than those that bound to the distal region (e.g., mAb 8E3) (Kaever et al., 2016).

2.8. A17

The precursor of A17 has a relative molecular mass of 2.3×10^4 Da and contains 203 amino acids. It is hydrolyzed by protease at the AA17 site to obtain the A17 protein. A17 has two hydrophobic peptide segments, thus both its N-terminus and C-terminus were once thought to be located inside the membrane to act as a membrane-anchoring helper of the A27 molecule, not as a membrane protein and antibody recognition epitope of MV. Wallengren et al. (2001) identified a series of rabbit polyclonal antibodies against different segments of A17 via immunoelectron microscopy, immunoblotting, and neutralization assays in BSC-40 cells. Their investigations indicated that the polyclonal antibodies against the C-terminus of the A17 protein had no protective effects, whereas anti-N-terminus and

anti-A17 protein antibodies had good protective effects. These observations suggested that the extracellular N-terminus of A17 contained the neutralizing epitopes, whereas the C-terminus was located inside the MV membrane and did not induce neutralizing antiserum.

2.9. A28

The poxvirus cell/membrane complex consists of at least nine transmembrane proteins (including A28 and H2) that are conserved among all poxviruses, although the physical structure and immunogenicity of each component are not well understood. Nelson et al. (2008) expressed and purified soluble A28 protein in an insect expression system and generated rabbit anti-A28 polyclonal antibody. This antibody neutralized VACV and prevented it from entering cells. In an *in vivo* intranasal inoculation mouse model the virus caused significant weight loss that was inhibited by administration of the polyclonal antibody. Its neutralizing effects were similar to those exerted against VACV; however, the anti-H2 polyclonal antibody had no neutralizing effects. ELISA results derived from peptides of 20 amino acids in length designed based on A28 indicated that the polyclonal antibody is recognized mainly at the C-terminal amino acids, encompassing approximately one third of the total length. Antibodies binding to each peptide were obtained by affinity purification, and the antibody recognizing residues 73–92 of A28 had the best neutralizing activity (EC_{50} was 0.11 μg/mL); which was better than that of the original polyclonal antibody. The activity of other antibodies was similar to or worse than that of the polyclonal antibody, indicating that the sequence is key to epitope recognition. Shinoda et al. (2010) investigated the effects interaction between A28 and H2 on the production of anti-A28 neutralizing antibodies. Higher titers of antibodies were obtained with simultaneous immunization of A28 and H2 genes, and neutralizing activity *in vitro* and *in vivo* was stronger than that obtained via a single immunization with either A28 or H2, or even anti-A28 antiserum mixed with anti-H2 antiserum. This suggests that on the virus surface, interaction between H2 and A28 can stabilize the conformation of A28. Thus the epitope recognized by the anti-A28 antibody is mainly located at the C-terminal of A28, consistent with Nelson's above-described study.

3. Multivalent antibodies and recombinant polyclonal antibodies

The body produces billions of antibodies against different antigens and different antigenic epitopes of the same antigen. Isolated antiserum has a good curative effect that is typically better than some mAbs, particularly when the antigenic epitopes are mutated. Antiserum also has obvious shortcomings however, including heterogeneity of animal origin, low safety, low proportions of effective antibodies, limited supply, and poor batch-to-batch consistency. Antisera contain multiple neutralizing antibody components (Bell et al., 2004; Goldsmith et al., 2004; Davies et al., 2005, 2007; He et al., 2007; Benhnia et al., 2008). In vaccine studies immunization with subunit vaccines of A27/L1 (MV particles) and B5/A33 (EV particles) can protect mice and rhesus monkeys from poxvirus challenge (Hooper et al., 2003, 2004; Sakhatskyy et al., 2006). A33, B5, and L1 fusion proteins can also protect mice from lethal doses of virus infection (Fogg et al., 2004). Therefore, to obtain a similar or better therapeutic effect than that derived from antiserum, it is best to combine two or more antibodies targeting both EV and MV proteins. Two human monoclonal antibodies obtained from transgenic mice, hV26 and h101, recognized the H3 protein of MV and the B5 protein of EV, respectively (McCausland et al., 2010). A dose of 20 μg hV26 was as effective as 1.25 mg antiserum in the treatment of SCID mice. The efficacy of 50 μg h101 was similar to that of 1.25 mg antiserum, and the lowest dose of 25 μg antibody was superior to 1.25 mg VIG in terms of body weight loss and clinical score. In an *in vivo* evaluation of antibody combinations 50% of mice were protected by 50 μg mAb, 30% of mice were protected by 25 μg mAb, and all mice died in the control group and the 1.25 mg antiserum group.

With the development of human antibody library and site-specific integration technology, it is possible to generate recombinant polyclonal antibodies with all the advantages of antiserum and mAbs. Moreover, recombinant polyclonal antibodies have the advantage of batch-to-batch stability, making them the best choice for treating complex infectious diseases and cancers (Haurum and Bregenholt, 2005). The company Symphogen (Lyngby, Denmark) is currently working on recombinant polyclonal antibody drugs. The first fully human recombinant polyclonal antibody formulation, Sym001 against RhD, is composed of 25 antibodies. A phase II clinical trial was done in 2012 in which Sym001 was used for the treatment of hemolytic diseases in newborns, and congenital thrombocytopenic purpura. Several other recombinant polyclonal antibody drugs are in various stages of development. These include the anti-VACV recombinant polyclonal antibody formulation Sym002 (Haurum, 2006), anti-RSV Sym003, anti-*Pseudomonas aeruginosa* Sym006, Sym008, and Sym009 (all against infectious diseases with undisclosed targets), anti-EGFR Sym004 for tumor treatment (of which a phase II clinical trial is soon to commence), and the anti-Her family member Sym013.

4. Conclusion

Smallpox is a severe infectious disease caused by the variola virus. Traditional vaccinations should usually be injected before exposure to viruses, and sometimes the vaccines might have unpredictable side effects. Human-sourced antiserum supply is limited, and its anti-viral efficacy is insufficient because of the low proportion of effective antibodies (Hopkins and Lane, 2004; Wittek, 2006). Thus, the development of anti-smallpox antibodies is worthwhile. To date the development of mAbs against smallpox has yielded numerous drug candidates with good efficacy *in vivo* and *in vitro*, and notably antibody cocktails targeting multiple epitopes have proven more effective than monoclonal antibodies alone. Given epitope escape caused by virus mutation, the development of multivalent antibody drugs capable of recognizing multiple epitopes will be beneficial for treating viral infections. The neutralizing epitopes of vaccinia virus reviewed herein could be used as candidate fragments for epitope combinations. Moreover, we suggest that epitope combinations should include both EV and MV proteins, such as those targeted by anti-B5 and anti-L1 antibodies, to better block the transmission of the virus between and within individuals. With continued research, new

neutralizing epitopes may be discovered. The study of epitopes, their associated mechanisms and antigenicity, and their application has important practical significance with respect to preparing for potential bioterrorism involving the smallpox virus, and with regard to preventing and treating similar infectious pathogens such as severe acute respiratory syndrome viruses, H1N1 and H5N1 influenza strains, and West Nile virus.

Author contributions

FP: Writing – original draft, Writing – review & editing. NH: Writing – original draft, Writing – review & editing. YL: Writing – original draft. CX: Writing – original draft. LL: Writing – review & editing. XL: Writing – review & editing. JW: Writing – review & editing. GC: Writing – review & editing. HX: Writing – review & editing. CL: Writing – review & editing. BS: Writing – original draft, Writing – review & editing. JF: Writing – original draft, Writing – review & editing. CQ: Writing – original draft, Writing – review & editing.

Funding

This work was supported by the National Natural Sciences Foundation of China (Grant No. 31771010).

Conflict of interest

The authors declare that the research was conducted in the absence of any commercial or financial relationships that could be construed as a potential conflict of interest.

Publisher's note

References

Addeo, A., Friedlaender, A., Giovannetti, E., Russo, A., De Miguel-Perez, D., Arrieta, O., et al. (2021). A new generation of vaccines in the age of immunotherapy. *Curr. Oncol. Rep.* 23:137. doi: 10.1007/s11912-021-01130-x

Aldaz-Carroll, L., Whitbeck, J. C., Ponce de Leon, M., Lou, H., Hirao, L., Isaacs, S. N., et al. (2005). Epitope-mapping studies define two major neutralization sites on the vaccinia virus extracellular enveloped virus glycoprotein B5R 49. *J. Virol.* 79, 6260–6271. doi: 10.1128/JVI.79.10.6260-6271.2005

Aldaz-Carroll, L., Xiao, Y., Whitbeck, J. C., de Leon, M. P., Lou, H., Kim, M., et al. (2007). Major neutralizing sites on vaccinia virus glycoprotein B5 are exposed differently on variola virus ortholog B6 15. *J. Virol.* 81, 8131–8139. doi: 10.1128/JVI.00374-07

Amanna, I. J., Slifka, M. K., and Crotty, S. (2006). Immunity and immunological memory following smallpox vaccination. *Immunol. Rev.* 211, 320–337. doi: 10.1111/j.0105-2896.2006.00392.x

Beachkofsky, T. M., Carrizales, S. C., Bidinger, J. J., Hrncir, D. E., Whittemore, D. E., and Hivnor, C. M. (2010). Adverse events following smallpox vaccination with ACAM2000 in a military population. *Arch. Dermatol.* 146, 656–661. doi: 10.1001/archdermatol.2010.46

Bell, E., Shamim, M., Whitbeck, J. C., Sfyroera, G., Lambris, J. D., and Isaacs, S. N. (2004). Antibodies against the extracellular enveloped virus B5R protein are mainly responsible for the EEV neutralizing capacity of vaccinia immune globulin 54. *Virology* 325, 425–431. doi: 10.1016/j.virol.2004.05.004

Benhnia, M. R., McCausland, M. M., Moyron, J., Laudenslager, J., Granger, S., Rickert, S., et al. (2009). Vaccinia virus extracellular enveloped virion neutralization in vitro and protection in vivo depend on complement 53. *J. Virol.* 83, 1201–1215. doi: 10.1128/JVI.01797-08

Benhnia, M. R., McCausland, M. M., Su, H. P., Singh, K., Hoffmann, J., Davies, D. H., et al. (2008). Redundancy and plasticity of neutralizing antibody responses are cornerstone attributes of the human immune response to the smallpox vaccine 73. *J. Virol.* 82, 3751–3768. doi: 10.1128/JVI.02244-07

Bisht, H., Weisberg, A. S., and Moss, B. (2008). Vaccinia virus l1 protein is required for cell entry and membrane fusion 46. *J. Virol.* 82, 8687–8694. doi: 10.1128/JVI.00852-08

Blouch, R. E., Byrd, C. M., and Hruby, D. E. (2005). Importance of disulphide bonds for vaccinia virus L1R protein function 62. *Virol. J.* 2:91. doi: 10.1186/1743-422X-2-91

Breiman, A., Carpentier, D. C. J., Ewles, H. A., and Smith, G. L. (2013). Transport and stability of the vaccinia virus A34 protein is affected by the A33 protein. *J. Gen. Virol.* 94, 720–725. doi: 10.1099/vir.0.049486-0

Breiman, A., and Smith, G. L. (2010). Vaccinia virus B5 protein affects the glycosylation, localization and stability of the A34 protein. *J. Gen. Virol.* 91, 1823–1827. doi: 10.1099/vir.0.020677-0

Chen, Z., Earl, P., Americo, J., Damon, I., Smith, S. K., Yu, F., et al. (2007). Characterization of chimpanzee/human monoclonal antibodies to vaccinia virus A33 glycoprotein and its variola virus homolog in vitro and in a vaccinia virus mouse protection model 58. *J. Virol.* 81, 8989–8995. doi: 10.1128/JVI.00906-07

Chen, Z., Earl, P., Americo, J., Damon, I., Smith, S. K., Zhou, Y. H., et al. (2006). Chimpanzee/human mAbs to vaccinia virus B5 protein neutralize vaccinia and smallpox viruses and protect mice against vaccinia virus 56. *Proc. Natl. Acad. Sci. U. S. A.* 103, 1882–1887. doi: 10.1073/pnas.0510598103

Chung, C. S., Hsiao, J. C., Chang, Y. S., and Chang, W. (1998). A27L protein mediates vaccinia virus interaction with cell surface heparan sulfate 40. *J. Virol.* 72, 1577–1585. doi: 10.1128/JVI.72.2.1577-1585.1998

Condit, R. C., Moussatche, N., and Traktman, P. (2006). In a nutshell: structure and assembly of the vaccinia virion. *Adv. Virus Res.* 66, 31–124. doi: 10.1016/S0065-3527(06)66002-8

Davies, D. H., McCausland, M. M., Valdez, C., Huynh, D., Hernandez, J. E., Mu, Y., et al. (2005). Vaccinia virus H3L envelope protein is a major target of neutralizing antibodies in humans and elicits protection against lethal challenge in mice 33. *J. Virol.* 79, 11724–11733. doi: 10.1128/JVI.79.18.11724-11733.2005

Davies, D. H., Molina, D. M., Wrammert, J., Miller, J., Hirst, S., Mu, Y., et al. (2007). Proteome-wide analysis of the serological response to vaccinia and smallpox 26. *Proteomics* 7, 1678–1686. doi: 10.1002/pmic.200600926

Engelstad, M., and Smith, G. L. (1993). The vaccinia virus 42-kDa envelope protein is required for the envelopment and egress of extracellular virus and for virus virulence 50. *Virology* 194, 627–637. doi: 10.1006/viro.1993.1302

Fang, M., Cheng, H., Dai, Z., Bu, Z., and Sigal, L. J. (2006). Immunization with a single extracellular enveloped virus protein produced in bacteria provides partial protection from a lethal orthopoxvirus infection in a natural host 16. *Virology* 345, 231–243. doi: 10.1016/j.virol.2005.09.056

Fogg, C., Lustig, S., Whitbeck, J. C., Eisenberg, R. J., Cohen, G. H., and Moss, B. (2004). Protective immunity to vaccinia virus induced by vaccination with multiple recombinant outer membrane proteins of intracellular and extracellular virions 19. *J. Virol.* 78, 10230–10237. doi: 10.1128/JVI.78.19.10230-10237.2004

Fogg, C. N., Americo, J. L., Earl, P. L., Resch, W., Aldaz-Carroll, L., Eisenberg, R. J., et al. (2008). Disparity between levels of in vitro neutralization of vaccinia virus by antibody to the A27 protein and protection of mice against intranasal challenge 70. *J. Virol.* 82, 8022–8029. doi: 10.1128/JVI.00568-08

Froude, J. W., Stiles, B., Pelat, T., and Thullier, P. (2011). Antibodies for biodefense 57. *MAbs* 3, 517–527. doi: 10.4161/mabs.3.6.17621

Fulginiti, V. A., Papier, A., Lane, J. M., Neff, J. M., Henderson, D. A., Henderson, D. A., et al. (2003). Smallpox vaccination: a review, part II. Adverse events. *Clin. Infect. Dis.* 37, 251–271. doi: 10.1086/375825

Galmiche, M. C., Goenaga, J., Wittek, R., and Rindisbacher, L. (1999). Neutralizing and protective antibodies directed against vaccinia virus envelope antigens 5. *Virology* 254, 71–80. doi: 10.1006/viro.1998.9516

Goldsmith, J. C., Eller, N., Mikolajczyk, M., Manischewitz, J., Golding, H., and Scott, D. E. (2004). Intravenous immunoglobulin products contain neutralizing antibodies to vaccinia 74. *Vox Sang.* 86, 125–129. doi: 10.1111/j.0042-9007.2004.00397.x

Hansel, T. T., Kropshofer, H., Singer, T., Mitchell, J. A., and George, A. J. (2010). The safety and side effects of monoclonal antibodies 6. *Nat. Rev. Drug Discov.* 9, 325–338. doi: 10.1038/nrd3003

Haurum, J., and Bregenholt, S. (2005). Recombinant polyclonal antibodies: therapeutic antibody technologies come full circle 77. *IDrugs* 8, 404–409.

Haurum, J. S. (2006). Recombinant polyclonal antibodies: the next generation of antibody therapeutics? 78. *Drug Discov. Today* 11, 655–660. doi: 10.1016/j.drudis.2006.05.009

He, Y., Manischewitz, J., Meseda, C. A., Merchlinsky, M., Vassell, R. A., Sirota, L., et al. (2007). Antibodies to the A27 protein of vaccinia virus neutralize and protect against infection but represent a minor component of Dryvax vaccine--induced immunity 69. *J. Infect. Dis.* 196, 1026–1032. doi: 10.1086/520936

Hooper, J. W., Custer, D. M., and Thompson, E. (2003). Four-gene-combination DNA vaccine protects mice against a lethal vaccinia virus challenge and elicits appropriate antibody responses in nonhuman primates 17. *Virology* 306, 181–195. doi: 10.1016/s0042-6822(02)00038-7

Hooper, J. W., Thompson, E., Wilhelmsen, C., Zimmerman, M., Ichou, M. A., Steffen, S. E., et al. (2004). Smallpox DNA vaccine protects nonhuman primates against lethal monkeypox 75. *J. Virol.* 78, 4433–4443. doi: 10.1128/jvi.78.9.4433-4443.2004

Hopkins, R. J., and Lane, J. M. (2004). Clinical efficacy of intramuscular vaccinia immune globulin: a literature review. *Clin. Infect. Dis.* 39, 819–826. doi: 10.1086/422999

Howard, A. R., Senkevich, T. G., and Moss, B. (2008). Vaccinia virus A26 and A27 proteins form a stable complex tethered to mature virions by association with the A17 transmembrane protein 68. *J. Virol.* 82, 12384–12391. doi: 10.1128/JVI.01524-08

Hsiao, J. C., Chung, C. S., and Chang, W. (1999). Vaccinia virus envelope D8L protein binds to cell surface chondroitin sulfate and mediates the adsorption of intracellular mature virions to cells 43. *J. Virol.* 73, 8750–8761. doi: 10.1128/JVI.73.10.8750-8761.1999

Ichihashi, Y., and Oie, M. (1996). Neutralizing epitope on penetration protein of vaccinia virus 31. *Virology* 220, 491–494. doi: 10.1006/viro.1996.0337

Ichihashi, Y., Takahashi, T., and Oie, M. (1994). Identification of a vaccinia virus penetration protein 63. *Virology* 202, 834–843. doi: 10.1006/viro.1994.1405

Kaever, T., Matho, M. H., Meng, X., Crickard, L., Schlossman, A., Xiang, Y., et al. (2016). Linear epitopes in vaccinia virus A27 are targets of protective antibodies induced by vaccination against smallpox. *J. Virol.* 90, 4334–4345. doi: 10.1128/JVI.02878-15

Kaever, T., Meng, X., Matho, M. H., Schlossman, A., Li, S., Sela-Culang, I., et al. (2014). Potent neutralization of vaccinia virus by divergent murine antibodies targeting a common site of vulnerability in L1 protein. *J. Virol.* 88, 11339–11355. doi: 10.1128/JVI.01491-14

Kennedy, J. S., and Greenberg, R. N. (2009). IMVAMUNE: modified vaccinia Ankara strain as an attenuated smallpox vaccine. *Expert Rev. Vaccines* 8, 13–24. doi: 10.1586/14760584.8.1.13

Lefkowitz, E. J., Upton, C., Changayil, S. S., Buck, C., Traktman, P., and Buller, R. M. (2005). Poxvirus bioinformatics resource center: a comprehensive Poxviridae informational and analytical resource. *Nucleic Acids Res.* 33, D311–D316. doi: 10.1093/nar/gki110

Lin, C. L., Chung, C. S., Heine, H. G., and Chang, W. (2000). Vaccinia virus envelope H3L protein binds to cell surface heparan sulfate and is important for intracellular mature virion morphogenesis and virus infection in vitro and in vivo 14. *J. Virol.* 74, 3353–3365. doi: 10.1128/jvi.74.7.3353-3365.2000

Matho, M. H., De Val, N., Miller, G. M., Brown, J., Schlossman, A., Meng, X., et al. (2014). Murine anti-vaccinia virus D8 antibodies target different epitopes and differ in their ability to block D8 binding to CS-E. *PLoS Pathog.* 10:e1004495. doi: 10.1371/journal.ppat.1004495

Matho, M. H., Maybeno, M., Benhnia, M. R., Becker, D., Meng, X., Xiang, Y., et al. (2012). Structural and biochemical characterization of the vaccinia virus envelope protein D8 and its recognition by the antibody LA5 65. *J. Virol.* 86, 8050–8058. doi: 10.1128/JVI.00836-12

Matho, M. H., Schlossman, A., Gilchuk, I. M., Miller, G., Mikulski, Z., Hupfer, M., et al. (2018). Structure-function characterization of three human antibodies targeting the vaccinia virus adhesion molecule D8. *J. Biol. Chem.* 293, 390–401. doi: 10.1074/jbc.M117.814541

Matho, M. H., Schlossman, A., Meng, X., Benhnia, M. R., Kaever, T., Buller, M., et al. (2015). Structural and functional characterization of anti-A33 antibodies reveal a potent cross-species Orthopoxviruses neutralizer. *PLoS Pathog.* 11:e1005148. doi: 10.1371/journal.ppat.1005148

Mayr, A. (2003). Smallpox vaccination and bioterrorism with pox viruses 70. *Comp. Immunol. Microbiol. Infect. Dis.* 26, 423–430. doi: 10.1016/S0147-9571(03)00025-0

McCausland, M. M., Benhnia, M. R., Crickard, L., Laudenslager, J., Granger, S. W., Tahara, T., et al. (2010). Combination therapy of vaccinia virus infection with human anti-H3 and anti-B5 monoclonal antibodies in a small animal model 76. *Antivir. Ther.* 15, 661–675. doi: 10.3851/IMP1573

Meng, X., Zhong, Y., Embry, A., Yan, B., Lu, S., Zhong, G., et al. (2011). Generation and characterization of a large panel of murine monoclonal antibodies against vaccinia virus 25. *Virology* 409, 271–279. doi: 10.1016/j.virol.2010.10.019

Meyer, H., Ehmann, R., and Smith, G. L. (2020). Smallpox in the post-eradication era 70. *Viruses* 12:138. doi: 10.3390/v12020138

Monticelli, S. R., Earley, A. K., Stone, R., Norbury, C. C., and Ward, B. M. (2020). Vaccinia virus glycoproteins A33, A34, and B5 form a complex for efficient endoplasmic reticulum to trans-Golgi network transport. *J. Virol.* 94:e02155. doi: 10.1128/JVI.02155-19

Mucker, E. M., Lindquist, M., and Hooper, J. W. (2020). Particle-specific neutralizing activity of a monoclonal antibody targeting the poxvirus A33 protein reveals differences between cell associated and extracellular enveloped virions. *Virology* 544, 42–54. doi: 10.1016/j.virol.2020.02.004

Nafziger, S. D. (2005). Smallpox. *Crit. Care Clin.* 21, 739–746. doi: 10.1016/j.ccc.2005.06.004

Nalca, A., and Zumbrun, E. E. (2010). ACAM 2000: the new smallpox vaccine for United States strategic National Stockpile. *Drug Des. Devel. Ther.* 4, 71–79. doi: 10.2147/dddt.s3687

Nelson, G. E., Sisler, J. R., Chandran, D., and Moss, B. (2008). Vaccinia virus entry/fusion complex subunit A28 is a target of neutralizing and protective antibodies 37. *Virology* 380, 394–401. doi: 10.1016/j.virol.2008.08.009

Paran, N., Lustig, S., Zvi, A., Erez, N., Israely, T., Melamed, S., et al. (2013). Active vaccination with vaccinia virus A33 protects mice against lethal vaccinia and ectromelia viruses but not against cowpoxvirus; elucidation of the specific adaptive immune response. *Virol. J.* 10:229. doi: 10.1186/1743-422X-10-229

Parrino, J., and Graham, B. S. (2006). Smallpox vaccines: Past, present, and future 72. *J. Allergy Clin. Immunol.* 118, 1320–1326. doi: 10.1016/j.jaci.2006.09.037

Pennington, H. (2003). Smallpox and bioterrorism 3. *Bull. World Health Organ.* 81, 762–767.

Rao, A. K., Petersen, B. W., Whitehill, F., Razeq, J. H., Isaacs, S. N., Merchlinsky, M. J., et al. (2022). Use of JYNNEOS (smallpox and Monkeypox vaccine, live, nonreplicating) for Preexposure vaccination of persons at risk for occupational exposure to Orthopoxviruses: recommendations of the advisory committee on immunization practices-United States, 2022. *MMWR Morb. Mortal. Wkly Rep.* 71, 734–742. doi: 10.15585/mmwr.mm7122e1

Roberts, K. L., and Smith, G. L. (2008). Vaccinia virus morphogenesis and dissemination 2. *Trends Microbiol.* 16, 472–479. doi: 10.1016/j.tim.2008.07.009

Rodriguez, J. F., Janeczko, R., and Esteban, M. (1985). Isolation and characterization of neutralizing monoclonal antibodies to vaccinia virus 4. *J. Virol.* 56, 482–488. doi: 10.1128/JVI.56.2.482-488.1985

Russo, A. T., Grosenbach, D. W., Chinsangaram, J., Honeychurch, K. M., Long, P. G., Lovejoy, C., et al. (2021). An overview of tecovirimat for smallpox treatment and expanded anti-orthopoxvirus applications. *Expert Rev. Anti-Infect. Ther.* 19, 331–344. doi: 10.1080/14787210.2020.1819791

Sakhatskyy, P., Wang, S., Chou, T. H., and Lu, S. (2006). Immunogenicity and protection efficacy of monovalent and polyvalent poxvirus vaccines that include the D8 antigen 36. *Virology* 355, 164–174. doi: 10.1016/j.virol.2006.07.017

Senkevich, T. G., Ward, B. M., and Moss, B. (2004). Vaccinia virus entry into cells is dependent on a virion surface protein encoded by the A28L gene 45. *J. Virol.* 78, 2357–2366. doi: 10.1128/jvi.78.5.2357-2366.2004

Shinoda, K., Wyatt, L. S., and Moss, B. (2010). The neutralizing antibody response to the vaccinia virus A28 protein is specifically enhanced by its association with the H2 protein 71. *Virology* 405, 41–49. doi: 10.1016/j.virol.2010.05.025

Su, H. P., Golden, J. W., Gittis, A. G., Hooper, J. W., and Garboczi, D. N. (2007). Structural basis for the binding of the neutralizing antibody, 7D11, to the poxvirus L1 protein 64. *Virology* 368, 331–341. doi: 10.1016/j.virol.2007.06.042

Theves, C., Crubezy, E., and Biagini, P. (2016). History of smallpox and its spread in human populations. *Microbiol. Spectr.* 4:4. doi: 10.1128/microbiolspec.PoH-0004-2014

Vázquez, M̀.. I., and Esteban, M. (1999). Identification of functional domains in the 14-kilodalton envelope protein (A27L) of vaccinia virus 42. *J. Virol.* 73, 9098–9109. doi: 10.1128/JVI.73.11.9098-9109.1999

Wallengren, K., Risco, C., Krijnse-Locker, J., Esteban, M., and Rodriguez, D. (2001). The A17L gene product of vaccinia virus is exposed on the surface of IMV 38. *Virology* 290, 143–152. doi: 10.1006/viro.2001.1131

Walper, S. A., Liu, J. L., Zabetakis, D., Anderson, G. P., and Goldman, E. R. (2014). Development and evaluation of single domain antibodies for vaccinia and the L1 antigen. *PLoS One* 9:e106263. doi: 10.1371/journal.pone.0106263

Wang, D. R., Hsiao, J. C., Wong, C. H., Li, G. C., Lin, S. C., Yu, S. S., et al. (2014). Vaccinia viral protein A27 is anchored to the viral membrane via a cooperative interaction with viral membrane protein A17. *J. Biol. Chem.* 289, 6639–6655. doi: 10.1074/jbc.M114.547372

Wittek, R. (2006). Vaccinia immune globulin: current policies, preparedness, and product safety and efficacy. *Int. J. Infect. Dis.* 10, 193–201. doi: 10.1016/j.ijid.2005.12.001

Wolffe, E. J., Vijaya, S., and Moss, B. (1995). A myristylated membrane protein encoded by the vaccinia virus L1R open reading frame is the target of potent neutralizing monoclonal antibodies 32. *Virology* 211, 53–63. doi: 10.1006/viro.1995.1378

Xu, C., Meng, X., Yan, B., Crotty, S., Deng, J., and Xiang, Y. (2011). An epitope conserved in orthopoxvirus A13 envelope protein is the target of neutralizing and protective antibodies 67. *Virology* 418, 67–73. doi: 10.1016/j.virol.2011.06.029

Zajonc, D. M. (2017). Antibody recognition of Immunodominant vaccinia virus envelope proteins 151. *Subcell. Biochem.* 83, 103–126. doi: 10.1007/978-3-319-46503-6_4

frontiers | Frontiers in Microbiology

TYPE Review
PUBLISHED 20 November 2023
DOI 10.3389/fmicb.2023.1321116

OPEN ACCESS

EDITED BY
Cécile E. Malnou,
Université Toulouse III Paul Sabatier, France

REVIEWED BY
Hang Su,
Albert Einstein College of Medicine,
United States
Beatrice Mercorelli,
University of Padua, Italy

*CORRESPONDENCE
Claire Gourin
✉ claire.gourin@unilim.fr
Sophie Alain
✉ sophie.alain@unilim.fr
Sébastien Hantz
✉ sebastien.hantz@unilim.fr

RECEIVED 13 October 2023
ACCEPTED 06 November 2023
PUBLISHED 20 November 2023

CITATION
Gourin C, Alain S and Hantz S (2023) Anti-CMV therapy, what next? A systematic review. *Front. Microbiol.* 14:1321116. doi: 10.3389/fmicb.2023.1321116

Anti-CMV therapy, what next? A systematic review

Claire Gourin[1]*, Sophie Alain[1,2]* and Sébastien Hantz[1,2]*

[1]INSERM, CHU Limoges, University of Limoges, RESINFIT, Limoges, France, [2]CHU Limoges, Laboratoire de Bactériologie-Virologie-Hygiène, National Reference Center for Herpesviruses, Limoges, France

Human cytomegalovirus (HCMV) is one of the main causes of serious complications in immunocompromised patients and after congenital infection. There are currently drugs available to treat HCMV infection, targeting viral polymerase, whose use is complicated by toxicity and the emergence of resistance. Maribavir and letermovir are the latest antivirals to have been developed with other targets. The approval of letermovir represents an important innovation for CMV prevention in hematopoietic stem cell transplant recipients, whereas maribavir allowed improving the management of refractory or resistant infections in transplant recipients. However, in case of multidrug resistance or for the prevention and treatment of congenital CMV infection, finding new antivirals or molecules able to inhibit CMV replication with the lowest toxicity remains a critical need. This review presents a range of molecules known to be effective against HCMV. Molecules with a direct action against HCMV include brincidofovir, cyclopropavir and anti-terminase benzimidazole analogs. Artemisinin derivatives, quercetin and baicalein, and anti-cyclooxygenase-2 are derived from natural molecules and are generally used for different indications. Although they have demonstrated indirect anti-CMV activity, few clinical studies were performed with these compounds. Immunomodulating molecules such as leflunomide and everolimus have also demonstrated indirect antiviral activity against HCMV and could be an interesting complement to antiviral therapy. The efficacy of anti-CMV immunoglobulins are discussed in CMV congenital infection and in association with direct antiviral therapy in heart transplanted patients. All molecules are described, with their mode of action against HCMV, preclinical tests, clinical studies and possible resistance. All these molecules have shown anti-HCMV potential as monotherapy or in combination with others. These new approaches could be interesting to validate in clinical trials.

KEYWORDS

cytomegalovirus, letermovir, maribavir, direct antivirals, indirect antivirals, immunomodulatory molecules, immunoglobulins

1 Introduction

Human cytomegalovirus (CMV) is an opportunistic pathogen in the immunocompromised host. Not only in transplant recipients, but also in AIDS patients or highly immunocompromised patients with congenital immunodeficiency or immunosuppressive biotherapies. Such infections can lead to graft rejection and organ damages (Kotton et al., 2018; Ljungman et al., 2019). Due to the use of preventive strategies, either preemptive treatment or prophylaxis, CMV disease frequency has decreased. But in solid organ recipients, late disease may occur in up to 18% of patients after stopping prophylaxis (Kotton et al., 2018). In stem cell recipients, it decreased from 10–40% to 2–3% in randomized trials but 5–10% in real life cohorts despite efficient preemptive

treatment (Ljungman et al., 2019). Currently, available antivirals are limited to virostatic polymerase inhibitors (ganciclovir, its oral prodrug valganciclovir, cidofovir and foscarnet). Neutropenia limits efficacy of ganciclovir or valganciclovir and this hematological toxicity prevents its use as a prophylaxis in the stem cell recipients. Cidofovir and foscarnet are highly nephrotoxic and restricted to second line treatment. The second limitation of these molecules is the emergence of resistance, favored by prolonged treatments in highly immunocompromised hosts, and use of lower doses due to renal impairment (Razonable et al., 2019).

Congenital CMV infection (cCMV) is also a leading cause of hearing loss and neurological sequelae in children. During pregnancy, the prevalence of primary CMV infection ranges from 1 to 2% in the United States and Western Europe (Hyde et al., 2010; Leruez-Ville et al., 2020), with an average cCMV birth prevalence of 0.65% (Kenneson and Cannon, 2007). If the primary maternal infection occurs during pregnancy, especially during the first trimester, more severe sequelae, including complete hearing loss, are to be feared. The risk of maternal transmission occurs in 30–40% of case with CMV primary infection. Thus, during the first trimester of pregnancy, it is essential to prevent viral transmission to the fetus to avoid neurological disability in newborns (Ornoy and Diav-Citrin, 2006; Ross et al., 2006; Chatzakis et al., 2020). Among infected neonates, 12.7% will have symptoms at birth and 40 to 58% develop permanent sequelae. As a whole, long-term sequelae from sensorineural hearing loss to neurodevelopmental disabilities may occur in 17 to 19% of infected newborns, 51 to 57% of them following maternal primary infection (Dollard et al., 2007; Leruez-Ville and Ville, 2020). Ganciclovir (GCV) and its prodrug valganciclovir (VGCV), foscarnet (FOS) and cidofovir (CDV), are proscribed during pregnancy, due to their toxicity (e.g., neutropenia, nephrotoxicity). Although a randomized study has demonstrated the efficacy of a high dose (8 g per day) of valaciclovir (VACV), a prodrug of acyclovir, in preventing transmission, only 50% of periconceptional or 1st trimester primary infection transmissions were avoided, and more efficient anti-CMV drugs are thus needed (Shahar-Nissan et al., 2020). Treatment of symptomatic newborns for 6 weeks GCV or 6 months with VGCV was shown to improve hearing skills, and is now recommended, although 49 to 63% of the treated neonates developed grade 3 or 4 neutropenia with treatment (Kimberlin et al., 2015).

The burden of long-term therapies for immunocompromised patients, and the emergence of new resistance mechanisms (Chou, 2020), the unmet need for low toxic treatments to prevent or cure cCMV, make it essential to find new antiviral targets and to develop new therapies, in order to treat CMV infections more efficiently while reducing side effects.

Recently, two antiviral drugs with new targets, high specificity and low toxicity, reached clinical development: letermovir targets the highly virus-specific terminase complex (UL56, UL98 and UL51) and maribavir inhibits the UL97 viral kinase. Letermovir (LMV) was approved in 2017 by the Food and Drug Administration (FDA) for the prophylaxis of CMV infection in hematopoietic stem cell transplant patients with high risk of CMV infections (Marty et al., 2017). This new antiviral inhibits the terminase complex, a viral component not found in human cells, thereby reducing its toxicity. Similarly, maribavir (MBV) was approved in 2021 for the treatment of adults and children presenting post-transplant CMV infections refractory or resistant to antivirals (Food and Drug Administration, 2021). It targets the viral kinase UL97 (Biron et al., 2002). Both LMV and MBV have a high oral bioavailability and a low toxicity profile. Nevertheless, resistance mutations have already been described with these new antivirals, making it crucial to continue to develop new therapies.

This is why it is necessary to find new molecules with an anti-CMV spectrum. In this context, this review summarizes the panel of molecules with antiviral activity, including direct inhibitors (brincidofovir, cyclopropavir, anti-terminase benzimidazole analogs), molecules acting through cellular pathways inhibition (artemisinin derivatives, flavonoids, leflunomide, everolimus, or anti Cox) and immunoglobulins (Figures 1, 2 and Table 1).

2 Newly approved antivirals target the late stage of the viral cycle

2.1 Letermovir

Letermovir (LMV; AIC246; Prevymis™; Figure 2), an antiviral of the quinazoline class, was developed by Aicuris and further marketed by Merck. LMV acts at the late stage of the viral cycle by direct inhibition of the human CMV terminase complex (Goldner et al., 2011). This viral terminase complex has no functional equivalent in the mammalian cells and the drug is therefore highly specific.

It appears to be very specific of CMV, and has a high activity against resistant strains to DNA polymerase inhibitors (Lischka et al., 2010). In 2017, LMV has been approved by the FDA for CMV prophylaxis in stem cell transplant patients seropositive for CMV (Marty et al., 2017).

2.1.1 Mechanism of action

LMV targets pUL56, the large subunit of the CMV terminase complex that cleaves DNA prior to encapsidation of the genome in neoformed capsids. In addition, it has high specificity against CMV, even if other herpesviruses also possess a terminase complex. This could possibly be explained by a particular mode of action, as LMV probably disrupts the interaction between the subunits of the terminase complex: pUL56, pUL89 and pUL51 unlike other antivirals, which often act by blocking functional domains. LMV has been shown to inhibit primarily the viral step of genome encapsidation (Lischka et al., 2010). Moreover, it was demonstrated that LMV prevents cleavage of concatemeric DNA into units of genomes and formation of CMV mature virions (Goldner et al., 2011).

2.1.2 Preclinical studies

Preclinical studies showed its very high antiviral activity (range: 1.6–5.1 nM; 1,000-fold more potent than GCV) against clinical and laboratory strains included refractory-resistant isolates to current drugs (Marschall et al., 2012) with low toxicity levels at high doses over the EC_{90}. LMV has a high specificity to HCMV and is well tolerated in various cell types with a mean selectivity index of 18,000. LMV has *in vivo* efficacy in a mouse xenograft model (Lischka et al., 2010) and shows an anti-CMV activity in histoculture of third trimester placenta (Hamilton et al., 2020). It reached concentrations above EC_{50} at the fetal face when perfused across a third trimester placenta (Faure Bardon et al., 2020). However, its efficacy during the

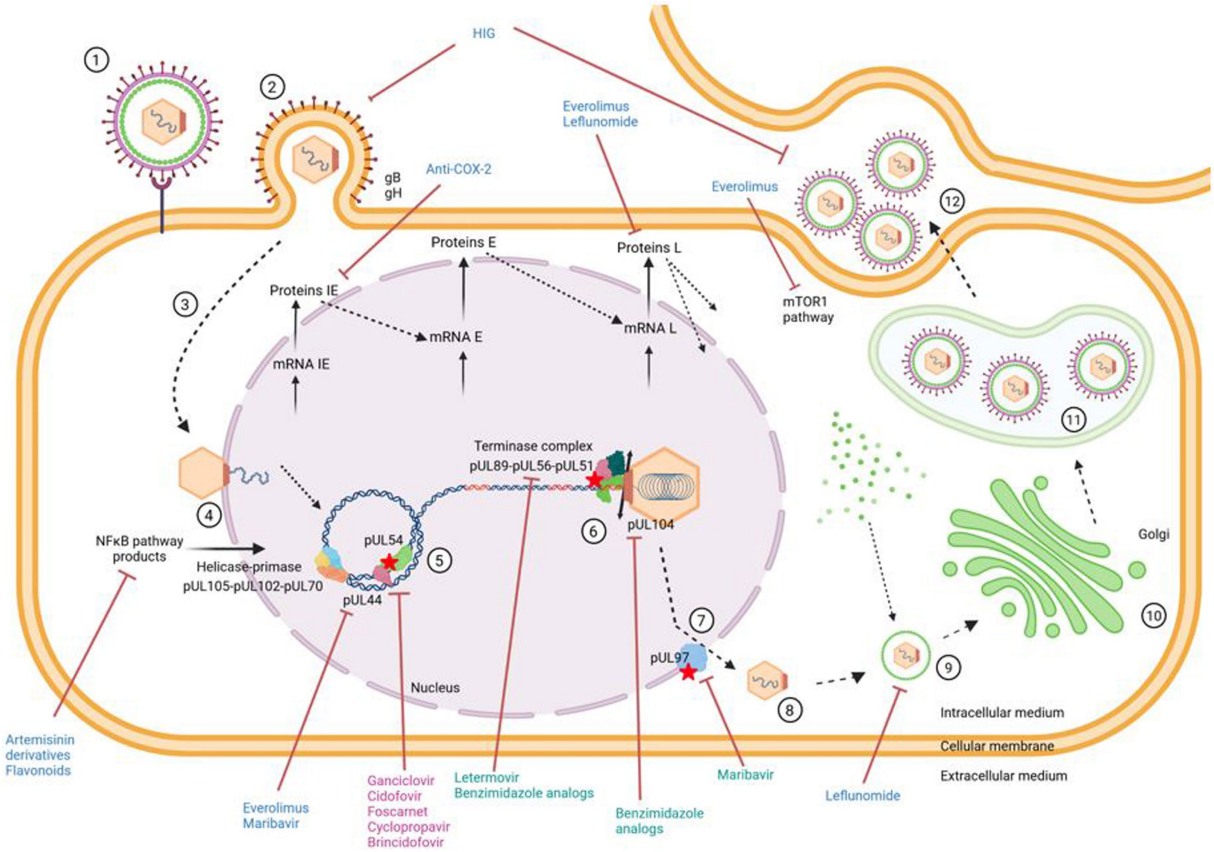

FIGURE 1
Antiviral targets in relication cycle of CMV. ① Virus attaches to cell. ② Entry of virus into cell and release of capsid into cytoplasm. ③ Migration of capsid to cell nucleus. ④ Release of viral genome from capsid through nuclear pore. ⑤ Replication of viral DNA by the rolling circle method using the viral polymerase pUL54. ⑥ Encapsidation of the genome into neoformed capsids via the encapsidation complex. ⑦ Nuclear exit. ⑧ Release of newly formed virions into cell cytoplasm. ⑨ Tegumentation of newly formed virions. ⑩ Passage of virions through Golgi apparatus. ⑪ Acquisition of a primary envelope and transport of virions in a vesicle to the extracellular medium. ⑫ Budding, release of infectious virus particles and infection of a new cell. Indirect antivirals, direct antivirals and antivirals targeting the viral polymerase are in blue, green and pink, respectively. Created with BioRender.com

first trimester is not yet validated. Drug combination assays showed additive effect and no synergistic toxicity with current CMV drugs and no effect with anti-HIV drugs (Wildum et al., 2015).

2.1.3 Clinical studies

LMV is a highly lipophilic molecule with a C_{max} of between 45 min and 2.25 h and a half-life of 12 h. After administration, LMV is highly protein-bound and eliminated via the biliary tract. The efficacy, safety and pharmacokinetic parameters of oral LMV were studied in a Phase IIa trial: LMV 40 mg twice daily or 80 mg once daily was administered to patients for 14 days as a preventive treatment against CMV infection in kidney and kidney/pancreas transplant recipients (Stoelben et al., 2014). This study demonstrated that all patients responded to LMV treatment. Chemaly et al. conducted a Phase IIb variable-dose prophylaxis trial in 2014: LMV was administered daily orally at 60 mg, 120 mg or 240 mg for 12 weeks post-transplant in CMV-seropositive allogeneic hematopoietic cell recipients. The incidence of prophylaxis failure (with or without virological failure) was significantly lower in the LMV-treated groups than in the placebo group (32% for the 120 mg group, 29% for the 240 mg group vs. 64%). The incidence of virological failure was lower in the 240 mg group (6%) than in the placebo group (36%). This study demonstrated that LMV was well tolerated and that a dose of 240 mg once daily was effective in suppressing viremia (Chemaly et al., 2014).

The Phase III prophylaxis trial (NCT02137772) evaluated the efficacy of a daily oral or intravenous dose of LMV of 480 mg/day (or 240 mg/day in patients taking ciclosporin) for 14 weeks after transplantation. A significant reduction in the number of patients developing CMV infection was observed. Indeed, at week 24, 38% of patients in the LMV group developed an HCMV infection versus 61% in the placebo group. In addition, the mortality rate was higher in the placebo group (16%) compared to the LMV group (10%). This study confirms the efficacy of LMV in the prophylaxis of CMV infection after HSCT in R+ patients (Marty et al., 2017). Used as primary and secondary prophylaxis in the French Compassionate Use Program (CUP) for high-risk patients, it was well tolerated and reduced the number of CMV infections compared with historical studies (Robin et al., 2020; Beauvais et al., 2022).

LMV has also been tested in case-series for prophylaxis or treatment in organ transplanted patients. It had good virologic outcomes and was well tolerated in patient with few side effects (Aryal et al., 2019; Veit et al., 2020; Linder et al., 2021). Recently, a large study conducted in 94 centers with kidney recipients showed that LMV was non-inferior to valganciclovir for prophylaxis of CMV disease for

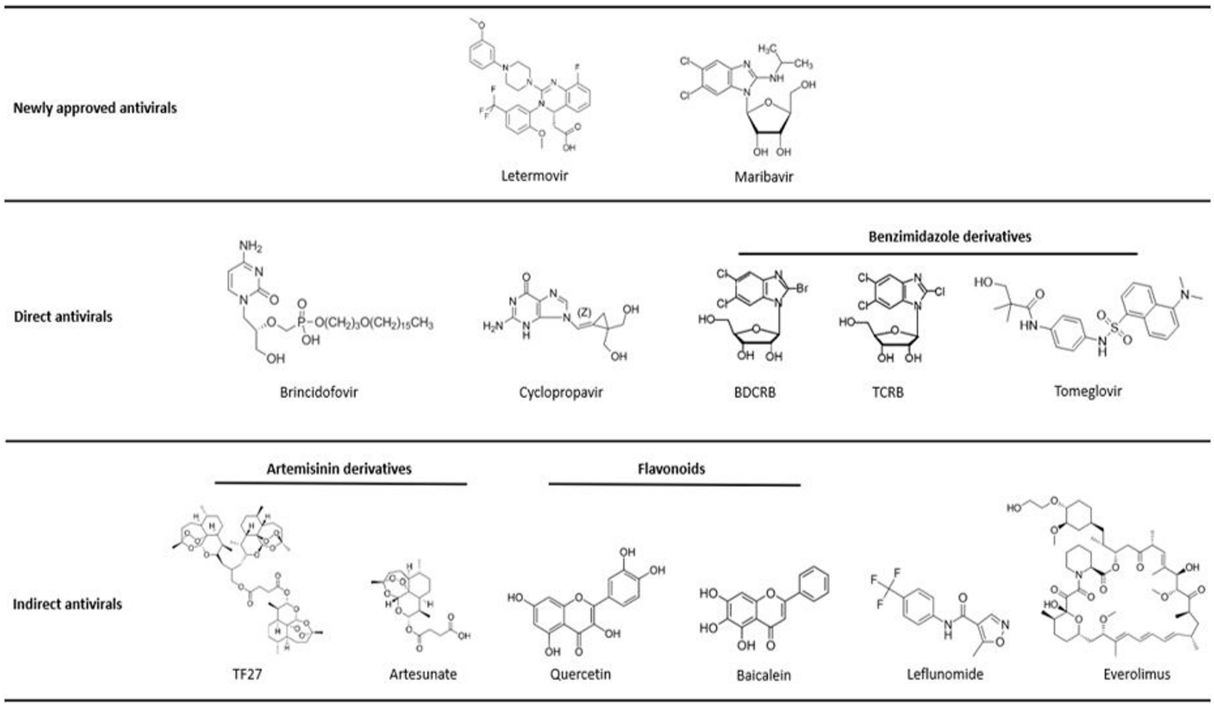

FIGURE 2
Molecule structures. Structures of chemical molecules with their corresponding order in the review. All molecules are classified as approved antivirals, molecules with direct antiviral activity or molecules with indirect antiviral activity.

52 weeks, with lower rates of leukopenia or neutropenia, arguing in favor of its use in this indication (Limaye et al., 2023).

2.1.4 Resistance

In less than 5 passages, the selection of resistant strains is rapidly achieved *in vitro* with UL56 mutations conferring high or absolute LMV resistance (Chou, 2017). *In vitro* studies have also revealed mutations in the genes encoding pUL51 and pUL89. In clinical trials, the first resistant isolate appeared after a sub-optimal dose of 60 mg/day (Chemaly et al., 2014; Lischka et al., 2016). Resistant mutants can emerge rapidly under LMV if treatment is interrupted or underdosed (Alain et al., 2020). pUL56 is the main target of LMV, which explains why mutations occur more frequently in this protein than in other proteins of the terminize complex (Cherrier et al., 2018; Frietsch et al., 2019; Alain et al., 2020). A new resistance mutation A95V in pUL51 was also described *in vivo* after LMV treatment in combination with a L257I mutation in pUL56 (Muller et al., 2022; Figure 3).

2.2 Maribavir

Maribavir (MBV; 1,263 W94; LIVTENCITY™) [formerly 1,263 W94, 5,6-dichloro-2-(isopropylamino)-1,β-l-ribofuranosyl-1-H-benzimidazole] (Figure 2) is an oral bioavailable benzimidazole riboside initially developed by Glaxo Smith Kline (Biron et al., 2002), then Viropharma, now marketed by Takeda Pharmaceuticals/a Shire company for treatment of refractory or resistant CMV infections. In November 2021, the FDA approved MBV for 400 mg twice a day-treatment of adults and children (12 years of age or older, weight > 35 kg) with post-transplant CMV infection/illness refractory/resistant to GCV, VGCV, CDV and FOS (Food and Drug Administration, 2021; Halpern-Cohen and Blumberg, 2022). In 2022, the European Commission approved MBV in the same indications.

2.2.1 Mechanism of action

Maribavir does not require activation or intracellular processing. Unlike other anti-CMV drugs, MBV targets the viral kinase *UL97* and its natural substrates, which are involved in the DNA replication and viral capsid nuclear egress (Biron et al., 2002; Hamirally et al., 2009; Prichard, 2009). This mechanism of action confers MBV an *in vitro* and *in vivo* activity against GCV, FOS and CDV resistant CMV strains (Biron et al., 2002; Drew et al., 2006). The combination of MBV and GCV is therefore not recommended, as GCV activation requires three phosphorylation, the first of which being mediated by pUL97. Indeed, MBV antagonizes anti-CMV effect of GCV by increasing the 50% inhibitory concentration (IC50) of a GCV-sensitive strain by 13 fold (Chou and Marousek, 2006).

MBV competitively inhibits pUL97 (Biron et al., 2002) and blocks the phosphorylation of several downstream proteins including cellular components and the viral proteins pp65 and pUL44 the DNA polymerase accessory protein (Prichard, 2009). Like Cdc2/Cyclin-dependent kinase 1 (CDK1) in CMV-uninfected cells, the viral kinase pUL97 phosphorylates nuclear lamina components (lamin A/C), facilitating the removal of mature virions from the nucleus. Consequently, MBV treatment results in the accumulation of immature virions in the nucleus (Hamirally et al., 2009). It also inhibits CMV DNA replication through pUL44 inhibition. *In vitro* drug combination assays showed additive effect with foscarnet, and synergy with artesunate (Morère et al., 2015). Additive effect was also observed with cidofovir or letermovir (quinazoline), while association

TABLE 1 Summary of molecules and their main characteristics.

Molecule	Preclinical testing		Clinical trials				EC50	EC90	Selectivity index (EC50/CC50)
	In vitro	*Ex vivo*	Animal model	Phase I	Phase II	Phase III			
Letermovir	Lischka et al. (2010) and Marschall et al. (2012)	-	Mouse xenograft (Lischka et al., 2010)		Chemaly et al. (2014), Stoelben et al. (2014), and Lischka et al. (2016)	NCT02137772 (Marty et al., 2017)	0.0038 ± 0.0009 µM (Lischka et al., 2010)	0.0051 ± 0.0014 µM (Lischka et al., 2010)	>18,000 (median SI) (Lischka et al., 2010)
Maribavir	Lu and Thomas (2000) and Chou et al. (2012a)	-	Mouse, rats, monkeys, guinea pig, rabbit, dog (Koszalka et al., 2002)	Wang et al. (2003), Swan et al. (2007), and Winston et al. (2008)	Papanicolaou et al. (2019), Maertens et al. (2020), and Song et al. (2023)	NCT02931539 (Avery et al., 2021)	0.54 ± 0.06 µM (Biron et al., 2002) 19.4 ± 18.6 (Williams et al., 2003)	-	13 (Williams et al., 2003)
Brincidofovir	Beadle et al. (2002)	-	Guinea pig Bravo et al., 2011 Monkeys, mice, rabbits, rats, cynomolgous monkeys	Painter et al. (2012)	NCT00942305 (Marty et al., 2013) NCT00942305 (Lanier et al., 2016)	NCT01769170 (Marty et al., 2019)	0.0009 µM (Beadle et al., 2002) 0.001 ± 0.001 µM (Williams-Aziz et al., 2005)	-	1×10^5 (Beadle et al., 2002)
Cyclopropavir	Kern et al. (2004a), Komazin-Meredith et al. (2014), Zhou et al. (2004), Kern et al. (2005), and Brooks and Bowlin (2013)	-	SCID mice (Bidanset et al., 2004; Kern et al., 2004a) dog, rat (Brooks and Bowlin, 2013)	(NTC01433835) (Brooks et al., 2015) (NCT02454699) (Rouphael et al., 2019)	-	-	1.2 ± 0.8 µM (Kern et al., 2005) 0.27–0.49 µM (Zhou et al., 2004)	-	1×10^5 (Beadle et al., 2002)
Flavonoids: Quercetin Baicalein	Cotin et al. (2012)	-	-	Polansky et al. (2016) and Polansky et al. (2018)	-	-	4.8 ± 1.2 (Cotin et al., 2012)	-	1.3 (Cotin et al., 2012)
	Cotin et al. (2012)	-	Rats, mouse (Lai et al., 2003; Dou et al., 2011; Tian et al., 2012)	Li et al. (2014) and Li et al. (2021)	-	-	2.2 ± 0.5 (Cotin et al., 2012)	-	3 (Cotin et al., 2012)
Anti-COX-2	Cotin et al. (2012), Andouard et al. (2021), and Baryawno et al. (2011)	Baryawno et al. (2011)	Mice (Baryawno et al., 2011)				8,6–22,1 ± 3,6–10,1 µM (Andouard et al., 2021)	-	3–10 (Andouard et al., 2021)

(Continued)

10.3389/fmicb.2023.1321116

TABLE 1 (Continued)

Molecule	Preclinical testing		Clinical trials				EC50	EC90	Selectivity index (EC50/CC50)
	In vitro	*Ex vivo*	Animal model	Phase I	Phase II	Phase III			
Artemisinin derivatives: Artesunate TF27	Hutterer et al. (2015)	-	mice, rats and dogs (Efferth et al., 2002; Kaptein et al., 2006)	Shapira et al. (2008) and Germi et al. (2014)	-	-	18.5 ± 5.2 µM (Arav-Boger et al., 2010) 3.9 ± 0.6 µM (Hutterer et al., 2015)	-	4 ± 2 (Arav-Boger et al., 2010)
	Hutterer et al. (2015)	Placental vili (Jacquet et al., 2020)	immunodefective mouse strain Rag−/− (Sonntag et al., 2019)	-	-	-	0.04 ± 0.01 µM (Reiter et al., 2015) 0.04 ± 0.01 µM (Hutterer et al., 2015)	0.08 ± 0.03 µM (Hutterer et al., 2015)	-
Benzimidazole analogs: BDCRB TRCB Tomeglovir	Townsend et al. (1995)	-	Guinea pig (Nixon and McVoy, 2004; Kern et al., 2004a; Ourahmane et al., 2018)	-	-	-	0.7 µM (Townsend et al., 1995) 0.31 ± 0.06 (Biron et al., 2002) 2.7 ± 0.8 (Evers et al., 2002) 0.4 ± 0.3 µM (Williams et al., 2003)	0.9 ± 0.2 (Evers et al., 2002)	425 (Williams et al., 2003)
	Townsend et al. (1995)	-		-	-	-	1.4 (Migawa et al., 1998) 2.9 µM (Townsend et al., 1995)	1.4 µM (Townsend et al., 1995)	-
	Evers et al. (2002), Reefschlaeger et al. (2001), and McSharry et al. (2001)	-	Guinea pigs (Schleiss et al., 2005) SCID mice (Reefschlaeger et al., 2001; Weber et al., 2001)	-	-	-	0.52 ± 0.14 µM (Reefschlaeger et al., 2001)	-	300 (Reefschlaeger et al., 2001)
Leflunomide	Waldman et al. (1999a)	-	Nude rats (Waldman et al., 1999a) Nude rats allograft (Chong et al., 2006)	Williams et al. (2002) and John et al. (2005)	-	-	40-60 µM (Waldman et al., 1999a)	-	-
Everolimus									
Immunoglobulins	Coste Mazeau et al. (2022), Germer et al. (2016), Miescher et al. (2015), and Schampera et al. (2017)	Placental vili (Coste Mazeau et al., 2022)	Guinea pig (Bia et al., 1980; Bratcher et al., 1995; Chatterjee et al., 2001; Schleiss, 2008) Mouse (Cekinović et al., 2008)	Alsuliman et al. (2018)	NCT00881517 (Revello et al., 2014; Chiaie et al., 2018)	NCT01376778 (Hughes et al., 2021)	0.024 µM (Coste Mazeau et al., 2022)	-	-

10.3389/fmicb.2023.1321116

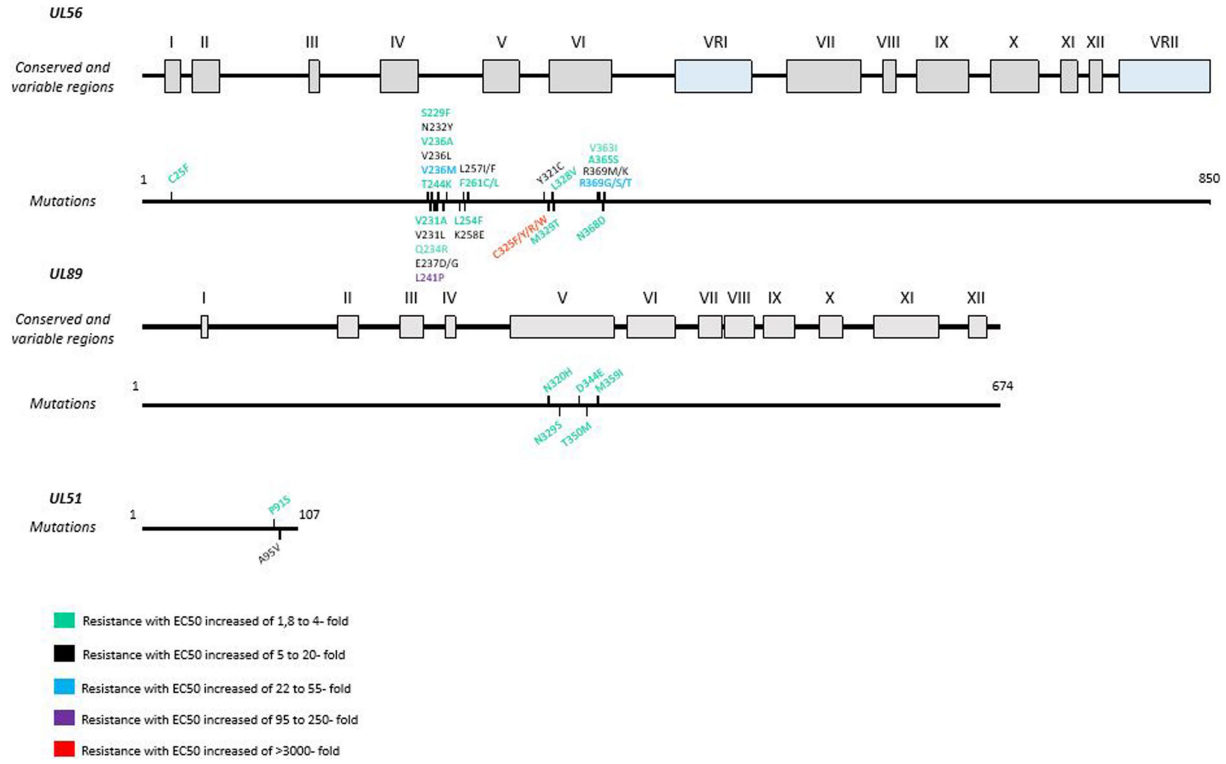

FIGURE 3
Resistance mutations to letermovir in *UL56*, *UL89* and *UL51* genes. LMV resistance mutations according to EC50 values. Mutations are referenced on genes under the map of conserved and variable regions. Scaled representation.

with BDCRB, a benzimidazole inhibitor of the terminase, or with sirolimus, a mTor inhibitor, was synergistic (Chou et al., 2019).

2.2.2 Preclinical studies

In vitro, MBV has selective activity against CMV. Its activity has been demonstrated against Epstein–Barr virus (EBV), however it is not active against herpes simplex virus, varicella-zoster virus (VZV) or human herpesviruses 6 and 8 (HHV-6 and HHV-8) (Prichard, 2009).

Preclinical studies showed that MBV has a better oral bioavailability, a better safety profile and a lower toxicity for host cells than current drugs (GCV, FOS and CDV) with theoretical benefits for the viral inhibition and cross-resistances appearing (Lu and Thomas, 2000; Koszalka et al., 2002; Chou et al., 2012a). MBV also reached concentrations above EC_{50} at the fetal face when perfused across a third trimester placenta (Faure Bardon et al., 2020). In addition, it inhibits CMV replication in first trimester placental villi models in histoculture, with the same EC_{50} as *in vitro* (Morère et al., 2015).

In animal models, the oral bioavailability of MBV is 90% in rats and 50% in monkeys. MBV is excreted via the biliary route and, to a lesser extent, via the metabolic and renal pathways. The minimum effect dose in rats was 100 mg/kg/day and the no-effect dose in monkeys was 180 mg/kg/day (Wang et al., 2003). It was initially distributed in the gastrointestinal tract of rats, but did not cross the blood–brain barrier. This study showed favorable results for MBV's safety profile (Koszalka et al., 2002). In addition, Kern et al. (2004a) demonstrated that oral MBV significantly reduced HCMV replication at concentrations of 75 mg/kg twice daily in SCID-humanized mice with human fetal retinal tissue implants or thymus/liver implants. However, MBV was more effective in treating thymus/liver infection, as it was shown to be poorly absorbed by ocular tissues.

2.2.3 Clinical studies

Several Phase I clinical trials have been conducted with MBV to evaluate its safety, pharmacokinetics and efficacy against CMV infection. In fact, two Phase I clinical trials with escalating single doses of MBV (50 mg to 1,600 mg) were conducted in healthy and human immunodeficiency virus (HIV)-infected patients. 30–40% of an oral dose of MBV was absorbed, and C_{max} was reached 1–3 h after administration (Wang et al., 2003). MBV was rapidly eliminated. At the 400 mg dose, no statistical difference was observed whatever the renal functions of patients (Wang et al., 2003; Swan et al., 2007). The main side effect of MBV is dysgeusia. A Phase I study with multiple oral doses of MBV was carried out to evaluate its antiviral activity. MBV was administered orally at doses of 100 mg twice daily, 400 mg once daily or 400 mg twice daily to CMV-seropositive HSCT recipients. One hundred days after transplantation, pp65 antigenemia was lower in all groups than in the placebo group (15, 19, 15% vs. 39% respectively). In addition, pharmacokinetic analysis of the 400 mg twice-daily dose showed higher C_{max} and area under the curve (AUC) values than the 100 mg twice-daily dose, but with no improvement in antiviral activity and more side effects (Winston et al., 2008).

At low doses, MBV failed to meet the primary endpoints of the initial Phase III study for prophylaxis in hematopoietic stem cell allograft and liver transplant recipients. However, in a Phase II dose-ranging clinical trial, MBV ≥ 400 mg twice was active against

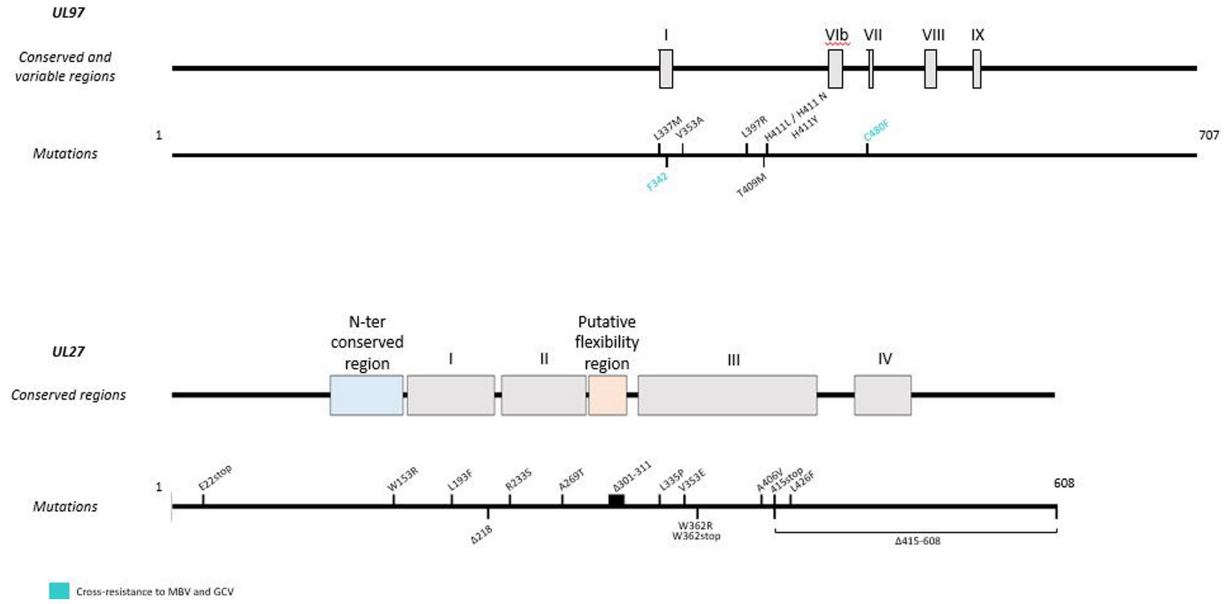

FIGURE 4
Resistance mutations to maribavir in *UL97* and *UL27* genes. Mutations responsible for cross-resistance with GCV are represented in blue. Mutations are referenced on genes under the map of conserved and variable regions. Scaled representation.

refractory or resistant CMV infections in transplant recipients (Papanicolaou et al., 2019). This dosing also showed similar efficacy to those of valganciclovir in pre-emptive treatment of solid organ transplant and HSCT recipients (Maertens et al., 2020). MBV is mainly metabolized in the liver, and moderate hepatic impairment increased total MBV concentrations. This suggests that dose adjustment of MBV may not be necessary for individuals with mild to moderate hepatic impairment (Song et al., 2023).

A randomized Phase III trial, the Solstice study (NCT02931539), demonstrated the efficacy of MBV in SOT and HSCT patients with refractory CMV infections with or without resistance. The study was conducted on 352 patients (235 patients receiving MBV 400 mg twice daily versus 117 patients receiving investigator-assigned therapy (IAT): GCV, VGCV, FOS or CDV) for 8 weeks with a 12-week follow-up. Endpoints were CMV disappearance at the end of week 8 and MBV disappearance and symptom control at the end of week 8, maintained until week 16. Significantly, more patients in the MBV group achieved the primary endpoint (55.7% vs. 23.9%; $p < 0.001$) and the secondary endpoint (18.7% vs. 10.3%; $p < 0.01$). Side effects were less frequent in the MBV group than in the IAT group. Acute kidney injury was more frequent in patients treated with FOS (21.3% vs. 8.5%), and neutropenia was more frequent in patients treated with GCV/GCV (9.4% vs. 33.9%). In the MBV group, 13.2% of patients discontinued treatment due to drug-related adverse events, compared with 31.9% in the IAT group (Avery et al., 2021).

2.2.4 Resistance

Although MBV is a newly approved antiviral, resistance mutations (Figure 4) have already been found in viral genes *UL97* and *UL27*. Indeed, some pUL97 mutations (V353A, L397R, L337M, T409M, H411L, H411N, H411Y, F342, C480F) confer moderate to high-level resistance to MBV, with a 3.5 to 200 fold increase of the EC_{50} (Chou et al., 2007, 2019; Chou and Marousek, 2008; Chou, 2020). These mutations are close to the kinase ATP-binding and catalytic domains upstream the GCV resistance mutations (Chou and Marousek, 2008). Mutations F342Y and C480F are responsible for cross-resistance to ganciclovir and may be present before MBV treatment (Chou et al., 2023). In addition, mutations in the UL27 gene confer low resistance to MBV with a 2- to 3-fold increase in EC50. These mutations (R233S, W362R, W153R, L193F, A269T, V353E, L426F, E22stop, W362stop, 218delC, and 301-311del) compensate for pUL97 inhibition by destabilizing Tip60 (histone acetyltransferase), increase p21 expression and inhibit cyclin-dependent cellular kinases (Chou et al., 2004; Chou, 2009; Kamil and Coen, 2011; Reitsma et al., 2011). In phase II and phase III clinical trials, resistance to MBV emerged in 52 and 26% of treated patients, respectively (Papanicolaou et al., 2019; Chou et al., 2023).

3 New molecules with activity against CMV

3.1 Direct-acting antivirals

3.1.1 Brincidofovir

Brincidofovir (BCV, CMX001; HDP-CDV) [[(S)-2-(4-amino-2-oxo-1(2H)-pyrimidinyl)-1-(hydroxymethyl)ethoxy]methyl]mono[3-(hexadecyloxy)propyl] ester (Figure 2) developed by Chimerix is a lipid antiviral conjugate (LAC) composed of a lipid [1-0-hexadecyl-oxypropyl (HDP)] covalently linked to the acyclic nucleotide analog CDV, enabling the drug to utilize the natural absorption pathways of lysophosphatidylcholine in the small intestine (i.e., passive diffusion and flipases; Lanier et al., 2016). Currently, the United-States FDA approves BCV for treatment of smallpox.

3.1.2 Mechanism of action

BCV was designed to remain intact in plasma and deliver the drug directly to target cells. It enabled enhanced cellular uptake and high

intracellular levels of the converted active antiviral agent, CDV-diphosphate (CDV-PP), increasing antiviral activity against CMV by 2 to 3 orders of magnitude compared with CDV alone (Aldern et al., 2003; Williams-Aziz et al., 2005). BCV is cleaved to release CDV. Then, CDV is converted by intracellular anabolic kinases to CDV-PP, the active inhibitor of viral DNA synthesis. Unlike CDV, BCV is not a substrate for the human organic anion transporter 1, which mechanistically explains the absence of renal toxicity observed in clinical trials with BCV (Tippin et al., 2016; Figure 5).

3.1.3 Preclinical tests

BCV has been developed for the treatment of infections by double-stranded DNA viruses. It has broad-spectrum efficacy against herpesviruses, polyomaviruses, adenoviruses, papillomaviruses and orthopoxviruses (Beadle et al., 2002; Bidanset et al., 2004; Williams-Aziz et al., 2005). BCV is effective against clinical isolates of HCMV (EC50 of 0.0009 µM against HCMV strain AD169) and HSV, including isolates resistant to GCV and ACV (Williams-Aziz et al., 2005; James et al., 2013). In addition, BCV has been shown to be 10 to 100 times more active than CDV against murine CMV (Kern et al., 2004b).

In vivo tests were carried out on animal models to evaluate its efficacy in congenital CMV infection. BCV showed antiviral activity of 0.004 µM ± 0.001 µM against guinea pig CMV (GPCMV). At the end of the second or beginning of the third trimester of gestation, guinea pigs were infected with GPCMV. Significant pup survival was observed in the BCV group (93–100% vs. 50–60%; $p \leq 0.019$). Viral load was significantly reduced in the spleen and liver of pups after BCV treatment ($p = 0.017$ and $p = 0.029$ respectively). Although pup survival was improved with 4 mg/kg treatment, virus levels in fetal tissues were related to those in control tissues. This suggests that BCV could have been a good candidate for the treatment of congenital CMV infections in humans, with high tolerance (Bravo et al., 2011).

3.1.4 Clinical trials

Painter et al. evaluated the pharmacokinetics and safety of BCV in the first Phase I clinical trial in 2012. This was a randomized, double-blind, placebo-controlled, parallel-group, dose-escalation trial in healthy adults. There were no adverse events during the trial. No significant changes in pharmacokinetic parameters were reported. Gastrointestinal analyzes showed no BCV-related mucosal changes. After multiple doses, no accumulation of BCV was observed. Maximum plasma concentrations of BCV were observed 2 to 3 h after dosing. This trial showed that BCV was relatively well tolerated and had a high bioavailability with a dose of approximately 140 mg in adults (2 mg/kg) (Painter et al., 2012).

From 2009 to 2011, Marty et al. (2013) conducted a phase II clinical trial (NCT00942305) on 230 adult CMV-seropositive hematopoietic stem cell transplant recipients at 27 centers. Five sequential study cohorts were planned according to a double-blind ascending dose schedule (3:1 ratio to receive BCV or matching

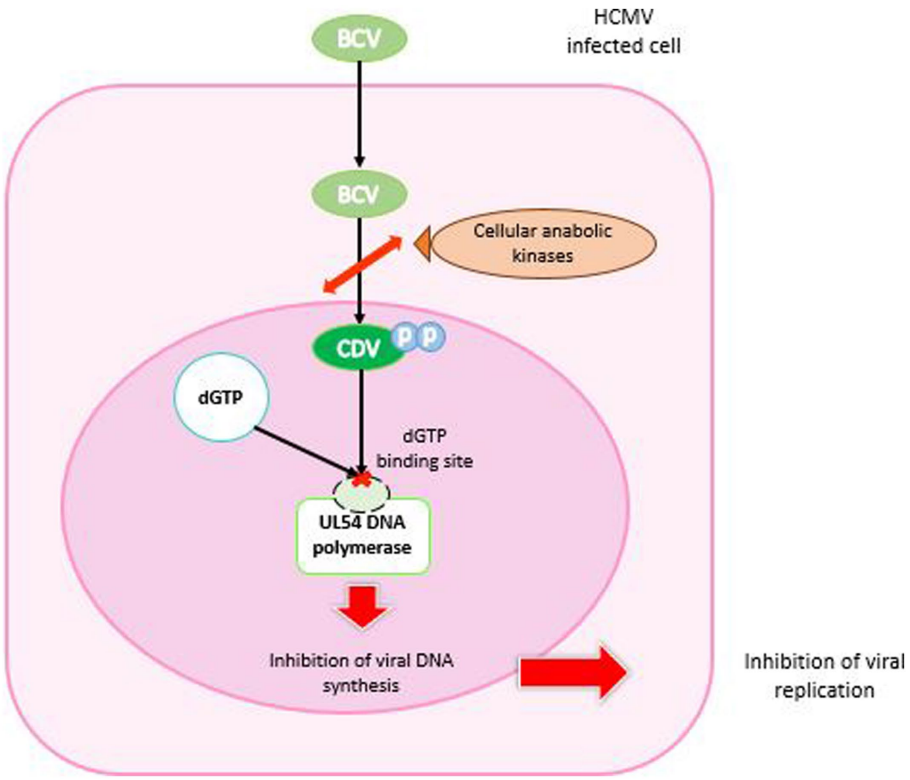

FIGURE 5
Mechanism of action of brincidofovir. BCV enters the HCMV-infected cell, is cleaved and phosphorylated by cellular anabolic kinases to cidofovir diphosphate. In the nucleus, CDV-PP binds competitively to the dGTP binding site of UL54 DNA polymerase. The result is inhibition of DNA synthesis and arrest of viral replication.

placebo). Drugs were administered for 9 to 11 weeks post-transplant. The primary endpoint was a CMV-related event, i.e., CMV disease or a plasma CMV DNA level above 200 copies/ml. In the BCV 100 mg twice weekly group, the incidence of CMV-related events was significantly lower than in the placebo group (10% vs. 37%; $p = 0.002$). The most frequent side effect of treatment was diarrhea in the BCV 200 mg weekly group. There were no reports of myelosuppression or nephrotoxicity (Marty et al., 2013).

The Phase III clinical trial (NCT01769170) was a randomized, double-blind, placebo-controlled (2:1) trial for CMV prophylaxis in 452 CMV-seropositive adults with HCT without CMV viremia. Patients received BCV or placebo until week 14 after HCT. The primary endpoint was the proportion of patients who developed clinically significant CMV infection (CS-CMVi: CMV viremia requiring preemptive treatment or CMV disease) up to week 24 after HCT. This proportion was similar in both groups (51.2% vs. 52.3%; $p = 0.805$). Fewer BCV-treated patients developed CMV viremia up to week 14 than placebo-treated patients (41.6%; $p < 0.001$). BCV resulted in more frequent adverse events (51.1% vs. 37.6%) such as acute graft-versus-host disease (32.3% vs. 6.0%) and diarrhea (6.9% vs. 2.7%). All-cause mortality at week 24 was 15.5 and 10.1% in the BCV and placebo groups, respectively. In conclusion, BCV did not reduce CMV viremia at week 24 post-transplant, and was associated with gastrointestinal toxicities (Marty et al., 2019). BCV is not available to date for the treatment of CMV infection.

3.1.5 Resistance

Since 2013, CDV resistance mutations in UL54 DNA polymerase have been shown to confer resistance to BCV. *In vitro*, increasing concentrations of BCV over 10 months conferred CDV and BCV resistance on a wild-type strain. Genotyping of the strain revealed a D542E mutation in pUL54, which was responsible for a more than 10-fold reduction in susceptibility to BCV and CDV in marker-transfer experiments. This mutation did not confer resistance to GCV or FOS. A smaller plaque phenotype and slower replication kinetics than the parent viruses were also demonstrated. This is the first mutation described under BCV selective pressure. This suggests that BCV may have a unique resistance profile associated with reduced viral replication and maintenance of sensitivity to FOS and GCV (James et al., 2013).

In vitro experiments under BCV pressure selected the N408K and V812L mutations in CMV DNA polymerase, which were already known to confer resistance to CDV. In addition, new substitutions in the exonuclease domain were identified: D413Y, E303D and E303G, which confer resistance to GCV and CDV, with 6- to 11-fold resistance to BCV, or 17-fold when E303G is combined with V812L. This confirmed the expected pattern of cross-resistance (Chou et al., 2016).

In a clinical study, Lanier et al. investigated CMV genotypes from a Phase II trial comparing BCV to placebo for prophylaxis of CMV infections in HCT recipients. Two mutations (M827I and R1052C) were reported in pUL54 in a small number of patients, but did not confer resistance to BCV, CDV, GCV or FOS. This study suggests that the first-line use of BCV for the prevention of CMV infection may preserve downstream options for patients (Lanier et al., 2016). Nevertheless, A987G and F412L mutations in pUL54 have been reported in other studies using BCV as rescue therapy (Kaul et al., 2011; Vial et al., 2017). These mutations were known to confer resistance to CDV, suggesting that the emergence of resistance could occur after BCV treatment.

3.2 Metylenecyclopropane analog: cyclopropavir

Cyclopropavir (CPV, Filociclovir (FCV), ZSM-I-62), (Z)-9-{[2,2-bis-(hydroxymethyl)cyclopropylidene]methyl}guanine (Figure 2) is a new analog of methylenecyclopropane (MCPN) (Zhou et al., 2004). This antiviral showed a good activity against HCMV and murine CMV in animal models (Kern et al., 2004b). In addition, CPV proved highly potent against HCMV (wild-type and GCV-resistant mutants in pUL97 and pUL54), EBV, both variants of HHV-6, HHV-7 and HHV-8 (Kern et al., 2005).

3.2.1 Mechanism of action

As with other nucleoside analogs such as GCV, activation of CPV by tri-phosphorylation is required (Littler et al., 1992). The primary phosphorylation is performed by the viral kinase pUL97 (HCMV) or pU69 (HHV-6), whereas the second and third phosphorylations are made by the guanosine monophosphate kinase (GMPK), thus resulting in tri-phosphate CPV (CPV-TP) (Kern et al., 2005; Gentry et al., 2011; Komazin-Meredith et al., 2014). Therefore, the conversion mechanism of CPV is different from that of GCV; it necessitates a single cellular enzyme to have CPV-triphosphate (CPV-TP; Figure 6).

CPV inhibits HCMV replication by a dual mechanism, inhibiting both pUL54 DNA polymerase and UL97 kinase (James et al., 2011). Indeed, some mutations on pUL54 confer a resistance to CPV, which confirms that the viral polymerase is a target of CPV (Chou et al., 2012b). CPV-TP inhibits pUL54 by competition with dGTP and takes place as chain terminator that stops the DNA synthesis. Interestingly, of the two CPV enantiomers, (+)-CPV-TP could have a twenty-fold higher affinity with pUL54 (Chen et al., 2016). In addition, (+)-CPV is preferencially converted in (+)-CPV-TP than (−)-CPV-TP by the GMP kinase (Gentry et al., 2011). Besides this mechanism, the inhibition of normal function of pUL97 kinase by CPV was assessed by cell transfection with plasmids expressing pUL97 and a reporter plasmid expressing pp65-GFP. CPV prevented the pUL97 capacity to inhibit aggresomes formation, as MBV (James et al., 2011).

3.2.2 Preclinical tests

A study on immunocompromised SCID mice (BALB/c) infected with MCMV, orally administered CPV showed a good effectiveness compared with GCV. Mortality rates were significantly reduced with CPV. Indeed, reducing of viral replication was much more effective in CMV target organs like liver, spleen and lung (Kern et al., 2004c).

Additionally, CPV showed a greater efficacy *in vitro* and *in vivo* than GCV without any increase of toxicity (Zhou et al., 2004; Kern et al., 2005) and achieved therapeutic concentrations *in vivo* without prodrug modification (Wu et al., 2009). In addition, CPV was used in combination with BDCRB and produced a statistically significant synergistic effect against HCMV *in vitro* (O'Brien et al., 2018). On the other hand, the introduction of 1.0 or 10 nM MBV demonstrated a competitive inhibition of CPV phosphorylation with a Ki of 3.0 ± 0.3 nM (Gentry et al., 2010).

Pharmacokinetics, toxicokinetics and absorption, distribution, metabolism and excretion (ADME) datas of CPV showed good results

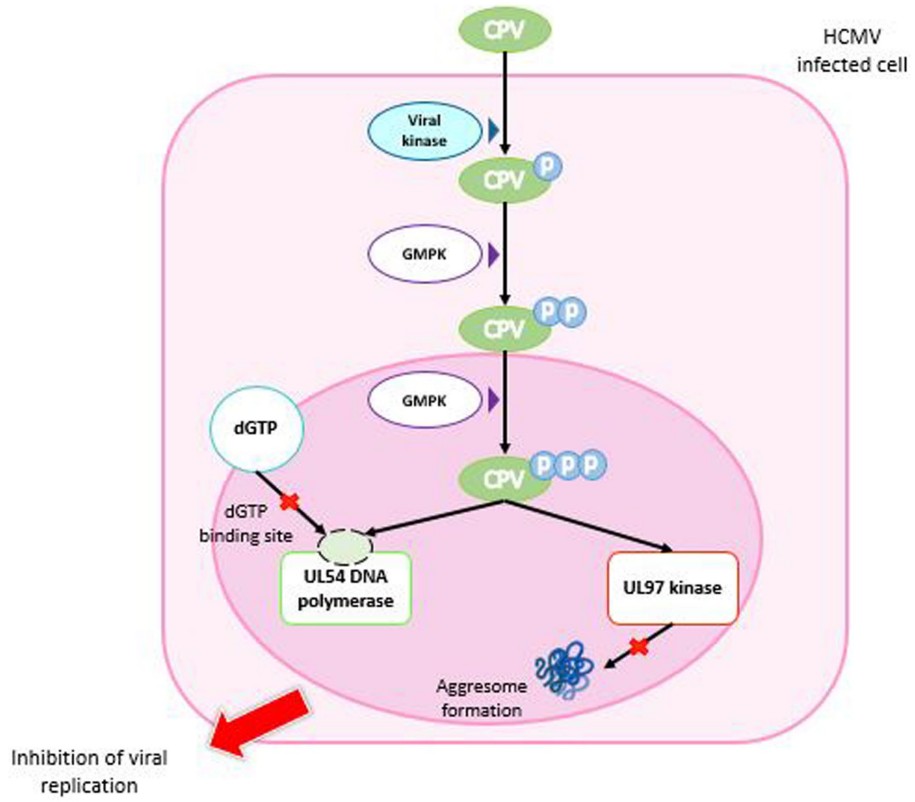

FIGURE 6
Mechanism of action of cyclopropavir. CPV enters the HCMV-infected cell and is phosphorylated by a viral kinase to CPV monophosphate. Two successive phosphorylations by GMPK are required to obtain CPV triphosphate. In the nucleus, CPV-triP binds competitively to the dGTP binding site of DNA polymerase UL54 and inhibits DNA synthesis. It also inhibits the ability of the viral UL97 kinase to prevent aggresome formation. Both mechanisms lead to inhibition of viral replication. GMPK: guanosine monophosphate kinase.

in animals. CPV has a high oral biodisponibility. It also shown that plasma concentration were higher after the first dose of CPV than after the fourteenth daily dose. CPV did not induce or inhibit cytochrome P450 and was minimily metabolized by liver microsomes (Brooks and Bowlin, 2013).

The safety study showed that CPV did not present adverse effects on central nervous system, respiratory and cardiovasular systems. Besides, toxicology studies demonstrated that CPV did not cause haemolysis *ex vivo* (Brooks and Bowlin, 2013).

3.2.3 Clinical trials

The first phase 1A clinical trial (NTC01433835) included 48 healthy adults (3 males, 45 females) with a main age of 50.3 years. This randomized, placebo-controlled (3:1) trial evaluated CPV safety and pharmacokinetics after the administration of various doses ranging from 35 to 1,350 mg. No serious adverse effects were classified. C_{max} were reached after 1 to 2 h after oral administration and the CPV was not detectable 24 h after last dose of treatment (Brooks et al., 2015).

A phase 1B, double blind, randomized, placebo-controlled (3:1), single center, multiple ascending doses, clinical trial (NCT02454699) was done to assess safety, tolerability and pharmacokinetics of CPV at various doses in 24 healthy adult volunteers monitored for 22 days (7 males and 17 females; main age 47.4 years). Doses of CPV were 100, 350 and 750 mg for 7 days. During this study, no serious adverse effect was highlighted. Indeed, main adverse events concerned gastrointestinal tract (17%), nervous system (11%) and skin and subcutaneous tissues (11%). The only severe adverse event appeared in the 750-mg cohort was a reversible grade 3 elevation in serum creatinine and bilirubin associated with a 1-log increase of CPV in plasma after 24 h of the initial dose. The C_{max} was reached at 2 to 3 h following administration and CPV was undetectable in plasma 24 h after the last dose, as phase 1A trial. Finally, authors concluded that, *in vivo*, doses as low as 100 mg were sufficient to inhibit CMV (Rouphael et al., 2019).

So far, no phase II or III clinical trials are in progress (source: ClinicaTrials.gov).

3.2.4 A new antiviral against adenoviruses

Adenoviruses are responsible for a variety of infections in children, and can cause acute hepatitis with high morbidity and mortality (Kajon and St George, 2022). Recent studies have also demonstrated the antiviral activity of CPV against adenovirus (HAdV) by inhibition of the adenovirus-encoded DNA polymerase (Toth et al., 2020). Hartline et al. (2018), have shown that the strain human adenovirus type 5 (HAdV5) of the American Type Culture Collection (ATCC) was sensitive to CPV. CPV has shown a high potential to inhibit *in vitro* HAdV replication with a higher efficacy than CDV (5- to 10- fold higher) (Tollefson et al., 2022).

The same potential against adenoviruses has been observed with BCV. It has been demonstrated in several clinical trials, notably in the

treatment of severe adenovirus infection and disease in 2022 (NTC02596997) (Alvarez-Cardona et al., 2020; Chimerix, 2022).

3.2.5 Resistance

Mutations are known to confer CPV resistance (Figure 7). Indeed, a recombinant virus with Δ498 bp mutation in the *UL97* open reading frame (ORF) is resulting in a protein with a missing kinase domain (Gentry et al., 2013). The K355M mutation confers to the virus a moderate 5- to 7- fold increase in EC_{50} versus a 13- to 25- fold increase for FCV and GCV, respectively, (Komazin-Meredith et al., 2014). Recombinant virus lacking pUL97 kinase domain is 20 times more resistant to CPV (Kern et al., 2005), which can be explained by the need for the first phosphorylation of CPV by pUL97, essential for activation of the molecule (Gentry et al., 2013). Mutations have been identified *in vitro*, ranging from insignificant mutations to resistance mutation confering cross-resistance to GCV, MBV and CPV.

Mutations close to critical functional residues were also identified: F342S and V356G. These mutations are close to the highly conserved residues involved in the kinase ATP-binding P-loop G338, G340 and G343 (Chou et al., 2013). The L595S mutants are resistant to GCV but remain susceptible to CPV (Chou and Bowlin, 2011). On the other hand, M460V, A594V, C592G and C603W, which confer low resistance to GCV, increase EC50 by 3 to 5-fold; M460I and H520Q induce high resistance to CPV, with a 12- to 20-fold increase in EC50 (Chou and Bowlin, 2011; James et al., 2011).

In addition, D456N, C480R and Δ617 confer resistance to GCV, MBV and all the MCPNs including CPV (Komazin-Meredith et al., 2014).

The combination H520Q-M488V (UL97-UL54) induced the highest level of resistance to CPV. Resistance mutations are close to finger and palm domains of the polymerase catalytic core (Chou et al., 2012b). Two other mutations in pUL54 were shown to confer a lower resistance to CPV: E756D and E756K. Both are involved in FOS resistance (Lurain and Chou, 2010).

3.3 Benzimidazole analogs: BDCRB, TCRB and tomeglovir

BDCRB or 2-Bromo-5,6-dichloro-1-(beta-d-ribofuranosyl) benzimidazole and TRCB or 2,5,6-Trichloro-1-(beta-D-ribofuranosyl) benzimidazole (Figure 2) are benzimidazole ribofuranoside. These two molecules are potent and selective inhibitors of HCMV replication (Townsend et al., 1995). Tomeglovir (BAY 38–4,766) or {3-hydroxy-2,2-dimethyl-N[4({[5-(dimethylamino)-1-naphthyl]sulfonyl}amino)-phenyl] propanamide} (Figure 2) is an oral, non-nucleoside compound related to the D-benzimidazole ribonucleosides. It is a potent and selective inhibitor of HCMV replication by inhibition of viral DNA concatemers processing (Reefschlaeger et al., 2001; Weber et al., 2001).

3.3.1 Mechanism of action

The mechanism of action of BDCRB and TCRB (Figure 8) does not need phosphorylation at the 5′ position and does not involve the inhibition of DNA synthesis (Krosky et al., 2002). It prevents the cleavage of high molecular weight viral DNA concatemers to monomeric genomic lengths (Underwood et al., 1998). Resistance mutations were found in HCMV genes *UL56* and *UL89* suggesting that BDCRB and TCRB target the encapsidation step (Krosky et al., 1998; Underwood et al., 1998). BDCRB partially inhibits the ATPase activity of pUL56 and the pUL89-associated nuclease activity at high concentrations (Scholz et al., 2003). Furthermore, it has been suggested that BDCRB causes HCMV terminase to skip the normal cleavage site and continue packing DNA until a second cleavage site is encountered 30 kb further (McVoy and Nixon, 2005). In GPCMV, monomer-length genomes are plentifully produced under BDCRB, but are slightly truncated at the left end (Nixon and McVoy, 2004). This is in accordance with the fact that BDCRB alters recognition and cleavage of DNA by the terminase complex.

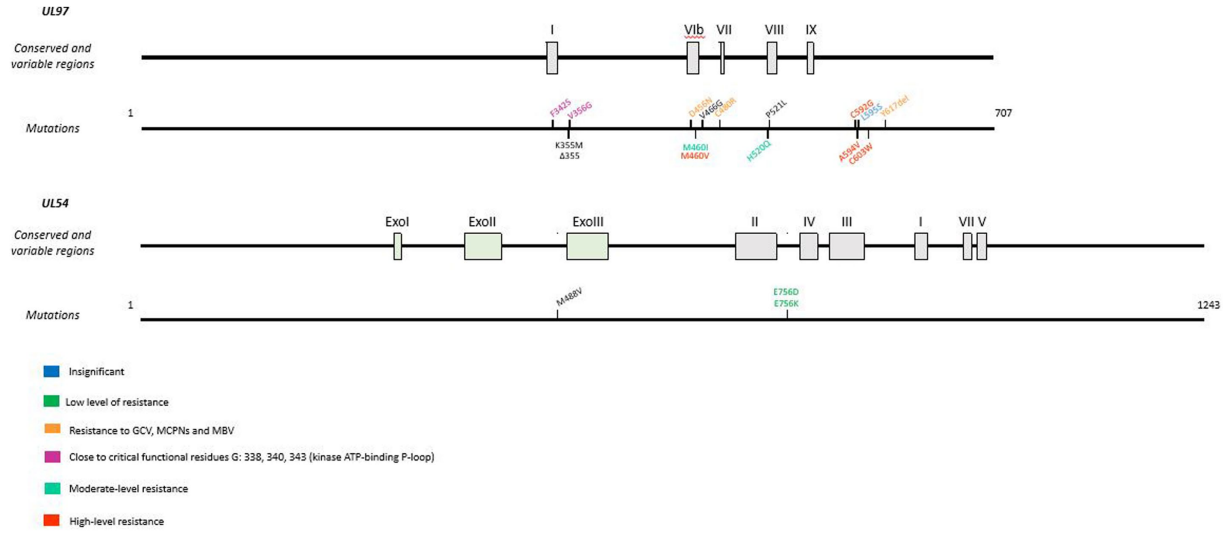

FIGURE 7
Resistance mutations to cyclopropavir in UL97 and UL54 genes. CPV resistance mutations according to EC50 values. In *UL97*, cross-resistance mutations are represented in orange and mutations next to the ATP-binding P-loop are in pink. Mutations are referenced on genes under the map of conserved and variable regions. Scaled representation.

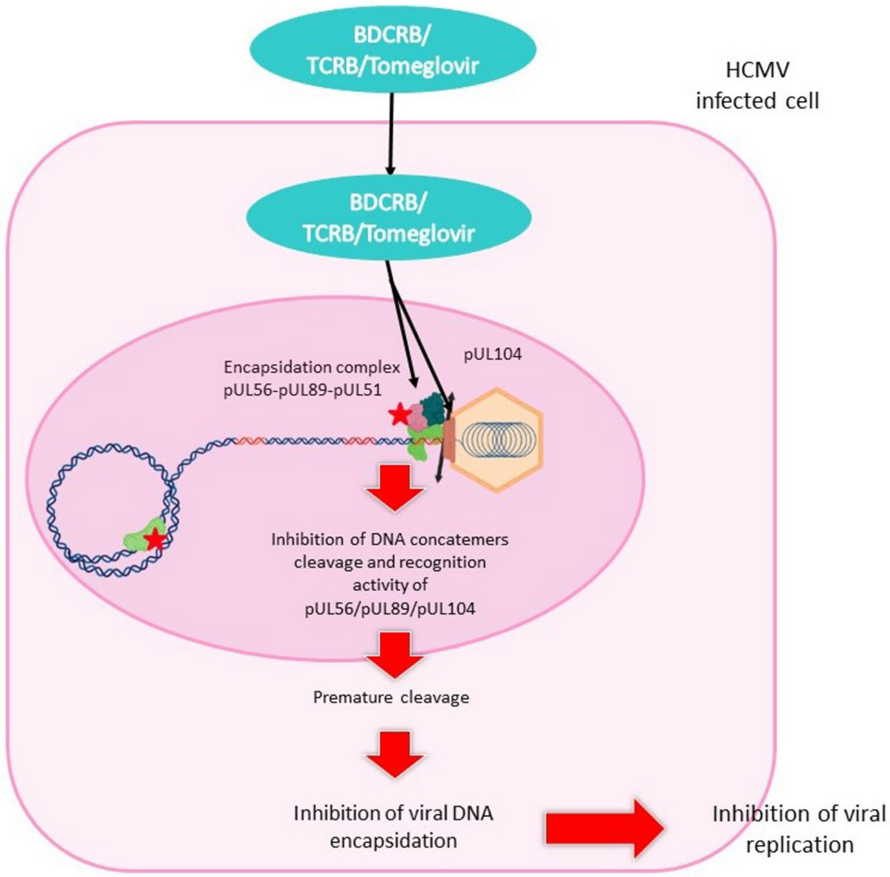

FIGURE 8
Mechanism of action of benzimidazol analogs. BDCRB, TCRB and tomeglovir enter the HCMV-infected cell and travel to the nucleus. They inhibit the encapsidation complex composed of pUL56, pUL89 and pUL51, and inhibit the portal protein pUL104. This mechanism leads to inhibition of DNA cleavage and concatemer recognition, or to premature cleavage. Encapsidation is interrupted and viral replication halted.

Tomeglovir mode of action (Figure 7) is the same as that of BDCRB and TCRB described above. This molecule targets HCMV-specific proteins required for cleavage and packaging of viral DNA, transforming high molecular weight viral DNA concatemers into monomeric genomes length (Reefschlaeger et al., 2001).

3.3.2 Preclinical tests

BDCRB and TCRB were effective against HCMV with EC_{50} of 0.7 μM and 2.9 μM in plaque assays, respectively. It was also proved that BDCRB and TCRB were inactive against HSV-1. However, the incorporation of Cl and Br into these two molecules improved dramatically their therapeutic index (Townsend et al., 1995). It was also shown that BDCRB is inactive against HHV-6 and HHV-7 (Yoshida et al., 1998). Another study demonstrated the inefficacy of BDCRB against HSV-1, HSV-2, VZV, HHV-8 but an activity against EBV (Williams et al., 2003). Furthermore, it was demonstrated that conformational changes in BDCRB structure could increase its spectrum against herpesviruses. Indeed, the L-analog of BDCRB was effective against HHV-6 (Prichard et al., 2011). Tomeglovir was effective against HCMV strains ($EC_{50} = 0.52 \pm 0.014$ μM) (Reefschlaeger et al., 2001). GCV-resistant clinical isolates were also susceptible to tomeglovir (McSharry et al., 2001).

Interestingly, HCMV strain AD169 was more sensitive to benzimidazole than the strain Towne (Krosky et al., 2000). Although TCRB and BDCRB showed excellent activity *in vitro*, their glycosidic bonds are hydrolyzed *in vivo* to less active metabolites that reduce their activity (Good et al., 1994).

In addition, BDCRB showed synergy in combination with MBV, synergy at low concentrations and antagonism at higher concentrations with tomeglovir (Evers et al., 2002). Furthermore, tomeglovir had an antagonistic effect when combined with GCV (Evers et al., 2002).

The toxicity of benzimidazole analogs was tested in bone marrow cells. One hundred μM BDCRB inhibited cell proliferation by 20% over a 10-day period, while 100 μM GCV inhibited it by 52%. In other experiments on hematopoietic progenitor cell colony-forming assays, 100 μM BDCRB affected BFU-E and CFU-GM (burst forming units-erythroid and colony forming units-granulocyte/macrophage) by 31 and 47%, respectively. In contrast, GCV inhibited BFU-E by 54% and CFU-GM by 86%. However, TCRB was less effective than BDCRB. This study concludes that certain benzimidazole nucleosides are less toxic than conventional drugs (Reza Nassiri et al., 1996).

Additionally, *in vitro* study with BDCRB in guinea pig embryo or lung fibroblasts showed that GPCMV was sensitive to BDCRB

(EC_{50} = 4.7 μM). BDCRB did not inhibit the formation of genome-sized GPCMV DNA, which was packaged but not protected from nuclease. Termini formed on GPCMV genome were altered by BDCRB. Then, BDCRB participated to the retention of C capsids in the nucleus (McVoy and Nixon, 2005). However, more recently, a GPCMV resistant to BDRCRB was generated and characterized. Genetic alterations were reported: an L406P substitution in GP89, the HCMV UL89 homolog; a 13.4 kb internal deletion of the GP131-GP143 non-essential ORFs; and a dramatic increase in the number of iterations of a 1 kb terminal repetitive sequence, from 0 or 1 to up to 9 at either genomic end (Ourahmane et al., 2018).

In animal model experiments, efficacy was evaluated in an ocular model of SCID-humanized mice infected with the Toledo strain of HCMV. BDCRB was administered at doses of 50 mg/kg for 28 days or 25 mg/kg twice daily for 1 week and once daily for 2 weeks. A slight but non-significant reduction in HCMV titers was observed in the 50 mg/kg group, and no reduction in mean titers was observed in the 25 mg/kg group. These results showed that BDCRB could only be active against HCMV at high concentrations. In the second experiment, HCMV-infected SCID-humanized retinal implants were treated with BDCRB or CDV for 28 days. Mice were treated with 75 mg/kg BDCRB from day one post-infection. BDCRB had no effect on reducing viral titers in retinal implant tissues. These results demonstrated the ineffectiveness of BDCRB in crossing the blood-ocular barrier in *in vivo* models. In addition, the same experiments were carried out with visceral organs (fetal thymus and liver) implanted in the kidney capsule. Doses of BDCRB blocked viral replication by around 2 to 3 log^{10} PFU/g (Kern et al., 2004a).

Tomeglovir was evaluated in MCMV-infected immunodeficient mice and reduced viral load in target organs in a manner comparable to GCV. Weight loss (consequence of viral infection) is reduced after tomeglovir administration (Reefschlaeger et al., 2001). Another study on murine model with *per os* administration of tomeglovir at dose ≥10 mg/kg showed similar results (Weber et al., 2001). A study in guinea pigs also demonstrated that peak plasma tomeglovir levels were 26.7 mg/mL 1 h after dosing. It reduced both viremia and DNAemia, as well as mortality following lethal GPCMV challenge in immunocompromised guinea pigs, from 83 to 17% ($p < 0.0001$). This study demonstrated the safety, pharmacokinetics and favorable therapeutic profiles of tomeglovir (Schleiss et al., 2005).

3.3.3 Clinical trials

Currently, no published clinical trial was performed to assess BDCRB, TCRB and tomeglovir in human (source: ClinicaTrials.gov).

3.3.4 Resistance

Resistance mutations to BDRCRB and TCRB (Table 2) are located in pUL56 (Q204R) and in pUL89 (D344E and A355T). If combined, these mutations showed a greater resistance to benzimidazole analogs than alone. Nevertheless, these mutations did not confer resistance to GCV (Krosky et al., 1998; Underwood et al., 1998; Evers et al., 2002). Additionally, mutations M360I in M89 exon II and P202A and I208N in M56 confer murine CMV resistance to tomeglovir. Mutation in M89 exon II had analogous mutations in HCMV pUL89 mentioned for BDCRB and TCRB but those in M56 did not have it in HCMV pUL56. Thus, pUL89 could be directly targeted by tomeglovir and pUL56 could compensate for restricted activities of Buerger et al. (2001). More recently, Chou (2017) highlighted new mutations in *UL89* gene and *UL56* responsible for tomeglovir resistance. In pUL89 N329S, T350M, H389N, N405D, D344E, C347S and V362M conferred moderate to high drug resistance. The mutation I334V did not conferred tomeglovir resistance but affected growth fitness when combined with N405D. Then, in pUL56, Q204R was shown as lower-grade resistance mutation (Chou, 2017).

The L406P mutation described in GPCMV QP89 was more than 50 residues away from the positions of the confirmed resistance mutations in HCMV pUL89. This mutation does not confer significant resistance of GPCMV to BDCRB but may have a compensatory function in enhancing replication by making easier genomic cleavage at cleavage sites containing multiple repeats. Furthermore, deletion of the E region of *HindIII* is unlikely to contribute directly to resistance to BDCRB. Thus, the accumulation of terminal repeats could be a response to BDCRB pressure and the resulting increase in genome length resulted in compensatory deletion of the *HindIII* E region (Ourahmane et al., 2018).

BDCRB and TCRB do not show any cross-resistance with GCV because of their different mechanisms of action and their different gene targets. Surprisingly, a cross-resistance with MBV is responsible for an increase of 2-3-fold EC_{50} even if these molecules do not have the same mechanism of action. Indeed, BDCRB and TCRB are DNA processing inhibitors and MBV is a DNA synthesis inhibitor (Evers et al., 2002).

In addition, a mutation was described in pUL104, the portal protein of HCMV, which is colocalized with pUL56, in resistant strains to benzimidazole nucleosides. However, this L21F pUL104 mutation alone did not prove sufficient to ensure resistance of HCMV to BDCRB (Komazin et al., 2004; Table 2).

4 Host-targeting antivirals

Several molecules targeting cellular metabolism have antiviral activity by interfering with cellular components participating in the viral replication cycle. These components have various targets, efficacy, and share the absence of identified viral resistance.

4.1 Artemisinin derivatives: artesunate, artemisone, and TF27

Artemisinin is an antimalarial drug that is an active compound of *A. annua* (1972). Many derivatives of this drug were developed. In this context, Saokim Ltd. (Hanoi, Vietnam) synthesized artesunate (Figure 2), a semisynthetic drug of artemisinin. This compound is available as intravenous or oral formulation to treat life-threatening malaria access. In 2010, the World Health Organization (WHO) recommended this drug as quinine to treat severe malarial infections during the first trimester of pregnancy (McGready et al., 2012; Roussel et al., 2017). Besides this activity, artesunate (ART) was shown as a good inhibitor of HCMV infections *in vitro* (Efferth et al., 2002, 2008). The laboratory of Sensitive Biology Therapy (S.B.T) synthesized its trimeric derived compound, TF27 (Figure 2; Hutterer et al., 2015; Reiter et al., 2015; Hahn et al., 2018). Recently, LH54, the heterologous hybrid compound of artesunate was developed in the laboratory of S.B.T. and has also a good antiviral activity (Wild et al., 2020). All these artesunate derivatives have shown good efficacy.

TABLE 2 Resistance mutations to benzimidazol analogs in UL56 and UL89 genes.

Gene		Resistance EC_{50} (μm; Fold change)			Reference
UL56	UL89	BDCRB	Tomeglovir	TCRB	
Q204R		**17 (14)**	**1.2 (2.7)**	**57 (23)**	Chou (2017), Krosky et al. (1998), and Evers et al. (2002)
L208M			**0.8 (3.4)**		Chou (2017)
N232Y			**1.2 (2.7)**		Chou (2017)
E407D			**1.3 (6.0)**		Chou (2017)
H637Q			**0.9 (2.0)**		Chou (2017)
V639M			**4.6 (10)**		Chou (2017)
L764M			0.19 (0.4)		Chou (2017)
	Q11H				
	I334V		1.1 (0.9)		Chou (2017)
	N320H		**3.0 (6.5)**		
	N329S		**2.0 (15)**		Chou (2017)
	D344E	**20,3 (10)**	**1.8 (1.7)**	**6–18 (10)**	Chou (2017), Underwood et al. (1998), and Krosky et al. (1998)
	C347S		0.6 (0.3)		Chou (2017)
	T350M		**2.8 (8.7)**		Chou (2017)
	A355T				
	M359I		**3.4 (7.4)**		Chou (2017)
	V362M		**1.2 (98)**		Chou (2017)
	H389N		**1.1 (29)**		Chou (2017)
	N405D		**6.9 (15)**		Chou (2017)
	I334V-N405D		**5.6 (12)**		Chou (2017)
	D344E-A355T	**20 (30)**		**>50**	Underwood et al. (1998)
H637Q-V639M			**7.5 (17)**		Chou (2017)
Q204R	D344E	**32 (13)**	**2.5 (5.8)**	**68 (30)**	Chou (2017) and Krosky et al. (1998)
F261L	D344E		**0.91 (2.1)**		Chou (2017)
M329T	D344E		**0.98 (2.2)**		Chou (2017)

Bold values are significant values for resistance.

4.1.1 Mechanism of action

Artemisin and its derivatives are primarily metabolized in dihydroartemisin (DHA) by cytochrome P-450 monooxygenase enzyme (CYP) 2B6 in human liver microsomes. This step is followed by the conversion into inactive metabolites via other enzyme systems. DHA has a half-life of about 45 min and is also an anti-malarial drug.

In HCMV infections, ART inhibits cellular transcription factors Sp1 and NF-κB (Hutterer et al., 2015). Indeed, its derivatives, TF79 and TF27, inhibit NF-κB signaling by approximatively 90% at concentration of 3 μM to 0.3 μM, with a correlation between the diminution of NF-κB pathway and the antiviral activity (Hahn et al., 2018). Previous studies have suggested that sustained NF-κB activation is necessary for viral replication (Hiscott et al., 2001; Figure 9).

4.1.2 Preclinical tests

Artemisinin derivatives are well tolerated in humans (Ribeiro and Olliaro, 1998; Adjuik et al., 2004). Rarely, slight and reversible adverse effects were observed such as first-degree heart block and neutropenia (Ribeiro and Olliaro, 1998; Adjuik et al., 2004). However, in animal models like mice, rats and dogs, neurotoxic effects were reported (Toovey, 2006). Studies showed that a shorter exposure to artemisinin derivatives with higher concentrations was less neurotoxic than a longer exposure with lower concentrations (Li et al., 2002).

ART was shown to be efficient against all types of herpesviruses, more than artemisinin. ART inhibits HCMV *in vitro* and *in vivo* (Efferth et al., 2002; Kaptein et al., 2006), both HHV-6 variants (Milbradt et al., 2009; Hakacova et al., 2013), Epstein–Barr virus (Auerochs et al., 2011) and Herpes simplex virus 1 (Efferth et al., 2008).

In addition, ART can be combined with other conventional anti-CMV drugs such as GCV, CDV and FOS to decrease risk of resistance mutation emergence. ART also shows a pronounced synergistic effect with MBV (Chou et al., 2011). Furthermore, its activity was confirmed in a model of 1st trimester placental villi infection (Morère et al., 2015). In combination with MBV, ART

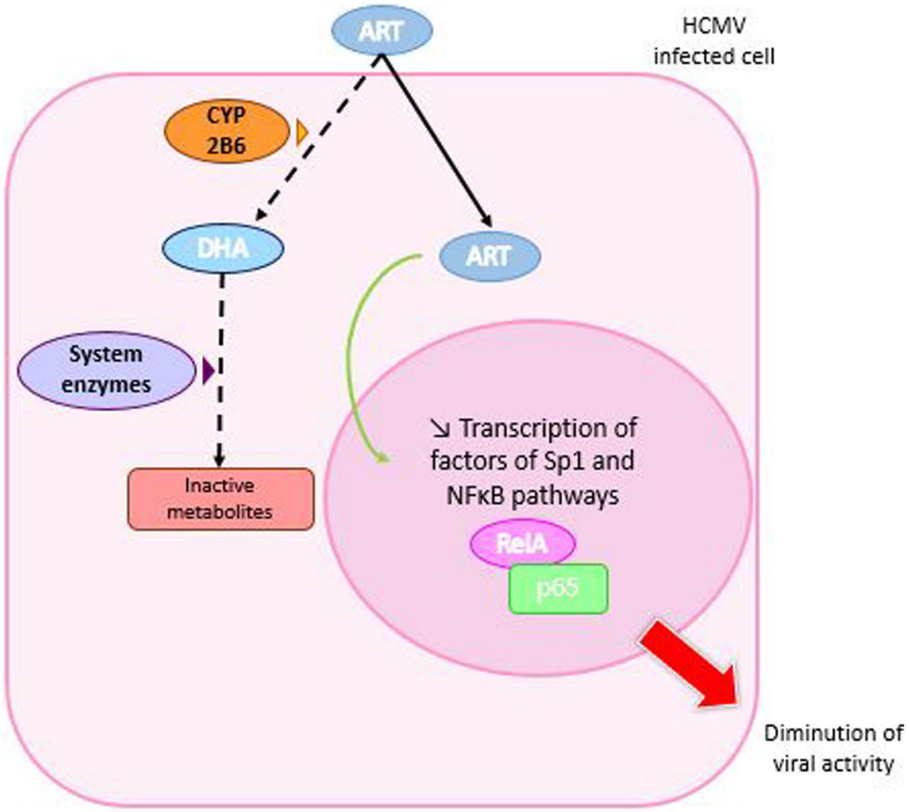

FIGURE 9
Mechanism of action of artemisinin derivatives. Artemisinin derivatives enter HCMV-infected cells and are metabolized to dihydroartemisin (DHA) by the cytochrome P-450 monooxygenase 2B6 (CYP 2B6) enzyme, which is then converted to inactive metabolites. In addition, ART moves to the cell nucleus where it inhibits the production of RelA and p65 involved in the NFκ-B pathway, which is necessary for viral replication.

showed a synergistic effect at low concentrations, with IC_{50} of 0.25 and 2 μM for the two molecules, respectively. However, the combination with baicalein had an antagonistic effect (Morère et al., 2015). In the same year, Drouot et al. (2016) demonstrated that combining ART with GCV, CDV and MBV was associated with synergy, while combining it with FOS or LMV produced only moderate synergy.

Artemisin was also tested against HCMV in different ratios in combination with the anti-HCMV drugs BDCRB, LMV, GCV, CDV, BCV and MBV. This study revealed synergistic antiviral activity with no microscopically apparent cell toxicity or reduction in cell viability (Oiknine-Djian et al., 2019).

ART derivative, TF27, also showed an anti-HCMV activity at nanomolar concentrations (Hutterer et al., 2015; Reiter et al., 2015; Fröhlich et al., 2018). Besides, antiviral activity against HCMV infections was also shown in *ex vivo* placental villi explant model (Jacquet et al., 2020). Recently, Sonntag et al., demonstrated its antiviral efficacy *in vivo* by using an established model of murine CMV infection of an immunodeficient mouse strain Rag−/− (Sonntag et al., 2019). TF27 has a higher antiviral activity than ART: the EC_{50} of 0.04 ± 0.01 μM against HCMV strain (Hutterer et al., 2015) was 100 fold lower than the EC50 of artesunate (Hahn et al., 2018).

4.1.3 Clinical tests

ART is a good inhibitor for clinical use in the treatment of drug-resistant HCMV infection. The first report of treatment of CMV infection with ART in a HCT recipient with resistance to foscarnet and ganciclovir (DNA polymerase L776M mutation) dates back to 2008. Treatment with GCV, CDV and intravenous immunoglobulin had failed. ART was started at a dose of 100 mg daily after other treatments had been discontinued. A favorable response was observed, followed by a rapid reduction in viral load and improvement in hematopoiesis. During the 30 days of treatment, there were no adverse events and no increase in viremia. The patient received a third transplant with a recurrent episode of viremia but controlled by a new antiretroviral treatment regimen. Nevertheless, retinitis was diagnosed during treatment, reflecting the limited penetration of ART into the eye. Combining ART with GCV resolved this local infection and controlled the viral load. This study demonstrates the potential of ART to control CMV infection (Shapira et al., 2008).

ART was used in a case series of 6 SCT recipients as a preventive treatment for CMV infection to calculate its antiviral efficacy by studying viral kinetics. Two patients showed a decrease in viral load (0.8 to 2.1 log after 7 days). Antiviral efficacy was described as heterogeneous, ranging from 43 to 90%, and depended on the basic growth dynamics of the virus (Wolf et al., 2011).

In another study, ART was evaluated in five patients with resistant CMV infection. ART was unsuccessful in two cases of severe CMV disease with high CMV viral load and pulmonary involvement. However, these patients also suffered from diseases (Wegener's granulomatosis and Hodgkin's lymphoma) that may have accounted

for some of the deaths. In conclusion, ART may be useful in the treatment of mild CMV disease due to multidrug-resistant strains. However, further data are needed on the risk factors associated with ART failure. In addition, it should be noted that ART is not sufficient to treat serious CMV disease with pulmonary involvement due to its poor diffusion in lung tissue, as has been reported in animal models (Zhao and Song, 1993; Germi et al., 2014).

4.1.4 Resistance

To date, no resistance to artemisinin derivatives has been reported in CMV.

4.2 Flavonoids

Flavonoids are metabolites found in fruits and vegetables with high biological activity and low toxicity. Flavonoids with well-classified structures and well-defined structure–function relationships include flavans, flavanones, flavones, flavanonols, flavonols, catechins, anthocyanidins, isoflavones and chalcons (Tsao, 2010). Over 5,000 flavonoids were defined as molecules with potential health benefits as antioxidative, anti-inflammatory, antitumoral, antiviral and antibacterial effects (Middleton, 1998; Beecher, 2003; Cazarolli et al., 2008). Besides, flavonoids can specially modulate activities of cellular enzymes and inhibit protein kinases (Middleton, 1998). These metabolites are therefore a real option for current antiviral therapies. Indeed, it was shown that kaempferol inhibits herpes simplex virus (Amoros et al., 1992) and that baicalein and genistein interact with the first steps of HCMV infection (Evers et al., 2005). In an exploratory *in vitro* study, Cotin et al. (2012) showed that baicalein and quercetin were the most potent flavonoids to inhibit HCMV *in vitro*. Their combination had an additive effect. In addition, the combination of these two molecules with chalcone to reduce toxicity was tested against HCMV. The result was a synergistic effect for baicalein, while an antagonistic effect was observed with quercetin (Andouard et al., 2016). Both molecules were also combined with MBV, and quercetin did not improve the efficacy of MBV alone, unlike baicalein, which reduced infection by 90% at low concentrations (2.2 μM baicalein; 1 μM MBV; Morère et al., 2015). In this review, quercetin and baicalein will be explored for their potential antiviral activity.

4.2.1 Quercetin

Quercetin or (3,3′,4′,5,7-pentahydroxy-2-phenylchromen-4-one; Figure 2) is the main representative of the flavonoid subclass, flavonols. The fruits and vegetables with the highest concentration of quercetin are apples, cherries, onions, asparagus and red leaf lettuce (Nishimuro et al., 2015). It is also found in herbs such as licorice.

In food, quercetin is present as quercetin glycosides that are hydrolyzed and released as aglycone. Then, aglycone is absorbed and metabolized into glucuronidated, methylated and sulfated derives (Kawabata et al., 2015). However, the stability of quercetin and its derivatives in the organism can be influenced by pH, temperature, metal ions and other compound as glutathione (GSH) (Boots et al., 2005; Moon et al., 2008). This could affect the efficacy of the molecule.

4.2.1.1 Mechanism of action

Quercetin was shown to act by inhibition of early viral proteins IE-1and IE-2 expression (Cotin et al., 2012). Through the downregulation of IE-2 of VZV and HCMV, it inhibits viral lytic gene expression and replication (Kim et al., 2020) and modulates NF-κB, mitochondrial and ROS pathways (Hung et al., 2015; De Oliveira et al., 2016). Quercetin also inhibits the activation of IRF3 and NF-kB induced by HSV-1 infection in a TLR3-dependent manner that results in a lower production of TNF-α (Lee et al., 2017). Quercetin was then shown to prevent EBV-induced B cell immortalization and proliferation of lymphoblastoid cell lines by interrupting the dialectic between IL-6 and STAT3, promoting autophagy and reducing ROS levels and p62 accumulation (Granato et al., 2019; Figure 10).

4.2.1.2 Preclinical tests

Many studies showed the antiviral activity of quercetin. Indeed, quercetin inhibits HBsAg and HBeAg secretion in Hepatitis B virus infected cells (Wu et al., 2007). It is also an active agent against HIV-1 reverse transcriptase, protease and α-glucosidase with an EC_{50} value of 60 μM (Yu et al., 2007).

Quercetin was tested *in vitro* against herpesvirus, reducing intracellular replication of HSV-1 and HCMV. The antiviral activity against HCMV infected cells was 4.8 μM and 145 μM against HSV-1 (Cotin et al., 2012). In 2022, a formulation of polyxamer 188 and quercetin (QP188) amplified the *in vitro* GCV antiviral activity against HCMV. Indeed, QP188 was tunable, bioactive and rapidly internalized in NIH/3 T3 cells. This formulation had a dose-dependent activity combined synergistically with GCV. These results could be interesting for finding means to reduce GCV toxicities (Kjar et al., 2022).

4.2.1.3 Clinical study

In 2018, an herbal treatment (Gene-Eden-VIR/Novirin) composed of five ingredients including quercetin was tested in a clinical trial for the treatment of oral herpes. The study included 68 participants who took 1 to 4 capsules a day for an average duration of 10.4 months. Efficacy was assessed from symptom onset to complete resolution and also included analysis of recurrence rates. Treatment was compared with two conventional drugs: valaciclovir (VAVC) and aciclovir (ACV). Gene-Eden-VIR/Novirin was more effective in reducing the number and duration of oral herpes epidemics, and more secure than ACV and VAVC. Gene-Eden-VIR/Novirin reduced the duration of outbreaks from 5.83 days to 3.21 days in the treated group ($p < 0.0001$). In addition, 46.4% of patients on herbal treatment were relapse-free ($p < 0.0001$), and no adverse events were observed (Polansky et al., 2018). However, results of this study must be confirmed with further investigations. The same comparison was done with famciclovir (FCV) in 2016 (Polansky et al., 2016).

4.2.1.4 Resistance

Currently, no resistance mutation to quercetin was documented.

4.2.2 Baicalein

Baicalein (5,6,7-trihydroxyflavone; C15H10O5) (Figure 2) belongs to the flavone sub-family of flavonoids. This molecule is isolated from the roots of *Scutellaria baicalensis* with different properties: antioxidant, anti-inflammatory, anticancer, antidiabetic, antithrombotic, anxiolytic, anti-convulsive, cardioprotective, hepatoprotective and neuroprotective agent (Chang et al., 2016; Gao et al., 2016; Dinda et al., 2017; Cristelli et al., 2019; Tuli et al., 2020).

4.2.2.1 Mechanism of action

Pretreatment with baicalein failed in suppressing viral replication in cells while post-treatment was effective. These results suggest that

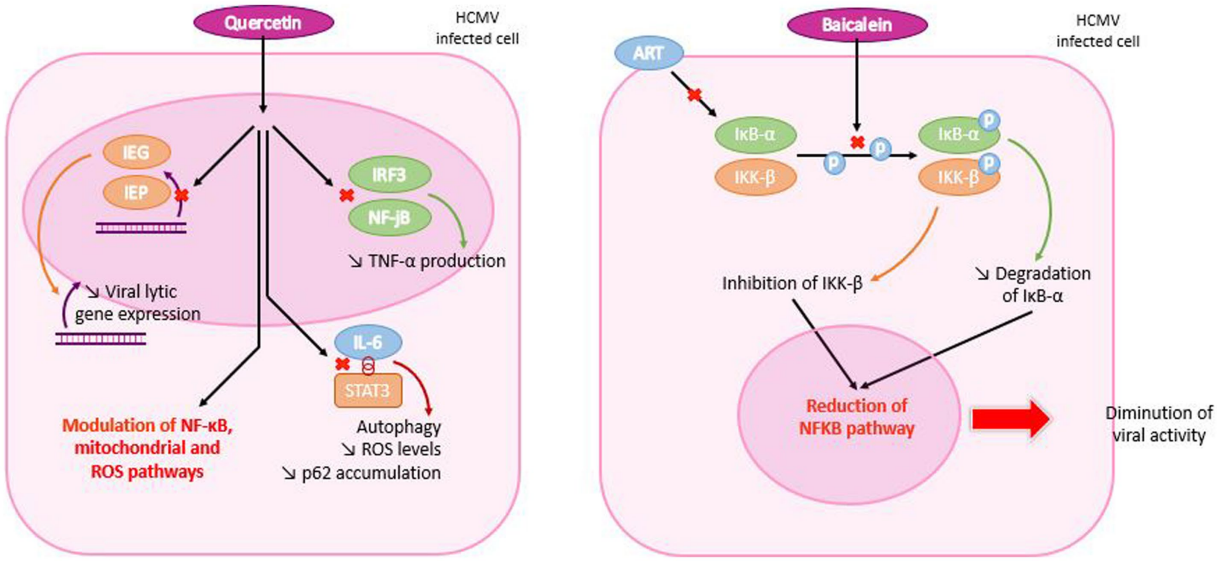

FIGURE 10
Mechanism of action of quercetin and baicalein in HCMV infected cells. Quercetin enters the HCMV-infected cell and travels to the nucleus, where it inhibits early viral protein and TNF-α production. It also inhibits contact between interleukin 6 (IL-6) and STAT3, resulting in reduced ROS levels and p62 accumulation. Both mechanisms are responsible for modulating NF-κB, mitochondrial and ROS pathways. In the case of baicalein, the molecule penetrates the cell and inhibits phosphorylation of IκB-α and IKK-β, which are degraded and inhibited, respectively. Each molecular mechanism leads to a reduction in the NF-κB pathway and, consequently, in viral activity.

baicalein may be effective at the post-entry stage of viral infection (Luo et al., 2020). Previous studies indicated that baicalein had an inhibitory effect on NF-κB activation induced by pathological factors (Li et al., 2016).

In vitro, baicalein has been shown to act on IκB-α and therefore to have an antagonistic effect with ART, as they share the same target, which could lead to competitive inhibition (Morère et al., 2015). In agreement, Luo et al., reported that baicalein blocks NF-κB activation by inhibiting phosphorylation of IKK-β and IκB-α. By reducing IκB-α degradation, baicalein could inhibit viral replication (Luo et al., 2020). Thus, HSV-1 infections are prevented by a dual mechanism: the suppression of IKK-β phosphorylation and the decrease of NF-κB activation. This study also demonstrated that baicalein inactivates HSV-1 particles in a direct manner (Luo et al., 2020). However, further studies are needed to explain how baicalein acts on IKK-β phosphorylation (Figure 10).

4.2.2.2 Preclinical tests

Baicalein has a poor oral bioavailability and a low aqueous solubility, which are the major disadvantage of this molecule. Studies of oral administration of baicalein have demonstrated that it is glucuronized in the intestinal wall and livers of rats and humans (Nagashima et al., 2000; Zhang et al., 2005, 2007). Additionally, baicalein is well absorbed by the small intestine and stomach (Taiming and Xuehua, 2006).

Some studies demonstrated baicalein is metabolized to baicalein and baicalein 6-O-sulfate in blood (Muto et al., 1998; Zhang et al., 2004; Dou et al., 2011). Following intravenous administration in rats, 75.7% of circulating baicalein in blood was as conjugated metabolites form (Lai et al., 2003). The bioavailability of baicalein in monkeys reached 23.0% after oral and intravenous administrations (Tian et al., 2012).

Cotin et al. (2012) demonstrated that baicalein inhibits *in vitro* CMV early proteins production. The inhibition of the tyrosine kinase activity of the EGF factor was already proved in a previous study (Evers et al., 2005). Additionally, combinations of quercetins and baicalein revealed additive effects particularly when baicalein was added at fixed quercetin concentrations. That reflected the probably higher efficacy of baicalein (Cotin et al., 2012).

4.2.2.3 Clinical study

A randomized, double-blind, single-dose phase I trial of baicalein (100–2,800 mg) was conducted in 72 healthy adults. Analysis of baicalein and baicalin (baicalein's 1st metabolite) was performed by liquid chromatography–tandem mass spectrometry on various biological fluids. Urinary clearance of baicalein and baicalin was 1, and 27% of baicalein was eliminated unchanged in feces. Eleven treatment-related side effects were recorded, but these were defined as moderated and resolved without further treatment. Baicalein is well tolerated by healthy patients, and no liver or kidney toxicity was observed (Li et al., 2014).

In 2021, another trial was conducted by Li et al. using data from the 2014 Phase I clinical trial. It was a randomized, placebo-controlled, multi-dose, and escalating trial of 36 healthy subjects who received 200, 400, and 600 mg of baicalein or placebo tablets. The drug was administered once on days 1 and 10, and three times daily from day 4 to 9. To analyze the pharmacokinetics of baicalein, blood and urine samples were taken from the 600 mg group. This study showed that baicalein tablets were safe and well tolerated. Mild adverse effects were observed, but none were not resolved. Maximum plasma concentrations were observed within 2 h of baicalein administration. Urinary excretion of baicalein and its metabolites peaked in 2 h, followed by a tendency to double the peak in 12 h. These results support the launch of a Phase II clinical trial (Li et al., 2021).

4.2.2.4 Resistances

No resistance mutation to baicalein was reported in CMV.

4.3 Anti-COX-2

COX-2 inhibitors (cyclooxygenase-2) have been developed to reduce the adverse effects associated with the use of aspirin and indomethacin (gastric hemorrhage or perforation and hepatotoxicity; Nagi et al., 2015). Structural studies have highlighted the inhibitory activity of COX-2 as a heterocyclic or carbocyclic structure and substituting sulfonamide or methylsulfonyl in position para on one of the aromatic rings (Chakraborti et al., 2010). Nevertheless, some anti-COX-2 agents have been shown to cause serious adverse effects and have been withdrawn from the market (Mukherjee, 2002). Thus, certain anti-COX-2 agents have been identified in plants with fewer side effects than polyphenols. In this category, chalcones are a sub-category of the flavonoid family (Cerella et al., 2010).

4.3.1 Mechanism of action

HCMV has been shown to increase the amount of COX-2 enzyme in infected cells, establishing an inflammatory state to promote replication (Speir et al., 1998). As part of the analysis of anti-inflammatory activity, certain chalcone derivatives and those of 2′-hydroxychalocone were determined to inhibit COX-2 and the production of PGE2 catalyzed by this enzyme. Chalcones appear to act before the early stage of viral replication, by reducing the production of IE-1 and IE-2 proteins (Andouard et al., 2021).

4.3.2 Preclinical study

Celecoxib, a COX-2 inhibitor, was evaluated against HCMV in *in vitro* and *in vivo* (mouse) models of medulloblastoma. Its efficacy was compared with that of VGC. Both drugs inhibited HCMV replication *in vitro*, inhibited PGE2 production and reduced growth of medulloblastoma tumor cell *in vitro* and *in vivo* (Baryawno et al., 2011).

In a study carried out in 2021, the anti-HCMV activity of new 2′-hydroxychalcone compounds was assessed. These molecules were designed to inhibit PGE2 synthesis. To achieve this, a COX-2 pharmacophore (sulfonamide motif) and other substituents (chlorine, fluorine and methyl group) were introduced into the 2′-hydroxychalcone backbone (Zarghi and Arfaei, 2011). The selection of 4 anti-COX-2 agents was based on their significant activity against PGE2 production. However, three of them proved to be toxic to cells and one had a CC50 of 1,500 µM in growing cells and 185 µM in static cells, which was related to indomethacin (a non-specific cyclooxygenase inhibitor). Toxicity was potentially increased by the presence of the SO_2NH_2 group in the molecules, whereas the presence of the chlorine atom reduced it. These 2'hydroxychalcones were defined as less toxic than the tri-hydroxychalcones (Cotin et al., 2012). The molecules were tested against strain AD169-GFP. EC50s were up to 16 times higher than GCV (EC50 = 19.6 ± 10.1 µM; 8.6 ± 10.1 µM; 10.5 ± 3.6 µM; 22.1 ± 7.7 µM; 15.1 ± 5.9 µM for the 4 chalcones and indomethacin respectively). EC50s were also determined on clinical isolates and proved effective against resistant strains. Three chalcones tested proved capable of inhibiting IE1-72 production (Andouard et al., 2021).

In addition, a synthesized anti-COX-2 was combined with other anti-CMV drugs such as GCV, MBV, baicalein, quercetin and ART. This resulted in a synergistic effect with MBV or baicalein. An additive effect was demonstrated with GCV or ART, and an antagonistic effect was observed with quercetin (Andouard et al., 2021).

4.3.3 Clinical study

No clinical study was done for anti-COX-2 molecules against HCMV (source: ClinicaTrials.gov).

4.3.4 Resistances

So far, no resistance mutations in HCMV genome were defined.

5 Immunomodulating molecules

5.1 Leflunomide

Leflunomide (LEF) (HWA 486; A77 1726, Arava®) or N-(4-trifluoromethylphenyl)-5-methylisoxazol-4-carboxamide (Figure 2) is an antirheumatic agent used to treat rheumatoid arthritis. It was also demonstrated as effective in HCMV infection in HCT and renal transplant.

5.1.1 Mechanism of action

After administration, LEF is converted to an active matabolite, teriflunomide (A77 1726) that blocks lymphocyte enzyme dihydroorotate dehydrogenase and the pyrimidine biosynthetic pathway (Williamson et al., 1996). This activity results in a lower T-cell proliferation and changes in immune response (Dayer and Cutolo, 2005; Chong et al., 2006). At a later stage in virion assembly, it prevents viral nucleocapsides from acquiring integument. LEF has a dose-dependent effect on the infectious production of HCMV (Waldman et al., 1999a). Unlike polymerase inhibitors, LEF did not inhibit HCMV DNA replication, but it did appear to interfere with tegument assembly by inhibiting protein phosphorylation (Xu et al., 1995; Waldman et al., 1999b; Figure 11).

5.1.1.1 Preclinical tests

HCMV isolates in human fibroblats and endothelial cells, including multidrug-resistant viruses (EC_{50} 40–60 µM), are inhibited by LEF (Waldman et al., 1999b). LEF also inhibits HSV-1 with same mechanism of action than with HCMV (Knight et al., 2001).

Furthermore, the LEF was evaluated *in vivo* using animal models. Immunodeficient rats were inoculated with rat CMV (Maastricht strain of RCMV) and administered 15 mg/kg/day LEF for 14 days, 10 mg/kg/day GCV for 5 days, or a drug-free vehicle. Plaque assay from tissue homogenates (salivary glands, spleen and lung) showed a decrease of 75 to 99% of viral load in the organs of animals treated with LEF, and 85 to 99% in those treated with GCV. Thus, LEF is an effective agent in decreasing viral load *in vivo* (Waldman et al., 1999a). After that, it was demonstrated the efficacy of LEF in an allogenic cardiac transplant model of RCMV infection with low toxicity (Chong et al., 2006).

5.1.1.2 Clinical study

Due to its synergy with calcineurin phosphatase inhibitors and its inhibitory effects on herpesvirus replication, LEF was presented as a promising drug for experimental transplantation (Williams et al.,

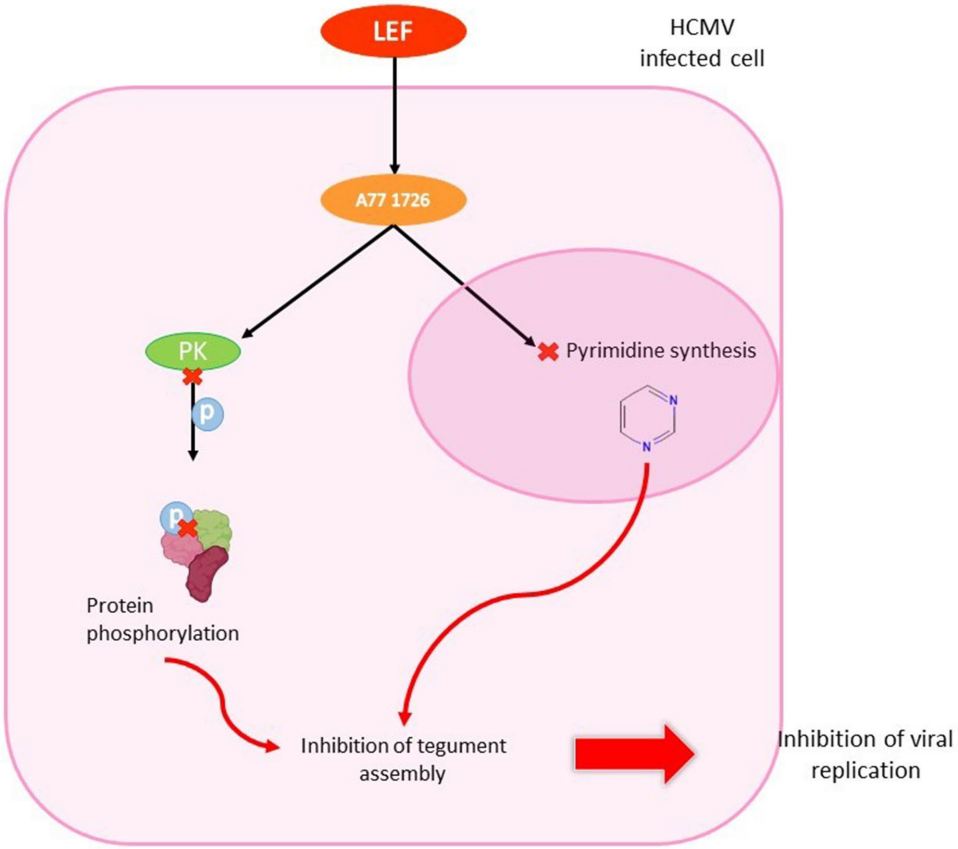

FIGURE 11
Antiviral effect of leflunomide in HCMV infected cell. LEF enters the HCMV-infected cell and is converted to teriflunomide (A77 1726). The metabolite inhibits protein kinase, which is unable to phosphorylate proteins. It also penetrates the nucleus to inhibit pyrimidine synthesis. These two mechanisms are involved in inhibiting tegument assembly, thereby stopping viral replication.

2002). Fifty-three recipients of LEF were analyzed in a retrospective study. A single-dose pharmacokinetic study was performed in stable renal transplant recipients with a target serum concentration of 100 µg/mL to require a loading dose of 1,200 to 1,400 mg over a 7-day period. Anemia in the renal transplant patients and increase of liver enzymes in liver-transplanted patients were the major observed toxicities (Williams et al., 2002). Another study reported same side effects and diarrhea after a therapy with a mean duration of 3.5 months. The recommended dose of LEF was 100 mg/day for 5 days followed by 40 mg/day, based on the serum metabolite levels of A77 1726 teriflunomide (Avery et al., 2010).

In one study, John and colleagues analyzed 17 patients who underwent kidney transplantation and were infected with CMV. Patients were treated with monitored doses of leflunomide. Among these 17 patients, 88% responded clinically to leflunomide therapy with viral clearance in the blood and healing of the organs involved. The cost of treatment was cheaper than that of ganciclovir: 64 $ for 6 months against 721 $ for 2 weeks, respectively, (John et al., 2005).

Three cases of resistant HCMV infections were reported with LEF treatment. It was showed that LEF is not efficient enough in monotherapy and should be combined with GCV or FOS to better control CMV infection. It was also only used for CMV maintenance therapy (El Chaer et al., 2016). As an oral treatment, LEF is also a convenient alternative that does not need to stay in hospital to reach undetectable viral load (Gómez Valbuena et al., 2016). Then, after lung transplant, LEF was assessed in a case of drug resistant CMV retinitis. In spite of intravitreal FOS administration and oral VACV, HCMV disease progressed. Oral LEF helped in control of retinitis and allowed cessation of intravitreal treatment. No recurrence of infection was noticed (Rifkin et al., 2017).

A more recent study on case series assessed LEF in patients treated with GCV and FOS with adverse effects reported in 50% of cases. In 66.67% of cases, resistance mutations to polymerase inhibitors were present before LEF treatment. LEF was prescribed to treat HCMV infection in 75% of patients and as secondary prophylaxis in 25% of them. A primary reduction of HCMV viremia was observed after the beginning of LEF treatment in 77.7% of recipients but was transient in 22.2%. In 58.3% of recipients, LEF suppressed HCMV infection for long-term. Adverse effects were responsible for treatment discontinuation in 25% of cases. This study showed that LEF can be an effective treatment for transplant recipients with GCV-resistant infections, whether alone or combined with other drugs, even though the small number of subjects was a limitation. It can also be used as a secondary prophylaxis (Silva et al., 2018). LEF was also proposed in combination with hyperimmune globulins in cardiothoracic grafts and was associated with decreasing viremia (Santhanakrishnan et al., 2019).

In other hand, there is few numbers of studies with LEF in allogeneic HCT. One reported that LEF had efficacy in HCMV clearance in 38% of cases. Nevertheless, treatment significantly succeeded (53%; $p = 0.022$) only when LEF was used in patients with HCMV viral load <2.10^{3}copies/mL. Furthermore, it was demonstrated as ineffective in patients with terminal organ disease. Thus, LEF could be used in prophylaxis in stem cell transplants (Gokarn et al., 2019).

5.1.1.3 Resistance

Currently, there is no reported resistance mutation to leflunomide in HCMV.

5.2 mTOR inhibitor: everolimus

Everolimus (SDZ RAD; Certican®, ZORTRESS®; EVR) or 40-O-(2-hydroxyethyl)-rapamycin (Figure 2) is an oral mammalian target of a sirolimus-derived rapamycin inhibitor. It is used in immunosuppressive therapy after SOT. FDA approved it for the prevention of rejection in kidney transplant recipients at low to moderate risk (Gabardi and Baroletti, 2010).

5.2.1 Mechanism of action

Intracellular immunophilin (FKBP12) is bound by EVR, but it does not inhibit calcineurin, it binds to the mechanistic target of Rapamycin (mTOR). It is at the origin of the inhibition of a multifunctional serine–threonine kinase, preventing both the synthesis of DNA and proteins that leads to a cell cycle shutdown. More precisely, after stimulation of the IL-2 receptor on the activated T-cell, EVR inhibits p70S6 kinase which acts at a later stage in the T-cell mediated response (Roy and Arav-Boger, 2014). EVR inhibits HCMV through improved CD8+/CD4+ T cell responses specific to HCMV (Havenith et al., 2013; Roy and Arav-Boger, 2014; Figure 12).

5.2.1.1 Preclinical tests

So far, no preclinical test of the *in vitro* anti-HCMV efficacy of EVR was done because it is not the primary function of this molecule.

5.2.1.2 Clinical study

The effectiveness of EVR against HCMV has been demonstrated for several years. A multicenter Phase III trial included 634 heart transplant patients receiving immunosuppressive therapies (1.5 mg/day EVR; 3 mg/day EVR or azathioprine). The EVR groups had significant lower HCMV incidence ($p < 0.001$). Thus, the use of EVR suggests an additional benefit in cardiac transplant recipients as it is linked to lower rates of HCMV infection, syndrome or organ damage (Hill et al., 2007). In accordance with these results, same doses of EVR were assessed in heart and renal transplants recipients compared to mycophenolic acid (MPA). A significantly lower HCMV incidence was observed in the EVR group at 3.0 mg (3%) than in the MPA group (7%) ($p < 0.04$). The same observation was made for organ involvement in the EVR 1.5 mg group (0.9%) than in the MPA group (3%) ($p < 0.04$). Therefore, the EVR was associated with a decrease in EVR events compared to the MPA (Brennan et al., 2011). In a study of data from 3 randomized trials of *de novo* cardiac transplant recipients, Kobashigawa et al. reported that EVR was linked to a significantly lower incidence of HCMV infections compared to azathioprine and mycophenolate mofetil by combining its immunosuppressive efficacy with antiproliferative effects that may have a positive impact on long-term results (Kobashigawa et al., 2013).

In another study, EVR was compared with valganciclovir (VGC) in heart transplant recipients. EVR was introduced at 1.5 mg/day to discontinue the use of mycophenolate mophetil in combination with VGC that caused neutropenia. HCMV antigenemia was negative even after discontinuation of VGC and both renal function and neutrophil counts were normalized. No major side effects or rejection due to EVR were observed. Thus, EVR was described as an alternative or additive option in immunosuppressive therapy for heart transplant recipients because of maintenance of immune tolerance, prophylactic potency against HCMV, reduced myelosuppression and potential sparing of renal function (Imamura et al., 2012).

The impact of EVR on HCMV infection at both systemic or pulmonary level was also evaluated in lung transplant recipients ($n = 32$ patients). Eighteen patients were on EVR-immunosuppressive regimens. No differences were described in HCMV viremia occurrence between EVR-based and EVR-free immunosuppressive regimens. However, patients with EVR treatment experienced fewer high-load HCMV episodes defined as $\geq 10^5$ copies/mL during EVR administration. It validate the reduction of HCMV events in EVR-based regimens transplanted patients, as lung transplant recipients (Rittà et al., 2015).

The international randomized phase IV TRANSFORM trial (NCT01950819) was conducted in *de novo* renal transplant patients randomized to RVE with reduced exposure to CNI or MPA with standard exposure to CNI, treated with induction and corticosteroids. EVR caused more adverse reactions than MPA, such as hyperlipidemia, interstitial lung disease, peripheral edema, proteinuria, stomatitis/mouth ulceration, thrombocytopenia and wound healing complications. However, EVR has been associated with viral infections less frequently than MPA. Indeed, HCMV infections and HCMV syndrome were lower (8.1% vs. 20.1%; $p < 0.001$ and 13.6% vs. 23.0%; $p < 0.044$ respectively). The same result was observed for BKV infections. EVR was more often stopped due to rejection or delayed healing (Tedesco-Silva et al., 2019). Another phase IV trial (NCT02096107) with EVR in kidney transplants was also conducted and reported that EVR with low tacrolimus exposure produced related efficacy to tacrolimus and MPA with significantly lower BK and HCMV levels (Taber et al., 2019). A more recent Phase IV trial was conducted with 186 seropositive HCMV kidney recipients randomized (1:1) to receive EVR or MPA in combination with basiliximab, cyclosporine and steroids. In seropositive recipients, HCMV DNAemia is prevented by EVR treatment until it is no longer tolerated or stopped (Kaminski et al., 2022a). In addition, the same authors reported that the T-cell phenotype may offer a new biomarker for predicting post-transplant infection and classifying patients who should be eligible for EVR treatment (Kaminski et al., 2022b).

5.2.1.3 Resistances

Currently, there is no resistance mutation to EVR that was reported in CMV.

6 Immunoglobulins

Two types of immunoglobulins are available in therapy: intravenous administered immunoglobulins (IVIG) and

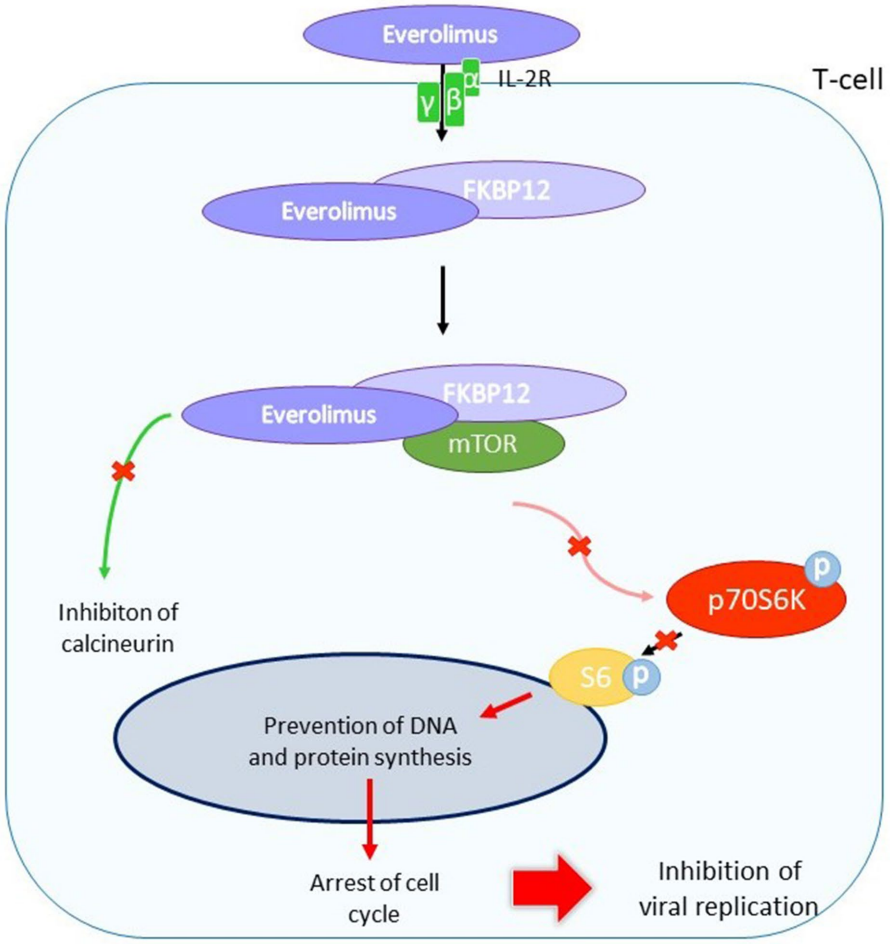

FIGURE 12
Indirect antiviral action of everolimus in HCMV infected T-cell. EVR binds to the interleukin-2 receptor (IL-2R) on HCMV-infected T cells. The molecule enters the cell and binds to the immunophilin FKBP12. The complex binds to mTOR, which is unable to phosphorylate the p70S6 kinase. The kinase does not phosphorylate S6, which is involved in DNA and protein synthesis. HCMV replication is inhibited by cell cycle arrest.

hyperimmune immunoglobulins (CMV-HIG). We will focus on HCMV-specific immunoglobulins which are able to neutralize viral infectivity (Aiba et al., 2017). Immunoglobulins may be used in preventing congenital infections or in association with other antivirals to cure HCMV infection in transplantation (El-Qushayri et al., 2021).

CMV-HIG are obtained by purification of adult human plasma-derived immunoglobulin products in pools selected for high levels of anti-HCMV antibodies. IVIG are acquired from the plasmas of healthy blood donors on the basis of a high level of antibodies against HCMV (Maniez-Montreuil et al., 1984). Using a correlation test between HCMV antibody titer and viral neutralization titer, it was shown that HIG has a higher level of anti-HCMV IgG than IVIG (Germer et al., 2016; Schampera et al., 2017). Currently, there is two options of HCMV-HIG which are, respectively, authorized in United States and Europe: Cytogam® (CMVIG CG; CSL Behring, Berne, Switzerland) and Cytotect CP® (Biotest AG).

Cytogam® is an HCMV-HIG derived from human plasma with high titers of anti-HCMV antibodies [112,5 PEIU/mL (Paul Ehrlich Institute Units)] (Germer et al., 2016). It contains a standardized amount of Ig (5 ± 0.1%). In the United States, it is approved for the prophylaxis of HCMV disease in heart, liver, lung, kidney and pancreas transplant recipients.

Cytotect CP® contains 5% Ig (50 mg/mL), 96% of which is IgG (110.1 PEIU/mL) (Germer et al., 2016). Its maximum IgA level is 2 mg/mL, and its anti-HCMV antibody level is 100 U/mL. It is approved in Europe for the prophylaxis of HCMV infection in patients treated with immunosuppressants and in solid organ transplant patients. In France, this solution is available as part of a patient-nominated program for the prevention or treatment of HCMV infection.

Cytotect CP® and Cytogam® preparations have high avidity indexes (90.5 and 91.0% respectively) and both have been tested in immunoblot assays against antigenic HCMV glycoproteins with similar results (Germer et al., 2016).

6.1 Mechanism of action

HCMV-HIG involve the neutralization of viral particles in extracellular environment, opsonization for phagocytosis (ADP),

activation of the cellular immune system (ADCC) and immune adaptation with complement activation (Carbone, 2016; Figure 13).

6.2 Preclinical tests

Efficacy of HCMV-HIG was proved *in vitro* with a higher HCMV neutralizing activity than IVIG (Miescher et al., 2015; Germer et al., 2016; Schampera et al., 2017).

In 2022 and 2023, an *in vitro* and *ex vivo* (in placental villi of the first trimester) study analyzed the efficacy and mode of action of Cytotect CP® and showed good efficacy and low toxicity in different routes of HCMV infection (Coste Mazeau et al., 2022, 2023). The development of infection foci was blocked by Cytotect CP® with a DN50 of 0.011 to 0.033 U/mL on endothelial strains (TB40E/VHLE) in *in vitro* neutralization assays. Samely, on day 7, Cytotect CP® prevents CMV infection with an EC_{50} of 0.024 U/mL in placental villi. Although, once infected, viral growth was not inhibited in explants. The viability of villi has not been affected. An additional study shows the need for renewing Cytotect CP® every 7 days in the medium to maintain efficacy at day 14 in the explants. This was coherent with the recent pharmacokinetics study from Kagan et al. showing the decrease of plasma concentrations within 2 weeks (Kagan et al., 2021).

Potency of CMV-HIGs during pregnacy was assessed in animal models. Guinea pigs were used as model to study HCMV-HIG because congenital infection has similarities between HCMV and GPCMV. The placental barrier can be crossed by both viruses that can create an *in utero* infection. In guinea pig experiments, pup survival is the endpoint as GPCMV causes their death (Schleiss, 2008). This model evaluated passive immunization of the fetus. Indeed, studies have used pregnant guinea pigs with GPCMV infection prior to HIG administration or after to assess the inhibition of viral particle and gB. In two studies, fetal survival was increased after administration of CMV-HIG but the viral load was not affected (Bia et al., 1980; Chatterjee et al., 2001). Thus, anti-gB CMV-HIG were used in another study and allowed a reduction in fetal infection, inflmmation of placenta, death of the fetus and increased fetal development. Results were independent of CMV-HIG administration time. Infection rate of fetuses was significantly reduced with the administration of CMV-HIG from 39 to 0%. Anti-gB HIG also reduced inflammation of placenta and increased fetal development (Bratcher et al., 1995).

The mouse model was used to assess passive immunization in the fetal brain because the mouse CMV (mCMV) does not pass through the placental barrier. Peritoneal cavity of new-born mice was infected with mCMV. The viral infection was disseminated in mice brains with associated inflammatory lesions such as infiltrations of mononuclear

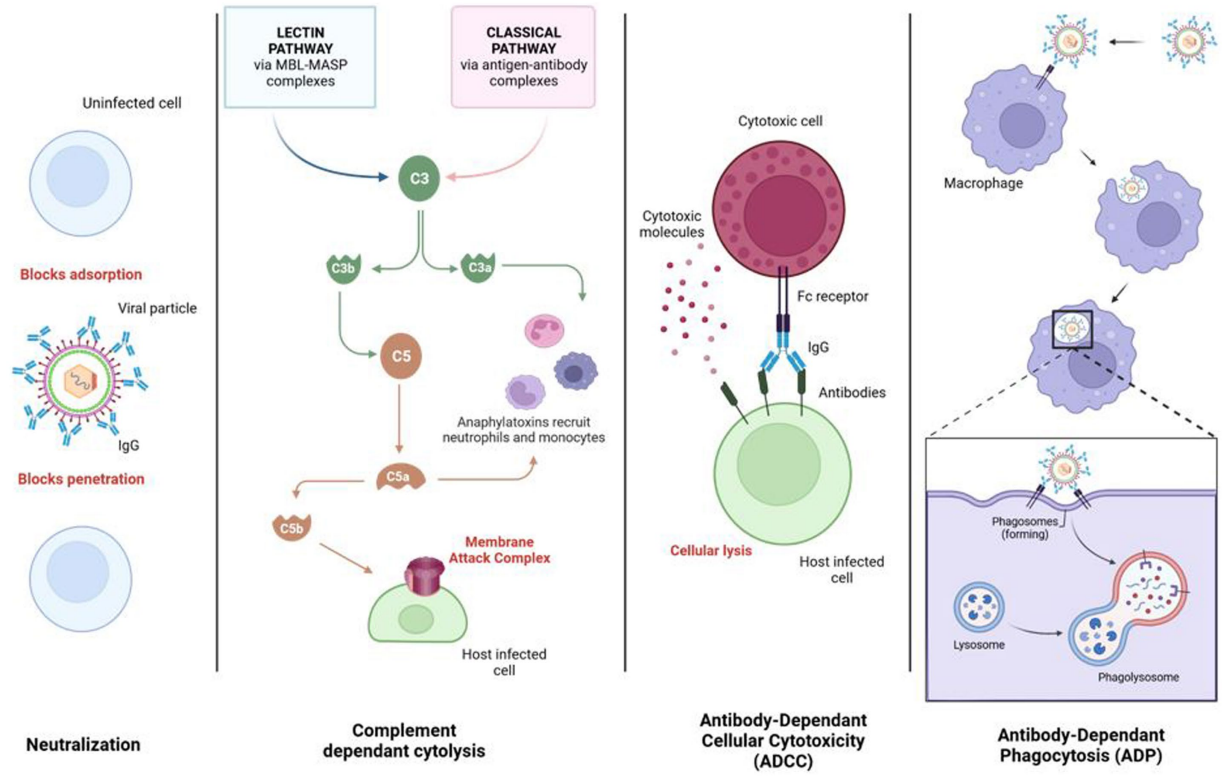

FIGURE 13
The four modes of action of anti-CMV immunoglobulins. In the first mechanism, HIGs neutralize the viral particle by binding its epitope to viral envelope glycoproteins. Virus adsorption and cellular penetration are inhibited. In the second mechanism, HIGs induce complement pathways leading to the formation of the membrane attack complex (MAC), which creates a hole in the cell membrane leading to cytolysis. In the third mechanism (ADCC), the Fc fraction of the HIG-neutralizing viral particle is recognized by the cytotoxic cell's Fc receptor (FcR). This leads to the release of cytotoxic molecules that create a cytolysis signal. In the final mechanism, after neutralization of the viral particle by HIGs, macrophage FcRs recognize HIG Fc, resulting in a phagocytosis signal. The viral particle-HIG complex is phagocytosed. The phagosome fuses with the lysosome, forming a phagolysosome and destroying the complex. Created with BioRender.com

cells and prominent glial nodules. Treatment with HIG or monoclonal antibody specific of gB glycoprotein led to decrease of viral load in the brains and a 5-fold reduction of inflammatory lesions. This study showed that CMV-HIG are responsible for a limitation of viral replication and its associated lesions in the brain (Cekinović et al., 2008).

6.3 Clinical trials

CMV-HIG treatments were shown to be effective against severe HCMV infections in immunocompromised patients and congenital infections. Whereas, retrospective studies assessed the potency of the HCMV-HIG for the prevention of cCMV infection. To date, the only two published trials have reported that anti-HCMV IgG has not been effective (Revello et al., 2014; Hughes et al., 2021). The effectiveness of treatment is determined according to the frequency of treatment, the concentration of HCMV-HIG and the time of seroconversion of the patient (Kagan et al., 2019, 2021). A new administration protocol with higher concentrations at the first stage of pregnancy will begin as a third Phase III trial (NCT 05170269).

Concerning adverse events, in the phase II study, Cytotect® CP was associated with a tendancy to a low birth weight for treated newborns (Revello et al., 2014). Nevertheless, these results were disclaimed by a newer investigation of Chiaie et al. that was conducted in 50 women with a dose of 200 unit/kg taken twice during pregnancy. No side effects caused by HCMV-HIG were reported in this study (Chiaie et al., 2018).

Recently, an observational study was undertaken in 149 pregnant women to assess the effectiveness of Cytotect CP® in pregnant women with HCMV primary infection during the first trimester or periconceptional period. This study was based on pharmacokinetics results showing the half-life of HCMV-HIGs, which is about 10 days. Every 2 weeks, a dose of 200 IU/kg body weight of Cytotect CP® was injected to women with primary infection before 14 weeks of amenorrhea. Intravenous injection should begin within 3 weeks of discovery of the primary infection. HCMV-HIG injections were made until the 18th week of amenorrhea. A significantly lower rate of maternal infection transmitted to the fetus was observed with 7.5% in the intervention group and 35.2% in the control group (Kagan et al., 2021).

In comparison with the historical cohort of Feldman, Seidel et al. conducted an observational survey using the same doses as Kagan et al. and found a significant reduction in the rate of mother-to-fetus transmission, regardless of the term of pregnancy (23.9% versus 39.9% for the Feldman control group; $p = 0.026$; Feldman et al., 2011; Seidel et al., 2020).

Some observational studies suggest that HCMV-HIG may have a protecting effect on the fetus after maternal primary infection (Buxmann et al., 2012). Cytotect® CP was evaluated on 592 cases of maternal primary infection before the 19th week of amenorrhea. After an administration of 200 unit/kg, HCMV-linked symptoms in the newborn decreased (Visentin et al., 2012).

Nevertheless, Cytotect CP® has also been evaluated in rescue therapy for hematopoietic stem cell recipients with resistant refractory infections. One study determined the safety and efficacy profiles of Cytotect CP® in 23 patients with refractory HCMV and GVHD (74%) and/or steroid treatment (64%). After 15 days, a response was observed in 18 patients. Of the 18, four had CMV reactivation, one died of CMV infection, and 4 died of CMV-related causes within 100 days of starting treatment. Total 100-day survival was 69.6% after Cytotect CP®. However, no statistical difference between respondents and non-respondents was reported. Thus, it showed that Cytotect CP® was well tolerated and effective as a recovery treatment (Alsuliman et al., 2018).

Another rescue therapy study was conducted in cardiothoracic transplant recipients. This was a 6-year retrospective single-center experiment in 35 patients. The rescue therapy consisted of Cytotect CP® supplemented by antiviral treatment (GCV/VGCV/LEF). HCMV-HIGs were well tolerated by patients and safe; only two patients had adverse events, but their symptoms were resolved after reducing HCMV-HIG doses to 1.5 mg/kg. CMV DNA was reduced in all patients and, after 4 weeks, undetectable in 73% of them. HCMV-HIG were shown as effective to control viral replication in cardiothoracic transplant recipients (Santhanakrishnan et al., 2019).

6.4 Resistances

So far, there is no reported case of resistant CMV to HIG.

7 Discussion

The CMV DNA polymerase inhibitors (GCV, FOS, and CDV) are essential molecules for decreasing the morbidity and mortality rate associated with CMV infection in transplant recipients (SOT or HSCT). However, they are often responsible for toxicity (hematologic or renal) and emergence of resistance that may limit their use. Nevertheless, they are always the most used in clinical practice. The approval of letermovir represents an important innovation for CMV prevention in HSCT. A decisive step forward in the management of refractory and/or resistant infections has been achieved with the validation of maribavir in transplant recipients. However, in case of multidrug resistance, or in non-transplanted patient or also in the prevention and treatment of cCMV infection, finding new antivirals or molecules able to inhibit CMV replication with the lowest toxicity remains a critical need.

In this review, we have listed the main compounds with potential activity against CMV. They belong to different families of molecules, some with specific antiviral activity, others known for their antimicrobial or immunosuppressive activities but with anti-CMV efficacy, and still others with a completely different mode of action, such as immunoglobulins.

Some direct antivirals like brincidofovir or cyclopropavir have an interesting profile for CMV treatment, but the development of the first was stopped after emergence of toxicity in a phase II clinical trial whereas the second did not enter in phase II trials until now. The search of cidofovir derivatives or pro-drugs is not yet stopped: recently, a new family of antiviral acyclonucleoside analogs with high bioavailability and potential activity against HCMV was patented (Roy and Agrofoglio, 2022) and are under evaluation (personal data). Concerning anti-terminase benzimidazole analogs, their poor biodisponibility limited their clinical use. As the effectiveness of letermovir validates terminase inhibitors as a clinically relevant class of antiviral agents, the development of other terminase inhibitors may

be considered and research on these inhibitors should be encouraged (Ligat et al., 2018; Gentry et al., 2019). Indirect antivirals are also an interesting area to explore because of their cellular targets, which do not select for resistance to direct antivirals. Artemisin derivatives have shown their efficacy to control HCMV replication in some transplant patients but with varying degrees of effectiveness. A degree of uncertainty therefore remains when these treatments are used as monotherapy but artesunate is still an alternative alone or in association in multidrug resistant infections. Other indirect antivirals like flavonoids or anti-cox derivatives have demonstrated good efficacy *in vitro* but few or no study were performed until now with these molecules. Expanding these families of chemical compounds could be a complementary approach. Concerning immunomodulating agents, leflunomide, mTOR inhibitors and immunoglobulins could be used in combination with other antiviral drugs, as their use as monotherapy is not sufficiently effective to be recommended for the control of high level HCMV replication.

With agents acting by new modes of action as LTV and MBV available in clinical use, association therapy for the treatment of CMV infection and disease can move from concept to reality. *In vitro* studies support at least one additive (and sometimes synergistic) effect of association of LTV or MBV with DNA polymerase inhibitors. MBV targeting the kinase pUL97, his mode of action differs from the DNA polymerase or terminase inhibitors, but pUL97 being the kinase essential for GCV activation, association of both antivirals are antagonist. Moreover, we and others have already demonstrated *in vitro* that combination of indirect antiviral with DNA polymerase inhibitors have additive or synergistic activity (Morère et al., 2015; Wildum et al., 2015; Drouot et al., 2016; Chou et al., 2019). So far, clinical studies are needed to assess which combination therapy for HCMV is superior to monotherapy and which combination regimens are most effective. Combination therapy has already proved its relevance to treat other viral infections such as human immunodeficiency virus and hepatitis C virus (Hepatitis, 2018; Saag et al., 2020). Use of immunoglobulins in addition with antiviral therapy should also be considered in immunosuppressed patients, especially those with weak or null cellular response against CMV. Nevertheless, the effectiveness of this approach must be confirmed in clinical trials to better define the indications according to the patient profile, the history of CMV infection and the antivirals already used. Since few agents are currently being studied in humans, a combination therapy with existing agents and possibly with indirect acting anti-HCMV molecules approved for other indications not suitable for use in monotherapy should be considered.

Author contributions

CG: Writing – original draft. SA: Writing – review & editing. SH: Writing – review & editing.

Funding

The author(s) declare financial support was received for the research, authorship, and/or publication of this article. This work was granted by the University of Limoges and Santé Publique France (National Reference Center for Herpesviruses).

Conflict of interest

SA is an expert for Takeda, MSD, Merck and Biotest with no personal link.

The remaining authors declare that the research was conducted in the absence of any commercial or financial relationships that could be construed as a potential conflict of interest.

Publisher's note

References

Adjuik, M., Babiker, A., Garner, P., Olliaro, P., Taylor, W., and White, N. (2004). Artesunate combinations for treatment of malaria: meta-analysis. *Lancet* 363, 9–17. doi: 10.1016/S0140-6736(03)15162-8

Aiba, N., Shiraki, A., Yajima, M., Oyama, Y., Yoshida, Y., Ohno, A., et al. (2017). Interaction of immunoglobulin with cytomegalovirus-infected cells. *Viral Immunol.* 30, 500–507. doi: 10.1089/vim.2016.0151

Alain, S., Feghoul, L., Girault, S., Lepiller, Q., Frobert, E., Michonneau, D., et al. (2020). Letermovir breakthroughs during the French named patient Programme: interest of monitoring blood concentration in clinical practice. *J. Antimicrob. Chemother.* 75, 2253–2257. doi: 10.1093/jac/dkaa135

Aldern, K. A., Ciesla, S. L., Winegarden, K. L., and Hostetler, K. Y. (2003). Increased antiviral activity of 1-O-hexadecyloxypropyl-[2-(14)C]cidofovir in MRC-5 human lung fibroblasts is explained by unique cellular uptake and metabolism. *Mol. Pharmacol.* 63, 678–681. doi: 10.1124/mol.63.3.678

Alsuliman, T., Kitel, C., Dulery, R., Guillaume, T., Larosa, F., Cornillon, J., et al. (2018). Cytotect®CP as salvage therapy in patients with CMV infection following allogeneic hematopoietic cell transplantation: a multicenter retrospective study. *Bone Marrow Transplant.* 53, 1328–1335. doi: 10.1038/s41409-018-0166-9

Alvarez-Cardona, J. J., Whited, L. K., and Chemaly, R. F. (2020). Brincidofovir: understanding its unique profile and potential role against adenovirus and other viral infections. *Future Microbiol.* 15, 389–400. doi: 10.2217/fmb-2019-0288

Amoros, M., Simões, C. M., Girre, L., Sauvager, F., and Cormier, M. (1992). Synergistic effect of flavones and flavonols against herpes simplex virus type 1 in cell culture. Comparison with the antiviral activity of propolis. *J. Nat. Prod.* 55, 1732–1740. doi: 10.1021/np50090a003

Andouard, D., Gueye, R., Hantz, S., Fagnère, C., Liagre, B., Bernardaud, L., et al. (2021). Impact of new cyclooxygenase 2 inhibitors on human cytomegalovirus replication in vitro. *Antivir. Ther.* 26, 117–125. doi: 10.1177/13596535211064078

Andouard, D., Mazeron, M. C., Ligat, G., Couvreux, A., Pouteil-Noble, C., Cahen, R., et al. (2016). Contrasting effect of new HCMV pUL54 mutations on antiviral drug susceptibility: benefits and limits of 3D analysis. *Antivir. Res.* 129, 115–119. doi: 10.1016/j.antiviral.2016.02.004

Arav-Boger, R., He, R., Chiou, C. J., Liu, J., Woodard, L., Rosenthal, A., et al. (2010). Artemisinin-derived dimers have greatly improved anti-cytomegalovirus activity compared to artemisinin monomers. *PLoS One* 5:e10370. doi: 10.1371/journal.pone.0010370

Aryal, S., Katugaha, S. B., Cochrane, A., Brown, A. W., Nathan, S. D., Shlobin, O. A., et al. (2019). Single-center experience with use of letermovir for CMV prophylaxis or treatment in thoracic organ transplant recipients. *Transpl. Infect. Dis.* 21:e13166. doi: 10.1111/tid.13166

Auerochs, S., Korn, K., and Marschall, M. (2011). A reporter system for Epstein-Barr virus (EBV) lytic replication: anti-EBV activity of the broad anti-herpesviral drug artesunate. *J. Virol. Methods* 173, 334–339. doi: 10.1016/j.jviromet.2011.03.005

Avery, R. K., Alain, S., Alexander, B. D., Blumberg, E. A., Chemaly, R. F., Cordonnier, C., et al. (2021). Maribavir for refractory cytomegalovirus infections with or without resistance post-transplant: results from a phase 3 randomized clinical trial. *Clin. Infect. Dis.* 75, 690–701. doi: 10.1093/cid/ciab988

Avery, R. K., Mossad, S. B., Poggio, E., Lard, M., Budev, M., Bolwell, B., et al. (2010). Utility of Leflunomide in the treatment of complex cytomegalovirus syndromes. *Transplantation* 90, 419–426. doi: 10.1097/TP.0b013e3181e94106

Baryawno, N., Rahbar, A., Wolmer-Solberg, N., Taher, C., Odeberg, J., Darabi, A., et al. (2011). Detection of human cytomegalovirus in medulloblastomas reveals a potential therapeutic target. *J. Clin. Invest.* 121, 4043–4055. doi: 10.1172/JCI57147

Beadle, J. R., Hartline, C., Aldern, K. A., Rodriguez, N., Harden, E., Kern, E. R., et al. (2002). Alkoxyalkyl esters of Cidofovir and cyclic Cidofovir exhibit multiple-log enhancement of antiviral activity against cytomegalovirus and herpesvirus replication in vitro. *Antimicrob. Agents Chemother.* 46, 2381–2386. doi: 10.1128/AAC.46.8.2381-2386.2002

Beauvais, D., Robin, C., Thiebaut, A., Alain, S., Coiteux, V., Ducastelle-Lepretre, S., et al. (2022). Effective Letermovir prophylaxis of CMV infection post allogeneic hematopoietic cell transplantation: results from the French temporary authorization of use compassionate program. *J. Clin. Virol.* 148:105106. doi: 10.1016/j.jcv.2022.105106

Beecher, G. R. (2003). Overview of dietary flavonoids: nomenclature, occurrence and intake. *J. Nutr.* 133, 3248S–3254S. doi: 10.1093/jn/133.10.3248S

Bia, F. J., Griffith, B. P., Tarsio, M., and Hsiung, G. D. (1980). Vaccination for the prevention of maternal and fetal infection with Guinea pig cytomegalovirus. *J. Infect. Dis.* 142, 732–738. doi: 10.1093/infdis/142.5.732

Bidanset, D. J., Beadle, J. R., Wan, W. B., Hostetler, K. Y., and Kern, E. R. (2004). Oral activity of ether lipid Ester prodrugs of Cidofovir against experimental human cytomegalovirus infection. *J. Infect. Dis.* 190, 499–503. doi: 10.1086/421912

Biron, K. K., Harvey, R. J., Chamberlain, S. C., Good, S. S., Smith, A. A. III, Davis, M. G., et al. (2002). Potent and selective inhibition of human cytomegalovirus replication by 1263W94, a Benzimidazole l-riboside with a unique mode of action. *Antimicrob. Agents Chemother.* 46, 2365–2372. doi: 10.1128/AAC.46.8.2365-2372.2002

Boots, A. W., Balk, J. M., Bast, A., and Haenen, G. R. M. M. (2005). The reversibility of the glutathionyl-quercetin adduct spreads oxidized quercetin-induced toxicity. *Biochem. Biophys. Res. Commun.* 338, 923–929. doi: 10.1016/j.bbrc.2005.10.031

Bratcher, D. F., Bourne, N., Bravo, F. J., Schleiss, M. R., Slaoui, M., Myers, M. G., et al. (1995). Effect of passive antibody on congenital cytomegalovirus infection in Guinea pigs. *J. Infect. Dis.* 172, 944–950. doi: 10.1093/infdis/172.4.944

Bravo, F. J., Bernstein, D. I., Beadle, J. R., Hostetler, K. Y., and Cardin, R. D. (2011). Oral Hexadecyloxypropyl-Cidofovir therapy in pregnant Guinea pigs improves outcome in the congenital model of cytomegalovirus infection. *Antimicrob. Agents Chemother.* 55, 35–41. doi: 10.1128/AAC.00971-10

Brennan, D. C., Legendre, C., Patel, D., Mange, K., Wiland, A., McCague, K., et al. (2011). Cytomegalovirus incidence between Everolimus versus mycophenolate in De novo renal transplants: pooled analysis of three clinical trials. *Am. J. Transplant.* 11, 2453–2462. doi: 10.1111/j.1600-6143.2011.03674.x

Brooks, J. L., and Bowlin, T. L. (2013). *Preclinical pharmacokinetic, safety pharmacology and in vitro and Oral toxicology studies of MBX-400, a potent inhibitor of human cytomegalovirus*.

Brooks, J., Bowlin, T., and Usa, M.. (2015). *Phase 1A clinical trial results of MBX-400; a potent antiviral in development for CMV and HHV-6*.

Buerger, I., Reefschlaeger, J., Bender, W., Eckenberg, P., Popp, A., Weber, O., et al. (2001). A novel nonnucleoside inhibitor specifically targets cytomegalovirus DNA maturation via the UL89 and UL56 gene products. *J. Virol.* 75, 9077–9086. doi: 10.1128/JVI.75.19.9077-9086.2001

Buxmann, H., Stackelberg, O. M., Schlößer, R. L., Enders, G., Gonser, M., Meyer-Wittkopf, M., et al. (2012). Use of cytomegalovirus hyperimmunoglobulin for prevention of congenital cytomegalovirus disease: a retrospective analysis. *J. Perinat. Med.* 40, 439–446. doi: 10.1515/jpm-2011-0257

Carbone, J. (2016). The immunology of Posttransplant CMV infection: potential effect of CMV immunoglobulins on distinct components of the immune response to CMV. *Transplantation* 100, S11–S18. doi: 10.1097/TP.0000000000001095

Cazarolli, L. H., Zanatta, L., Alberton, E. H., Bonorino Figueiredo, M. S., Folador, P., Damazio, R. G., et al. (2008). Flavonoids: prospective drug candidates. *Mini-Rev. Med. Chem.* 8, 1429–1440. doi: 10.2174/138955708786369564

Cekinović, D., Golemac, M., Pugel, E. P., Tomac, J., Čičin-Šain, L., Slavuljica, I., et al. (2008). Passive immunization reduces murine cytomegalovirus-induced brain pathology in newborn mice. *J. Virol.* 82, 12172–12180. doi: 10.1128/JVI.01214-08

Cerella, C., Sobolewski, C., Dicato, M., and Diederich, M. (2010). Targeting COX-2 expression by natural compounds: a promising alternative strategy to synthetic COX-2 inhibitors for cancer chemoprevention and therapy. *Biochem. Pharmacol.* 80, 1801–1815. doi: 10.1016/j.bcp.2010.06.050

Chakraborti, A. K., Garg, S. K., Kumar, R., Motiwala, H. F., and Jadhavar, P. S. (2010). Progress in COX-2 inhibitors: a journey so far. *Curr. Med. Chem.* 17, 1563–1593. doi: 10.2174/092986710790979980

Chang, Y., Lu, C. W., Lin, T. Y., Huang, S. K., and Wang, S. J. (2016). Baicalein, a constituent of Scutellaria baicalensis, reduces glutamate release and protects neuronal cell against Kainic acid-induced excitotoxicity in rats. *Am. J. Chin. Med.* 44, 943–962. doi: 10.1142/S0192415X1650052X

Chatterjee, A., Harrison, C. J., Britt, W. J., and Bewtra, C. (2001). Modification of maternal and congenital cytomegalovirus infection by anti–glycoprotein B antibody transfer in Guinea pigs. *J. Infect. Dis.* 183, 1547–1553. doi: 10.1086/320714

Chatzakis, C., Ville, Y., Makrydimas, G., Dinas, K., Zavlanos, A., and Sotiriadis, A. (2020). Timing of primary maternal cytomegalovirus infection and rates of vertical transmission and fetal consequences. *Am. J. Obstet. Gynecol.* 223, 870–883.e11. doi: 10.1016/j.ajog.2020.05.038

Chemaly, R. F., Ullmann, A. J., Stoelben, S., Richard, M. P., Bornhäuser, M., Groth, C., et al. (2014). Letermovir for cytomegalovirus prophylaxis in hematopoietic-cell transplantation. *N. Engl. J. Med.* 370, 1781–1789. doi: 10.1056/NEJMoa1309533

Chen, H., Li, C., Zemlicka, J., Gentry, B. G., Bowlin, T. L., and Coen, D. M. (2016). Potency and Stereoselectivity of Cyclopropavir triphosphate action on human cytomegalovirus DNA polymerase. *Antimicrob. Agents Chemother.* 60, 4176–4182. doi: 10.1128/AAC.00449-16

Cherrier, L., Nasar, A., Goodlet, K. J., Nailor, M. D., Tokman, S., and Chou, S. (2018). Emergence of letermovir resistance in a lung transplant recipient with ganciclovir-resistant cytomegalovirus infection. *Am. J. Transplant.* 18, 3060–3064. doi: 10.1111/ajt.15135

Chiaie, L. D., Neuberger, P., Vochem, M., Lihs, A., Karck, U., and Enders, M. (2018). No evidence of obstetrical adverse events after hyperimmune globulin application for primary cytomegalovirus infection in pregnancy: experience from a single Centre. *Arch. Gynecol. Obstet.* 297, 1389–1395. doi: 10.1007/s00404-018-4703-y

Chimerix. (2022) *An intermediate-size, expanded access protocol to provide Brincidofovir for the treatment of serious adenovirus infection or disease*. Report No.: NCT02596997. Available at: https://clinicaltrials.gov/study/NCT02596997. (Accessed Jan 1, 2023).

Chong, A. S., Zeng, H., Knight, D. A., Shen, J., Meister, G. T., Williams, J. W., et al. (2006). Concurrent antiviral and immunosuppressive activities of Leflunomide in vivo. *Am. J. Transplant.* 6, 69–75. doi: 10.1111/j.1600-6143.2005.01152.x

Chou, S. (2009). Diverse cytomegalovirus UL27 mutations adapt to loss of viral UL97 kinase activity under Maribavir. *Antimicrob. Agents Chemother.* 53, 81–85. doi: 10.1128/AAC.01177-08

Chou, S. (2017). Comparison of cytomegalovirus Terminase gene mutations selected after exposure to three distinct inhibitor compounds. *Antimicrob. Agents Chemother.* 61:e01325. doi: 10.1128/AAC.01325-17

Chou, S. (2020). Advances in the genotypic diagnosis of cytomegalovirus antiviral drug resistance. *Antivir. Res.* 176:104711. doi: 10.1016/j.antiviral.2020.104711

Chou, S., Alain, S., Cervera, C., Chemaly, R. F., Kotton, C. N., Lundgren, J., et al. (2023). Drug resistance assessed in a phase 3 clinical trial of Maribavir therapy for refractory or resistant cytomegalovirus infection in transplant recipients. *J. Infect. Dis.*:jiad293. doi: 10.1093/infdis/jiad293

Chou, S., and Bowlin, T. L. (2011). Cytomegalovirus UL97 mutations affecting Cyclopropavir and ganciclovir susceptibility. *Antimicrob. Agents Chemother.* 55, 382–384. doi: 10.1128/AAC.01259-10

Chou, S., Ercolani, R. J., and Lanier, E. R. (2016). Novel cytomegalovirus UL54 DNA polymerase gene mutations selected in vitro that confer Brincidofovir resistance. *Antimicrob. Agents Chemother.* 60, 3845–3848. doi: 10.1128/AAC.00214-16

Chou, S., Ercolani, R. J., Marousek, G., and Bowlin, T. L. (2013). Cytomegalovirus UL97 kinase catalytic domain mutations that confer multidrug resistance. *Antimicrob. Agents Chemother.* 57, 3375–3379. doi: 10.1128/AAC.00511-13

Chou, S., Hakki, M., and Villano, S. (2012a). Effects on maribavir susceptibility of cytomegalovirus UL97 kinase ATP binding region mutations detected after drug exposure in vitro and in vivo. *Antivir. Res.* 95, 88–92. doi: 10.1016/j.antiviral.2012.05.013

Chou, S., and Marousek, G. I. (2006). Maribavir antagonizes the antiviral action of ganciclovir on human cytomegalovirus. *Antimicrob. Agents Chemother.* 50, 3470–3472. doi: 10.1128/AAC.00577-06

Chou, S., and Marousek, G. I. (2008). Accelerated evolution of Maribavir resistance in a cytomegalovirus exonuclease domain II mutant. *J. Virol.* 82, 246–253. doi: 10.1128/JVI.01787-07

Chou, S., Marousek, G., Auerochs, S., Stamminger, T., Milbradt, J., and Marschall, M. (2011). The unique antiviral activity of artesunate is broadly effective against human cytomegaloviruses including therapy-resistant mutants. *Antivir. Res.* 92, 364–368. doi: 10.1016/j.antiviral.2011.07.018

Chou, S., Marousek, G., and Bowlin, T. L. (2012b). Cyclopropavir susceptibility of cytomegalovirus DNA polymerase mutants selected after antiviral drug exposure. *Antimicrob. Agents Chemother.* 56, 197–201. doi: 10.1128/AAC.05559-11

Chou, S., Marousek, G. I., Senters, A. E., Davis, M. G., and Biron, K. K. (2004). Mutations in the human cytomegalovirus UL27 gene that confer resistance to Maribavir. *J. Virol.* 78, 7124–7130. doi: 10.1128/JVI.78.13.7124-7130.2004

Chou, S., Van Wechel, L. C., and Marousek, G. I. (2007). Cytomegalovirus UL97 kinase mutations that confer Maribavir resistance. *J. Infect. Dis.* 196, 91–94. doi: 10.1086/518514

Chou, S., Wu, J., Song, K., and Bo, T. (2019). Novel UL97 drug resistance mutations identified at baseline in a clinical trial of maribavir for resistant or refractory cytomegalovirus infection. *Antivir. Res.* 172:104616. doi: 10.1016/j.antiviral.2019.104616

Coste Mazeau, P., Berto, L., Andouard, D., El Hamel, C., Chianea, T., Hantz, S., et al. (2023). New therapeutic perspective in the prevention of congenital cytomegalovirus infection. *Antivir. Res.* 216:105661. doi: 10.1016/j.antiviral.2023.105661

Coste Mazeau, P., Jacquet, C., Muller, C., Courant, M., El Hamel, C., Chianea, T., et al. (2022). Potential of anti-CMV immunoglobulin Cytotect CP® in vitro and ex vivo in a first-trimester placenta model. *Microorganisms* 10:694. doi: 10.3390/microorganisms10040694

Cotin, S., Calliste, C. A., Mazeron, M. C., Hantz, S., Duroux, J. L., Rawlinson, W. D., et al. (2012). Eight flavonoids and their potential as inhibitors of human cytomegalovirus replication. *Antivir. Res.* 96, 181–186. doi: 10.1016/j.antiviral.2012.09.010

Cristelli, M. P., Felipe, C. R., Prizmic, P. S. S., De Azevedo, V. F. D., Viana, L. A., Tavares, M. G., et al. (2019). Use of mTOR inhibitor as prophylaxis for cytomegalovirus disease after kidney transplantation: a natural experiment. *Clin. Transpl.* 33:e13689. doi: 10.1111/ctr.13689

Dayer, J. M., and Cutolo, M. (2005). Is there a rationale to using leflunomide in early rheumatoid arthritis? *Clin. Exp. Rheumatol.* 23, 404–412.

De Oliveira, M. R., Nabavi, S. M., Braidy, N., Setzer, W. N., Ahmed, T., and Nabavi, S. F. (2016). Quercetin and the mitochondria: a mechanistic view. *Biotechnol. Adv.* 34, 532–549. doi: 10.1016/j.biotechadv.2015.12.014

Dinda, B., Dinda, S., DasSharma, S., Banik, R., Chakraborty, A., and Dinda, M. (2017). Therapeutic potentials of baicalin and its aglycone, baicalein against inflammatory disorders. *Eur. J. Med. Chem.* 131, 68–80. doi: 10.1016/j.ejmech.2017.03.004

Dollard, S. C., Grosse, S. D., and Ross, D. S. (2007). New estimates of the prevalence of neurological and sensory sequelae and mortality associated with congenital cytomegalovirus infection. *Rev. Med. Virol.* 17, 355–363. doi: 10.1002/rmv.544

Dou, J., Chen, L., Xu, G., Zhang, L., Zhou, H., Wang, H., et al. (2011). Effects of baicalein on Sendai virus in vivo are linked to serum baicalin and its inhibition of hemagglutinin-neuraminidase. *Arch. Virol.* 156, 793–801. doi: 10.1007/s00705-011-0917-z

Drew, W. L., Miner, R. C., Marousek, G. I., and Chou, S. (2006). Maribavir sensitivity of cytomegalovirus isolates resistant to ganciclovir, cidofovir or foscarnet. *J. Clin. Virol.* 37, 124–127. doi: 10.1016/j.jcv.2006.07.010

Drouot, E., Piret, J., and Boivin, G. (2016). Artesunate demonstrates in vitro synergism with several antiviral agents against human cytomegalovirus. *Antivir. Ther.* 21, 535–539. doi: 10.3851/IMP3028

Efferth, T., Marschall, M., Wang, X., Huong, S. M., Hauber, I., Olbrich, A., et al. (2002). Antiviral activity of artesunate towards wild-type, recombinant, and ganciclovir-resistant human cytomegaloviruses. *J. Mol. Med.* 80, 233–242. doi: 10.1007/s00109-001-0300-8

Efferth, T., Romero, M. R., Wolf, D. G., Stamminger, T., Marin, J. J. G., and Marschall, M. (2008). The antiviral activities of artemisinin and Artesunate. *Clin. Infect. Dis.* 47, 804–811. doi: 10.1086/591195

El Chaer, F., Mori, N., Shah, D., Oliver, N., Wang, E., Jan, A., et al. (2016). Adjuvant and salvage therapy with leflunomide for recalcitrant cytomegalovirus infections in hematopoietic cell transplantation recipients: a case series. *Antivir. Res.* 135, 91–96. doi: 10.1016/j.antiviral.2016.08.027

El-Qushayri, A. E., Ghozy, S., Abbas, A. S., Dibas, M., Dahy, A., Mahmoud, A. R., et al. (2021). Hyperimmunoglobulin therapy for the prevention and treatment of congenital cytomegalovirus: a systematic review and meta-analysis. *Expert Rev. Anti-Infect. Ther.* 19, 661–669. doi: 10.1080/14787210.2021.1846521

Evers, D. L., Chao, C. F., Wang, X., Zhang, Z., Huong, S. M., and Huang, E. S. (2005). Human cytomegalovirus-inhibitory flavonoids: studies on antiviral activity and mechanism of action. *Antivir. Res.* 68, 124–134. doi: 10.1016/j.antiviral.2005.08.002

Evers, D. L., Komazin, G., Shin, D., Hwang, D. D., Townsend, L. B., and Drach, J. C. (2002). Interactions among antiviral drugs acting late in the replication cycle of human cytomegalovirus. *Antivir. Res.* 56, 61–72. doi: 10.1016/S0166-3542(02)00094-3

Faure Bardon, V., Peytavin, G., Lê, M. P., Guilleminot, T., Elefant, E., Stirnemann, J., et al. (2020). Placental transfer of Letermovir and Maribavir in the ex vivo human cotyledon perfusion model. New perspectives for in utero treatment of congenital cytomegalovirus infection. *PLoS One* 15:e0232140. doi: 10.1371/journal.pone.0232140

Feldman, B., Yinon, Y., Tepperberg Oikawa, M., Yoeli, R., Schiff, E., and Lipitz, S. (2011). Pregestational, periconceptional, and gestational primary maternal cytomegalovirus infection: prenatal diagnosis in 508 pregnancies. *Am. J. Obstet. Gynecol.* 205, 342.e1–342.e6. doi: 10.1016/j.ajog.2011.05.030

Food and Drug Administration. (2021). *FDA approves first treatment for common type of post-transplant infection that is resistant to other drugs*. US Food Drug Administration. Available at: https://www.fda.gov/news-events/press-announcements/fda-approves-first-treatment-common-type-post-transplant-infection-resistant-other-drugs.

Frietsch, J. J., Michel, D., Stamminger, T., Hunstig, F., Birndt, S., Schnetzke, U., et al. (2019). In vivo emergence of UL56 C325Y cytomegalovirus resistance to Letermovir in a patient with acute myeloid leukemia after hematopoietic cell transplantation. *Mediterr. J. Hematol. Infect. Dis.* 11:e2019001. doi: 10.4084/MJHID.2019.001

Fröhlich, T., Hahn, F., Belmudes, L., Leidenberger, M., Friedrich, O., Kappes, B., et al. (2018). Synthesis of artemisinin-derived dimers, trimers and dendrimers: investigation of their antimalarial and antiviral activities including putative mechanisms of action. *Chemistry* 24, 8103–8113. doi: 10.1002/chem.201800729

Gabardi, S., and Baroletti, S. A. (2010). Everolimus: a proliferation signal inhibitor with clinical applications in organ transplantation, oncology, and cardiology. *Pharmacotherapy* 30, 1044–1056. doi: 10.1592/phco.30.10.1044

Gao, Y., Snyder, S. A., Smith, J. N., and Chen, Y. C. (2016). Anticancer properties of baicalein: a review. *Med. Chem. Res.* 25, 1515–1523. doi: 10.1007/s00044-016-1607-x

Gentry, B. G., Bogner, E., and Drach, J. C. (2019). Targeting the terminase: an important step forward in the treatment and prophylaxis of human cytomegalovirus infections. *Antivir. Res.* 161, 116–124. doi: 10.1016/j.antiviral.2018.11.005

Gentry, B. G., Gentry, S. N., Jackson, T. L., Zemlicka, J., and Drach, J. C. (2011). Phosphorylation of antiviral and endogenous nucleotides to di- and triphosphates by guanosine monophosphate kinase. *Biochem. Pharmacol.* 81, 43–49. doi: 10.1016/j.bcp.2010.09.005

Gentry, B. G., Kamil, J. P., Coen, D. M., Zemlicka, J., and Drach, J. C. (2010). Stereoselective phosphorylation of Cyclopropavir by pUL97 and competitive inhibition by Maribavir. *Antimicrob. Agents Chemother.* 54, 3093–3098. doi: 10.1128/AAC.00468-10

Gentry, B. G., Vollmer, L. E., Hall, E. D., Borysko, K. Z., Zemlicka, J., Kamil, J. P., et al. (2013). Resistance of human cytomegalovirus to Cyclopropavir maps to a base pair deletion in the open Reading frame of UL97. *Antimicrob. Agents Chemother.* 57, 4343–4348. doi: 10.1128/AAC.00214-13

Germer, M., Herbener, P., and Schüttrumpf, J. (2016). Functional properties of human cytomegalovirus Hyperimmunoglobulin and standard immunoglobulin preparations. *Ann. Transplant.* 21, 558–564. doi: 10.12659/AOT.898050

Germi, R., Mariette, C., Alain, S., Lupo, J., Thiebaut, A., Brion, J. P., et al. (2014). Success and failure of artesunate treatment in five transplant recipients with disease caused by drug-resistant cytomegalovirus. *Antivir. Res.* 101, 57–61. doi: 10.1016/j.antiviral.2013.10.014

Gokarn, A., Toshniwal, A., Pathak, A., Arora, S., Bonda, A., Punatar, S., et al. (2019). Use of Leflunomide for treatment of cytomegalovirus infection in recipients of allogeneic stem cell transplant. *Biol. Blood Marrow Transplant.* 25, 1832–1836. doi: 10.1016/j.bbmt.2019.04.028

Goldner, T., Hewlett, G., Ettischer, N., Ruebsamen-Schaeff, H., Zimmermann, H., and Lischka, P. (2011). The novel Anticytomegalovirus compound AIC246 (Letermovir) inhibits human cytomegalovirus replication through a specific antiviral mechanism that involves the viral Terminase. *J. Virol.* 85, 10884–10893. doi: 10.1128/JVI.05265-11

Gómez Valbuena, I., Alioto, D., Serrano Garrote, O., and Ferrari Piquero, J. M. (2016). Use of leflunomide in a cytomegalovirus infection resistant: a report of a case. *Farm Hosp.* 40, 52–54. doi: 10.7399/fh.2016.40.1.10161

Good, S. S., Owens, T. L. B., and Drach, J. C. (1994). The disposition in rats and monkeys of 2-bromo-5,6-dichloro-1-(β-D-ribofuranosyl)-benzimidazole (BDCRB) and its 4,5,6,-trichloro-cohner (TCRB). *Antivir. Res.* 23:103. doi: 10.1016/0166-3542(94)90251-8

Granato, M., Gilardini Montani, M. S., Zompetta, C., Santarelli, R., Gonnella, R., Romeo, M. A., et al. (2019). Quercetin interrupts the positive feedback loop between STAT3 and IL-6, promotes autophagy, and reduces ROS, preventing EBV-driven B cell immortalization. *Biomol. Ther.* 9:482. doi: 10.3390/biom9090482

Hahn, F., Fröhlich, T., Frank, T., Bertzbach, L. D., Kohrt, S., Kaufer, B. B., et al. (2018). Artesunate-derived monomeric, dimeric and trimeric experimental drugs – their unique mechanistic basis and pronounced antiherpesviral activity. *Antivir. Res.* 152, 104–110. doi: 10.1016/j.antiviral.2018.02.013

Hakacova, N., Klingel, K., Kandolf, R., Engdahl, E., Fogdell-Hahn, A., and Higgins, T. (2013). First therapeutic use of Artesunate in treatment of human herpesvirus 6B myocarditis in a child. *J. Clin. Virol.* 57, 157–160. doi: 10.1016/j.jcv.2013.02.005

Halpern-Cohen, V., and Blumberg, E. A. (2022). New perspectives on antimicrobial agents: Maribavir. *Antimicrob. Agents Chemother.* 66, e02405–e02421. doi: 10.1128/aac.02405-21

Hamilton, S. T., Marschall, M., and Rawlinson, W. D. (2020). Investigational antiviral therapy models for the prevention and treatment of congenital cytomegalovirus infection during pregnancy. *Antimicrob. Agents Chemother.* 65, e01627–e01620. doi: 10.1128/AAC.01627-20

Hamirally, S., Kamil, J. P., Ndassa-Colday, Y. M., Lin, A. J., Jahng, W. J., Baek, M. C., et al. (2009). Viral mimicry of Cdc2/cyclin-dependent kinase 1 mediates disruption of nuclear Lamina during human cytomegalovirus nuclear egress. *PLoS Pathog.* 5:e1000275. doi: 10.1371/journal.ppat.1000275

Hartline, C. B., Keith, K. A., Eagar, J., Harden, E. A., Bowlin, T. L., and Prichard, M. N. (2018). A standardized approach to the evaluation of antivirals against DNA viruses: Orthopox-, adeno-, and herpesviruses. *Antivir. Res.* 159, 104–112. doi: 10.1016/j.antiviral.2018.09.015

Havenith, S. H. C., Yong, S. L., van Donselaar-van der Pant, K. A. M. I., van Lier, R. A. W., ten Berge, I. J. M., and Bemelman, F. J. (2013). Everolimus-treated renal transplant recipients have a more robust CMV-specific CD8+ T-cell response compared with cyclosporine- or mycophenolate-treated patients. *Transplantation* 95, 184–191. doi: 10.1097/TP.0b013e318276a1ef

Hepatitis, C. (2018). Guidance 2018 update: AASLD-IDSA recommendations for testing, managing, and treating Hepatitis C virus infection. *Clin. Infect. Dis.* 67, 1477–1492. doi: 10.1093/cid/ciy585

Hill, J. A., Hummel, M., Starling, R. C., Kobashigawa, J. A., Perrone, S. V., Arizón, J. M., et al. (2007). A lower incidence of cytomegalovirus infection in De novo heart transplant

recipients randomized to Everolimus. *Transplantation* 84, 1436–1442. doi: 10.1097/01.tp.0000290686.68910.bd

Hiscott, J., Kwon, H., and Génin, P. (2001). Hostile takeovers: viral appropriation of the NF-kB pathway. *J. Clin. Invest.* 107, 143–151. doi: 10.1172/JCI11918

Hughes, B. L., Clifton, R. G., Rouse, D. J., Saade, G. R., Dinsmoor, M. J., Reddy, U. M., et al. (2021). A trial of Hyperimmune globulin to prevent congenital cytomegalovirus infection. *N. Engl. J. Med.* 385, 436–444. doi: 10.1056/NEJMoa1913569

Hung, C. H., Chan, S. H., Chu, P. M., and Tsai, K. L. (2015). Quercetin is a potent anti-atherosclerotic compound by activation of SIRT1 signaling under oxLDL stimulation. *Mol. Nutr. Food Res.* 59, 1905–1917. doi: 10.1002/mnfr.201500144

Hutterer, C., Niemann, I., Milbradt, J., Fröhlich, T., Reiter, C., Kadioglu, O., et al. (2015). The broad-spectrum antiinfective drug artesunate interferes with the canonical nuclear factor kappa B (NF-κB) pathway by targeting RelA/p65. *Antivir. Res.* 124, 101–109. doi: 10.1016/j.antiviral.2015.10.003

Hyde, T. B., Schmid, D. S., and Cannon, M. J. (2010). Cytomegalovirus seroconversion rates and risk factors: implications for congenital CMV. *Rev. Med. Virol.* 20, 311–326. doi: 10.1002/rmv.659

Imamura, T., Shiga, T., Kinugawa, K., Kato, N., Endo, M., Inaba, T., et al. (2012). Successful conversion to Everolimus after cytomegalovirus infection in a heart transplant recipient. *Int. Heart J.* 53, 199–201. doi: 10.1536/ihj.53.199

Jacquet, C., Marschall, M., Andouard, D., El Hamel, C., Chianea, T., Tsogoeva, S. B., et al. (2020). A highly potent trimeric derivative of artesunate shows promising treatment profiles in experimental models for congenital HCMV infection in vitro and ex vivo. *Antivir. Res.* 175:104700. doi: 10.1016/j.antiviral.2019.104700

James, S. H., Hartline, C. B., Harden, E. A., Driebe, E. M., Schupp, J. M., Engelthaler, D. M., et al. (2011). Cyclopropavir inhibits the Normal function of the human cytomegalovirus UL97 kinase∇. *Antimicrob. Agents Chemother.* 55, 4682–4691. doi: 10.1128/AAC.00571-11

James, S. H., Price, N. B., Hartline, C. B., Lanier, E. R., and Prichard, M. N. (2013). Selection and recombinant phenotyping of a novel CMX001 and Cidofovir resistance mutation in human cytomegalovirus. *Antimicrob. Agents Chemother.* 57, 3321–3325. doi: 10.1128/AAC.00062-13

John, G. T., Manivannan, J., Chandy, S., Peter, S., Fleming, D. H., Chandy, S. J., et al. (2005). A prospective evaluation of Leflunomide therapy for cytomegalovirus disease in renal transplant recipients. *Transplant. Proc.* 37, 4303–4305. doi: 10.1016/j.transproceed.2005.10.116

Kagan, K. O., Enders, M., Hoopmann, M., Geipel, A., Simonini, C., Berg, C., et al. (2021). Outcome of pregnancies with recent primary cytomegalovirus infection in first trimester treated with hyperimmunoglobulin: observational study. *Ultrasound Obstet. Gynecol.* 57, 560–567. doi: 10.1002/uog.23596

Kagan, K. O., Enders, M., Schampera, M. S., Baeumel, E., Hoopmann, M., Geipel, A., et al. (2019). Prevention of maternal–fetal transmission of cytomegalovirus after primary maternal infection in the first trimester by biweekly hyperimmunoglobulin administration. *Ultrasound Obstet. Gynecol.* 53, 383–389. doi: 10.1002/uog.19164

Kajon, A. E., and St George, K. (2022). Mysterious cases of acute hepatitis in children: is adenovirus still a lead suspect? Emerg. *Microbes Infect.* 11, 1787–1789. doi: 10.1080/22221751.2022.2095933

Kamil, J. P., and Coen, D. M. (2011). HATs On for drug resistance. *Cell Host Microbe* 9, 85–87. doi: 10.1016/j.chom.2011.02.001

Kaminski, H., Kamar, N., Thaunat, O., Bouvier, N., Caillard, S., Garrigue, I., et al. (2022a). Incidence of cytomegalovirus infection in seropositive kidney transplant recipients treated with everolimus: a randomized, open-label, multicenter phase 4 trial. *Am. J. Transplant.* 22, 1430–1441. doi: 10.1111/ajt.16946

Kaminski, H., Marseres, G., Yared, N., Nokin, M. J., Pitard, V., Zouine, A., et al. (2022b). mTOR inhibitors prevent CMV infection through the restoration of functional αβ and γδ T cells in kidney transplantation. *J. Am. Soc. Nephrol.* 33, 121–137. doi: 10.1681/ASN.2020121753

Kaptein, S. J. F., Efferth, T., Leis, M., Rechter, S., Auerochs, S., Kalmer, M., et al. (2006). The anti-malaria drug artesunate inhibits replication of cytomegalovirus in vitro and in vivo. *Antivir. Res.* 69, 60–69. doi: 10.1016/j.antiviral.2005.10.003

Kaul, D. R., Stoelben, S., Cober, E., Ojo, T., Sandusky, E., Lischka, P., et al. (2011). First report of successful treatment of multidrug-resistant cytomegalovirus disease with the novel anti-CMV compound AIC246. *Am. J. Transplant.* 11, 1079–1084. doi: 10.1111/j.1600-6143.2011.03530.x

Kawabata, K., Mukai, R., and Ishisaka, A. (2015). Quercetin and related polyphenols: new insights and implications for their bioactivity and bioavailability. *Food Funct.* 6, 1399–1417. doi: 10.1039/C4FO01178C

Kenneson, A., and Cannon, M. J. (2007). Review and meta-analysis of the epidemiology of congenital cytomegalovirus (CMV) infection. *Rev. Med. Virol.* 17, 253–276. doi: 10.1002/rmv.535

Kern, E. R., Bidanset, D. J., Hartline, C. B., Yan, Z., Zemlicka, J., and Quenelle, D. C. (2004c). Oral activity of a methylenecyclopropane analog, Cyclopropavir, in animal models for cytomegalovirus infections. *Antimicrob. Agents Chemother.* 48, 4745–4753. doi: 10.1128/AAC.48.12.4745-4753.2004

Kern, E. R., Collins, D. J., Wan, W. B., Beadle, J. R., Hostetler, K. Y., and Quenelle, D. C. (2004b). Oral treatment of murine cytomegalovirus infections with ether lipid esters of Cidofovir. *Antimicrob. Agents Chemother.* 48, 3516–3522. doi: 10.1128/AAC.48.9.3516-3522.2004

Kern, E. R., Hartline, C. B., Rybak, R. J., Drach, J. C., Townsend, L. B., Biron, K. K., et al. (2004a). Activities of Benzimidazole d- and l-Ribonucleosides in animal models of cytomegalovirus infections. *Antimicrob. Agents Chemother.* 48, 1749–1755. doi: 10.1128/AAC.48.5.1749-1755.2004

Kern, E. R., Kushner, N. L., Hartline, C. B., Williams-Aziz, S. L., Harden, E. A., Zhou, S., et al. (2005). In vitro activity and mechanism of action of methylenecyclopropane analogs of nucleosides against herpesvirus replication. *Antimicrob. Agents Chemother.* 49, 1039–1045. doi: 10.1128/AAC.49.3.1039-1045.2005

Kim, C. H., Kim, J. E., and Song, Y. J. (2020). Antiviral activities of quercetin and Isoquercitrin against human herpesviruses. *Molecules* 25:2379. doi: 10.3390/molecules25102379

Kimberlin, D. W., Jester, P. M., Sánchez, P. J., Ahmed, A., Arav-Boger, R., Michaels, M. G., et al. (2015). Valganciclovir for symptomatic congenital cytomegalovirus disease. *N. Engl. J. Med.* 372, 933–943. doi: 10.1056/NEJMoa1404599

Kjar, A., Wadsworth, I., Vargis, E., and Britt, D. W. (2022). Poloxamer 188 – quercetin formulations amplify in vitro ganciclovir antiviral activity against cytomegalovirus. *Antivir. Res.* 204:105362. doi: 10.1016/j.antiviral.2022.105362

Knight, D. A., Hejmanowski, A. Q., Dierksheide, J. E., Williams, J. W., Chong, A. S. F., and Waldman, W. J. (2001). Inhibition of herpes simplex virus type 1 by the experimental immunosuppressive agent leflunomide. *Transplantation* 71, 170–174. doi: 10.1097/00007890-200101150-00031

Kobashigawa, J., Ross, H., Bara, C., Delgado, J. F., Dengler, T., Lehmkuhl, H. B., et al. (2013). Everolimus is associated with a reduced incidence of cytomegalovirus infection following de novo cardiac transplantation. *Transpl. Infect. Dis.* 15, 150–162. doi: 10.1111/tid.12007

Komazin, G., Townsend, L. B., and Drach, J. C. (2004). Role of a mutation in human cytomegalovirus gene UL104 in resistance to Benzimidazole Ribonucleosides. *J. Virol.* 78, 710–715. doi: 10.1128/JVI.78.2.710-715.2004

Komazin-Meredith, G., Chou, S., Prichard, M. N., Hartline, C. B., Cardinale, S. C., Comeau, K., et al. (2014). Human cytomegalovirus UL97 kinase is involved in the mechanism of action of methylenecyclopropane analogs with 6-ether and -thioether substitutions. *Antimicrob. Agents Chemother.* 58, 274–278. doi: 10.1128/AAC.01726-13

Koszalka, G. W., Johnson, N. W., Good, S. S., Boyd, L., Chamberlain, S. C., Townsend, L. B., et al. (2002). Preclinical and toxicology studies of 1263W94, a potent and selective inhibitor of human cytomegalovirus replication. *Antimicrob. Agents Chemother.* 46, 2373–2380. doi: 10.1128/AAC.46.8.2373-2380.2002

Kotton, C. N., Kumar, D., Caliendo, A. M., Huprikar, S., Chou, S., Danziger-Isakov, L., et al. (2018). The third international consensus guidelines on the Management of Cytomegalovirus in solid-organ transplantation. *Transplantation* 102, 900–931. doi: 10.1097/TP.0000000000002191

Krosky, P. M., Borysko, K. Z., Nassiri, M. R., Devivar, R. V., Ptak, R. G., Davis, M. G., et al. (2002). Phosphorylation of β-d-Ribosylbenzimidazoles is not required for activity against human cytomegalovirus. *Antimicrob. Agents Chemother.* 46, 478–486. doi: 10.1128/AAC.46.2.478-486.2002

Krosky, P. M., Ptak, R. G., Underwood, M. R., Biron, K. K., Townsend, L. B., and Drach, J. C. (2000). Differences in DNA packaging genes and sensitivity to Benzimidazole Ribonucleosides between human cytomegalovirus strains AD169 and Towne. *Antivir. Chem. Chemother.* 11, 349–352. doi: 10.1177/095632020001100506

Krosky, P. M., Underwood, M. R., Turk, S. R., Feng, K. W. H., Jain, R. K., Ptak, R. G., et al. (1998). Resistance of human cytomegalovirus to Benzimidazole Ribonucleosides maps to two open Reading frames: UL89 and UL56. *J. Virol.* 72, 4721–4728. doi: 10.1128/JVI.72.6.4721-4728.1998

Lai, M. Y., Hsiu, S. L., Tsai, S. Y., Hou, Y. C., and Chao, P. D. L. (2003). Comparison of metabolic pharmacokinetics of baicalin and baicalein in rats. *J. Pharm. Pharmacol.* 55, 205–209. doi: 10.1211/002235702522

Lanier, E. R., Foster, S., Brundage, T., Chou, S., Prichard, M. N., Kleiboeker, S., et al. (2016). Analysis of mutations in the gene encoding cytomegalovirus DNA polymerase in a phase 2 clinical trial of Brincidofovir prophylaxis. *J. Infect. Dis.* 214, 32–35. doi: 10.1093/infdis/jiw073

Lee, S., Lee, H. H., Shin, Y. S., Kang, H., and Cho, H. (2017). The anti-HSV-1 effect of quercetin is dependent on the suppression of TLR-3 in raw 264.7 cells. *Arch. Pharm. Res.* 40, 623–630. doi: 10.1007/s12272-017-0898-x

Leruez-Ville, M., Foulon, I., Pass, R., and Ville, Y. (2020). Cytomegalovirus infection during pregnancy: state of the science. *Am. J. Obstet. Gynecol.* 223, 330–349. doi: 10.1016/j.ajog.2020.02.018

Leruez-Ville, M., and Ville, Y. (2020). Is it time for routine prenatal serological screening for congenital cytomegalovirus? *Prenat. Diagn.* 40, 1671–1680. doi: 10.1002/pd.5757

Li, L., Gao, H., Lou, K., Luo, H., Hao, S., Yuan, J., et al. (2021). Safety, tolerability, and pharmacokinetics of oral baicalein tablets in healthy Chinese subjects: a single-center, randomized, double-blind, placebo-controlled multiple-ascending-dose study. *Clin. Transl. Sci.* 14, 2017–2024. doi: 10.1111/cts.13063

Li, J., Ma, J., Wang, K. S., Mi, C., Wang, Z., Piao, L. X., et al. (2016). Baicalein inhibits TNF-α-induced NF-κB activation and expression of NF-κB-regulated target gene products. *Oncol. Rep.* 36, 2771–2776. doi: 10.3892/or.2016.5108

Li, Q. G., Mog, S. R., Si, Y. Z., Kyle, D. E., Gettayacamin, M., and Milhous, W. K. (2002). Neurotoxicity and efficacy of arteether related to its exposure times and exposure levels in rodents. *Am. J. Trop. Med. Hyg.* 66, 516–525. doi: 10.4269/ajtmh.2002.66.516

Li, M., Shi, A., Pang, H., Xue, W., Li, Y., Cao, G., et al. (2014). Safety, tolerability, and pharmacokinetics of a single ascending dose of baicalein chewable tablets in healthy subjects. *J. Ethnopharmacol.* 156, 210–215. doi: 10.1016/j.jep.2014.08.031

Ligat, G., Cazal, R., Hantz, S., and Alain, S. (2018). The human cytomegalovirus terminase complex as an antiviral target: a close-up view. *FEMS Microbiol. Rev.* 42, 137–145. doi: 10.1093/femsre/fuy004

Limaye, A. P., Budde, K., Humar, A., Vincenti, F., Kuypers, D. R. J., Carroll, R. P., et al. (2023). Letermovir vs Valganciclovir for prophylaxis of cytomegalovirus in high-risk kidney transplant recipients: a randomized clinical trial. *JAMA* 330, 33–42. doi: 10.1001/jama.2023.9106

Linder, K. A., Kovacs, C., Mullane, K. M., Wolfe, C., Clark, N. M., La Hoz, R. M., et al. (2021). Letermovir treatment of cytomegalovirus infection or disease in solid organ and hematopoietic cell transplant recipients. *Transpl. Infect. Dis.* 23:e13687. doi: 10.1111/tid.13687

Lischka, P., Hewlett, G., Wunberg, T., Baumeister, J., Paulsen, D., Goldner, T., et al. (2010). In vitro and in vivo activities of the novel Anticytomegalovirus compound AIC246. *Antimicrob. Agents Chemother.* 54, 1290–1297. doi: 10.1128/AAC.01596-09

Lischka, P., Zhang, D., Holder, D., and Zimmermann, H. (2016). Impact of glycoprotein B genotype and naturally occurring ORF UL56 polymorphisms upon susceptibility of clinical human cytomegalovirus isolates to letermovir. *Antivir. Res.* 132, 204–209. doi: 10.1016/j.antiviral.2016.06.008

Littler, E., Stuart, A. D., and Chee, M. S. (1992). Human cytomegalovirus UL97 open reading frame encodes a protein that phosphorylates the antiviral nucleoside analogue ganciclovir. *Nature* 358, 160–162. doi: 10.1038/358160a0

Ljungman, P., De la Camara, R., Robin, C., Crocchiolo, R., Einsele, H., Hill, J. A., et al. (2019). Guidelines for the management of cytomegalovirus infection in patients with haematological malignancies and after stem cell transplantation from the 2017 European conference on infections in Leukaemia (ECIL 7). *Lancet Infect. Dis.* 19, e260–e272. doi: 10.1016/S1473-3099(19)30107-0

Lu, H., and Thomas, S. (2000). Maribavir (ViroPharma). *Curr. Opin. Investig. Drugs* 5, 898–906.

Luo, Z., Kuang, X. P., Zhou, Q. Q., Yan, C. Y., Li, W., Gong, H. B., et al. (2020). Inhibitory effects of baicalein against herpes simplex virus type 1. *Acta Pharm. Sin. B* 10, 2323–2338. doi: 10.1016/j.apsb.2020.06.008

Lurain, N. S., and Chou, S. (2010). Antiviral drug resistance of human cytomegalovirus. *Clin. Microbiol. Rev.* 23, 689–712. doi: 10.1128/CMR.00009-10

Maertens, J., Logan, A. C., Jang, J., Long, G., Tang, J. L., Hwang, W. Y. K., et al. (2020). Phase 2 study of anti-human cytomegalovirus monoclonal antibodies for prophylaxis in hematopoietic cell transplantation. *Antimicrob. Agents Chemother.* 64, e02467–e02419. doi: 10.1128/AAC.02467-19

Maniez-Montreuil, M., Dupressoir-Burlet, M. V., Martinache, L., and Goudemand, M. (1984). Preparation of a specific anti-cytomegalovirus immunoglobulin for intravenous injection. *Rev. Fr. Transfus. Immunohematol.* 27, 375–382. doi: 10.1016/S0338-4535(84)80178-6

Marschall, M., Stamminger, T., Urban, A., Wildum, S., Ruebsamen-Schaeff, H., Zimmermann, H., et al. (2012). In vitro evaluation of the activities of the novel Anticytomegalovirus compound AIC246 (Letermovir) against herpesviruses and other human pathogenic viruses. *Antimicrob. Agents Chemother.* 56, 1135–1137. doi: 10.1128/AAC.05908-11

Marty, F. M., Ljungman, P., Chemaly, R. F., Maertens, J., Dadwal, S. S., Duarte, R. F., et al. (2017). Letermovir prophylaxis for cytomegalovirus in hematopoietic-cell transplantation. *N. Engl. J. Med.* 377, 2433–2444. doi: 10.1056/NEJMoa1706640

Marty, F. M., Winston, D. J., Chemaly, R. F., Mullane, K. M., Shore, T. B., Papanicolaou, G. A., et al. (2019). A randomized, double-blind, placebo-controlled phase 3 trial of Oral Brincidofovir for cytomegalovirus prophylaxis in allogeneic hematopoietic cell transplantation. *Biol. Blood Marrow Transplant.* 25, 369–381. doi: 10.1016/j.bbmt.2018.09.038

Marty, F. M., Winston, D. J., Rowley, S. D., Vance, E., Papanicolaou, G. A., Mullane, K. M., et al. (2013). CMX001 to prevent cytomegalovirus disease in hematopoietic-cell transplantation. *N. Engl. J. Med.* 369, 1227–1236. doi: 10.1056/NEJMoa1303688

McGready, R., Phyo, A. P., Rijken, M. J., Tarning, J., Lindegardh, N., Hanpithakpon, W., et al. (2012). Artesunate/dihydroartemisinin pharmacokinetics in acute falciparum malaria in pregnancy: absorption, bioavailability, disposition and disease effects. *Br. J. Clin. Pharmacol.* 73, 467–477. doi: 10.1111/j.1365-2125.2011.04103.x

McSharry, J. J., McDonough, A., Olson, B., Hallenberger, S., Reefschlaeger, J., Bender, W., et al. (2001). Susceptibilities of human cytomegalovirus clinical isolates to BAY38-4766, BAY43-9695, and ganciclovir. *Antimicrob. Agents Chemother.* 45, 2925–2927. doi: 10.1128/AAC.45.10.2925-2927.2001

McVoy, M. A., and Nixon, D. E. (2005). Impact of 2-Bromo-5,6-Dichloro-1-β-d-Ribofuranosyl Benzimidazole riboside and inhibitors of DNA, RNA, and protein synthesis on human cytomegalovirus genome maturation. *J. Virol.* 79, 11115–11127. doi: 10.1128/JVI.79.17.11115-11127.2005

Middleton, E. (1998). Effect of plant flavonoids on immune and inflammatory cell function. *Adv. Exp. Med. Biol.* 439, 175–182. doi: 10.1007/978-1-4615-5335-9_13

Miescher, S. M., Huber, T. M., Kühne, M., Lieby, P., Snydman, D. R., Vensak, J. L., et al. (2015). In vitro evaluation of cytomegalovirus-specific hyperimmune globulins vs. standard intravenous immunoglobulins. *Vox Sang.* 109, 71–78. doi: 10.1111/vox.12246

Migawa, M. T., Girardet, J. L., Walker, J. A., Koszalka, G. W., Chamberlain, S. D., Drach, J. C., et al. (1998). Design, synthesis, and antiviral activity of α-nucleosides: d- and l-isomers of Lyxofuranosyl- and (5-Deoxylyxofuranosyl)benzimidazoles. *J. Med. Chem.* 41, 1242–1251. doi: 10.1021/jm970545c

Milbradt, J., Auerochs, S., Korn, K., and Marschall, M. (2009). Sensitivity of human herpesvirus 6 and other human herpesviruses to the broad-spectrum antiinfective drug artesunate. *J. Clin. Virol.* 46, 24–28. doi: 10.1016/j.jcv.2009.05.017

Moon, Y., Wang, L., DiCenzo, R., and Morris, M. E. (2008). Quercetin pharmacokinetics in humans. *Biopharm. Drug Dispos.* 29, 205–217. doi: 10.1002/bdd.605

Morère, L., Andouard, D., Labrousse, F., Saade, F., Calliste, C. A., Cotin, S., et al. (2015). Ex vivo model of congenital cytomegalovirus infection and new combination therapies. *Placenta* 36, 41–47. doi: 10.1016/j.placenta.2014.11.003

Mukherjee, D. (2002). Selective cyclooxygenase-2 (COX-2) inhibitors and potential risk of cardiovascular events. *Biochem. Pharmacol.* 63, 817–821. doi: 10.1016/S0006-2952(02)00842-0

Muller, C., Tilloy, V., Frobert, E., Feghoul, L., Garrigue, I., Lepiller, Q., et al. (2022). First clinical description of letermovir resistance mutation in cytomegalovirus UL51 gene and potential impact on the terminase complex structure. *Antivir. Res.* 204:105361. doi: 10.1016/j.antiviral.2022.105361

Muto, R., Motozuka, T., Nakano, M., Tatsumi, Y., Sakamoto, F., and Kosaka, N. (1998). The chemical structure of new substance as the metabolite of baicalin and time profiles for the plasma concentration after oral administration of sho-saiko-to in human. *Yakugaku Zasshi* 118, 79–87. doi: 10.1248/yakushi1947.118.3_79

Nagashima, S., Hirotani, M., and Yoshikawa, T. (2000). Purification and characterization of UDP-glucuronate: baicalein 7-O-glucuronosyltransferase from Scutellaria baicalensis Georgi. Cell suspension cultures. *Phytochemistry* 53, 533–538. doi: 10.1016/S0031-9422(99)00593-2

Nagi, R., Yashoda Devi, B. K., Rakesh, N., Reddy, S. S., and Patil, D. J. (2015). Clinical implications of prescribing nonsteroidal anti-inflammatory drugs in oral health care—a review. *Oral Surg. Oral Med. Oral Pathol. Oral Radiol.* 119, 264–271. doi: 10.1016/j.oooo.2014.12.002

Nishimuro, H., Ohnishi, H., Sato, M., Ohnishi-Kameyama, M., Matsunaga, I., Naito, S., et al. (2015). Estimated Daily intake and seasonal food sources of quercetin in Japan. *Nutrients* 7, 2345–2358. doi: 10.3390/nu7042345

Nixon, D. E., and McVoy, M. A. (2004). Dramatic effects of 2-Bromo-5,6-Dichloro-1-β-d-Ribofuranosyl Benzimidazole riboside on the genome structure, packaging, and egress of Guinea pig cytomegalovirus. *J. Virol.* 78, 1623–1635. doi: 10.1128/JVI.78.4.1623-1635.2004

O'Brien, M. S., Markovich, K. C., Selleseth, D., DeVita, A. V., Sethna, P., and Gentry, B. G. (2018). In vitro evaluation of current and novel antivirals in combination against human cytomegalovirus. *Antivir. Res.* 158, 255–263. doi: 10.1016/j.antiviral.2018.08.015

Oiknine-Djian, E., Bar-On, S., Laskov, I., Lantsberg, D., Haynes, R. K., Panet, A., et al. (2019). Artemisone demonstrates synergistic antiviral activity in combination with approved and experimental drugs active against human cytomegalovirus. *Antivir. Res.* 172:104639. doi: 10.1016/j.antiviral.2019.104639

Ornoy, A., and Diav-Citrin, O. (2006). Fetal effects of primary and secondary cytomegalovirus infection in pregnancy. *Reprod. Toxicol.* 21, 399–409. doi: 10.1016/j.reprotox.2005.02.002

Ourahmane, A., Sauer, A., Nixon, D. E., Murphy, C., Mondello, M., Douglass, E., et al. (2018). A Guinea pig cytomegalovirus resistant to the DNA maturation inhibitor BDCRB. *Antivir. Res.* 154, 44–50. doi: 10.1016/j.antiviral.2018.04.006

Painter, W., Robertson, A., Trost, L. C., Godkin, S., Lampert, B., and Painter, G. (2012). First pharmacokinetic and safety study in humans of the novel lipid antiviral conjugate CMX001, a broad-Spectrum Oral drug active against double-stranded DNA viruses. *Antimicrob. Agents Chemother.* 56, 2726–2734. doi: 10.1128/AAC.05983-11

Papanicolaou, G. A., Silveira, F. P., Langston, A. A., Pereira, M. R., Avery, R. K., Uknis, M., et al. (2019). Maribavir for refractory or resistant cytomegalovirus infections in hematopoietic-cell or solid-organ transplant recipients: a randomized, dose-ranging, double-blind, phase 2 study. *Clin. Infect. Dis.* 68, 1255–1264. doi: 10.1093/cid/ciy706

Polansky, H., Javaherian, A., and Itzkovitz, E. (2016). Clinical study in genital herpes: natural Gene-Eden-VIR/Novirin versus acyclovir, valacyclovir, and famciclovir. *Drug Des. Devel. Ther.* 10, 2713–2722. doi: 10.2147/DDDT.S112852

Polansky, H., Javaherian, A., and Itzkovitz, E. (2018). Clinical trial of herbal treatment Gene-Eden-VIR/Novirin in Oral herpes. *J. Evid. Based Integr. Med.* 23:2515690X1880626. doi: 10.1177/2515690X18806269

Prichard, M. N. (2009). Function of human cytomegalovirus UL97 kinase in viral infection and its inhibition by maribavir. *Rev. Med. Virol.* 19, 215–229. doi: 10.1002/rmv.615

Prichard, M. N., Frederick, S. L., Daily, S., Borysko, K. Z., Townsend, L. B., Drach, J. C., et al. (2011). Benzimidazole Analogs Inhibit Human Herpesvirus 6▽. *Antimicrob. Agents Chemother.* 55, 2442–2445. doi: 10.1128/AAC.01523-10

Razonable, R. R., Amer, H., and Mardini, S. (2019). Application of a new paradigm for cytomegalovirus disease prevention in Mayo Clinic's first face transplant. *Mayo Clin. Proc.* 94, 166–170. doi: 10.1016/j.mayocp.2018.09.017

Reefschlaeger, J., Bender, W., Hallenberger, S., Weber, O., Eckenberg, P., Goldmann, S., et al. (2001). Novel non-nucleoside inhibitors of cytomegaloviruses (BAY 38-4766): in vitro and in vivo antiviral activity and mechanism of action. *J. Antimicrob. Chemother.* 48, 757–767. doi: 10.1093/jac/48.6.757

Reiter, C., Fröhlich, T., Gruber, L., Hutterer, C., Marschall, M., Voigtländer, C., et al. (2015). Highly potent artemisinin-derived dimers and trimers: synthesis and evaluation of their antimalarial, antileukemia and antiviral activities. *Bioorg. Med. Chem.* 23, 5452–5458. doi: 10.1016/j.bmc.2015.07.048

Reitsma, J. M., Savaryn, J. P., Faust, K., Sato, H., Halligan, B. D., and Terhune, S. S. (2011). Antiviral inhibition targeting the HCMV kinase pUL97 requires pUL27-dependent degradation of Tip60 acetyltransferase and cell-cycle arrest. *Cell Host Microbe* 9, 103–114. doi: 10.1016/j.chom.2011.01.006

Revello, M. G., Lazzarotto, T., Guerra, B., Spinillo, A., Ferrazzi, E., Kustermann, A., et al. (2014). A randomized trial of hyperimmune globulin to prevent congenital cytomegalovirus. *N. Engl. J. Med.* 370, 1316–1326. doi: 10.1056/NEJMoa1310214

Reza Nassiri, M., Emerson, S. G., Devivar, R. V., Townsend, L. B., Drach, J. C., and Taichman, R. S. (1996). *Comparison of benzimidazole nucleosides and ganciclovir on the in vitro proliferation and colony formation of human bone marrow progenitor cells*. Available at: http://deepblue.lib.umich.edu/handle/2027.42/72204. (Accessed April 4, 2023).

Ribeiro, I. R., and Olliaro, P. (1998). Safety of artemisinin and its derivatives. A review of published and unpublished clinical trials. *Med. Trop.* 58, 50–53.

Rifkin, L. M., Minkus, C. L., Pursell, K., Jumroendararasame, C., and Goldstein, D. A. (2017). Utility of Leflunomide in the treatment of drug resistant cytomegalovirus retinitis. *Ocul. Immunol. Inflamm.* 25, 93–96. doi: 10.3109/09273948.2015.1071406

Rittà, M., Costa, C., Solidoro, P., Sidoti, F., Libertucci, D., Boffini, M., et al. (2015). Everolimus-based immunosuppressive regimens in lung transplant recipients: impact on CMV infection. *Antivir. Res.* 113, 19–26. doi: 10.1016/j.antiviral.2014.10.016

Robin, C., Thiebaut, A., Alain, S., Sicre de Fontbrune, F., Berceanu, A., D'Aveni, M., et al. (2020). Letermovir for secondary prophylaxis of cytomegalovirus infection and disease after allogeneic hematopoietic cell transplantation: results from the French compassionate program. *Biol. Blood Marrow Transplant.* 26, 978–984. doi: 10.1016/j.bbmt.2020.01.027

Ross, S. A., Fowler, K. B., Ashrith, G., Stagno, S., Britt, W. J., Pass, R. F., et al. (2006). Hearing loss in children with congenital cytomegalovirus infection born to mothers with preexisting immunity. *J. Pediatr.* 148, 332–336. doi: 10.1016/j.jpeds.2005.09.003

Rouphael, N. G., Hurwitz, S. J., Hart, M., Beck, A., Anderson, E. J., Deye, G., et al. (2019). Phase Ib trial to evaluate the safety and pharmacokinetics of multiple ascending doses of Filociclovir (MBX-400, Cyclopropavir) in healthy volunteers. *Antimicrob. Agents Chemother.* 63, e00717–e00719. doi: 10.1128/AAC.00717-19

Roussel, C., Caumes, E., Thellier, M., Ndour, P. A., Buffet, P. A., and Jauréguiberry, S. (2017). Artesunate to treat severe malaria in travellers: review of efficacy and safety and practical implications. *J. Travel Med.* 24:93. doi: 10.1093/jtm/taw093

Roy, V., and Agrofoglio, L. A. (2022). Nucleosides and emerging viruses: a new story. *Drug Discov. Today* 27, 1945–1953. doi: 10.1016/j.drudis.2022.02.013

Roy, S., and Arav-Boger, R. (2014). New cell-signaling pathways for controlling cytomegalovirus replication. *Am. J. Transplant.* 14, 1249–1258. doi: 10.1111/ajt.12725

Saag, M. S., Gandhi, R. T., Hoy, J. F., Landovitz, R. J., Thompson, M. A., Sax, P. E., et al. (2020). Antiretroviral drugs for treatment and prevention of HIV infection in adults: 2020 recommendations of the international antiviral society–USA panel. *JAMA* 324, 1651–1669. doi: 10.1001/jama.2020.17025

Santhanakrishnan, K., Yonan, N., Callan, P., Karimi, E., Al-Aloul, M., and Venkateswaran, R. (2019). The use of CMVIg rescue therapy in cardiothoracic transplantation: a single-center experience over 6 years (2011-2017). *Clin. Transpl.* 33:e13655. doi: 10.1111/ctr.13655

Schampera, M. S., Schweinzer, K., Abele, H., Kagan, K. O., Klein, R., Rettig, I., et al. (2017). Comparison of cytomegalovirus (CMV)-specific neutralization capacity of hyperimmunoglobulin (HIG) versus standard intravenous immunoglobulin (IVIG) preparations: impact of CMV IgG normalization. *J. Clin. Virol.* 90, 40–45. doi: 10.1016/j.jcv.2017.03.005

Schleiss, M. R. (2008). Comparison of vaccine strategies against congenital CMV infection in the guinea pig model. *J. Clin. Virol.* 41, 224–230. doi: 10.1016/j.jcv.2007.10.008

Schleiss, M. R., Bernstein, D. I., McVoy, M. A., Stroup, G., Bravo, F., Creasy, B., et al. (2005). The non-nucleoside antiviral, BAY 38-4766, protects against cytomegalovirus (CMV) disease and mortality in immunocompromised guinea pigs. *Antivir. Res.* 65, 35–43. doi: 10.1016/j.antiviral.2004.09.004

Scholz, B., Rechter, S., Drach, J. C., Townsend, L. B., and Bogner, E. (2003). Identification of the ATP-binding site in the terminase subunit pUL56 of human cytomegalovirus. *Nucleic Acids Res.* 31, 1426–1433. doi: 10.1093/nar/gkg229

Seidel, V., Hackelöer, M., Rancourt, R. C., Henrich, W., and Siedentopf, J. P. (2020). Fetal and maternal outcome after hyperimmunoglobulin administration for prevention of maternal–fetal transmission of cytomegalovirus during pregnancy: retrospective cohort analysis. *Arch. Gynecol. Obstet.* 302, 1353–1359. doi: 10.1007/s00404-020-05728-7

Shahar-Nissan, K., Pardo, J., Peled, O., Krause, I., Bilavsky, E., Wiznitzer, A., et al. (2020). Valaciclovir to prevent vertical transmission of cytomegalovirus after maternal primary infection during pregnancy: a randomised, double-blind, placebo-controlled trial. *Lancet* 396, 779–785. doi: 10.1016/S0140-6736(20)31868-7

Shapira, M. Y., Resnick, I. B., Chou, S., Neumann, A. U., Lurain, N. S., Stamminger, T., et al. (2008). Artesunate as a potent antiviral agent in a patient with late drug-resistant cytomegalovirus infection after hematopoietic stem cell transplantation. *Clin. Infect. Dis.* 46, 1455–1457. doi: 10.1086/587106

Silva, J. T., Pérez-González, V., Lopez-Medrano, F., Alonso-Moralejo, R., Fernández-Ruiz, M., San-Juan, R., et al. (2018). Experience with leflunomide as treatment and as secondary prophylaxis for cytomegalovirus infection in lung transplant recipients: a case series and review of the literature. *Clin. Transpl.* 32:e13176. doi: 10.1111/ctr.13176

Song, I., Chen, G., Wu, J., and Ilic, K. (2023). Maribavir pharmacokinetics and safety in participants with moderate hepatic impairment: a phase 1, open-label, single-dose, parallel group study. *J. Clin. Pharmacol.* 63, 250–258. doi: 10.1002/jcph.2155

Sonntag, E., Hahn, F., Bertzbach, L. D., Seyler, L., Wangen, C., Müller, R., et al. (2019). In vivo proof-of-concept for two experimental antiviral drugs, both directed to cellular targets, using a murine cytomegalovirus model. *Antivir. Res.* 161, 63–69. doi: 10.1016/j.antiviral.2018.11.008

Speir, E., Yu, Z. X., Ferrans, V. J., Huang, E. S., and Epstein, S. E. (1998). Aspirin attenuates cytomegalovirus infectivity and gene expression mediated by Cyclooxygenase-2 in coronary artery smooth muscle cells. *Circ. Res.* 83, 210–216. doi: 10.1161/01.RES.83.2.210

Stoelben, S., Arns, W., Renders, L., Hummel, J., Mühlfeld, A., Stangl, M., et al. (2014). Preemptive treatment of cytomegalovirus infection in kidney transplant recipients with letermovir: results of a phase 2a study. *Transpl. Int.* 27, 77–86. doi: 10.1111/tri.12225

Swan, S. K., Smith, W. B., Marbury, T. C., Schumacher, M., Dougherty, C., Mico, B. A., et al. (2007). Pharmacokinetics of Maribavir, a novel Oral Anticytomegalovirus agent, in subjects with varying degrees of renal impairment. *J. Clin. Pharmacol.* 47, 209–217. doi: 10.1177/0091270006296765

Taber, D. J., Chokkalingam, A., Su, Z., Self, S., Miller, D., and Srinivas, T. (2019). Randomized controlled trial assessing the impact of everolimus and low-exposure tacrolimus on graft outcomes in kidney transplant recipients. *Clin. Transpl.* 33:e13679. doi: 10.1111/ctr.13679

Taiming, L., and Xuehua, J. (2006). Investigation of the absorption mechanisms of baicalin and baicalein in rats. *J. Pharm. Sci.* 95, 1326–1333. doi: 10.1002/jps.20593

Tedesco-Silva, H., Pascual, J., Viklicky, O., Basic-Jukic, N., Cassuto, E., Kim, D. Y., et al. (2019). Safety of Everolimus with reduced Calcineurin inhibitor exposure in De novo kidney transplants: an analysis from the randomized TRANSFORM study. *Transplantation* 103, 1953–1963. doi: 10.1097/TP.0000000000002626

Tian, S., He, G., Song, J., Wang, S., Xin, W., Zhang, D., et al. (2012). Pharmacokinetic study of baicalein after oral administration in monkeys. *Fitoterapia* 83, 532–540. doi: 10.1016/j.fitote.2011.12.019

Tippin, T. K., Morrison, M. E., Brundage, T. M., and Momméja-Marin, H. (2016). Brincidofovir is not a substrate for the human organic anion transporter 1: a mechanistic explanation for the lack of nephrotoxicity observed in clinical studies. *Ther. Drug Monit.* 38, 777–786. doi: 10.1097/FTD.0000000000000353

Tollefson, A. E., Hussein, I. T. M., Toth, K., and Bowlin, T. L. (2022). Filociclovir is a potent inhibitor of human adenovirus F41. *Antivir. Res.* 208:105431. doi: 10.1016/j.antiviral.2022.105431

Toovey, S. (2006). Are currently deployed artemisinins neurotoxic? *Toxicol. Lett.* 166, 95–104. doi: 10.1016/j.toxlet.2006.06.001

Toth, K., Hussein, I. T. M., Tollefson, A. E., Ying, B., Spencer, J. F., Eagar, J., et al. (2020). Filociclovir is a potent in vitro and in vivo inhibitor of human adenoviruses. *Antimicrob. Agents Chemother.* 64, e01299–e01220. doi: 10.1128/AAC.01299-20

Townsend, L. B., Devivar, R. V., Turk, S. R., Nassiri, M. R., and Drach, J. C. (1995). Design, synthesis, and antiviral activity of certain 2,5,6-trihalo-1-(beta-D-ribofuranosyl) benzimidazoles. *J. Med. Chem.* 38, 4098–4105. doi: 10.1021/jm00020a025

Tsao, R. (2010). Chemistry and biochemistry of dietary polyphenols. *Nutrients* 2, 1231–1246. doi: 10.3390/nu2121231

Tuli, H. S., Aggarwal, V., Kaur, J., Aggarwal, D., Parashar, G., Parashar, N. C., et al. (2020). Baicalein: a metabolite with promising antineoplastic activity. *Life Sci.* 259:118183. doi: 10.1016/j.lfs.2020.118183

Underwood, M. R., Harvey, R. J., Stanat, S. C., Hemphill, M. L., Miller, T., Drach, J. C., et al. (1998). Inhibition of human cytomegalovirus DNA maturation by a Benzimidazole Ribonucleoside is mediated through the UL89 gene product. *J. Virol.* 72, 717–725. doi: 10.1128/JVI.72.1.717-725.1998

Veit, T., Munker, D., Kauke, T., Zoller, M., Michel, S., Ceelen, F., et al. (2020). Letermovir for difficult to treat cytomegalovirus infection in lung transplant recipients. *Transplantation* 104, 410–414. doi: 10.1097/TP.0000000000002886

Vial, R., Zandotti, C., Alain, S., Decourt, A., Jourde-Chiche, N., Purgus, R., et al. (2017). Brincidofovir use after Foscarnet crystal nephropathy in a kidney transplant

recipient with multiresistant cytomegalovirus infection. *Case Rep. Transplant.* 2017, 1–7. doi: 10.1155/2017/3624146

Visentin, S., Manara, R., Milanese, L., Da Roit, A., Forner, G., Salviato, E., et al. (2012). Early primary cytomegalovirus infection in pregnancy: maternal Hyperimmunoglobulin therapy improves outcomes among infants at 1 year of age. *Clin. Infect. Dis.* 55, 497–503. doi: 10.1093/cid/cis423

Waldman, W. J., Knight, D. A., Blinder, L., Shen, J., Lurain, N. S., Miller, D. M., et al. (1999a). Inhibition of cytomegalovirus in vitro and in vivo by the experimental immunosuppressive agent Leflunomide. *Intervirology* 42, 412–418. doi: 10.1159/000053979

Waldman, W. J., Knight, D. A., Lurain, N. S., Miller, D. M., Sedmak, D. D., Williams, J. W., et al. (1999b). Novel mechanism of inhibition of cytomegalovirus by the experimental immunosuppressive agent leflunomide. *Transplantation* 68, 814–825. doi: 10.1097/00007890-199909270-00014

Wang, L. H., Peck, R. W., Yin, Y., Allanson, J., Wiggs, R., and Wire, M. B. (2003). Phase I safety and pharmacokinetic trials of 1263W94, a novel Oral anti-human cytomegalovirus agent, in healthy and human immunodeficiency virus-infected subjects. *Antimicrob. Agents Chemother.* 47, 1334–1342. doi: 10.1128/AAC.47.4.1334-1342.2003

Weber, O., Bender, W., Eckenberg, P., Goldmann, S., Haerter, M., Hallenberger, S., et al. (2001). Inhibition of murine cytomegalovirus and human cytomegalovirus by a novel non-nucleosidic compound in vivo. *Antivir. Res.* 49, 179–189. doi: 10.1016/S0166-3542(01)00127-9

Wild, M., Bertzbach, L. D., Tannig, P., Wangen, C., Müller, R., Herrmann, L., et al. (2020). The trimeric artesunate derivative TF27 exerts strong anti-cytomegaloviral efficacy: focus on prophylactic efficacy and oral treatment of immunocompetent mice. *Antivir. Res.* 178:104788. doi: 10.1016/j.antiviral.2020.104788

Wildum, S., Zimmermann, H., and Lischka, P. (2015). In vitro drug combination studies of Letermovir (AIC246, MK-8228) with approved anti-human cytomegalovirus (HCMV) and anti-HIV compounds in inhibition of HCMV and HIV replication. *Antimicrob. Agents Chemother.* 59, 3140–3148. doi: 10.1128/AAC.00114-15

Williams, S. L., Hartline, C. B., Kushner, N. L., Harden, E. A., Bidanset, D. J., Drach, J. C., et al. (2003). In vitro activities of Benzimidazole d- and l-Ribonucleosides against herpesviruses. *Antimicrob. Agents Chemother.* 47, 2186–2192. doi: 10.1128/AAC.47.7.2186-2192.2003

Williams, J. W., Mital, D., Chong, A., Kottayil, A., Millis, M., Longstreth, J., et al. (2002). Experiences with LEFLUNOMIDE in solid organ transplantation. *Transplantation* 73, 358–366. doi: 10.1097/00007890-200202150-00008

Williams-Aziz, S. L., Hartline, C. B., Harden, E. A., Daily, S. L., Prichard, M. N., Kushner, N. L., et al. (2005). Comparative activities of lipid esters of Cidofovir and cyclic Cidofovir against replication of herpesviruses in vitro. *Antimicrob. Agents Chemother.* 49, 3724–3733. doi: 10.1128/AAC.49.9.3724-3733.2005

Williamson, R. A., Yea, C. M., Robson, P. A., Curnock, A. P., Gadher, S., Hambleton, A. B., et al. (1996). Dihydroorotate dehydrogenase is a target for the biological effects of leflunomide. *Transplant. Proc.* 28, 3088–3091.

Winston, D. J., Young, J. A. H., Pullarkat, V., Papanicolaou, G. A., Vij, R., Vance, E., et al. (2008). Maribavir prophylaxis for prevention of cytomegalovirus infection in allogeneic stem cell transplant recipients: a multicenter, randomized, double-blind, placebo-controlled, dose-ranging study. *Blood* 111, 5403–5410. doi: 10.1182/blood-2007-11-121558

Wolf, D. G., Shimoni, A., Resnick, I. B., Stamminger, T., Neumann, A. U., Chou, S., et al. (2011). Human cytomegalovirus kinetics following institution of Artesunate after hematopoietic stem cell transplantation. *Antivir. Res.* 90, 183–186. doi: 10.1016/j.antiviral.2011.03.184

Wu, Z., Drach, J. C., Prichard, M. N., Yanachkova, M., Yanachkov, I., Bowlin, T. L., et al. (2009). L-valine Ester of Cyclopropavir - a new antiviral prodrug. *Antivir. Chem. Chemother.* 20, 37–46. doi: 10.3851/IMP782

Wu, L. L., Yang, X. B., Huang, Z. M., Liu, H. Z., and Wu, G. X. (2007). In vivo and in vitro antiviral activity of hyperoside extracted from *Abelmoschus manihot* (L) medik. *Acta Pharmacol. Sin.* 28, 404–409. doi: 10.1111/j.1745-7254.2007.00510.x

Xu, X., Williams, J. W., Bremer, E. G., Finnegan, A., and Chong, A. S. F. (1995). Inhibition of protein tyrosine phosphorylation in T cells by a novel immunosuppressive agent, Leflunomide (∗). *J. Biol. Chem.* 270, 12398–12403. doi: 10.1074/jbc.270.21.12398

Yoshida, M., Yamada, M., Tsukazaki, T., Chatterjee, S., Lakeman, F. D., Nii, S., et al. (1998). Comparison of antiviral compounds against human herpesvirus 6 and 7. *Antivir. Res.* 40, 73–84. doi: 10.1016/S0166-3542(98)00049-7

Yu, Y. B., Miyashiro, H., Nakamura, N., Hattori, M., and Park, J. C. (2007). Effects of triterpenoids and flavonoids isolated from *Alnus firma* on HIV-1 viral enzymes. *Arch. Pharm. Res.* 30, 820–826. doi: 10.1007/BF02978831

Zarghi, A., and Arfaei, S. (2011). Selective COX-2 inhibitors: a review of their structure-activity relationships. *Iran J. Pharm. Res.* 10, 655–683. doi: 10.1016/j.bmc.2005.11.041

Zhang, L., Lin, G., Chang, Q., and Zuo, Z. (2005). Role of intestinal first-pass metabolism of baicalein in its absorption process. *Pharm. Res.* 22, 1050–1058. doi: 10.1007/s11095-005-5303-7

Zhang, L., Lin, G., and Zuo, Z. (2004). High-performance liquid chromatographic method for simultaneous determination of baicalein and baicalein 7-glucuronide in rat plasma. *J. Pharm. Biomed. Anal.* 36, 637–641. doi: 10.1016/j.jpba.2004.07.024

Zhang, L., Lin, G., and Zuo, Z. (2007). Involvement of UDP-glucuronosyltransferases in the extensive liver and intestinal first-Pass metabolism of flavonoid Baicalein. *Pharm. Res.* 24, 81–89. doi: 10.1007/s11095-006-9126-y

Zhao, K. C., and Song, Z. Y. (1993). Pharmacokinetics of dihydroqinghaosu in human volunteers and comparison with qinghaosu. *Yao Xue Xue Bao* 28, 342–346.

Zhou, S., Breitenbach, J. M., Borysko, K. Z., Drach, J. C., Kern, E. R., Gullen, E., et al. (2004). Synthesis and antiviral activity of (Z)- and (E)-2,2-[Bis(hydroxymethyl) cyclopropylidene]methylpurines and -pyrimidines: second-generation methylenecyclopropane analogues of nucleosides. *J. Med. Chem.* 47, 566–575. doi: 10.1021/jm030316s

frontiers | Frontiers in Microbiology

TYPE Original Research
PUBLISHED 23 November 2023
DOI 10.3389/fmicb.2023.1269869

OPEN ACCESS

EDITED BY
Gaëtan Ligat,
Université Toulouse III Paul Sabatier, France

REVIEWED BY
Joseph Atia Ayariga,
Alabama State University, United States
Jai K. Kaushik,
National Dairy Research Institute (ICAR), India

*CORRESPONDENCE
Shi-Hua Xiang
✉ sxiang2@unl.edu

†These authors have contributed equally to this work

RECEIVED 31 July 2023
ACCEPTED 20 October 2023
PUBLISHED 23 November 2023

CITATION
Wiggins J, Nguyen N, Wei W, Wang LL, Hollingsead Olson H and Xiang S-H (2023) Lactic acid bacterial surface display of scytovirin inhibitors for anti-ebolavirus infection.
Front. Microbiol. 14:1269869.
doi: 10.3389/fmicb.2023.1269869

Lactic acid bacterial surface display of scytovirin inhibitors for anti-ebolavirus infection

Joshua Wiggins[1,2†], Ngan Nguyen[1,3†], Wenzhong Wei[1,3], Leah Liu Wang[1,3], Haley Hollingsead Olson[1,3] and Shi-Hua Xiang[1,3*]

[1]Nebraska Center for Virology, Lincoln, NE, United States, [2]School of Biological Sciences, University of Nebraska-Lincoln, Lincoln, NE, United States, [3]School of Veterinary Medicine and Biomedical Sciences, University of Nebraska-Lincoln, Lincoln, NE, United States

Scytovirin (SVN) is a lectin from cyanobacteria which has a strong inhibitory activity against Ebola virus infection. We engineered scytovirin as the inhibitor for surface display of lactic acid bacteria to block Ebola virus infection. Two different bacterial strains (*Lactobacillus casei* and *Lactococcus lactis*) were successfully engineered for scytovirin expression on the bacterial surface. These bacteria were found to be effective at neutralizing pseudotyped Ebolavirus in a cell-based assay. This approach can be utilized for prophylactic prevention, as well as for treatment. Since lactic acid bacteria can colonize the human body, a long-term efficacy could be achieved. Furthermore, this approach is also simple and cost-effective and can be easily applied in the regions of Ebola outbreaks in the developing countries.

KEYWORDS

scytovirin, lectins, lactic acid bacteria, Ebola virus, bacterial engineering, surface display

1 Introduction

Ebola virus (EBOV) is an enveloped negative-stranded RNA virus which can cause severe Ebola viral disease (EVD) in humans and nonhuman primates (Jacob et al., 2020). EBOV belongs to the family *Filoviridae* along with Marburg virus that also causes a similar disease. Ebolavirus in Zaire was first identified in 1976 in Africa (Bowen et al., 1980), now five Ebola species have been recognized (Kuhn et al., 2019): Zaire ebolavirus (ZEBOV or EBOV), Sudan ebolavirus (SUDV), Tai Forest ebolavirus (TAFV), Reston ebolavirus (RESTV) and Bundibugyo ebolavirus (BDBV). Ebolavirus has produced more than 20 outbreaks in humans with high mortality rates from 25 to 90% (Feldmann and Geisbert, 2011;WHO, n.d.). The recent large Ebola outbreak in 2014 in West Africa infected more than 28,000 people and more than 11,000 died (Cenciarelli et al., 2015). It is evident that this emerging and reemerging viral pathogen represents a great threat to human health. However, we do not have any medicines to treat this lethal viral disease until December 2019, when a vaccine (rVSVΔG-ZEBOV-GP) was approved by FDA for limited use against Zaire Ebolavirus, and in 2020, two antibody drugs (mAb114 and REGN-EB3) were approved for treating this viral infection. It is apparent that more medicines are required for fighting against this deadly, infectious viral disease.

Scytovirin (SVN) is a small protein of 95 amino acids which was first identified from cyanobacteria of *Scytonema varium* (Bokesch et al., 2003). Scytovirin is a type of lectin which are known carbohydrate-binding proteins with non-immunologic nature (Fernandez Romero et al., 2021). Because lectins recognize the carbohydrates on the glycoproteins of viral particles, they usually exhibit antiviral activities (Akkouh et al., 2015; Naik and Kumar, 2022). Lectins

from algae, plants and cyanobacteria show strong inhibitory activity against HIV infection (Li et al., 2008; Akkouh et al., 2015). Due to their inhibitory effect and immunosuppressive properties, lectins such as cyanovirin-N (CV-N) (Colleluori et al., 2005; Li et al., 2011; O'Keefe et al., 2015; Vamvaka et al., 2016) and griffithsin (GRFT) (Emau et al., 2007; Girard et al., 2018; Alexandre et al., 2020), have been used as microbicides for treating viral diseases (Abdool Karim and Baxter, 2012; Huskens and Schols, 2012; Koharudin and Gronenborn, 2014) and have been investigated for pre-exposure prophylaxis (PrEP) against HIV-1 infection. Like the well-studied lectins CV-N and GRFT in HIV research, SVN has also shown highly specific activity to the high mannose moieties that exist on the surface of glycoproteins of HIV, Ebola, and Marburg viruses (Barrientos and Gronenborn, 2005, Mori et al., 2005, Alexandre et al., 2010). More studies have demonstrated that scytovirin has much stronger activity against Ebola than HIV *in vitro* and *in vivo* (Garrison et al., 2014).

Because scytovirin demonstrated potent antiviral activity against Ebola infection, we used it to develop a novel live microbicide for Ebola infection control. This approach displayed scytovirin on the surface of Lactic acid bacteria (LAB) for delivery against Ebola virus infection. These bacteria can be delivered into mucosal surfaces of the body (e.g., mouth, nose, and GI tract) that are the ports of viral entry where they can colonize and replicate. Previous studies using LAB expressing the antiviral lectin CV-N demonstrated that the bacteria can pass through the GI tract unharmed and stably produce lectins to inhibit HIV (Lagenaur et al., 2011, Li et al., 2011, Brichacek et al., 2013). Therefore, this approach for application of viral inhibition should be safe, long-lasting and effective. Furthermore, this approach is cost-effective and easy-to-use, so it is especially valuable for use in those outbreak regions in Africa. Here, we reported the *in vitro* data we have achieved successfully in this research direction.

2 Methods and materials

2.1 Strains, cell lines, and plasmids

Escherichia coli DH5α and *E. coli BL21 DE3* were used for cloning and initial protein verification, respectively. Both were cultured in LB media (FisherSci, BP1427-500) overnight in a shaker at 250 rpm and 37°C. The antibiotics used for plasmid selection were 50 μg/mL kanamycin for pET28a and 250 μg/mL erythromycin for pLSVN3 and pLSVN7 (Table 1). *L. casei* and *L. lactis* were cultured statically in MRS media (FisherSci, CM0359) at 37°C and 5% CO2 for 2–3 days until reaching log phase. For engineered bacterial culturing, 5 μg/mL erythromycin was added to the MRS media for applying selection pressure. HEK 293 T and TZM-bl mammalian cell lines were grown in Dulbecco Minimum Essential Media (DMEM) (Gibco, 11,965,092) supplemented with 10% FBS (Gibco, 10,082), 1 mM L-glutamine (Gibco, 25,030), and 100 μg/mL penicillin/streptomycin (Gibco, 15,140). Cells were cultured in a humidified cell culture incubator at 37°C with 5% CO2 using T-75 flasks.

2.2 Scytovirin gene expression in *E. coli*.

The scytovirin (SVN) gene sequence (GenBank: P86041.1) (Bokesch et al., 2003) with an added E-tag sequence (total 348 bp) was synthesized with *SacI*/*XhoI* restriction sites by GenScript and inserted into the vector pET28a (Novagen, Inc.) to test protein expression in *E. coli BL21 (DE3)* bacterial cells. SVN was overexpressed in *E. coli* previously by Xiong et al. (2006). SVN expression was induced by IPTG (1 mM) to increase protein production which was verified by Western blotting using an anti-E-tag (ab3397, Abcam), anti-His-tag (HRP-66005, Proteintech) or anti-SVN (A64238-050, Epigentek) polyclonal antibodies.

2.3 Scytovirin constructs for surface display on LAB

To express the SVN protein on the surface of LAB, constructs were created which included the *Lactate dehydrogenase* promoter (*Pldh*), signal peptide (SP), cell membrane anchor protein (ANC), E-tag marker (E), and the protein marker (GFP). The constructs were built up based on our previous plasmid pWZ486 (Wei et al., 2019) derived from pTRKH3-ldhGFP (Addgene). The SVN-E-tag-GFP fusion sequence replaced the CD4 gene sequence in pWZ486 using the *SacI*/*XhoI* restriction sites. The constructs pLSVN3 and pLSVN7 were verified by DNA sequencing and PCR using the specific primers (Table 1) marked in the construct maps.

2.4 Electroporation

Plasmids were transformed into the Lactic acid bacteria (LAB) by electroporation as previously described (Wei et al., 2019; Welker et al., 2019). Briefly, overnight cultures of LAB cells were diluted (1:50) into fresh MRS media with 1% glycine and incubated at 37°C without shaking for 2 h. Cells were harvested and treated with 50 mM EDTA (pH 8.0) for 15 min, followed by two washes with ice-cold electroporation buffer (0.5 M sucrose) and resuspended in electroporation buffer (1/100 volume of the initial culture). 50 μL of cells were mixed with plasmid DNA and incubated on ice for 15 min. The mixture was added to an ice-cold 0.2 cm GenePulser (Biorad) cuvette and pulse was immediately applied at the conditions of 10 KV/cm, 200 Ω, and 25 μF. Cells were suspended in 1 mL MRS broth with 2 mM CaCl2 and 20 mM MgCl2 and then incubated at 37°C for 4 h. Cells were pooled on MRS plates with 5 μg/mL erythromycin and cultured as described above. To verify transformation, single colonies were picked and added to 25 μL PCR master mix (Promega, M791B) containing 1 μM forward and reverse primers (Table 1). PCR amplification occurred in a SimpliAmp thermocycler (Applied BioSystems, A24811) under the following conditions: Stage 1; 95°C for 5 min, Stage 2 (35 cycles); 95°C for 30 s, 55°C for 30 s, 72°C for 1 min, Stage 3; 72°C for 7 min. PCR products were visualized on 1% agarose gel electrophoresis.

2.5 Flow cytometry

For the pLSVN3 construct transformed into *L. casei*, the fusion protein was detected based on the GFP fluorescence. Bacteria were washed three times with PBS and analyzed on a BD FACSAria using a 488 nm laser. For the pLSVN7 construct transformed into *L. lactis*, the bacteria were first stained for 1 h

TABLE 1 List of strains, cell lines, plasmids, and primers used in this study.

Materials	Relevant characteristics	Source or reference
Strains		
Lactobacillus casei	host strain for SVN engineering	ATCC
Lactococcus lactis	host strain for SVN engineering	ATCC
E. coli BL21 DE3	For SVN expression	Previous study
E. coli DH5α	For plasmid amplification	Previous study
Cell lines		
HEK 293 T	human embryonic kidney 293 cells for making pseudotyped viruses	Previous study
TZM-bl	HIV permissive cells under Tat-responsive long terminal repeat (LTR) promoter driving the expression of firefly luciferase and beta-galactosidase used as report cells.	NIH HIV Research reagents program
Plasmids		
pSG3$^{\Delta Env}$	An envelope gene defective HIV clone (cat no. ARP-11051, GenBank: L02317) used as the backbone for pseudotyping viruses.	NIH HIV Research reagents program
pWZ486	pTRKH-Pldh-SP1-GFP-CD4-ANC, Erm^r	Previous study (Wei et al., 2019)
pET28a-SVN	for SVN-E-tag expression in *E. coli*	This study
pLSVN3	for *Lactobacillus casei* engineering	This study
pLSVN7	for *Lactococcus lactis* engineering	This study
Primers		
037	GCGCCTGCAGCTATTCTTCACGTTGTTTCCGTTTC	ANC, reverse
048	GCGCGAATTCGCAGTCGACAAGCTTTTTAGTC	*Pldh*, forward
057	AATTCTCGAGTCCTGAGCCTTTGTATAGTTCATCCATG	GFP, reverse
141	GCGACTCGAGGATAAGAAGACTTCGCTGC	ANC, forward
154	GCAGCAACCATAGAAAGCGGAGGTAGTAAAGGAGAAG	*Pldh*-SP-GFP, forward
155	CTTCTCCTTTACTACCTCCGCTTTCTATGGTTGCTGC	*Pldh*-SP-GFP, reverse
198	GCGCGAGCTCATGGGAGCACCACTACC	SVN Forward primer to test integration
199	GCGCCTGCAGCTACTCGAGTGCGG	SVN Reverse primer to test integration

Erm^r, erythromycin resistance gene; SP, signal peptide; GFP, green fluorescent protein, ANC, anchor (prtP) (Wei et al., 2019). SVN, scytovirin; Restriction enzymatic sites are underlined.

with two primary antibodies: mouse monoclonal anti E-tag (Novus NBP2-67081) and rabbit polyclonal anti SVN (A64238-050, Epigentek). Goat anti mouse conjugated with AlexaFluor488 (A-11011, ThermoFisher) and goat anti rabbit conjugated with AlexaFluor594 (A-11012, ThermoFisher) were used as secondary antibodies, respectively. Bacteria were analyzed on a Beckman Coulter CytoFLEX FX at 488 nm and 561 nm. Unstained bacteria and stained wild-type bacteria were used in all experiments for an appropriate gating strategy.

2.6 Confocal microscopy

Confocal microscopy was performed using the same fluorescent fusion protein or antibody combinations as described for flow cytometry (above). Following the antibody staining, bacteria were pelleted, resuspended in 10 μL PBS, and transferred to a microscope slide with cover slip. Images were captured using a Nikon A1R-Ti2 (Nikon Instruments, NY, USA) inverted confocal system.

2.7 Pseudotyping viruses

The Ebola pseudotyped viruses were made from a HIV-1 backbone plasmid, pSG3$^{\Delta Env}$ (NIH HIV Reagent Program). The Ebola Envelope gene (GP, Zaire ebolavirus, GenBank: AIO11753.1), was synthesized by GenScript and cloned into pcDNA3.1(+). Both plasmids were co-transfected into 293 T cells in a 10 cm plate using transfection reagent polyethyleneimine (PEI). Three days post transfection, the medium was harvested and centrifuged at 500 g to remove cell debris, and then the supernatants were stored at −80°C (Platt et al., 2009; Wang et al., 2022). The viral titers were determined by reverse transcriptase assay.

2.8 Reverse transcriptase assay

The titers of pseudotyped viruses were determined by Reverse transcriptase assay (RTA) (Wei et al., 2019). 500 μL of pseudotyped virus stock was spun at 14,000 g for 2 h at 4°C to precipitate the virus. The viral pellet was resuspended in a Triton X-100-based suspension

buffer and vortexed, followed by three rapid freeze–thaw cycles to lyse the viruses. 50 μL of reaction mix [Oligo-dT Poly-A and ^{3}H-dTTP (PerkinElmer)] was added, and the samples were incubated at 37°C for 1 h in a heating block. Then, the samples were pipetted onto DEAE Filter mat circle papers (PerkinElmer), followed by three 10 min washes in 2X SSC buffer, and one 10 s wash in 100% ethanol. The filters were dried at room temperature and analyzed using a scintillation counter to measure the incorporation of ^{3}H-dTTP into cDNA. The average CPM values from duplicates were determined.

2.9 Virus adsorption

Pseudotyped Ebola virus stocks were mixed with wild-type bacteria or engineered bacteria (~5×10^{7}/mL) in 1.5 mL micro-centrifuge tubes. The mixtures of bacteria and viruses were incubated for 1 h at room temperature. Then the tubes were spun for 1 min at a 13,000 g to remove the bacteria and bound pseudotyped virus. The supernatants were collected, and the viral titers determined by RTA.

2.10 Virus neutralization

For the neutralization assay, pseudotyped Ebola virus was mixed with wild-type or engineered bacteria in the same manner as the adsorption assay described above. After centrifugation to remove the bacteria and bound pseudovirus, the remaining supernatants were applied to TZM-bl cells which were used as the target cells due to their ability to express luciferase when infected (Platt et al., 2009). The TZM-bl cells were set at a density of 6.0 × 10^{3} per well in a 96-well plate. Each neutralization assay was performed in triplicate with 5,000 RT units of pseudovirus per well used as the starting titer. Two days post-infection, the supernatants were removed, the cells were washed once with PBS, lysed in 1x Passive Lysis Buffer, and frozen at −80°C. The plates were then thawed, and luciferase activity was measured using beetle luciferin substrate (Promega) in a Veritas Luminometer.

2.11 Statistical analyses

Statistical analyses were conducted for virus adsorption and virus neutralization data using GraphPad Prism software (version 9.0). The significances were determined by using unpaired two-tailed Student's *t*-test at *p*-value ≤0.05.

3 Results

3.1 SVN gene cloning and expression

The scytovirin gene was initially synthesized by adding an E-tag at the N-terminus and cloned into pET28a with *SacI/XhoI* sites. The SVN plasmid was transformed to *E. coli* BL21 (DE3) cells for protein expression. The SVN fusion protein was observed under induction of 1 mM IPTG by Coomassie blue staining. The induced band of ~16kD fusion protein was noticed clearly (Figure 1A). To further confirm this protein, Western blotting was carried out by using E-tag, His-tag, and SVN specific antibodies. Positive bands were observed from all three different specific antibodies (Figure 1B), suggesting that the ~16kD SVN-E-tag fusion protein is expressed correctly. Figure 1C shows the construct design including the two His-tags encoded by the pET28a vector, as well the SVN ribbon structure with two highly similar domains (D1 and D2) for carbohydrate binding (Moulaei et al., 2007). Thus, the SVN-E-tag expressing construct can be further utilized for following bacterial engineering.

3.2 SVN gene engineering for surface display on *Lactobacillus casei*

The SVN-E-tag construct was cloned into our previous plasmid (pWZ486) through *SacI/XhoI* sites to produce a new construct designated as pLSVN3 (Figure 2A). This GFP-E-tag-SVN fusion protein with the anchor has been modeled and shown in Figure 2B, which should be flexible for capturing viral particles. The construct

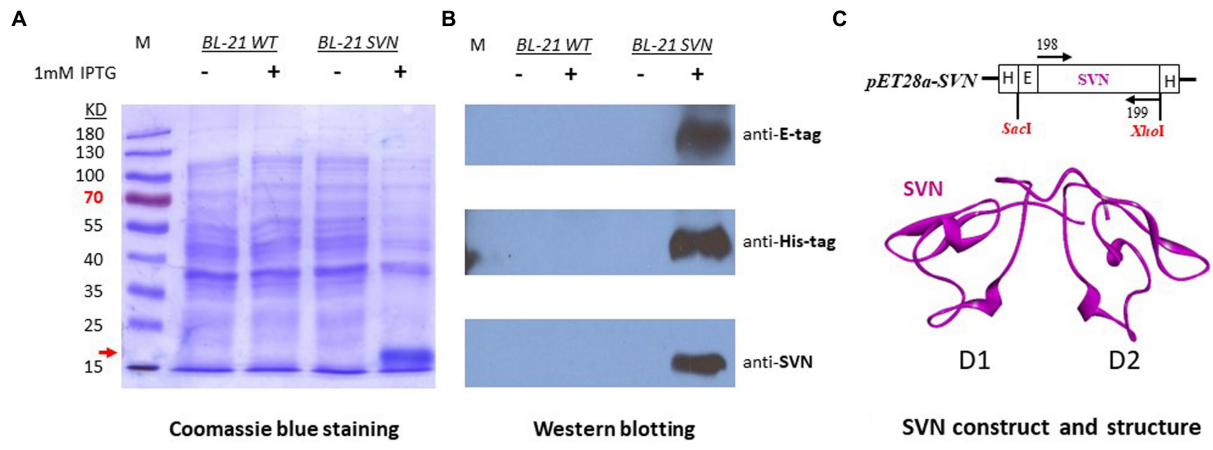

FIGURE 1
Expression of SVN-E-tag-His-tag in bacterial *Escherichia coli K12 BL21* cells. **(A)** Coomassie blue staining, the induced fusion protein band was marked with the red arrow. **(B)** Western blots showing the specific positive bands. The specific antibody for anti-SVN is a scytovirin polyclonal antibody. **(C)** The SVN construct in pET28a and the SVN 3D structure, showing the two similar domains (D1 and D2) in magenta. H, His-tag, E, E-tag.

10.3389/fmicb.2023.1269869

was created first in *E. coli DH5α* cells and demonstrated the PCR fragment of ~1800 bp of GFP-E-tag-SVN sequence was correctly amplified using primers 154 and 037 (Figure 2C). To engineer the *L. casei* strain, the SVN construct pLSVN3 was transformed by electroporation into the *L. casei* for protein expression. The transformants were verified by PCR. A ~ 1800 bp PCR band from the amplification with primers 154 and 037 revealed that the pLSVN3 plasmid was transformed into the *L. casei* cells (Figure 2D). A ~ 75kD band corresponding to the fusion protein size (GFP-E-SVN-ANC) was detected by Western blotting using specific GFP and SVN antibodies (Figure 2E), suggesting that the SVN-GFP based fusion protein was produced from the *L. casei* cells. The smaller size band (~43kD) that appeared is the partial fragment of the fusion protein complex without the anchor domain (ANC). Flow cytometry analysis revealed the rate of SVN-GFP positive cells was 33.5% (Figure 2F a and b). To determine whether these protein inhibitors are displayed on the bacterial surface, confocal microscopy was used to visualize these SVN-GFP fused proteins. The pictures from confocal microscopy exhibited the fusion protein in green (GFP) displayed on the surface of bacteria (Figure 2F b). The biological functional studies were conducted for virus binding and neutralization. The engineered bacteria showed a moderate binding activity to the pseudotyped Ebola particles, reduced 37.2% of virus load, but the wild-typed (WT) bacteria also showed weak binding to the pseudotyped viruses because of the unspecific binding, reduced 21.8% (Figure 3A). The virus inhibition assay indicated that SVN-expressing bacteria had a moderate inhibition activity against pseudotyped Ebola virus infection which was 39.1%, but the WT-bacteria also had 23% inhibition (Figure 3B). These moderate functions may be due to the lower positive rate of SVN-expressing cells and the GFP interference of SVN binding in the SVN-GFP-ANC fusion protein complex.

3.3 SVN gene engineering for surface display on *Lactococcus lactis*

Lactococcus lactis is another type of LAB which has a round shape and is widely used in the production of buttermilk and cheese. Thus, it is a very safe host strain candidate for anti-Ebola infection. We created the construct to remove the protein marker GFP but keep the E-tag marker from the construct pLSVN3, and this new construct was designated as pLSVN7 (Figure 2A). The construct pLSVN7 was transformed into the *L. lactis* using electroporation method. Positive bacterial colonies in the erythromycin selection plates were picked for further evaluation. The PCR method was first used to confirm the pLSVN7 plasmid was in the bacterium of *L. lactis* using primers 048 and 199. The expected ~700 bp band was identified (Figure 4A). Western blotting further demonstrated that SVN fusion protein (E-tag-SVN-ANC) was shown and in the correct molecular weight of 55kD both in anti-E-tag and anti-SVN specific antibodies. The 16kD SVN-E-tag fusion protein from the *E. coli* BL-21 (DE3) lysate as the positive control was also shown in the Western blots (Figures 4B,C). These Western blotting data demonstrated that the E-tag-SVN-ANC fusion protein was expressed in *L. lactis*. Next, the Confocal microscopy method was used to verify the surface display. Two colors of fluorescence were used for labeling E-tag (green) and SVN (red), respectively. The results demonstrated that the SVN fusion protein is clearly expressed on the surface of the bacterium. The single color, green or red and the merged color of green and red indicated the overlapping presence of fusion protein surface expression (Figure 5). Furthermore, Flow cytometry analysis was also conducted, and the data presented in Figure 6, shows that the positive rate of bacteria has reached 92.4%. The results demonstrated that the SVN-fusion protein is unambiguously expressed on the surface of these bacteria.

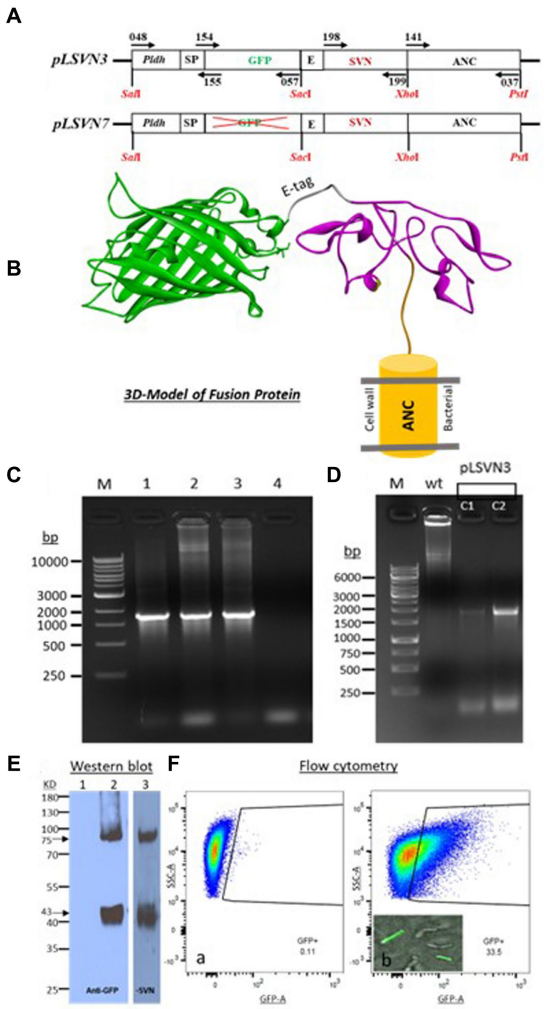

FIGURE 2
Plasmid constructs and characterizations of SVN-fusion protein expression in *Lactobacillus casei*. **(A)** Maps of scytovirin (SVN) plasmid constructs. Promoter, *Pldh*; SP, signal peptide; GFP, green fluorescent protein; E, E-tag; SVN, scytovirin; ANC, anchor domain. **(B)** Three-dimensional (3D) model of fusion protein of ANC-SVN-E-tag-GFP. **(C)** DNA gels showing the PCR bands with the pair of primers 154/037, indicating the total 1797 bp band from the positive colonies of *E. coli*: 1. pLSVN3 plasmid, 2. pLSVN3 C1 (colony 1), 3. pLSVN3 C2 (colony 2). 4. *E. coli* WT. **(D)** Verification of pLSVN3 plasmid in *L. casei* after electroporation using PCR primers 154/037. wt, wild-type *L. casei*; 1. pLSVN3 C1 (colony 1); 2. pLSVN3 C2 (colony 2). **(E)** Western blot for detecting the SVN-GFP fusion protein. 1. *L. casei* wild-type bacteria only. 2. Engineered *L. casei* (using anti-GFP antibody). 3. Engineered *L. casei* (using anti-SVN HRP conjugated polyclonal antibody, MBS7005164). **(F)** Flow cytometry analysis: (a), Wild-type *L. casei* (negative control), (b). Engineered *L. casei* and the images of SVN-GFP surface displayed bacteria.

Functional studies were performed against the pseudotyped Ebola viruses. First, we used the viral particles adsorption method to evaluate the bacterial ability for capturing the viruses. We then tested

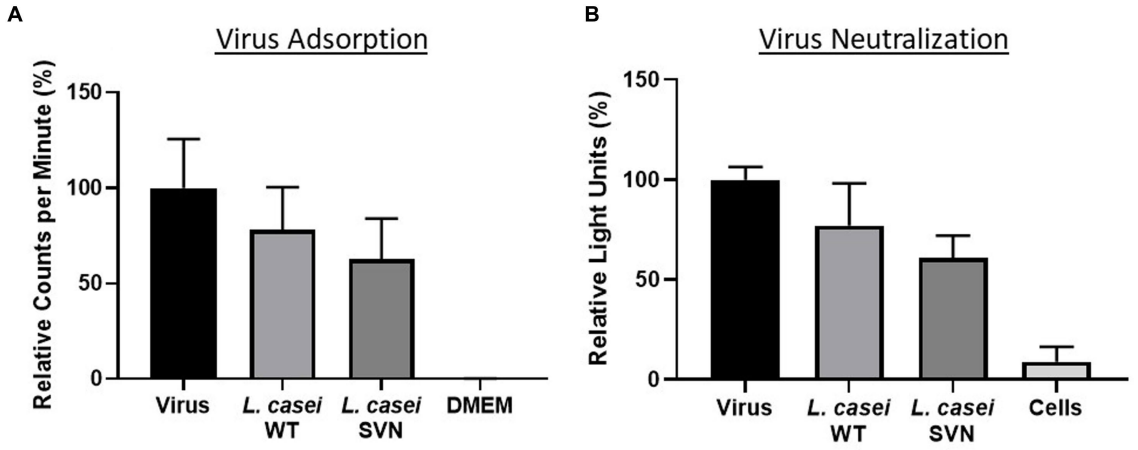

FIGURE 3
Functional studies of SVN-engineered *L. casei* bacteria. **(A)** Virus adsorption assay. **(B)** Virus neutralization assay. Wild-type (WT) *L. casei* as the negative bacterial control; virus only used as the positive control; DMEM medium or cells as the negative control.

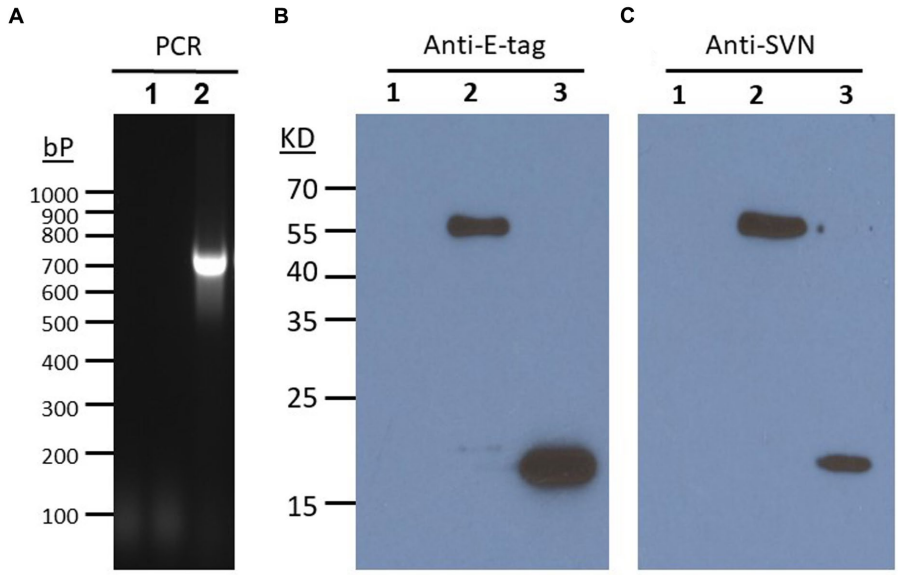

FIGURE 4
Characterizations of SVN expression in *L. lactis*. **(A)** PCR verification of SVN plasmid in *L. lactis*. PCR verified a positive band of ~700 bp from primers of 048 and SVN reverse primer 199. **(B)** Western blots showing anti-E-tag and Anti-SVN positive bands. 1. *L. lactis* WT, 2, *L. lactis* SVN. 3. *E. coil* SVN (positive control). SVN specific polyclonal antibody A64238-050 (Epigentek).

the engineered strain activity to inhibit Ebola virus infection using TZM-bl cells. The virus adsorption and neutralization data are shown in Figure 7. Compared to the wild-type control bacteria, *L. lactis*, SVN engineered bacteria demonstrated improved functional abilities, absorbing 22.1% more pseudoviral particles and reducing infection by 28.5%. Overall, the SVN expressing *L. lactis* was able to adsorb 37.6% and neutralize 53.5% of the total pseudotyped Ebola virus, reducing infection in half compared to the virus only positive control (Figures 7A,B). In comparison, the wild-type *L. lactis* also demonstrated some ability to bind pseudotyped Ebola virus and reduce infection (15.5% adsorption and 24.7% neutralization) through non-specific binding, but the specific binding of the engineered bacteria to the viruses and are more than twice as effective, suggesting the SVN-expressing *L. lactis* bacteria can offer better protection against Ebola virus infection.

4 Discussion

Bacterial therapy is a promising approach for human health and the common use of probiotics demonstrates its great potential (Yadav et al., 2020; Tegegne and Kebede, 2022). Using commensal bacteria for treating viral diseases has received broad attention since the bacterial microbicide has its advantages such as easy-to-use, cost-effective, and long-term

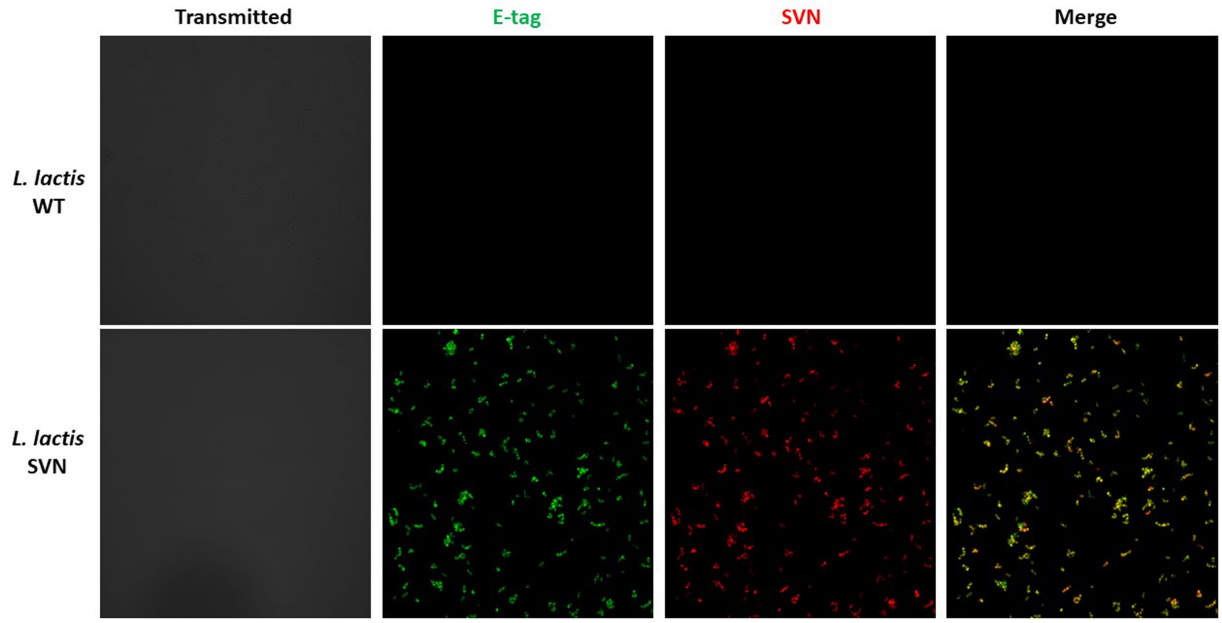

FIGURE 5
Confocal analysis of SVN-engineered *Lactococcus lactis*. Antibodies used for staining: AF-488 (green) for E-tag; AF-594 (red) for SVN. For more details, please see the Method section.

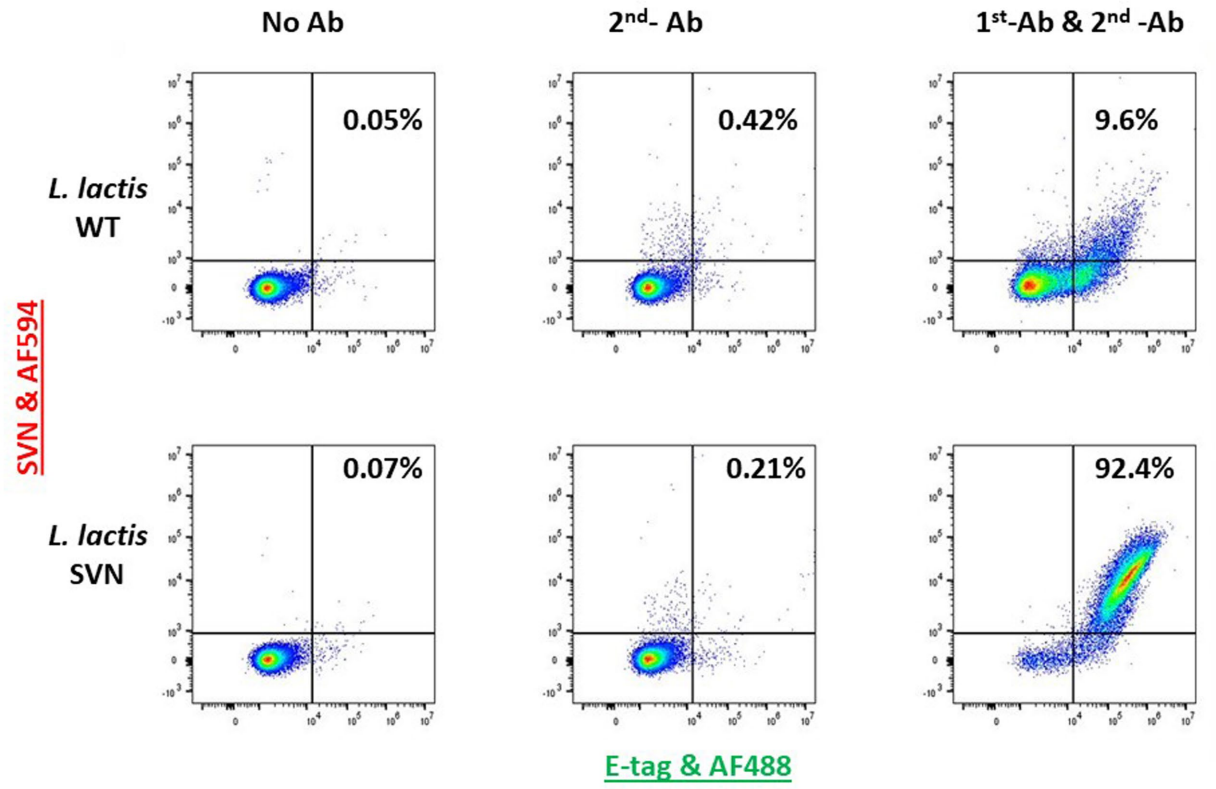

FIGURE 6
Flow cytometry analysis of SVN-engineered *Lactococcus lactis*. The 1st antibody (AF-488 conjugated, green) used is for staining E-tag; The 2nd antibody used (AF-594, red) is for staining SVN.

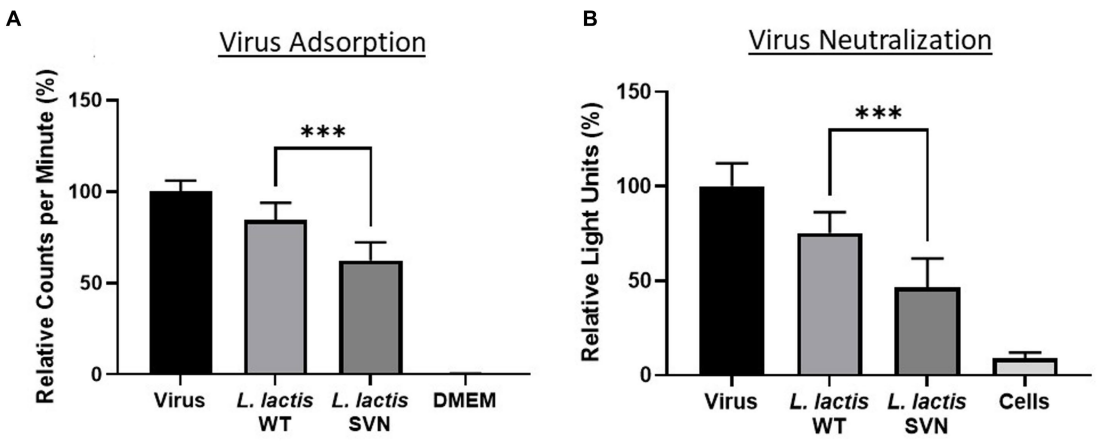

FIGURE 7
Functional studies of SVN-engineered *L. lactis*. **(A)** Virus adsorption assay. **(B)** Virus neutralization assay. Wild-type (WT) *L. lactis* as the negative bacterial control; virus only used as the positive control; DMEM medium or cells as the negative control. Significances were determined by using unpaired two-tailed Student's *t*-test at *p*-value ≤0.05.

efficacy (Ramachandran and Shanmughavel, 2009; Obiero et al., 2012). Especially, natural lectins as inhibitors can reduce unnecessary immune responses and enhance specific inhibiting activities for therapeutic applications (Akkouh et al., 2015; Mitchell et al., 2017; El-Maradny et al., 2021; Fernandez Romero et al., 2021; Mazur-Marzec et al., 2021; Naik and Kumar, 2022). For developing this method to use bacteria for antiviral diseases, bacterial engineering is a critical step. In this report, we engineered two types of Lactic acid bacteria (LAB) for surface display of the Ebola inhibitor scytovirin (SVN). Both bacterial strains successfully displayed scytovirin on the surface, suggesting the applicability of our constructs for surface expression of SVN fusion protein in lactic acid bacteria. The fluorescence of the SVN lectin fusion molecules when stained with GFP or SVN antibodies perfectly overlapped on the surface of the bacterium indicating a high display of inhibitors. The positive rate of engineered bacteria is higher in *L. lactis* (92.4%) than in *L. casei* (33.5%), suggesting that lower positive rate in *L. casei* is due to the higher genetic instability because certain bacteria may lose the SVN plasmid or SVN gene during the replication, especially when the antibiotic pressure is reduced. Another possibility is the genetic recombination between the SVN plasmid and host genome by which the plasmid composition could be changed or damaged. We found that LAB were capable of quickly developing resistance to erythromycin (5μg/mL) selective pressure, especially when grown in stationary, liquid culturing conditions, suggesting that the bacteria lose the plasmid (data not shown). Thus, increased erythromycin concentration is usually needed to get more genetically stable strains. In general, using a genomic integration method for engineering would be better than plasmid transformation for making genetically stable strains, which is essential for clinical or therapeutic use. In this research, *L. lactis* was found to be highly stable and would be assessed for *in vivo* (mice) colonization, and for protective efficacy against challenge with infectious Ebola viruses conducted in the BSL-4 containment.

In the construction of fusion protein plasmids, the GFP protein marker seems unnecessary. Small protein tags such as E-tag appear to be adequate for detection and evaluation during the studies. Removing GFP reduced the size of the fusion protein by ~27kD, nearly 3x the size of SVN, maximizing the exposure of SVN inhibitor and preventing possible steric hindrance from GFP. Eliminating GFP from the fusion protein also presents another advantage for *in vivo* applications by avoiding the potential for immunogenicity and cytotoxicity caused by the GFP protein (Ansari et al., 2016).

In this report, our data from the *in vitro* study with pseudotyped Ebola virus serves as a proof of concept of using engineered commensal bacteria for blocking Ebola infection. Commensal bacteria have previously been demonstrated to inhibit HIV-1 infection (Nahui Palomino et al., 2017), and it is likely they provide a similar baseline level of protection at mucosal surfaces against other viral infections. This study indicates that this baseline level of protection is around 20–25% for WT *L. lactis*. Our data shows that lectin displaying bacteria can bind and neutralize significantly more viruses compared to the wild-type commensal bacteria, suggesting that engineered bacteria could be used prophylactically to improve upon the health benefit already provided by commensal bacteria by decreasing the likelihood of contracting a viral disease. This is contingent upon the engineered bacteria successfully colonizing various mucosal surfaces in the body and stably producing recombinant protein. To investigate this, we will test different routes of administration in mice (oral, nasal, rectal, etc.) to determine the stability of the *L. lactis* strain under different physiological conditions, as well as determining the efficacy of the bacteria to prevent *in vivo* infection prior to advancing to clinical trials. In conclusion, the commensal bacterial based anti-Ebola approach is promising and will be beneficial for combating this deadly viral disease.

Data availability statement

The datasets presented in this study can be found in online repositories. The names of the repository/repositories and accession number(s) can be found in the article/supplementary material.

Ethics statement

Ethical approval was not required for the studies on humans in accordance with the local legislation and institutional requirements because only commercially available established cell lines were used. Ethical approval was not required for the studies on animals in accordance with the local legislation and institutional

requirements because only commercially available established cell lines were used.

Author contributions

JW: Data curation, Methodology, Writing – review & editing, Formal analysis, Investigation, Validation, Visualization. NN: Data curation, Formal analysis, Investigation, Methodology, Validation, Writing – review & editing, Visualization. WW: Data curation, Formal Analysis, Investigation, Methodology, Writing – review & editing. LW: Formal Analysis, Investigation, Methodology, Writing – review & editing. HH: Investigation, Writing – review & editing. S-HX: Data curation, Investigation, Writing – review & editing, Conceptualization, Formal Analysis, Funding acquisition, Methodology, Project administration, Resources, Supervision, Writing – original draft.

Funding

The author(s) declare financial support was received for the research, authorship, and/or publication of this article. JW was supported by the NIH T-32 grant (5T32NS105594). This project was supported by the NIH R21 grant (1R21AI126299-01A1).

Acknowledgments

We thank the University of Nebraska - Lincoln Microscopy Core facility (You Zhou, Terri Fangman) and Flow Cytometry Core facility (Dirk Anderson) for helping with sample analyses.

Conflict of interest

The authors declare that the research was conducted in the absence of any commercial or financial relationships that could be construed as a potential conflict of interest.

Publisher's note

References

Abdool Karim, S. S., and Baxter, C. (2012). Overview of microbicides for the prevention of human immunodeficiency virus. *Best Pract. Res. Clin. Obstet. Gynaecol.* 26, 427–439. doi: 10.1016/j.bpobgyn.2012.01.010

Akkouh, O., Ng, T. B., Singh, S. S., Yin, C., Dan, X., Chan, Y. S., et al. (2015). Lectins with anti-HIV activity: a review. *Molecules* 20, 648–668. doi: 10.3390/molecules20010648

Alexandre, K. B., Gray, E. S., Lambson, B. E., Moore, P. L., Choge, I. A., Mlisana, K., et al. (2010). Mannose-rich glycosylation patterns on HIV-1 subtype C gp120 and sensitivity to the lectins, Griffithsin, Cyanovirin-N and Scytovirin. *Virology* 402, 187–196. doi: 10.1016/j.virol.2010.03.021

Alexandre, K., Malatji, K., and Mulaudzi, T. (2020). Comparison of the antiviral activity of the microbicide candidate griffithsin and its tandemers derivatives against different modes of HIV-1 transmission. *Virology* 544, 12–20. doi: 10.1016/j.virol.2020.01.017

Ansari, A. M., Ahmed, A. K., Matsangos, A. E., Lay, F., Born, L. J., Marti, G., et al. (2016). Cellular GFP toxicity and immunogenicity: potential confounders in in vivo cell tracking experiments. *Stem Cell Rev. Rep.* 12, 553–559. doi: 10.1007/s12015-016-9670-8

Barrientos, L. G., and Gronenborn, A. M. (2005). The highly specific carbohydrate-binding protein cyanovirin-N: structure, anti-HIV/Ebola activity and possibilities for therapy. *Mini Rev. Med. Chem.* 5, 21–31. doi: 10.2174/1389557053402783

Bokesch, H. R., O'Keefe, B. R., McKee, T. C., Pannell, L. K., Patterson, G. M., Gardella, R. S., et al. (2003). A potent novel anti-HIV protein from the cultured cyanobacterium *Scytonema varium*. *Biochemistry* 42, 2578–2584. doi: 10.1021/bi0205698

Bowen, E. T., Platt, G. S., Lloyd, G., Raymond, R. T., and Simpson, D. I. (1980). A comparative study of strains of Ebola virus isolated from southern Sudan and northern Zaire in 1976. *J. Med. Virol.* 6, 129–138. doi: 10.1002/jmv.1890060205

Brichacek, B., Lagenaur, L. A., Lee, P. P., Venzon, D., and Hamer, D. H. (2013). In vivo evaluation of safety and toxicity of a *Lactobacillus jensenii* producing modified cyanovirin-N in a rhesus macaque vaginal challenge model. *PLoS One* 8:e78817. doi: 10.1371/journal.pone.0078817

Cenciarelli, O., Pietropaoli, S., Malizia, A., Carestia, M., D'Amico, F., Sassolini, A., et al. (2015). Ebola virus disease 2013-2014 outbreak in West Africa: an analysis of the epidemic spread and response. *Int J Microbiol* 2015:769121

Colleluori, D. M., Tien, D., Kang, F., Pagliei, T., Kuss, R., McCormick, T., et al. (2005). Expression, purification, and characterization of recombinant cyanovirin-N for vaginal anti-HIV microbicide development. *Protein Expr. Purif.* 39, 229–236. doi: 10.1016/j.pep.2004.10.009

El-Maradny, Y. A., El-Fakharany, E. M., Abu-Serie, M. M., Hashish, M. H., and Selim, H. S. (2021). Lectins purified from medicinal and edible mushrooms: insights into their antiviral activity against pathogenic viruses. *Int. J. Biol. Macromol.* 179, 239–258. doi: 10.1016/j.ijbiomac.2021.03.015

Emau, P., Tian, B., O'keefe, B. R., Mori, T., McMahon, J. B., Palmer, K. E., et al. (2007). Griffithsin, a potent HIV entry inhibitor, is an excellent candidate for anti-HIV microbicide. *J. Med. Primatol.* 36, 244–253. doi: 10.1111/j.1600-0684.2007.00242.x

Feldmann, H., and Geisbert, T. W. (2011). Ebola haemorrhagic fever. *Lancet* 377, 849–862. doi: 10.1016/S0140-6736(10)60667-8

Fernandez Romero, J. A., Paglini, M. G., Priano, C., Koroch, A., Rodriguez, Y., Sailer, J., et al. (2021). Algal and cyanobacterial lectins and their antimicrobial properties. *Mar. Drugs* 19. doi: 10.3390/md19120687

Garrison, A. R., Giomarelli, B. G., Lear-Rooney, C. M., Saucedo, C. J., Yellayi, S., Krumpe, L. R., et al. (2014). The cyanobacterial lectin scytovirin displays potent in vitro and in vivo activity against Zaire Ebola virus. *Antivir. Res.* 112, 1–7. doi: 10.1016/j.antiviral.2014.09.012

Girard, L., Birse, K., Holm, J. B., Gajer, P., Humphrys, M. S., Garber, D., et al. (2018). Impact of the griffithsin anti-HIV microbicide and placebo gels on the rectal mucosal proteome and microbiome in non-human primates. *Sci. Rep.* 8:8059. doi: 10.1038/s41598-018-26313-8

Huskens, D., and Schols, D. (2012). Algal lectins as potential HIV microbicide candidates. *Mar. Drugs* 10, 1476–1497. doi: 10.3390/md10071476

Jacob, S. T., Crozier, I., Fischer, W. A. 2nd, Hewlett, A., Kraft, C. S., Vega, M. A., et al. (2020). Ebola virus disease. *Nat. Rev. Dis. Primers.* 6:13. doi: 10.1038/s41572-020-0147-3

Koharudin, L. M., and Gronenborn, A. M. (2014). Antiviral lectins as potential HIV microbicides. *Curr. Opin. Virol.* 7, 95–100. doi: 10.1016/j.coviro.2014.05.006

Kuhn, J. H., Adachi, T., Adhikari, N. K. J., Arribas, J. R., Bah, I. E., Bausch, D. G., et al. (2019). New filovirus disease classification and nomenclature. *Nat. Rev. Microbiol.* 17, 261–263. doi: 10.1038/s41579-019-0187-4

Lagenaur, L. A., Sanders-Beer, B. E., Brichacek, B., Pal, R., Liu, X., Liu, Y., et al. (2011). Prevention of vaginal SHIV transmission in macaques by a live recombinant Lactobacillus. *Mucosal Immunol.* 4, 648–657. doi: 10.1038/mi.2011.30

Li, M., Patton, D. L., Cosgrove-Sweeney, Y., Ratner, D., Rohan, L. C., Cole, A. M., et al. (2011). Incorporation of the HIV-1 microbicide cyanovirin-N in a food product. *J. Acquir. Immune Defic. Syndr.* 58, 379–384. doi: 10.1097/QAI.0b013e31823643fe

Li, Y., Zhang, X., Chen, G., Wei, D., and Chen, F. (2008). Algal lectins for potential prevention of HIV transmission. *Curr. Med. Chem.* 15, 1096–1104. doi: 10.2174/092986708784221421

Mazur-Marzec, H., Ceglowska, M., Konkel, R., and Pyrc, K. (2021). Antiviral Cyanometabolites-A review. *Biomol. Ther.* 11. doi: 10.3390/biom11030474

Mitchell, C. A., Ramessar, K., and O'Keefe, B. R. (2017). Antiviral lectins: selective inhibitors of viral entry. *Antivir. Res.* 142, 37–54. doi: 10.1016/j.antiviral.2017.03.007

Mori, T., O'Keefe, B. R., Sowder, R. C. 2nd, Bringans, S., Gardella, R., Berg, S., et al. (2005). Isolation and characterization of griffithsin, a novel HIV-inactivating protein, from the red alga *Griffithsia* sp. *J. Biol. Chem.* 280, 9345–9353. doi: 10.1074/jbc.M411122200

Moulaei, T., Botos, I., Ziolkowska, N. E., Bokesch, H. R., Krumpe, L. R., McKee, T. C., et al. (2007). Atomic-resolution crystal structure of the antiviral lectin scytovirin. *Protein Sci.* 16, 2756–2760. doi: 10.1110/ps.073157507

Nahui Palomino, R. A., Zicari, S., Vanpouille, C., Vitali, B., and Margolis, L. (2017). Vaginal lactobacillus inhibits HIV-1 replication in human tissues ex vivo. *Front. Microbiol.* 8:906. doi: 10.3389/fmicb.2017.00906

Naik, S., and Kumar, S. (2022). Lectins from plants and algae act as anti-viral against HIV, influenza and coronaviruses. *Mol. Biol. Rep.* 49, 12239–12246. doi: 10.1007/s11033-022-07854-8

Obiero, J., Mwethera, P. G., Hussey, G. D., and Wiysonge, C. S. (2012). Vaginal microbicides for reducing the risk of sexual acquisition of HIV infection in women: systematic review and meta-analysis. *BMC Infect. Dis.* 12:289. doi: 10.1186/1471-2334-12-289

O'Keefe, B. R., Murad, A. M., Vianna, G. R., Ramessar, K., Saucedo, C. J., Wilson, J., et al. (2015). Engineering soya bean seeds as a scalable platform to produce cyanovirin-N, a non-ARV microbicide against HIV. *Plant Biotechnol. J.* 13, 884–892. doi: 10.1111/pbi.12309

Platt, E. J., Bilska, M., Kozak, S. L., Kabat, D., and Montefiori, D. C. (2009). Evidence that ecotropic murine leukemia virus contamination in TZM-bl cells does not affect the outcome of neutralizing antibody assays with human immunodeficiency virus type 1. *J. Virol.* 83, 8289–8292. doi: 10.1128/JVI.00709-09

Ramachandran, R., and Shanmughavel, P. (2009). Role of microbicides in the prevention of HIV and sexually transmitted diseases – a review. *Curr. HIV Res.* 7, 279–286. doi: 10.2174/157016209788347921

Tegegne, B. A., and Kebede, B. (2022). Probiotics, their prophylactic and therapeutic applications in human health development: a review of the literature. *Heliyon* 8:e09725. doi: 10.1016/j.heliyon.2022.e09725

Vamvaka, E., Evans, A., Ramessar, K., Krumpe, L. R., Shattock, R. J., O'Keefe, B. R., et al. (2016). Cyanovirin-N produced in rice endosperm offers effective pre-exposure prophylaxis against HIV-1BaL infection in vitro. *Plant Cell Rep.* 35, 1309–1319. doi: 10.1007/s00299-016-1963-5

Wang, L. L., Estrada, L., Wiggins, J., Anantpadma, M., Patten, J. J., Davey, R. A., et al. (2022). Ligand-based design of peptide entry inhibitors targeting the endosomal receptor binding site of filoviruses. *Antivir. Res.* 206:105399. doi: 10.1016/j.antiviral.2022.105399

Wei, W., Wiggins, J., Hu, D., Vrbanac, V., Bowder, D., Mellon, M., et al. (2019). Blocking HIV-1 infection by chromosomal integrative expression of human CD4 on the surface of *Lactobacillus acidophilus* ATCC 4356. *J. Virol.* 93. doi: 10.1128/JVI.01830-18

Welker, D. L., Coburn, B. M., McClatchy, J. H., and Broadbent, J. R. (2019). Multiple pulse electroporation of lactic acid bacteria *Lactococcus lactis* and *Lactobacillus casei*. *J. Microbiol. Methods* 166:105741. doi: 10.1016/j.mimet.2019.105741

WHO (n.d.). Available at: https://www.who.int/health-topics/ebola/

Xiong, C., O'Keefe, B. R., Botos, I., Wlodawer, A., and McMahon, J. B. (2006). Overexpression and purification of scytovirin, a potent, novel anti-HIV protein from the cultured cyanobacterium *Scytonema varium*. *Protein Expr. Purif.* 46, 233–239. doi: 10.1016/j.pep.2005.09.019

Yadav, M., Mandeep, , and Shukla, P. (2020). Probiotics of diverse origin and their therapeutic applications: a review. *J. Am. Coll. Nutr.* 39, 469–479. doi: 10.1080/07315724.2019.1691957

Frontiers in Microbiology

Explores the habitable world and the potential of microbial life

The largest and most cited microbiology journal which advances our understanding of the role microbes play in addressing global challenges such as healthcare, food security, and climate change.

Discover the latest Research Topics

See more →

Frontiers

Avenue du Tribunal-Fédéral 34
1005 Lausanne, Switzerland
frontiersin.org

Contact us

+41 (0)21 510 17 00
frontiersin.org/about/contact